

AD _____

Award Number: DAMD17-03-1-0343

TITLE: Breast Cancer Gene Therapy: Development of Novel Non-Invasive Magnetic Resonance Assay to Optimize Efficacy

PRINCIPAL INVESTIGATOR: Ralph P. Mason, Ph.D.

CONTRACTING ORGANIZATION: The University of Texas Southwestern Medical Center
at Dallas
Dallas, TX 75390-9058

REPORT DATE: May 2007

TYPE OF REPORT: Final

PREPARED FOR: U.S. Army Medical Research and Materiel Command
Fort Detrick, Maryland 21702-5012

DISTRIBUTION STATEMENT: Approved for Public Release;
Distribution Unlimited

The views, opinions and/or findings contained in this report are those of the author(s) and should not be construed as an official Department of the Army position, policy or decision unless so designated by other documentation.

REPORT DOCUMENTATION PAGE				Form Approved OMB No. 0704-0188	
Public reporting burden for this collection of information is estimated to average 1 hour per response, including the time for reviewing instructions, searching existing data sources, gathering and maintaining the data needed, and completing and reviewing this collection of information. Send comments regarding this burden estimate or any other aspect of this collection of information, including suggestions for reducing this burden to Department of Defense, Washington Headquarters Services, Directorate for Information Operations and Reports (0704-0188), 1215 Jefferson Davis Highway, Suite 1204, Arlington, VA 22202-4302. Respondents should be aware that notwithstanding any other provision of law, no person shall be subject to any penalty for failing to comply with a collection of information if it does not display a currently valid OMB control number. PLEASE DO NOT RETURN YOUR FORM TO THE ABOVE ADDRESS.					
1. REPORT DATE 01-05-2007		2. REPORT TYPE Final		3. DATES COVERED 1 May 2003– 30 Apr 2007	
4. TITLE AND SUBTITLE Breast Cancer Gene Therapy: Development of Novel Non-Invasive Magnetic Resonance Assay to Optimize Efficacy				5a. CONTRACT NUMBER	
				5b. GRANT NUMBER DAMD17-03-1-0343	
				5c. PROGRAM ELEMENT NUMBER	
6. AUTHOR(S) Ralph P. Mason, Ph.D. Email: Ralph.Mason@UTSouthwestern.edu				5d. PROJECT NUMBER	
				5e. TASK NUMBER	
				5f. WORK UNIT NUMBER	
7. PERFORMING ORGANIZATION NAME(S) AND ADDRESS(ES) The University of Texas Southwestern Medical Center at Dallas Dallas, TX 75390-9058				8. PERFORMING ORGANIZATION REPORT NUMBER	
9. SPONSORING / MONITORING AGENCY NAME(S) AND ADDRESS(ES) U.S. Army Medical Research and Materiel Command Fort Detrick, Maryland 21702-5012				10. SPONSOR/MONITOR'S ACRONYM(S)	
				11. SPONSOR/MONITOR'S REPORT NUMBER(S)	
12. DISTRIBUTION / AVAILABILITY STATEMENT Approved for Public Release; Distribution Unlimited					
13. SUPPLEMENTARY NOTES Original contains colored plates: ALL DTIC reproductions will be in black and white.					
14. ABSTRACT Gene therapy holds great promise for treatment of breast cancer. In particular clinical trials are underway to apply therapeutic genes related to pro-drug activation or to modulate the activity of oncogenes by blocking promoter sites. However, there are major problems in terms of assessing the delivery to target tissue, assessing the uniformity (versus heterogeneity) of biodistribution, and determining whether the genes are expressed. We designed, evaluated and tested a novel approach to gene activity detection- specifically, using fluorinated substrates of β -galactosidase to reveal gene activity. Our prototype molecule PFONPG (p-fluoro-o-nitro-phenyl β -D-galactopyranoside) is a direct analog of the traditional "yellow" biochemical indicator ONPG (o- nitro-phenyl β -D-galactopyranoside). Analogs of this prototype were developed to optimize MR and biological characteristics and explore the feasibility of tailoring the reporter to specific applications, e.g., exploiting β -gal activity to deliver specific physiological reporter molecules such as pH and potentially specific cytotoxic agents. The agents have been tested in solution, applied to cultured breast cancer cells, and used to examine β -gal activity in vivo in transfected breast tumors.					
15. SUBJECT TERMS Gene therapy, fluorine NMR, β -galactosidase, pH					
16. SECURITY CLASSIFICATION OF:			17. LIMITATION OF ABSTRACT	18. NUMBER OF PAGES	19a. NAME OF RESPONSIBLE PERSON
a. REPORT	b. ABSTRACT	c. THIS PAGE			USAMRMC
U	U	U	UU	270	19b. TELEPHONE NUMBER (include area code)

Table of Contents

Introduction.....	4
Body.....	5
Key Research Accomplishments.....	37
Reportable Outcomes.....	38
Conclusions.....	41
References.....	43
Appendices.....	45

Introduction

Gene therapy holds great promise for treatment of breast cancer (1, 2). In particular, clinical trials are underway to apply therapeutic genes related to pro-drug activation or modulation of the activity of oncogenes by blocking promoter sites. However, there are major problems in terms of assessing the delivery to target tissue, assessing the uniformity (versus heterogeneity) of biodistribution, and determining whether the genes are expressed. We proposed to design, evaluate and apply a novel approach to gene activity detection- specifically, using fluorinated substrates of β -galactosidase to reveal gene activity. Our prototype molecule PFONPG (para- fluoro- ortho- nitro- phenyl β -D-galactopyranoside) is a direct analog of the traditional “yellow” biochemical indicator ONPG (ortho- nitro- phenyl β -D-galactopyranoside).. We synthesized analogs of this prototype to optimize MR and biological characteristics and explore the feasibility of tailoring the reporter to specific applications, *e.g.*, exploiting β -gal activity to deliver specific physiological reporter molecules such as pH and potentially specific cytotoxic agents. The agents were tested in solution, applied to cultured breast cancer cells, and ultimately used to reveal β -gal activity *in vivo* in transfected breast tumors in mice.

Body

Task 1 Synthesize novel molecules to report activity of the β -galactosidase gene- minimum 8 novel agents: completed Year 1.

We successfully synthesized twelve simple novel fluorine substituted phenylgalactosides, as potential ^{19}F NMR reporter molecules for β -galactosidase activity. These all include an aglycone with a fluorine atom of trifluoromethyl group sensitive to β -gal activity. Approaches and results have been published in two primary manuscripts (3, 4) and in two reviews (5, 6).

- 1 “A Novel NMR Platform for Detecting Gene Transfection: Synthesis and Evaluation of Fluorinated Phenyl β -D-Galactosides with Potential Application for Assessing LacZ Gene Expression”, J. Yu, P. Otten, Z. Ma, W. Cui, L. Liu, R. P. Mason, *Bioconjug. Chem.* 15 (6): 1334-1341 (2004),
- 2 “Synthesis and Evaluation of Novel Enhanced Gene Reporter Molecules: Detection of β -Galactosidase Activity Using ^{19}F NMR of Trifluoromethylated Aryl β -D-Galactopyranosides”, J. Yu, L. Liu, V. D. Kodibagkar, W. Cui, R. P. Mason, *Bioorg. Med. Chem.*, 14, 326-33 (2006).
- 3 “ ^{19}F : a versatile reporter for non-invasive physiology and pharmacology using magnetic resonance”, J. Yu, V. D. Kodibagkar, W. Cui, R. P. Mason, *Curr. Med. Chem.* 12 (7) 819-848 (2005) + cover figure and editorial
- 4 “Non-invasive physiology and pharmacology using ^{19}F magnetic resonance” J-X. Yu, W. Cui, D. Zhao, and R. P. Mason, *Adv. Fluorine Chem.*, in the press 2007

The results are also summarized below. Molecular structures are in Figures 1 and 2.

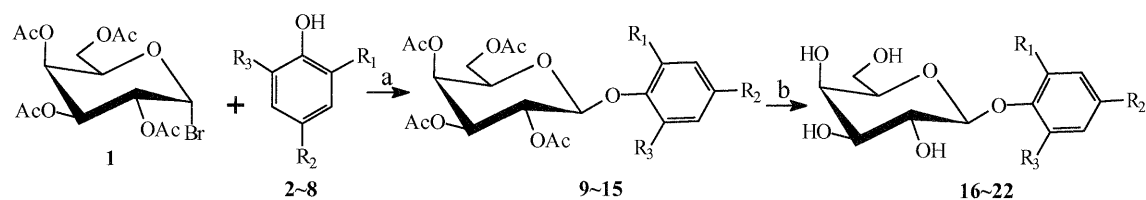


Figure 1. The reactions and structures of 1~22 (fluorophenylgalactosides) (4).

Reaction conditions: (a) CH_2Cl_2 - H_2O , pH 8~9, 50 °C, TBAB, ~1 h, near quantitative yield; (b) NH_3 -MeOH, 0 °C→r.t., 24 h, quantitative yields. R groups are defined in chart below

Compounds	R ₁	R ₂	R ₃
2, 9, 16	NO ₂	F	H
3, 10, 17	F	NO ₂	H
4, 11, 18	F	H	NO ₂
5, 12, 19	F	H	H
6, 13, 20	H	F	H
7, 14, 21	Cl	F	H
8, 15, 22	Br	F	H

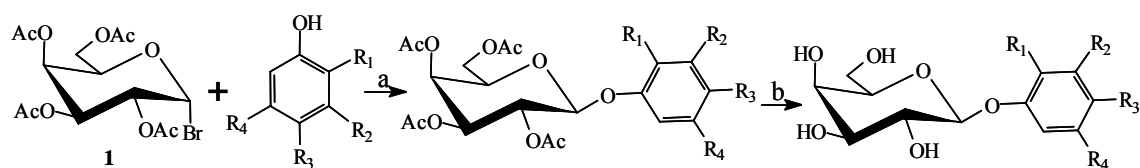


Figure 2. The reactions and structures of trifluorophenylgalactosides with structures defined below (3) .

Reaction conditions: (a) CH₂Cl₂-H₂O, pH 8~9, 50 °C, TBAB, ~1 h, near quantitative yield except **13** in only 20% yield; (b) NH₃-MeOH, 0 °C → r.t., 24 h, quantitative yields.

Compounds	R ₁	R ₂	R ₃	R ₄
	NO ₂	H	CF ₃	H
	H	CF ₃	NO ₂	H
	Cl	CF ₃	H	H
	Cl	H	H	CF ₃
	CF ₃	H	H	H
	H	CF ₃	H	H
	H	H	CF ₃	H

Task 2 Characterize novel agents (NMR, mass spec, colorimetric analysis): completed Year 1.

Each of the molecules described in Task 1 was fully characterized and structure validated by mass spectrometry, high resolution NMR, and other techniques, as appropriate. Details are provided in manuscripts 1 and 2 listed as for Task 1 (3, 4) and representative results follow:

Fluorinated phenyl β -D-galactopyranoside tetraacetates 9-15.

General procedure (Fig. 1). A solution of **1** (1 mmol; 2, 3, 4, 6-tetra-O-acetyl- α -D-galactopyranosyl bromide, Sigma) in CH_2Cl_2 (5 ml) was added dropwise to a vigorously stirred solution of fluorophenol **2 - 8** (1.2 mmol) and tetrabutylammonium bromide (0.48 g, 1.5 mmol) in H_2O (5 ml; pH 8~9) at 50 °C in 3-neck round-bottom flask equipped with condenser and thermometer. After TLC showed complete reaction (~1 h) the organic layer was separated, washed, dried, evaporated under reduced pressure and recrystallized ($\text{EtOH-H}_2\text{O}$) or purified by column chromatography on silica gel to give fluorinated aryl β -D-galactopyranoside tetraacetates **9 - 15**, as white crystals.

2-Nitro-4-fluorophenyl 2, 3, 4, 6-tetra-O-acetyl- β -D-galactopyranoside 9 (0.5 g, 99%), R_f 0.31(3:2 cyclohexane-EtOAc), δ_H : 7.55(1H, dd, $J=3.0, 8.4$ Hz, Ar-H), 7.42(1H, dd, $J=4.8, 9.0$ Hz, Ar-H), 7.27(1H, m, Ar-H), 5.04(1H, d, $J_{1,2}=7.8$ Hz, H-1), 5.52(1H, dd, $J_{2,3}=8.4$ Hz, H-2), 5.11(1H, dd, $J_{3,4}=3.0$ Hz, H-3), 5.47(1H, d, $J_{4,5}=2.6$ Hz, H-4), 4.07(1H, m, H-5), 4.26(1H, dd, $J_{5,6a}=4.2$ Hz, $J_{6a,6b}=11.4$ Hz, H-6a), 4.17(1H, dd, $J_{5,6b}=5.4$ Hz, H-6b), 2.20, 2.14, 2.07, 2.02(12H, 4s, 4 \times CH₃CO)ppm; δ_C : 170.43, 170.31, 170.24, 169.62(4 \times CH₃CO), 157.70(d, $J_{F-C}=164.8$ Hz, Ar-C), 145.66(Ar-C), 141.86(d, $J_{F-C}=5.7$ Hz, Ar-C), 122.68(d, $J_{F-C}=4.9$ Hz, Ar-C), 120.77(d, $J_{F-C}=15.2$ Hz, Ar-C), 112.60(d, $J_{F-C}=18.3$ Hz, Ar-C), 101.40(C-1), 68.01(C-2), 70.63(C-3), 66.86(C-4), 71.58(C-5), 61.45(C-6), 21.25, 21.10, 20.38, 20.25(4 \times CH₃CO)ppm; HRMS: $[\text{M}+\text{Na}]^+$, $\text{C}_{20}\text{H}_{22}\text{NO}_{12}\text{FNa}$, Calcd: 510.1024, Found: 510.1014; $[\text{M}+\text{K}]^+$, $\text{C}_{20}\text{H}_{22}\text{NO}_{12}\text{FK}$, Calcd: 526.0763, Found: 526.0751.

Fluorinated aryl β -D-galactopyranosides 16 - 22. *General procedure*---- A solution of fluorophenyl 2,3,4,6-tetra-O-acetyl- β -D-galactopyranoside (**9 - 15**) (0.4 g) in anhydrous MeOH (15 ml) containing 0.5M NH_3 was vigorously stirred from 0 °C to room temperature overnight

until TLC showed complete reaction. Following solvent removal *in vacuo*, chromatography on silica gel (EtOAc/MeOH) afforded the free galactopyranosides **16 - 22** in near quantitative yield, as white crystalline materials

2-Nitro-4-fluorophenyl β -D-galactopyranoside 16, R_f 0.40(1:9 MeOH-EtOAc), δ_H : 7.84(1H, dd, $J=2.8, 8.0$ Hz, Ar-H), 7.53(1H, ddd, $J=1.6, 1.0, 2.8$ Hz, Ar-H), 7.43(1H, dd, $J=4.4, 9.2$ Hz, Ar-H), 4.96(1H, d, $J_{1,2}=7.6$ Hz, H-1), 3.60(1H, dd, $J_{2,3}=10.6$ Hz, H-2), 3.51(1H, dd, $J_{3,4}=5.2$ Hz, H-3), 3.47(1H, d, $J_{4,5}=5.6$ Hz, H-4), 3.43(1H, m, H-5), 3.67(2H, m, H-6), 5.16(1H, d, $J_{H-2,OH-2}=5.2$ Hz, HO-2), 4.67(1H, d, $J_{H-3,OH-3}=4.4$ Hz, HO-3), 4.90(1H, d, $J_{H-4,OH-4}=6.0$ Hz, HO-4), 4.67(1H, t, $J_{H-6,OH-6}=5.2, 5.4$ Hz, HO-6)ppm; δ_C : 155.41(d, $J_{F-C}=239.6$ Hz, Ar-C), 146.19(d, $J_{F-C}=3.1$ Hz, Ar-C), 140.17(d, $J_{F-C}=9.1$ Hz, Ar-C), 120.91(d, $J_{F-C}=22.1$ Hz, Ar-C), 119.03(d, $J_{F-C}=7.7$ Hz, Ar-C), 111.89(d, $J_{F-C}=27.5$ Hz, Ar-C), 101.65(C-1), 70.07(C-2), 73.37(C-3), 68.06(C-4), 75.87 (C-5), 60.33(C-6)ppm; HRMS: $[M+Na]^+$, $C_{12}H_{14}NO_8FNa$, Calcd: 342.0601, Found: 342.0589; $[M+K]^+$, $C_{12}H_{14}NO_8FK$, Calcd: 358.0341, Found: 358.0328.

The titration curve of each aglycone was analyzed, as presented in Figure 3 and Table 1. Although there were eight product aryl galactosides, one comprised α and β anomers, so that there are 7 aglycones for assessment.

Titration Curves of the aglycones 2~8

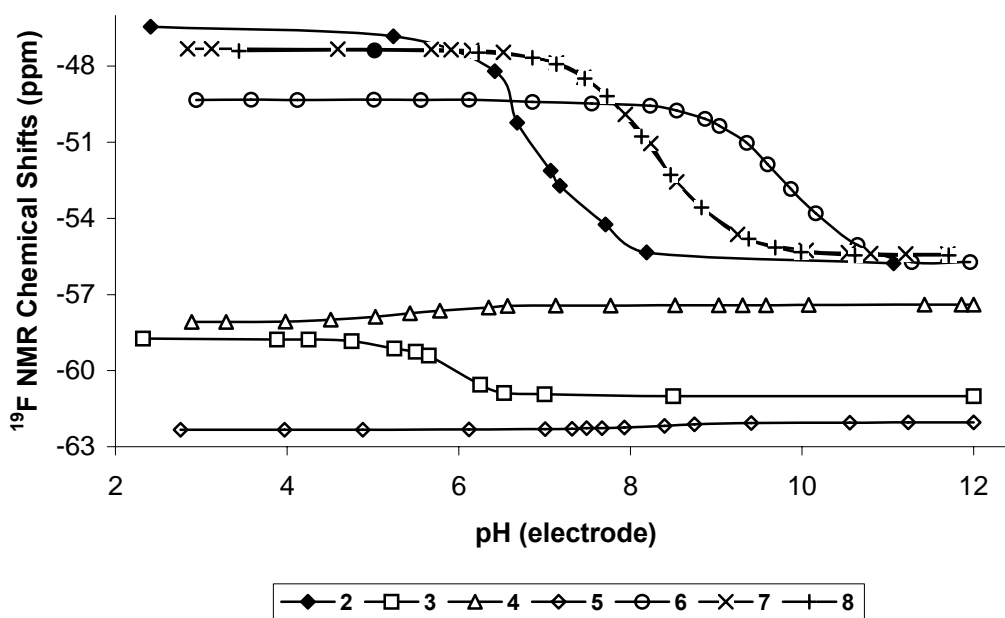


Figure 3 ^{19}F NMR chemical shift pH titration curves of 2-8 in saline at 25 °C, summarized in Table 1

Table 1 ^{19}F NMR pH characterization of aglycones at 25 °C

Compd.	2	3	4	5	6	7	8
<i>pKa</i>	6.87	6.03	5.44	8.33	9.80	8.31	8.28
$\delta_{(\text{acid})}$	-44.44	-58.77	-58.07	-62.33	-49.33	-47.32	-47.40
$\delta_{(\text{base})}$	-55.76	-61.01	-57.39	-62.04	-57.72	-55.40	-55.45
$\Delta\delta(\text{ppm})$	11.32	2.24	0.68	0.29	6.39	8.08	8.05

Task 3 Test agents for enzyme activity in solution: completed Year 1.

Each of the agents was evaluated for β -gal enzyme activity. Details are provided in manuscripts as for Task 1 (3, 4) and summarized in Figure 4 and Table 2 below. All β -anomers were substrate for β -gal, whereas the α -anomer 18B was not cleaved.

As a further test of enzyme/substrate specificity β -galactosidase was added to a mixture of 2-nitro-4-fluorophenyl β -D-glucopyranoside (PFONPGu) and 2-nitro-4-fluorophenyl β -D-galactopyranoside (PFONPG). While the β -galactopyranoside was fully cleaved within 10 mins, no activity was seen for the β -D-glucopyranoside (Figure 5). The para fluoro glucopyranoside and galactopyranoside were barely resolved, but noting the range of chemical shifts of substrates, we also compared 2-nitro-4-fluorophenyl β -D-glucopyranoside (PFONPGu) and 4-nitro-2-fluorophenyl β -D-galactopyranoside (OFPNPG). Now substrates were well resolved. As before, the β -galactopyranoside was readily cleaved (< 10 mins; Figure 6). Six hours later some β -D-glucopyranoside was seen to be cleaved. We also sought to test β -galactopyranoside with β -glucosidases, but have not been able to find any which are active in the physiological range.

Table 2. ^{19}F chemical shifts (ppm) of 16 - 22 before and after the hydrolysis by β -gal*

Compd.	16	17	18A	18B	19	20	21	22
$\delta_{\text{F}}(\text{substrate})$	-42.87	-54.93	-50.67	-49.37	-58.74	-45.87	-43.56	-43.82
$\delta_{\text{F}}(\text{product})$	-52.71	-61.04	-58.67		-62.30	-49.59	-48.13	-48.24
Observed $\Delta\delta_{\text{F}}$	9.84	6.11	8.00		3.56	3.72	4.57	4.42
Min $\Delta\delta_{\text{F}}$	1.57	3.84	6.72		3.3	3.46	3.76	3.58
Max $\Delta\delta_{\text{F}}$	12.89	6.11	8.1		3.59	11.85	11.84	11.63

* β -gal (E801A, 20 units at 37°C in 0.1M PBS, pH 7.4).

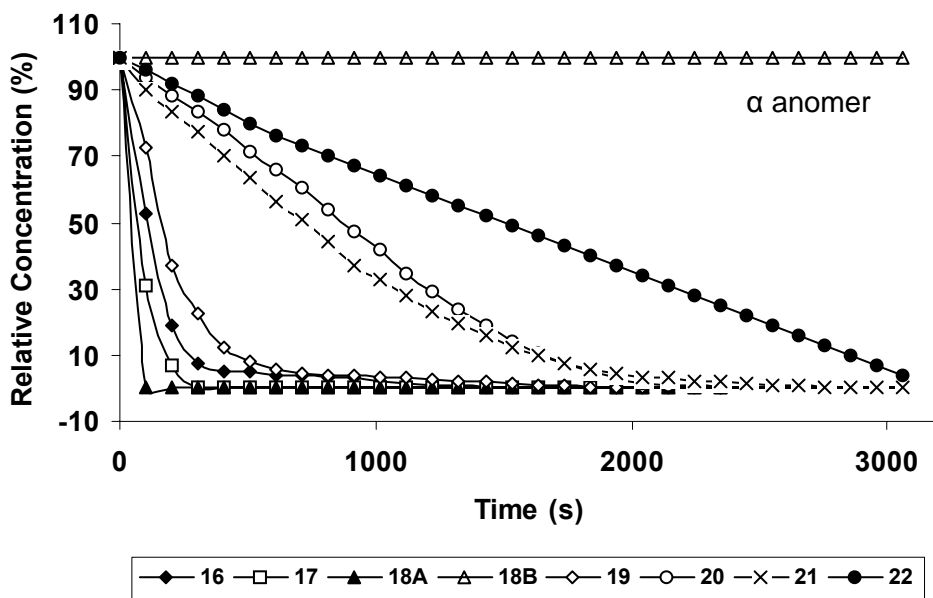


Figure 4 Hydrolysis time courses of the fluorinated phenyl D-galactopyranoside 16-22 (15 mmol) by β -gal (E801A, 20 units) in PBS (0.1M, 0.6 ml) at 37 °C

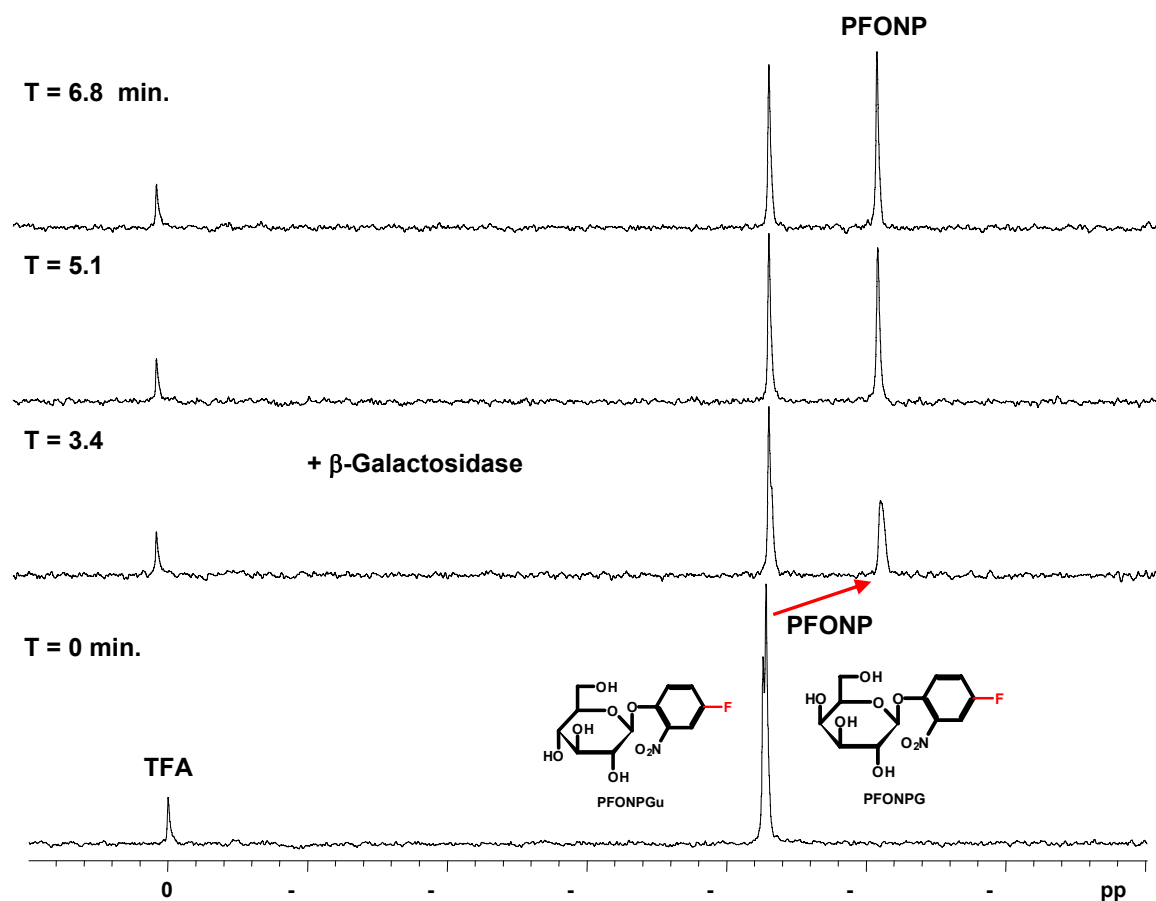


Figure 5. Testing substrate specificity. Para-fluoro-ortho-nitro aglycones conjugated with glucose (PFONPGu) or galactose (PFONPG) were evaluated by ^{19}F NMR with respect to addition of β -galactosidase. PFONPGu (2.9 mg, 9.1 mmol) and PFONPG (3.0 mg, 9.4 mmol) in PBS (0.1 M, pH 7.4, 600 μL) at 22°C with respect to addition of β -gal (E801A, 10 μL , 1 unit/ μL). PFONPG was cleaved rapidly whereas PFONPGu showed no change.

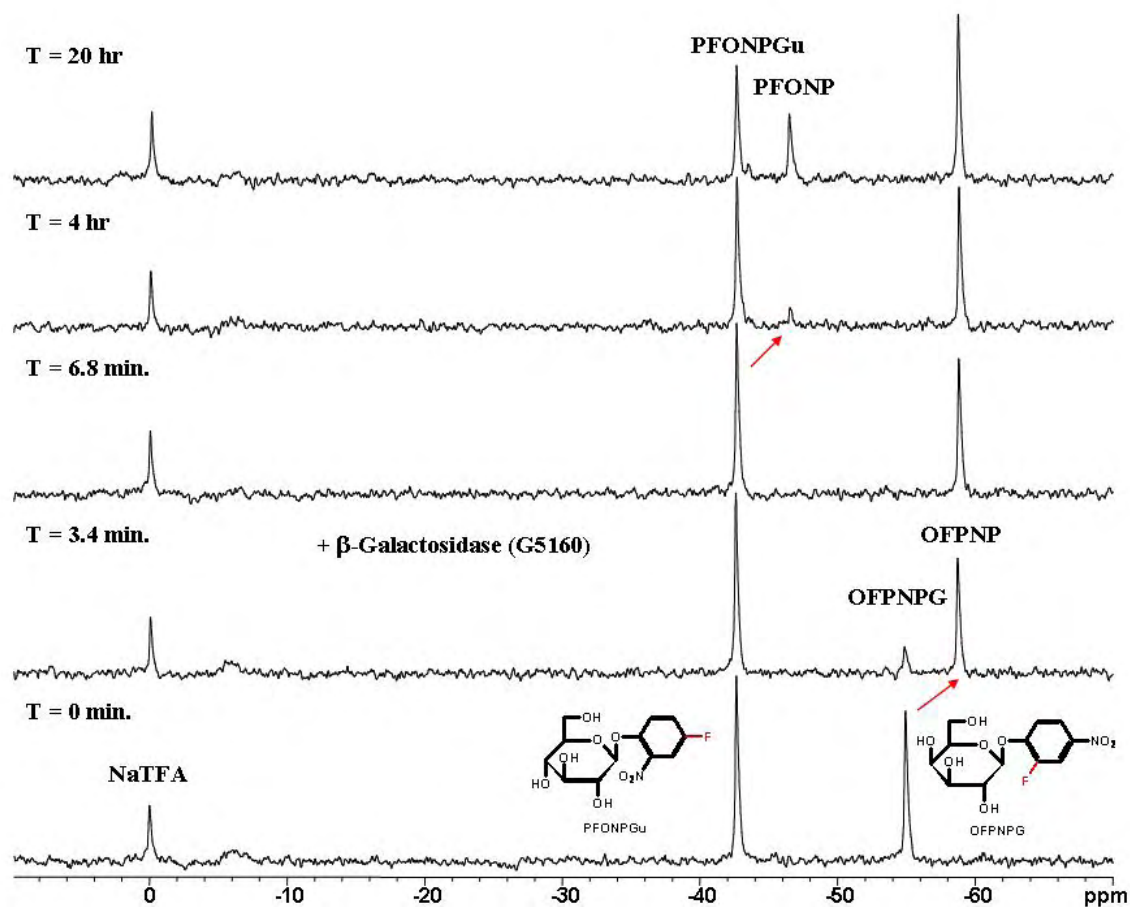


Figure 6. Comparing substrate specificity. OFPNPG (2.2 mg, 6.8 mmol) plus PFONPGu (2.5 mg, 7.7 mmol) in PBS (0.1 M, pH 4.5, 600uL) at 37°C with addition of β -galactosidase (G5160, 15 uL, 38 units/100uL). The glucoside reacted very slowly.

Task 4 Test initial indicators in cultured breast cancer cells (control + transfected): completed in Year 2.

We had expected to be able to readily acquire β -gal expressing breast tumor cells from tissue banks, but available cells were found to exhibit very low expression. Thus, in year 1 we were forced to undertake tests in PC3, LNCaP, MAT-Lu, and 9L glioma cells expressing β -gal. Establishing high expressing lacZ (β -gal) breast cancer cell lines became a high priority and Dr. Liu established several tumors in our laboratory (*e.g.*, MTLn3-lacZ, MCF7-lacZ). Results were published in the papers mentioned for Task 1 together with additional papers (3, 4, 7, 8).

- 5 “A novel NMR approach to assessing gene transfection: 4-fluoro-2-nitrophenyl- β -D-galactopyranoside as a prototype reporter molecule for β -galactosidase”, W. Cui, P. Otten, Y. Li, K. S. Koeneman, J. Yu and R. P. Mason, *Magn. Reson. Med.*, **51**, 616-20 (2004)
- 6 “Imaging β -galactosidase activity using ^{19}F CSI of lacZ gene-reporter molecule 2-fluoro-4-nitrophenol- β -D-galactopyranoside (OFPNPG)” V. D. Kodibagkar, J. Yu, L. Liu, H. Hetherington, R. P. Mason *Magn. Reson. Imaging* 24: 959-962 (2006)

Initially we established stably transfected rat MTLn3-lacZ and their activity was described in Yu *et al. Bioconjug. Chem.* (2004) (4) and shown in Figure 7, but activity was low. Much higher activity was achieved in MCF7 cells (Figure 8)

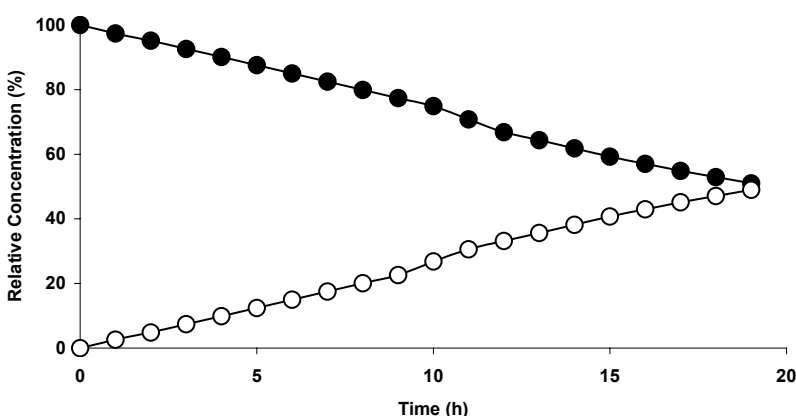


Figure 7 Hydrolysis of 2-fluoro-4-nitrophenyl- β -D-galactopyranoside (open symbols) to 2-fluoro-4-nitrophenol (solid symbols) by stably transfected rat breast tumor MTLn3-lacZ (9.8×10^6) in PBS at 37 °C.

Characterization and use of the new transfected MCF7 cells follows.

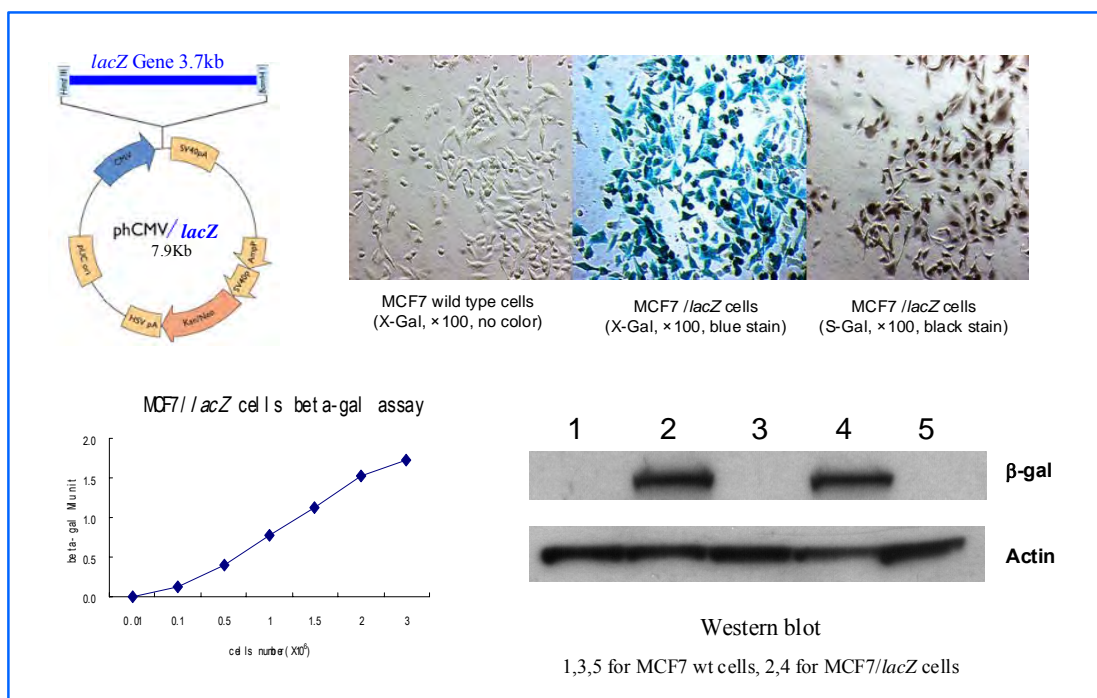


Figure 8 Stable expression of β-gal MCF7 cell lines. The phCMV/*lacZ* plasmid map is top left. MCF7-*lacZ* cells were stained using X-Gal (blue) and S-Gal (black), MCF7 wild type cell did not stain (no color). More than 90% MCF7-*lacZ* cells were stained after passage for 30 generations. *LacZ* gene expression in stably MCF7-*lacZ* cells was confirmed by β-gal assay and Western blot. The definition of β-gal unit is that one unit will hydrolyze 1.0 μmol of o-nitrophenyl β-*D*-galactoside (ONPG) to o-nitrophenol and *D*-galactose per min.

The cells showed activity on the ¹⁹F NMR reporters (Figure 9), but we have found some toxicity associated with the nitrophenol aglycones (Figure 10). This set a foundation for gene activated broad spectrum chemotherapy, which was further evaluated in Task 8. We found that the toxicity of the aglycone was masked in the conjugate substrate for wild type cells, but toxicity occurs in β-gal expressing cells (Figure 10). This prompted us to seek less toxic agents as part of Task 5.

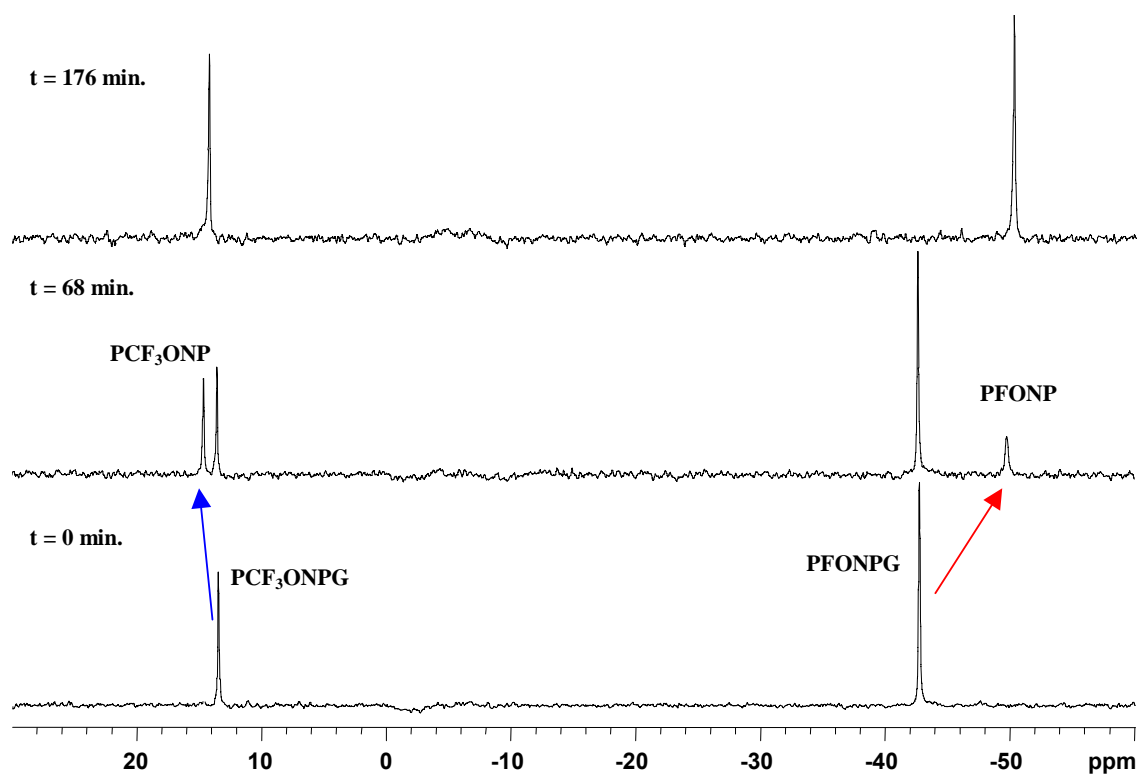


Figure 9. ^{19}F NMR spectra of PCF_3ONPG (1.4 mg, 4.5 mmol) and PFONPG (6.0 mg, 18.8 mmol) showing simultaneous hydrolysis by stably transfected MCF7-lacZ cells (1.75×10^6) in PBS (0.1M, pH=7.4, 600 μL) at 37 $^\circ\text{C}$. Each spectrum acquired in 51 s.

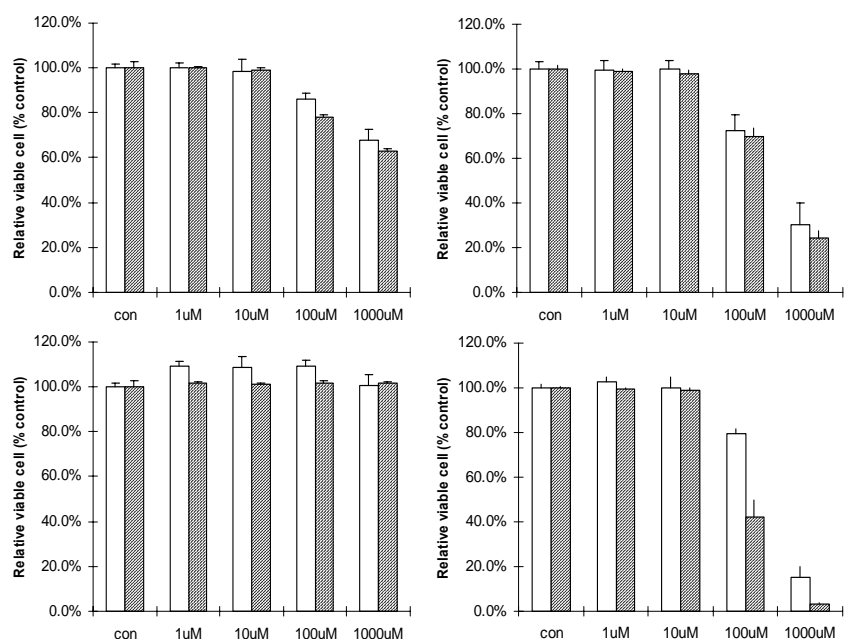


Figure 10. Viability of human breast cancer cells with respect to exposure to substrate 2-nitro-4-trifluoromethylphenyl β -D-galactopyranoside (left panels) or aglycone (2-nitro-4-trifluoromethylphenol) (right panels). Upper panels MCF7-lacZ cells; lower panels MCF7-WT .

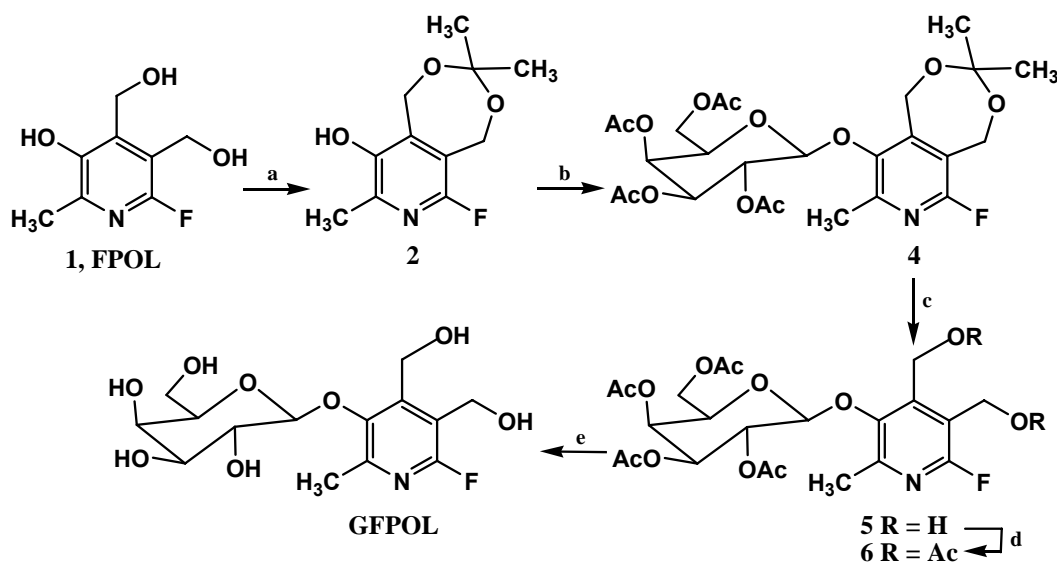
Open bars 48 h exposure; hatched bars 96 h exposure.

Task 5 Scale up synthesis of most promising indicator for animal investigations: completed in Year 2.

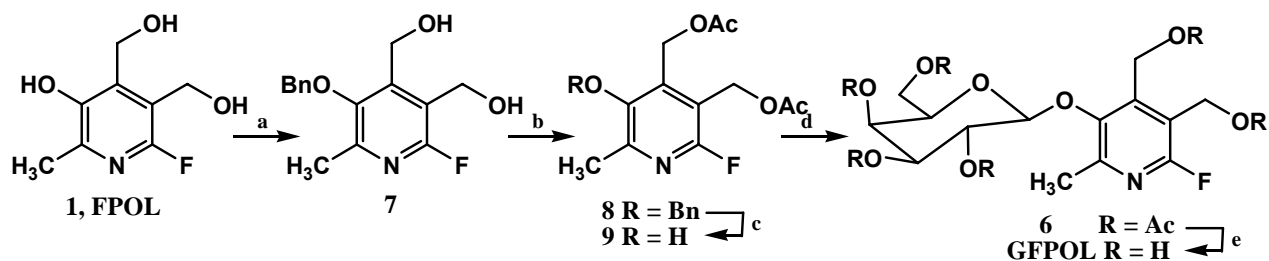
Synthesis of reporter molecules was scaled up to provide materials for *in vivo* evaluation. In particular, Dr. Yu developed novel synthetic strategies, which gave higher yields and fewer synthetic steps. As described in Yu *et al. Bioconjug. Chem.* (2004) (4) the use of phase transfer catalysis provided high yields, high stereo specificity, and mild reaction conditions for the synthesis of the fluorophenyl β -D-galactopyranosides. Optimization of procedures was particularly significant for the second generation reporter molecule GFPOL (Figure 11) (9), which was developed to exhibit lower toxicity, as described in

“Synthesis and Evaluation of a Novel Gene Reporter Molecule: Detection of β -galactosidase activity Using ^{19}F NMR of a Fluorinated Vitamin B₆ conjugate” J. Yu, Z. Ma, Y. Li, K. S. Koeneman, L. Liu, R. P. Mason, *Med. Chem.* 1(3) 255-262 (2005)

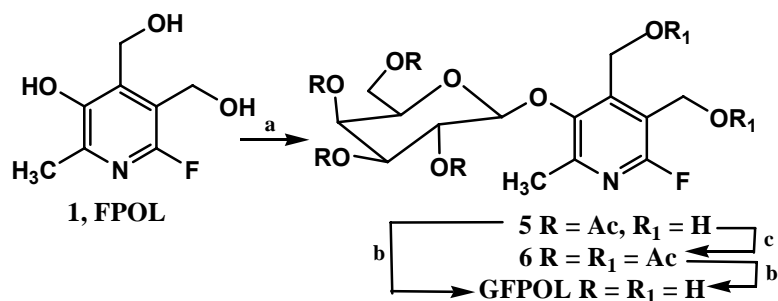
The overall yield of the original five-step route was ~3% (Scheme 1, below). A revised strategy gave 68% overall yield (Scheme 2) and direct galactopyranosylation using 2, 3, 4, 6-tetra-*O*-acetyl- α -D-galactopyranosyl bromide and phase-transfer catalysis gave (88%) (Scheme 3).



Scheme 1



Scheme 2



Scheme 3

Figure 11 Synthetic approaches to GFPOL

Task 6 Evaluate in mice (constitutively expressing β -gal ROSA animals); test dosing protocols, timing, MR detection protocols: completed in Year 3.

We found that administration of PFONPG (4-fluoro-2-nitrophenol- β -D-galactopyranoside) to ROSA mice caused rapid death. We believe this was due to release of toxic aglycone (nitrophenol) causing rapid depolarization of the heart. Indeed, perfusion of a heart with the PFONP aglycone caused immediate cardiac arrest. However, we were able to show effective conversion of reporter molecules by tissues (heart, liver, and muscle) excised from ROSA mice, but not wild type mice. Fluorophenylgalactopyranoside substrates could be administered systemically in normal mice without apparent toxicity.

A problem with systemic delivery was competing wash-in and wash-out phenomena. In some cases, we were able to detect signal from tumors following IP administration, but substrate signal was weak and washed out again. Thus, any conversion of substrate to aglycone product by β -gal competed with substrate clearance. Likewise product cleared, and thus, signal was difficult to detect. However, we established that direct intra tumoral injection of substrate provided

excellent signal to noise (>10), which could be detected within 5 minutes by spectroscopy. Some substrate clearance occurred, but in β -gal expressing tumors, conversion to aglycone product was much faster and the product signal was readily detected. We examined multiple mice expressing MCF7-lacZ or -WT tumors. Following direct intra tumoral injection, the presence of β -gal was obvious as revealed by appearance of new signal (Figure 12).

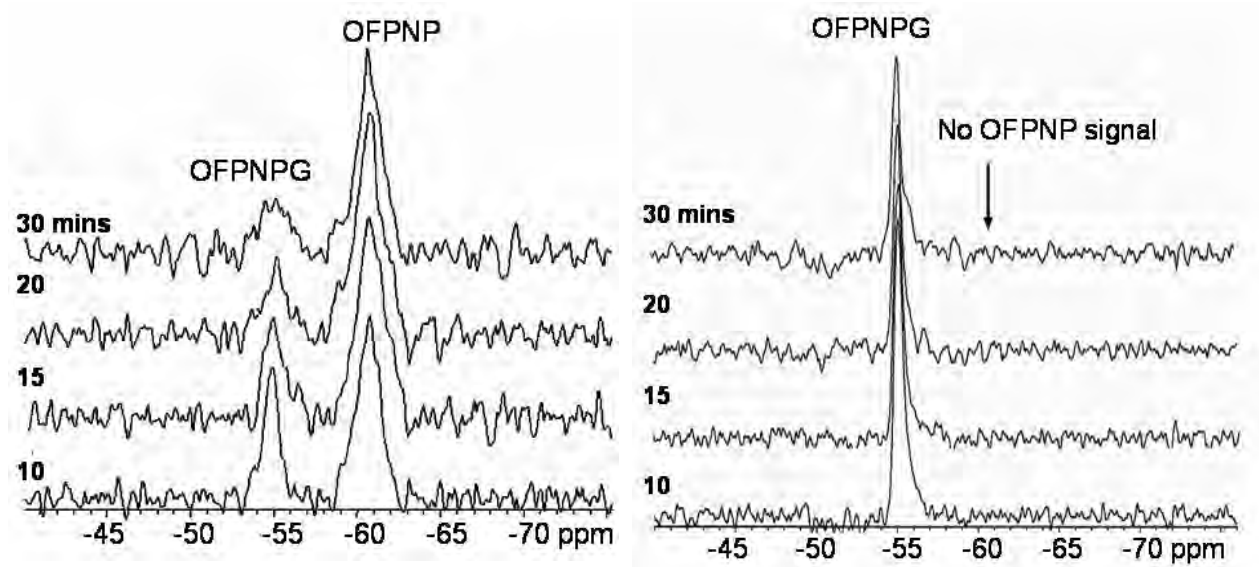


Figure 12. In vivo detection of β -gal in breast tumors.

Partial ^{19}F NMR spectra acquired following introduction of OFPNPG into tumors (signals for TFA and isoflurane occurred downfield and are not shown).

a) A solution (0.24 M, 100 μL DMSO/PBS (V/V' 1:1) with 10 mg/ml NaTFA) was injected intra tumorally in a “fan” pattern in an MCF7-lacZ tumor ($0.8 \times 1.1 \times 1.2 \text{ cm}^3$) in a mouse. Serial spectra were acquired at 4.7 T (188 MHz) with $\text{TR}=1.0 \text{ s}$ and 256 acquisitions (5 min. each) showing liberation of aglycone.

b) As for a, but wild type tumor ($0.4 \times 0.6 \times 0.9 \text{ cm}^3$).

Task 7 Evaluate in rodents with stably transfected tumors and compare with traditional assays: completed in Year 4.

Since we developed several reporter molecules with similar characteristics, but separate well resolved ^{19}F NMR signals it occurred to us that we could use pairs of reporters to examine pairs of tumors simultaneously. As proof of principle we examined the conversion of three reporters simultaneously by MCF7-lacZ cells (Figure 13). Based on the successful interrogation of multiple reporters in cells *in vitro*, we examined paired tumor xenografts on opposite flanks of female mice. While there was insufficient signal for imaging, pairs of reporter molecules as developed in Tasks 1-4, revealed differential activity. LacZ tumors were readily identified by conversion of substrate to release aglycone product, whereas no conversion was seen in the wild type tumors (Figure 14). While our original goal was systemic IV or IP delivery of reporter molecules, direct intra tumoral injection represents considerable progress over the previous NMR approaches (10), which required intra cellular micro injection. We have been able to identify breast tumors expressing lacZ (β -gal) *in vivo* and differentiate them from wild type (Figure 14). Since different substrates have different hydrolysis kinetics, we also tested alternating substrates, as shown in Figure 15, which demonstrated consistent results. For validation histology, Western blots, and enzyme activity following tumor excision (*e.g.*, Figure 16).

To place our new ^{19}F NMR approach in context of existing technologies we also tested other reporter molecules for the ability to detect β -gal activity in tumors in mice *in vivo*. A new near infrared fluorescent approach was presented by Tung *et al.* in 2004 (11). The method exploits a so-called molecular switch and reveals β -gal activity by a modest change in fluorescent emission wavelength following cleavage of substrate (Figure 17). Wild type and lacZ tumors could also be identified using β -glo (12), although this requires additional administration of luciferase or transfection with luciferase. In this case β -gal acts on the substrate to release luciferin serving as the second substrate. To test this approach we generated a new MCF7-lacZ-luciferase cell line, which provides correlative studies by bioluminescent imaging of tumor location and extent (Figure 18). An optical imaging approach based on a single reporter gene would be more convenient and we have now tested Galacto-Light PlusTM. *In vitro* deglycosylation releases a reactive oxitene which spontaneously decomposes emitting light. As proposed in our original application, we have demonstrated that this approach is feasible *in vivo* (Figure 19).

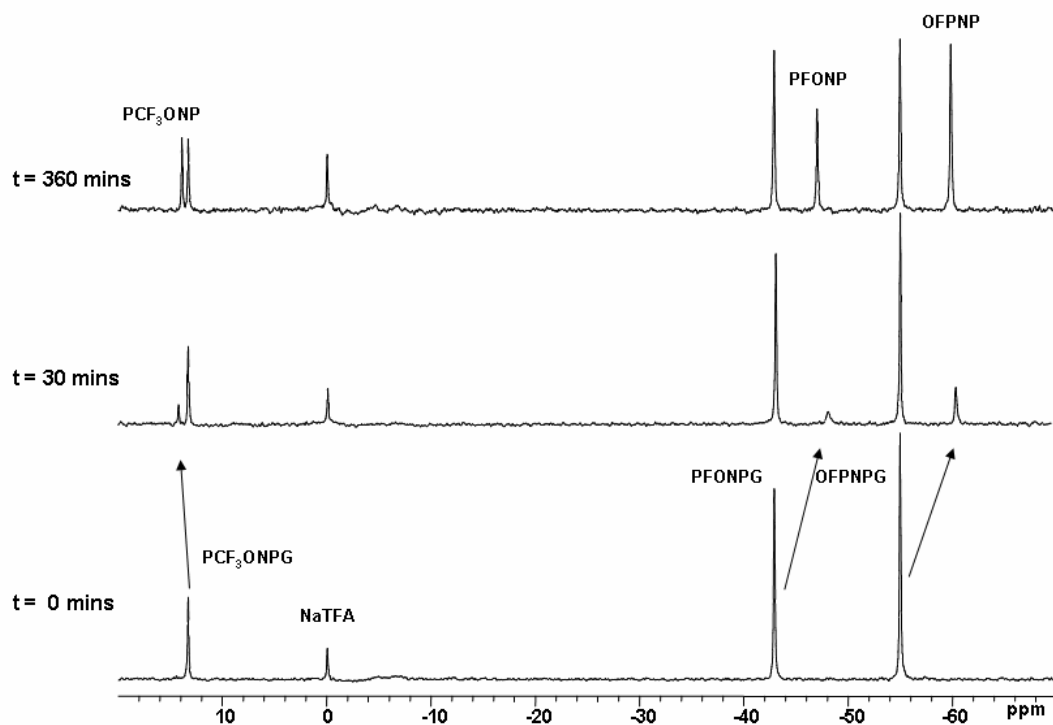


Figure 13. Detection of β -gal using multiple reporter molecules simultaneously in breast tumor cells.

^{19}F NMR (376 MHz) spectra of PCF_3ONPG (1.7 mg, 4.6 mmol), PFONPG (4.6 mg, 14.5 mmol) and OFPNPG (4.8 mg, 15.1 mmol) with stably transfected MCF7-lacZ cells (3.0×10^6) in PBS (0.1 M, pH=7.4, 600 μL) at 37 $^\circ\text{C}$. Each ^{19}F NMR spectrum was acquired in 16 min, and enhanced with an exponential line broadening (40 Hz). In this case the presence of high concentrations of the three reporter molecules seemed to inhibit activity, likely due to acidification. Within 30 minutes the pH sensitive aglycone product chemical shifts were $\delta_{\text{F}}(\text{PCF}_3\text{ONPG}) = 14.26$ ppm, $\delta_{\text{F}}(\text{PFONPG}) = -47.82$ ppm, and $\delta_{\text{F}}(\text{OFPNPG}) = -59.92$ ppm each corresponding to pH = 6.10 ± 0.05 .

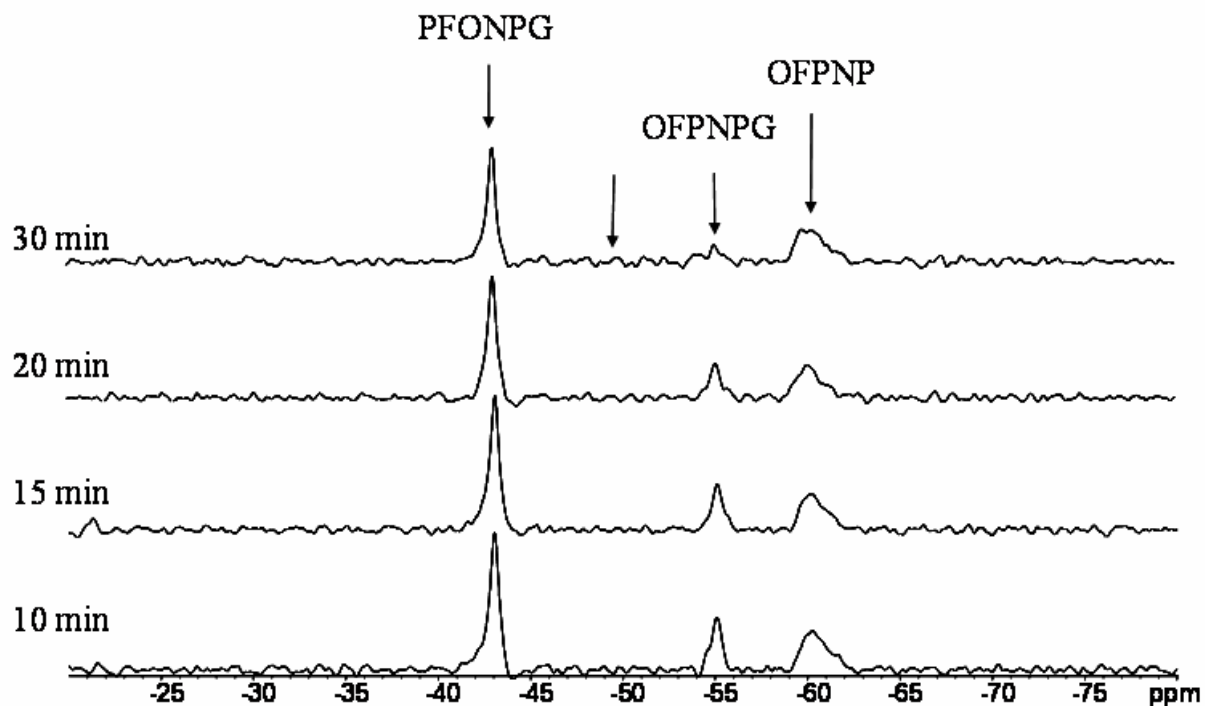


Figure 14. Differentiating lacZ and WT breast tumors *in vivo*

^{19}F NMR spectra (188 MHz) of a mouse bearing two MCF7 thigh tumors. Following intratumoral injection of an aqueous DMSO solution of PFONPG (50 μl) in wild type (WT) tumor and OFPNPG (50 μl) in lacZ transfected tumor, complete conversion of OFPNPG was seen in 30 min, while no conversion of PFONPG was observed. Each spectrum was acquired in 5 mins and 60 Hz exponential line broadening was applied.

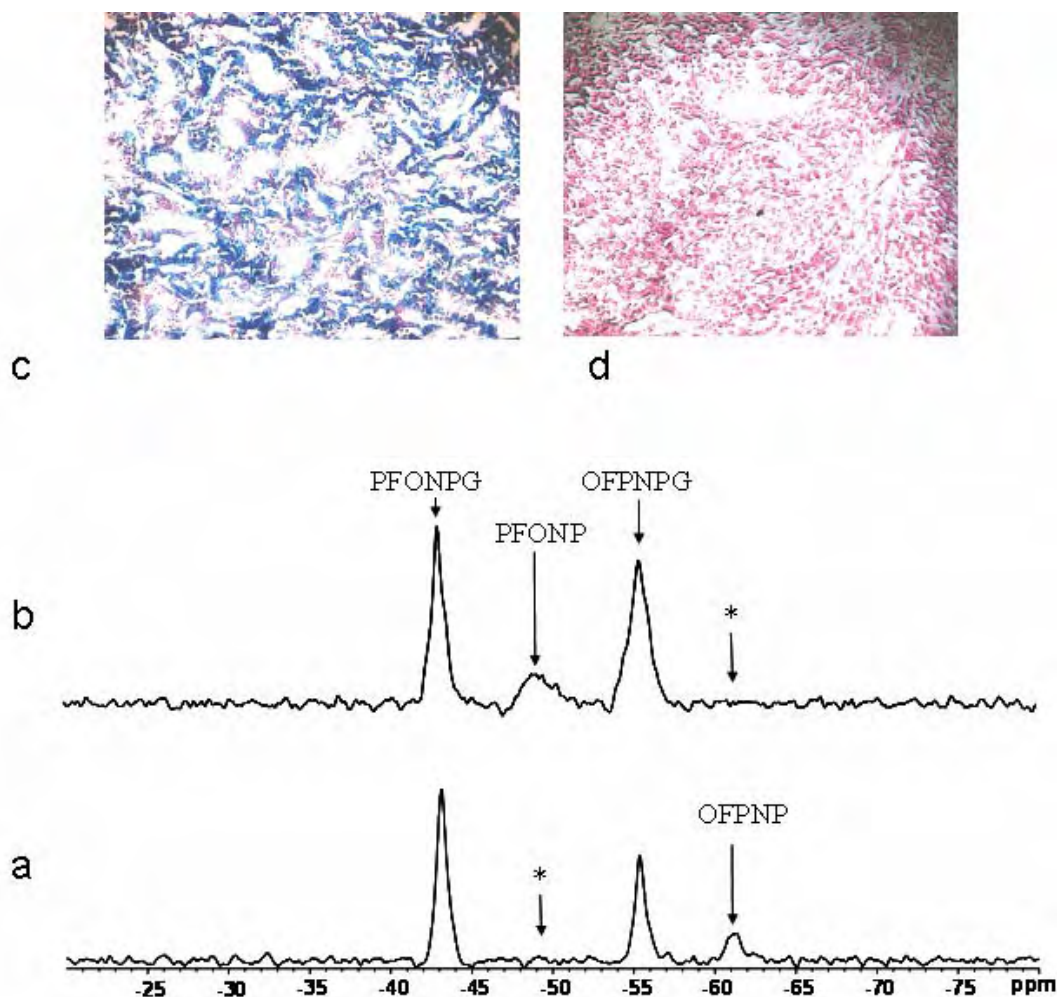


Figure 15 Assessing expression of β -gal in tumors *in vivo* and histological confirmation

- a)** Solutions of PFONPG and OFPNPG were injected into MCF7 tumors, as for Figure 14. Release of OFPNP was observed confirming β -gal expression. * shows location of other aglycone, which was not observed.
- b)** Five hours later, following clearance of substrates and product, agents were again injected, but into the opposite tumors. Now PFONP was observed, but no OFPNP.
- X-gal and Nuclear fast staining of slices from the tumors obtained post mortem **(c)** MCF7-lacZ (100X) and **(d)** MCF7-WT(100X). Intense blue stain showed β -gal activity for the MCF7-lacZ tumor section only.

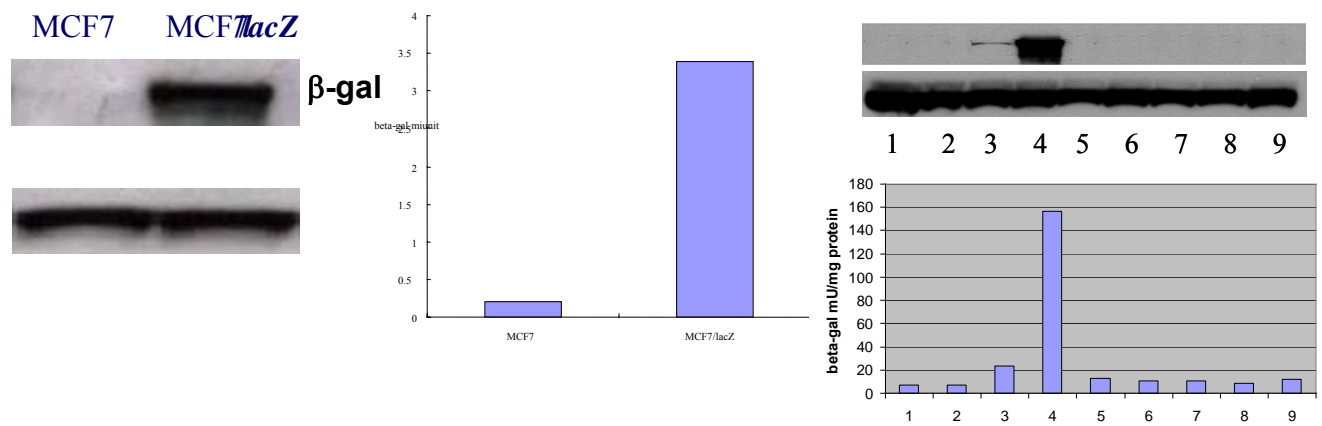


Figure 16 Verification of β -gal expression in tumors growing in mice using Western blot and enzyme activity analysis. Left and center: comparison of MCF7-WT and -LacZ tumors. Right Comparison with other mouse tissues 1. Liver; 2. Muscle; 3. MCF7-WT tumor; 4. MCF7-lacZ tumor; 5 Heart; 6. Spleen; 7. Lung; 8. Kidney; 9. Tail.

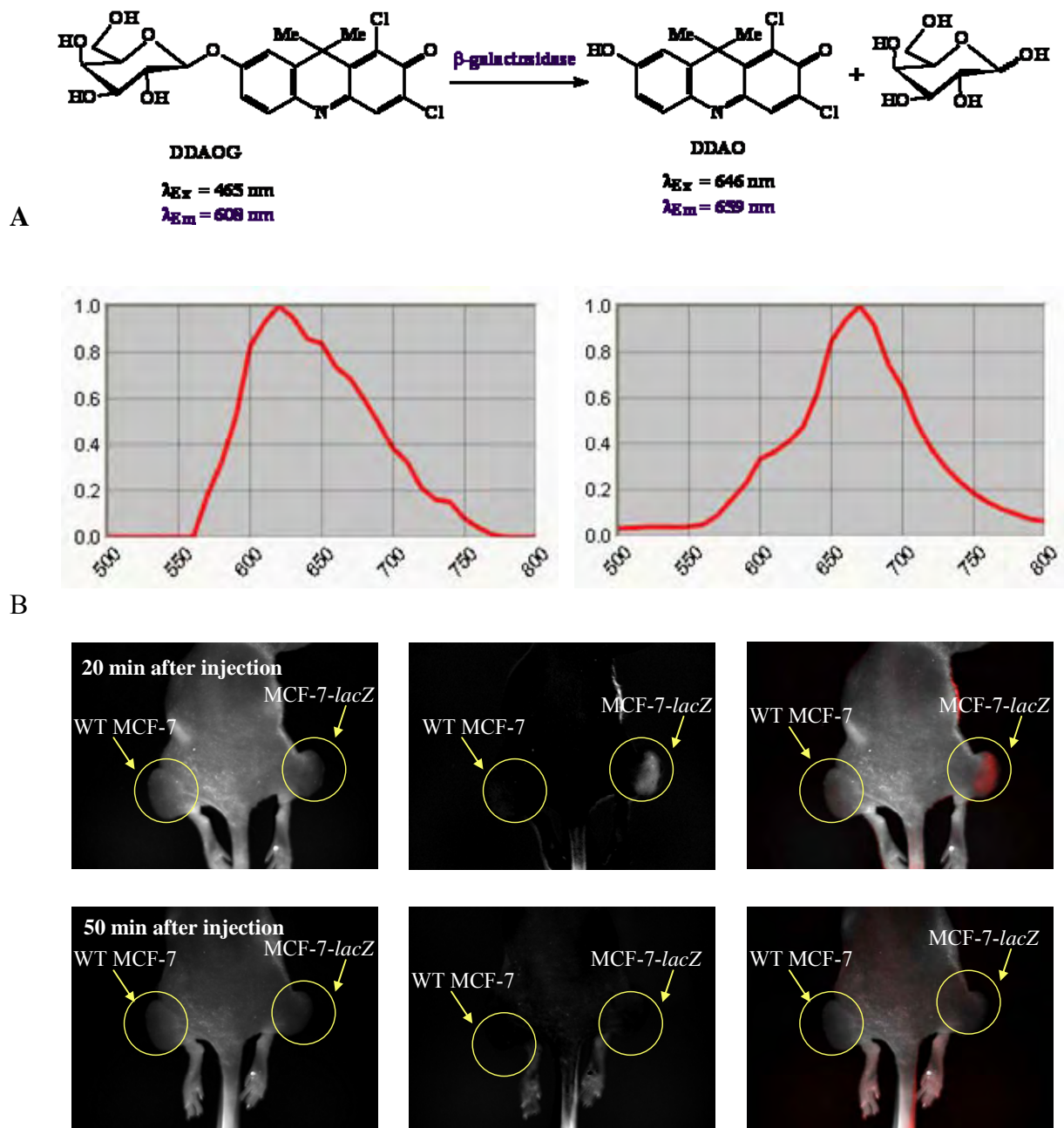


Figure 17 Detecting β -gal activity using fluorescence.

A) Action of β -gal on DDAOG (9*H*-(1,3-dichloro-9,9-dimethylacridin-2-one-7-yl) β -D-galactopyranoside) to release DDAO accompanied by changes in fluorescent emission.

B) Emission spectra of substrate (DDAOG) and product (DDAO) observed using CRi Maestro.

C) Fluorescent imaging of mouse with MCF7-WT (left) and -LacZ (right) tumors in contra lateral thighs, following administration of DDAOG I.V. At 20 mins the tumors were readily discriminated, but by 50 mins signal had cleared. DDAOG: (0.5 mg in 100 μ L DMSO/PBS (1:1 V/V')) was injected I.V. and the mouse observed by fluorescence using a CRi MaestroTM

imaging device. Images acquired in 1.0 ms, wavelength: 646 nm with acquisition settings: 500~800 nm/10 nm.

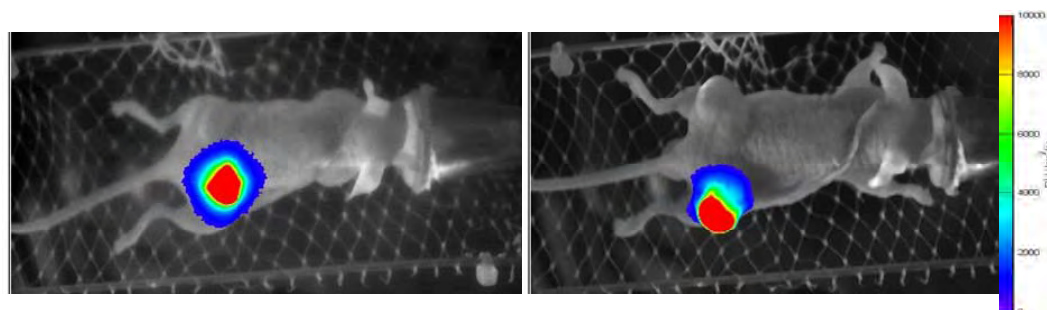


Figure 18 Detecting β -gal activity using beta-glo.

Nude mouse had two tumors: left thigh: MCF7-WT and right thigh MCF7-lacZ-Luc

Left image: BLI following SC injection of 200 μ l (40 mg/ml) D-Luciferin. Image obtained in 5 min. Right image: BLI following SC injection 100 μ l totally 5 mg) D-Luciferin-6-O-Beta-D-Galactopyranoside. Image acquired in 5 min ten minutes after injection.

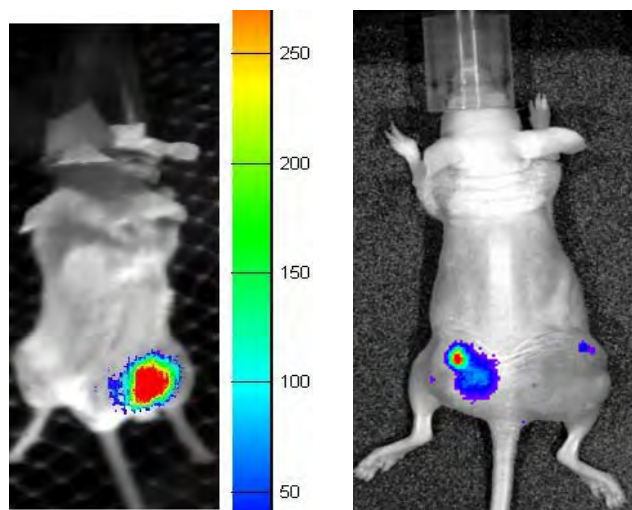


Figure 19 Detecting β -gal activity using Galacto-Light PlusTM. Cells were implanted in contra lateral thighs of female SCID or nude mice. When tumors reached 5 mm diameter 50 μ l of Galacto-Light Plus were injected intra tumorally and the anesthetized mice observed using a Xenogen Lumina, Berthold Nightowl, or homebuilt bioluminescent imaging system. Images were acquired over 5 mins. 5 mins after injection.

Wild type cells gave no detectable light emission, but strong signal was obtained from lacZ tumors. The results have been submitted for presentation at SMI.

Task 8 Synthesize second generation “smart” β -gal substrates as reporters of physical parameters such as pH or as cytotoxic agents (Completed in Year 3)

Several “second” generation gene reporters were synthesized representing diverse classes of agents (Figures 20 & 21). I). GFPOL uses fluorinated vitamin B6 as the aglycone to reduce toxicity of product and results were published (9). GFPOL was indeed much less toxic, but also rather insensitive to β -gal activity. Additional sugar moieties improved water solubility and response to β -gal and detection of the polyglycosylated agents (13). Results of enzyme activity and MCF7-lacZ cells are described under Task 10.

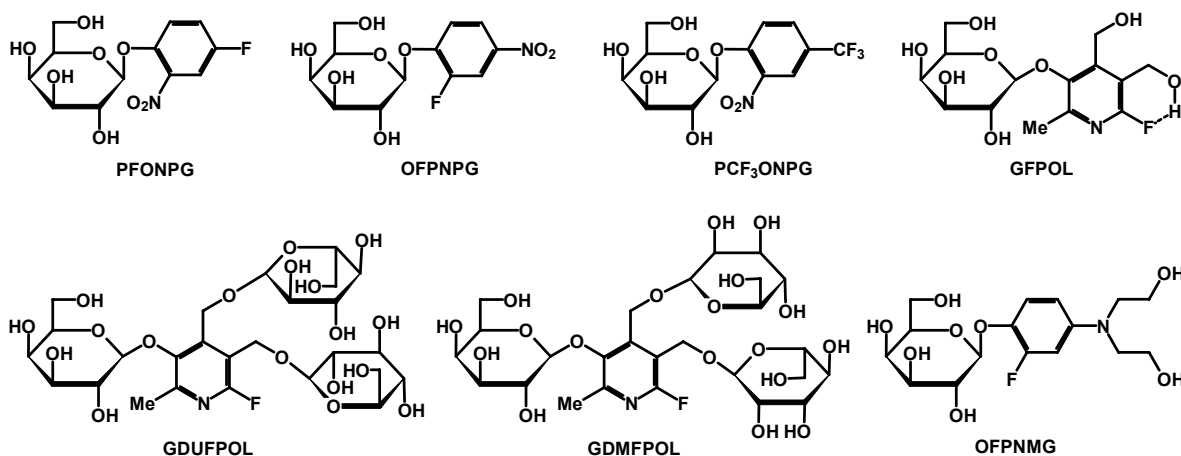


Figure 20 Second generation gene reporter molecules. Each has been successfully synthesized.

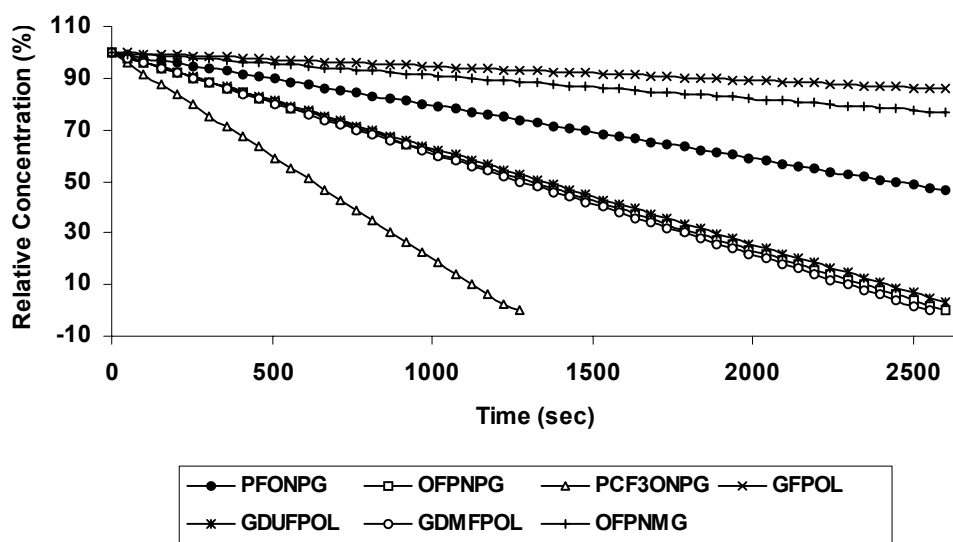


Figure 21. The relative cleavage rates of PFONPG, OFPNPG, PCF₃ONPG, GFPOL, GDUFPOL, GDMFPOL and OFPNMG (5.0 mmol) by MCF7-lacZ cells in culture.

A problem with the ^{19}F NMR approach is that product aglycones are not trapped at site of activity, but washed out, and hence, difficult to detect. It occurred to us that fluoroaryl agents could be trapped by generating insoluble complexes as with the commercial black stain S-gal. A novel class of ^{19}F NMR *lacZ* gene reporter molecule based on fluorocatechols was designed (**LCD-1**), synthesized and tested (Figure 22), as described for Task 10 (Figure 31) and presented at ISMRM (14).

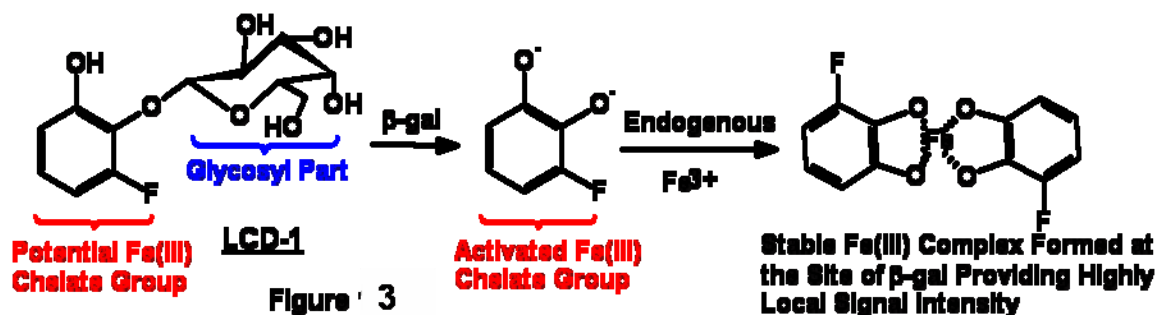


Figure 22 Overcoming reporter product clearance by trapping.

In addition to seeking to reduce toxicity of reporter molecules, we also sought to exploit enzyme activated release of toxic aglycones. We have achieved modest success (Figure 23), but while *lacZ* cells showed greater toxicity the 100 μM concentrations are too high to provide effective activity *in vivo*.

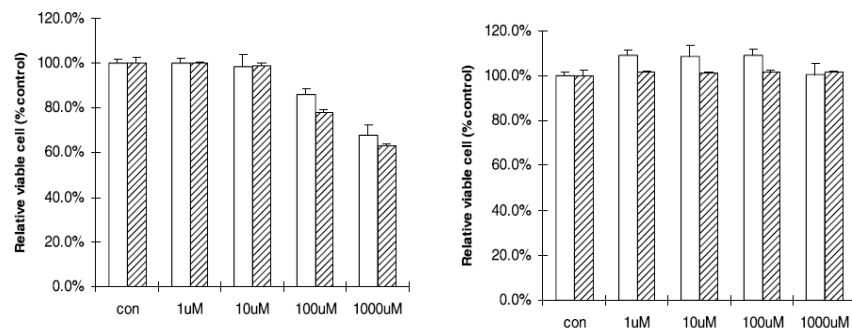


Figure 23. Cell viability of human MCF7 breast cancer cells in PBS (pH 7.4) with respect to exposure to substrate 2-nitro-4-trifluoromethylphenyl β -D-galactopyranoside. Left panel MCF7-*lacZ* cells; right panel: MCF7-WT. Open bars 48 h exposure; hatched bars 96 h exposure.

We had proposed to synthesize a conjugate of 5FU with galactose. Parts of the synthesis were successful, but inseparable mixture resulted (Figure 24) and enzyme activated toxicity in cell culture was not clear. However, we recently found that a conjugate of 5FU with galactose is commercially available and this was tested on MCF7-lacZ and –WT cells (Figure 25).

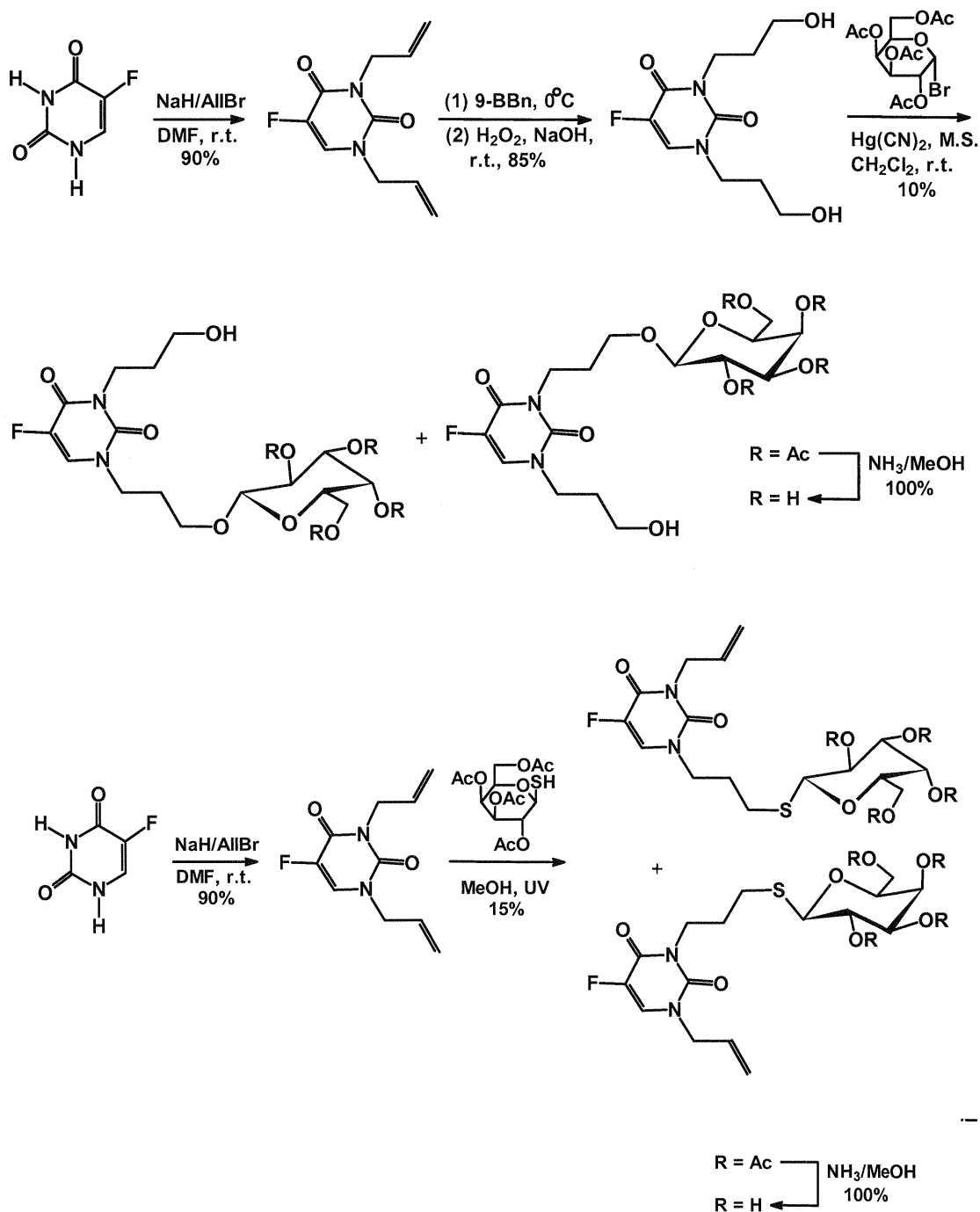


Figure 24 Approaches to generate enzyme automatable conjugates of 5FU with galactose.

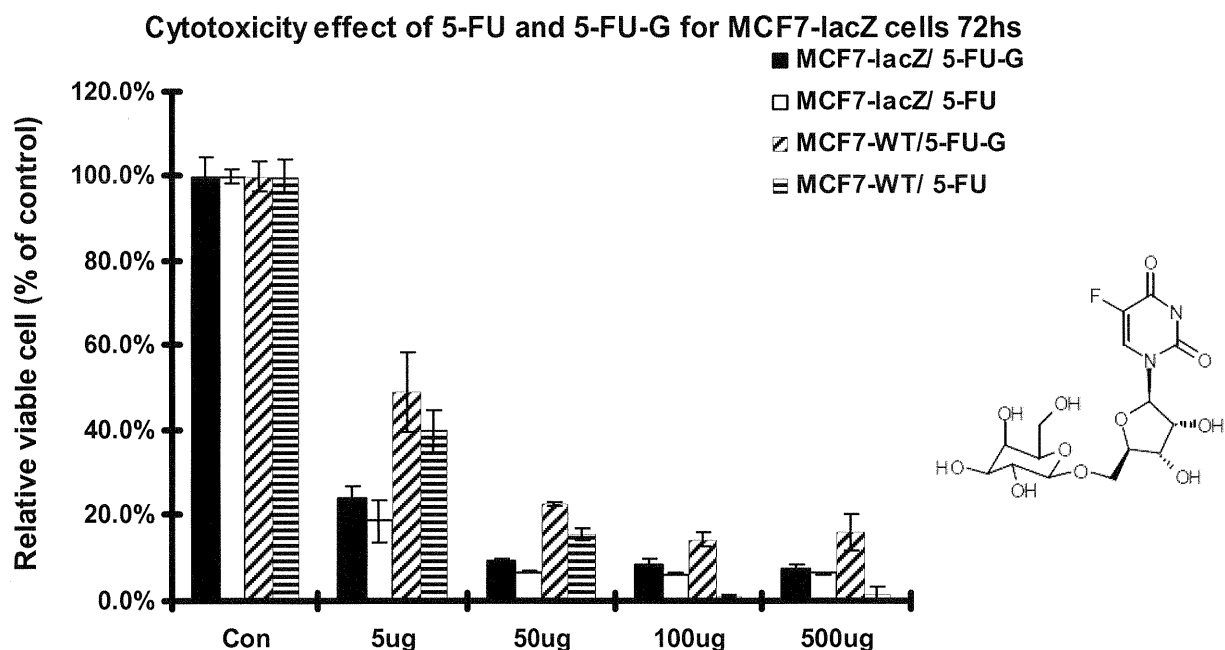


Figure 25 Gene/enzyme activated pro-drug toxicity.

5FU has a notoriously narrow window of efficacy. High concentrations cause systemic toxicity. We proposed to test whether lacZ/ β -gal could be used to activate and release 5FU in breast tumors. Synthesis of pro-drugs was not successful in our lab. However, we recently became aware of a commercial source of 5-Fluorouridine-5'-O- β -D-Galactopyranoside, which we tested. Intriguingly the lacZ expressing cells were more susceptible to both 5FU and the pro-drug. This may be a result of clonal selection during the transfection process. As expected both cells types were more susceptible to 5FU than the pro-drug. However, both types were susceptible to the pro-drug. This may be due to low level constitutive expression in the wild type cells and would require further investigation.

Task 9 Apply optimal β -gal reporters to assess transfection efficiency, gene expression (spatial and temporal) in tumors *in vivo*: completed in Year 4.

In solution Dr. Kodibagkar developed NMR methods to enhance detection of reporter molecules, particularly to allow chemical shift selective imaging to reveal substrate and product by imaging (Figure 26) (8). In phantom studies the techniques are effective, but to date there is insufficient signal to noise for ^{19}F MRI *in vivo*. However, we are able to achieve spatially resolved measurements by using ^{19}F NMR spectroscopy with separate reporter molecules placed at different locations as shown in Figure 14 and 15 above. We tested this approach to examine transient transfection *in situ* in tumors of living mice, but to date have been unsuccessful in observing β -gal expression (Figure 28).

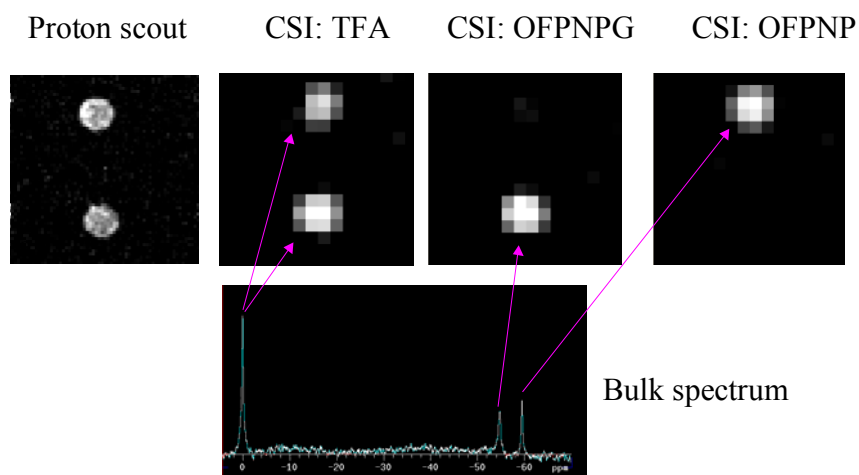


Figure 26

Selective imaging of substrate and aglycone product. Two vials containing TFA and substrate or product as aqueous solutions.

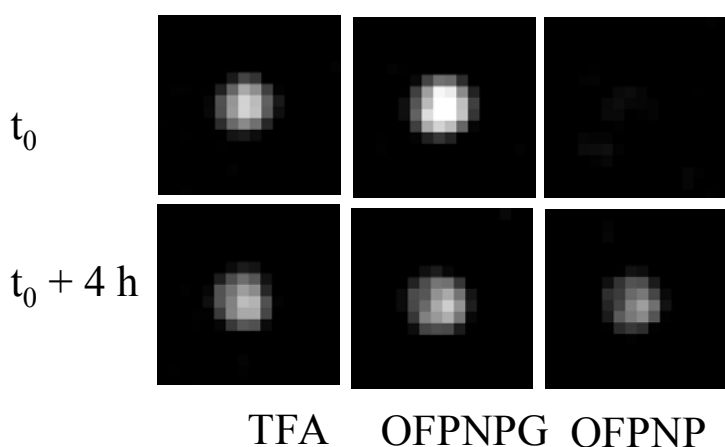


Figure 27 Imaging β -gal activity in cells. A vial containing OFPNPG was imaged at t_0 . 10^7 lacZ transfected MCF7 cells were added to the vial and imaged. ^{19}F CSI detects the conversion of OFPNPG to OFPNP by the MCF7-LacZ cells.

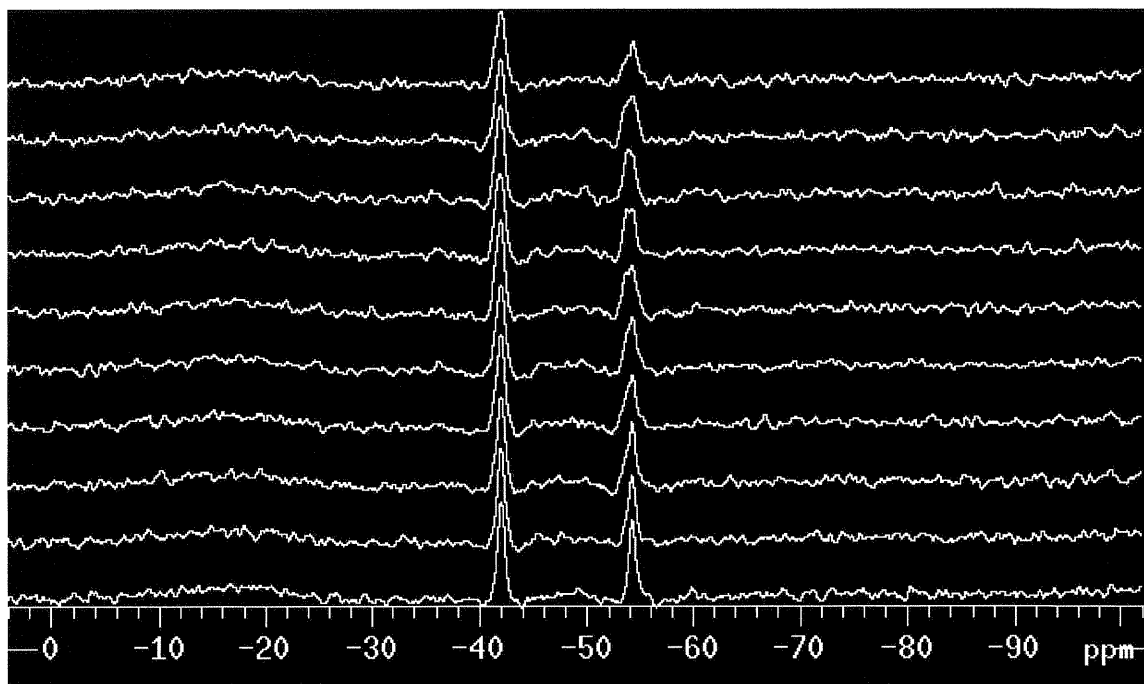


Figure 28 ^{19}F MRS detection of transient transfection in situ. MCF7-WT tumors were in contra-lateral thighs of nude mice. 24 hr after transfection with adenovirus in situ OFPNPG was administered. PFONPG was administered to the other tumor. Neither showed any β -gal activity. Spectral parameters: $T_r = 1\text{ s}$, 256 averages, $5\frac{1}{2}$ min per spectrum, 1st spectrum (bottom) 10 min after injection

Task 10 Evaluate “smart agents” *in vitro*: completed in Year 3.

Polyglycosylated FPOL substrates were added to β -gal enzyme or MCF7-lacZ cells and results published (13). It became apparent that use of multiple galactose moieties was not appropriate since enzyme acted on each of them generating complex NMR spectra (Figure 29). However, when secondary sugar moieties were glucose or mannose, there was selective enzyme activity (Figure 30). We also determined the titration curves for each of the polyglycosylated substrates and products. (Table 3).

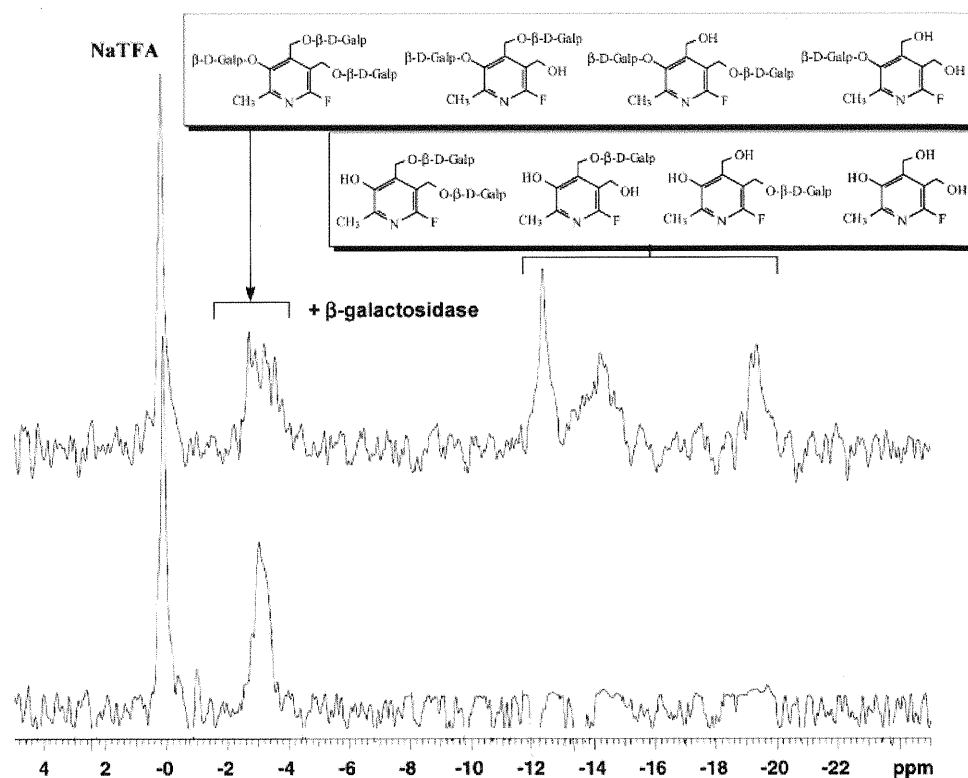


Figure 29. ^{19}F NMR spectra of 3,α⁴,α⁵-tri-*O*-(β-*D*-galactopyranosyl)-6-fluoropyridoxol (10.1 mg, 15 mmol, lower trace) and its products resulting from addition of β-gal (E801A, 15 units) in PBS (pH) 7.4 at 37 °C (upper trace). Spectra were acquired in 51 s and enhanced with an exponential line broadening 40 Hz; β-*D*-Galp: β-*D*-galactopyranosyl.

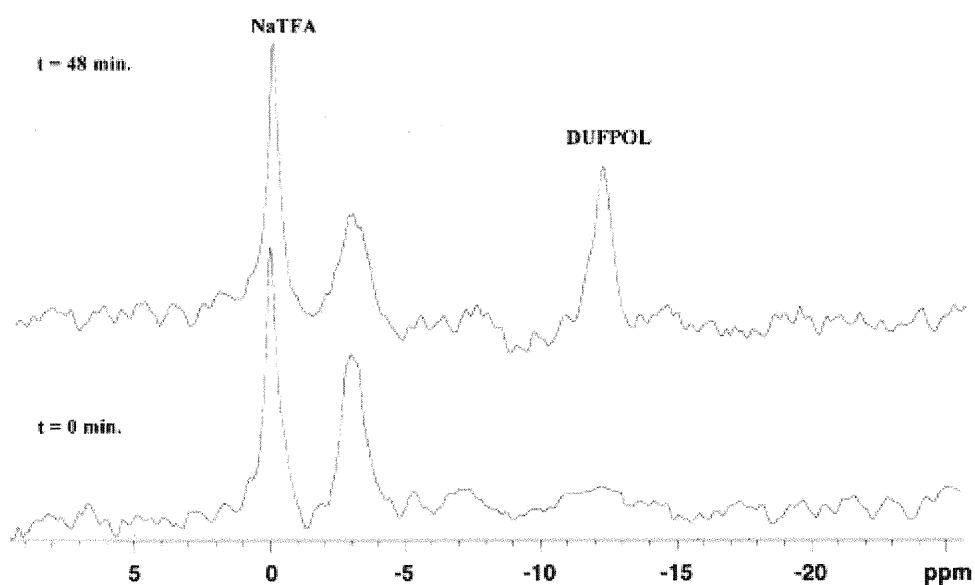


Figure 30. ^{19}F NMR spectra of 3-*O*-(β -D-galactopyranosyl)- α^4 , α^5 -di- *O*-(β -D-glucopyranosyl)-6-fluoropyridoxol 12 (5.1 mg, 7.5 mmol) with stably transfected MCF7-*lacZ* cells (5×10^6) in PBS (0.1 M, pH) 7.4, 600 μL) at 37 °C. Spectra were acquired in 51 s and enhanced with an exponential line broadening) 100 Hz. [DUFPOL) α^4 , α^5 - di-*O*-(β -D-glucopyranosyl)-6-fluoropyridoxol.]

Table 3 Acidities and ^{19}F NMR/pH Properties of DGFPOL, DUFPOL, DMFPOL, and FPOL in Saline at 25 °C^a

pH indicators	DGFPOL	DUFPOL	DMFPOL	FPOL ²⁴
$\text{p}K_a$	7.95	8.08	8.18	8.20
δ_{Facid}	−8.34	−8.15	−7.44	−9.85
δ_{Fbase}	−19.05	−18.85	−18.15	−19.61

^a Chemical shifts are given in parts per million (ppm) with respect to sodium trifluoroacetate.

^{19}F NMR chemical shift pH titration curve of DGFPOL, DUFPOL, and DMFPOL in 0.9% saline at 37 °C. [DGFPOL) α^4 , α^5 - di-*O*-(β -D-galactopyranosyl)-6-fluoropyridoxol; DUFPOL) α^4 , α^5 - di-*O*-(β -D-glucopyranosyl)-6-fluoropyridoxol; DMFPOL) α^4 , α^5 -di-*O*- (β -D-mannopyranosyl)-6-fluoropyridoxol.]

LCD-1 was examined with MCF7-*lacZ* cells and showed conversion yielding two signals (Figure 31). In the presence of ferric ions a purple gelatinous precipitate was formed, but there was still a single narrow ^{19}F NMR signal. These preliminary data demonstrate the feasibility of a novel approach to detecting β -gal activity, *i.e.*, generating complexes to trap the released reporter molecule products. Reassuringly, the product signals remained narrow and detectable, and we believe this approach shows promise for developing ^{19}F NMR approaches to gene reporter molecules.

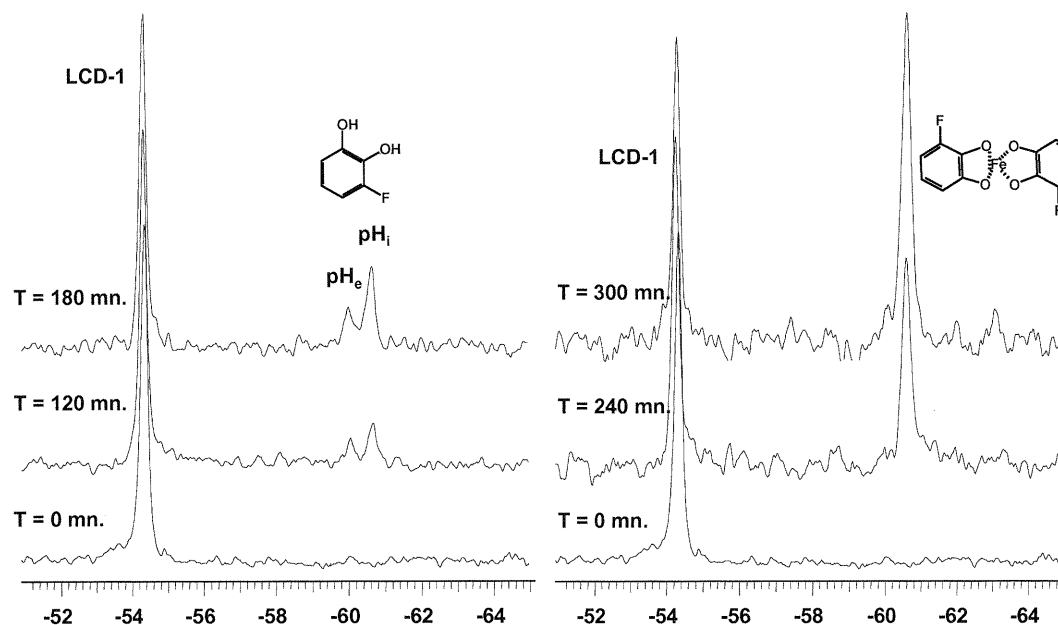


Figure 31 LCD-1 was stable in solution and gave a single sharp ^{19}F NMR signal. Addition of LCD-1 to MCF7-*lacZ* cells caused rapid cleavage (8 $\mu\text{mol}/\text{min}$ per million cells) generating two new signals (left spectra). When ferric ammonium citrate (FAC) was included, cells generated a purple solution indicative of Fe-complex formation (right spectra). Now only a single resonance was observed, which we believe represents the trapped complex. We continue to explore the nature of these signals

Task 11 Evaluate “smart agents” *in vivo*: completed in Year 4.

PFONPG and OFPNPG were examined *in vivo* (Figures 12, 14 and 15). During our research we became aware of the commercial histological “black stain” S-GalTM. Given the precipitation of Fe^{3+} we hypothesized that this could serve as a potential proton T_2^* MRI reporter for β -gal (Figure 32). We then undertook preliminary tests with β -gal enzyme, bacterial and breast tumor cells and the work will be continued as a new R21 to be funded by NCI. Upon cleavage by beta-galactosidase in the presence of ferric ions (Fe^{3+}), the aglycone chelates iron to produce an intense black stain, which is not only visible, but also paramagnetic (Figures 33 and

34). For *in vivo* experiments 1.5×10^6 MCF7/WT or MCF7/LacZ tumor cells were implanted in both flanks of nude mice and allowed to grow to about 0.7 cm^3 . Then 50 mg/kg S-gal-Na (3,4-cyclohexenoescluletin- β -D-galactopyranoside) sodium) and 25 mg/kg FAC (ferric ammonium citrate) in saline were injected intra tumorally. The whole abdomen was observed using a 2 cm volume coil at 4.7 T. Following intra tumor injection of S-gal + FAC into MCF7-LacZ tumor there was rapid development of intense contrast in the form of signal loss in T2 weighted images (Figure 35)

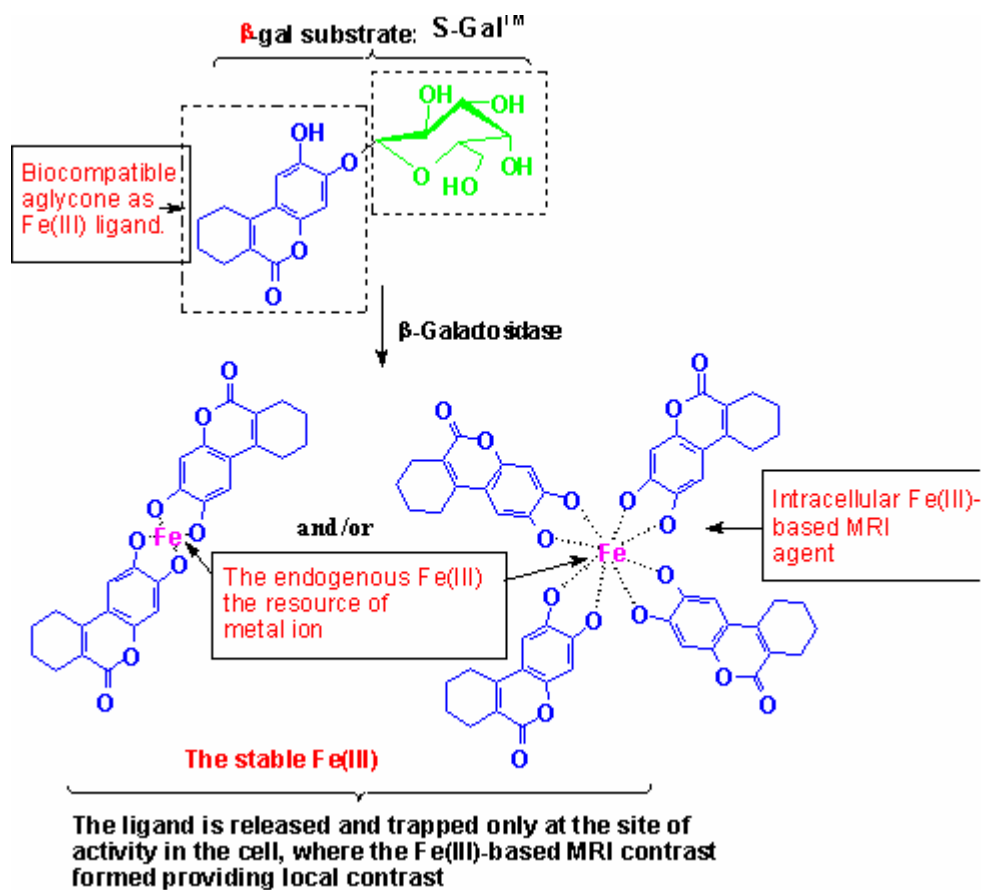


Figure 32 Formation of black paramagnetic precipitate by the action of β -gal on S-GalTM

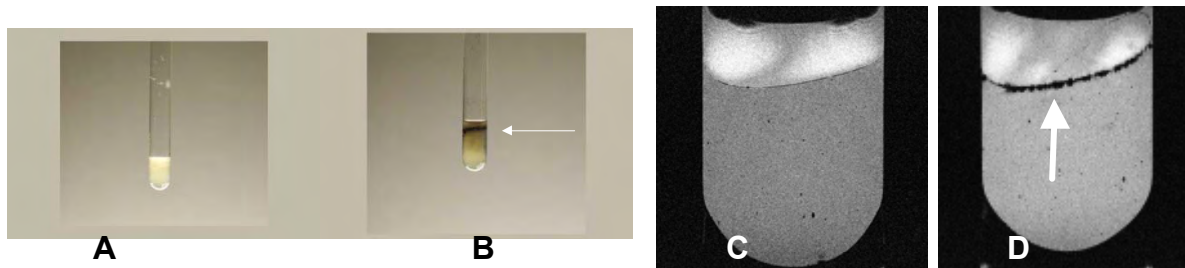


Figure 33 Detection of β -gal in *E.coli*

Left panel: photographs of *E.coli* grown on agar, which included S-GalTM. A) control cells; B) cells induced to express β -gal. A black precipitate is obvious (arrow). Right panel: C and D) Corresponding MRI (9.4 T). The intense black contrast is due to signal loss from the paramagnetic precipitate (arrow). Images acquired in 4 mins with 0.3 mg/ml S-GalTM and FAC in the agar.

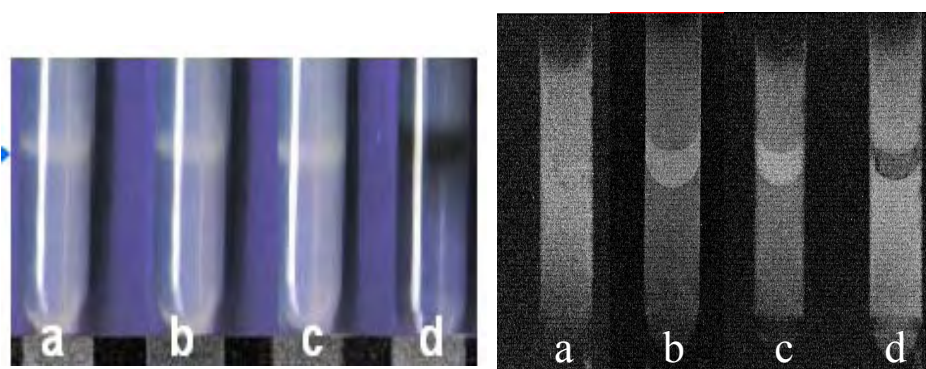


Figure 34 The use of S-gal to detect β -gal activity in breast cancer cells. Left panel- photograph; right MRI. MRI (4.7 T) of MCF7 breast tumor cells (10^6) in agarose TR=1 s, TE=30 ms, 60 μ m in plane resolution with 2 mm thickness.

- a) wild type tumor MCF7 cells with S-GalTM and FAC.
- b) MCF7-lacZ cells with FAC (ferric ammonium citrate) only
- c) MCF7-lacZ cells with S-GalTM only
- d) MCF7-lacZ cells with S-GalTM and FAC

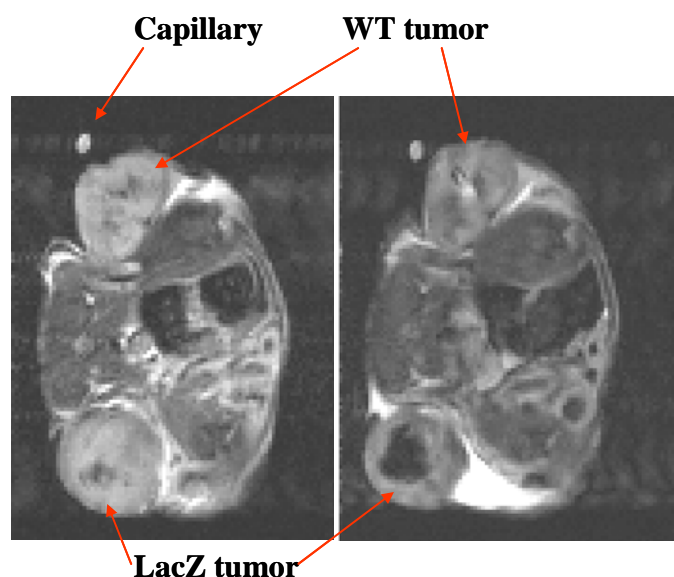


Figure 35. Mouse bearing MCF7 and MCF7-LacZ tumors was imaged using a 4.7T MR Scanner. The T2* weighted images were obtained before (left) and after (right) the intratumoral injection of S-gal-Na and FAC. (TR =500 ms, TE=15 ms, Flip angle=20, matrix=128x128)

Task 12 Prepare manuscripts and final report: completed in Year 4.

The final report is provided here and two further, manuscripts are being prepared based on abstracts presented at conferences.

“Detection of Transgene Expression in Tumors *in Vivo*: A ^{19}F NMR Approach using Dual Reporters to Assess β -Galactosidase” J.X. Yu, V. D. Kodibagkar, Li Liu and R. P. Mason, and
 “Novel *lacZ* Gene Reporter for Dual Modalities: ^{19}F MRS and ^1H MRI” J. Yu, Vikram D. Kodibagkar, and R. P. Mason

KEY RESEARCH ACCOMPLISHMENTS:

- We have demonstrated ^{19}F NMR detection of β -gal activity in breast tumor cells *in vitro* and in tumors growing in mice. Meanwhile little activity was found in wild type cells and tumors.
- We generated breast tumor cell lines stably expressing high activity of β -galactosidase.
- We successfully synthesized a series of novel fluorine substituted phenylgalactosides as potential ^{19}F NMR reporter molecules for β -galactosidase activity.
- The fluorophenyl β -D-galactopyranosides are stable in saline, but are rapidly cleaved by the enzyme β -galactosidase.

- The fluorophenyl β -D-galactopyranosides provide a single ^{19}F NMR signal, which is invariant with pH. Enzyme cleavage produces a new signal well removed from the parent compound.
- **Direct intra tumoral injection of ^{19}F NMR substrates allows detection of lacZ expressing breast tumors versus wild type.**
- Incorporation of trifluoromethyl groups enhances NMR signal to noise, though there is a smaller chemical shift response to cleavage.
- Prototype “smart” β -gal substrates have been synthesized using the pH reporter molecule 6-fluoropyridoxol (FPOL) in place of fluorophenol aglycones. FPOL is less toxic, but also less reactive with β -gal.
- Introduction of sugar moieties onto the FPOL skeleton enhances water solubility and reactivity with β -gal.
- A problem with the first generation substrates and products is that they are washed out of tumors. Based on observations with S-gal we synthesized a novel agent (LCD1), which forms a gel upon cleavage in the presence of Fe^{3+} ions and becomes trapped.
- We have found that S-gal provides a proton MRI contrast agent for detecting β -gal activity in tumors. The product is an insoluble paramagnetic precipitate.

REPORTABLE OUTCOMES:

New Cells lines

New MCF7-LacZ stably transfected cell line.

New MCF7-LacZ-luc stably doubly transfected breast tumor cell line.

New Grants to continue studies

U24 CA126608 – SAIRP

04/2007 – 03/2012

NIH/National Cancer Institute

UT Southwestern Small Animal Imaging Resource

Principal Investigator Mason

1R21CA120774-01A1

05/2007 – 04/2010

NIH/National Cancer Institute

MAGIC – Magnetic Resonance Assessment of Gene Imaging Constructs

Principal Investigator Mason

Published manuscripts

- 1 “A novel NMR approach to assessing gene transfection: 4-fluoro-2-nitrophenyl- β -D-galactopyranoside as a prototype reporter molecule for β -galactosidase”, W. Cui, P. Otten, Y. Li, K. S. Koeneman, J. Yu and R. P. Mason, *Magn. Reson. Med.*, 51, 616-20 (2004)
- 2 “A Novel NMR Platform for Detecting Gene Transfection: Synthesis and Evaluation of Fluorinated Phenyl β -D-Galactosides with Potential Application for Assessing LacZ Gene Expression”, J. Yu, P. Otten, Z. Ma, W. Cui, L. Liu, R. P. Mason, *Bioconjug. Chem.* 15 (6): 1334-1341 (2004)
- 3 “Synthesis and Evaluation of a Novel Gene Reporter Molecule: Detection of β -galactosidase activity Using ^{19}F NMR of a Fluorinated Vitamin B₆ conjugate” J. Yu, Z. Ma, Y. Li, K. S. Koeneman, L. Liu, R. P. Mason, *Med. Chem.* 1(3) 255-262 (2005)
- 4 “ ^{19}F : a versatile reporter for non-invasive physiology and pharmacology using magnetic resonance”, J. Yu, V. D. Kodibagkar, W. Cui, R. P. Mason, *Curr. Med. Chem.* 12 (7) 819-848 (2005) + cover figure and editorial
- 5 “Synthesis and Evaluation of Novel Enhanced Gene Reporter Molecules: Detection of β -Galactosidase Activity Using ^{19}F NMR of Trifluoromethylated Aryl β -D-Galactopyranosides”, Yu J, Liu L, Kodibagkar VD, Cui W, Mason RP: *Bioorg. Med. Chem.*, 14, 326-33 (2006).
- 6 “Synthesis and Characterization of Novel *lacZ* Gene Reporter Molecules: Detection of β -Galactosidase Activity Using ^{19}F NMR of Polyglycosylated Fluorinated Vitamin B₆”, Yu JX, Mason RP: *J. Med. Chem.* 49:1991-9 (2006)
- 7 “Imaging β -galactosidase activity using ^{19}F CSI of *lacZ* gene-reporter molecule 2-fluoro-4-nitrophenol- β -D-galactopyranoside (OFPNPG)” Kodibagkar VD, Yu J, Liu L, Hetherington H, Mason RP *Magn. Reson. Imaging* 24: 959-962 (2006)
- 8 “Non-invasive physiology and pharmacology using ^{19}F magnetic resonance” .Yu, J.-X., Cui, W., Zhao, D., and Mason, R. P. *Adv. Fluorine Sci.*, in the press (2007).

Conference presentations

- 1 "Stereoselective synthesis and evaluation of fluorinated vitamin B6 β -D-galactosides as potential novel substrates for *in vivo* and non-invasive detection of lacZ gene expression", J. Yu, R. P. Mason, 38th National Organic Symposium, B3, Bloomington, Indiana, June 2003.
- 2 "Gene Reporter Molecules: a new platform using ^{19}F NMR substrates for β -galactosidase", J. Yu, W. Cui & R. P. Mason, Proc. 16th International NMR Spectroscopy Conference, C-7, Cambridge, England, July 2003
- 3 "Novel *in vivo* Gene Reporter Molecule Using Fluorinated Vitamin B6 as ^{19}F NMR indicator", J. Yu and R. P. Mason, Proc. Intl. Soc. Magn. Reson. Med. 11, 674 (2003)
- 4 "Synthesis and Characterization of Novel Probes for *in vivo* Detection of LacZ Gene Expression", J. Yu, V. Kodibagkar, L. Liu, R. P. Mason, *Third Meeting of the Society for Molecular Imaging*, St. Louis, MO, September 2004
- 5 "Magnetic resonance chemical shift imaging of gene-reporter molecule OFPNPG", V. Kodibagkar, J. Yu, L. Liu, H. P. Hetherington and R. P. Mason, *Third Meeting of the Society for Molecular Imaging*, St. Louis, MO, September 2004
- 6 "Novel Magnetic resonance Assays of Gene Imaging Constructs (MAGIC)" R. P. Mason, J. Yu, L. Liu, W. Cui and V. Kodibagkar, Molecular Medicine Symposium, Houston, Feb. 2005
- 7 " ^{19}F CSI of gene-reporter molecule OFPNPG", V. Kodibagkar, J. Yu, L. Liu, S. Brown, H. P. Hetherington, R. D. Gerard, and R. P. Mason, ISMRM 13th Scientific Meeting in Miami Beach, Florida, USA May 2005.
- 8 "Breast cancer gene therapy: development of novel non-invasive magnetic resonance assay to optimize efficacy", R. P. Mason, J. Yu., L. Liu, V. D. Kodibagkar, W Cui, and S. L. Brown, Era of Hope, accepted as poster and oral, Philadelphia June 2005
- 9 "Magnetic resonance assays of gene imaging constructs (MAGIC)", R. P. Mason, J. Yu, L. Liu, W. Cui V. Kodibagkar, Imaging in 2020, Jackson Hole, WY September (2005)
- 10 "A Novel Approach in the Development of ^{19}F NMR Reporter to Assess *LacZ* Gene Expression" J. X. Yu, Y. Ren, and R. P. Mason, Proc 14th ISMRM, 191, Seattle, May (2006)

- 11 “Detection of LacZ and luciferin double gene expression in breast cancer xenograft by BLI and ¹H MRI “ L. Liu, W. Cui, A. Contero and R. P. Mason, *Proc SMI*, Waikoloa Village, Hawai’i, August 2006
- 12 “Detection of LacZ expression *in vivo* in MCF7 breast tumors using multiple gene-reporter molecules” V. Kodibagkar, J. Yu, L. Liu, R. P. Mason, *Proc. SMI*, Waikoloa Village, Hawai’i 2006
- 13 “Novel *lacZ* Gene Reporter for Dual Modalities: ¹⁹F MRS and ¹H MRI” J. Yu, Vikram D. Kodibagkar, R. P. Mason, *Proc SMI*, Waikoloa Village, Hawai’i, August 2006
- 14 “A MAGIC approach to gene expression (Magnetic resonance Assay of Gene Imaging Constructs)” R. P. Mason, J.-X. Yu, L. Liu, W. Cui, J. McAnally, V. D. Kodibagkar *ISMRM workshop of Molecular Imaging*
- 15 “Detection of LacZ and luciferase double gene expression in breast cancer xenograft by MRI and BLI”, W. Cui, L. Liu, and R. Mason, *ISMRM* Berlin Germany, May 2007

Personnel

Adam, Ammar
 Cui, Wei-Na
 Kodibagkar, Vikram
 Liu, Li
 Mason, Ralph
 McAnally, Jennifer
 Ren, Ya
 Richer, Edmond
 Yu, Jian-Xin

CONCLUSIONS:

Gene therapy holds great promise for treating breast cancer. A major current obstacle to implementation is assessment of gene expression in terms of heterogeneity and longevity in tissues. Reporter genes and associated molecules should allow assessment of gene expression. To date successful reporters have been developed for nuclear imaging, but radionuclides can be difficult to handle and decay limiting shelf life detectability (15). Optical techniques are favored for gene assessment in small animals, but light penetration can limit utility (16). NMR facilitates assessment of deep tissues without radiation exposure. We have demonstrated the feasibility of synthesizing NMR reporter molecules to reveal activity of β -galactosidase, the primary tool of

molecular biologists to assess gene transfection. Significantly the molecules enter cells and are effective substrates. Moreover the ^{19}F NMR chemical shift unequivocally reveals enzyme activity. Differences in chemical shift associated with small molecular changes allow two tumors to be interrogated simultaneously using unlocalized spectroscopy. Potentially substrates to different enzymes could also allow multiple genes to be interrogated simultaneously. Appropriate NMR pulse sequences allow distribution of substrate and product to be observed by imaging in phantoms. Second generation agents exhibit enhanced sensitivity to enzyme activity, accompanied by modified toxicity.

The investigations funded by this grant have substantially enhanced our laboratory skills and capabilities relevant to breast cancer facilitating enhanced future investigations. We have several stably transfected cell lines and the skills to generate further transfectants. We have gained experience with beta-gal and diverse substrates. We gained experience in designing and use of substrates for ^{19}F NMR and ^1H MRI, fluorescence, bioluminescence and chemoluminescent imaging. We have greater appreciation for the characteristics required for a useful gene-reporter molecule.

Reporter molecules must respond to the target, *e.g.*, enzyme. Substrates must reach the target and product and should be trapped. Neither should be toxic. Adding sugar residues can enhance water-solubility and reactivity. Trifluoromethyl groups enhance SNR, but at the expense of chemical shift sensitivity. Judicious use of ^{19}F NMR reporters with differing chemical shifts can *de facto* reveal spatial distribution and could reveal multiple enzyme activities. We validated the use of DDAOG and beta-glo and demonstrated the feasibility of using Galacton-Plus for chemoluminescent imaging of β -galactosidase.

Proton MRI should provide enhanced capabilities and we have identified S-gal as a prototype molecule for future investigations. While optical reporters exist, MRI could be pertinent to deep tissues in larger animals and ultimately patients. MRI avoids radioactive exposure and handling. Several research groups throughout the world have expressed interest in exploring the agents we have developed, though the synthesis of materials for distribution may be a roadblock.

REFERENCES:

1. Zwiebel, J. A. Cancer gene and oncolytic virus therapy. [Review]. *Semin. Oncol.*, 28: 336-343, 2001.
2. Vlachaki, M. T., Chhikara, M., Aguilar, L., Zhu, X., Chiu, K. J., Woo, S., Teh, B. S., Thompson, T. C., Butler, E. B., and Aguilar-Cordova, E. Enhanced therapeutic effect of multiple injections of HSV-TK + GCV gene therapy in combination with ionizing radiation in a mouse mammary tumor model. *Int J Radiat Oncol Biol Phys*, 51: 1008-1017, 2001.
3. Yu, J. X., Liu, L., Kodibagkar, V. D., Cui, W., and Mason, R. P. Synthesis and Evaluation of Novel Enhanced Gene Reporter Molecules: Detection of b-Galactosidase Activity Using ^{19}F NMR of Trifluoromethylated Aryl b-D-Galactopyranosides. *Bioorg. Med. Chem.*, 14: 326-333, 2006.
4. Yu, J. X., Otten, P., Ma, Z., Cui, W., Liu, L., and Mason, R. P. A Novel NMR Platform for Detecting Gene Transfection: Synthesis and Evaluation of Fluorinated Phenyl b-D-Galactosides with Potential Application for Assessing LacZ Gene Expression. *Bioconj. Chem.*, 15: 1334-1341, 2004.
5. Yu, J. X., Kodibagkar, V., Cui, W., and Mason, R. P. ^{19}F : a versatile reporter for non-invasive physiology and pharmacology using magnetic resonance. *Curr. Med. Chem.*, 12: 818-848, 2005.
6. Yu, J.-X., Cui, W., Zhao, D., and Mason, R. P. Non-invasive physiology and pharmacology using ^{19}F magnetic resonance. *Adv. Fluorine Sci.*, in the press 2007.
7. Cui, W., Otten, P., Li, Y., Koeneman, K., Yu, J., and Mason, R. P. A novel NMR approach to assessing gene transfection: 4-fluoro-2-nitrophenyl-b-D-galactopyranoside as a prototype reporter molecule for b-galactosidase. *Magn. Reson. Med.*, 51: 616-620, 2004.
8. Kodibagkar, V. D., Yu, J., Liu, L., Hetherington, H. P., and Mason, R. P. Imaging b-galactosidase activity using ^{19}F chemical shift imaging of LacZ gene-reporter molecule 2-fluoro-4-nitrophenol-b-D-galactopyranoside. *Magn. Reson. Imaging*, 24: 959-962, 2006.
9. Yu, J. X., Ma, Z., Li, Y., Koeneman, K. S., Liu, L., and Mason, R. P. Synthesis and Evaluation of a Novel Gene Reporter Molecule: Detection of b-galactosidase activity Using ^{19}F NMR of a Fluorinated Vitamin B6 conjugate. *Med. Chem*, 1: 255-262, 2005.
10. Louie, A. Y., Huber, M. M., Ahrens, E. T., Rothbacher, U., Moats, R., Jacobs, R. E., Fraser, S. E., and Meade, T. J. In vivo visualization of gene expression using magnetic resonance imaging. *Nature Biotechnol.*, 18: 321-325, 2000.
11. Tung, C. H., Zeng, Q., Shah, K., Kim, D. E., Schellingerhout, D., and Weissleder, R. In vivo imaging of beta-galactosidase activity using far red fluorescent switch. *Cancer Res.*, 64: 1579-1583, 2004.
12. Wehrman, T. S., von Degenfeld, G., Krutzik, P., Nolan, G. P., and Blau, H. M. Luminescent imaging of beta-galactosidase activity in living subjects using sequential reporter-enzyme luminescence. *Nature Methods*, 3: 295-301, 2006.
13. Yu, J. X. and Mason, R. P. Synthesis and Characterization of Novel lacZ Gene Reporter Molecules: Detection of b-Galactosidase Activity Using ^{19}F NMR of Polyglycosylated Fluorinated Vitamin B6. *J. Med. Chem.*, 49: 1991-1999, 2006.
14. Yu, J.-X., Ren, Y., and Mason, R. P. A Novel Approach in the Development of ^{19}F NMR Reporter to Assess LacZ Gene Expression. *In: Proceedings 14th International Society of Magnetic Resonance in Medicine Seattle, WA, 2006*, pp. 191.

15. Berger, F. and Gambhir, S. S. Recent advances in imaging endogenous or transferred gene expression utilizing radionuclide technologies in living subjects: applications to breast cancer. [Review]. *Breast Cancer Res.*, 3: 28-35, 2001.
16. Contag, C. H. and Ross, B. D. It's not just about anatomy: In vivo bioluminescence imaging as an eyepiece into biology. *JMRI*, 16: 378-387, 2002.

Appendices

1. Cui, W., Otten, P., Li, Y., Koeneman, K., Yu, J., and Mason, R. P. A novel NMR approach to assessing gene transfection: 4-fluoro-2-nitrophenyl- β -D-galactopyranoside as a prototype reporter molecule for β -galactosidase. *Magn. Reson. Med.*, **51**: 616-620, 2004.
2. Yu, J. X., Ma, Z., Li, Y., Koeneman, K. S., Liu, L., and Mason, R. P. Synthesis and Evaluation of a Novel Gene Reporter Molecule: Detection of β -galactosidase activity Using ^{19}F NMR of a Fluorinated Vitamin B6 conjugate. *Med. Chem.*, **1**: 255-262, 2005.
3. Yu, J. X., Otten, P., Ma, Z., Cui, W., Liu, L., and Mason, R. P. A Novel NMR Platform for Detecting Gene Transfection: Synthesis and Evaluation of Fluorinated Phenyl β -D-Galactosides with Potential Application for Assessing LacZ Gene Expression. *Bioconj. Chem.*, **15**: 1334-1341, 2004.
4. Yu, J. X., Kodibagkar, V., Cui, W., and Mason, R. P. ^{19}F : a versatile reporter for non-invasive physiology and pharmacology using magnetic resonance. *Curr. Med. Chem.*, **12**: 818-848, 2005.
5. Yu, J. X., Liu, L., Kodibagkar, V. D., Cui, W., and Mason, R. P. Synthesis and Evaluation of Novel Enhanced Gene Reporter Molecules: Detection of β -Galactosidase Activity Using ^{19}F NMR of Trifluoromethylated Aryl β -D-Galactopyranosides. *Bioorg. Med. Chem.*, **14**: 326-333, 2006.
6. Yu, J. X. and Mason, R. P. Synthesis and Characterization of Novel lacZ Gene Reporter Molecules: Detection of β -Galactosidase Activity Using ^{19}F NMR of Polyglycosylated Fluorinated Vitamin B6. *J. Med. Chem.*, **49**: 1991-1999, 2006.
7. Kodibagkar, V. D., Yu, J., Liu, L., Hetherington, H. P., and Mason, R. P. Imaging β -galactosidase activity using ^{19}F chemical shift imaging of LacZ gene-reporter molecule 2-fluoro-4-nitrophenol- β -D-galactopyranoside. *Magn. Reson. Imaging*, **24**: 959-962, 2006.
8. Yu, J.-X., Cui, W., Zhao, D., and Mason, R. P. Non-invasive physiology and pharmacology using ^{19}F magnetic resonance. *Adv. Fluorine Sci.*, in the press 2007.
9. Yu, J.-X., Ren, Y., and Mason, R. P. A Novel Approach in the Development of ^{19}F NMR Reporter to Assess LacZ Gene Expression. *In: Proceedings 14th International Society of Magnetic Resonance in Medicine Seattle, WA, 2006*, pp. 191.
10. Liu, L., Cui, W., Contero, A., and Mason, R. P. Detection of LacZ and luciferin double gene expression in breast cancer xenograft by BLI and ^1H MRI *In: Proc SMI, Waikoloa Village, Hawai'i, 2006*, pp. 271, #312.
11. Yu, J., Kodibagkar, V. D., and Mason, R. P. Novel lacZ Gene Reporter for Dual Modalities: ^{19}F MRS and ^1H MRI. *In: Proc SMI, Waikoloa Village, Hawai'i, 2006*.
12. Kodibagkar, V., Yu, J., Liu, L., and Mason, R. P. Detection of LacZ expression in vivo in MCF-7 breast tumors using multiple gene-reporter molecules. *In: Proc. Society of Molecular Imaging, Waikoloa Village, Hawai'i 2006*, pp. #290.
13. Mason, R. P., Yu, J.-X., Liu, L., Cui, W., McAnally, J., and Kodibagkar, V. D. A MAGIC approach to gene expression (Magnetic resonance Assay of Gene Imaging Constructs). *In: ISMRM workshop of Molecular Imaging, Cozumel, 2007*.

Novel NMR Approach to Assessing Gene Transfection: 4-Fluoro-2-Nitrophenyl- β -D-Galactopyranoside as a Prototype Reporter Molecule for β -Galactosidase

Weina Cui,¹ Pieter Otten,¹ Yingming Li,² Kenneth S. Koeneman,² Jianxin Yu,¹ and Ralph P. Mason^{1*}

Gene therapy holds great promise for the treatment of diverse diseases. However, widespread implementation is hindered by difficulties in assessing the success of transfection in terms of spatial extent, gene expression, and longevity of expression. The development of noninvasive reporter techniques based on appropriate molecules and imaging modalities may help to assay gene expression. 4-Fluoro-2-nitrophenyl- β -D-galactopyranoside (PFONPG) is a novel prototype NMR-sensitive molecule, which is highly responsive to the action of β -galactosidase (β -gal), the product of the *lacZ* gene. The molecule is stable in solution and with respect to wild-type cells, but the enzyme causes very rapid liberation of the aglycone, accompanied by color formation and a ^{19}F NMR chemical shift of 5–10 ppm, depending on pH. Since the product is pH-sensitive, this opens the possibility for direct pH determinations at the site of enzyme activity. Molecular and ^{19}F NMR characteristics of PFONPG in solution, blood, and prostate tumor cells are presented. This prototype molecule facilitates a novel approach for assaying gene activity in vivo. *Magn Reson Med* 51:616–620, 2004. © 2004 Wiley-Liss, Inc.

Key words: β -galactosidase; gene reporter molecule; *lacZ*; ^{19}F NMR; nitrophenyl- β -D-galactopyranoside; prostate cancer

Gene therapy holds great promise for the treatment of various diseases, including cancer, cystic fibrosis, and immunodeficiency. However, a major obstacle to widespread successful implementation is the need to verify successful transfection—in particular, the spatial extent of expression in the target tissue—together with assays of the longevity of expression. An image-based assay would greatly facilitate optimal gene therapy vector dosing, in a precise temporal and spatial manner. Numerous preclinical studies have indicated that this therapy shows promise for the treatment of solid tumors. However, useful reporter molecules could accelerate the effective transition to human clinical trials.

Many promising methods are being developed to image (i.e., assay noninvasively) tissue gene expression, often by including a reporter gene in tandem with the therapeutic gene (1–4). A critical criterion is that the reporter gene is not normally present or expressed in the cells of interest. One of the earliest examples of gene transfection was the introduction of creatine kinase into the liver of mice, and the subsequent detection of phosphocreatine (PCr) by ^{31}P NMR (5). This particular case involved a benign product and natural substrates, but the technique would be inappropriate in most tissues, where PCr is normally present at high levels. Perhaps the most popular reporter genes today are associated with optical imaging, since this is a cheap modality and highly sensitive results are rapidly obtained. Thus, bioluminescent imaging (BLI) of luciferase (1), and fluorescent imaging of green fluorescent protein (GFP) and longer-wavelength variants (6) are popular. These techniques are very useful in superficial tissues and have extensive applications in mice, but application to larger bodies is limited by the depth of light penetration.

Several nuclear medicine approaches have been demonstrated that employ thymidine kinase with a variety of substrates, including iodo- and fluoronucleosides (such as FIAU and gancyclovir) and various radionuclide labels (e.g., 123-, 124-, 125-I, and ^{18}F) (3,7). An alternative approach uses the sodium iodine symporter (hNIS), which works well with both iodide and pertechnetate substrates (2). For cancer, thymidine kinase is advantageous because the gene serves as a reporter and the gene products themselves may have therapeutic value.

The *lac* operon was the first gene expression system to be well characterized, some 40 years ago by Jacob and Monod (8). One component, *lacZ*, which produces β -galactosidase, has been the primary choice of reporter gene to verify effective transfection in biochemistry, and many reporter molecules are available for biological and histological analysis. Diverse agents are commercially available with specific characteristics, such as developed color, thermal stability, and cellular retention (e.g., X-gal, o-nitrophenylgalactoside (ONPG), and S-Galacton-star) (9–11). However, β -galactosidase was largely neglected for in vivo work until the elegant studies of Meade et al. (12) were published. The galactose bridged cyclic gadolinium contrast agent ((1-(2-(galactopyranosyloxy)propyl)-4,7,10-tris(carboxymethyl)-1,4,7,10-tetraazacyclo dodecane) gadolinium(III) (EgadMe) shows considerable change in water relaxivity upon exposure to β -galactosidase. While the molecule is a poor substrate for the enzyme (on the order of 500 times less efficient than the colorimetric biochemical agent ONPG) and does not penetrate cells, it can

¹Department of Radiology, University of Texas Southwestern Medical Center at Dallas, Dallas, Texas.

²Department of Urology, University of Texas Southwestern Medical Center at Dallas, Dallas, Texas.

Presented in part at the 10th Annual Meeting of ISMRM, Honolulu, 2002.

Grant sponsor: Department of Defense; Grant numbers: BC980020 DAMD17-99-1-9381; BC022001 DAMD17-03-1-0343-01; DAMD17-01-1-0107; Grant sponsor: NIH Cancer Imaging Program; Grant number: P20 CA 86354.

Weina Cui and Pieter Otten contributed equally to this work.

*Correspondence to: Ralph P. Mason, Ph.D., University of Texas Southwestern Medical Center at Dallas, 5323 Harry Hines Blvd., Dallas, TX 75390-9058. E-mail: Ralph.Mason@UTSouthwestern.edu

Received 17 April 2003; revised 9 October 2003; accepted 9 October 2003. DOI 10.1002/mrm.10719

Published online in Wiley InterScience (www.interscience.wiley.com).

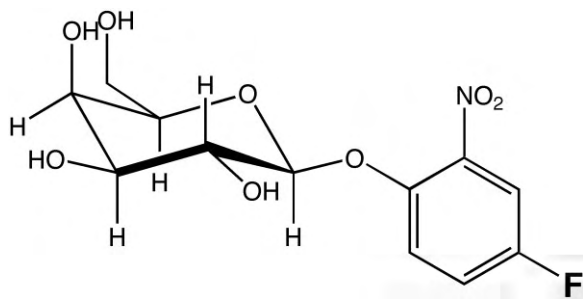


FIG. 1. The structure of PFONPG.

facilitate effective investigations of cell lineages following direct intracellular microinjections (12). These previous findings prompted us to consider other NMR active analogs, and we hypothesized that introducing a fluorine atom into the popular colorimetric biochemical indicator ONPG would produce a strong candidate molecule. We now report the successful synthesis of the reporter molecule, together with NMR characterization and examples of activity in solution and cell culture.

MATERIALS AND METHODS

4-Fluoro-2-nitrophenyl- β -D-galactopyranoside (PFONPG; Fig. 1) was prepared from a reaction of acetobromo- α -D-galactose and the potassium salt of 4-fluoro-2-nitrophenol (PFONP) followed by deprotection with triethylamine using methods similar to those reported by Yoon et al. (13). Details regarding the chemical synthesis will be published in a future work.

^{19}F NMR experiments were performed at 564 MHz using a Varian INOVA Unity spectrometer, and a capillary of sodium trifluoroacetate served as an external chemical shift reference standard (δ 0 ppm). Spectra were obtained from both PFONPG and the aglycone PFONP in saline, buffers, heparinized whole rabbit blood, and prostate cancer cells. The titration curves of PFONP were measured at 25°C and 37°C in saline, and aliquots of HCl (0.2N) and NaOH (0.25N) were added to alter pH, which was independently measured in the NMR tube using a pH electrode.

For single-component kinetic enzyme experiments, PFONPG (5 mg) was dissolved in buffer-I (0.6 ml, pH = 4.5, prepared with 10 mM sodium hydrogen phosphate and 5 mM citric acid). A solution of β -galactosidase (G5160 from *Aspergillus oryzae* (Aldrich); 10 μl of a solution of 19 mg (152 units) in 2 ml buffer-I) was added, and NMR data were acquired immediately at 30°C. Each spectrum was acquired in 36 s and the kinetic curve was

assessed over 11 min. A similar experiment was performed using β -gal isolated from *Escherichia coli* (G6008; 250–600 U/mg) in buffer-II at 37°C. Buffer-II was prepared with HEPES (2 mM) and hydrogen phosphate (7 mM), providing the higher pH (7.3) that is optimal for this enzyme.

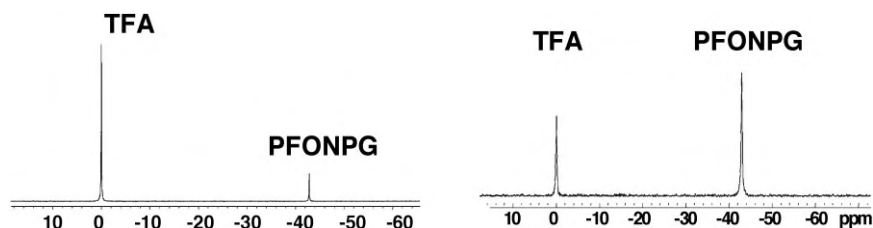
To test substrate efficacy, a substrate competition experiment was undertaken. NMR experiments were performed with various concentrations of PFONPG (28.8–262 μmol) added to a solution of β -gal (G5160). In a second series, 2-nitrophenyl- β -D-galactopyranoside (ONPG, 65 μmol) was added simultaneously to each sample.

For cell studies, 5×10^6 human prostate tumor cells PC-3 (American Type Culture Collection, Manassas, VA) and LNCAP C4-2 (UroCor, Oklahoma City, OK) were grown on 150-mm culture dishes in T-medium (Invitrogen) with 5% fetal bovine serum at 37°C with 5% CO_2 . Control (wild-type) cells and transfected cells (infected by replication defective adenovirus harboring *lacZ* gene under the control of the cytomegalovirus (CMV) or bone sialo protein (BSP) promoter at 10 or 100 multiplicity of infection (MOI), with transfection times of 24 or 48 hr), were harvested. The cells were trypsinized for 2 min and neutralized with medium for harvesting. The cell pellet was obtained by gentle centrifugation, washed twice with phosphate-buffered saline (PBS), and resuspended in 1 ml PBS. PFONPG (2 mg) was added to a suspension of $10^7/\text{ml}$ cells, and ^{19}F NMR spectra were acquired after various incubation times at 30°C or 37°C.

RESULTS

PFONPG is hydrophilic and readily dissolves in saline or whole blood, giving a single narrow ^{19}F NMR signal at δ –42.75 ppm with respect to $\delta_{\text{Na-TFA}}$ 0 ppm (Fig. 2). This signal is essentially invariant in the range of pH 1–11 with a change of <0.05 ppm. The signal appeared stable in solution and whole rabbit blood for a period of 2 days. The addition of β -galactosidase caused rapid cleavage and released the aglycone PFONP, which appeared at δ –46.49 ppm for β -gal G5160 at 30°C and at δ –51.07 ppm for β -gal G6008 at 37°C (Fig. 3), and was accompanied by the development of yellow color. The addition of β -gal (G5160) to PFONPG showed a rapid exponential loss of the substrate accompanied by the appearance of the aglycone over a period of 10 min, as shown by the curves in Fig. 4. Similar activity was seen with G6008, although the change was less rapid under comparable conditions. The substrate competition kinetics showed that ONPG acts as a competitive inhibitor of β -gal with respect to PFONPG: the Michaelis constant increased from 91 μmol to 200 μmol , but V_{max} remained unchanged (Fig. 5).

FIG. 2. ^{19}F NMR spectra of PFONPG (2 mg \equiv 8 μmol , 10 mM) in saline (left) and fresh heparinized whole rabbit blood (right). ^{19}F NMR spectra were obtained in 36 s and apodized with a 10-Hz exponential line-broadening prior to Fourier transformation. Sodium trifluoroacetate was used as a chemical shift reference (δ 0 ppm).



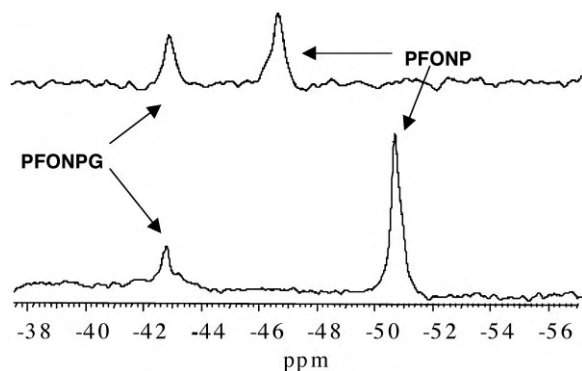


FIG. 3. PFONPG (-42.75 ppm) was rapidly cleaved by β -gal G5160 (pH = 4.5, upper spectrum) and G6008 (initial pH = 7.3, but acidified to 6.8 during reaction, lower spectrum) releasing the aglycone PFONP. Since the product has a pH-sensitive chemical shift, PFONP occurs at different positions for each buffer.

When PFONPG was added to wild-type prostate cancer cells (PC-3 or LNCAP C4-2), there were no spectral changes after incubation for 3 hr at 37°C . When PC-3 cells were transfected with a first-generation adenovirus vector encoding the β -gal gene driven by the CMV promoter for 24 hr, 12.7% PFONPG was converted to PFONP after incubation for 3 hr at 37°C (Table 1). When PC-3 cells or LNCAP C4-2 cells were transfected with the CMV system, but for 48 hr, 74% and 100% of PFONPG was converted by PC-3 and LNCAP C4-2 cells, respectively, after incubation for 15 min at room temperature. CMV may be considered a universal promoter, so we also tested the β -gal gene under control of the specific BSP promoter. In this case, the substrate cleavage was lower, with only 5% conversion after incubation with PFONPG for 3 hr at 37°C for cells with 10-fold MOI viral transfection, and 14% for 100 MOI.

The ^{19}F NMR signal of the aglycone (PFONP) is very sensitive to pH, exhibiting a range of 9.3 ppm. The titration curves (Fig. 6) were identical at 25°C and 37°C , and gave the Henderson Hasselbalch coefficients $\text{pK}_a = 6.85$, $\delta_{\text{acid}} -46.44$ ppm, $\delta_{\text{base}} -55.73$ ppm.

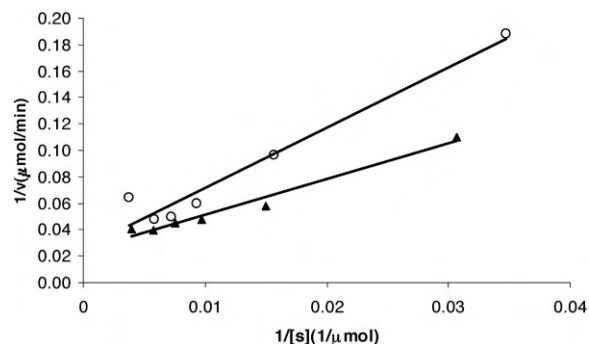


FIG. 5. Lineweaver-Bourke plot showing kinetics of β -gal activity on PFONPG, and competitive inhibition by addition of ONPG (○).

DISCUSSION

We have demonstrated the potential utility of a novel class of gene reporter molecules—fluoro-phenyl-galactopyranosides (specifically, PFONPG)—as an effective substrate for β -galactosidase. This molecule is an excellent substrate for the enzyme and acts competitively with traditional biochemical indicators. It provides a single ^{19}F NMR signal with a narrow linewidth and good stability in solution. It is apparently stable in normal wild-type cells and whole blood, but exposure to the enzyme or cells transfected to express β -galactosidase causes rapid cleavage, in line with anticipated levels of transfection.

Upon cleavage of the glycosidic bond, a chemical shift difference of >3.6 ppm is observed. However, the chemical shift of the product may have a range of about 9 ppm, since the released aglycone is pH-sensitive and the pK_a is in the physiological range. Significantly, there is no overlap between the chemical shift of the substrate and the product. This presents the interesting possibility of selective determination of pH at the site of enzyme activity. Indeed, we have demonstrated that if the aglycone (PFONP) is added to a suspension of red blood cells, two signals are rapidly observed representing the intra- and extracellular pH (14). However, PFONP is somewhat toxic

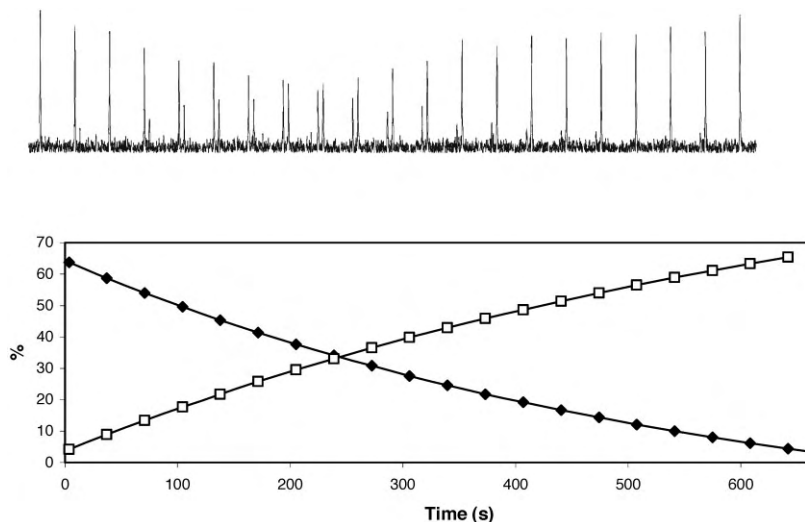


FIG. 4. Kinetic curves showing cleavage of PFONPG to PFONP by β -gal G5160. The upper trace shows the spectral time course, and the amplitudes are plotted below.

and causes lysis of less robust cells, such as cultured tumor cells. Thus, PFONPG may be regarded as an interesting prototype molecule that is primarily representative of a new approach to the use of NMR gene reporter molecules in association with β -galactosidase. Given the well-known promiscuity (lack of specificity) of β -galactosidase (15), many commercial colorimetric molecular substrates are available for this enzyme. We believe that other NMR-sensitive aglycone analogs may readily be introduced in place of the PFONP, and can display preferable characteristics. In particular, analogs may be selected to be less toxic, to be selectively trapped in cells, or to have particular activities as specific reporters or drugs. Indeed, preliminary investigations show the feasibility of conjugating the pH reporter 6-fluoropyridoxol (16) to galactose, and thereby generating an effective substrate for β -gal (17).

While the toxicity of PFONP appears to severely limit the application of PFONPG as a gene reporter molecule, it does present the intriguing possibility of a broad-spectrum, gene-activated chemotherapeutic. Indeed, PFONP is clearly analogous to the classic biochemical uncoupler dinitrophenol. While specific traditional chemotherapeutic drugs may be subject to multidrug resistance and become ineffective, we believe that nitrophenols could exert local cytotoxic effects on many tissues. Gene-activated drug therapy (often termed gene-directed enzyme prodrug therapy (GDEPT)) (18), has been demonstrated by others using the cytosine deaminase (CD) gene. Specifically, CD activates the minimally toxic 5-fluorocytosine (5-FC) to the highly toxic 5-fluorouracil (5-FU). This is being widely exploited in gene therapy trials, in the hope that it may mitigate the toxicity threshold associated with systemic 5-FU delivery (18,19). The conversion of 5-FC to 5-FU causes a chemical shift of ~ 1.5 ppm, revealing gene activity. This has been demonstrated in a number of systems *in vivo* (18,20). It is also interesting to note that some of the major metabolic products of 5-FU exhibit chemical shift sensitivity to pH, which may provide an indication of local tissue pH (21).

NMR reporters have a long shelf life and are easy to handle, both of which are great advantages over radioactive substrates. Functional paramagnetic agents are attractive because they interact with large numbers of water molecules generating amplification, as previously shown for various "smart" contrast agents (22). However, the prototype proton NMR substrate for β -gal (EgadMe) fails to enter cells and is a poor substrate for the enzyme. Introducing a fluorine atom minimally perturbs the structure and reactivity of the traditional efficient biochemical substrate (ONPG), and offers a new approach. Given that there

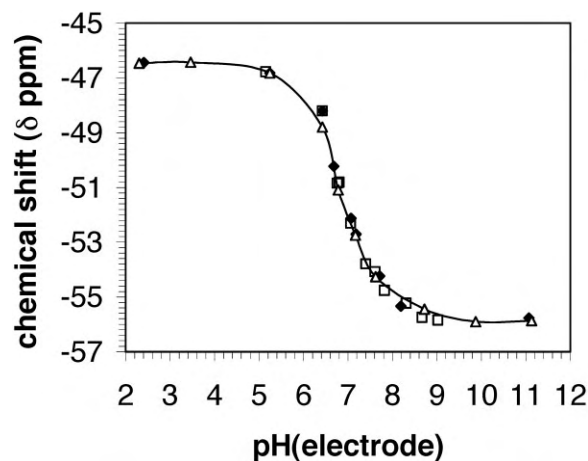


FIG. 6. Titration curves of PFONP in saline (\blacklozenge), and plasma at 30°C (\square), and 37°C (\triangle).

is essentially no ^{19}F NMR background signal in tissues, fluorinated reporter molecules may be assessed by changes in chemical shift. Our ability to detect these molecules is dependent on the signal-to-noise ratio (SNR), rather than the contrast-to-noise ratio (CNR). The chemical shift difference between substrate and aglycone product reveals the unambiguous detection of enzyme activity. This approach was previously demonstrated for the cytosine deaminase reporter gene system (18,20). Spatial resolution will require chemical shift imaging, rather than merely selective excitation, since the PFONP can have a wide pH-dependent chemical shift range. Detectability could be enhanced by the introduction of a trifluoromethyl (CF_3) reporter group, as opposed to the single F-atom. However, a CF_3 group will likely perturb the water solubility to a greater extent, and the chemical shift response is expected to be considerably smaller due to transmission of the electron density redistribution through an additional carbon-carbon bond.

PFONPG is readily synthesized using simple organic chemistry methods. It is water-soluble and appears to enter cells easily. However, the product aglycone is not trapped and in some cases causes cell lysis. Thus, while cleavage provides clear evidence of β -galactosidase activity, it would be difficult to localize this information to specific tissues *in vivo*. This may limit the ultimate application of this prototype molecule for widespread studies.

ACKNOWLEDGMENTS

This research was supported by grants from the Department of Defense (Breast Cancer Initiative IDEA awards BC980020 DAMD17-99-1-9381 and BC022001 DAMD17-03-1-0343-01 to R.P.M., and Prostate Cancer Initiative IDEA award DAMD17-01-1-0107 to K.S.K.). The NMR experiments were conducted at the Mary Nell and Ralph B. Rogers NMR Center, an NIH BTRP facility (#P41-RR02584). We are grateful to Dr. Anca Constantinescu for technical assistance, and Drs. Ralph Shohet, J.T. Hsieh, and Peter Peschke (Deutsches Krebsforschungszentrum

Table 1
Relative Gene Expression of Transfected Cells Determined Using PFONPG

Cell line Promoter	PC3 BSP	PC3 CMV	PC3 CMV	C4(2) CMV
Transfection time	24 hr	24 hr	48 hr	48 hr
Incubation temperature	37°C	37°C	Room	Room
Incubation time	3 hr	3 hr	15 min	15 min
Cleaved portion	5.3%	12.7%	74%	100%

(DKFZ), German Cancer Center) for stimulating discussions.

REFERENCES

- Contag CH, Ross BD. It's not just about anatomy: in vivo bioluminescence imaging as an eyepiece into biology. *J Magn Reson Imaging* 2002;16:378–387.
- Haberkorn U, Altmann A, Jiang S, Morr I, Mahmut M, Eisenhut M. Iodide uptake in human anaplastic thyroid carcinoma cells after transfer of the human thyroid peroxidase gene. *Eur J Nucl Med* 2001;28:633–638.
- Tjuvajev JG, Doubrovina M, Akhurst T, Cai S, Balatoni J, Alauddin MM, Finn R, Bornmann W, Thaler H, Conti PS, Blasberg RG. Comparison of radiolabeled nucleoside probes (FIAU, FHBG, and FHPG) for PET imaging of HSV1-tk gene expression. *J Nucl Med* 2002;43:1072–1083.
- Ichikawa T, Hogemann D, Saeki Y, Tyminski E, Terada K, Weissleder R, Chiocca EA, Basilion JP. MRI of transgene expression: correlation to therapeutic gene expression. *Neoplasia* (NY) 2002;6:523–530.
- Koretsky AP, Brosnan MJ, Chen LH, Chen JD, Vandyke T. NMR detection of creatine-kinase expressed in liver of transgenic mice—determination of free ADP levels. *Proc Natl Acad Sci USA* 1990;87:3112–3116.
- Hoffman R. Green fluorescent protein imaging of tumour growth, metastasis, and angiogenesis in mouse models. *Lancet Oncol* 2002;3:546–556.
- Herschman HR. Non-invasive imaging of reporter genes. *J Cell Biochem* 2002;39:36–44.
- Jacob F, Monod J. Genetic regulatory mechanisms in the synthesis of proteins. *J Mol Biol* 1961;3:318–356.
- Kawaguchi J, Wilson V, Mee PJ. Visualization of whole-mount skeletal expression patterns of LacZ reporters using a tissue clearing protocol. *Biotechniques* 2002;32:68–73.
- Heuermann K, Cosgrove J. S-Gal: an autoclavable dye for color selection of cloned DNA inserts. *Biotechniques* 2001;30:1142–1147.
- Bronstein I, Edwards B, Voyta JC. 1,2-Dioxetanes—novel chemiluminescent enzyme substrates—applications to immunoassays. *J Biolumin Chemilumin* 1989;4:99–111.
- Louie AY, Huber MM, Ahrens ET, Rothbacher U, Moats R, Jacobs RE, Fraser SE, Meade TJ. In vivo visualization of gene expression using magnetic resonance imaging. *Nat Biotechnol* 2000;18:321–325.
- Yoon S, Kim HG, Chun KH, Shin JEN. 4-deoxy-analogs of p-nitrophenyl β -D-galactopyranosides for specificity study with β -galactosidase from *Escherichia coli*. *Bull Korean Chem Soc* 1996;17:599–604.
- Cui W, Otten P, Merritt M, Mason RP. A novel NMR reporter molecule for transmembrane pH gradients: para-fluoro-ortho-nitrophenol. In: *Proceedings of the 10th Annual Meeting of ISMRM, Honolulu, 2002*. p 385.
- Posci I, Taylor SA, Richardson AC, Smith BV, Price RG. Comparison of several new chromogenic galactosides as substrates for various β -D-galactosidases. *Biochem Biophys Acta* 1993;1163:54–60.
- Mason RP. Transmembrane pH gradients *in vivo*: measurements using fluorinated vitamin B6 derivatives. *Curr Med Chem* 1999;6:481–499.
- Yu X, Mason RP. Novel *in vivo* gene reporter molecule using fluorinated vitamin B6 as ^{19}F NMR indicator. In: *Proceedings of the 11th Annual Meeting of ISMRM, Toronto, Canada, 2003*. p 675.
- Stegman LD, Rehemtulla A, Beattie B, Kievit E, Lawrence TS, Blasberg RG, Tjuvajev JG, Ross BD. Noninvasive quantitation of cytosine deaminase transgene expression in human tumor xenografts with in vivo magnetic resonance spectroscopy. *Proc Natl Acad Sci USA* 1999;96:9821–9826.
- Freytag SO, Khil M, Stricker H, Peabody J, Menon M, DePeralta-Venturina M, Nafziger D, Pegg J, Paielli D, Brown S, Barton K, Lu M, Aguilar-Cordova E, Kim JH. Phase I study of replication-competent adenovirus-mediated double suicide gene therapy for the treatment of locally recurrent prostate cancer. *Cancer Res* 2002;62:4968–4976.
- Corban-Wilhelm H, Hull WE, Becker G, Bauder-Wust U, Greulich D, Debus J. Cytosine deaminase and thymidine kinase gene therapy in a Dunning rat prostate tumour model: absence of bystander effects and characterisation of 5-fluorocytosine metabolism with ^{19}F -NMR spectroscopy. *Gene Ther* 2002;9:1564–1575.
- Lutz NW, Hull WE. Assignment and pH dependence of the ^{19}F -NMR resonances from the fluorouracil anabolites involved in fluoropyrimidine chemotherapy. *NMR Biomed* 1999;12:237–248.
- Aime S, Cabella C, Colombatto S, Geninatti Crich S, Gianolio E, Maggioni F. Insights into the use of paramagnetic Gd(III) complexes in MR-molecular imaging investigations. *J Magn Reson Imaging* 2002;16:394–406.

Synthesis and Evaluation of a Novel Gene Reporter Molecule: Detection of β -galactosidase Activity Using ^{19}F NMR of a Fluorinated Vitamin B₆ Conjugate⁺

Jianxin Yu¹, Zhenyi Ma¹, Yingming Li^{2§}, Kenneth S. Koeneman^{2§}, Li Liu¹,
Ralph P. Mason^{1*}

Departments of Radiology¹ and Urology², UT Southwestern Medical Center, Dallas, TX, USA, [§]Current address: Dept. of Urologic Surgery and Comprehensive Cancer Center, University of Minnesota, Minneapolis, MN, USA

Abstract: Gene therapy has emerged as a promising strategy for treatment of various diseases. However, widespread implementation is hampered by difficulties in assessing the success of transfection, in particular, the spatial extent of expression in the target tissue and the longevity of expression. Thus, the development of non-invasive reporter techniques based on appropriate molecules and imaging modalities may help to assay gene expression. We now **report the design, synthesis and evaluation of a novel *in vivo* gene transfection reporter molecule 3-O-(β -D-galactopyranosyl)-6-fluoropyridoxol (GFPOL) using fluorinated vitamin B₆ as the ^{19}F NMR sensitive aglycone.** GFGPOL exhibits the following strengths as an *in vivo* ^{19}F NMR gene expression reporter: (a) large chemical shift response to enzyme cleavage (Δ = 8.00 ppm); (b) **minimal** toxicity for substrate or aglycone; (c) **good** water solubility; (d) good blood stability; (e) pH responsiveness of aglycone.

Key Words: β -galactosidase, ^{19}F NMR, gene reporter, pyridoxol, pH.

INTRODUCTION

Gene therapy shows promise for the treatment various disorders and clinical trials are underway. However, non-invasive detection of transgenes *in vivo* would be of considerable value for assessing the location, magnitude and persistence of expression. Generally, therapeutic genes are not readily detected, and thus, various reporter genes have been developed and are widely applied in molecular biology, *e.g.*, β -galactosidase (β -gal), β -glucuronidase, chloramphenicol acetyltransferase, and firefly luciferase [1]. Among these, the *lacZ* gene, encoding β -gal, is the most attractive reporter gene, because β -gal activity is readily assessed *in vitro* in hosts as evolutionarily diverse as bacteria, yeast, and mammals, and its introduction has become a standard means of assaying clonal insertion, transcriptional activation, protein expression, and protein interaction [2]. Many chromogenic or fluorogenic substrates are well-established, but they are generally limited to histology or *in vitro* assays [3-8].

Recently, Weissleder et al. [9] presented a near infrared approach based on 9H-(1, 3-dichloro-9, 9-dimethylacridin-2-one-7-yl) β -D-galactopyranoside (DDAOG), and Meade et al. [10] reported an NMR approach using 1-[2-(β -galactopyranosyloxy) propyl]-4, 7, 10-tris (carboxymethyl)-1, 4, 7, 10-tetraazacyclododecane) gadolinium (III) (EgadMe),

to assess β -gal activity *in vivo*. These diverse substrates emphasize the promiscuity (lack of substrate specificity) of β -gal activity. However, EgadMe was found to be 500 times less sensitive to β -gal than the traditional "yellow" biochemical indicator ortho-nitrophenol- β -D-galactopyranoside (ONPG) and failed to enter cells, necessitating direct microinjection. We realized that introduction of a fluorine atom into the traditional nitrophenol aglycones could generate NMR indicator molecules with minimal perturbation to a well-established molecular structure. Indeed, we successfully demonstrated the use of p-fluoro-o-nitrophenyl β -D-galactopyranoside (PFONPG) to detect enzyme activity in solution and transfected tumor cells [11]. PFONPG exhibits virtually identical sensitivity to cleavage by β -gal as compared with ONPG [12]. However, the liberated aglycone p-fluoro-o-nitrophenol (PFONP) exhibits some cytotoxicity, likely by analogy to the well known uncoupler of oxidative phosphorylation 2, 4-dinitrophenol [13]. More recently, we showed that various analogs of the aglycone structure (halophenols) showed significant differences in rate of response to enzyme action and some of these alternate aglycones exhibit much lower toxicity [12]. We now report the design, synthesis, and evaluation of another novel *in vivo* gene transfection reporter molecule using fluorinated vitamin B₆ as a stable aglycone and sensitive ^{19}F NMR indicator.

RESULTS AND DISCUSSION

Design

^{19}F NMR signals are exquisitely sensitive to molecular changes and often also to the microenvironment, and thus, there are many reporter molecules exploiting fluorine atoms

*Address correspondence to this author at the Department of Radiology, The University of Texas Southwestern Medical Center at Dallas, 5323 Harry Hines Blvd, Dallas, Texas 75390-9058, USA; Tel: (214)-648-8926; Fax: (214)-648-4538; E-mail: Ralph.Mason@UTSouthwestern.edu

⁺Presented in part at the 11th ISMRM in Toronto, Canada, 2003

[14]. We have previously shown that 6-fluoropyridoxol (**1**, **FPOL**) exhibits exceptional sensitivity to changes in pH with ~10 ppm acid/base ^{19}F NMR shift [15]. We recognized that **1** could serve as a replacement for fluorophenol aglycones offering similar steric and electrostatic properties. The fluorine atom located para to the phenolic group should provide sensitive response to enzyme induced cleavage of the substrate GFPOL. FPOL exhibits little toxicity and can reveal local pH in a similar manner to the prototype aglycone PFONP.

Synthesis

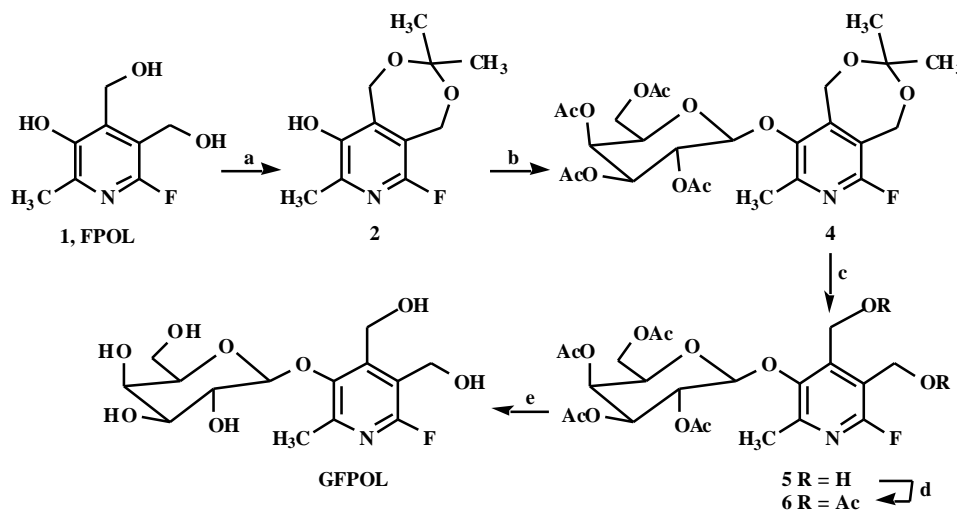
Condensation of **FPOL** and galactose has regioselectivity requirements and Scheme 1 outlines a synthetic route exploiting regioselective protection of the $^4, ^5$ -hydroxyl groups through ketal condensation. However, the ketal addition of **1** with acetone using standard conditions gave 6-fluoro-3, 4 -isopropylidenepyridoxol, as major product and the desired 6-fluoro- $^4, ^5$ -isopropylidenepyridoxol **2**, as minor by-product. Testing various acids as catalysts showed 2% H_2SO_4 acetone solution to provide the best yield of **2** (26%). The regioselectivity of the acetonation reaction was confirmed by analyzing ^1H -NMR spectra of **2** and 6-fluoro-3, 4 -isopropylidenepyridoxol, in which the 5-CH_2 signal of **2** appeared at 5.03 ppm as singlet and of 6-fluoro-3, 4 -isopropylidenepyridoxol at 4.97 ppm, but as doublet ($J_{\text{H-5}, \text{HO-5}} = 1.2$ Hz) due to the coupling of the 5-OH. The inefficient reaction is presumably due to the unfavorable seven member ring, as opposed to alternate six member ring.

Treatment of **2** with 2, 3, 4, 6-tetra-*O*-acetyl- β -D-galactopyranosyl bromide **3** using the Koenigs-Knorr glycosylation method gave 3-*O*-(2, 3, 4, 6-tetra-*O*-acetyl- β -D-galactopyranosyl)- $^4, ^5$ -isopropylidene-6-fluoropyridoxol **4** in 85% yield. NMR verified that the galactose was in the β -configuration ($J_{\text{H-1}', \text{HO-4}} = 8.0$ Hz) and C-1' 100.03 ppm). The correlation between 2-CH_3 and H-1' of sugar ring from the NOSEY spectrum of **4** verified that 2, 3,

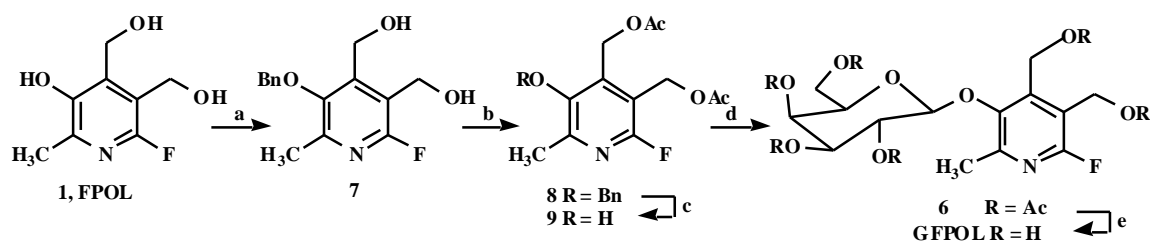
4, 6-tetra-*O*-acetyl- β -D-galactopyranosyl residue connected at the 3 phenolic site provided further evidence that acetonation reaction did occur regioselectively on 4, 5 hydroxymethyl groups.

Cleavage of acetonide **4** for synthesis of 3-*O*-(2, 3, 4, 6-tetra-*O*-acetyl- β -D-galactopyranosyl)-6-fluoropyridoxol **5** was achieved, however, the yields were low (15%), based on several hydrolysis conditions, such as 80% AcOH, 1% HCl or 90% $\text{CF}_3\text{CO}_2\text{H}$ in MeOH, CH_2Cl_2 or 1, 4-dioxane at various temperatures (60–100 °C). A moderate amount of **1** was recoverable indicating that the β -D-galactopyranosyl C-1' (gal)-O_3 bond became weak and sensitive to acid hydrolysis presumably due to the presence of 6-fluorine atom. Acetylation of **5** to **6** facilitated purification and structural characterization by NMR. Finally, deacetylation of **6**, in NH_3/MeOH from 0 °C to room temperature yielded the target molecule **GFPOL** in quantitative yield. The overall yield for **GFPOL** through this five-step route was ~3% with limiting steps in the $^4, ^5$ -isopropylidene group formation and hydrolysis procedures (a and c).

We thus considered alternate approaches, *e.g.*, Scheme 2. Particularly, the acidic phenolic group *para* to the 6-fluorine atom should be ionized under mild base conditions to selectively react with benzyl bromide affording the expected 3-mono benzylated product under carefully controlled conditions. When benzyl bromide (1.1 equiv.) was added dropwise over a period of 4–5 h to the well-stirred reaction mixture of compound **1** in a biphasic dichloromethane-aqueous system (pH 10–11) using tetrabutylammonium bromide (TBAB) as the phase-transfer catalyst (PTC), 3-*O*-benzyl-6-fluoropyridoxol **7** was isolated as major product in 76% yield with small amounts of di-*O*-benzyl derivatives 3, 4 -di-*O*-benzyl-6-fluoropyridoxol (16%) and 3, 5 -di-*O*-benzyl-6-fluoropyridoxol (8%). The structure of **7** was established on the basis of the coupling characteristics of $^4, ^5\text{-CH}_2$ as doublets ($J_{\text{H-4}, \text{HO-4}} = 6.0$ Hz, $J_{\text{H-5}, \text{HO-5}} = 5.4$ Hz) and $^4, ^5\text{-OH}$ as triplets in the ^1H -NMR spectrum. Treatment of



Scheme 1. Reagents and conditions: (a) 2% H_2SO_4 , acetone, r.t. 4–5 h, 26%; (b) 2, 3, 4, 6-tetra-*O*-acetyl- β -D-galactopyranosyl bromide (**3**), $\text{Hg}(\text{CN})_2$, 4Å M.S., CH_2Cl_2 , r.t., 12 h, 85%; (c) 80% AcOH, 80 °C, 4–5 h, 15%; (d) Ac_2O -Pyridine, 0 °C r.t., 24 h, quantitative yield; (e) NH_3 -MeOH, 0 °C r.t., 24 h, quantitative yield.



Scheme 2. Reagents and conditions: (a) benzyl bromide (1.1 equiv.), CH_2Cl_2 - H_2O , pH 10–11, 50 °C, TBAB, 4–5 h, 76%; (b) Ac_2O -Pyridine, 0 °C r.t., 24 h, quantitative yield; (c) H_2 , Pd/C, r.t., 12 h, quantitative yields; (d) 2, 3, 4, 6-tetra-*O*-acetyl- β -D-galactopyranosyl bromide (**3**), $\text{Hg}(\text{CN})_2$, 4 Å M.S., CH_2Cl_2 , r.t., 12 h, 90%; (e) NH_3 -MeOH, 0 °C r.t., 24 h, quantitative yield.

7 with acetic anhydride in pyridine from 0 °C to r.t. overnight gave 3-*O*-benzyl-4,5-di-*O*-acetyl-6-fluoropyridoxol **8** in quantitative yield. The 3-benzyl protecting group was removed under 5% Pd/C hydrogenation overnight affording nucleophile 4,5-di-*O*-acetyl-6-fluoropyridoxol **9** in quantitative yield. **9** was then subjected to a procedure similar to that described for the preparation of galactoside **4** giving 3-*O*-(2, 3, 4, 6-tetra-*O*-acetyl- β -D-galactopyranosyl)-4,5-di-*O*-acetyl-6-fluoropyridoxol **6** in 90% yield. After work up and deacetylation, the target compound **GFPOL** was obtained in 68% overall yield over five steps.

Recognizing the differential reactivity of the 3 phenolic group over the hydroxymethyl groups suggested a more direct synthesis. Direct galactopyranosylation of **1** with 2, 3, 4, 6-tetra-*O*-acetyl- β -D-galactopyranosyl bromide **3** failed as a result of the very low selectivity of the Koenigs-Knorr glycosylation reaction for the 3 phenolic group in the presence of the two free active hydroxymethyl groups. Product **5** could not be isolated, but using 2, 3, 4, 6-tetra-*O*-acetyl- β -D-galactopyranosyl bromide **3** phase-transfer catalysis gave **5** (88%) directly, and **GFPOL** (88%) through only two reaction steps (Scheme 3).

In conclusion, Scheme 3 provided a very efficient and direct method to stereo- and regioselectively synthesize 3-*O*-(β -D-galactopyranosyl)-6-fluoropyridoxol **GFPOL** in high yields. Large-scale preparation of **GFPOL** can be performed by these PTC methods.

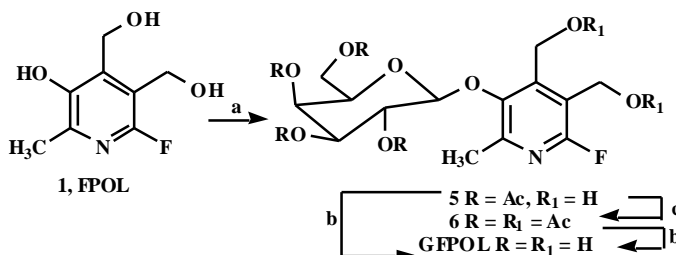
Characteristics

As expected, **GFPOL** readily dissolves in saline, whole blood, or PBS buffer, and is much more soluble than the aglycone **1**. **GFPOL** was stable in aqueous solutions in the pH range 3 to 12 at temperatures from 25 to 37 °C for at

least 5 days. Cell viability assays [16] showed that neither **GFPOL** nor **FPOL** exhibited significant cytotoxicity (Fig. 1). For **GFPOL** viability exceeded 98% at all concentrations tested and for **FPOL** survival was > 80% up to 2 mM.

Proton decoupling was applied to simplify ^{19}F NMR spectra and sodium trifluoroacetate (NaTFA) in a capillary was used as an external standard. **GFPOL** gave a single narrow ^{19}F NMR signal at -3.22 ppm essentially invariant (0.06 ppm) with pH in the range 3 to 12 and temperatures from 25 to 37 °C. Addition of β -gal (E801A) in PBS buffer (0.1M, pH=7.4) at 37 °C caused hydrolysis releasing the pH indicator aglycone **FPOL** appearing also as a single narrow ^{19}F signal shifted up-field to -11.21 ppm (Fig. 2), consistent with our previous titration curve of **FPOL** [15]. Sequential ^{19}F NMR spectra showed that **GFPOL** decreased monotonically, releasing free **FPOL** with an initial rate of 4.3 $\mu\text{mol}/\text{min}/\text{unit}$ (Fig. 3). For comparison **PFONPG** gave 19 $\mu\text{mol}/\text{min}/\text{unit}$ and **OFNPG** gave 32 $\mu\text{mol}/\text{min}/\text{unit}$ [12]. **PFONPG** was previously shown to exhibit very similar substrate activity to the traditional yellow biochemical indicator **ONPG** [12]. When **GFPOL** was incubated with wild type human cancer cells (prostate PC-3 or C4-2 (LNCaP lineage derived androgen independent subline)) or (breast MCF-7) for 5 h in PBS buffer at 37 °C under 5% CO_2 in air with 95% humidity, no changes were observed in the ^{19}F NMR spectra. However, addition of **GFPOL** to cells from these lines, which had been transfected transiently or stably to express β -gal led to cleavage of **GFPOL**, as detected over a period of hours (Fig. 4).

GFPOL provides further evidence for the ^{19}F NMR approach to assessing enzyme activity *in situ*. We are currently extending applications to imaging based on



Scheme 3. Reagents and conditions: (a) 2, 3, 4, 6-tetra-*O*-acetyl- β -D-galactopyranosyl bromide (**3**), CH_2Cl_2 - H_2O , pH 10–11, r.t., TBAB, 4–5 h, 88%; (b) NH_3 -MeOH, 0 °C r.t., 24 h, quantitative yield; (c) Ac_2O -Pyridine, 0 °C r.t., 24 h, quantitative yield.

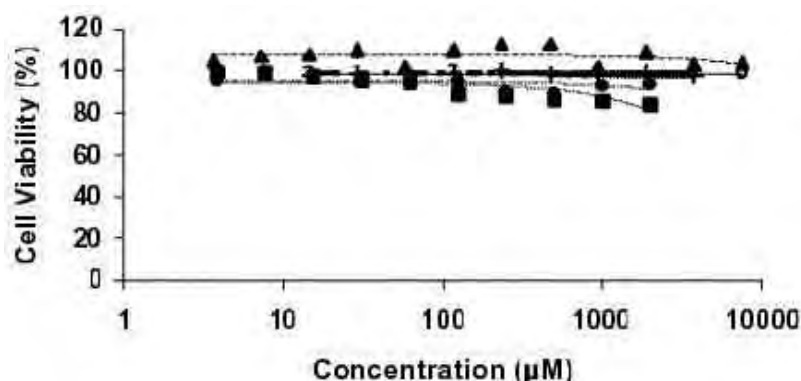


Fig. (1). Cellular toxicity of reporter molecules o C4-2 cells (GFPOL), + PC3 cells (GFPOL), • MAT-Lu cells (FPOL), MAT-Lu-LacZ cells (FPOL), ■ MAT-Lu-LacZ cells (GFPOL).

chemical shift selective excitation exploiting the large chemical shift difference between the substrate and product. We are also initiating studies in living animals and exploring the utility of enzyme activated pH measurements.

EXPERIMENTAL

General Methods

NMR spectra were recorded on a Varian Inova 400 spectrometer (400 MHz for ^1H , 100 MHz for ^{13}C) with CDCl_3 , acetone- d_6 or $\text{DMSO}-d_6$, as solvents, and chemical shifts referenced to TMS, as internal standard. ^{19}F NMR (376 MHz) signals are referenced to dil. sodium trifluoroacetate (NaTFA) in an external capillary. 2, 3, 4, 6-tetra-O-acetyl- β -D-galactopyranosyl bromide (**3**) was purchased from Sigma. Reactions requiring anhydrous conditions were performed under nitrogen or argon. $\text{Hg}(\text{CN})_2$ was dried before use at 50 $^\circ\text{C}$ for 1 h, CH_2Cl_2 was dried over Drierite. Solutions in organic solvents were dried with anhydrous sodium sulfate, and concentrated *in vacuo* below 45 $^\circ\text{C}$. Column chromatography was performed on silica gel (200–300 mesh) by elution with cyclohexane-EtOAc and silica gel GF $_{254}$ used for analytical TLC (Aldrich). Detection was effected by spraying the plates with 5% EtOH/ H_2SO_4 (followed by heating at 110 $^\circ\text{C}$ for 10 min.) or by direct UV. Microanalyses were performed on a Perkin-Elmer 2400 CHN microanalyser.

-Gal (E801A) was purchased from Promega and enzymic reactions performed at 37 $^\circ\text{C}$ in PBS buffer (0.1M, pH 7.4). For enzyme kinetic experiments, **GFPOL** (5.25 mg) was dissolved in PBS buffer (600 μL , pH=7.4), a PBS solution of -gal (20 μL , E801A, 1unit/ μL) was added and NMR data were acquired immediately at 37 $^\circ\text{C}$.

Both PC-3 and C4-2 were plated at 5 million cells per dish (P150) and grown for 24 h. Then PC-3 and C4-2 were transfected for 48 h with a first generation adenovirus vector encoding the lacZ gene driven by the CMV promoter. PC-3 was transfected with 50 moi and C4-2 with 10 moi of Ad-CMV-lacZ. After 48 h incubation and washing, cells were trypsinized and concentrated to 10 million cells per ml. for further use (NMR).

Human breast cancer cells MCF-7 were stably co-transfected with pCMV (Clontech, Palo Alto, CA, USA), using TransFastTM Transfection Reagent (Promega, Madison, WI, USA) comprising the *E.coli lacZ* gene located under the human cytomegalovirus (CMV) immediate-early enhancer/promoter region and pCI-neo (Promega, Madison, WI, USA) carrying the neomycin phosphotransferase gene. For MCF-7 cells clonal selection was applied to identify those cells with highest -gal expression.

Control wild type and transfected human prostate tumor cells (PC3 and C4-2 (LNCaP lineage derived androgen independent subline)) and human breast tumor cells MCF-7

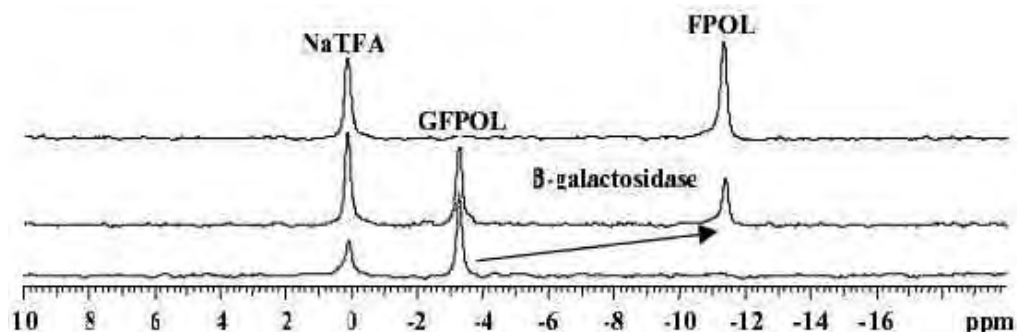


Fig. (2). ^{19}F NMR spectra of **GFPOL** during the hydrolysis by -gal in PBS buffer at 37 $^\circ\text{C}$.

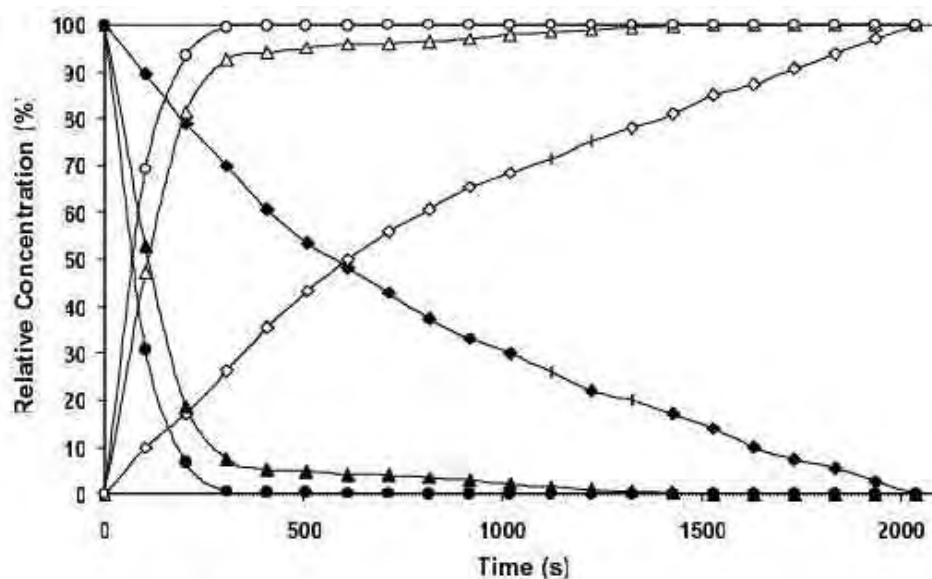


Fig. (3). Relative action of β -gal (E801A) on **GFPOL** (\blacklozenge), **PFONPG** (\square) and **OFPNP** (O) in PBS buffer at 37 °C yielding **FPOL** (\square), **PFONP** (\square) and **OFPNP** (\bullet), respectively. In each case 20 units of β -gal (E801A) were added to 15 mmol substrate in PBS at 37 °C.

were grown in culture dishes under standard conditions and harvested. **GFPOL** (1.84 mg) in PBS buffer (70 μL) was added to suspension of 10^7 cells in PBS buffer (530 μL) and NMR data were acquired immediately, and again after incubation for various times up to 5 h at 37 °C (prostate tumor cells PC3 and C4-2) or at 22 °C (breast tumor cells MCF-7).

The sensitivities of human prostate cancer cells PC3, C4-2 and their LacZ transfected counterparts to **GFPOL** and **FPOL** were quantified using a colorimetric CellTiter 96 Aqueous Nonradioactive MTS Cell Proliferation Assay (Promega, Madison, WI, USA). The assays were performed in triplicate using 24-well plates seeded with 10^3 cells per well in 500 μL RPMI 1640 without phenol red and supplemented with 10% FCS and 2 mM glutamine. After 24 h incubation, the medium was replaced with fresh RPMI 1640 containing various concentrations of **GFPOL**. For the

determination of IC_{50} drug concentrations, incubations with **GFPOL** (0–7.5 mM) and **FPOL** (0–2 mM) were performed for 72 h, followed by the MTS assay (Figure 1).

Syntheses

$4, 5\text{-O-isopropylidene-6-fluoropyridoxol } 2$

A suspension of 6-fluoropyridoxol **1** (0.50 g, 2.67 mmol) in anhydrous acetone (40 ml) containing 2% $\text{c.H}_2\text{SO}_4$ was stirred until TLC (4:1 cyclohexane-EtOAc) indicated complete reaction (4–5 h), then cold saturated Na_2CO_3 solution was added with vigorous stirring up to pH 8–9. The precipitate was filtered, the reaction mixture concentrated under reduced pressure followed by purification on flash silica gel column (4:1 cyclohexane-EtOAc) yielding the acetone **2** (0.64 g, 26%) as a syrup, R_f 0.34(4:1 cyclohexane-EtOAc), δ_{H} : 7.45(1H, s, HO-3), 5.03(2H, s,

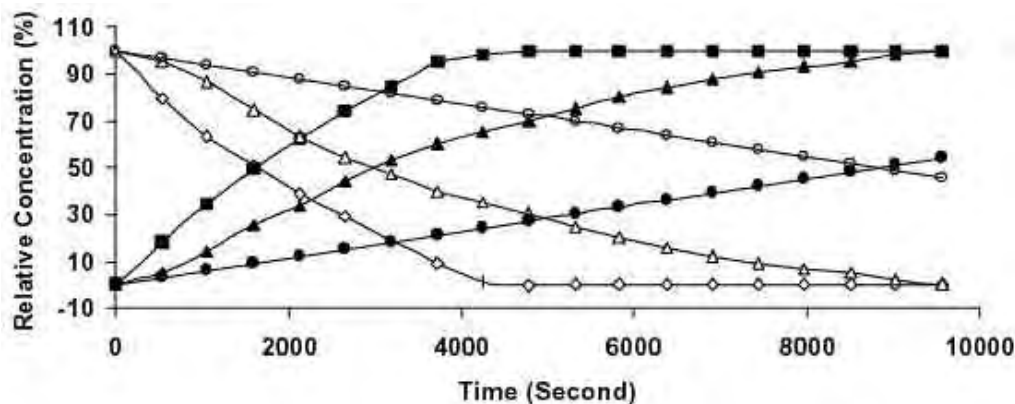


Fig. (4). Kinetic curves showing changes in **GFPOL** (open symbols) and **FPOL** (closed symbols) during incubation with human C4-2 (square) and PC-3 (triangle) prostate and MCF-7 breast (circle) cancer cells transfected to express β -gal. Prostate cells were investigated at 37 °C, while breast cells were examined at 22 °C in PBS buffer.

CH₂-5), 4.57(2H, s, CH₂-4), 2.33(3H, s, CH₃-2), 1.55(6H, s, 2×CH₃)ppm; δ_{C} : 154.49(s, Py-C), 152.20(s, Py-C), 144.14(d, $J_{\text{F-C}}=14.5$ Hz, Py-C), 131.37(d, $J_{\text{F-C}}=3.8$ Hz, Py-C), 114.01(d, $J_{\text{F-C}}=32.9$ Hz, Py-C), 99.51(s, CMe₂), 59.04(d, $J_{\text{F-C}}=3.8$ Hz, CH₂-5), 54.51(s, CH₂-4), 31.62(s, C(CH₃)₂), 17.58(s, CH₃-2)ppm.

Anal. Calcd. for C₁₁H₁₄NO₃F(%): C, 58.13, H, 6.21, N, 6.17; Found: C, 58.08, H, 6.16, N, 6.11.

3-O-(2, 3, 4, 6-tetra-O-acetyl- -D-galactopyranosyl)- ⁴, ⁵-O-isopropylidene-6-fluoropyridoxol **4**

To a solution of ⁴, ⁵-O-isopropylidene-6-fluoropyridoxol **2** (0.62 g, 2.72mmol) and Hg(CN)₂ (0.88 g, 3.50 mmol) in dry CH₂Cl₂ (10 mL) containing freshly activated 4Å molecular sieve (2 g) was added dropwise **3** (1.23 g, 3.0 mmol, 1.1 equiv. in CH₂Cl₂). The mixture was stirred overnight in the dark at r.t. under N₂ until TLC indicated complete reaction. The mixture was diluted with CH₂Cl₂ (30 mL), filtered through Celite, washed, dried (Na₂SO₄) and concentrated *in vacuo*. The residue was purified on a silica gel column (2:3 cyclohexane-EtOAc) to yield **4** (1.29 g, 85%) as syrup, R_f 0.40(2:3 cyclohexane-EtOAc), δ_{H} : 4.64(1H, d, $J_{1', 2'}=8.0$ Hz, H-1'), 5.25(1H, dd, $J_{2', 3'}=10.0$ Hz, H-2'), 5.02(1H, dd, $J_{3', 4'}=3.6$ Hz, H-3'), 5.41(1H, dd, $J_{4', 5'}=3.2$ Hz, H-4'), 3.97(1H, m, H-5'), 4.21(1H, dd, $J_{5', 6a'}=4.4$ Hz, $J_{6a', 6b'}=11.2$ Hz, H-6a'), 4.13(1H, dd, $J_{5', 6b'}=7.2$ Hz, H-6b'), 5.10(1H, d, $J_{\text{CH}_2\text{-4a}, \text{CH}_2\text{-4b}}=8.0$ Hz, CH₂-4a), 4.67(1H, d, $J_{\text{CH}_2\text{-4a}, \text{CH}_2\text{-4b}}=8.0$ Hz, CH₂-4b), 5.14(1H, d, $J_{\text{CH}_2\text{-5a}, \text{CH}_2\text{-5b}}=9.6$ Hz, CH₂-5a), 5.12(1H, d, $J_{\text{CH}_2\text{-5a}, \text{CH}_2\text{-5b}}=9.6$ Hz, CH₂-5b), 2.42(3H, s, CH₃-2), 2.17, 2.09, 2.08, 1.99(12H, 4s, 4×CH₃CO), 1.61, 1.59(6H, 2s, 2×CH₃)ppm; δ_{C} : 170.78, 170.39, 170.26, 170.11(4s, 4×CH₃CO), 155.44(s, Py-C), 153.15(s, Py-C), 145.48(d, $J_{\text{F-C}}=15.2$ Hz, Py-C), 133.16(d, $J_{\text{F-C}}=4.0$ Hz, Py-C), 116.95(d, $J_{\text{F-C}}=32.1$ Hz, Py-C), 101.41(s, CMe₂), 100.03(s, C-1'), 68.70(s, C-2'), 70.82(s, C-3'), 67.12(s, C-4'), 71.53(s, C-5'), 64.28(s, C-6'), 55.38(s, CH₂-4), 61.58(s, CH₂-5), 31.88(s, C(CH₃)₂), 20.90, 20.89, 20.82, 20.77(4s, 4×CH₃CO), 18.77(s, CH₃-2)ppm.

Anal. Calcd. for C₂₅H₃₂NO₁₂F(%): C, 53.84, H, 5.79, N, 2.51; Found: C, 53.79, H, 5.74, N, 2.49.

3-O-(2, 3, 4, 6-tetra-O-acetyl- -D-galactopyranosyl)-6-fluoropyridoxol **5**

A mixture of 3-O-(2, 3, 4, 6-tetra-O-acetyl- -D-galactopyranosyl)- ⁴, ⁵-O-isopropylidene-6-fluoropyridoxol **4** (1.25 g, 2.50 mmol) in 80% AcOH (40 mL) was stirred at 80 °C for 4~5 h, until TLC (1:3 cyclohexane-EtOAc) showed complete reaction. The cooled mixture was neutralized with cold saturated Na₂CO₃, extracted (EtOAc, 4×30 mL), concentrated and purified by flash silica gel column (1:4 cyclohexane-EtOAc) yielding **5** (0.17 g, 15%) as a syrup, R_f 0.18(1:4 cyclohexane-EtOAc), δ_{H} : 4.79(1H, d, $J_{1', 2'}=8.0$ Hz, H-1'), 5.55(1H, dd, $J_{2', 3'}=10.6$ Hz, H-2'), 5.10(1H, dd, $J_{3', 4'}=3.6$ Hz, H-3'), 5.41(1H, dd, $J_{4', 5'}=3.6$ Hz, H-4'), 3.88(1H, m, H-5'), 4.24(1H, dd, $J_{5', 6a'}=4.4$ Hz, $J_{6a', 6b'}=12.0$ Hz, H-6a'), 4.09(1H, dd, $J_{5', 6b'}=6.0$ Hz, H-6b'), 5.01(2H, d, $J_{\text{CH}_2\text{-4a}, \text{CH}_2\text{-4b}}=12.4$ Hz, CH₂-4a, CH₂-4b), 4.66(1H, d, $J_{\text{CH}_2\text{-5a}, \text{CH}_2\text{-5b}}=12.4$

Hz, CH₂-5b), 3.50(1H, m, HO-4, exchangeable with D₂O), 3.56(1H, m, HO-5, exchangeable with D₂O), 2.47(3H, s, CH₃-2), 2.23, 2.17, 2.02, 2.00(12H, 4s, 4×CH₃CO)ppm; δ_{C} : 170.32, 170.28, 170.18, 169.48(4×CH₃CO), 158.78(s, Py-C), 156.42(s, Py-C), 150.33(d, $J_{\text{F-C}}=15.2$ Hz, Py-C), 147.62(d, $J_{\text{F-C}}=4.6$ Hz, Py-C), 120.17(d, $J_{\text{F-C}}=32.0$ Hz, Py-C), 102.39(s, C-1'), 68.91(s, C-2'), 70.74(s, C-3'), 67.19(s, C-4'), 71.93(s, C-5'), 61.98(s, C-6'), 55.91(s, CH₂-4), 59.60(s, CH₂-5), 20.99, 20.85, 20.70, 20.67(4s, 4×CH₃CO), 19.46(s, CH₃-2)ppm.

Anal. Calcd. for C₂₂H₂₈NO₁₂F(%): C, 51.05, H, 5.46, N, 2.71; Found: C, 51.00, H, 5.39, N, 2.68.

As an alternative, **5** was synthesized from **1** directly by phase transfer catalysis. To a well stirred CH₂Cl₂ (10 mL)-H₂O (10 mL) biphasic mixture (pH 10~11) of **1** (0.5 g, 2.67mmol) and tetrabutylammonium bromide (TBAB; 0.1 g, 0.31mmol) as the phase-transfer catalyst, a solution of 2, 3, 4, 6-tetra-O-acetyl- -D-galactopyranosyl bromide (**3**) (1.21 g, 2.94 mmol, 1.1equiv.) in CH₂Cl₂ (10 mL) was added dropwise over a period of 4~5 h at r.t., and the stirring continued for an additional hour. The products were extracted (EtOAc, 4×20 mL), washed free of alkali, dried (Na₂SO₄), concentrated and the residue purified by column chromatography on silica gel (1:4 cyclohexane-EtOAc) to afford **5** (1.08 g, 88%) as a syrup, which was identical in all respects to the product obtained above.

3-O-(2, 3, 4, 6-tetra-O-acetyl- -D-galactopyranosyl)- ⁴, ⁵-di-O-acetyl-6-fluoropyridoxol **6**

A solution of **5** (1.20 g, 2.64mmol) in pyridine (30 mL) was treated with Ac₂O (15 mL). The reaction mixture was stirred from 0 °C to r.t. overnight, coevaporated with toluene under reduced pressure and the residue purified by flash silica gel column chromatography (1:1 cyclohexane-EtOAc) to give **6** (1.56 g, 100%) as a foamy solid, R_f 0.32(1:2 cyclohexane-EtOAc), δ_{H} : 5.15(1H, d, $J_{1', 2'}=7.8$ Hz, H-1'), 5.18(1H, dd, $J_{2', 3'}=10.8$ Hz, H-2'), 4.17(1H, dd, $J_{3', 4'}=6.0$ Hz, H-3'), 5.41(1H, dd, $J_{4', 5'}=5.6$ Hz, H-4'), 5.31(1H, m, H-5'), 4.06(1H, dd, $J_{5', 6a'}=5.2$ Hz, $J_{6a', 6b'}=12.0$ Hz, H-6a'), 4.01(1H, dd, $J_{5', 6b'}=6.8$ Hz, H-6b'), 5.28(2H, m, CH₂-5), 5.12(2H, s, CH₂-4), 2.44(3H, s, CH₃-2), 2.17, 2.12, 2.03, 2.02, 1.99, 1.96(18H, 6s, 6×CH₃CO)ppm; δ_{C} : 170.42, 170.41, 170.29, 170.25, 170.00, 169.68(6×CH₃CO), 158.91(s, Py-C), 156.57(s, Py-C), 152.36(d, $J_{\text{F-C}}=16.0$ Hz, Py-C), 147.05(d, $J_{\text{F-C}}=4.6$ Hz, Py-C), 115.53(d, $J_{\text{F-C}}=32.0$ Hz, Py-C), 101.97 (s, C-1'), 69.10(s, C-2'), 70.51(s, C-3'), 67.63(s, C-4'), 70.84(s, C-5'), 60.20(s, C-6'), 57.13(s, CH₂-4), 61.44(s, CH₂-5), 21.15, 20.88, 20.86, 20.84, 20.80, 20.76(6s, 6×CH₃CO), 19.83(s, CH₃-2)ppm.

Anal. Calcd. for C₂₆H₃₂NO₁₄F(%): C, 51.90, H, 5.37, N, 2.33; Found: C, 51.88, H, 5.31, N, 2.29.

3-O-(-D-galactopyranosyl)-6-fluoropyridoxol GFPOL

Compound **6** (1.25 g, 2.1 mmol) was deacetylated with 0.5M NH₃/MeOH (30 mL) from 0 °C to r.t. giving the free galactopyranoside **GFPOL** (0.75 g) as a foamy solid in quantitative yield, R_f 0.21 (1:9 MeOH-EtOAc), δ_{H} : 4.43(1H, d, $J_{1', 2'}=8.0$ Hz, H-1'), 3.63(1H, dd, $J_{2', 3'}=8.8$ Hz, H-2'),

3.39(1H, dd, $J_{3',4'}=3.2$ Hz, H-3'), 4.54(1H, dd, $J_{4',5'}=2.8$ Hz, H-4'), 4.69(1H, m, H-5'), 3.45(1H, dd, $J_{5',6a'}=4.4$ Hz, $J_{6a',6b'}=10.8$ Hz, H-6a'), 3.07(1H, dd, $J_{5',6b'}=6.0$ Hz, H-6b'), 5.20~4.70(4H, br, HO-2', 3', 4', 6', exchangeable with D_2O), 4.53(2H, s, CH_2 -4), 4.71(2H, s, CH_2 -5), 3.39(2H, br, HO-4, 5, exchangeable with D_2O), 2.42(3H, s, CH_3 -2)ppm; ^{13}C : 158.03(s, Py-C), 155.71(s, Py-C), 150.28(d, $J_{\text{F-C}}=15.3$ Hz, Py-C), 147.61(d, $J_{\text{F-C}}=5.3$ Hz, Py-C), 119.71 (d, $J_{\text{F-C}}=31.3$ Hz, Py-C), 105.62(s, C-1'), 70.90(s, C-2'), 73.06(s, C-3'), 68.14(s, C-4'), 75.47(s, C-5'), 60.58(s, C-6'), 53.79(s, CH_2 -4), 54.65(s, CH_2 -5), 19.40(s, CH_3 -3)ppm.

Anal. Calcd. for $\text{C}_{14}\text{H}_{20}\text{NO}_8\text{F}$ (%): C, 48.12, H, 5.77, N, 4.01; Found: C, 48.08, H, 5.75, N, 3.97.

3-O-Benzyl-6-fluoropyridoxol 7

To a well stirred CH_2Cl_2 (15 mL)- H_2O (20 mL) biphasic mixture (pH 10~11) of 1 (1.0 g, 5.34 mmol) and TBAB (0.3 g, 0.93 mmol), a solution of benzyl bromide (1.02 g, 5.88 mmol, 1.1 equiv.) in CH_2Cl_2 (15 mL) was added dropwise over a period of 4~5 h, while the reaction temperature was maintained at 50 °C, and the stirring continued for an additional hour. The products were extracted (CH_2Cl_2 , 4×30 mL), washed free of alkali, dried (Na_2SO_4), concentrated and the residue purified by column chromatography on silica gel (1:2 cyclohexane-EtOAc) to afford major product 7 and small amounts of di-O-benzyl-6-fluoropyridoxol derivatives.

3-O-Benzyl-6-fluoropyridoxol 7

(1.12 g, 76%), white crystalline, R_f 0.38(1:2 cyclohexane-EtOAc), ^1H : 7.39(5H, m, Ar-H), 4.90(2H, s, PhCH_2), 4.75(2H, d, $J_{\text{H-5}, \text{HO-5}}=5.4$ Hz, CH_2 -5), 4.72(2H, d, $J_{\text{H-4}, \text{HO-4}}=6.0$ Hz, CH_2 -4), 3.57(1H, t, $J_{\text{H-5}, \text{HO-5}}=5.4$ Hz, HO-5, exchangeable with D_2O), 3.49(1H, t, $J_{\text{H-4}, \text{HO-4}}=6.0$ Hz, HO-4, exchangeable with D_2O), 2.44(3H, s, CH_3 -2)ppm; ^{13}C : 157.38(s, Py-C), 155.82(s, Py-C), 149.55(d, $J_{\text{F-C}}=4.7$ Hz, Py-C), 146.97(d, $J_{\text{F-C}}=4.0$ Hz, Py-C), 119.09(d, $J_{\text{F-C}}=31.2$ Hz, Py-C), 136.33, 128.96, 128.88, 128.87(Ph-C), 55.99(s, PhCH_2 , CH_2 -4), 56.76(s, CH_2 -5), 19.31(s, CH_3 -2)ppm.

Anal. Calcd. for $\text{C}_{15}\text{H}_{16}\text{NO}_5\text{F}$ (%): C, 64.96, H, 5.82, N, 5.05; Found: C, 64.95, H, 5.79, N, 5.04.

3, 4-Di-O-benzyl-6-fluoropyridoxol

(0.30 g, 16%), syrup, R_f 0.30(1:2 cyclohexane-EtOAc), ^1H : 7.46~7.33(10H, m, Ar-H), 4.90(2H, s, PhCH_2 -3), 4.69(2H, s, PhCH_2 -4), 4.64(2H, d, $J_{\text{H-5}, \text{HO-5}}=4.8$ Hz, CH_2 -5), 4.62(2H, s, CH_2 -4), 3.37(1H, t, $J_{\text{H-5}, \text{HO-5}}=4.8$ Hz, HO-5, exchangeable with D_2O), 2.44(3H, s, CH_3 -2)ppm; ^{13}C : 157.98(s, Py-C), 155.65(s, Py-C), 152.10(d, $J_{\text{F-C}}=14.5$ Hz, Py-C), 150.04(d, $J_{\text{F-C}}=4.6$ Hz, Py-C), 116.16(d, $J_{\text{F-C}}=31.3$ Hz, Py-C), 136.91, 136.59, 128.92, 128.76, 128.56, 128.48, 128.44(Ph-C), 77.21(s, PhCH_2 -3), 73.48(s, PhCH_2 -4), 56.73(s, CH_2 -4), 63.30(s, CH_2 -5), 19.65(s, CH_3 -2)ppm.

Anal. Calcd. for $\text{C}_{22}\text{H}_{22}\text{NO}_3\text{F}$ (%): C, 71.90, H, 6.04, N, 3.81; Found: C, 71.86, H, 5.99, N, 3.77.

3, 5-Di-O-benzyl-6-fluoropyridoxol

(0.16 g, 8%), syrup, R_f 0.25(1:2 cyclohexane-EtOAc), ^1H : 7.39~7.30(10H, m, Ar-H), 4.77(2H, s, PhCH_2 -3),

4.66(2H, d, $J_{\text{H-4}, \text{HO-4}}=6.8$ Hz, CH_2 -4), 4.63(2H, s, CH_2 -5), 4.58(2H, s, PhCH_2 -5), 2.95(1H, t, $J_{\text{H-4}, \text{HO-4}}=6.8$ Hz, HO-5, exchangeable with D_2O), 2.46(3H, s, CH_3 -2)ppm; ^{13}C : 158.39(s, Py-C), 156.04(s, Py-C), 151.04(d, $J_{\text{F-C}}=14.5$ Hz, Py-C), 149.72(d, $J_{\text{F-C}}=4.6$ Hz, Py-C), 120.36(d, $J_{\text{F-C}}=32.8$ Hz, Py-C), 136.78, 136.30, 128.92, 128.77, 128.60, 128.55, 128.27(Ph-C), 77.05(s, PhCH_2 -3), 73.97(s, PhCH_2 -5), 56.09(s, CH_2 -4), 63.66(s, CH_2 -5), 19.43(s, CH_3 -2)ppm.

Anal. Calcd. for $\text{C}_{22}\text{H}_{22}\text{NO}_3\text{F}$ (%): C, 71.90, H, 6.04, N, 3.81; Found: C, 71.88, H, 6.01, N, 3.78.

3-O-Benzyl- 4, 5-di-O-acetyl-6-fluoropyridoxol 8

Acetylation of 7 (1.10 g, 4.0 mmol) was carried out as described above for 6 to give 8 (1.43 g, 100%), white crystalline, R_f 0.44(3:2 cyclohexane-EtOAc), ^1H : 7.40(5H, m, Ar-H), 4.98(2H, s, CH_2 -5), 4.92(2H, s, PhCH_2), 4.85(2H, s, CH_2 -4), 2.46(3H, s, CH_3 -2), 2.20, 2.17(6H, 2s, 2× CH_3CO)ppm; ^{13}C : 170.58, 170.46(2× CH_3CO), 158.48(s, Py-C), 155.98(s, Py-C), 150.35(d, $J_{\text{F-C}}=5.0$ Hz, Py-C), 147.68(d, $J_{\text{F-C}}=4.4$ Hz, Py-C), 120.06(d, $J_{\text{F-C}}=31.6$ Hz, Py-C), 137.43, 129.66, 129.38, 128.88(Ph-C), 56.69(s, PhCH_2 , CH_2 -4), 57.66(s, CH_2 -5), 21.45, 20.98(2s, 2× CH_3CO), 19.36(s, CH_3 -2)ppm.

Anal. Calcd. for $\text{C}_{19}\text{H}_{20}\text{NO}_5\text{F}$ (%): C, 63.13, H, 5.58, N, 3.88; Found: C, 63.09, H, 5.53, N, 3.86.

4, 5-di-O-acetyl-6-fluoropyridoxol 9

A mixture of 8 (1.20 g, 3.32 mmol) and 5% Pd-C (500 mg) in MeOH (100 mL) was stirred for 24 h at r.t. under H_2 atmosphere. After filtration, the filtrate was evaporated to afford 9 in quantitative yields (white crystals), R_f 0.24(3:2 cyclohexane-EtOAc), ^1H : 7.56(1H, s, HO-3), 5.08(2H, s, CH_2 -5), 4.91(2H, s, CH_2 -4), 2.48(3H, s, CH_3 -2), 2.22, 2.18(6H, 2s, 2× CH_3CO)ppm; ^{13}C : 170.56, 170.50(2× CH_3CO), 158.68(s, Py-C), 156.00(s, Py-C), 150.75(d, $J_{\text{F-C}}=5.1$ Hz, Py-C), 147.88(d, $J_{\text{F-C}}=4.2$ Hz, Py-C), 120.09(d, $J_{\text{F-C}}=31.9$ Hz, Py-C), 56.88(s, CH_2 -4), 57.94(s, CH_2 -5), 21.65, 20.89(2s, 2× CH_3CO), 19.44(s, CH_3 -2)ppm.

Anal. Calcd. for $\text{C}_{12}\text{H}_{14}\text{NO}_5\text{F}$ (%): C, 53.11, H, 5.20, N, 5.17; Found: C, 53.08, H, 5.17, N, 5.14.

ACKNOWLEDGEMENTS

Supported by grants from the Department of Defense Breast Cancer Initiative IDEA award DAMD 17-03-1-0343-01, Department of Defense Prostate Cancer Initiative IDEA awards DAMD 17-01-1-0107 (KSK) and DAMD17-02-1-0148 (KSK) and Prostate Cancer Consortium DAMD17-03-2-0033 (KSK), a post doc award from the DOD Prostate Cancer Initiative W81XWH-04-10331 (LL) and the Cancer Imaging Program, NIH P20 CA 86354 (pre-ICMIC). NMR experiments were conducted at the Mary Nell and Ralph B. Rogers NMR Center, an NIH BTRP facility #P41-RR02584.

REFERENCES

- [1] Wood, K.V. *Curr. Opin. Biotechnol.* **1995**, 6, 50.
- [2] Serebriiskii, I.G.; Golemis, E.A. *Anal. Biochem.* **2000**, 285, 1.
- [3] Nolan, G.P.; Fiering, S.; Nicholas, J.-F.; Herzenberg, L.A. *Proc. Natl. Acad. Sci. USA* **1988**, 85, 2603.

- [4] James, A.L.; Perry, J.D.; Ford, M.; Armstrong, L.; Gould, F.K. *Appl. Environ. Microbiol.* **1996**, *62*, 3868.
- [5] James, A.L.; Perry, J.D.; Chilvers, K.; Robson, I.S.; Armstrong, L.; Orr, K.E. *Letters in Applied Microbiol.* **2000**, *30*, 336.
- [6] Heuermann, K.; Cosgrove, J. *Biotechniques* **2001**, *30*, 1142.
- [7] Manafi, M.; Kneifel, W.; Bascomb, S. *Microbiol. Rev.* **1991**, *55*, 335.
- [8] Perry, J.D.; Ford, M.; Taylor, J.; Jones, A.L.; Freeman, R.; Gould, F.K. *J. Clin. Microbiol.* **1999**, *37*, 766.
- [9] Tung, C.H.; Zeng, Q.; Shah, K.; Kim, D.E.; Schellingerhout, D.; Weissleder, R. *Cancer Res.* **2004**, *64*, 1579.
- [10] Louie, A.Y.; Huber, M.M.; Ahrens, E.T.; Rothbacher, U.; Moats, R.; Jacobs, R.E.; Fraser, S.E.; Meade, T.J. *Nature Biotechnol.* **2000**, *18*, 321.
- [11] Cui, W.; Otten, P.; Li, Y.; Koeneman, K.; Yu, J.; Mason, R.P. *Magn. Reson. Med.* **2004**, *51*, 616.
- [12] Yu, J.; Otten, P.; Ma, Z.; Cui, W.; Liu, L.; Mason, R.P. *Bioconj. Chem.* **2004**, *15*, 1334.
- [13] Slater, E.C., In , S. P. Colowick and N. O. Kaplan, Ed.; Academic Press: New York, **1967** 48.
- [14] Mason, R.P. *Curr. Med. Chem.* **1999**, *6*, 481.
- [15] Mehta, V.D.; Kulkarni, P.V.; Mason, R.P.; Constantinescu, A.; Aravind, S.; Goomer, N.; Antich, P.P. *FEBS Letters* **1994**, *349*, 234.
- [16] Mosmann, T. *Immunol. Methods* **1983**, *65*, 55.

Novel NMR Platform for Detecting Gene Transfection: Synthesis and Evaluation of Fluorinated Phenyl β -D-Galactosides with Potential Application for Assessing LacZ Gene Expression[†]

Jianxin Yu, Pieter Otten, Zhenyi Ma, Weina Cui, Li Liu, and Ralph P. Mason*

Department Radiology, The University of Texas Southwestern Medical Center at Dallas, Dallas, Texas 75390-9058. Received March 12, 2004; Revised Manuscript Received October 1, 2004

Gene therapy holds great promise for the treatment of diverse diseases, but widespread implementation is hindered by difficulties in assessing the success of transfection. The development of noninvasive reporter techniques based on appropriate molecules and imaging modalities may help to assay gene expression. Fluorophenyl- β -D-galactopyranosides provide a novel class of NMR active molecules, which are highly responsive to the action of β -galactosidase (β -gal), the product of the lacZ gene. The reporter molecules are stable in solution and with respect to wild-type cells, but the enzyme causes liberation of the aglycon, a fluorophenol, accompanied by distinct color formation and a ^{19}F NMR chemical shift of 5–10 ppm, depending on pH. Synthetic strategy, experimental methods, and molecular and ^{19}F NMR characteristics are reported for a series of molecules in solution, blood, and tumor cells. This class of molecules presents a new strategy for assaying gene expression with a highly versatile molecular structural platform.

INTRODUCTION

Gene therapy holds great promise for the treatment of diseases including cancer, cystic fibrosis, and immunodeficiency. However, a major hurdle to widespread successful implementation is the need to verify successful transfection, in particular, the spatial distribution of gene expression in the target tissue, together with assays of the longevity of expression. An image-based assay could greatly facilitate optimal gene therapy vector dosing, in a precise temporal and spatial manner.

Two approaches are gaining popularity for reporter genes. One method favors the use of genes producing reporter molecules such as green fluorescent protein, which are directly detectable by physical methods such as fluorescence. The second approach uses genes to produce enzymes, which act upon substrates administered to specifically interrogate gene expression. A critical criterion is that the reporter gene not be normally present or expressed in the cells of interest. The most popular reporter genes today are associated with optical imaging, because this is a cheap modality and is highly sensitive and the results are rapidly available (1, 2). Thus, fluorescent imaging of green fluorescent protein [GFP¹ and longer wavelength variants (3)] and bioluminescent imaging (BLI) of luciferase activity on administered D-luciferin (4) are popular. These techniques are useful only in superficial tissues and have extensive applications

in mice, but application to larger bodies is limited by shallow light penetration.

Several nuclear medicine approaches have been demonstrated by exploiting the action of thymidine kinase on a variety of substrates including iodo- and fluoro-nucleosides, such as FIAU and gancyclovir, and various radionuclide labels including ^{123}I , ^{124}I , ^{125}I , and ^{18}F (5, 6). For cancer, thymidine kinase has the advantage that not only does the gene serve as a reporter, but the gene products can themselves have therapeutic value. An alternative approach uses the sodium iodine symporter (hNIS), which works well with both iodide and pertechnetate substrates (7).

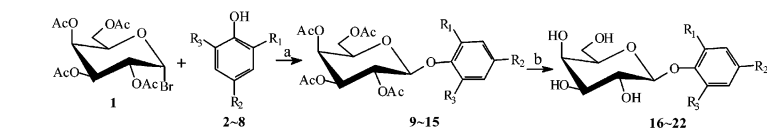
NMR has been applied to cells transfected to express melanin or transferrin resulting in iron accumulation, which produces proton MRI contrast (8, 9). ^{19}F NMR has been used to detect conversion of 5-fluorocytosine to 5-fluorouracil following introduction of cytosine deaminase (10).

Historically, the bacterial lacZ gene, encoding the enzyme β -galactosidase (β -gal, EC 3.2.1.23), has been the most popular reporter gene. The lac operon was the first gene expression system to be well characterized, some 40 years ago by Jacob and Monod (11), and it is a recognized tool for the study of problems in cell and molecular biology and the recently emerging fields of genomics and proteomics (12). Its induction has become a standard means of assaying clonal insertion and transcriptional activation (13). The long-established tests for β -gal based on colorimetric assay of *o*- and *p*-nitrophenyl- β -galactopyranoside hydrolysis to release yellow *o*- or *p*-nitrophenols remain popular (14). However, because of the broad substrate specificity of the enzyme, alternate reporter substrates have been proposed (15–19), and many are commercially available. Fluorogenic galactosides based on fluorescein and resorufin, such as *p*-naphtholbenzein, 1,2-dihydroxyanthraquinone, 4-methylumbelliferone, 5-bromo-4-chloro-3-indoxyl- β -galactopyranoside (X-Gal), and 3,4-cyclohexenoescoletin- β -galactopyranoside (S-Gal) are well established (16, 20–

[†]Presented in part at the 16th International NMR Spectroscopy Conference, Cambridge, U.K., July 2003.

* Address correspondence to this author at the Department of Radiology, The University of Texas Southwestern Medical Center at Dallas, 5323 Harry Hines Blvd., Dallas, TX 75390-9058 [telephone (214) 648-8926; fax (214) 648-2991; e-mail Ralph.Mason@UTSouthwestern.edu].

¹ Abbreviations: β -gal, β -galactosidase; BLI, bioluminescent imaging; GFP, green fluorescent protein; ONPG, *o*-nitrophenyl- β -galactopyranoside; PFONPG, 4-fluoro-2-nitrophenyl- β -D-galactopyranoside; S-Gal, 3,4-cyclohexenoescoletin- β -galactopyranoside; X-Gal, 5-bromo-4-chloro-3-indoxyl- β -galactopyranoside.



Reaction conditions: (a) $\text{CH}_2\text{Cl}_2\text{-H}_2\text{O}$, pH 8–9, 50 °C, TBAB, ~1 hr, near quantitative yield; (b) $\text{NH}_3\text{-MeOH}$, 0 °C \rightarrow r.t., 24 hr, quantitative yields.

Compounds	R ₁	R ₂	R ₃
2, 9, 16	NO ₂	F	H
3, 10, 17	F	NO ₂	H
4, 11, 18	F	H	NO ₂
5, 12, 19	F	H	H
6, 13, 20	H	F	H
7, 14, 21	Cl	F	H
8, 15, 22	Br	F	H

Figure 1. Reactions and structures of 1–22.

23). The staining methodologies described above are effective for histological specimens and in vitro, but in vivo capabilities would promise new applications to study, and clinically evaluate, gene transfection.

Recently, Louie et al. (24) demonstrated an elegant MRI assessment of β -gal activity based on 1-[2-(β -D-galactopyranosyloxy)propyl]-4,7,10-tris(carboxymethyl)-1,4,7,10-tetraazacyclododecane(gadolinium(III) (EgadMe). Access of water to the first coordination sphere of the paramagnetic Gd^{3+} is blocked by a galactopyranose bridge, but β -gal cleaves the bridge, yielding a 20% increase in relaxivity. Whereas EgadMe is a poor substrate for the enzyme (several orders of magnitude less efficient than the colorimetric biochemical agent ONPG) and does not penetrate cells, it facilitated effective investigation of cell lineage following direct intracellular microinjections (24). These studies prompted us to consider other NMR active analogues, and it appeared that introduction of a fluorine atom into the popular colorimetric biochemical indicator ONPG could produce a strong candidate molecule. Diverse fluorinated reporter molecules have been successfully applied previously to metabolic and physiological studies (25, 26). ^{19}F -labeled molecules exploit the high NMR visibility of fluorine, the great NMR sensitivity of ^{19}F to the environmental milieu, and the lack of background signal. We recently reported the successful synthesis of a prototype reporter molecule, *p*-fluoro-*o*-nitrophenyl β -D-galactopyranoside (PFONPG; 16), and demonstrated initial NMR applications (27). We have now synthesized and evaluated a series of analogues and provide structural characterization, together with evaluation of their activity in solution and in cell culture, and compare the relative merits of the substrates.

EXPERIMENTAL SECTION

General Methods. NMR spectra were recorded on Varian Inova spectrometers (400 or 600 MHz for ^1H , 100 or 150 MHz for ^{13}C) with CDCl_3 (for 9–15) or $\text{DMSO-}d_6$ (for 16–22) as solvents, and ^1H and ^{13}C chemical shifts were referenced to TMS, as internal standard. Compounds were characterized by acquisition of ^1H , ^{13}C , DEPT, ^1H – ^1H COSY, or NOESY experiments at 25 °C. ^{19}F NMR (376 MHz) measurements were performed at 25–37 °C in aqueous solution with ^{19}F signals referenced to dilute sodium trifluoroacetate (NaTFA) in a capillary, as an external standard. High-resolution mass spectra were obtained on an ABI Voyager STR MALDI-TOF mass spectrometer in reflector mode (service provided by Dr.

Tichy, Department of Chemistry, Texas A&M University).

Reactions requiring anhydrous conditions were performed under nitrogen or argon. Solutions in organic solvents were dried with anhydrous sodium sulfate and concentrated in vacuo below 45 °C. Column chromatography was performed on silica gel (200–300 mesh) with cyclohexane–EtOAc. Analytical TLC (silica gel GF₂₅₄; Aldrich Chemical Co.) used detection by UV or staining with 5% ethanolic H_2SO_4 at 110 °C for 10 min.

Although many nitrophenol glycosides have been described (28, 29) including nitrophenyl fluorogalactoside (30), to our knowledge there have been no published syntheses of the β -D-galactosides 16–22. For the construction of *O*-glycosidic linkages, many strategies are available using anhydrous zinc chloride (for the α anomer) or *p*-toluenesulfonic acid (for the β anomer), but the *p*-nitrophenyl glycosides were usually obtained in low yield (31–33).

We initially tested the method of Yoon et al. (30), which involves the reaction of a potassium salt of an acidic phenol with an α -D-galactopyranosyl bromide. Aryl β -D-galactopyranosides 16 and 17 were prepared by a nucleophilic substitution reaction of a phenolate ion on acetobromo- α -D-galactose 1 followed by saponification of the acetyl groups. We applied two different procedures for generating the phenolate ion, depending on the acidity of the phenol. The brightly colored solid potassium salts of fluoronitrophenols 2 and 3 could be isolated by lyophilizing an aqueous solution of phenol with a slight excess of aqueous KOH. The salts were subsequently used directly in excess for the synthesis of the corresponding fluoronitrophenyl tetra-*O*-acetyl β -D galactopyranosides 9 and 10. Compounds 9 and 10 were isolated pure in moderate yields (58–77%) after basic extractive workup and flash chromatography. A different strategy had to be applied for the less acidic 2-fluorophenol 5. The phenolate was generated in situ with K_2CO_3 in refluxing acetone in the presence of a catalytic amount of 18-crown-6 (34).

However, given the reported high yields, mild reaction conditions, and high stereospecificity, we ultimately explored phase-transfer catalysis for the synthesis of our desired glycosides (Figure 1) (30, 34).

Fluorophenyl β -D-Galactopyranoside Tetraacetates 9–15. *General Procedure (Figure 1).* A solution of 1 (1 mmol; 2,3,4,6-tetra-*O*-acetyl- α -D-galactopyranosyl bromide, Sigma) in CH_2Cl_2 (5 mL) was added dropwise

to a vigorously stirred solution of fluorophenol **2–8** (1.2 mmol) and tetrabutylammonium bromide (0.48 g, 1.5 mmol) in H₂O (5 mL; pH 8–9) at 50 °C in a three-neck round-bottom flask equipped with a condenser and thermometer. After TLC showed complete reaction (~1 h), the organic layer was separated, washed, dried, evaporated under reduced pressure, and recrystallized (EtOH–H₂O) or purified by column chromatography on silica gel to give fluorinated aryl β -D-galactopyranoside tetraacetates **9–15**, as white crystals.

2-Nitro-4-fluorophenyl 2,3,4,6-tetra-O-acetyl- β -D-galactopyranoside 9: 0.5 g, 99%; R_f 0.31 (3:2 cyclohexane–EtOAc); δ_H 7.55 (1H, dd, $J = 3.0, 8.4$ Hz, Ar–H), 7.42 (1H, dd, $J = 4.8, 9.0$ Hz, Ar–H), 7.27 (1H, m, Ar–H), 5.04 (1H, d, $J_{1,2} = 7.8$ Hz, H-1), 5.52 (1H, dd, $J_{2,3} = 8.4$ Hz, H-2), 5.11 (1H, dd, $J_{3,4} = 3.0$ Hz, H-3), 5.47 (1H, d, $J_{4,5} = 2.6$ Hz, H-4), 4.07 (1H, m, H-5), 4.26 (1H, dd, $J_{5,6a} = 4.2$ Hz, $J_{6a,6b} = 11.4$ Hz, H-6a), 4.17 (1H, dd, $J_{5,6b} = 5.4$ Hz, H-6b), 2.20, 2.14, 2.07, 2.02 (12H, 4s, 4 \times CH₃CO); δ_C 170.43, 170.31, 170.24, 169.62 (4 \times CH₃CO), 157.70 (d, $J_{F-C} = 164.8$ Hz, Ar–C), 145.66 (Ar–C), 141.86 (d, $J_{F-C} = 5.7$ Hz, Ar–C), 122.68 (d, $J_{F-C} = 4.9$ Hz, Ar–C), 120.77 (d, $J_{F-C} = 15.2$ Hz, Ar–C), 112.60 (d, $J_{F-C} = 18.3$ Hz, Ar–C), 101.40 (C-1), 68.01 (C-2), 70.63 (C-3), 66.86 (C-4), 71.58 (C-5), 61.45 (C-6), 21.25, 21.10, 20.38, 20.25 (4 \times CH₃CO); HRMS, [M + Na]⁺, C₂₀H₂₂NO₁₂FNa, calcd 510.1024, found 510.1014; [M + K]⁺, C₂₀H₂₂NO₁₂-FK, calcd 526.0763, found 526.0751.

2-Fluoro-4-nitrophenyl 2,3,4,6-tetra-O-acetyl- β -D-galactopyranoside 10: 0.5 g, 99%; R_f 0.35 (3:2 cyclohexane–EtOAc); δ_H 8.03 (2H, m, Ar–H), 7.32 (1H, m, Ar–H), 5.13 (1H, d, $J_{1,2} = 7.8$ Hz, H-1), 5.58 (1H, dd, $J_{2,3} = 10.2$ Hz, H-2), 5.15 (1H, dd, $J_{3,4} = 3.6$ Hz, H-3), 5.40 (1H, dd, $J_{4,5} = 3.6$ Hz, H-4), 4.10 (1H, ddd, $J_{5,6a} = 4.5$ Hz, $J_{5,6b} = 5.0$ Hz, H-5), 4.26 (1H, dd, $J_{6a,6b} = 11.0$ Hz, H-6a), 4.19 (1H, dd, H-6b), 2.21, 2.11, 2.08, 2.04 (12H, 4s, 4 \times CH₃CO); δ_C 170.45, 170.26, 170.21, 169.44 (4 \times CH₃CO), 152.23 (d, $J_{F-C} = 252.0$ Hz, Ar–C), 150.07 (d, $J_{F-C} = 10.6$ Hz, Ar–C), 120.51 (d, $J_{F-C} = 9.2$ Hz, Ar–C), 118.53 (d, $J_{F-C} = 11.7$ Hz, Ar–C), 113.11 (d, $J_{F-C} = 23.7$ Hz, Ar–C), 100.28 (d, $J_{F-C} = 3.1$ Hz, C-1), 68.34 (C-2), 70.57 (C-3), 66.81 (C-4), 71.83 (C-5), 61.45 (C-6), 20.80, 20.77, 20.72, 20.33 (4 \times CH₃CO); HRMS, [M + Na]⁺, C₂₀H₂₂NO₁₂FNa, calcd 510.1010, found 510.1014; [M + K]⁺, C₂₀H₂₂NO₁₂-FK, calcd 526.0763, found 526.0751.

2-Nitro-6-fluorophenyl 2,3,4,6-tetra-O-acetyl- β -D-galactopyranoside 11: 0.49 g, 98%; R_f 0.30 (3:2 cyclohexane–EtOAc); δ_H 7.58 (1H, ddd, $J = 1.2, 1.4, 8.8$ Hz, Ar–H), 7.39 (1H, ddd, $J = 1.8, 8.4, 9.8$ Hz, Ar–H), 7.29 (1H, m, Ar–H), 5.02 (1H, d, $J_{1,2} = 8.0$ Hz, H-1), 5.48 (1H, dd, $J_{2,3} = 10.4$ Hz, H-2), 5.08 (1H, dd, $J_{3,4} = 5.4$ Hz, H-3), 5.41 (1H, dd, $J_{4,5} = 3.6$ Hz, H-4), 3.90 (1H, m, H-5), 4.11 (1H, dd, $J_{5,6a} = 7.8$ Hz, $J_{6a,6b} = 10.2$ Hz, H-6a), 4.08 (1H, dd, $J_{5,6b} = 7.2$ Hz, H-6b), 2.20, 2.14, 2.01, 2.00 (12H, 4s, 4 \times CH₃CO); δ_C 170.45, 170.19, 169.61 (4 \times CH₃CO), 155.84 (d, $J_{F-C} = 251.8$ Hz, Ar–C), 146.01 (Ar–C), 137.17 (d, $J_{F-C} = 15.3$ Hz, Ar–C), 125.66 (d, $J_{F-C} = 7.6$ Hz, Ar–C), 121.11 (d, $J_{F-C} = 20.6$ Hz, Ar–C), 120.22 (d, $J_{F-C} = 3.8$ Hz, Ar–C), 102.84 (d, $J_{F-C} = 2.3$ Hz, C-1), 68.75 (C-2), 70.76 (C-3), 66.74 (C-4), 71.41 (C-5), 61.02 (C-6), 20.82, 20.79, 20.70, 20.66 (4 \times CH₃CO); HRMS, [M + Na]⁺, C₂₀H₂₂NO₁₂FNa, calcd 510.1024, found 510.1011; [M + K]⁺, C₂₀H₂₂NO₁₂-FK, calcd 526.0763, found 526.0750.

2-Fluorophenyl 2,3,4,6-tetra-O-acetyl- β -D-galactopyranoside 12: 0.45 g, 98%; R_f 0.40 (3:2 cyclohexane–EtOAc); δ_H 7.48 (1H, dd, $J = 2.0, 10$ Hz, Ar–H), 7.36 (1H, m, Ar–H), 7.30 (1H, m, Ar–H), 7.22 (1H, m, Ar–H), 5.54 (1H, d, $J_{1,2} = 8.4$ Hz, H-1), 5.48 (1H, dd, $J_{2,3} = 10.0$ Hz, H-2), 5.09 (1H, dd, $J_{3,4} = 4.4$ Hz, H-3), 5.40 (1H, d, $J_{4,5} = 3.0$

Hz, H-4), 4.24 (1H, m, H-5), 4.18 (1H, dd, $J_{5,6a} = 7.5$ Hz, $J_{6a,6b} = 10.4$ Hz, H-6a), 4.08 (1H, dd, $J_{5,6b} = 7.0$ Hz, H-6b), 2.19, 2.10, 2.04, 2.02 (12H, 4s, 4 \times CH₃CO); δ_C 170.66, 170.23, 170.10, 169.58 (4 \times CH₃CO), 156.14 (Ar–C), 146.01 (d, $J_{F-C} = 245.9$ Hz, Ar–C), 136.58 (d, $J_{F-C} = 14.8$ Hz, Ar–C), 126.08 (d, $J_{F-C} = 7.9$ Hz, Ar–C), 122.33 (d, $J_{F-C} = 26.3$ Hz, Ar–C), 121.33 (d, $J_{F-C} = 6.8$ Hz, Ar–C), 101.89 (d, $J_{F-C} = 2.6$ Hz, C-1), 68.85 (C-2), 70.58 (C-3), 66.79 (C-4), 71.56 (C-5), 61.33 (C-6), 20.77, 20.70, 20.60, 20.58 (4 \times CH₃CO); HRMS, [M + Na]⁺, C₂₀H₂₃NO₁₀FNa, calcd 465.1173, found 465.1169; [M + K]⁺, C₂₀H₂₃NO₁₀-FK, calcd 481.0912, found 481.0907.

4-Fluorophenyl 2,3,4,6-tetra-O-acetyl- β -D-galactopyranoside 13: 0.42 g, 95%; R_f 0.45 (3:2 cyclohexane–EtOAc); δ_H 6.99 (4H, m, Ar–H), 4.98 (1H, d, $J_{1,2} = 8.0$ Hz, H-1), 5.48 (1H, dd, $J_{2,3} = 10.0$ Hz, H-2), 5.11 (1H, dd, $J_{3,4} = 4.2$ Hz, H-3), 5.45 (1H, d, $J_{4,5} = 2.4$ Hz, H-4), 4.06 (1H, m, H-5), 4.24 (1H, dd, $J_{5,6a} = 7.2$ Hz, $J_{6a,6b} = 10.4$ Hz, H-6a), 4.16 (1H, dd, $J_{5,6b} = 6.4$ Hz, H-6b), 2.19, 2.09, 2.06, 2.02 (12H, 4s, 4 \times CH₃CO); δ_C 170.45, 170.36, 170.28, 169.48 (4 \times CH₃CO), 160.08 (Ar–C), 157.69 (Ar–C), 153.10 (d, $J_{F-C} = 20.0$ Hz, Ar–C), 118.82–115.97 (m, Ar–C), 100.62 (C-1), 68.68 (C-2), 70.71 (C-3), 66.90 (C-4), 71.06 (C-5), 61.44 (C-6), 20.79, 20.72, 20.68, 20.64 (4 \times CH₃CO); HRMS, [M + Na]⁺, C₂₀H₂₃NO₁₀FNa, calcd 465.1173, found 465.1170; [M + K]⁺, C₂₀H₂₃NO₁₀-FK, calcd 481.0912, found 481.1014.

2-Bromo-4-fluorophenyl 2,3,4,6-tetra-O-acetyl- β -D-galactopyranoside 14: 0.50 g, 97%; R_f 0.48 (3:2 cyclohexane–EtOAc); δ_H 7.28 (1H, ddd, $J = 3.2, 2.8, 3.2$ Hz, Ar–H), 7.16 (1H, dd, $J = 4.8, 9.2$ Hz, Ar–H), 6.97 (1H, m, Ar–H), 4.91 (1H, d, $J_{1,2} = 8.0$ Hz, H-1), 5.56 (1H, dd, $J_{2,3} = 10.8$ Hz, H-2), 5.10 (1H, dd, $J_{3,4} = 3.6$ Hz, H-3), 5.46 (1H, d, $J_{4,5} = 4.0$ Hz, H-4), 4.24 (1H, m, H-5), 4.25 (1H, dd, $J_{5,6a} = 7.2$ Hz, $J_{6a,6b} = 11.4$ Hz, H-6a), 4.08 (1H, dd, $J_{5,6b} = 6.0$ Hz, H-6b), 2.19, 2.11, 2.06, 2.02 (12H, 4s, 4 \times CH₃CO); δ_C 170.52, 170.43, 170.34, 169.57 (4 \times CH₃CO), 159.80 (Ar–C), 157.35 (Ar–C), 150.22 (Ar–C), 120.91–13.93 (m, Ar–C), 101.36 (C-1), 68.33 (C-2), 70.66 (C-3), 67.03 (C-4), 71.49 (C-5), 61.51 (C-6), 21.28, 21.15, 21.10, 20.91 (4 \times CH₃CO); HRMS, [M + Na]⁺, C₂₀H₂₂O₁₀F⁷⁹BrNa, calcd 543.0279, found 543.0266; C₂₀H₂₂O₁₀F⁸¹BrNa, calcd 545.0259, found 545.0205; [M + K]⁺, C₂₀H₂₂O₁₀F⁷⁹-BrK, calcd 559.0043, found 559.0043; C₂₀H₂₂O₁₀F⁸¹BrNa, calcd 560.9997, found 560.9892.

2-Chloro-4-fluorophenyl 2,3,4,6-tetra-O-acetyl- β -D-galactopyranoside 15: 0.48 g, 99%; R_f 0.46 (3:2 cyclohexane–EtOAc); δ_H 7.21 (1H, dd, $J = 4.8, 8.8$ Hz, Ar–H), 7.13 (1H, dd, $J = 3.2, 8.0$ Hz, Ar–H), 6.92 (1H, m, Ar–H), 4.90 (1H, d, $J_{1,2} = 8.0$ Hz, H-1), 5.54 (1H, dd, $J_{2,3} = 10.8$ Hz, H-2), 5.12 (1H, dd, $J_{3,4} = 3.2$ Hz, H-3), 5.46 (1H, d, $J_{4,5} = 3.6$ Hz, H-4), 4.04 (1H, m, H-5), 4.26 (1H, dd, $J_{5,6a} = 6.8$ Hz, $J_{6a,6b} = 11.4$ Hz, H-6a), 4.16 (1H, dd, $J_{5,6b} = 6.4$ Hz, H-6b), 2.19, 2.11, 2.06, 2.02 (12H, 4s, 4 \times CH₃CO); δ_C 170.40, 170.32, 170.21, 169.49 (4 \times CH₃CO), 159.72 (Ar–C), 157.25 (Ar–C), 149.14 (d, $J_{F-C} = 3.1$ Hz, Ar–C), 125.55 (d, $J_{F-C} = 9.9$ Hz, Ar–C), 120.62–114.34 (m, Ar–C), 101.46 (C-1), 68.29 (C-2), 70.51 (C-3), 66.97 (C-4), 71.38 (C-5), 61.40 (C-6), 20.99, 20.87, 20.77, 20.66 (4 \times CH₃CO); HRMS, [M + Na]⁺, C₂₀H₂₂O₁₀F³⁵ClNa, calcd 499.0783, found 499.0761; C₂₀H₂₂O₁₀F³⁷ClNa, calcd 501.0754, found 501.0701; [M + K]⁺, C₂₀H₂₂O₁₀F³⁵ClK, calcd 515.0523, found 515.0495; C₂₀H₂₂O₁₀F³⁷ClK, calcd 517.0494, found 517.0488.

Fluoroaryl β -D-Galactopyranosides 16–22. General Procedure. A solution of fluorophenyl 2,3,4,6-tetra-O-acetyl- β -D-galactopyranoside (**9–15**) (0.4 g) in anhydrous MeOH (15 mL) containing 0.5 M NH₃ was vigorously stirred from 0 °C to room temperature overnight until

TLC showed complete reaction. Following solvent removal in vacuo, chromatography on silica gel (EtOAc/MeOH) afforded the free galactopyranosides **16–22** in nearly quantitative yield, as white crystalline materials.

2-Nitro-4-fluorophenyl β -D-galactopyranoside 16: R_f 0.40 (1:9 MeOH–EtOAc); δ_H 7.84 (1H, dd, $J = 2.8, 8.0$ Hz, Ar–H), 7.53 (1H, ddd, $J = 1.6, 1.0, 2.8$ Hz, Ar–H), 7.43 (1H, dd, $J = 4.4, 9.2$ Hz, Ar–H), 4.96 (1H, d, $J_{1,2} = 7.6$ Hz, H-1), 3.60 (1H, dd, $J_{2,3} = 10.6$ Hz, H-2), 3.51 (1H, dd, $J_{3,4} = 5.2$ Hz, H-3), 3.47 (1H, d, $J_{4,5} = 5.6$ Hz, H-4), 3.43 (1H, m, H-5), 3.67 (2H, m, H-6), 5.16 (1H, d, $J_{H-2,OH-2} = 5.2$ Hz, HO-2), 4.67 (1H, d, $J_{H-3,OH-3} = 4.4$ Hz, HO-3), 4.90 (1H, d, $J_{H-4,OH-4} = 6.0$ Hz, HO-4), 4.67 (1H, t, $J_{H-6,OH-6} = 5.2, 5.4$ Hz, HO-6); δ_C 155.41 (d, $J_{F-C} = 239.6$ Hz, Ar–C), 146.19 (d, $J_{F-C} = 3.1$ Hz, Ar–C), 140.17 (d, $J_{F-C} = 9.1$ Hz, Ar–C), 120.91 (d, $J_{F-C} = 22.1$ Hz, Ar–C), 119.03 (d, $J_{F-C} = 7.7$ Hz, Ar–C), 111.89 (d, $J_{F-C} = 27.5$ Hz, Ar–C), 101.65 (C-1), 70.07 (C-2), 73.37 (C-3), 68.06 (C-4), 75.87 (C-5), 60.33 (C-6); HRMS, $[M + Na]^+$, $C_{12}H_{14}NO_8FNa$, calcd 342.0601, found 342.0589; $[M + K]^+$, $C_{12}H_{14}NO_8FK$, calcd 358.0341, found 358.0328.

2-Fluorine-4-nitrophenyl β -D-galactopyranoside 17: R_f 0.45 (1:9 MeOH–EtOAc); δ_H 7.58 (1H, dd, $J = 3.3, 8.0$ Hz, Ar–H), 7.42 (1H, dd, $J = 4.2, 8.7$ Hz, Ar–H), 7.28 (1H, m, Ar–H), 5.16 (1H, d, $J_{1,2} = 7.8$ Hz, H-1), 4.60 (1H, dd, $J_{2,3} = 8.8$ Hz, H-2), 3.70 (1H, dd, $J_{3,4} = 3.2$ Hz, H-3), 3.63 (1H, d, $J_{4,5} = 3.1$ Hz, H-4), 3.60 (1H, m, H-5), 3.50 (2H, m, H-6), 4.98 (1H, d, $J_{H-2,OH-2} = 7.2$ Hz, HO-2), 4.66 (1H, d, $J_{H-3,OH-3} = 4.0$ Hz, HO-3), 4.80 (1H, d, $J_{H-4,OH-4} = 5.0$ Hz, HO-4), 4.90 (1H, t, $J_{H-6,OH-6} = 5.5, 5.8$ Hz, HO-6); δ_C 156.80 (d, $J = 160.4$ Hz, Ar–C), 146.55 (Ar–C), 140.68 (d, $J = 5.5$ Hz, Ar–C), 123.44 (d, $J = 4.2$ Hz, Ar–C), 121.33 (d, $J = 18.2$ Hz, Ar–C), 114.80 (d, $J = 17.9$ Hz, Ar–C), 101.73 (C-1), 68.33 (C-2), 70.86 (C-3), 66.90 (C-4), 71.47 (C-5), 61.77 (C-6); HRMS, $[M + Na]^+$, $C_{12}H_{14}NO_8FNa$, calcd 342.0601, found 342.0585; $[M + K]^+$, $C_{12}H_{14}NO_8FK$, calcd 358.0341, found 358.0320.

2-Nitro-6-fluorophenyl β -D-galactopyranoside 18A: R_f 0.40 (1:9 MeOH–EtOAc); δ_H 7.73 (1H, ddd, $J = 1.6, 3.2, 8.4$ Hz, Ar–H), 7.63 (1H, ddd, $J_{HH} = 1.2, 4.0, 8.4$ Hz, $J_{HF} = 19.2$ Hz, Ar–H), 7.46 (1H, ddd, $J_{HH} = 5.2, 8.4$ Hz, $J_{HF} = 16.8$ Hz, Ar–H), 5.00 (1H, d, $J_{1,2} = 7.6$ Hz, H-1), 3.88 (1H, dd, $J_{2,3} = 9.2$ Hz, H-2), 3.82 (1H, dd, $J_{3,4} = 4.0$ Hz, H-3), 3.70 (1H, dd, $J_{4,5} = 3.2$ Hz, H-4), 3.66 (1H, m, H-5), 4.00 (2H, m, H-6), 3.80 (1H, d, $J_{H-2,OH-2} = 4.2$ Hz, HO-2), 3.69 (1H, d, $J_{H-3,OH-3} = 3.0$ Hz, HO-3), 3.86 (1H, d, $J_{H-4,OH-4} = 1.6$ Hz, HO-4), 3.62 (1H, dd, $J_{H-6,OH-6} = 4.6, 5.0$ Hz, HO-6); δ_C 156.66 (d, $J_{F-C} = 246.2$ Hz, Ar–C), 145.78 (Ar–C), 138.54 (d, $J_{F-C} = 12.2$ Hz, Ar–C), 125.83 (d, $J_{F-C} = 8.4$ Hz, Ar–C), 121.65 (d, $J_{F-C} = 19.9$ Hz, Ar–C), 120.80 (d, $J_{F-C} = 3.8$ Hz, Ar–C), 106.06 (d, $J_{F-C} = 3.8$ Hz, C-1), 70.59 (C-2), 74.48 (C-3), 69.30 (C-4), 77.00 (C-5), 61.73 (C-6); HRMS, $[M + Na]^+$, $C_{12}H_{14}NO_8FNa$, calcd 342.0601, found 342.0599; $[M + K]^+$, $C_{12}H_{14}NO_8FK$, calcd 358.0341, found 358.0337.

2-Nitro-6-fluorophenyl α -D-galactopyranoside 18B: R_f 0.47 (1:9 MeOH–EtOAc); δ_H 7.76 (1H, ddd, $J = 1.6, 2.8, 8.4$ Hz, Ar–H), 7.62 (1H, ddd, $J_{HH} = 0.4, 4.8, 8.4$ Hz, $J_{HF} = 12.0$ Hz, Ar–H), 7.40 (1H, ddd, $J_{HH} = 4.8, 8.4$ Hz, $J_{HF} = 13.2$ Hz, Ar–H), 5.85 (1H, d, $J_{1,2} = 3.2$ Hz, H-1), 4.01 (1H, dd, $J_{2,3} = 8.9$ Hz, H-2), 4.03 (1H, dd, $J_{3,4} = 3.6$ Hz, H-3), 4.11 (1H, dd, $J_{4,5} = 3.6$ Hz, H-4), 3.74 (1H, m, H-5), 3.63 (2H, m, H-6), 3.92 (1H, d, $J_{H-2,OH-2} = 3.2$ Hz, HO-2), 3.74 (1H, d, $J_{H-3,OH-3} = 3.6$ Hz, HO-3), 3.83 (1H, d, $J_{H-4,OH-4} = 2.0$ Hz, HO-4), 3.80 (1H, t, $J_{H-6,OH-6} = 5.6, 6.0$ Hz, HO-6); δ_C 157.06 (d, $J_{F-C} = 248.7$ Hz, Ar–C), 146.05 (Ar–C), 139.20 (d, $J_{F-C} = 13.8$ Hz, Ar–C), 124.59 (d, $J_{F-C} = 8.4$ Hz, Ar–C), 122.05 (d, $J_{F-C} = 19.9$ Hz, Ar–C), 121.37 (d, $J_{F-C} = 3.0$ Hz, Ar–C), 104.14 (d, $J_{F-C} =$

7.6 Hz, C-1), 70.23 (C-2), 70.59 (C-3), 69.94 (C-4), 74.21 (C-5), 62.03 (C-6); HRMS, $[M + Na]^+$, $C_{12}H_{14}NO_8FNa$, calcd 342.0601, found 342.0590; $[M + K]^+$, $C_{12}H_{14}NO_8FK$, calcd 358.0341, found 358.0333.

2-Fluorophenyl β -D-galactopyranoside 19: R_f 0.48 (1:9 MeOH–EtOAc); δ_H 7.26 (1H, m, Ar–H), 7.21 (1H, ddd, $J = 1.2, 3.6, 8.0$ Hz, Ar–H), 7.11 (1H, ddd, $J_{HH} = 1.2, 7.2, J_{HF} = 14.4$ Hz, Ar–H), 6.98 (1H, m, Ar–H), 4.91 (1H, d, $J_{1,2} = 7.6$ Hz, H-1), 3.41 (1H, dd, $J_{2,3} = 9.6$ Hz, H-2), 3.47 (1H, dd, $J_{3,4} = 4.0$ Hz, H-3), 3.71 (1H, d, $J_{4,5} = 3.2$ Hz, H-4), 3.54 (1H, m, H-5), 3.60 (2H, m, H-6), 3.58 (1H, d, $J_{H-2,OH-2} = 4.0$ Hz, HO-2), 3.48 (1H, d, $J_{H-3,OH-3} = 3.1$ Hz, HO-3), 3.57 (1H, d, $J_{H-4,OH-4} = 2.2$ Hz, HO-4), 3.54 (1H, t, $J_{H-6,OH-6} = 4.0, 5.2$ Hz, HO-6); δ_C 152.28 (d, $J_{F-C} = 242.7$ Hz, Ar–C), 145.50 (d, $J_{F-C} = 9.9$ Hz, Ar–C), 125.10 (d, $J_{F-C} = 3.8$ Hz, Ar–C), 122.60 (d, $J_{F-C} = 6.9$ Hz, Ar–C), 117.73 (Ar–C), 116.66 (d, $J_{F-C} = 18.3$ Hz, Ar–C), 101.53 (C-1), 70.59 (C-2), 73.81 (C-3), 68.52 (C-4), 76.04 (C-5), 60.74 (C-6); HRMS, $[M + Na]^+$, $C_{12}H_{15}O_6FNa$, calcd 297.0750, found 297.0739; $[M + K]^+$, $C_{12}H_{15}O_6FK$, calcd 313.0490, found 313.0486.

4-Fluorophenyl β -D-galactopyranoside 20: R_f 0.40 (1:9 MeOH–EtOAc); δ_H 7.14–7.03 (4H, m, Ar–H), 4.74 (1H, d, $J_{1,2} = 7.6$ Hz, H-1), 3.54 (1H, dd, $J_{2,3} = 10.6$ Hz, H-2), 3.50 (1H, dd, $J_{3,4} = 3.6$ Hz, H-3), 3.72 (1H, d, $J_{4,5} = 3.2$ Hz, H-4), 3.43 (1H, m, H-5), 3.58 (2H, m, H-6), 5.30–4.4 (4H, br, HO-2,3,4,6); δ_C 157.25 (d, $J_{F-C} = 235$ Hz, Ar–C), 153.98 (Ar–C), 117.93–115.69 (Ar–C), 101.88 (C-1), 70.40 (C-2), 73.32 (C-3), 68.30 (C-4), 75.60 (C-5), 60.46 (C-6); HRMS, $[M + Na]^+$, $C_{12}H_{15}O_6FNa$, calcd 297.0750, found 297.0731.

2-Bromo-4-fluorophenyl β -D-galactopyranoside 21: R_f 0.52 (1:9 MeOH–EtOAc); δ_H 7.54 (1H, dd, $J = 2.4, 8.0$ Hz, Ar–H), 7.22 (2H, m, Ar–H), 4.90 (1H, d, $J_{1,2} = 7.6$ Hz, H-1), 3.41 (1H, dd, $J_{2,3} = 9.6$ Hz, H-2), 3.47 (1H, dd, $J_{3,4} = 4.0$ Hz, H-3), 3.71 (1H, d, $J_{4,5} = 3.2$ Hz, H-4), 3.54 (1H, m, H-5), 3.60 (2H, m, H-6), 5.11 (1H, d, $J_{H-2,OH-2} = 5.6$ Hz, HO-2), 4.58 (1H, d, $J_{H-3,OH-3} = 4.8$ Hz, HO-3), 4.89 (1H, d, $J_{H-4,OH-4} = 5.2$ Hz, HO-4), 4.67 (1H, t, $J_{H-6,OH-6} = 5.2, 5.2$ Hz, HO-6); δ_C 157.38 (d, $J_{F-C} = 240.4$ Hz, Ar–C), 151.09 (Ar–C), 120.79–121.32 (m, Ar–C), 101.96 (C-1), 70.87 (C-2), 73.78 (C-3), 68.84 (C-4), 76.13 (C-5), 61.13 (C-6); HRMS, $[M + Na]^+$, $C_{12}H_{14}O_6F^{79}BrNa$, calcd 374.9855, found 374.9851; $C_{12}H_{14}O_6F^{81}BrNa$, calcd 376.9835, found 376.9665; $[M + K]^+$, $C_{12}H_{14}O_6F^{79}BrK$, calcd 390.9595, found 390.9803; $C_{12}H_{14}O_6F^{81}BrK$, calcd 392.9575, found 392.9687.

2-Chloro-4-fluorophenyl β -D-galactopyranoside 22: R_f 0.45 (1:9 MeOH–EtOAc); δ_H 7.42 (1H, dd, $J = 2.8, 8.4$ Hz, Ar–H), 7.28 (1H, dd, $J = 5.2, 9.6$ Hz, Ar–H), 7.17 (1H, m, Ar–H), 4.90 (1H, d, $J_{1,2} = 7.6$ Hz, H-1), 3.57 (1H, dd, $J_{2,3} = 11.6$ Hz, H-2), 3.52 (1H, dd, $J_{3,4} = 5.2$ Hz, H-3), 3.72 (1H, m, H-4), 3.17 (1H, m, H-5), 3.60 (1H, dd, $J_{5,6a} = 8.8$ Hz, $J_{6a,6b} = 12.4$ Hz, H-6a), 3.45 (1H, dd, $J_{5,6b} = 6.0$ Hz, H-6b), 5.17 (1H, d, $J_{H-2,OH-2} = 4.0$ Hz, HO-2), 4.59 (1H, d, $J_{H-3,OH-3} = 3.2$ Hz, HO-3), 4.89 (1H, d, $J_{H-4,OH-4} = 7.0$ Hz, HO-4), 4.69 (1H, br, HO-6); δ_C 156.38 (d, $J_{F-C} = 238.80$ Hz, Ar–C), 149.62 (Ar–C), 122.55 (d, $J_{F-C} = 10.7$ Hz, Ar–C), 117.45–114.54 (m, Ar–C), 101.45 (C-1), 70.25 (C-2), 73.47 (C-3), 68.23 (C-4), 75.75 (C-5), 60.39 (C-6); HRMS, $[M + Na]^+$, $C_{12}H_{14}O_6F^{35}ClNa$, calcd 331.0361, found 331.0349; $C_{12}H_{14}O_6F^{37}ClNa$, calcd 333.0331, found 333.0249.

Kinetic Experiments. Relative substrate efficacies of **16–22** were compared using ^{19}F NMR. Enzyme reactions were conducted at 37 °C in PBS (0.1 M, pH 7.4) using β -gal (E801A, Promega, Madison, WI). Fluorophenyl β -D-galactopyranosides **16–22** (15 mmol) were dissolved in PBS (600 μ L, pH 7.4) and β -gal (20 μ L, 1 unit/

μL E801A in PBS) was added, followed by immediate ^{19}F NMR data acquisition at 37°C with subsequent spectra every 101 s providing a kinetic curve over 51 min.

Substrate efficacy relative to traditional indicators was assessed by spectrophotometry. PFONPG **16** and ONPG (2.5 $\mu\text{mol/mL}$), respectively, were dissolved in buffer (pH 4.5, 10 mM sodium hydrogen phosphate, 5 mM citric acid). A solution of β -gal [G5160 from *Aspergillus oryzae* (Aldrich), 95 μg in 10 μL of buffer] was added and the absorption ($\lambda = 420\text{ nm}$) measured every 30 s for 10 min at room temperature.

Cell Culture and Cell Proliferation Assay. Dunning R3327-MAT-Lu rat prostate cancer cells (isolated for growth in culture by us from solid tumor tissues originally provided by Dr. Peter Peschke of the DKFZ, Heidelberg, Germany) and MTLn3 rat breast cancer cells (ATCC, Manassas, VA) were maintained in RPMI-1640 medium supplemented with 100 units/mL penicillin, 100 $\mu\text{g/mL}$ streptomycin, and 10% fetal bovine serum (FBS) at 37°C , with 5% CO_2 and 95% humidified air. Using TransFast transfection reagent (Promega), MAT-Lu and MTLn3 cells were cotransfected with pCMV β (Clontech, Palo Alto, CA) comprising the *Escherichia coli lacZ* gene located under the human cytomegalovirus (CMV) immediate-early enhancer/promoter region and pCI-neo (Promega) carrying the neomycin phosphotransferase gene and were selected in growth medium containing 400 $\mu\text{g/mL}$ G418 (Cellgro, Merndon, VA). Cells were harvested, trypsinized and resuspended in PBS, pH 7.4. **17** (1.9 mg, 100 μL) was added to cell suspension in PBS (10^8 cells in 600 μL), and ^{19}F NMR spectra were acquired immediately at 37°C and again at various times up to 72 h. The β -gal activity of MAT-Lu-LacZ cells was 196 milliunits/ 10^7 cells and that for MTLn3-LacZ cells, 67 milliunits/ 10^7 cells.

The toxicity of aglycons and conjugates was assessed in both wild-type and LacZ-transfected MAT-Lu cells using a colorimetric CellTiter 96 Aqueous Nonradioactive MTS Cell Proliferation Assay (Promega). Assays were performed in triplicate using 24-well plates seeded with 10^3 cells per well in 500 μL of RPMI-1640 without phenol red and supplemented with 10% FCS and 2 mM glutamine. After 24 h of incubation, the medium was replaced with fresh medium. To determine IC_{50} , cells were incubated (72 h) with molecules **2–8** (0–1.6 mM) and **16–22** (0–4.5 mM), followed by the MTS assay. In each case successive dilutions were 2-fold. In some cases maximum tested doses were lower because some molecules showed poor solubility.

RESULTS

The methodology presented by Yoon et al. (30) to synthesize phenyl fluorogalactoside tetraacetates using potassium salts of the phenol produced mediocre yields for the fluorophenyl analogues **9** and **10**. By contrast, the phase-transfer approach using TBAB produced fluorophenyl β -D-galactopyranoside tetraacetates **9–15** in nearly quantitative yields. The anomeric β -D-configuration of compounds **9–15** in the $^4\text{C}_1$ chair conformation was unambiguously established on the basis of the observed ^1H NMR chemical shifts (δ_{H} 5.00–5.25) of the anomeric protons and the $J_{1,2}$ ($J \sim 8\text{ Hz}$) and $J_{2,3}$ ($J \sim 10\text{ Hz}$) coupling constants (34). The signals of the ^{13}C NMR spectra of **9–15** were assigned by comparison with the chemical shifts of *p*-nitrophenyl β -D-galactopyranoside (30). As expected, the anomeric carbon resonances appeared at $\sim 100\text{ ppm}$ in accord with the β -D-configuration.

Deacetylation of **9–15** gave the free galactopyranosides **16–22** in nearly quantitative yields. ^1H NMR spectra of

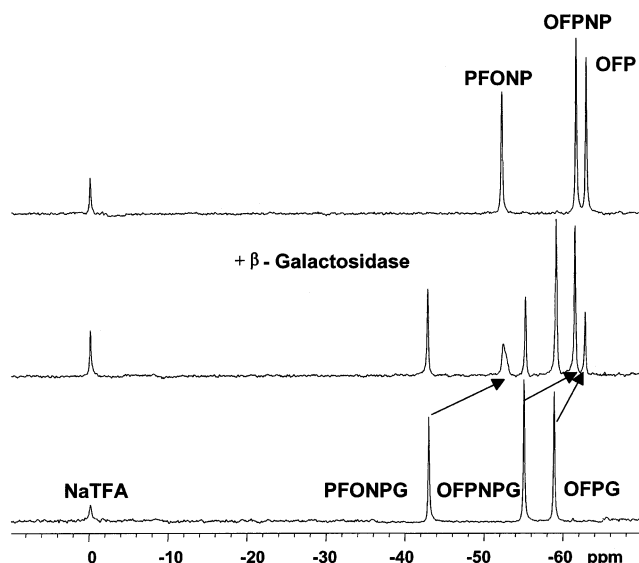


Figure 2. ^{19}F NMR spectra of β -D-galactopyranosides **16** (PFONPG), **17** (OFPNPG), and **19** (OFPNG) in PBS at 37°C (a) and following addition of β -gal [2 min (b) and 34 min (c)].

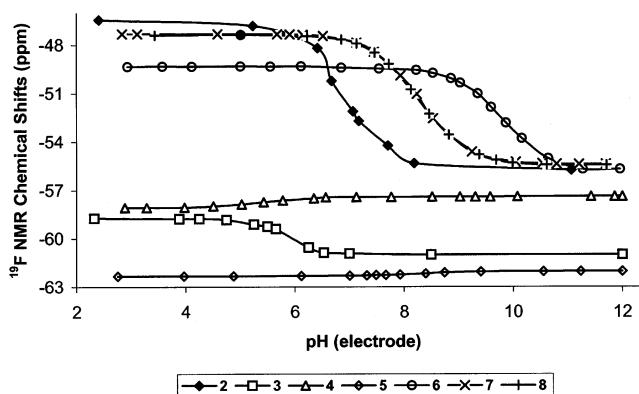


Figure 3. ^{19}F NMR chemical shift pH titration curves of **2–8** in saline at 25°C .

16–22 were assigned by ^1H – ^1H COSY spectra and D_2O exchange. The ^1H NMR chemical shifts (δ_{H} 4.91–5.85) of the anomeric protons and the coupling constants ($J_{1,2} \sim 8\text{ Hz}$; $J_{2,3} \sim 10\text{ Hz}$) showed that the free galactopyranosides **16–22** (except **18**) retained the anomeric β -D-configuration with the $^4\text{C}_1$ chair conformation. The synthesis of **18** was more complex with the isolation of two distinct and separable isomers **18A** and **18B** in a 1:1 ratio, which also gave distinct ^{19}F NMR spectra. The downfield shifts of **18B** $\delta_{\text{H}1}$ at 5.85 with $J_{1,2} = 3.2\text{ Hz}$ and δ_{C} at 104.14 compared to those of **18A** at 5.00 ppm with $J_{1,2} = 7.6\text{ Hz}$ and δ_{C} at 106.06 suggest α and β isomers, respectively (35–38). Further evidence supporting the structural assignment of **18B** is that the α anomer resists activity of β -gal (Figure 4). Epimerization likely occurs during removal of the acetyl groups, possibly via a carbocation pathway due to the excellent leaving group ability of the 2-fluoro-6-nitrophenol anion group.

All except **18A** were stable in saline (0.9%), PBS (0.1 M), and fresh whole rabbit blood, at 25 and 37°C , for extended periods showing no breakdown by ^{19}F NMR even after 1 week. **18A** hydrolyzed completely within 2 h in 0.1 M PBS buffer solution (pH 7.4) at 25°C . By contrast, **18B** was stable even at 60 or 100°C . As expected, the more polar substituted phenyl β -D-galactopyranosides **16–18** were most soluble and **19–21** quite

Table 1. ^{19}F Chemical Shifts (Parts per Million) of **16**–**22** before and after Hydrolysis by β -gal^a

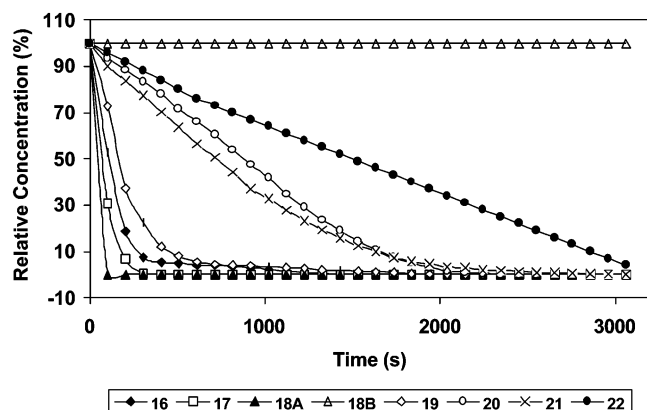
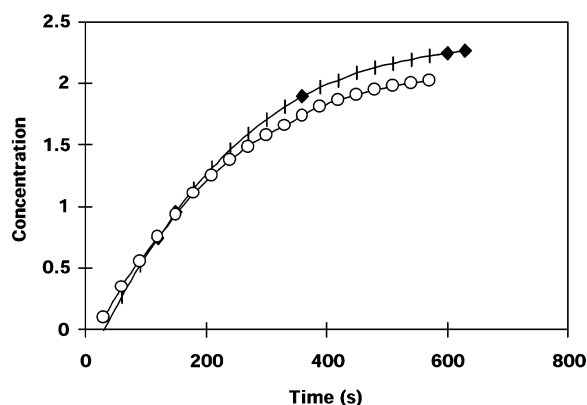
	compound							
	16	17	18A	18B	19	20	21	22
$\delta_{\text{F}}(\text{substrate})$	−42.87	−54.93	−50.67	−49.37	−58.74	−45.87	−43.56	−43.82
$\delta_{\text{F}}(\text{product})$	−52.71	−61.04	−58.67	−58.67	−62.30	−49.59	−48.13	−48.24
observed $\Delta\delta_{\text{F}}$	9.84	6.11	8.00	9.30	3.56	3.72	4.57	4.42
min $\Delta\delta_{\text{F}}$	1.57	3.84	6.72	8.7	3.3	3.46	3.76	3.58
max $\Delta\delta_{\text{F}}$	12.89	6.11	8.1	9.4	3.59	11.85	11.84	11.63

^a β -gal (E801A, 20 units at 37 °C in 0.1 M PBS, pH 7.4).**Table 2.** ^{19}F NMR pH Characterization of Aglycons at 25 °C

	compound							
	2	3	4	5	6	7	8	
pK_{a}	6.87	6.03	5.44	8.33	9.80	8.31	8.28	
$\delta_{\text{(acid)}}$	−46.44	−58.77	−58.07	−62.33	−49.33	−47.32	−47.40	
$\delta_{\text{(base)}}$	−55.76	−61.01	−57.39	−62.04	−57.72	−55.40	−55.45	
$\Delta\delta$	9.3	2.24	0.68	0.29	6.39	8.08	8.05	

soluble in water, buffer, and whole blood, but 2-bromo-4-fluorophenyl β -D-galactopyranoside **22** was poorly soluble.

^{19}F NMR. Compounds **16**–**22** each gave a single, narrow ^{19}F NMR signal essentially invariant ($\Delta\delta \leq 0.03$) in rabbit whole blood, 0.9% saline, and PBS in the pH range 3–12 and at various temperatures ranging from 25 to 37 °C. The liberated aglycons display a chemical shift range of ~ 16 ppm (Table 1; Figure 2). Addition of β -galactosidase (E801A) in PBS (0.1 M, pH 7.4) at 37 °C caused each substrate to hydrolyze, releasing the pH sensitive aglycons **2**–**8** appearing also as a single narrow ^{19}F NMR signal (Figure 2; Table 1), consistent with the titration curves of **2**–**8** (Figure 3; Table 2). The minimum

**Figure 4.** Hydrolysis time courses of **16**–**22** (15 mmol) by β -gal (E801A, 20 units) in PBS (0.1 M, 0.6 mL) at 37 °C.**Figure 5.** Colorimetric comparison of enzyme (G5160, pH 4.5) sensitivity for **16** and ONPG.

^{19}F NMR chemical shift response observed was 3.56 ppm for **19** and maximum was 9.84 ppm for **16** at pH 7.4 (Table 1).

The various substrates **16**–**22** exhibited differential sensitivity to β -galactosidase in PBS (pH 7.4), and kinetics were monitored by changes in the integration of the ^{19}F NMR signals (Figures 2 and 4). The shapes of the kinetic curves suggest straightforward first-order kinetics for all substrates. The best substrate was **18A**, with an initial rate of 0.74 mM/min/unit, although this molecule hydrolyzed spontaneously within 2 h. **16**, **17**, and **19** also showed rapid cleavage, whereas **20**–**22** were somewhat slower and **18B** resisted enzyme action (as expected for an α anomer). By colorimetric assay **16** was essentially equivalent to ONPG as a substrate (Figure 5).

Several of the aglycons (**2**, **3**, **6**–**8**) exhibit a large ^{19}F NMR chemical shift in response to pH with $\Delta\delta$ reaching 9.3. However, **4** and **5** showed little response (Figure 3). The observed pK_{a} values were found to be in the range of 5.4–9.8 (Table 2). There was a strong linear correlation between initial rate of enzymatic hydrolysis of the substrates and pK_{a} of the aglycon (Figure 6).

When **17** was incubated with wild-type MAT-Lu rat prostate cancer cells (4 h, PBS, 37 °C under air–5% CO_2 with 95% humidity), ^{19}F NMR spectra showed no changes. When **17** was incubated with MAT-Lu-LacZ cells ($92 \times$

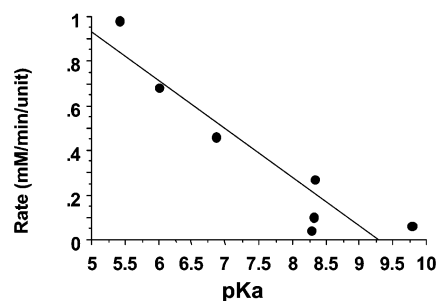
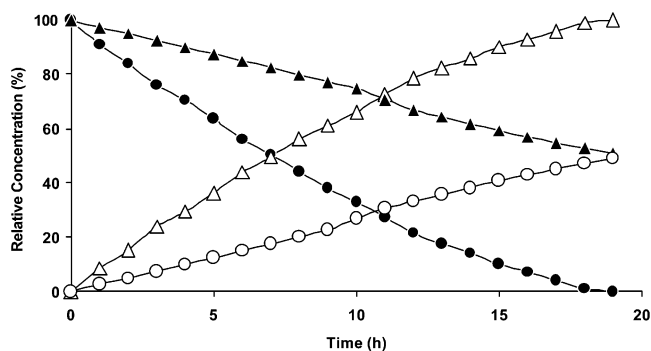
**Figure 6.** Brønsted plot of substrate susceptibility to β -gal (E801A, pH 7.4) versus of pK_{a} of liberated aglycon ($r^2 > 0.85$).**Figure 7.** Hydrolysis of **17** (open symbols) to **3** (solid symbols) by stably transfected Dunning prostate R3327 MAT-Lu-lacZ cells (Δ , 92×10^6) and MTLn3-lacZ (\circ , 9.8×10^6) suspended in PBS at 37 °C.

Table 3. Toxicity of 2–8 and 16–22 to MAT-Lu -WT and -LacZ Cells (PBS, pH 7.4)

		molecule													
		2	3	4	5	6	7	8	16	17	18A/B	19	20	21	22
IC ₅₀ mM	MAT-Lu	<0.4	>1.6 ^a	>1.3	<0.003	<1.6	<0.003	>0.9	>3.6 ^a	<3	<4.5	>4.5	>4.5	>4.5 ^a	>0.3 ^a
	MAT-Lu-LacZ	<0.8	>1.6 ^a	>1.3 ^a	<0.003	<0.8	<0.003	>0.9	>3.6 ^a	>6	>4.5	>4.5	>4.5	>4.5 ^a	>0.3 ^a

^a Greater than 90% survival at the highest dose tested.

10⁶, 1803 milliunits of β -gal) in PBS, cleavage proceeded in a smooth monotonic manner with hydrolysis complete after 19 h (Figure 7). MTLn3-LacZ breast cancer cells (9.8×10^6 , 67 milliunits of β -gal) hydrolyzed ~50% of **17** in 19 h.

Toxicity was evaluated for both aglycons and conjugates using both wild-type and lacZ expressing MAT-Lu cells (Table 3). **5** and **7** were severely cytotoxic, **2** was somewhat toxic (IC₅₀ < 0.4 mM), and the other aglycons, **3**, **4**, **6**, and **8**, were less toxic (IC₅₀ > 1 mM), making them more suitable for in vivo NMR investigations. Most conjugates were much less toxic; in particular, the toxicity of the aglycons was masked in **19** and **21**.

DISCUSSION

We have presented a method to efficiently and stereoselectively synthesize a series of fluorophenyl β -D-galactopyranosides **16**–**22** as potential ¹⁹F NMR-based gene reporter molecules. We previously demonstrated that **16** could be used to assess β -gal activity in transiently transfected human prostate cancer cells (27). We have now assessed the relative substrate efficacy of a series of analogues and demonstrated the utility of **17** to assess β -gal activity in stably transfected rat breast and prostate tumor cells.

¹⁹F NMR provides a large chemical shift response to small changes in molecular structure or microenvironment (25, 26). Here, hydrolysis provided a minimum $\Delta\delta$ 3.56 between the substrate and the aglycon at pH 7.4, although depending on the pH, it could range from 1.6 to 12.9 ppm. Significantly, because of the chemical shift range of the ¹⁹F signals of the aglycons **2**–**8** (up to 9.3 ppm), several substrates and aglycons can be detected simultaneously, allowing direct comparison of substrate efficacy (Figure 2). Preliminary data suggest that the approach used here could also be applied to glucosidases and glucuronides. Indeed, Schmidt and Monneret (39) presented ¹⁹F NMR analysis of a fluorine-tagged nitrogen mustard pro-drug activated by glucuronidase. ¹⁹F NMR spectroscopy lacks the spatial resolution of ¹H MRI, but the chemical shift accompanying substrate cleavage by β -gal unequivocally reveals enzyme activity. Comparing the substrates shows a 10-fold range in rate of substrate reaction at pH 7.4, the optimal pH for activity of β -gal derived from *Escherichia coli*. The observed initial rates were found to have a strong linear correlation with the pK_a of the aglycon (Figure 6), consistent with previous work by Richard et al. (40), who examined a series of alkyl β -galactosides. At pH 4.5—the optimal pH for β -gal derived from *Aspergillus oryzae*—**16** showed very similar activity in comparison with the traditional colorimetric indicator ONPG.

Substrates **16** and **17** share many attributes with similar sensitivity to β -gal at pH 7.4 (Figure 4), a large chemical shift range, and effective response to cells expressing β -gal (Figure 7) (27). All of the aglycons are electronically similar to the classic biochemical uncoupler dinitrophenol, raising potential concerns of toxicity. We have found extensive cell lysis upon direct exposure to the product aglycon **2** (IC₅₀ < 0.4 mM), but **16** has allowed us to assess β -gal expression in culture (27). Other

aglycons, **3**, **4**, **6**, and **8**, are less toxic, making them more suitable for in vivo NMR investigations, although **5** and **7** are severely cytotoxic. The conjugates are generally much less toxic, and indeed **19** and **21** showed essentially no toxicity up to the highest concentrations tested in wild-type or lacZ-expressing cells. Intriguingly, the conjugate **17** was more toxic than its aglycon. Similar toxicity was observed for all materials in wild-type or LacZ cells. Release of the less toxic, pH-sensitive aglycons suggests a novel approach to measuring pH at the site of enzyme activity. Moreover, noting the broad specificity of β -gal, we have synthesized an alternative galactoside with the ¹⁹F NMR pH indicator fluoropyridoxol (25), as the aglycon and preliminary data show that it is also sensitive to enzyme activity (41).

We believe that noninvasive detection of gene reporter molecules will become increasingly important in biomedicine. It will be important to have diverse agents, genes, and modalities for specific applications. Fluorophenyl β -D-galactosides offer a novel approach for addressing β -gal activity. Moreover, we believe the concept of using ¹⁹F NMR to monitor gene transfection, together with the molecular approach presented here, can serve as a platform technology with widespread application to many diverse genes and enzymes.

ACKNOWLEDGMENT

Supported in part by DOD Breast Cancer Initiative IDEA Award BC022001 DAMD17-03-1-0343-01, a DOD Prostate Cancer Initiative Postdoctoral Award W81XWH-04-10331 (L.L.), and the Cancer Imaging Program, NCI Pre-ICMIC P20 CA086354. NMR experiments were conducted at the Mary Nell and Ralph B. Rogers NMR Center, an NIH BTRP facility (P41-RR02584).

LITERATURE CITED

- (1) Bronstein, I., Fortin, J., Stanley, P. E., Stewart, G. S., and Kricka, L. J. (1994) Chemiluminescent and bioluminescent reporter gene assays. *Anal. Biochem.* 219, 169–181.
- (2) Contag, C. H., Jenkins, D., Contag, P. R., and Negrin, R. S. (2000) Use of reporter genes for optical measurements of neoplastic disease in vivo. *Neoplasia* 2, 41–52.
- (3) Hoffman, R. (2002) Green fluorescent protein imaging of tumour growth, metastasis, and angiogenesis in mouse models. *Lancet Oncol.* 3, 546–556.
- (4) Contag, C. H., and Ross, B. D. (2002) It's not just about anatomy: In vivo bioluminescence imaging as an eyepiece into biology. *J. Magn. Reson. Imag.* 16, 378–387.
- (5) Herschman, H. R. (2002) Non-invasive imaging of reporter genes. *J. Cell. Biochem.* 39, 36–44.
- (6) Tjuvavej, J. G., Doubrovina, M., Akhurst, T., Cai, S., Balatoni, J., Alauddin, M. M., Finn, R., Bornmann, W., Thaler, H., Conti, P. S., and Blasberg, R. G. (2002) Comparison of radiolabeled nucleoside probes (FIAU, FHBG, and FHPG) for PET imaging of HSV1-tk gene expression. *J. Nucl. Med.* 43, 1072–1083.
- (7) Haberkorn, U., Altmann, A., Jiang, S., Morr, I., Mahmut, M., and Eisenhut, M. (2001) Iodide uptake in human anaplastic thyroid carcinoma cells after transfer of the human thyroid peroxidase gene. *Eur. J. Nucl. Med.* 28, 633–638.
- (8) Weissleder, R., Simonova, M., Bogdanova, A., Bredow, S., Enochs, W. S., and Bogdanov, A. J. (1997) MR imaging and

- scintigraphy of gene expression through melanin induction. *Radiology* 204, 425–429.
- (9) Moore, A., Josephson, L., Bhorade, R. M., Basilion, J. P., and Weissleder, R. (2001) Human transferrin receptor gene as a marker gene for MR imaging. *Radiology* 221, 244–250.
- (10) Stegman, L. D., Rehemtulla, A., Beattie, B., Kievit, E., Lawrence, T. S., Blasberg, R. G., Tjuvajev, J. G., and Ross, B. D. (1999) Noninvasive quantitation of cytosine deaminase transgene expression in human tumor xenografts with in vivo magnetic resonance spectroscopy. *Proc. Natl. Acad. Sci. U.S.A.* 96, 9821–9826.
- (11) Beckwith, J. R., and Zipser, D. (1970) in *The Lactose Operon*, Cold Spring Harbor, Cold Spring Harbor, NY.
- (12) Serebriiskii, I. G., and Golemis, E. A. (2000) Uses of lacZ to study gene function: evaluation of β -galactosidase assays employed in the yeast two-hybrid system. *Anal. Biochem.* 285, 1–15.
- (13) Kruger, A., Schirmmacher, V., and Khokha, R. (1999) The bacterial lacZ gene: An important tool for metastasis research and evaluation if new cancer therapies. *Cancer Metastasis Rev.* 17, 285–294.
- (14) Pulvin, S., Friboulet, A., and Thomas, D. (1990) Substrate inhibition or activation kinetics of the β -galactosidase from the extreme thermoacidophile archaeobacterium *Caldariella acidophila*. *Biochim. Biophys. Acta* 1041, 97–100.
- (15) Poci, I., Taylor, S. A., Richardson, A. C., Smith, B. V., and Price, R. G. (1993) Comparison of several new chromogenic galactosides as substrates for various β -D-galactosidases. *Biochim. Biophys. Acta* 1163, 54–60.
- (16) James, A. L., Perry, J. D., Ford, M., Armstrong, L., and Gould, F. K. (1996) Evaluation of cyclohexenoesucetin- β -D-galactoside and -hydroxyquinoline- β -D-galactoside as substrates for the detection of β -galactosidase. *Appl. Environ. Microbiol.* 62, 3868–3870.
- (17) James, A. L., Perry, J. D., Chilvers, K., Robson, I. S., Armstrong, L., and Orr, K. E. (2000) Alizarin- β -D-galactoside: a new substrate for the detection of bacterial β -galactosidase. *Lett. Appl. Microbiol.* 30, 336–340.
- (18) Manafi, M., Kneifel, W., and Bascomb, S. (1991) Fluorogenic and chromogenic substrates used in bacterial diagnostics. *Microbiol. Rev.* 55, 335–348.
- (19) Buller, C. J., Zang, X. P., Howard, E. W., and Pento, J. T. (2003) Measurement of β -galactosidase tissue levels in a tumor cell xenograft model. *Methods Findings Exp. Clin. Pharmacol.* 25, 713–716.
- (20) Youngman, P., Zuber, P., Perkins, J. B., Sandman, K., Igo, M., and Losick, R. (1985) New ways to study developmental genes in spore-forming bacteria. *Science* 228, 285–290.
- (21) Alam, J., and Cook, J. L. (1990) Reporter genes: Application to the study of mammalian gene transcription. *Anal. Biochem.* 188, 245–254.
- (22) Horwitz, J. P., Chua, J., Curby, R. J., Tomson, A. J., DaRooge, M. A., Fisher, B. E., Mauricio, J., and Klundt, I. (1964) Substrates for cytochemical demonstration of enzyme activity. I. Some substituted 3-indolyl- β -D-glycopyranosides. *J. Med. Chem.* 7, 574–575.
- (23) Heuermann, K., and Cosgrove, J. (2001) S-Gal: an autoclavable dye for color selection of cloned DNA inserts. *Biotechniques* 30, 1142–1147.
- (24) Louie, A. Y., Huber, M. M., Ahrens, E. T., Rothbacher, U., Moats, R., Jacobs, R. E., Fraser, S. E., and Meade, T. J. (2000) In vivo visualization of gene expression using magnetic resonance imaging. *Nat. Biotechnol.* 18, 321–325.
- (25) Mason, R. P. (1999) Transmembrane pH gradients in vivo: measurements using fluorinated vitamin B6 derivatives. *Curr. Med. Chem.* 6, 481–499.
- (26) Mason, R. P., Ran, S., and Thorpe, P. E. (2002) Quantitative assessment of tumor oxygen dynamics: molecular imaging for prognostic radiology. *J. Cell. Biochem.* 87S, 45–53.
- (27) Cui, W., Otten, P., Li, Y., Koenenman, K., Yu, J., and Mason, R. P. (2004) A novel NMR approach to assessing gene transfection: 4-fluoro-2-nitrophenyl- β -D-galactopyranoside as a prototype reporter molecule for β -galactosidase. *Magn. Reson. Med.* 51, 616–620.
- (28) Hwang, D. R., and Scott, M. E. A. (1988) Chromogenic Substrates for β -Galactosidase, Eur. Pat. Appl. EP 88-304173 19880509.
- (29) Guder, H. J., Herrmann, R. Z., and Zdunek, D. (1992) Preparation of Nitrophenyl β -D-Galactopyranosides as β -Galactosidase Substrates for Cloned Enzyme Donor Immunoassay (CEDIA), DE 4021063 A1 19920109; assignee: Boehringer Mannheim G.m.b.H.
- (30) Yoon, S., Kim, H. G., Chun, K. H., and Shin, J. E. N. (1996) 4-deoxy-analogs of *p*-nitrophenyl β -D-galactopyranosides for specificity study with β -galactosidase from *Escherichia coli*. *Bull. Korean Chem. Soc.* 17, 599–604.
- (31) Garegg, P. I. (1997) Thioglycosides as glycosyl donors in oligosaccharide synthesis. *Adv. Carbohydr. Chem. Biochem.* 52, 179–205.
- (32) Ernst, B., Hart, G. W., and Sinäy, P. (2000) in *Chemistry of Saccharides; Chemical Syntheses of Glycosides and Glycomimetics*, Wiley-VCH, Weinheim, Germany.
- (33) Lam, S. N., and Gervay-Hague, J. (2002) Solution-phase hexasaccharide synthesis using glucosyl iodides. *Org. Lett.* 4, 2039–2042.
- (34) Dushin, R. G., and Danishefsky, S. J. (1992) Stereospecific synthesis of aryl β -glucosides: an application to the synthesis of a prototype corresponding to the aryloxy carbohydrate domain of vancomycin. *J. Am. Chem. Soc.* 114, 3471–3475.
- (35) Ding, Y. L., and Liu, Y. T. (1991) Stereoselective syntheses of acetylated *o*-tolyl 1-thioglycosides. *Carbohydr. Res.* 209, 306–310.
- (36) Mizutani, K., Kasai, R., and Tanaka, O. (1980) ¹³C-NMR spectroscopy of α - and β -anomeric series of alkyl L-arabinopyranosides. *Carbohydr. Res.* 87, 19–26.
- (37) Kasai, R., Okihara, M., Asakawa, J., Mizutani, K., and Tanaka, O. (1979) ¹³C-NMR study of α - and β -anomeric pairs of D-mannopyranosides and L-rhamnopyranosides. *Tetrahedron* 35, 1427–1432.
- (38) Duus, J. O., Gotfredsen, C. H., and Bock, K. (2000) Carbohydrate structural determination by NMR spectroscopy: modern methods and limitations. *Chem. Rev.* 100, 4589–4614.
- (39) Schmidt, F., and Monneret, C. (2002) In vitro fluorine-19 nuclear magnetic resonance study of the liberation of anti-tumor nitrogen mustard from prodrugs. *J. Chem. Soc., Perkin Trans 1* 1302–1308.
- (40) Richard, J. P., Westerfeld, J. G., and Lin, S. (1995) Structure–reactivity relationships for β -galactosidase (*Escherichia coli*, lac Z). 1. Bronsted parameters for cleavage of alkyl β -D-galactopyranosides. *Biochemistry* 34, 11703–11712.
- (41) Yu, X., and Mason, R. P. (2003) Novel in vivo gene reporter molecule using fluorinated vitamin B6 as ¹⁹F NMR indicator. In *Proceedings of the International Society for Magnetic Resonance in Medicine*, Toronto, Canada, p 675 ISMRM, Berkeley, CA.

¹⁹F: A Versatile Reporter for Non-Invasive Physiology and Pharmacology Using Magnetic Resonance

Jian-xin Yu⁺, Vikram D. Kodibagkar⁺, Weina Cui and Ralph P. Mason*

Department of Radiology, The University of Texas Southwestern Medical Center at Dallas, Texas, USA

Abstract: The fluorine atom provides an exciting tool for diverse spectroscopic and imaging applications using Magnetic Resonance. The organic chemistry of fluorine is widely established and it can provide a stable moiety for interrogating many aspects of physiology and pharmacology *in vivo*. Strong NMR signal, minimal background signal and exquisite sensitivity to changes in the microenvironment have been exploited to design and apply diverse reporter molecules. Classes of agents are presented to investigate gene activity, pH, metal ion concentrations (*e.g.*, Ca²⁺, Mg²⁺, Na⁺), oxygen tension, hypoxia, vascular flow and vascular volume. In addition to interrogating speciality reporter molecules, ¹⁹F NMR may be used to trace the fate of fluorinated drugs, such as chemotherapeutics (*e.g.*, 5-fluorouracil, gemcitabine), anesthetics (*e.g.*, isoflurane, methoxyflurane) and neuroleptics. NMR can provide useful information through multiple parameters, including chemical shift, scalar coupling, chemical exchange and relaxation processes (R1 and R2). Indeed, the large chemical shift range (~ 300 ppm) can allow multiple agents to be examined, simultaneously, using NMR spectroscopy or chemical shift selective imaging.

Keywords: Oxygen, pH, gene reporter, metal ions, 5FU, FDG, anesthetics.

1. INTRODUCTION

Nuclear magnetic resonance (NMR) was originally a curiosity for physicists, but its demonstration led to Nobel Prizes for Purcell and Bloch [1]. During the 1960's to 1980's NMR was embraced by the chemistry community for its power to discriminate chemical structures. Demand fed development with increasingly sophisticated instruments, including higher magnetic fields, faster and more precise electronics and more powerful computers, combined with innovations in data acquisition (*e.g.*, Fourier transform [2], echo planar imaging [2]) and radiofrequency coils (quadrature [3], SMASH [4], SENSE [5]). In biomedicine, the intense water signal (55 M H₂O) is exploited for high resolution, anatomical MR Imaging providing 3D tomography non-invasively in living systems. Millimeter resolution is routine and microscopy is feasible [6]). For many diseases, proton MRI has become the modality of choice for the radiologist. Increasingly, manipulation of the water signal through appropriate spin physics provides insight into physiology, such as, blood flow (arterial spin labeling (ASL) [7]), diffusion (diffusion tensor imaging (DTI) [8]), and oxygenation (Blood oxygen level dependent (BOLD) contrast [9]). Chemists have exploited NMR, but increasingly they also contribute in the form of contrast agents and reporter molecules, as described in this Hot Topics issue. Diagnostic value is added by applying paramagnetic contrast agents: several are in clinical use today, including Gd-DTPA (diethylenetriaminepentaacetic acid, Magnevist[®]) and Gd-DTPA-BMA (gadodiamide, OmniScan[®]), and Gd-HP-DO3A (1,4,7-tricarboxymethyl-

1,4,7,10-tetraazacyclododecane, ProHance[®]) and Gd-DOTA (1,4,7,10-tetraazacyclododecane-1,4,7,10-tetraacetic acid, Dotarem[®]), and new generations of "smart" agents are being developed, as reviewed in the accompanying paper by McMurphy, *et al.* [10].

Use of proton NMR to detect metabolites other than water is severely complicated by the relative signal intensity, since many metabolites occur at millimolar concentrations. Thus, hetero-nuclear approaches have been developed to explore other endogenous molecules and ³¹P NMR has been widely applied in the pre-clinical setting, with limited clinical application, to assess metabolites such as phosphocreatine, ATP, and inorganic phosphate, providing insight into both bioenergetics and pH [11, 12]. ²³Na NMR is also very sensitive, but is essentially limited to the Na⁺ ion; though application of contrast agents may differentiate intra- and extra-cellular sodium ions and these can be sensitive to edema and potentially reveal tumors [13-15]¹. Tissues also have extensive carbon, though 98.9% exists as NMR invisible ¹²C. ¹³C may be detected directly, but more significantly provides an opportunity for the use of isotopically enriched substrates (*e.g.*, acetate, formaldehyde), which are readily available and detectable [16, 17]. Isotopic substitutions may also be applied to protons, with replacement by deuterium or tritium to examine metabolic pathways and kinetic isotope effects [18, 19].

An alternative approach is ¹⁹F NMR, as described below. Some common drugs include a fluorine atom [20], and are obvious candidates for investigation (*e.g.*, 5FU [21, 22], flurbiprofen [23, 24], isoflurane [25], fluoxetine [26]). In other cases, a fluorine atom may be added as a simple tracking label, or by judicious placement in a carefully designed reporter molecule to interrogate some parameter, such as pO₂ [27], pH [28] or gene activity [29].

*Address correspondence to this author at the Laboratory of Prognostic Radiology, Department of Radiology, The University of Texas Southwestern Medical Center at Dallas, 5323 Harry Hines Blvd, Dallas, Texas 75390-9058, USA; Tel: (214)-648-8926, Fax: (214)-648-2991; E-mail: Ralph.Mason@UTSouthwestern.edu

⁺Contributed equally to this review.

¹ Kalyanapuram, R.; Winter, P.; Mason, R.P.; Bansal, N., Proc. 5th ISMRM, Vancouver, 1997, p. 2116.

NMR has many virtues compared with other modalities:

- 1 It is intrinsically non-invasive, though ^{19}F requires infusion of reporter molecules.
- 2 There is no radioactivity, so the substrates (reporter molecules) are inherently stable with a long shelf life and are not associated with problems of radioactive waste disposal.
- 3 Any tissues of arbitrary depth may be interrogated.
- 4 Multiple signals may be detected simultaneously from separate reporter molecules. By analogy, one may consider multi-wavelength fluorescent optical imaging or energy selective γ -ray detection in a gamma camera.
- 5 Clinical anatomical ^1H MRI is readily acquired together with ^{19}F -reporter molecule signals, providing context in terms of organs and tissue heterogeneity.

NMR is endowed with multiple characteristics including parameters such as signal intensity (SI), chemical shift (δ) and changes therein ($\Delta\delta$), transverse dephasing rate (R_2^*), spin-spin relaxation rate (R_2) and longitudinal relaxation rate (R_1). This provides both a wealth of potential information and complexity in optimal experimental planning. The signal intensity of a particular peak (more specifically integral of area under the peak) in the NMR spectrum is proportional to the amount of the corresponding substance in the region excited by the NMR coil. This provides qualitative and often quantitative assessment of the dynamic changes in the concentration of endogenous or exogenous probes.

NMR has certain drawbacks in terms of cost of instrumentation (much higher than optical methods), sensitivity (typically, mM vs. μM for optical or radionuclide studies), and acquisition time. Acquisition time depends on substrate concentration, magnetic field, and volume of interrogation. Traditional NMR sensitivity is quoted in the mM range. There are indications that specific contrast agents may be effective at lower concentrations by manipulating spin thermodynamics [30, 31] or exploiting activatable paramagnetic magnetization transfer contrast agents (PARACEST) [32].

^{19}F NMR has been used since the eighties for *in vivo* studies. In the past, various reviewers have discussed diverse applications of *in vivo* ^{19}F NMR [21, 27, 28, 33-41]. Thomas [33], Selinsky and Burt [34], Prior *et al.* [35] and London [36] reviewed the contemporary state-of-the-art, covering the entire spectrum of *in vivo* applications. Mason reviewed the use of perfluorocarbons for measuring pO_2 [27, 37] and the use of fluorinated derivatives of vitamin B₆ as probes for measuring *in vivo* cellular transmembrane pH gradients [28]. McSheehy *et al.* [38] discussed applications of ^{19}F magnetic resonance spectroscopy (MRS) to oncology. Menon [39] focused on the studies involving fluorinated anesthetic agents. Passe *et al.* [40] reviewed neuropsychiatric applications of NMR, which included a discussion on ^{19}F NMR applications. Bachert [42], Martino *et al.* [41] and Wolf *et al.* [21] gave comprehensive reviews of pharmacokinetics of fluoropyrimidine drugs using ^{19}F NMR. The continuing appearance of reports of the use of

^{19}F NMR and development of novel reporter molecules justifies a current review. Moreover, ^{19}F NMR has made inroads into some new areas (Table 1). The purpose of this article is to review the applications of ^{19}F NMR to *in vivo* studies especially from a chemical standpoint.

Table 1. Fluorinated Reporter Molecules

Parameter	Indicator (example)	References (representative)
Gene activity	PFONPG, 5FC	[29, 74]
pO_2	Fluorocarbons, <i>e.g.</i> , hexafluorobenzene	[27, 218]
Hypoxia	F-Misonidazoles	[150, 347]
pH	FPOL, ONPG, ZK 150471	[28, 29, 87, 105, 107, 348]
$[\text{Na}^+]$	F-cryp-1	[145]
$[\text{Ca}^{2+}]$	5F-BAPTA	[128, 130, 135]
$[\text{Mg}^{2+}]$	5F-APTRA	[36, 140]
Membrane/Chloride potential	TFA	[349, 350]
Temperature	PFCs	[33, 167, 351]
Blood flow	Freon FC-23	[292, 293]
Cell volume	TFM	[349]
Diffusion	FDG	[352]
Glycolysis	FDG	[302]
Drug metabolism	5-FU, gemcitabine	[21, 42]
Vascular volume	Fluorocarbon emulsion	[284, 285]
Protein catabolism	DLBA	[353]
Artherosclerotic plaques	nanoparticles	[354]
Lung function	PFC; SF_6	[269, 355]
GI function	PFC	[277, 278]

2. ^{19}F AS AN *IN VIVO* NMR PROBE

^{19}F has a nuclear spin 1/2 and a gyromagnetic ratio (γ) of 40.05 MHz/T. Being the only stable isotope of fluorine, it is 100 % naturally abundant. The NMR sensitivity of ^{19}F is 0.83 relative to ^1H . The high γ (only about 6% lower than protons) generally allows the use of existing proton NMR instrumentation with a minimum of component adjustments. While fluorine occurs in the body, it is present mostly in the form of solid fluorides in bones and teeth [43]. Endogenous fluorine has a very short T_2 relaxation time [43] and the resulting signal is below the limits of NMR detection in most biological systems of interest. Thus, exogenously administered fluorine containing compounds are observed without interference from background signals.

The ¹⁹F NMR chemical shift is exquisitely sensitive to perturbations in the chemical microenvironment. The range of chemical shifts of ¹⁹F is greater than 300 parts per million (ppm), as opposed to about 10 ppm for proton NMR [44]. The sensitivity and range of chemical shifts ensure that fluorinated probes and their metabolites, if any, are easily differentiated. While signals can be interpreted in isolation, it is often preferable to include a reference signal. There is no single fluorine-containing compound that is suitable as a universal chemical shift reference for *in vivo* studies. The IUPAC standard for ¹⁹F chemical shift reference is fluorotrichloromethane (CFCl₃). The range of chemical shifts of most organic fluorinated compounds is about -50 ppm to +250 ppm relative to CFCl₃. However, CFCl₃ is not convenient for most biomedical applications, and hence, secondary reference materials are commonly used. Chemical shifts can be strongly solvent dependent and vary with dilution [44]. CF₃CO₂H is quoted as -76.530 ppm on the δ scale (extrapolated to infinite dilution). Many investigators favor aqueous sodium trifluoroacetate (NaTFA) as a chemical shift reference for biological studies [28, 45-47]. NaTFA has the advantage of being quite nontoxic, and hence, can be introduced together with a fluorinated probe, as an internal chemical shift reference *in vivo*. This is preferable to an external reference, if total signal quantification is not an issue, since susceptibility effects may cause errors in estimation of chemical shifts of *in vivo* probes relative to an external standard.

To obtain detectable signals, spectra, or images, sufficient fluorinated probe must be administered, though the concentration of probe in studies of living organisms should be as low as possible to avoid physiological perturbations or toxic side effects. Unlike ¹H and ¹³C NMR, ¹⁹F chemical shift can appear quite unpredictable though theoretical treatments have attempted to rationalize values [44, 48] (+ refs therein). Extensive tables of ¹⁹F NMR chemical shifts and coupling constants have been published [49]. Molecules may include a single fluorine atom, in which case F-H coupling may be observed. For multiple F atoms, F-F coupling also occurs (Table 2). Unlike ¹H or ¹³C NMR, the coupling constants do not decrease monotonically with increasing separation, and negative coupling constants are sometimes observed [44, 50]. While C-F coupling is seen in ¹³C NMR spectroscopy, the low natural abundance of ¹³C is not generally apparent in ¹⁹F NMR spectroscopy. F-H coupling can be removed by proton de-coupling, however, fluorine detection is often accomplished by retuning the proton NMR channel, and thus, proton de-coupling is often not practical. F-F coupling is often unresolved, particularly in the broader signals encountered *in vivo*, but it can, nonetheless, give rise to J modulation in echo acquisitions [51]. While this may distort signals, it has also been exploited for signal editing providing resonance selective imaging [52]. The easiest way to avoid J_{FF} coupling is to ensure symmetry, *e.g.*, CF₃ groups. Moreover, this avoids the potential toxicity associated with mono- and di-fluoroacetate groups [53]. In addition to chemical shift, relaxation rates are exploited in ¹⁹F NMR. In particular, the ¹⁹F spin-lattice relaxation rate (R₁=1/T₁) of many perfluorocarbons (PFCs) is linearly related to the partial pressure of oxygen (pO₂) [27].

Fluorine may be introduced in many forms, though chemical reaction conditions are often quite severe and reagents include HF [54], various metal halides [55], SeF₄ [56], WF₆ [57], XeF₂ [58], SbF₅ [59], F₂ [60, 61], S-ethyltrifluorothioacetate [62] and trifluoroacetic anhydride [63]. Thus, it may be preferable to incorporate a moiety into synthetic planning, which already includes the desired fluorine atoms, *e.g.*, trifluoromethyl. Typical reporter groups are shown in (Table 3), together with reported syntheses and applications. For biological activity, the F atom has a similar size to a hydroxyl group, but exhibits a strong carbon-fluorine bond, and low chemical reactivity. Fluorine is highly electro-negative, causing potential charge redistribution. Some of the earliest biomedical applications of ¹⁹F NMR used fluorine labeled substrates to explore enzyme activity and protein structures, *e.g.*, ribonuclease A, hemoglobin and lysozyme as reviewed by Dwek [64] and Gerig [65].

Table 2. Typical Values of Fluorine Coupling Constants Summarized From [44, 49]

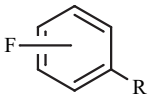
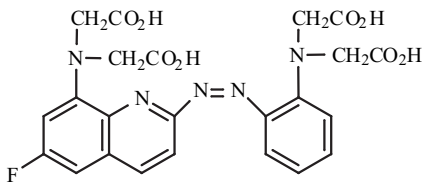
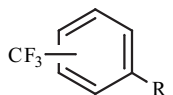
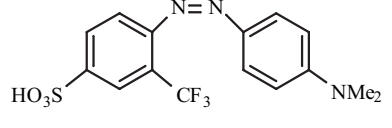
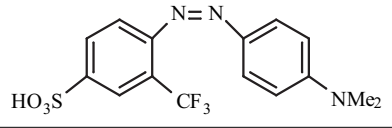
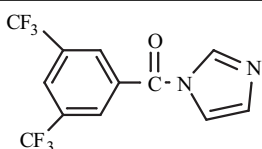
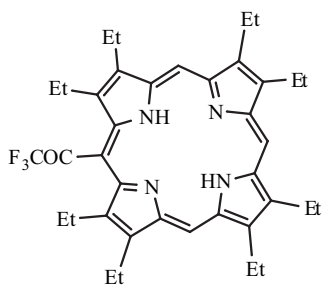
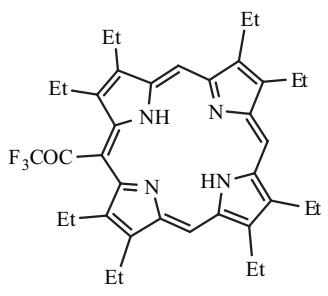
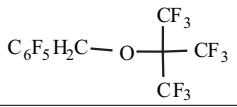
² J _{FH}	45-90 Hz
³ J _{FH}	0-53 Hz
² J _{FF}	200-800 Hz
³ J _{FF}	< 1 Hz
⁴ J _{FF}	1-20 Hz
⁵ J _{FF} - ⁶ J _{FF}	0-40 Hz
¹ J _{FC}	>200-312 Hz
² J _{FC}	(-25) 17-54 Hz

This review will consider three classes of molecular ¹⁹F NMR based on i) "Active agents", specifically designed to interact with the environment and including ¹⁹F atom(s), which respond to a specific parameter, such as enzyme activity, ion concentration or pO₂ (Section 3); ii) "Passive agents", which occupy space, thereby, revealing a tissue property, such as vascular volume based on NMR signal intensity, while remaining essentially inert (Section 4), iii) pharmaceuticals, which include a fluorine atom making them suitable for NMR investigations (Section 5).

3. ACTIVE AGENTS

Active agents typically fall into three categories; i) those which undergo irreversible interaction modifying their structure, as revealed by a change in chemical shift. These are represented by gene reporter molecules, where substrates are cleaved by specific enzyme activity (Section 3.1), and hypoxia agents (Section 3.4.2), which are modified by reductases and trapped. ii) Ligands designed to trap/bind specific entities, such as ions, specifically, but reversibly, *e.g.*, H⁺ (pH) (Section 3.2), metal ions (Ca²⁺, Mg²⁺) (Section 3.3); iii) perfluorocarbons, which exhibit exceptional gas solubility and reveal oxygen tension based on modification of relaxation parameters (Section 3.4.1).

Table 3. Synthetic Approaches to Fluorochemistry

Name	Structure	Synthesis	Example
Alkyl Fluoride	RCHFR'	SeF_4 [56], PhPF_4 [356], HF [54],	$\text{CH}_3\text{CH}_2\text{FCH}_3$
Difluoroalkane	$\text{RCH}_2\text{CF}_2\text{R}'$ or $\text{RCHF}(\text{CH}_2)_n\text{CHFR}'$	ClF [357], XeF_2 [58], KF [358], CF_2Br_2 [359],	$\begin{array}{c} \text{NH}_2 \quad \text{O} \\ \quad \\ \text{CHF}_2 - \text{C} - \text{C} - \text{OMe} \\ \\ \text{CH}_3 \end{array}$
Trifluoroalkane	RCH_2CF_3	CoF_3 [360], Bu_4NBF_4	$\begin{array}{c} \text{NH}_2 \\ \\ \text{CF}_3 - \text{C} - \text{CO}_2\text{H} \\ \\ \text{CH}_3 \end{array}$
Tetrafluoroalkane	$\text{RCF}_2(\text{CH}_2)_n\text{CF}_2\text{R}'$	HF , SF_4 [361]	$\text{MeCF}_2\text{CH}_2\text{CF}_2\text{Me}$
Trifluoroacetic compounds	$\text{CF}_3\text{CO}_2\text{R}$	EtSCOCF_3 or Trifluoroacetamido-succinic anhydride [62]	<p>Protein-NHCOCF₃ or $\begin{array}{c} \text{O} \\ \\ \text{NH} - \text{C} - \text{CF}_3 \end{array}$</p> <p>Protein-NH $\begin{array}{c} \text{O} \quad \text{O} \\ \quad \\ \text{CH}_2 - \text{CH} - \text{CH} - \text{OH} \\ \quad \\ \text{O} \quad \text{O} \end{array}$</p>
Monofluoro aromatic compounds		[362, 363]	
Trifluoromethyl aromatic compounds		[362, 363]	
Trifluoromethyl Aromatic Compounds		[65]	
Trifluoroacetyl compounds	CF_3COR	Me_3SiCF_3 , Bu_4NF [364]	
Di or tri-trifluoromethyl Derivatives		Me_3SiCF_3 , Bu_4NF [364, 365]	 <p>or</p> 

(Table 3). contd....

Name	Structure		Example
CF ₃ S- Derivatives	CF ₃ SR	Me ₃ SiCF ₃ , Bu ₄ NF [364, 365]	4-NO ₂ C ₆ H ₄ SCF ₃
CF ₃ SO- Derivatives	CF ₃ SOR	Me ₃ SiCF ₃ , Bu ₄ NF [364, 365]	
CF ₃ SO ₂ - Derivatives	CF ₃ SO ₂ R	Me ₃ SiCF ₃ , Bu ₄ NF [364, 365]	
(CF ₃) ₂ N- Derivatives	(CF ₃) ₂ NR	Me ₃ SiCF ₃ , Bu ₄ NF [364, 365]	

3.1 Gene Reporters

Gene therapy holds great promise for the treatment of diverse diseases. However, widespread implementation is hindered by difficulties in assessing the success of transfection in terms of spatial extent, gene expression, and longevity of expression. The development of non-invasive reporter techniques based on appropriate molecules and imaging modalities may help to assay gene expression and this is often achieved by including a reporter gene in tandem with the therapeutic gene [66-69]. A critical criterion is that the reporter gene not be normally present or expressed in the cells of interest. Popular reporter genes today are associated with optical imaging, since this is a cheap modality and highly sensitive results are rapidly available. Thus, bioluminescent imaging (BLI) of luciferase [66, 70] and fluorescent imaging of green fluorescent protein (GFP and longer wavelength variants [71]) are popular. These techniques are very useful in superficial tissues and have extensive applications in mice, but application to larger bodies is limited by depth of light penetration. Fluorescent imaging has been presented in a tomographic format, but to date BLI was limited to planar images. We have recently developed the first optical light emission tomography system (LETS) revealing luciferase expression in mice in 3D². Nuclear medicine approaches (see Haberkorn *et al.* this issue) exploit thymidine kinase with a variety of substrates including iodo- and fluoro-nucleosides, such as FIAU and gancyclovir, and various radionuclide labels including 123-, 124-, 125-I, and ¹⁸F [68, 72]. An alternative approach uses the sodium iodine symporter (hNIS), which works well with both iodide and pertechnetate substrates [67]. For cancer, thymidine kinase has the advantage that the gene serves not only as a reporter, but gene products can themselves have therapeutic value [73].

Gene activated drug therapy, often termed GDEPT (gene directed enzyme prodrug therapy) [74], has been demonstrated using the cytosine deaminase (CD) gene. Specifically, CD activates the minimally toxic 5-

fluorocytosine (5-FC) to the highly toxic 5-fluorouracil (5-FU). This is being widely exploited in gene therapy trials, in the hope of mitigating the toxicity threshold associated with systemic 5-FU delivery [73, 74]. The conversion of 5-FC to 5-FU causes a ¹⁹F NMR chemical shift ~1.5 ppm, hence, revealing gene activity, which has been demonstrated in a number of systems *in vivo* [74, 75]. NMR can be used to monitor conversion (gene activity) or conversely deduce lack of activity (Fig. 1). It is also interesting to note that some of the major metabolic products of 5-FU exhibit chemical shift sensitivity to pH and these could provide an indication of local tissue pH [47].

LacZ, which produces β-galactosidase, has been the primary choice of reporter gene to verify effective transfection in biochemistry and molecular biology for many years [76-78]. Diverse reporter agents are commercially available with specific characteristics, such as developed color, thermal stability, and cellular retention (*e.g.*, X-gal, ONPG (o-nitrophenylgalactoside), S-GalTM, and S-Galacton-starTM) for biological and histological analysis [79-81]. Representative agents (Fig. 2) show the broad range of substrate structures consistent with enzyme promiscuity (lack of substrate specificity). However, β-galactosidase had been largely neglected for *in vivo* work, until the elegant studies of Meade *et al.* [82]. As reviewed by McMurtry (this issue [10], Fig. 19) the galactose bridged cyclic gadolinium contrast agent ((1-(2-(galactopyranosyloxy)propyl)-4,7,10-tris(carboxymethyl)-1,4,7,10-tetraazacyclo dodecane) gadolinium(III) (EgadMe) shows considerable change in water relaxivity upon exposure to β-galactosidase. While the molecule is a poor substrate for the enzyme (about 500 times less efficient than the colorimetric biochemical agent ONPG) and does not penetrate cells, it facilitated effective investigation of cell lineage following direct intra-cellular microinjections [82]. These studies prompted us to consider other NMR active analogs, and it appeared that introduction of a fluorine atom into the popular colorimetric biochemical indicator ONPG could produce a strong candidate molecule. Fluoro-nitrophenol galactosides had previously been reported by Yoon *et al.* [83], though they placed the fluorine atom on the sugar moiety, which provided much less chemical shift response to cleavage.

² Richer, E., Slavine, N., Lewis, M. A., Tsyganov, E., Gellert, G. C., Gunnur Dikmen, Z., Bhagwandin, V., Shay, J. W., Mason, R. P., and Antich, P. P., Proc. 3rd Soc. Molecular Imaging, St. Louis, September 2004

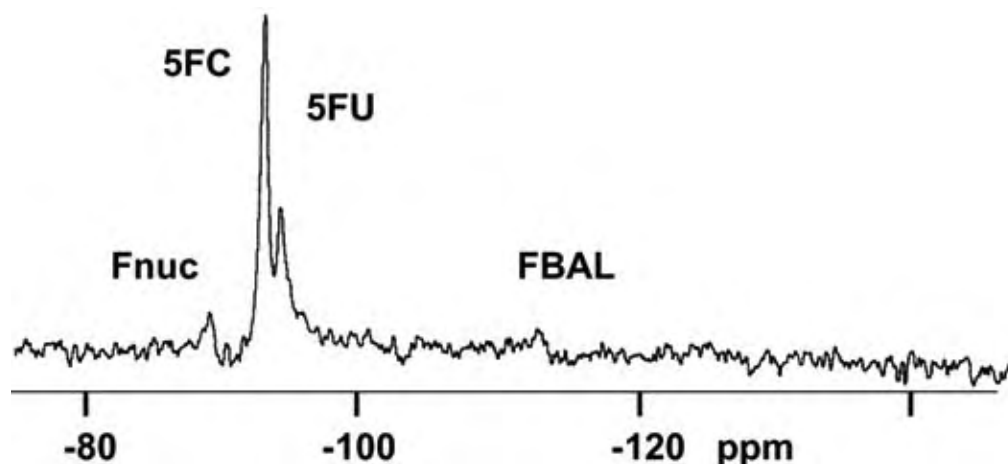


Fig. (1). Simultaneous detection of 5-fluorocytosine (5FC, prodrug) and 5-fluorouracil (5FU) by ^{19}F NMR in Dunning prostate R3327-AT1 cells. The tumor cells had been transfected in culture using adenovirus to express cytosine deaminase. However, following implantation into rat and growth, expression was lost and no conversion was detected *in vivo* following i.p. infusion of 5-FC. However, when 5-FU was administered in addition, both resonances could be resolved and metabolites of 5-FU were detectable. Thus, ^{19}F NMR can provide assay of gene expression (or lack thereof). (Data achieved in collaboration with Dr. Steven Brown, Henry Ford Hospital, Detroit).

We recently demonstrated 4-fluoro-2-nitrophenyl- β -D-galactopyranoside (PFONPG, (Fig. 3) as an effective substrate for β -galactosidase [29]. This molecule is an excellent substrate for the enzyme and acts competitively with traditional biochemical indicators. It provides a single ^{19}F NMR signal with a narrow linewidth and good stability in solution. It is stable in normal wild type cells and whole blood, but exposure to the enzyme or cells transfected to express β -galactosidase causes rapid cleavage in line with anticipated levels of transfection [29]. As with the traditional indicator ONPG, a color change accompanies release of the

aglycone, but this would be masked in tissue studies. Upon cleavage of the glycosidic bond a chemical shift difference $\Delta\delta > 3.6$ ppm is observed (Fig. 4). However, the chemical shift of the product may have a range of about 9 ppm, since the released aglycone is pH sensitive and the pKa is in the physiological range. Significantly, there is no overlap between the chemical shift of the substrate and the product and the chemical shift difference is sufficient to permit chemical shift selective imaging to reveal distribution of each entity separately (Fig. 5).

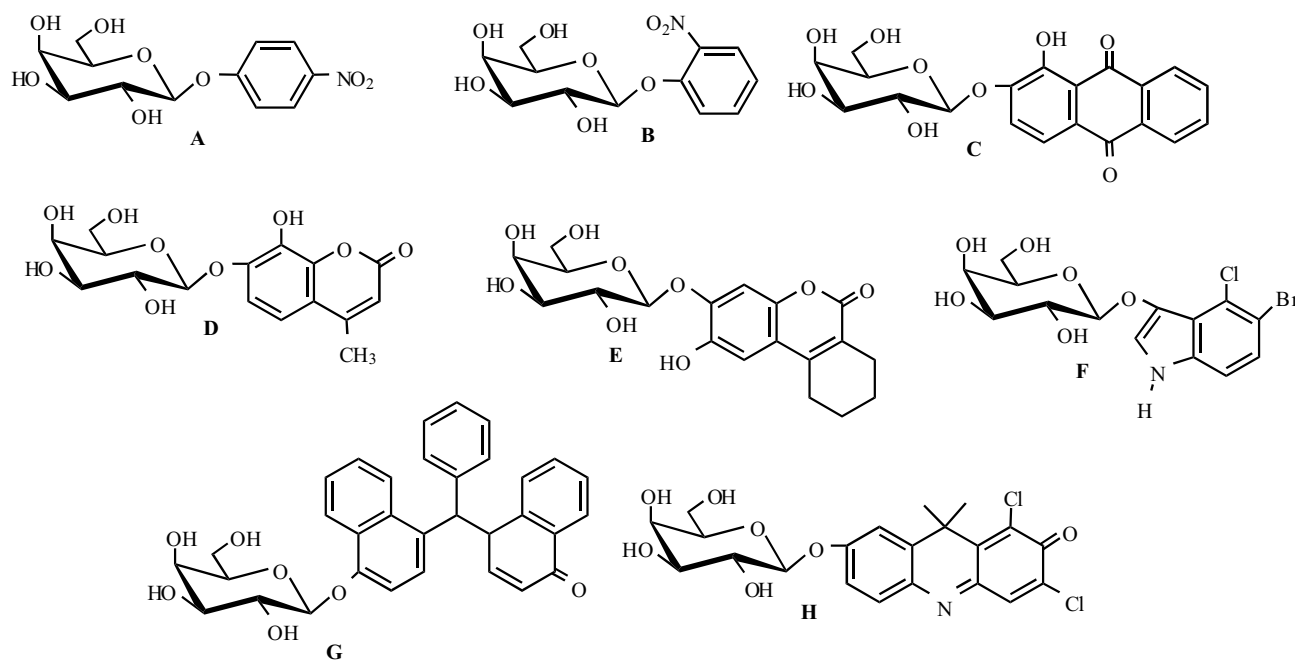


Fig. (2). Diverse substrates for β -galactosidase: 4-nitrophenyl β -D-galactopyranoside (A); 2-nitrophenyl β -D-galactopyranoside (B); p-naphtholbenzein β -D-galactopyranoside (C); 1,2-dihydroxyanthraquinone β -D-galactopyranoside (D); 4-methylumbelliferone β -D-galactopyranoside (E); 5-bromo-4-chloro-3-indoxyl β -D-galactopyranoside (X-gal) (F); 3,4-cyclohexenoescoletin β -D-galactopyranoside (G); 9H-(1,3-dichloro-9,9-dimethylacridin-2-one-7-yl)- β -D-galactopyranoside (DDAOG) (H).

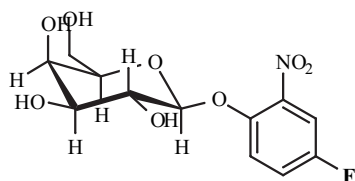


Fig. (3). 4-fluoro-2-nitrophenyl- β -D-galactopyranoside (PFONPG).

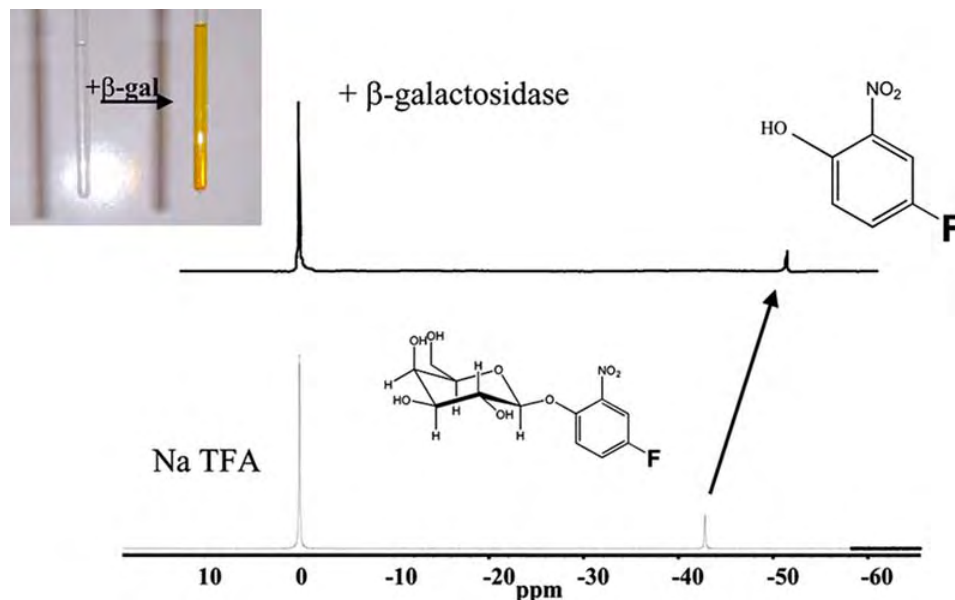


Fig. (4). Action of β -gal on PFONPG in saline. ^{19}F NMR showed a single narrow signal at δ -42.75 ppm and a chemical shift response $\Delta\delta > 5$ ppm upon cleavage, which was also accompanied by a colorimetric change to yellow (inset). Sodium trifluoroacetate was used as a chemical shift reference (δ 0 ppm).

The pH sensitivity of the product aglycone presents the interesting possibility of selective determination of pH at the site of enzyme activity. In some cases, we have observed a split peak in cells transfected to express β -gal, which may indicate a transmembrane pH gradient (Fig. 6). We have demonstrated that if the aglycone (PFONP) is added to a suspension of red blood cells, two signals are rapidly observed representing the intra and extra cellular pH³. However, PFONP is somewhat toxic and can cause lysis of less robust cells. Thus, PFONPG may be regarded as an interesting prototype molecule primarily representative of a new approach to NMR gene reporter molecules for use in association with β -galactosidase. We have synthesized series of analogues with the fluorine atom placed at various locations on the phenolic ring and incorporating alternate substituents, such as Cl and Br. Each adduct and aglycone provides a unique chemical shift allowing ready comparison of susceptibility to enzyme activity (manuscript in preparation). For the various substrates, the change in chemical shift ranged from a minimum of 1.57 ppm to a maximum of 12.89 ppm. The chemical shift accompanying cleavage depends strongly on the orientation of the F-atom with largest response for para-F and less for ortho-F. The rate of cleavage was closely related to the pK_a of the aglycone commensurate with enzyme studies reported

previously [84]. Although β -gal accepts a wide range of substrate structures, there was no activity on an alpha anomeric substrate. Ortho fluoro ortho nitrophenyl galactoside (OFONPG) was found to be substantially less toxic (preliminary studies Yu and Ma). Preliminary investigations also show the feasibility of conjugating other aglycones, such as the pH reporter 6-fluoropyridoxol [28] to galactose, generating an effective substrate for β -gal⁴. Given the different chemical shifts of individual substrates and

products, we believe there will be opportunities to establish optimized reporter molecules based on one-pot combinatorial approaches.

The chemical shift difference between substrate and aglycone product reveals unambiguous detection of enzyme activity. Signal to noise could be enhanced by introduction of a trifluoromethyl (CF₃) reporter group, as opposed to the single F-atom. However, a CF₃ group will likely perturb the water solubility to a greater extent and the chemical shift response is expected to be considerably smaller, due to transmission of the electron density redistribution through an additional carbon-carbon bond⁵.

The concept of ^{19}F NMR reporter molecules for detecting gene activity is in its infancy, but we believe it has great promise for future development.

3.2 pH

Development of ^{19}F NMR pH indicators (Table 4) has followed three strategies: i) development of molecules specifically designed for ^{19}F NMR, ii) fluorinated analogues of existing fluorescent indicators, iii) exploitation of the ^{19}F NMR chemical shift sensitivity inherent in cytotoxic drugs.

³ Cui, W., Otten, P., Merritt, M., and Mason, R. P., Proc. 10th ISMRM, Honolulu, Hawaii, USA, 2002, p. 385.

⁴ Yu, X. and Mason, R. P., Proc. 11th ISMRM, Toronto, Canada, 2003, p. 675.

⁵ Cui, W., Otten, P., Yu, J., Kodibagkar, V., and Mason, R. P., Proc. ISMRM, Toronto, Canada, 2003, p. 675.

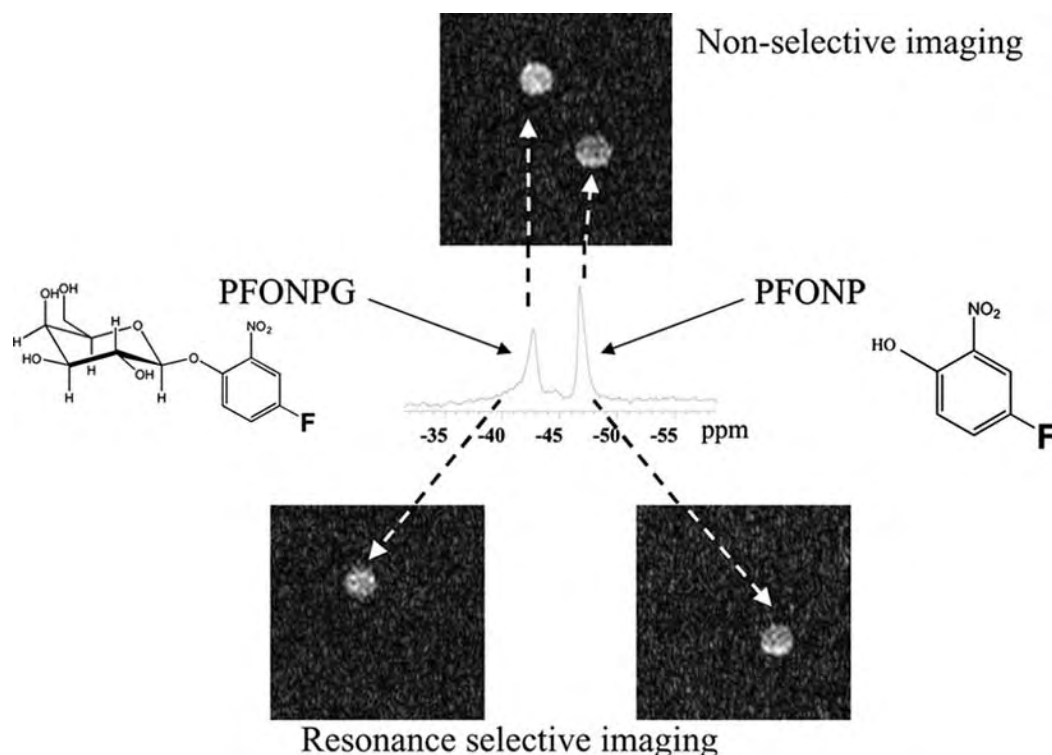


Fig. (5). ^{19}F MRI at 4.7 T of a phantom comprising vials of PFONPG and PFONP in buffer. Frequency selective excitation provides separate images of substrate (PFONPG) and aglycone product (PFONP).

The high sensitivity of ^{19}F NMR chemical shift to the microenvironment has prompted widespread application to pH indicators, as reviewed recently [28]. Many molecules exhibit chemical shift response to changes in pH, *e.g.*, the ^{19}F NMR resonance of 6-fluoropyridoxol. On the NMR time scale, protonated and deprotonated moieties are generally in fast exchange, so that a single signal is observed

representing the amplitude weighted mean of acid and base forms. As such, measurements of chemical shift may be directly related to pH in the form of a titration curve. pH values are calculated from the spectra on the basis of chemical shift of δ_{obs} with respect to a standard. The pH is measured using the Henderson-Hasselbalch equation:

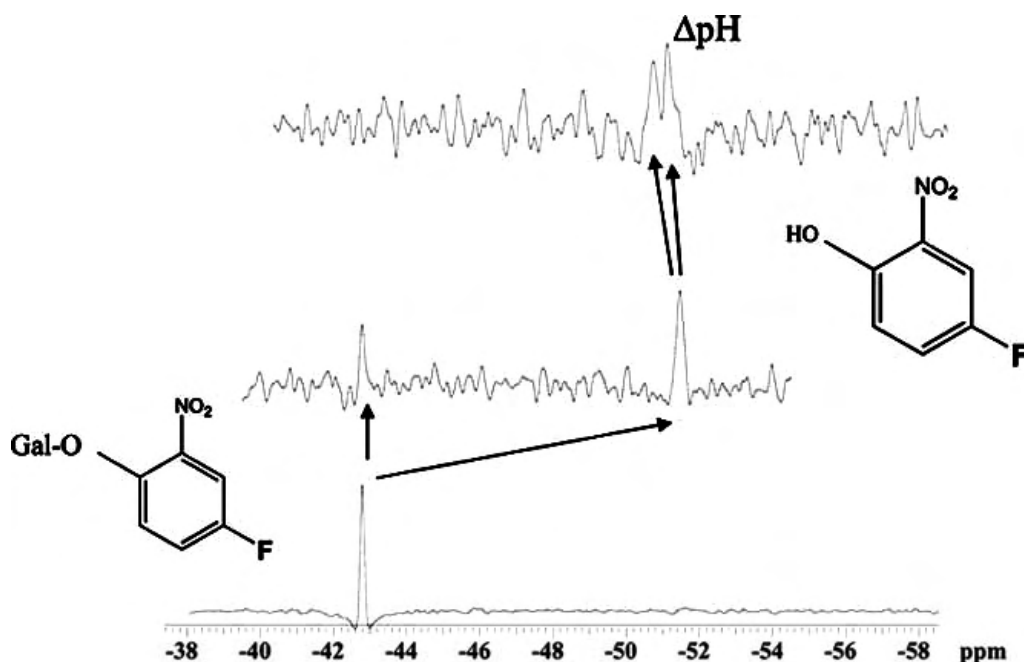
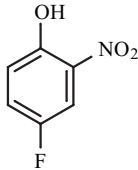
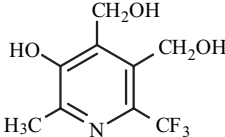


Fig. (6). Conversion of PFONPG by PC3 human prostate cancer cells transfected for 48 h using adenovirus to transiently express lacZ under CMV promoter. The split peak in the upper spectrum suggests a transmembrane pH gradient (Mason, Otten, Li and Koenenman, *Proc. ISMRM 10th Scientific Meeting*, 2002).

Table 4 ¹⁹F NMR pH indicators

Reporter	Structure	pKa	Chemical Shift Response (Δδ ppm)	References
3-fluoro-2-methylalanine		8.5	1.1	[86]
3,3-difluoro-2-methylalanine		7.3	2	[86]
3,3,3-trifluoro-2-methylalanine		5.9	2	[86]
2-difluoromethyl ornithine		6.4	0.4	[103]
N,N-(methyl-2-carboxyisopropyl)-4-fluoroaniline		5.8	17	[105]
FQuene		6.7	4.8	[102]
6-FPOL		8.2	9.7	[28, 45, 94]
5F-NEAP-1		6.9	11	[106]
5F-NEAP-2		6.6	11	[106]
ZK 150471		7.3	11	[109, 110]

(Table 4). contd.....

Reporter	Structure	pKa	Chemical Shift Response($\Delta\delta$ ppm)	References
PFONP		6.9	9.3	[29]
CF ₃ POL		6.8	1.7	6

Due to the non-linear form of the equation, greatest sensitivity is found close to the pKa. If exchange is slow on the NMR time scale both protonated and deprotonated structures provide separate signals simultaneously. In this case, the ratio of signals provides an indication of pH. Such is often the case in reporter molecules for metal ions (section 3.3, below). Another critical time scale is movement of reporter molecules between compartments, which gives rise to signal averaging as encountered for trifluoroethylamine [85]. Should exchange fall into an intermediate exchange regimen signal may be severely broadened or lost altogether. Such exchange rates are strongly temperature and magnetic field dependent.

$$\text{pH} = \text{pKa} + \log 10 \left[\frac{\delta_{\text{obs}} - \delta_{\text{acid}}}{\delta_{\text{base}} - \delta_{\text{obs}}} \right] \quad (1)$$

3.2.1 Fluoro Amino Acids

Deutsch *et al.* [86, 87] championed the use of ¹⁹F NMR of fluorinated indicators to measure intracellular pH. The first studies used trifluoroethylamine, which provided both intra- and extracellular signals in blood at 4 °C [85]. However, at room temperature transmembrane exchange accelerated and fell into the intermediate exchange regime causing severe line broadening. Based on this approach a series of fluorinated agents was developed, particularly, using mono-, di- and tri- D, L,- 2-amino- 3,3- difluoro-2-methyl propanoic acid (Table 4). These molecules have been successfully applied to pH measurements in peripheral blood lymphocytes [86, 88, 89], isolated hepatocytes [90], rabbit colon and frog skin [86]. Thoma and Ugurbil [91] used this approach in a perfused liver. Comparison of pH measurements determined using ³¹P NMR of inorganic phosphate (P_i) or difluoromethyl alanine showed close similarity. Toxicity was low and the molecules were stable, but loading indicators into cells is problematic. Generally, methyl esters have been used, which are relatively stable in water, but undergo non-specific enzymatic hydrolysis intracellularly, liberating the pH-sensitive molecules [87]. This approach can lead to complex spectra including overlapping multi-line ester and liberated free acid resonances from both intra- and extracellular compartments

[92]. For investigations in perfused organs or cell culture, extracellular indicator can be washed away with unlabeled perfusate, after loading the intracellular compartment, in order to simplify the NMR spectra. The mono- and trifluoro derivatives require an additional chemical shift reference standard, *e.g.*, sodium trifluoroacetate. An advantage of the difluoro derivative is that the relative chemical shifts of the resonances of the ¹⁹F AB quartet are pH sensitive obviating the need for a standard. However, the multiple signals do cause decreased SNR and both mono and difluoro derivatives require ¹H-decoupling for efficient utilization. Widespread use of these molecules has been hindered by the problem of loading the indicators into cells and the relatively small chemical shift range ~ 2 ppm.

3.2.2 Fluorinated Vitamin B6 Derivatives

Analogues of vitamin B6, *e.g.*, 6-FPOL (2-fluoro-5-hydroxy-6-methyl-3,4-pyridinedimethanol) are highly sensitive to pH [45, 93-95]. Synthesis of 6-FPOL is achieved in three steps starting from pyridoxine hydrochloride [96]. Diazotization of pyridoxine with benzene diazonium chloride yields 6-phenazopyridoxol and dithionite reduction produces 6-aminopyridoxol. 6-FPOL is then obtained using a modified Schieman reaction. 6-FPOL readily enters cells and provides well resolved resonances reporting both intra- and extracellular pH (pHi and pHe), simultaneously, in whole blood [45] and the perfused rat heart, as confirmed by ³¹P NMR and pH electrodes [93]. In contrast to other pH indicators, 6-FPOL readily enters certain cells without the need for loadable derivatives. For blood cells, this may be related to transport, since vitamin B6 is naturally stored, transported, and redistributed by erythrocytes [97]. *In vivo*, we have generally only observed a single signal from tumors implanted in rats or mice suggesting extra cellular signal only, and it is often broad suggesting tumor heterogeneity (Fig. 7). The molecule not only has a remarkable chemical shift range (~ 10 ppm), but in contrast to many pH indicators there is negligible response to changes in metal ion concentrations, the presence of proteins, or variations in temperature [93]. The somewhat basic pKa = 8.2 is appropriate for investigations of cellular alkalosis, but it is not ideal for studies in the normal physiological range (6.5-7.5).

⁶ Cui, W.; Otten, P.; Yu, J.; Kodibagkar, V.; Mason, R.P., Proc. ISMRM, Toronto, Canada, 2003, p. 675.

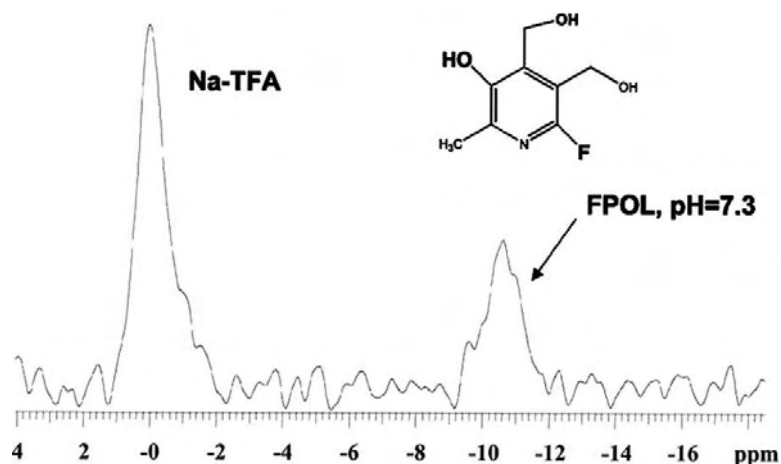


Fig. (7). 188 MHz ¹⁹F NMR of rat pedicle breast tumor 13762NF following administration of 470 μmol FPOL i.p. together with NaTFA. The broad ¹⁹F NMR signal indicates pH = 7.3.

The response of ¹⁹F NMR chemical shift to pH in the physiological range in these molecules is considered to be mainly due to protonation and deprotonation of the 3-phenolic OH [96, 98]. This affects the electronic environment around fluorine at the 6-position, which is particularly pronounced due to the para location. Extensive literature on modifications of vitamin B₆ suggested that the introduction of electron donating or withdrawing groups at the 4 and 5 positions of the pyridoxol ring could significantly alter the pK_a of the 3-phenolic group, and the NMR properties at the 6-position [95, 99, 100]. From a series of analogs 6-fluoropyridoxamine (6-FPAM) was identified as an enhanced pH indicator (pK_a 7.05) [94]. Other analogs had pK_a in the range 5.5 to 9.5 with chemical shift response of 7.5 to 12.1 ppm. 6-FPAM also has a single narrow resonance in solution with chemical shift independent of environment, other than pH. Like with 6FPOL, we have observed intra and extracellular signals in whole blood and perfused rat hearts [28, 94]. On rare occasions, we have seen evidence for intra and extra cellular signals in tumor cells (Fig. 8) ⁷. Given the large chemical shift range for ¹⁹F, signal interference is rare. However, there can be conflict between signals from the popular anesthetic gas isoflurane (δ = 5 and 11 ppm) and the Vitamin B₆ indicators (δ 9.8 - 20 ppm) (Fig. 9). Such interference can be avoided by using alternate anesthetics.

To enhance SNR, or reduce the required dose, a pH sensitive CF₃ moiety could be introduced in place of the F-atom. The chemical shift range decreases (Δδ~ 1.64 ppm)⁸, as expected since electronic sensing must be transmitted through an additional C-C bond. Importantly, the ¹⁹F NMR signal occurs downfield from NaTFA and there is no longer any interference from the isoflurane signals ⁶ (Fig. 9). While FPOL and FPAM provide both intra and extra cellular signals with varying ratios depending on cell type. CF₃POL

is found to occur exclusively in the extra cellular compartment, and thus reports pHe, or interstitial pH.

3.2.3. Fluorophenols

Many fluorophenols are commercially available facilitating ready evaluation as physiological indicators (Aldrich, Lancaster). Based on our observations with the fluorophenol galactosides, we explored the use of the aglycones as pH indicators. As expected, o-fluorophenols have a smaller chemical shift range (~ 0.3 to 2.2 ppm), as opposed to p-fluorophenols, which exhibit Δδ 6.4 to 11.3 ppm. pK_a was found in the range 5.4 to 9.8 ppm depending on substituents (Yu, Cui, Otten, unpublished observations). PFONP has Δδ 9.29 ppm and pK_a 6.85 [29]³. PFONP appears cytolytic for certain tumor cells and may act as an ionophore. However, we have obtained pH gradient measurements in whole blood, which were in agreement with FPOL and electrode measurements³. Trifluoromethylphenols also show titration response though typically, Δδ = 1.2 ppm (p-CF₃ArOH, pK_a 8.5) to 0.4 ppm (o-CF₃-Ar, pK_a 7.92) (Cui, Yu unpublished).

3.2.4. Other pH Reporters

By modifying known fluorescent pH indicators, Metcalfe *et al.* reported a series of fluorinated molecules, which were sensitive to various ions, *e.g.*, Ca²⁺, Zn²⁺ and H⁺ [101]. F-quene, a ¹⁹F NMR sensitive analog of the fluorescent pH indicator quene-1, was used to measure intracellular pH in a perfused heart [101] and liver [102]. The chemotherapeutic agent difluoromethyl ornithine has a small chemical shift range, which is also temperature sensitive, but it has been tested in rat tumors [103]. Bental and Deutsch [104] reported a fluoro-iso-butyric acid derivative, which has the advantage of a single ¹H decoupled-¹⁹F NMR resonance, improving the signal to noise ratio (SNR). Taylor and Deutsch [105] showed that N-methyl methoxyisopropyl fluoroaniline had a chemical shift range ~17 ppm, but the pK_a (5.8) was less suitable for *in vivo* investigations. Modification to methoxyisopropyl fluoroaniline [105] retained a substantial chemical shift range (Δδ 12 ppm) and produced a physiologically suitable pK_a, however, no biological studies have been reported. N-ethylaminophenol (NEAP) has been

⁷ Cui, C., Ma, Z., He, S., Peschke, P., and Mason, R. P., 8th Int. Conf. Tumor Microenvironment and Its Impact on Cancer Therapies, Miami (South Beach), FL, 2003, p. II-5.

⁸ Yu, J., Otten, P., Cui, W., and Mason, R. P., 38th National Organic Symp., Bloomington, IN, 2003, p. B2.

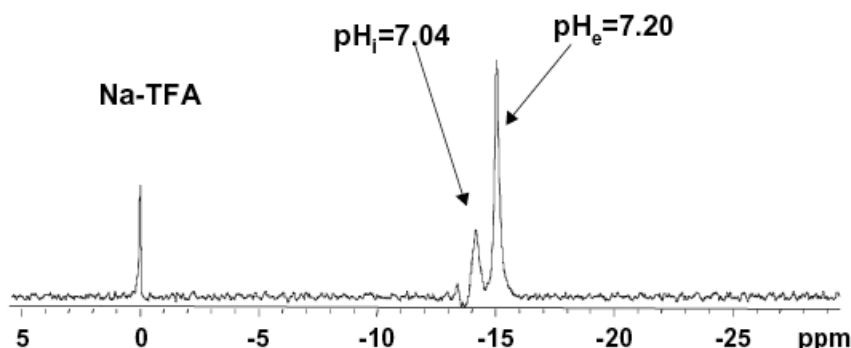


Fig. (8). ^{19}F NMR (9.4 T) of a suspension of 10^7 Morris hepatoma MH-Tk cells in buffer following addition of FPAM (58.3 mM) showed two signals attributed to intra and extra cellular compartments at -14.16 ppm and -15.04 ppm, corresponding to $\text{pH}_i = 7.04$ and $\text{pH}_e = 7.20$. (data obtained in collaboration with Drs. Peter Peschke and Uwe Haberkorn, DKFZ, Heidelberg, Germany).

described with various analogs to detect pH or metal ions [106]. Frenzel *et al.* [107] have described a fluoroaniline sulfonamide (ZK 150471) and its use has been demonstrated in mice and rats to investigate tumor pH [108, 109]. This molecule is restricted to the extracellular compartment only [107, 110], but combination with ^{31}P NMR of P_i to determine pH_i has been used to reveal the transmembrane pH gradient in mouse tumors [111]. A distinct problem with ZK150471 is that the pK_a differs in saline and plasma [110]. Both NEAP [106] and ZK150471 [107] have non-titrating intramolecular chemical shift references.

Wherever a difference exists between normal tissue and cancer there is an opportunity for selective therapy. For instance, molecular partitioning into cells is influenced by the pH gradient and many drugs are weak acids or bases [112-116]. However, the pH gradient (ΔpH) is often small and distinctly variable, and thus, the tumor microenvironment may need to be manipulated to further enhance cytotoxicity, *e.g.*, infusion of glucose or ionophores may cause tumor acidification [113, 117-120]. Inhalation of carbogen (5% CO_2 /95% O_2) was reported to reduce pH_e and generate a pH gradient ~ 0.1 units in large murine RIF-1 tumors [111]. This corresponded with the typical pH gradient found in small RIF-1 tumors, though they apparently did not respond to carbogen. Dietary alkaline load is reported to produce extracellular alkalization leading to

$\text{pH}_e > \text{pH}_i$ in nude mice bearing a xenografted breast tumor [115].

PH may be measured using ^{31}P NMR of endogenous P_i , though intra and extra cellular concentrations are variable and may not always be resolved [121, 122]. ^{19}F NMR agents can provide a much wider chemical shift range and in some cases report transmembrane pH gradient, though further development is needed for widespread application. Often, only a single global pH value is obtained, though chemical shift imaging (CSI) has been used to map pH based on ^1H and ^{31}P NMR [123, 124] and new ^1H pH sensitive relaxation contrast agents have been reported and reviewed [10, 32, 125, 126].

3.3. Metal Ions

Several metal ions are thought to play key roles in cellular physiological processes. Thus, there has been much interest in developing specific reporter molecules. The greatest availability is in the realm of fluorescent indicators, specifically, agents incorporating extended aromatic and conjugated structures, where the wavelength of fluorescence depends upon specific binding of a metal ion. Indeed, many agents are now commercially available (*e.g.*, Molecular Probes). The addition of fluorine atoms has yielded ^{19}F NMR reporters (Table 5).

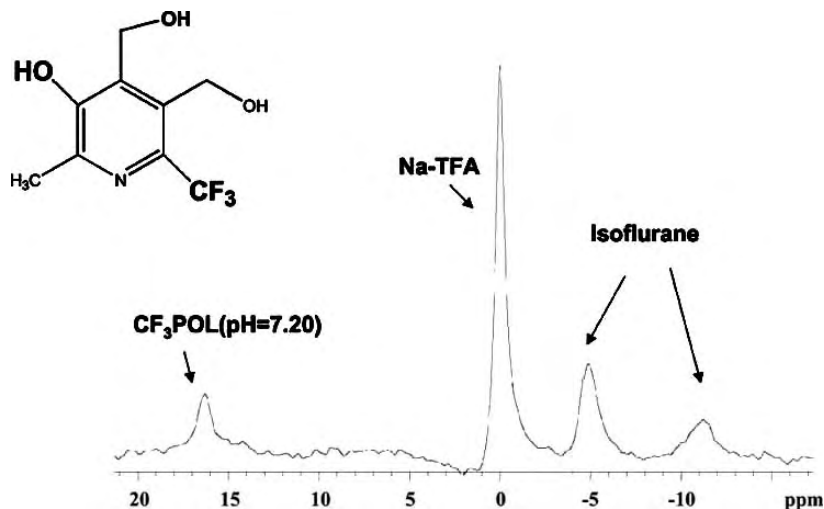
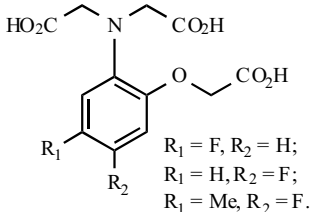
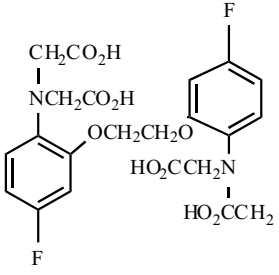
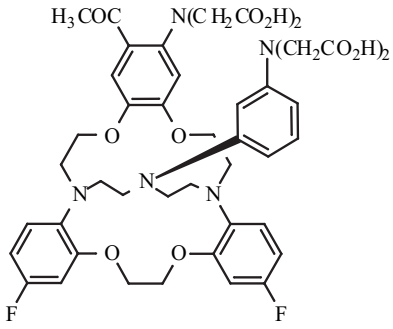
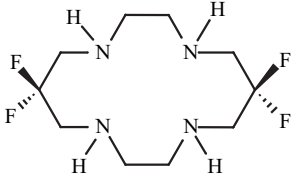
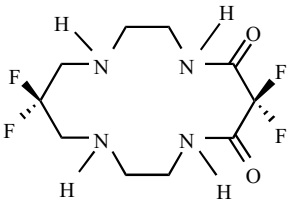
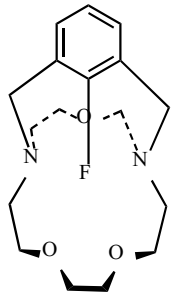
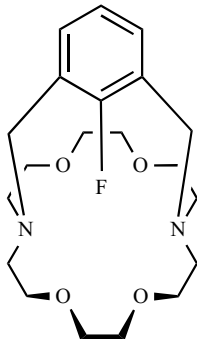
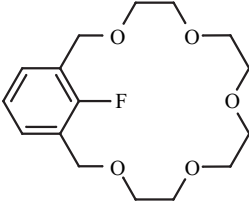
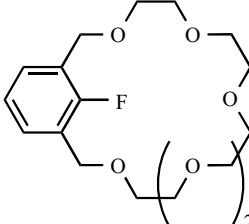


Fig. (9). 188 MHz ^{19}F NMR of Dunning prostate R3327-AT1 rat tumor ($\sim 1 \text{ cm}^3$) following administration of CF_3POL (320 mg/kg) with 17 min acquisition. NaTFA was used as chemical shift reference at 0 ppm and isoflurane anesthetic signals are also observed.

Table 5. ¹⁹F NMR Metal Ions Indicators

Detected Ion	Agent	Structure	Application
[Mg ²⁺]	F-APTRA	 <p> $R_1 = F, R_2 = H;$ $R_1 = H, R_2 = F;$ $R_1 = Me, R_2 = F.$ </p>	Erythrocytes [36, 142]
[Ca ²⁺]	5F-BAPTA		Tumors, cells, heart [36, 101, 130, 366, 367]
[Na ⁺]	F-cryp-1		Tumors, cells, heart [145]
[Ni ²⁺]	F-Cyclam		[368]
[Cu ²⁺]	F-Dioxocyclam		[368]
[Li ⁺]	FN ₂ O ₃		[136]

(Table 5). *contd..*

Detected Ion	Agent	Structure	Application
[K ⁺]	FN ₂ O ₄		[136]
[Sr ²⁺]	FO ₅		[136]
[Ba ²⁺]	FO ₆		[136]
Membrane/ Chloride Potential	TFA	CF ₃ CO ₂ ⁻	Cells, perfused heart [349, 350]

3.3.1 Detection of Calcium Ions

A fundamental development was that of Tsien, *et al.* [127], who proposed loading fluorescent metal ion chelators into cells using acetoxymethyl esters and demonstrated 1,2-bis(o-amino-phenoxy)ethane-N,N,N',N'-tetraacetic acid (BAPTA) for detecting intracellular calcium ions. Metcalfe, *et al.* [101] added para-fluoro atoms to the aromatic ring yielding a ¹⁹F NMR responsive agent (5,5-difluoro-1,2-bis(o-amino-phenoxy)ethane-N,N,N',N'-tetraacetic acid (5FBAPTA)) (Table 5). Upon binding calcium, there is a change in chemical shift. Ideally, such a reporter molecule would have high specificity for the metal ion of interest. In fact, the F-BAPTA agents are found to bind several divalent metal ions, including Ca²⁺, Zn²⁺, Pb²⁺, Fe²⁺, and Mn²⁺ [128, 129]. However, there is a very low affinity for Mg²⁺. Fortunately, each metal ion chelate has an individual chemical shift, so that they can be detected simultaneously [130] and do not directly interfere with measurements.

5FBAPTA includes two fluorine atoms symmetrically placed to provide a single signal. Upon binding there is slow exchange of Ca²⁺, on and off the indicator, on the NMR time scale, so that separate signals are seen for the free and metal ion bound moieties, with chemical shifts of several ppm. Calcium concentration may be calculated from the formula [130].

$$[\text{Ca}^{2+}] = K_D [\text{Ca-FBAPTA}] / [\text{FBAPTA}].$$

Typical calcium concentrations detected in cells, have been independently verified using fluorescence [130]. However, it is important to recognize that the dissociation constant (K_D) does depend on pH, ionic strength, and the concentration of free Mg²⁺, which need to be estimated independently. In many cases, pH can be estimated from the chemical shift of inorganic phosphate using ³¹P NMR. Of course, it can also be estimated using fluorinated pH indicators, as discussed above (Section 3.2). Magnesium ion concentrations may be estimated from the chemical shifts of the resonances of ATP, which vary upon binding magnesium [131, 132]. Signals from both bound and unbound forms allow ready identification of the moieties, avoiding the need for incorporation of a chemical shift reference. 5FBAPTA has been used extensively [130] in studies of tumor cells [133], osteoblastic cells [134] thymocytes [129], blood, and the perfused beating heart, where studies of calcium transients during the myocardial cycle have been reported [135]. A variant is 4F-BAPTA, which has a somewhat lower binding constant $K_D = 0.7 \mu\text{M}$, but more significantly at 94 MHz is found to be in fast exchange [130]. Thus, the signals from the bound and unbound forms are averaged, and it is the absolute chemical shift, which is related to the ratio of the two components. Plenio and Diodone have also reported fluorocrown ethers,

which exhibit chemical shift response upon binding Ca^{2+} [136]. Of course, calcium could potentially be analyzed directly by ^{43}Ca NMR, however, its natural abundance is <0.2%, its sensitivity is <1% that of ^1H , and being quadrupolar, it is liable to extensive line broadening [44]. Thus, the application of ^{19}F NMR with appropriately designed reporter molecules gives insight into cytosolic $[\text{Ca}^{2+}]$.

A critical issue for intracellular interrogation is loading the reporter molecule into cells. The tetra-carboxylates do not penetrate cells, however, derivatization as acetoxymethyl esters, which has been very widely used in association with analogous fluorescent indicators provides a more lipophilic entity, which can equilibrate across cell membranes [127]. These esters are specifically designed so that intra-cellular esterases cleave the acetoxy methyl ester, releasing the charged reporter molecule, which is then essentially trapped in the intracellular compartment. The release of acetic acid and formaldehyde are considered to be relatively innocuous.

3.3.2 Detection of Magnesium Ions

Magnesium ions can occur in tissues and cells at millimolar concentrations and play an important role in many physiological processes [137, 138]. There are many fluorescent indicators for detection, together with ion selective electrodes [139]. Magnesium can also be estimated based on the chemical shift difference of the resonances of ATP using ^{31}P NMR [131, 132]. However, ^{31}P NMR has intrinsically low signal to noise, exacerbated under many pathophysiological conditions, such as ischemia. Thus, there has been considerable interest in developing fluorinated NMR reporter molecules for detecting $[\text{Mg}^{2+}]$. The simplest is, perhaps, fluorocitrate [140]. Upon binding Mg^{2+} there is a change in chemical shift. However, fluorocitrate can be incorporated into the tri-carboxylic acid cycle as a potent highly toxic suicide inhibitor. Thus, it is critical that the reporter molecule be used as the plus isomer only, which shows little toxicity [141]. Given the difficulties in synthesis, and specifically isomeric isolation, alternative indicators have been sought. Levy, *et al.* [36, 142] developed classes of indicators based on the APTRA structure, both for fluorescent application and by incorporation of fluorine atoms for ^{19}F NMR. APTRA agents must be derivatized as acetoxymethyl esters in order to load tissues, and they have been reported for use in the perfused rat heart [143].

3.3.3 Other Biological Relevant Ligands

As described in 3.3.1, F-BAPTA provides a unique chemical shift with many divalent metal ions [128, 129] and has been used to estimate $[\text{Zn}^{2+}]$ [128], $[\text{Pb}^{2+}]$ [144], and $[\text{Cd}^{2+}]$ [128]. Other investigators have designed molecules to specifically interact with sodium ions. F-Cryp-1 was used to show that the total ^{23}Na NMR signal visible is less than 100% [145]. London and Gabel [146] reported fluorobenzene boronic acid, which interacted with specific sugars. Plenio and Diodone [147] reported fluorine containing cryptands, which interact with perchlorate. These investigators have also reported a series of fluorocyclophanes and fluoro crown ethers to explore specific cation binding (*e.g.*, K^+ , Li^+ , Na^+ , Ba^{2+} , Sr^{2+} , Ca^{2+} , and associated chemical shifts [136, 148].

Takamure [149] reported macrocycles designed to bind K^+ , NH_4^+ , and Ag^+ .

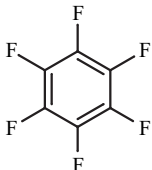
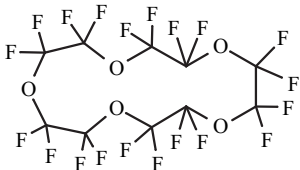
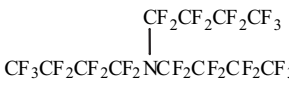
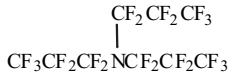
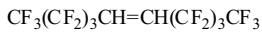
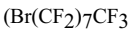
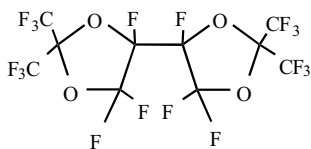
3.3.4 Reporter Molecules for Detection of Ions

In considering reporter molecules, a number of criteria are pertinent. The reporter molecule must in some way reach the cellular compartment of interest. Some molecules penetrate cells directly, for others it is facilitated by acetoxymethyl esters. In other cases specific cellular exclusion is important, so that any signal can unambiguously be attributed to the extra-cellular or interstitial compartment in a tissue. Such measurements would be analogous to electrode measurements. It is critical that the reporter molecule not perturb the system under investigation. For ions, there is inevitably some binding and complexation. Provided there is sufficient reservoir of the ions, there can be rapid re-equilibration, and the concentration may give a realistic indication of the free concentration. In unregulated systems, this may be less reliable. The fluorine NMR spectrum must be perturbed upon interaction with the ion of interest. This may be through the formation of a second signal, as in the slow exchange regime, or chemical shift in a fast exchange regime. Changes may be observed in coupling constants or relaxation times. For many ions, agents should be water soluble, although a degree of lipophilicity may help in transport. Signals should be narrow to enhance both the signal to noise and spectral resolution. The binding constant must be compatible with the typical concentration encountered *in vivo*. Ideally, the reporter ligand is highly selective for the ion of interest and of course the molecule should exhibit minimal toxicity. Further criteria are that the reporter molecule be readily available, particularly when complex synthesis is required. Reporter molecules, which are described in the literature, may not be readily available to other investigators.

3.4. Tissue Oxygenation and Hypoxia

While reporter molecules for enzyme activity and ions (Sections 3.1-3, above) are based almost exclusively on chemical shift response, measurement of pO_2 is based on variations of relaxation rates, as reviewed recently [27]. Hypoxia sensing agents rely on enzyme activated trapping [150]. It has long been appreciated that hypoxic tumor cells are more resistant to radiotherapy [151]. Indeed, a three fold increase in radio resistance may occur when cells are irradiated under hypoxic conditions compared with $\text{pO}_2 > 15$ torr for a given single radiation dose. However, recent modeling has indicated that the proportion of cells in the range 0 - 20 torr may be most significant in terms of surviving a course of fractionated radiotherapy [152]. Certain chemotherapeutic drugs also present differential efficacy depending on hypoxia [153, 154]. Increasingly, there is evidence that hypoxia also influences such critical characteristics as angiogenesis, tumor invasion and metastasis [155-158]. Given that hypoxic tumors are more resistant to certain therapies, it becomes important to assess tumor oxygenation as part of therapeutic planning. Patients could be stratified according to baseline hypoxia to receive adjuvant interventions designed to modulate pO_2 , or more intense therapy as facilitated by IMRT (Intensity Modulated Radiation Therapy). Tumors, which do not respond to

Table 6. ^{19}F NMR Characteristics and Applications of PFCs for Tissue Oximetry

Name	Structure	Sensitivity to pO_2 ^a	Temp. Sensitivity (torr/ $^{\circ}\text{C}$) ^b	Applications
HFB		A=0.0835 B=0.001876	0.13	Rat breast and prostate tumors, human lymphoma xenograft [27, 169, 173, 199-202, 215, 218]
Perfluoro-15-crown-5-ether		A=0.345 B=0.0034	0.94	Tumor cells, mouse tumor, spleen, liver, human glioma tumor in mice, rat breast tumor, rat brain [150, 170, 191, 194, 197, 198, 210]
FC-43		A=1.09 B=0.00623	4.43	Rodent liver, spleen, lung, eye, tumors, heart and human eye [168, 184, 189, 207, 214, 369, 370]
PFTP		A=0.314 B=0.002760 ⁻³		Rat subcutaneous tumor, spleen, lung, tumors, cells [46, 195]
F-44E		A=0.2525 B=0.16527	0.59	Alginate capsules, rodent spleen, liver, tumors [186, 196, 205]
PFOB		A=0.2677 B=0.12259	1.26	Rat heart, prostate tumor, rabbit liver, [162, 171, 172, 190, 371]
PTBD		A=0.50104 B=0.1672		phantom [372]

^a $R_1 \text{ (s}^{-1}\text{)} = A + B \cdot \text{pO}_2 \text{ (torr)}$ ^b variation in pO_2 per $^{\circ}\text{C}$ error in temperature estimate

interventions, may be ideal candidates for hypoxia selective cytotoxins (*e.g.*, tirapazamine [159]).

3.4.1. Fluorinated pO_2 Reporter Molecules

The ^{19}F NMR spin lattice relaxation rate R_1 of a perfluorocarbon varies linearly with pO_2 [27, 33, 160] and may be sensitive to temperature, and magnetic field. Importantly, R_1 of PFCs is essentially unresponsive to pH, CO_2 , charged paramagnetic ions, mixing with blood, or emulsification [46, 160-166]. For an emulsion of perfluorotributylamine, we have shown that the calibration curves obtained in solution are valid for PFC sequestered in tissue [167]. At any given magnetic field (B_0) and temperature (T), sensitivity of R_1 to changes in pO_2 is given by the linear relationship

$$R_1 = A + B \cdot \text{pO}_2.$$

The value of the intercept A represents the anoxic relaxation rate and the slope B represents the sensitivity of the reporter molecule to the paramagnetic contribution of

oxygen to the relaxation rate. The ratio $\eta = B/A$ has been proposed as a sensitivity index [168]. Small A , and hence long T_1 , potentially creates long imaging cycles, but this is readily overcome by applying single shot (echo planar) imaging techniques [169-171]. A particular PFC molecule may have multiple resonances, and each resonance has a characteristic R_1 response to pO_2 and temperature due to steric effects of O_2 , as it approaches the molecule [37, 50]. Characteristics of many reported PFCs are summarized in (Table 6).

R_1 is sensitive to temperature, although the response varies greatly between PFCs and between individual resonances of each individual PFC. Over small temperature ranges, a linear correction to calibration curves is appropriate, but over larger temperature ranges the response can be complex [50]. Differential sensitivity of pairs of resonances to pO_2 and temperature allowed Mason, *et al.* [167] to simultaneously determine both parameters by solving simultaneous equations. However, generally it is preferable for a pO_2 sensor to exhibit minimal response to

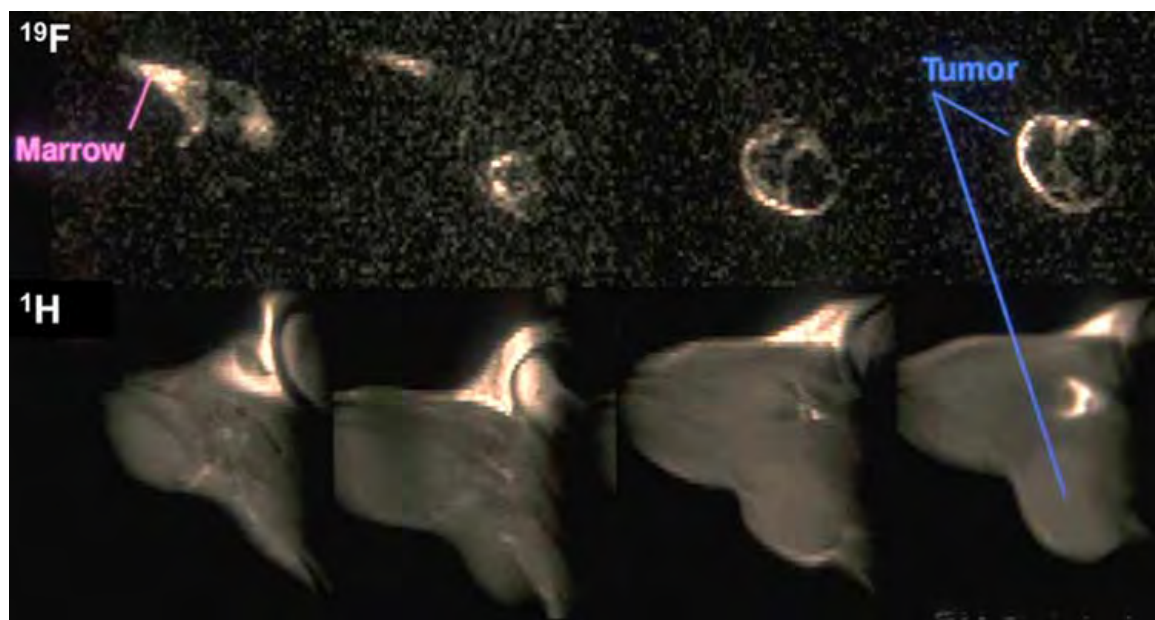


Fig. (10). ^{19}F MRI of Novikoff hepatoma in thigh of rat. Oxypherol emulsion was administered (4x4 ml over two days) and allowed to clear from the vasculature. ^1H MRI shows the tumor (~ 1 cm diameter) and thigh muscle. The corresponding ^{19}F MRI shows sequestered PFC in the bone marrow and around the periphery of this multi nodular tumor (image resolution 470 x 300 μm with 5 mm slice thickness) (From R. P. Mason, P. Peschke, E. W. Hahn, A. Constantinescu and P. P. Antich, Proc. 1st SMR, Dallas, S12-059, 1994).

temperature, since this is not always known precisely *in vivo* and temperature gradients may occur across tumors. Even a relatively small error in temperature estimate can introduce a sizable discrepancy into the apparent pO_2 based on some PFCs, *e.g.*, the relative error introduced into a pO_2 determination by a 1 $^\circ\text{C}$ error in temperature estimate ranges from 8 torr/ $^\circ\text{C}$ for perfluorotributylamine [167], to 3 torr/ $^\circ\text{C}$ for PFOB (perflubron) [172] or 15-Crown-5-ether [170], when pO_2 is actually 5 torr. HFB exhibits remarkable lack of temperature dependence and the comparative error would be 0.1 torr/ $^\circ\text{C}$ [173].

Thomas, *et al.* [33], pioneered the application of ^{19}F NMR relaxometry to measure pO_2 in tissues, *in vivo*, including lung, liver, and spleen with investigations relative to various interventions. PFCs are extremely hydrophobic and do not dissolve in blood directly, but may be formulated as biocompatible emulsions for intravenous (IV) infusion. Emulsion stability is critically dependent on the vapor pressure of the PFC and the emulsifying components, such as surfactants, and phospholipids. PFC emulsions have been developed commercially both as potential synthetic blood substitutes (*e.g.*, Oxygent[®], Fluosol[®], Therox[®], Oxypherol[®]) [174-177] and as ultrasound contrast agents (*e.g.*, Optison[®], Definity[®], Sonovue[®], Imagent[®] [178, 179]. Following IV infusion, a typical blood substitute emulsion (*e.g.*, Oxypherol[®], Imagent[®]) circulates in the vasculature with a half-life of 12 h providing substantial clearance within two days [175]. Primary clearance is by macrophage activity leading to extensive accumulation in the liver, spleen, and bone marrow [180, 181]. Indeed, this is a major shortcoming of IV delivery, since animals may exhibit extensive hepatomegaly or splenomegaly [175, 180, 182]. The emulsions are not toxic, and other than causing swelling, appear not to cause health problems [175]. PFC is retained in the liver with a typical half-life of 60 days for

perfluorotripropylamine and 3 days for perflubron, with primary clearance by migration to the lungs and exhalation [181]. Some investigators have examined pO_2 of tissues, while PFC remained in the blood, providing a vascular pO_2 measurement [163, 183-186]. Flow can generate artifacts and correction algorithms have been proposed ⁹. More extensive pO_2 measurements have been reported following clearance from the blood, in liver, spleen, abscess, perfused heart, and tumors [169, 170, 186-202].

Uptake and deposition of PFC emulsions in tumors is highly variable and heterogeneous (Fig. 10) typically, accounting for 1-5% of sequestered material [180]. Most signal occurs in well perfused regions, and indeed pO_2 values measured soon after intravenous infusion, but following vascular clearance, are generally high, approaching arterial pO_2 [187]. PFC does not seem to redistribute within tissue, but remains associated with specific locations. It has been shown that new tumor tissue grew around initially labeled tissue [187]. Peripheral distribution was also observed in a Novikoff hepatoma implanted in a rat (Fig. 10). Intriguingly, this tumor showed spontaneous regression following administration of PFC emulsion, but the tumor periphery remained labeled and signal coincided with tumor shrinkage (Fig. 11). The location of the tumor could still be identified even after the tumor had shrunk below palpable size. Such long term tissue marking has been proposed as a form of non-invasive histology and might have new applications for tracing stem cell grafts and cell migration ¹⁰. Recently, cell labeling has been developed based on cellular retention of superparamagnetic iron oxide particles

⁹ Higuchi, T., Naruse, S., Horikawa, Y., Hirakawa, K., and Tanaka, C. Proc. 7th SMRM (1988) p435

¹⁰ Antich, P. P., Mason, R. P., Constantinescu, A., Peschke, P., and Hahn, E. W. Proc. Soc. Nucl. Med. 35(5), (1994) p216

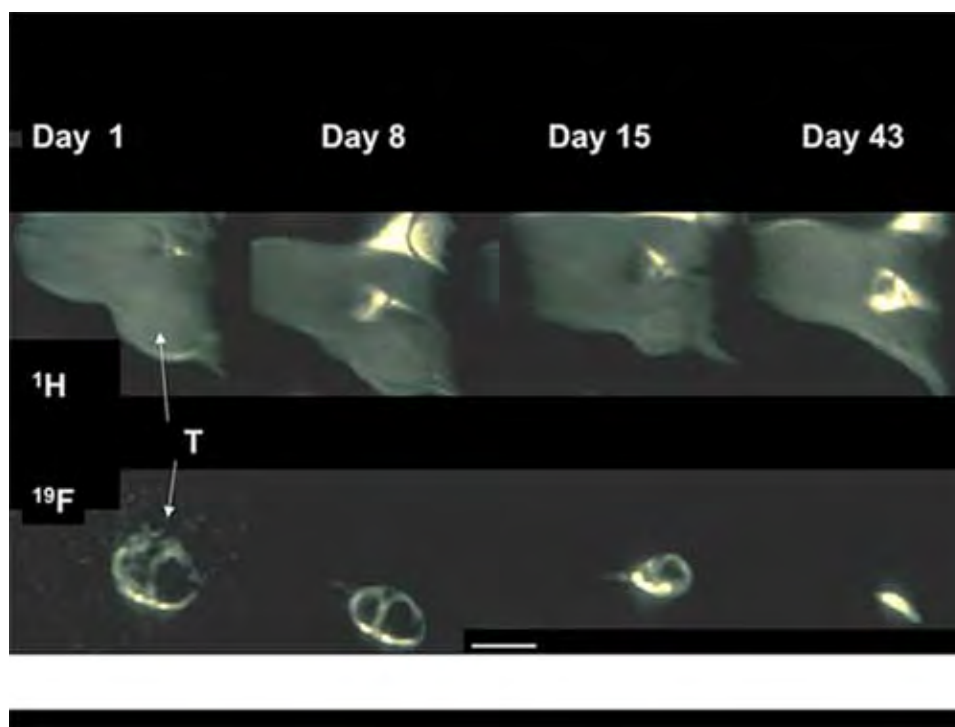


Fig. (11). ^{19}F MRI of Novikoff hepatoma in thigh of rat. The tumor in Fig. (10) regressed spontaneously over the next 43 days and residual PFC showed location.

[203]. Long tissue retention has the advantage of facilitating chronic studies during tumor development and progressive tumor hypoxia has been observed over many days [187, 192].

Two approaches have been applied to circumvent reticuloendothelial uptake. PFC has been incorporated in polyalginate beads for direct implantation at a site of interest [204, 205]. We favor direct intratumoral (IT) injection of neat PFC allowing any region of interest in a tumor to be interrogated immediately. Use of a fine needle ensures minimal tissue damage. Others have used direct injection of emulsions into tumors, but this increases the volume considerably making it more invasive [206]. Investigators have suggested that emulsification improves retention at the site of injection. Direct injection of neat PFC has also been used to investigate retinal oxygenation [207-209] and cerebral oxygenation in the interstitial and ventricular spaces [210].

Choice of PFC may be governed by practical considerations, such as cost and availability, since several products, particularly, proprietary emulsions may be difficult to obtain. Many PFCs (*e.g.*, perfluorotributylamine (PFTB), perflubron (formerly referred to as perfluorooctyl bromide; PFOB), TheroxTM (F44-E)) have several ^{19}F NMR resonances, which can be exploited to provide additional information in spectroscopic studies, but seriously hamper effective imaging. Multiple resonances can lead to chemical shift artifacts in images, which compromise the integrity of relaxation time measurements, though they can be avoided by selective excitation, or detection, chemical shift imaging, deconvolution or sophisticated tricks of NMR spin physics [52, 171, 190, 211-214]. These approaches add to experimental complexity and are generally associated with

lost signal to noise ratio (SNR). PFCs with a single resonance provide optimal SNR and simplify imaging: two agents hexafluorobenzene (HFB) [199-202, 215-218], and perfluoro-15-crown-5-ether (15C5) [170, 193, 206, 210] have found extensive use. HFB and 15C5 offer the immediate advantage of a high symmetry and a single ^{19}F NMR resonance. While 15C5 has 20 equivalent fluorine atoms per molecule and HFB has only 6, the difference in molecular weight (580 vs. 186) provides only 6% extra ^{19}F signal per unit volume (*i.e.*, μl administered dose) assuming equal density (1.62 g/ml).

Hexafluorobenzene has many virtues as a pO_2 reporter [173]. Symmetry provides a single narrow ^{19}F NMR signal and the spin lattice relaxation rate is highly sensitive to changes in pO_2 , yet minimally responsive to temperature [173]. Prior to our applications of HFB to tumor oximetry *in vivo*, several studies had examined the interaction of oxygen and HFB by NMR [219-221]. HFB also has a long spin spin relaxation time (T_2), which is particularly important for imaging investigations. From a practical perspective HFB is cheap (<\$2/g) and readily available commercially in high purity (>99%). HFB is well characterized in terms of lack of toxicity [222, 223], exhibiting no mutagenicity [224], teratogenicity or fetotoxicity [225] and the manufacturer's material data safety sheet indicates $\text{LD}_{50} > 25 \text{ g/kg}$ (oral- rat) and $\text{LC}_{50} 95 \text{ g/m}^3/2 \text{ hours}$ (inhalation-mouse). HFB had been proposed as a veterinary anesthetic and has been used in many species including ponies, sheep, cats, dogs, rats and mice, but was abandoned due to its high volatility (b.p. 81°C) and low flash point (10°C) [226]. It is not a problem in our studies, where small quantities of liquid (typically, $50 \mu\text{l}$) are injected directly into the tumor. HFB requires no special storage, other than a sealed bottle to prevent evaporation.

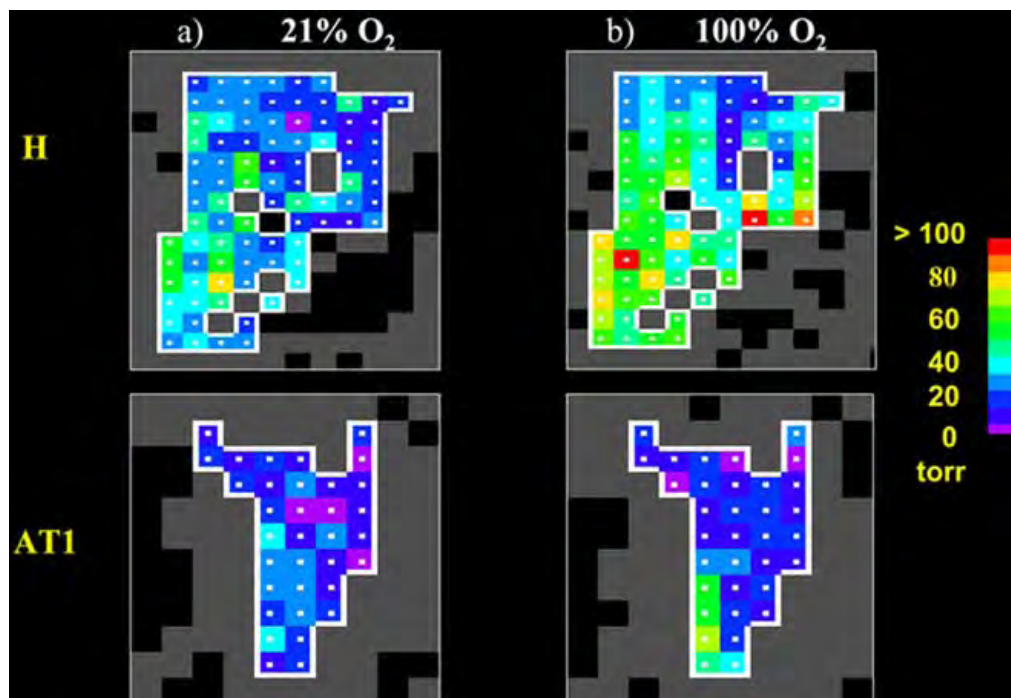


Fig. (12). pO_2 maps of Dunning prostate R3327 tumors in pedicles of Copenhagen rats obtained using *FREDOM* based on interrogation of the reporter molecule hexafluorobenzene. The H tumor (1.1 cm^3 ; baseline median $\text{pO}_2 = 26.7 \text{ torr}$) was better oxygenated than the AT1 tumor (2.6 cm^3 ; baseline median $\text{pO}_2 = 12.5 \text{ torr}$). In response to oxygen inhalation, pO_2 increased in both the H (median $\text{pO}_2 = 96.4 \text{ torr}$) and the AT1 tumors (median $\text{pO}_2 = 29.5 \text{ torr}$) and the largest response was observed in those areas initially well oxygenated. This approach allows oxygen dynamics to be observed in tissues in response to interventions based on small amounts of reporter molecule ($50 \mu\text{l}$ HFB, introduced i.t.) (Data obtained in collaboration with Dr. Dawen Zhao).

For initial studies, HFB ($10\text{--}20 \mu\text{l}$) was injected directly into the center or periphery of a tumor using a very fine sharp tipped needle (32 gauge). Local pO_2 measurements indicated tumor heterogeneity [169, 173]. The insertion of a needle is reminiscent of electrode studies, but importantly the HFB remains localized in the tumor for many hours (typical half life $\sim 600 \text{ mins}$) allowing repeat measurements from an individual location with respect to acute interventions, e.g., hyperoxic gas challenge. To overcome any potential artifacts from HFB clearance during a data acquisition, we instituted the *ARDVARC* (Alternating Relaxation Delays with Variable Acquisitions to Reduce Clearance effects) protocol, which improves SNR and reduces overall data acquisition time [169, 227]. *FREDOM* (Fluorocarbon Relaxometry using Echo planar imaging for Dynamic Oxygen Mapping) can provide 50 to 150 individual pO_2 measurements across a tumor simultaneously in about 6.5 mins with a local precision of 1 to 3 torr in relatively hypoxic regions based on $50 \mu\text{l}$ injected dose (Fig. 12) [27, 169]. NMR is also compatible with optical measurements and we have explored simultaneous NIR and MR approaches to measure vascular oxygenation in combination with pO_2 ^{11,12}. Other studies have examined the effects of vascular targeting agents [218], vasoactive agents [215] and hyperoxic gases [27, 169, 199–202, 215, 216, 228]. Results are consistent with hypoxia estimates

using the histological marker pimonidazole [199]. Most significantly, estimates of pO_2 and modulation of tumor hypoxia are found to be consistent with modified tumor response to irradiation [201]¹³. Such prognostic capability could be important in the clinic, since it is known that relatively hypoxic tumors tend to be more aggressive and respond less well to radiation therapy [155, 157, 159, 229, 230].

We have shown that measurements are consistent with sequential determinations made using electrodes [231, 232] and fiber optic systems (FOXYTM and OxyLite[®]) [216, 233]. Repeat measurements are highly reproducible and generally quite stable in tumors under baseline conditions. For PFCs, we believe that calibration curves determined in solution are valid *in vivo* and for an emulsion of perfluorotributylamine (Oxypherol[®]) measured in perfused rat heart, we have rigorously validated the measurements independently [167]. Others have shown that R1 of various PFCs was independent of emulsification [160, 161]. ^{19}F R1 of the emulsions was independent of dilution [162] and changes in pH [46, 163], common proteins [46, 163, 165] or blood [164]. R1 is unaffected by the presence of paramagnetic ions [165, 234], although certain lipophilic spin labels such as doxylsterate nitroxide did cause perturbation¹⁴. In essence the PFCs form droplets and are essentially immune to the influence of materials in the

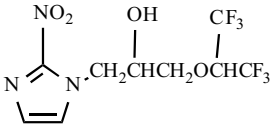
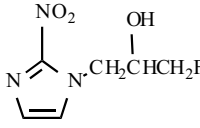
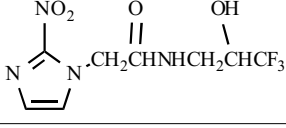
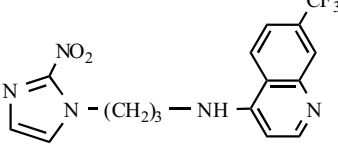
¹¹ Xia, M.; Kodibagkar, V.D.; Constantinescu, A.; Gu, Y.; Liu, H.; Mason, R.P., Proc. 12th ISMRM, Kyoto, Japan, 2004, p. 2004.

¹² Gu, Y.; Xia, M.; Liu, H.; Kodibagkar, V.; Constantinescu, A.; Mason, R.P., Biomedical Topical Meetings, Washington, DC, 2004, p. FB6.

¹³ Bourke, V., Gilio, J., Zhao, D., Constantinescu, A., Kodibagkar, V., Jiang, L., Hahn, E. W., and Mason, R. P., Radiat. Res. Meeting, St. Louis, MO, 2004.

¹⁴ Muller, R.N.; Brown, R.D.; Koenig, S.H., Society of Magnetic Resonance in Medicine 5th Annual Meeting, Montreal, 1986, p. 327

Table 7. ^{19}F NMR Hypoxia Indicators

Name	Structure	References
CCI 103F		[248-252]
RO 070741		[249, 253]
SR 4554		[254-259]
NLTQ-1		[373]

accompanying aqueous phase due to $1/r^6$ dipole effect. However, materials that dissolve in the PFC itself do alter the relaxation properties, hence, the strong effect of the highly soluble gas oxygen. For fluorohydrocarbons (not fully perfluorinated), the relaxation curves may be altered by additional environmental effects, since they may interact with lipids. For Therox F44E, we had problems achieving standard calibration curves [235] and others have also experienced unexpected values [205]. Specifically, Nöth *et al.* [205], found different calibration curves for the fluorohydrocarbon F44E in the pure state or when incorporated into polyalginate beads. This is likely a function of the partial fluorocarbon nature. Indeed, certain fluorohydrocarbons have been specifically designed to incorporate asymmetrically into membranes in order to explore micro regional pO_2 gradients [216].

3.4.2 Hypoxia

Nitroimidazoles are bioreductive agents that are reduced by intracellular reductases to generate reactive intermediates. In the presence of oxygen, the intermediates are rapidly reoxidised and may clear from cells. Under hypoxic conditions they become covalently bound to cellular constituents. These retained bioreduction products, therefore, indicate the presence of cellular hypoxia. Nitroimidazoles have been used extensively in the past as hypoxic cell radiosensitizers [236] and more recently have gained a role as markers of tumor hypoxia [237-240]. EF5 and pimonidazole are widely used to assess hypoxia in histological analysis of biopsy specimens [241-244], but non-invasive approaches would be preferable for therapeutic prognosis. Recent studies indicate that ^{18}F misonidazole and ^{64}Cu -ATSM correlate with patient survival [245, 246]. Hypoxia reporters have also been designed for PET using ^{18}F [247]. A potential problem is the relative time required for background clearance from oxygenated tissues, versus the rapid radioactive decay of

^{18}F . Non-radioactive approaches would be advantageous. By attaching a fluorine label to the nitroimidazole, it has become possible to detect the presence of hypoxic cells using *in vivo* NMR techniques [150]. Studies have reported the fluorinated nitroimidazoles CCI-103F [248-252], Ro 07-0741 [249, 253] and SR-4554 [254-259], which contain 6, 1 and 3 fluorine atoms per molecule, respectively (Table 7). Subsequent to administration, a washout period sufficient for elimination of unbound marker is required, since there is apparently no difference detectable *in vivo* in the chemical shifts of the parent molecule and the metabolites [150].

A comparative study of CCI-103F and Ro 07-0741 [249] showed similar tumor selective retention for the two agents in three different tumor types, while Ro 07-0741 had longer retention in liver. The variations in signal retention for each agent in different tumor types were consistent with known hypoxic fraction and *in vivo* nitroreductase activities. Li *et al.* [251] investigated the predictive potential of CCI-103F retention as an indicator of tumor radiosensitivity and found a weak correlation indicating that factors other than hypoxia are involved. Raleigh *et al.* [260] reported a correlation between ^{19}F MRS and scintillation counting measures of tumor-bound, tritium-labeled CCI-103F. Other studies suggest that glutathione concentration may be pertinent [150].

SR-4554 has been designed specifically for use as a noninvasive hypoxia marker detected by ^{19}F MRS and has already undergone preclinical evaluation *in vitro* [259] and *in vivo* [255, 261] and has completed a Phase I clinical trial [262]. The identification of hypoxia-dependent SR-4554 bioreduction products in tumor has been achieved in mice by comparing ^{19}F signal from retained bioreduction products acquired at a late time point (6 h), versus signal acquired at an early time point (45 min), when parent SR-4554 peaks in tumor [255, 262]. The Phase I clinical study [262] reported

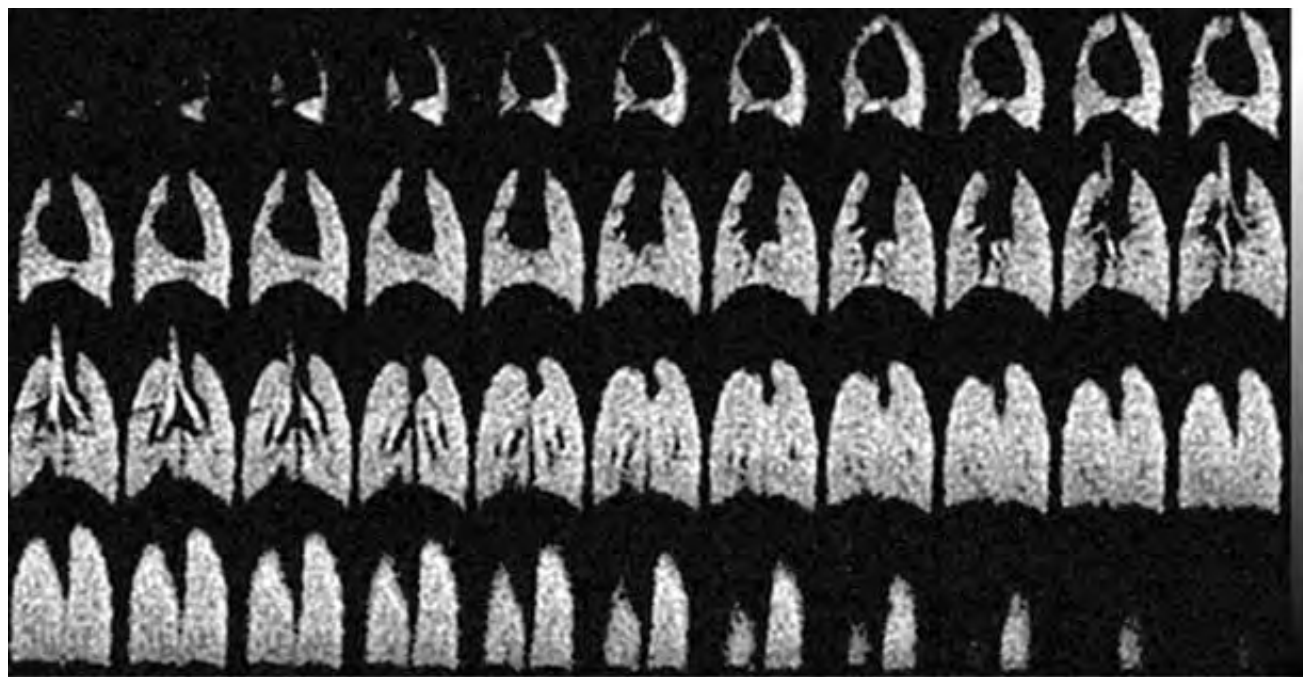


Fig. (13). Three dimensional ^{19}F MRI of SF_6 in the lungs of a large rat (594 g): 720 μm isotropic resolution obtained in 30 mins. using methods of Kuethe, *et al.*, [269, 346]. Frames, from top left to bottom right are successive planes of the image from chest to back. The large airways are brighter because the spin density of pure gas is higher than in the lungs, where 25% of the volume is occupied by tissue. Data kindly provided by Dr. Dean Kuethe *et al.*

the detection of SR-4554 by MRS in tumors immediately after infusion at doses of 400-1600 mg/m^2 . The high doses of nitroimidazoles required for NMR may have adverse side effects. The biggest problem with ^{19}F hypoxia agents is that they merely provide a qualitative impression of hypoxia rather than a definitive pO_2 .

Seddon *et al.* [262] reported a correlation between retention of SR4554 and pO_2 . Aboagye *et al.* [254] found increased retention in hypoxic tumors, but no linear correlation with pO_2 . Intriguingly administration of SR4554 was reported to reduce the hypoxic fraction in several tumor types, as determined polarographically [254]. Lack of correlation with pO_2 measurements [254, 262] and pimonidazole uptake [150] suggest that additional factors influence hypoxia marker retention and indeed flow has been implicated [150]. One must also consider the potential diversity of trapped adducts, and metabolites may exhibit multiple chemical shifts, each at very low concentration. There is also concern that polymeric adducts may have exceedingly short T_2 , so that they become essentially invisible for many NMR sequences.

4. PASSIVE REPORTER MOLECULES

While many active ^{19}F NMR reporter molecules have been designed, developed, and exploited, as described in Section 3, above, other methods use a passive approach, whereby fluorinated molecules occupy a space and a signal magnitude provides an indication of anatomical properties such as lung volume, bowel function, vascular volume or flow.

4.1 Lung Volume

Perfluorocarbons exhibit remarkable gas solubility, and based on the high carrying capacity for oxygen and carbon dioxide, have been developed in emulsion form as synthetic blood substitutes [179]. PFCs may also be relevant as pure liquids. In a classic experiment, Clark and Gollan [263] submersed a living mouse in PFC liquid and far from drowning, it inhaled the PFC facilitating effective oxygen transport to the lungs. Thus, PFCs have potential application as surfactants to aid breathing in extremely premature infants, as explored in clinical trials [264]. PFC may be administered as liquid or aerosols. Thomas, *et al.*, applied ^{19}F MRI to show the extent of lung filling. Further, by applying relaxation measurements (as described in Section 3.4, above) to estimate regional pO_2 in the lungs, while animals breathed various gases. Such measurements have been performed in mice, rats, dogs and pigs [168, 265]. Various perfluorocarbons and perfluorocarbon emulsions have been introduced into the lung as aerosols, sometimes with animals under forced ventilation, following thorocotomy [265]. The ^{19}F signal provides an opportunity to image lungs. By contrast ^1H MRI is handicapped by lack of water signal. In a novel approach, Huang, *et al.* [266] applied ^1H MRI to the water in a perfluorocarbon emulsion and found considerably enhanced structural information. Liquid and aerosol ventilation can be stressful, whereas inhalation of inert gas, may be more practical, as shown by proof of principal¹⁵ using CF_4 or C_2F_6 . More recent studies used SF_6 (Fig. 13) with potential application for detection

¹⁵ Heidelberger, E.; Lauterbur, P.C., 1st Meeting Soc. Magn. Reson. Med., Boston, MA, 1982, p. 70

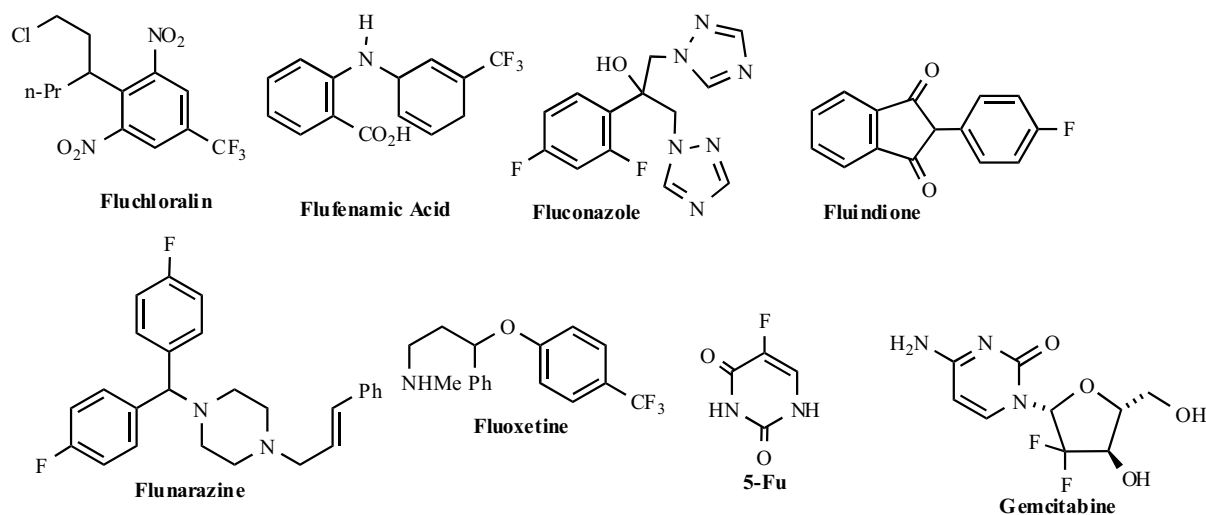


Fig. (14). Representative pharmaceuticals and industrial chemicals incorporating fluorine atoms.

of lung cancer, emphysema, or allograft rejection [267-269]. Gas detection does require special MR instrumentation, due to the exceedingly short T_1 and T_2 relaxation. ^{19}F MRI of lungs, has, to some extent, been superseded by inert gas approaches exploiting hyperpolarized gases, such as xenon and helium [270-272], though this requires expensive preparatory apparatus.

4.2 GI Imaging

Increasing awareness of colon cancer demands improved screening. Traditional barium meals provide contrast in CT, and virtual colonoscopy is competing with traditional fiber optic probes [273]. MR procedures have lagged behind CT, but several potential contrast agents have been presented, ranging from paramagnetic zeolite formulations [274] and ferric ammonium citrate [275] to PFC emulsions [276]. Emulsions of perflubron (PFOB) have been applied to multiple applications and are popular in ultrasound [178, 179]. For MRI, the multi-resonance spectrum requires extensive editing. PFOB has been tested in clinical trials [276, 277] and recently images were shown in mice based on perfluorononane [278].

4.3 Tumor Blood Volume

Angiogenesis is associated with tumor development and many clinical trials have found correlations between vascular density and prognosis. Traditionally, biopsy and histology are required to examine the vasculature. CD31 antibodies can provide blood vessel counts [279], while dyes such as India ink or Hoechst 33342 may reveal perfusion [280]. Small paramagnetic proton MRI contrast agents can indicate perfusion based on a first pass kinetic analysis, but interpretation is complicated by vascular permeability surface area [281, 282]. Thus, larger particulate agents (nanoparticles or USPIOs) have been developed with a view to vascular retention and definite tumor blood volume measurements [283]. Nonetheless, conflicting reports appear in the literature regarding true reliability, particularly the integrity of "vascular retention". ^{19}F NMR has provided a

robust indication of vascular volume based on intravenous perfluorocarbon emulsions. These are retained in the vasculature for a period of hours, and studies have validated signal based on traditional radioisotope labeled approaches and dyes [284, 285]. Non-invasive measurements based on long term vascular retention allows acute modulation of tumor blood volume to be assessed [284-289] ¹⁶. This approach has also been applied to other organs and tissues [290], *e.g.*, demonstrating reactive hyperemia in muscles [291].

4.4 Blood Flow

Fluorinated gases (*e.g.*, FC-23 (Tri-fluoromethane) and FC-22 (chlorofluoromethane)) have been used to examine cerebral blood flow based on inflow and outflow kinetics, sometimes with pulsed delivery to facilitate compartmental analysis [292, 293]. Such tracer studies are analogous to ^{133}Xe approaches in SPECT, but avoid radioactivity.

5. METABOLISM AND DRUG UPTAKE

The fluorine atom is exceedingly versatile for designing reporter molecules, as described above. In addition, many pharmaceuticals contain a fluorine atom allowing detection of pharmacokinetics and metabolism. Examination of the Merck Index [20] shows a range of pharmaceuticals and industrial agents containing a single fluorine atom, a trifluoromethyl group or other F-substituents with applications ranging from herbicides (*e.g.*, fluchloralin) to analgesics (*e.g.*, flufenamic acid), antifungals (*e.g.*, fluconazole), anticoagulants (*e.g.*, flutindione), vasodilators (*e.g.*, flunarazine), antidepressants (*e.g.*, fluoxetine) and several chemotherapeutics for cancer (5FU, gemcitabine) (Fig. 14). ^{19}F NMR analysis can be important both in drug development and applications. As described above, oxygen influences the relaxation of PFCs and facilitates accurate measurements of $p\text{O}_2$ *in vivo*. Oxygen has relatively little

¹⁶ Song, Y., Gu, Y., Kim, J. G., Liu, H., Constantinescu, A., and Mason, R. P., Proc. OSA Biomedical Topical Meetings, Miami, FL, 2002, p. 241-243.

effect on molecules in aqueous solution, however, in this case traditional paramagnetic ions, such as Gd³⁺ or Gd-DTPA may be applied [294-296]. Indeed, this approach has been used to differentiate signals from intra and extra cellular metabolites [297].

5.1 Metabolism of Fluorodeoxyglucose

Fluorodeoxyglucose (FDG) is a fluorinated glucose analogue used in Positron Emission Tomography (PET) to measure metabolic activity [298] (see Haberkorn *et al.*, this issue). Given the high glycolytic rate associated with tumors, FDG PET is also a powerful tool for detecting tumors and monitoring metastases and was recently approved for Medicare reimbursement. Substituting an F atom for the -OH in glucose leaves the structure intact, so that cells accumulate FDG based on glucose transporters. FDG is effectively phosphorylated, trapping it intracellularly, but FDG-P is not a substrate for phosphofructose isomerase. Thus, FDG accumulates in metabolically active cells, such as tumors, brain, and myocardium. The FDG isomer 2-fluoro-2-deoxy-D-glucose (2-FDG) has been used in metabolic studies using ¹⁹F NMR [299-304]. While PET can assess retention with great sensitivity, it provides no metabolic information, whereas ¹⁹F NMR can be used to differentiate individual metabolites from anabolic and catabolic processes. Significant metabolism of 2-FDG via the aldose reductase sorbitol pathway to the metabolites 2-fluoro-2-deoxy-D-sorbitol, 5-fluoro-5-deoxy-L-sorbose, 5-fluoro-5-deoxy-L-sorbose-1-phosphate, 2-fluoro-2-deoxy-L-glyceraldehyde, and 2-fluoro-2-deoxyglycerol was observed [299, 305-309]. It must be remembered that NMR studies typically require mM concentrations as opposed to μ M for PET, and thus, metabolic fates may differ. The 3-FDG isomer is a poor substrate for hexokinase and the binding affinity of phosphohexose isomerase is low relative to glucose. Kwee *et al.* [306] introduced 3-fluoro-3-deoxy-D-glucose (3-FDG) as a probe of aldose reductase activity in brain and demonstrated metabolism. The elimination of 3-FDG from brain is slow relative to 2-FDG [310] and it has been used to probe metabolic pathways [306, 311-313].

5.2. Metabolism of Fluoropyrimidine Drugs

5-fluorouracil (5FU) is one of the most popular drugs for chemotherapy, but it has a narrow range of efficacy/toxicity. It has been suggested that both response and toxicity may be related to pharmacokinetics and there is interest in assessing dynamics of uptake, biodistribution, and metabolism. Patients with enhanced retention of 5FU in tumors ("trappers") may be expected to exhibit better response [314]. Such trapping is apparently a requisite, though not in itself sufficient for efficacy [21].

5FU requires anabolic conversion to nucleosides (*e.g.*, FdUrd, FdUmp) and nucleotides for cytostatic activity, requiring the activity of various kinases and phosphorylases [21]. However, competing catabolic reactions convert 5FU to DHFU (5,6 dihydrofluorouracil) and FBAL (α -fluoro β -alanine), in liver in addition to several other molecules offering little toxicity [21, 42, 315]. FBAL is excreted by

the kidneys. However, when pH is >7.3 further conversion may liberate fluoride ion, which is cardio- and neuro-toxic [316, 317]. Pharmacokinetics have been extensively characterized by ¹⁸F Positron Emission Tomography and the metabolic processes by ¹⁹F NMR [22]. Chemical shifts of characterized products have been reported together with typical T1s. Studies have ranged from cells to rodents, and clinical studies in patients. Most studies have been limited to spectroscopy, though some imaging has been reported [22, 318-320].

The pharmacokinetics of 5FU are reported to be pH sensitive, and thus measurements of tumor pH may have prognostic value for drug efficacy. In tumors with lower pH the retention of 5-fluorouracil (5-FU) is considerably enhanced [321, 322] along with the cytotoxicity of several common drugs [113, 323-325]. Indeed, this prompted investigations of modulation of tumor pH to increase activity, *e.g.*, by breathing carbogen. Relevant is also the potential to monitor 5FU and tumor physiology simultaneously, based on ¹⁹F NMR signals of the drug and correlated signals from physiological reporter molecules. Intriguingly, fluoronucleotides derived *in vivo* from 5FU exhibit sensitivity to changes in pH and may be used to measure pH_i, although the presence of a mixture of products may complicate interpretation [111, 326]. Administration of 5-FU causes intracellular alkalinization and an increased transmembrane Δ pH.

Given the inherent dose-limiting toxicity of 5FU, various pro-drug approaches have been explored and ¹⁹F NMR has played a role in analysis and development. Pro-drug therapy has new impetus in conjunction with gene therapy, specifically the use of cytosine deaminase, to convert the relatively innocuous 5-fluorocytosine (5FC) to 5FU [73-75, 327, 328]. In this context, distribution, activity, and persistence of trans-genes is of critical importance (section 3.1). Several investigations have now reported ¹⁹F NMR of the conversion of 5FC to 5FU based on the ¹⁹F NMR chemical shift, $\Delta\delta$ 2 ppm [74, 75].

5.3. Other Drugs: Retention of Anesthetics

Many gaseous anesthetics are fluorinated, *e.g.*, halothane, enflurane, isoflurane, sevoflurane, and desflurane. These are listed in decreasing order of blood gas solubility, and hence, increasing wash in - wash out rates. NMR studies of fluorinated anesthetics form some of the earliest *in vivo* applications of ¹⁹F NMR. Issues regarding the use of anesthetics are site of anesthetic action, duration of residence in the brain and toxicity of metabolic byproducts. The results have been a source of debate and controversy.

Wyrwicz and co-workers [329-336] addressed the issue of residence times of anesthetics in the brain and observed signals for the anesthetics for prolonged durations after cessation of anesthesia. Both halothane [330] and isoflurane [331] showed bi-compartmental elimination from the rabbit brain with half-lives ($t_{1/2}$ of 25 and 320 mins for halothane and 26 and 174 mins for isoflurane). In the case of halothane, the findings were further supported with accompanying high resolution *in vitro* data, which showed two separate resonances with different relaxation times T₁ and T₂. One of the two resonances corresponded to

halothane, while the other was ascribed to a non-volatile metabolite possibly trifluoroacetate.

While global spectroscopy can be straightforward (Fig. 9), anesthetics have a short transverse relaxation time (T_2^*) and signals may be lost in localized spectroscopy or imaging approaches. Chew *et al.* [337], James *et al.* [24, 25], and Hashimoto *et al.* [338] failed to detect anesthetics in brain tissues presumably due to the short T_2 s. Lockhart *et al.* [339] reported a correlation between cerebral uptake and solubility, with desflurane (most soluble) having fastest uptake followed by isoflurane and halothane.

Very few clinical studies have reported ^{19}F MR of anesthetics in the brain. Menon *et al.* [39] demonstrated the feasibility of such studies and found halothane signal up to 90 min after the withdrawal of anesthetic. Lockwood *et al.* [31] studied isoflurane kinetics and showed biphasic elimination with decay halftimes of 9.5 and 130 min. They also studied the relation between the cerebral kinetics of isoflurane and cerebral function [32]. Another issue of interest regarding anesthetics is the site of action of the anesthetic agent in the brain and the availability of saturable binding sites. Artificially ventilated animals showed a linear relationship between inspired concentrations of halothane and cerebral halothane levels implying the absence of binding to specific sites [340, 341]. Selinsky *et al.* and Preece *et al.* [342-345] have studied the metabolism of volatile anesthetics showing generation of potentially toxic metabolites such as methoxydifluoroacetate, dichloroacetate, and fluoride ion from methoxyflurane.

6. CONCLUSIONS

Proton MRI is a mainstay of clinical Radiology. Several contrast agents are in routine use and other “smart” agents are being developed [10]. However, most investigations are limited to detection of fat and water signals, since they dominate. By contrast, there is essentially no ^{19}F NMR background signal in tissues, and thus, fluorinated reporter molecules may be assessed by changes in chemical shift and the detection ability is subject to the signal-to-noise ratio, as opposed to contrast-to-noise. Huge diversity of application has been demonstrated in the biochemical and small animal areas, with limited clinical application. To date clinical application is hindered by the lack of availability of clinical ^{19}F NMR. However, for about \$200k, such a capability can be added and will be straightforward as soon as there is a proven need and opportunity for medical reimbursement. Such a situation has occurred very recently for FDG PET providing access to equipment and incentive to generate novel reporters (see reviews by McQuade and Haberkorn, this issue). ^{19}F NMR offers the potential to investigate many diverse parameters (Table 1) and with a little imagination, together with thorough development will yield further applications.

7. ACKNOWLEDGEMENTS

Supported in part by the Cancer Imaging Program, NCI Pre-ICMIC P20 CA086354 and an IDEA awards from the DOD Breast Cancer Initiative DAMD179919381 and

170310343. NMR experiments were conducted at the Mary Nell and Ralph B. Rogers NMR Center, an NIH BTRP facility #P41-RR02584. We are grateful to Drs. Peter Antich, Eric Hahn, Dawen Zhao, Uwe Haberkorn, Peter Peschke, Ken Koeneman and Dean Kuethe for collegial support and Jocelyn Chafouleas for assistance in preparing this manuscript.

ABBREVIATIONS

ARDVARC	= Alternating Relaxation Delays with Variable Acquisitions to Reduce Clearance effects
ASL	= Arterial Spin Labeling
ATP	= Adenosine triphosphate
β -gal	= β -galactosidase
BAPTA	= 1,2-bis(o-amino-phenoxy)ethane-N,N,N',N'-tetraacetic acid
BLI	= Bioluminescent Imaging
BOLD	= Blood Oxygen Level Dependent
FDG	= Fluorodeoxyglucose
15C5	= Perfluoro-15-crown-5-ether
CD	= Cytosine Deaminase
CSI	= Chemical Shift Imaging
DTI	= Diffusion Tensor Imaging
DHFU	= 5,6 Dihydrofluorouracil
FBAL	= α -Fluoro β -alanine
5FBAPTA	= 5,5-Difluoro-1,2-bis(o-amino-phenoxy)-ethane-N,N,N',N'-tetraacetic acid
5-FC	= 5-fluorocytosine
FDG	= Fluorodeoxyglucose
6-FPAM	= 6-Fluoropyridoxamine
6-FPOL	= 2-Fluoro-5-hydroxy-6-methyl-3,4-pyridine-dimethanol
FREDOM	= Fluorocarbon Relaxometry using Echo planar imaging for Dynamic Oxygen Mapping
5FU	= 5-Fluorouracil
Gd-DTPA	= Diethylenetriaminepentaacetic Acid
GDEPT	= Gene Directed Enzyme Prodrug Therapy
GFP	= Green Fluorescent Protein
HFB	= Hexafluorobenzene
hNIS	= Sodium Iodine Symporter
LETS	= Light Emission Tomography System
MRS	= Magnetic Resonance Spectroscopy
NaTFA	= Sodium Trifluoroacetate
NEAP	= N-Ethylaminophenol
NMR	= Nuclear Magnetic Resonance

ONPG	= O-Nitrophenylgalactoside
pO ₂	= Partial Pressure of Oxygen
PARACEST	= Paramagnetic Magnetization Transfer Contrast Agents
PFCs	= Perfluorocarbons
PFOB	= Perflubron; Perfluorooctyl Bromide
PFTB	= Perfluorotributylamine
PFONPG	= 4-Fluoro-2-nitrophenyl-β-D-galactopyranoside
pHe	= Extracellular pH
pHi	= Intracellular pH
R ₁	= Spin lattice (longitudinal) relaxation rate (=1/T ₁)
R ₂	= Spin spin (transverse) relaxation rate (=1/T ₂)
SNR	= Signal to Noise Ratio

REFERENCES

- <http://www.nobel.se/physics/laureates/1952/>, in 'The Nobel Prize in Physics 1952'.
- <http://www.nobel.se/chemistry/laureates/1991/>, in 'The Nobel Prize in Chemistry 1991'; <http://www.nobel.se/medicine/laureates/2003/>.
- Wright, S.M.; Wald, L.L. *NMR Biomed.* **1997**, *10*, 394.
- Sodickson, D.K.; Griswold, M.A.; Jakob, P.M. *Magn. Reson. Imaging Clin. North America* **1999**, *7*, 237.
- van den Brink, J.S.; Watanabe, Y.; Kuhl, C.K.; Chung, T.; Muthupillai, R.; Van Cauteren, M.; Yamada, K.; Dymarkowski, S.; Bogaert, J.; Maki, J.H.; Matos, C.; Casselman, J.W.; Hoogeveen, R.M. *Eur. J. Radiol.* **2003**, *46*, 3.
- Blumlich, B.; Kuhn, W., *Magnetic Resonance Microscopy*, VCH, Weinheim, **1992**.
- Barbier, E.L.; Silva, A.C.; Kim, S.G.; Koretsky, A.P. *Magn. Reson. Med.* **2001**, *45*, 1021.
- Fasano, F.; Capuani, S.; Hagberg, G.E.; Branca, T.; Indovina, I.; Castriota-Scanderbeg, A.; Maraviglia, B. *Magn. Reson. Imaging* **2003**, *21*, 1151.
- Jiang, L.; Zhao, D.; Constantinescu, A.; Mason, R.P. *Magn. Reson. Med.* **2004**, *51*, 953.
- Zhang, Z.; Nair, S.A.; McMurtry, T.J. *Current Med. Chem.* **2004**, this issue.
- Gadian, D.G., *NMR and its applications to living systems*, OUP, Oxford, **1995**.
- Gillies, R.J., in 'NMR in physiology and medicine', San Diego, **1994**.
- Bansal, N.; Germann, M.J.; Seshan, V.; Shires III, G.T.; Malloy, C.R.; Sherry, A.D. *Biochemistry* **1993**, *32*, 5638.
- Seshan, V.; Bansal, N. In *In vivo ³¹P and ²³Na NMR spectroscopy and Imaging*, M. Bruch, Ed.; Marcel Dekker: New York, **1996** 557.
- Navon, G.; Shina, R.H.; Eliav, U.; Seo, Y. *NMR Biomed.* **2001**, *14*, 112.
- Mason, R.P.; Sanders, J.K.M.; Gidley, M.J. *Phytochem.* **1986**, *25*, 1567.
- Weis, B.C.; Margolis, D.; Burgess, S.C.; Merritt, M.E.; Wise, H.; Sherry, A.D.; Malloy, C.R. *Magn. Reson. Med.* **2004**, *51*, 649.
- Mason, R.P.; Sanders, J.K.M. *Biochemistry* **1989**, *28*, 2160.
- Burgess, S.C.; Nuss, M.; Chandramouli, V.; Hardin, D.S.; Rice, M.; Landau, B.R.; Malloy, C.R.; Sherry, A.D. *Anal. Biochem.* **2003**, *318*, 321.
- Budavari, S. *The Merck Index*, Rahway, NJ, **1989**.
- Wolf, W.; Presant, C.A.; Waluch, V. *Adv. Drug Del. Rev.* **2000**, *41*, 55.
- Brix, G.; Bellemann, M.E.; Haberkorn, U.; Gerlach, L.; Lorenz, W.J. *Nucl. Med. Biol.* **1996**, *23*, 897.
- Lee, D.J.; Burt, C.T.; Koch, R.L. *J. Invest. Dermatol.* **1992**, *99*, 431.
- Wade, K.E.; Wilson, I.D.; Troke, J.A.; Nicholson, J.K. *J. Pharm. Biomed. Anal.* **1990**, *8*, 401.
- Venkatasubramanian, P.N.; Shen, Y.J.; Wyrwicz, A.M. *NMR Biomed.* **1993**, *6*, 377.
- Strauss, W.L.; Unis, A.S.; Cowan, C.; Dawson, G.; Dager, S.R. *Am. J. Psych.* **2002**, *159*, 755.
- Zhao, D.; Jiang, L.; Mason, R.P. *Methods Enzymol.* **2004**, *386*, 378.
- Mason, R.P. *Curr. Med. Chem.* **1999**, *6*, 481.
- Cui, W.; Otten, P.; Li, Y.; Koenenman, K.; Yu, J.; Mason, R.P. *Magn. Reson. Med.* **2004**, *51*, 616.
- Golman, K.; Ardenkjaer-Larsen, J.H.; Petersson, J.S.; Mansson, S.; Leunbach, I. *PNAS USA* **2003**, *100*, 10435.
- Venkatesh, A.K.; Zhang, A.X.; Mansour, J.; Kubatina, L.; Oh, C.H.; Blasche, G.; Selim Unlu, M.; Balamore, D.; Jolesz, F.A.; Goldberg, B.B.; Albert, M.S. *Magn. Reson. Imaging* **2003**, *21*, 773.
- Zhang, S.; Merritt, M.; Woessner, D.E.; Lenkinski, R.E.; Sherry, A.D. *Acc. Chem. Res.* **2003**, *36*, 783.
- Thomas, S.R., In *The biomedical applications of Fluorine-19 NMR*, C. L. Partain, R. R. Price, J. A. Patton, M. V. Kulkarni, and A. E. J. James, Ed.; W.B. Saunders Co.: London, **1988**, 1536.
- Selinsky, B.S.; T., B.C. In *In vivo ¹⁹F NMR*, L. J. Berliner and J. Reuben, Ed.; Plenum: New York, **1992**, 241.
- Prior, M.J.W.; Maxwell, R.J.; Griffiths, J.R., In *Fluorine-¹⁹F NMR spectroscopy and imaging in-vivo*, M. Rudin, Ed.; Springer-Verlag: Berlin, **1992**, 103.
- London, R.E. In *In vivo NMR studies utilizing fluorinated NMR probes*, R. J. Gillies, Ed.; Academic: San Diego, **1994**, 263.
- Mason, R.P. *Art. Cells, Blood Sub. & Immob. Biotech.* **1994**, *22*, 1141.
- McSheehy, P.M.J.; Lemaire, L.P.; Griffiths, J.R., In *Fluorine-19 MRS: applications in oncology*, D. M. Grant and R. K. Harris, Ed.; Wiley: Chichester, **1996**, 2048.
- Menon, D.K. In *Fluorine-19 MRS: general overview and anesthesia*, R. K. Harris, Ed.; Wiley: Chichester, **1995**, 2052.
- Passe, T.J.; Charles, H.C.; Rajagopalan, P.; Krishnan, K.R. *Prog. Neuro-Psychopharmacol. Biol. Psych.* **1995**, *19*, 541.
- Martino, R.; Malet-Martino, M.; Gilard, V. *Curr. Drug Metab.* **2000**, *1*, 271.
- Bachert, P. *Prog. NMR Spectroscopy* **1998**, *33*, 1.
- Code, R.F.; Harrison, J.E.; McNeill, K.G.; Szyjowski, M. *Magn. Reson. Med.* **1990**, *13*, 358.
- Bovey, F.A. *Nuclear Magnetic Resonance Spectroscopy*, Academic Press, San Diego, **1988**.
- Mehta, V.D.; Kulkarni, P.V.; Mason, R.P.; Constantinescu, A.; Aravind, S.; Goomer, N.; Antich, P.P. *FEBS Letters* **1994**, *349*, 234.
- Taylor, J.; Deutsch, C.J. *Biophys. J.* **1988**, *53*, 227.
- Lutz, N.W.; Hull, W.E. *NMR Biomed.* **1999**, *12*, 237.
- Emsley, J.W.; Feeney, J.; Sutcliffe, L.H. *High Resolution Nuclear Magnetic Resonance Spectroscopy*, Pergamon Press, Oxford, **1966**.
- Emsley, J.W.; Phillips, L. *Prog. in NMR Spec.* **1976**, *10*, 83.
- Shukla, H.P.; Mason, R.P.; Woessner, D.E.; Antich, P.P. *J. Magn. Reson. Series B* **1995**, *106*, 131.
- Babcock, E.E.; Mason, R.P.; Antich, P.P. *Magn. Reson. Med.* **1991**, *17*, 178.
- Mason, R.P.; Bansal, N.; Babcock, E.E.; Nunnally, R.L.; Antich, P.P. *Magn. Reson. Imaging* **1990**, *8*, 729.
- Lantum, H.B.; Baggs, R.B.; Krenitsky, D.M.; Anders, M.W. *Toxicol. Sci.* **2002**, *70*, 261.
- Shainyan, B.A.; Danilevich, Y.S.; Grigor'eva, A.A.; Chuvashov, Y.A. *Russian J. Org. Chem. (Trans. Zh. Organ. Khim.)* **2004**, *40*, 513.
- Asovich, V.S.; Kornilov, V.; Maksimov, B.N. *Russ. Zh. Prikladnoi Kh.* **1994**, *67*, 107.
- Olah, G.A.; Nojima, M.; Kerekes, I. *J. Am. Chem. Soc.* **1974**, *96*, 925.
- Haas, A.; Maciej, T. *J. Fluorine Chem.* **1982**, *20*, 581.
- Patrick, T.B.; Zhang, L.; Li, Q. *J. Fluorine Chem.* **2000**, *102*, 11.
- Belen'kii, G.G.; Petrov, V.A.; Resnick, P.R. *J. Fluorine Chem.* **2001**, *108*, 15.

- [60] Rozen, S.; Brand, M. *J. Org. Chem.* **1986**, *51*, 3607.
- [61] Adachi, K.; Ohira, Y.; Tomizawa, G.; Ishihara, S.; Oishi, S. *J. Fluorine Chem.* **2003**, *120*, 173.
- [62] Mehta, V.; Kulkarni, P.V.; Mason, R.P.; Constantinescu, A.; Antich, P.P. *Bioorg. Med. Chem. Lett.* **1992**, *2*, 527.
- [63] Joubert, J.; Roussel, S.; Christophe, C.; Billard, T.; Langlois, B.R.; Vidal, T. *Angew. Chem. Int. Ed.* **2003**, *42*, 3133.
- [64] Dwek, R.A., In *The use of fluorine-19 as a detecting shift probe*, R. A. Dwek, Ed.; Clarendon: Oxford, **1975**, 158.
- [65] Gerig, J.T. *Methods Enzymol.* **1989**, *177*, 3.
- [66] Contag, C.H.; Ross, B.D. *JMRI* **2002**, *16*, 378.
- [67] Haberkorn, U.; Altmann, A.; Jiang, S.; Morr, I.; Mahmut, M.; Eisenhut, M. *Eur. J. Nucl. Med.* **2001**, *28*, 633.
- [68] Tjuvajev, J.G.; Doubrovina, M.; Akhurst, T.; Cai, S.; Balatoni, J.; Alauddin, M.M.; Finn, R.; Bornmann, W.; Thaler, H.; Conti, P.S.; Blasberg, R.G. *J. Nucl. Med.* **2002**, *43*, 1072.
- [69] Ichikawa, T.; Hogemann, D.; Saeki, Y.; Tyminski, E.; Terada, K.; Weissleder, R.; Chioocca, E.A.; Basilion, J.P. *Neoplasia (New York)* **2002**, *6*, 523.
- [70] Paroo, Z.; Bollinger, R.A.; Braasch, D.A.; Richer, E.; Corey, D.R.; Antich, P.P.; Mason, R.P. *Molecular Imaging* **2004**, *3*, 117.
- [71] Hoffman, R. *Lancet Oncol.* **2002**, *3*, 546.
- [72] Herschman, H.R. *J. Cell. Biochem.* **2002**, *39*, 36.
- [73] Freytag, S.O.; Khil, M.; Stricker, H.; Peabody, J.; Menon, M.; DePeralta-Venturina, M.; Nafziger, D.; Pegg, J.; Paielli, D.; Brown, S.; Barton, K.; Lu, M.; Aguilar-Cordova, E.; Kim, J.H. *Cancer Res.* **2002**, *62*, 4968.
- [74] Stegman, L.D.; Rehemtulla, A.; Beattie, B.; Kievit, E.; Lawrence, T.S.; Blasberg, R.G.; Tjuvajev, J.G.; Ross, B.D. *PNAS (USA)* **1999**, *96*, 9821.
- [75] Corban-Wilhelm, H.; Hull, W.E.; Becker, G.; Bauder-Wust, U.; Greulich, D.; Debus, J. *Gene Therapy* **2002**, *9*, 1564.
- [76] Kruger, A.; Schirmacher, V.; Khokha, R. *Cancer Metastasis Rev.* **1999**, *17*, 285.
- [77] Serebriiskii, I.G.; Golemis, E.A. *Anal. Biochem.* **2000**, *285*, 1.
- [78] Beckwith, J.R.; Zipser, D., in 'The Lactose operon', Cold Spring Harbor, **1970**.
- [79] Kawaguchi, J.; Wilson, V.; Mee, P.J. *Biotechniques* **2002**, *32*, 68.
- [80] Heuermann, K.; Cosgrove, J. *Biotechniques* **2001**, *30*, 1142.
- [81] Bronstein, I.; Edwards, B.; Voyta, J.C. *J. Chemilum. Biolum.* **1989**, *4*, 99-111.
- [82] Louie, A.Y.; Huber, M.M.; Ahrens, E.T.; Rothbacher, U.; Moats, R.; Jacobs, R.E.; Fraser, S.E.; Meade, T.J. *Nature Biotechnol.* **2000**, *18*, 321.
- [83] Yoon, S.; Kim, H.G.; Chun, K.H.; Shin, J.E.N. *Bull. Korean Chem. Soc.* **1996**, *17*, 599.
- [84] Richard, J.P.; Westerfeld, J.G.; Lin, S. *Biochemistry* **1995**, *34*, 11703.
- [85] Taylor, J.S.; Deutsch, C.J.; McDonald, G.G.; Wilson, D.F. *Anal. Biochem.* **1982**, *114*, 415.
- [86] Deutsch, C.J.; Taylor, J.S. In *¹⁹F NMR measurements of intracellular pH*, R. K. Gupta, Ed.; CRC Press: Boca Raton, **1987**, 55.
- [87] Deutsch, C.J.; Taylor, J.S. *Ann. NY Acad. Sci.* **1987**, *508*, 33.
- [88] Deutsch, C.; Taylor, J.S.; Wilson, D.F. *Proc. Natl. Acad. Sci. (USA)* **1982**, *79*, 7944.
- [89] Deutsch, C.; Taylor, J.S.; Price, M. *J. Cell Biol.* **1984**, *98*, 885.
- [90] Kashiwagura, T.; Deutsch, C.J.; Taylor, J.; Erecinska, M.; Wilson, D.F. *J. Biol. Chem.* **1984**, *259*, 237.
- [91] Thoma, W.J.; Ugurbil, K. *NMR Biomed.* **1988**, *1*, 95.
- [92] Taylor, J.A.; Deutsch, C.J. *Biophys. J.* **1983**, *43*, 261.
- [93] Hunjan, S.; Mason, R.P.; Mehta, V.D.; Kulkarni, P.V.; Aravind, S.; Arora, V.; Antich, P.P. *Magn. Reson. Med.* **1998**, *39*, 551.
- [94] He, S.; Mason, R.P.; Hunjan, S.; Mehta, V.D.; Arora, V.; Katipally, R.; Kulkarni, P.V.; Antich, P.P. *Bioorg. Med. Chem.* **1998**, *6*, 1631.
- [95] Korytnyk, W.; Singh, R.P. *J. Am. Chem. Soc.* **1963**, *85*, 2813.
- [96] Korytnyk, W.; Srivastava, S.C. *J. Med. Chem.* **1973**, *16*, 638.
- [97] Yamada, K.; Tsuji, M. *J. Vitaminol.* **1970**, *16*, 237.
- [98] Chang, Y.C.; Graves, D.J. *J. Biol. Chem.* **1985**, *260*, 2709.
- [99] Scott, R.D.; Chang, Y.-C.; Graves, D.J.; Metzler, D.E. *Biochemistry* **1985**, *24*, 7668.
- [100] Mantsch, H.H.; Smith, I.C.P. In *Carbon-13 nuclear magnetic resonance spectroscopy of the vitamin B₆ group* Ed.; Academic Press: **1979**, 422.
- [101] Metcalfe, J.C.; Hesketh, T.R.; Smith, G.A. *Cell Calcium* **1985**, *6*, 183.
- [102] Beech, J.S.; Iles, R.A. *Biochem. Soc. Trans.* **1987**, *15*, 871.
- [103] Joseph, A.; Davenport, C.; Kwock, L.; Burt, C.T.; London, R.E. *Magn. Reson. Med.* **1987**, *4*, 137.
- [104] Bental, M.; Deutsch, C. *Am. J. Physiol.* **1994**, *266*, C541.
- [105] Deutsch, C.J.; Taylor, J.S. *Biophys. J.* **1989**, *55*, 799.
- [106] Rhee, C.K.; Levy, L.A.; London, R.E. *Bioconj. Chem.* **1995**, *6*, 77.
- [107] Frenzel, T.; Koszler, S.; Bauer, H.; Niedballa, U.; Weinmann, H.J. *Invest. Radiol.* **1994**, *29*, S220.
- [108] Miyazawa, T.; Aoki, Y.; Akagi, K.; Takahashi, M.; Fritz-Zieroth, B.; Frenzel, T.; Weinmann, H.-J. *Acad. Radiol.* **1996**, *3*, S363.
- [109] Ojugo, A.S.; McSheehy, P.M.; McIntyre, D.J.; McCoy, C.; Stubbs, M.; Leach, M.O.; Judson, I.R.; Griffiths, J.R. *NMR Biomed.* **1999**, *12*, 495.
- [110] Aoki, Y.; Akagi, K.; Tanaka, Y.; Kawai, J.; Takahashi, M. *Invest. Radiol.* **1996**, *31*, 680.
- [111] McSheehy, P.M.J.; Robinson, S.P.; Ojugo, A.S.E.; Aboagye, E.O.; Cannell, M.B.; Leach, M.O.; Judson, I.R.; Griffiths, J.R. *Cancer Res.* **1998**, *58*, 1185.
- [112] Gerweck, L.E.; Seetharaman, K. *Cancer Res.* **1996**, *56*, 1194.
- [113] Tannock, I.F.; Rotin, D. *Cancer Res.* **1989**, *49*, 4373.
- [114] Kozin, S.V.; Gerweck, L.E. *Br. J. Cancer* **1998**, *77*, 1580.
- [115] Raghunand, N.; Mahoney, B.P.; Gillies, R.J. *Biochem. Pharmacol.* **2003**, *66*, 1219.
- [116] Mahoney, B.P.; Raghunand, N.; Baggett, B.; Gillies, R.J. *Biochem. Pharmacol.* **2003**, *66*, 1207.
- [117] Hwang, Y.C.; Kim, S.-G.; Evelhoch, J.L.; Ackerman, J.J.H. *Cancer Res.* **1992**, *52*, 1259.
- [118] Yamagata, M.; Tannock, I.F. *Br. J. Chem.* **1996**, *73*, 1328.
- [119] Prescott, D.M.; Charles, H.C.; Sostman, H.D.; Page, R.L.; Thrall, D.E.; Moore, D.; Oleson, J.R.; Dewhirst, M.W. *Int. J. Hypertherm.* **1993**, *9*, 745.
- [120] Jain, R.K.; Shah, S.A.; Finney, P.L. *JNCI* **1984**, *73*, 429.
- [121] Stubbs, M.; Rodrigues, L.; Howe, F.A.; Wang, J.; Jeong, K.-S.; Veech, R.L.; Griffiths, J.R. *Cancer Res.* **1994**, *54*, 4011.
- [122] Stubbs, M.; Bhujwalla, Z.M.; Tozer, G.M.; Rodrigues, L.M.; Maxwell, R.J.; Morgan, R.; Howe, F.A.; Griffiths, J.R. *NMR Biomed.* **1992**, *5*, 351.
- [123] Bhujwalla, Z.M.; Artemov, D.; Ballesteros, P.; Cerdan, S.; Gillies, R.J.; Solaiyappan, M. *NMR Biomed.* **2002**, *15*, 114.
- [124] Garcia-Martin, M.L.; Herigault, G.; Remy, C.; Farion, R.; Ballesteros, P.; Coles, J.A.; Cerdan, S.; Ziegler, A. *Cancer Res.* **2001**, *61*, 6524.
- [125] Raghunand, N.; Zhang, S.; Sherry, A.; Gillies, R. *Acad. Radiol.* **2002**, *9*, S481.
- [126] Raghunand, N.; Howison, C.; Sherry, A.D.; Zhang, S.; Gillies, R.J. *Magn. Reson. Med.* **2003**, *49*, 249.
- [127] Tsien, R.Y. *Nature* **1981**, *290*, 527.
- [128] Benders, J.; Flogel, U.; Schafer, T.; Leibfritz, D.; Hechtenberg, S.; Beyersmann, D. *Biochem. J.* **1997**, *322* (Pt 3), 793.
- [129] Smith, G.A.; Hesketh, R.T.; Metcalfe, J.C.; Feeney, J.; Morris, P.G. *Proc. Natl. Acad. Sci. (USA)* **1983**, *80*, 7178.
- [130] Gupta, R.K.; Gillies, R.J. In *¹⁹F NMR measurement of intracellular free calcium ions in intact cells and tissues*, R. K. Gupta, Ed.; CRC: Boca Raton, **1987**, 45.
- [131] Gupta, R.K.; Gupta, P. In *³¹P NMR measurement of intracellular free magnesium in cells and organisms*, R. K. Gupta, Ed.; CRC: Boca Raton, **1987**, 34.
- [132] Weller, E.; Bachert, P.; Meinck, H.M.; Friedmann, B.; Bartsch, P.; Mairbaurl, H. *Med. Sci. Sports Exe.* **1998**, *30*, 1584.
- [133] Schanne, F.A.; Moskal, J.R.; Gupta, R.K. *Brain Res.* **1989**, *503*, 308.
- [134] Schanne, F.A.; Dowd, T.L.; Gupta, R.K.; Rosen, J.F. *Proc. Natl. Acad. Sci. (USA)* **1989**, *86*, 5133.
- [135] Kusuoka, H.; Backx, P.H.; Camilion de Hurtado, M.C.; Azan-Backx, M.; Marban, E.; Cingolani, H.E. *Am. J. Physiol.* **1993**, *265*, H1696.
- [136] Plenio, H.; Diodone, R. *J. Am. Chem. Soc.* **1996**, *118*, 356.
- [137] Romani, A.M.; Scarpa, A. *Frontiers in Biosci.* **2000**, *5*, D720.
- [138] Noronha, J.L.; Matuschak, G.M. *Intensive Care Med.* **2002**, *28*, 667.
- [139] Murphy, E. *Mineral & Electrolyte Metab.* **1993**, *19*, 250.
- [140] Kirschenlohr, H.L.; Metcalfe, J.C.; Morris, P.G.; Rodrigo, G.C.; Smith, G.A. *Proc. Natl. Acad. Sci. (USA)* **1988**, *85*, 9017.
- [141] Tecle, B.; Casida, J.E. *Chem. Res. Toxicol.* **1989**, *2*, 429.

- [142] Levy, L.A.; Murphy, E.; Raju, B.; London, R.E. *Biochemistry* **1988**, *27*, 4041.
- [143] Murphy, E.; Steenbergen, C.; Levy, L.A.; Raju, B.; London, R.E. *J. Biol. Chem.* **1989**, *264*, 5622.
- [144] Long, G.J.; Rosen, J.F.; Schanne, F.A. *J. Biol. Chem.* **1994**, *269*, 834.
- [145] Smith, G.A.; Morris, P.G.; Hesketh, T.R.; Metcalfe, J.C. *Biochim. Biophys. Acta* **1986**, *889*, 72.
- [146] London, R.E.; Gabel, S.A. *J. Am. Chem. Soc.* **1994**, *116*, 2562.
- [147] Plenio, H.; Diodone, R. *Z. Naturforsch. Section B-J. Chem. Sci.* **1995**, *50*, 1075.
- [148] Plenio, H.; Hermann, J.; Diodone, R. *Inorg. Chem.* **1997**, *36*, 5722.
- [149] Takemura, H.; Kariyazono, H.; Yasutake, M.; Kon, N.; Tani, K.; Sako, K.; Shinmyozu, T.; Inazu, T. *Eur. J. Org. Chem.* **2000**, *1*, 141.
- [150] Robinson, S.P.; Griffiths, J.R. *Phil. Trans. R. Soc. London B Biol. Sci.* **2004**, *359*, 987.
- [151] Gray, L.; Conger, A.; Ebert, M.; Hornsey, S.; Scott, O. *Br. J. Radiol.* **1953**, *26*, 638.
- [152] Wouters, B.G.; Brown, J.M. *Radiat. Res.* **1997**, *147*, 514.
- [153] Sartorelli, A.C. *Cancer Res.* **1988**, *48*, 775.
- [154] Teicher, B.; Lazo, J.; Sartorelli, A. *Cancer Res.* **1981**, *41*, 73.
- [155] Höckel, M.; Vaupel, P. *J. Natl. Cancer Inst.* **2001**, *93*, 266.
- [156] Knowles, H.J.; Harris, A.L. *Breast Cancer Res.* **2001**, *3*, 318.
- [157] Rofstad, E.K.; Sundfor, K.; Lyng, H.; Trope, C.G. *Br. J. Cancer* **2000**, *83*, 354.
- [158] De Jaeger, K.; Kavanagh, M.C.; Hill, R.P. *Br. J. Cancer* **2001**, *84*, 1280.
- [159] Brown, J.M. *Molec. Med. Today* **2000**, *6*, 157.
- [160] Parhami, P.; Fung, B.N. *J. Phys. Chem.* **1983**, *87*, 1928.
- [161] Lai, C.-S.; Stair, S.; Mizioro, H.; Hyde, J.S. *J. Magn. Reson.* **1984**, *57*, 447.
- [162] Mattrey, R.F.; Schumacher, D.J.; Tran, H.T.; Guo, Q.; Buxton, R.B. *Biomater. Art. Cells Immob. Biotech.* **1992**, *20*, 917.
- [163] Eidelberg, D.; Johnson, G.; Barnes, D.; Tofts, P.S.; Delpy, D.; Plummer, D.; McDonald, W.I. *Magn. Reson. Med.* **1988**, *6*, 344.
- [164] Kong, C.F.; Holloway, G.M.; Parhami, P.; Fung, B.M. *J. Phys. Chem.* **1984**, *88*, 6308.
- [165] Thomas, S.R.; Pratt, R.G.; Millard, R.W.; Samarutunga, R.C.; Shiferaw, Y.; Clark, L.C. *Radiology* **1991**, *18*, 159.
- [166] Thomas, S.R.; Pratt, R.G.; Millard, R.W.; Samarutunga, R.C.; Shiferaw, Y.; Clark Jr., L.C.; Hoffmann, R.E. *JMRI* **1994**, *4*, 631.
- [167] Mason, R.P.; Shukla, H.P.; Antich, P.P. *Magn. Reson. Med.* **1993**, *29*, 296.
- [168] Thomas, S.R.; Pratt, R.G.; Millard, R.W.; Samarutunga, R.C.; Shiferaw, Y.; McGoron, A.J.; Tan, K.K. *Magn. Reson. Imaging* **1996**, *14*, 103.
- [169] Hunjan, S.; Zhao, D.; Constantinescu, A.; Hahn, E.W.; Antich, P.P.; Mason, R.P. *Int. J. Radiat. Oncol. Biol. Phys.* **2001**, *49*, 1097.
- [170] Dardzinski, B.J.; Sotak, C.H. *Magn. Reson. Med.* **1994**, *32*, 88.
- [171] Barker, B.R.; Mason, R.P.; Bansal, N.; Peshock, R.M. *JMRI* **1994**, *4*, 595.
- [172] Mason, R.P.; Shukla, H.P.; Antich, P.P. *Biomater. Artif. Cells Immob. Biotechnol.* **1992**, *20*, 929.
- [173] Mason, R.P.; Rodbumrung, W.; Antich, P.P. *NMR Biomed.* **1996**, *9*, 125.
- [174] Riess, J.G. *Biomater. Art. Cells Immob. Biotech.* **1992**, *20*, 183.
- [175] Kaufman, R.J.; In *Medical oxygen transport using perfluorochemicals*, J. Goldstein, Ed.; Butterworth-Heinemann: N.Y., **1991**, 127.
- [176] Zuck, T.F.; Riess, J.G. *Critical Rev. Clinical Lab. Sci.* **1994**, *31*, 295.
- [177] Krafft, M.P. *Adv. Drug Delivery Rev.* **2001**, *47*, 209.
- [178] Schutt, E.G.; Klein, D.H.; Mattrey, R.M.; Riess, J.G. *Angew. Chem. Int. Ed.* **2003**, *42*, 3218.
- [179] Riess, J.G. *Chem. Rev.* **2001**, *101*, 2797.
- [180] Mason, R.P.; Antich, P.P.; Babcock, E.E.; Gerberich, J.L.; Nunnally, R.L. *Magn. Reson. Imaging* **1989**, *7*, 475.
- [181] Mattrey, R.F.; Long, D.C. *Invest. Radiol.* **1988**, *23*, s298.
- [182] Rosenblum, W.I.; Hadfield, M.G.; Martinez, A.J.; Schatzki, P. *Arch. Pathol. Lab. Med.* **1976**, *100*, 213.
- [183] Fishman, J.E.; Joseph, P.M.; Floyd, T.F.; Mukherji, B.; Sloviter, H.S. *Magn. Reson. Imaging* **1987**, *5*, 279.
- [184] Fishman, J.E.; Joseph, P.M.; Carvlin, M.J.; Saadi-Elmandjra, M.; Mukherji, B.; Sloviter, H.S. *Invest. Radiol.* **1989**, *24*, 65.
- [185] Eidelberg, D.; Johnson, G.; Tofts, P.S.; Dobbin, J.; Crookard, H.A.; Plummer, D. *J. Cereb. Blood Flow Metab.* **1988**, *8*, 276.
- [186] Noth, U.; Morrissey, S.P.; Deichmann, R.; Adolf, H.; Schwarzbauer, C.; Lutz, J.; Haase, A. *Magn. Reson. Med.* **1995**, *34*, 738.
- [187] Mason, R.P.; Antich, P.P.; Babcock, E.E.; Constantinescu, A.; Peschke, P.; Hahn, E.W. *Int. J. Radiat. Oncol. Biol. Phys.* **1994**, *29*, 95.
- [188] Thomas, S.R.; Millard, R.W.; Pratt, R.G.; Shiferaw, Y.; Samarutunga, R.C. *Art. Cells, Blood Subst. Immob. Biotechnol.* **1994**, *22*, 1029.
- [189] Mason, R.P.; Nunnally, R.L.; Antich, P.P. *Magn. Reson. Med.* **1991**, *18*, 71.
- [190] Tran, H.T.; Guo, Q.; Schumacher, D.J.; Buxton, R.B.; Mattrey, R.F. *Acad. Radiol.* **1995**, *2*, 756.
- [191] Helmer, K.G.; Han, S.; Sotak, C.H. *NMR Biomed.* **1998**, *11*, 120.
- [192] Baldwin, N.J.; Ng, T.C. *Magn. Reson. Imaging* **1996**, *14*, 541.
- [193] van der Sanden, B.J.P.; Heerschap, A.; Hoofd, L.; Simonetti, A.W.; Nicolay, K.; van der Toorn, A.; Colier, W.N.M.; van der Kogel, A.J. *Magn. Reson. Med.* **1999**, *42*, 490.
- [194] Fan, X.; River, J.N.; Zamora, M.; Al-Hallaq, H.A.; Karczmar, G.S. *Int. J. Radiat. Oncol. Biol. Phys.* **2002**, *54*, 1202.
- [195] Holland, S.K.; Kennan, R.P.; Schaub, M.M.; D'Angelo, M.J.; Gore, J.C. *Magn. Reson. Med.* **1993**, *29*, 446.
- [196] Hees, P.S.; Sotak, C.H. *Magn. Reson. Med.* **1993**, *29*, 303.
- [197] McIntyre, D.J.O.; McCoy, C.L.; Griffiths, J.R. *Curr. Sci.* **1999**, *76*, 753.
- [198] van der Sanden, B.P.J.; Heerschap, A.; Simonetti, A.W.; Rijken, P.F.J.W.; Peters, H.P.W.; Stüben, G.; van der Kogel, A.J. *Int. J. Radiat. Oncol. Biol. Phys.* **1999**, *44*, 649.
- [199] Zhao, D.; Ran, S.; Constantinescu, A.; Hahn, E.W.; Mason, R.P. *Neoplasia* **2003**, *5*, 308.
- [200] Song, Y.; Constantinescu, A.; Mason, R.P. *Technol. Cancer Res. Treat.* **2002**, *1*, 471.
- [201] Zhao, D.; Constantinescu, A.; Chang, C.-H.; Hahn, E.W.; Mason, R.P. *Radiat. Res.* **2003**, *159*, 621.
- [202] Zhao, D.; Constantinescu, C.; Hahn, E.W.; Mason, R.P. *Int. J. Radiat. Oncol. Biol. Phys.* **2002**, *53*, 744.
- [203] Bulte, J.W.; Arbab, A.S.; Douglas, T.; Frank, J.A. *Methods Enzymol.* **2004**, *386*, 275.
- [204] Zimmermann, U.; Noth, U.; Grohn, P.; Jork, A.; Ulrichs, K.; Lutz, J.; Haase, A. *Artif. Cells, Blood Subst. Immob. Biotechnol.* **2000**, *28*, 129.
- [205] Noth, U.; Grohn, P.; Jork, A.; Zimmermann, U.; Haase, A.; Lutz, J. *Magn. Reson. Med.* **1999**, *42*, 1039.
- [206] Wang, Z.; Su, M.-Y.; Nalcioğlu, O. *Technol. Cancer Res. Treat.* **2002**, *1*, 29.
- [207] Berkowitz, B.A.; Wilson, C.A.; Hatchell, D.L. *Invest. Ophthalmol. Vis. Sci.* **1991**, *32*, 2382.
- [208] Wilson, C.A.; Berkowitz, B.A.; Hatchell, D.L. *Exp. Eye Res.* **1992**, *55*, 119.
- [209] Zhang, W.; Ito, Y.; Berlin, E.; Roberts, R.; Berkowitz, B.A. *Invest. Ophthalmol. Visual Sci.* **2003**, *44*, 3119.
- [210] Duong, T.Q.; Iadecola, C.; Kim, S.G. *Magn. Reson. Med.* **2001**, *45*, 61.
- [211] Nöth, U.; Deichmann, R.; Adolf, H.; Schwarzbauer, C.; Haase, A. *J. Magn. Reson. B.* **1994**, *105*, 233.
- [212] Lee, H.K.; Nalcioğlu, O. *JMRI* **1992**, *2*, 53.
- [213] Busse, L.J.; Pratt, R.G.; Thomas, S.R. *J. Comp. Ast. Tomogr.* **1988**, *12*, 824.
- [214] Pratt, R.G.; Zheng, J.; Stewart, B.K.; Shiferaw, Y.; McGoron, A.J.; Samarutunga, R.C.; Thomas, S.R. *Magn. Reson. Med.* **1997**, *37*, 307.
- [215] Zhao, D.; Constantinescu, A.; Jiang, L.; Hahn, E.W.; Mason, R.P. *Am. J. Clin. Oncol.* **2001**, *24*, 462.
- [216] Prosser, R.S.; Luchette, P.A.; Westerman, P.W.; Rozek, A.; Hancock, R.E. *Biophys. J.* **2001**, *80*, 1406.
- [217] Kim, J.G.; Zhao, D.; Constantinescu, A.; Mason, R.P.; Liu, H. *J. Biomed. Optics* **2003**, *8*, 53.
- [218] Mason, R.P.; Ran, S.; Thorpe, P.E. *J. Cell. Biochem.* **2002**, *87S*, 45.
- [219] Delpuech, J.-J.; Hamza, M.A.; Serraticce, G.; Stébé, M.-J. *J. Chem. Phys.* **1979**, *70*, 2680.
- [220] Hamza, M.A.; Serraticce, G.; Stebe, M.-J.; Delpuech, J.-J. *J. Am. Chem. Soc.* **1981**, *103*, 3733.
- [221] Hamza, M.A.; Serraticce, G.; Stebe, M.-J.; Delpuech, J.-J. *J. Magn. Reson.* **1981**, *42*, 227.

- [222] Rietjens, I.M.C.M.; Steensma, A.; den Besten, C.; van Tintelen, G.; Haas, J.; van Ommen, B.; van Bladeren, P.J. *Eur. J. Pharmacol.* **1995**, *293*, 292.
- [223] Gorsman, Y.S.; Kapitonenko, T.A. *Izv. Estestvennonauchu. Inst. Pevinsk.* **1973**, *15*, 155.
- [224] Mortelmans, K.M.; Simmon, V.F. *Gov. Rep. Announce Index (US)* **1981**, *81*, 2555.
- [225] Courtney, K.D.; Andrews, J.E. *J. Environ. Sci. Health B* **1984**, *19*, 83.
- [226] Hall, L.W.; Jackson, S.R.K.; Massey, G.M., In *Hexafluorobenzene in veterinary anaesthesia*, A. Arias, R. Llauro, M. A. Nalda, and J. N. Lunn, Ed.; Excerpta Medica: Oxford, **1975**, 201.
- [227] Hunjan, S.; Mason, R.P.; Constantinescu, A.; Peschke, P.; Hahn, E.W.; Antich, P.P. *Int. J. Radiat. Oncol. Biol. Phys.* **1998**, *40*, 161.
- [228] Le, D.; Mason, R.P.; Hunjan, S.; Constantinescu, A.; Barker, B.R.; Antich, P.P. *Magn. Reson. Imaging* **1997**, *15*, 971.
- [229] Brizel, D.M.; Sibly, G.S.; Prossnitz, L.R.; Scher, R.L.; Dewhirst, M.W. *Int. J. Radiat. Oncol. Biol. Phys.* **1997**, *38*, 285.
- [230] Fyles, A.W.; Milosevic, M.; Wong, R.; Kavanagh, M.-C.; Pintile, M.; Sun, A.; Chapman, W.; Levin, W.; Manchul, L.; Keane, T.J.; Hill, R.P. *Radiother. Oncol.* **1998**, *48*, 149.
- [231] Mason, R.P.; Hunjan, S.; Constantinescu, A.; Song, Y.; Zhao, D.; Hahn, E.W.; Antich, P.P.; Peschke, P., In *Tumor oximetry: Comparison of ¹⁹F MR EPI and electrodes*, J. F. Dunn and H. M. Swartz, Ed.; Kluwer: New York, **2003**, 19.
- [232] Mason, R.P.; Constantinescu, A.; Hunjan, S.; Le, D.; Hahn, E.W.; Antich, P.P.; Blum, C.; Peschke, P. *Radiat. Res.* **1999**, *152*, 239.
- [233] Gu, Y.; Bourke, V.; Kim, J.G.; Constantinescu, A.; Mason, R.P.; Liu, H. *Applied Optics* **2003**, *42*, 1.
- [234] Clark Jr., L.C.; Ackerman, J.; Thomas, S.R.; Millard, R.W.; Hoffmann, R.E.; Pratt, R.G.; Ragle-Cole, H.; Kinsey, R.A.; Janakiraman, R., In *Perfluorinated organic liquids and emulsions as biocompatible NMR imaging agents for ¹⁹F and dissolved oxygen*, D. Bruley, H. I. Bicher, and D. Reneau, Ed.; Plenum Press: New York, **1984**, 835.
- [235] Rodbumrung, W., 'Assessment of perfluorocarbons as probes for oximetry and thermometry', UT Southwestern, Dallas TX, 1994.
- [236] Stratford, I.J.; Adams, G.E., In *Radiation sensitizers and bioreductive drugs*, G. G. Steel, G. E. Adams, and A. Horwich, Ed.; Elsevier: Amsterdam, **1989**, 145.
- [237] Rasey, J.S.; Casciari, J.J.; Hofstrand, P.D.; Muzi, M.; Graham, M.M.; Chin, L.K. *Radiat. Res.* **2000**, *153*, 84.
- [238] Franko, A.; Koch, C.; Boisvert, D. *Cancer Res.* **1992**, *52*, 3831.
- [239] Ballinger, J.R. *Semin. Nucl. Med.* **2001**, *31*, 321.
- [240] Hodgkiss, R.J. *Anti-cancer Drug Design* **1998**, *13*, 687.
- [241] Evans, S.M.; Hahn, S.; Pook, D.R.; Jenkins, W.T.; Chalian, A.A.; Zhang, P.; Stevens, C.; Weber, R.; Weinstein, G.; Benjamin, I.; Mirza, N.; Morgan, M.; Rubin, S.; McKenna, W.G.; Lord, E.M.; Koch, C.J. *Cancer Res.* **2000**, *60*, 2018.
- [242] Koch, C.J.; Hahn, S.M.; Rockwell, K.J.; Covey, J.M.; McKenna, W.G.; Evans, S.M. *Cancer Chemother. Pharmacol.* **2001**, *48*, 177.
- [243] Ljungkvist, A.S.E.; Bussink, J.; Rijken, P.F.J.W.; Raleigh, J.A.; Denekamp, J.; Van Der Kogel, A.J. *Int. J. Radiat. Oncol. Biol. Phys.* **2000**, *48*, 1529.
- [244] Raleigh, J.A.; Chou, S.C.; Arteel, G.E.; Horsman, M. *Radiat. Res.* **1999**, *151*, 580.
- [245] Dehdashti, F.; Mintun, M.A.; Lewis, J.S.; Bradley, J.; Govinda, R.; Laforest, R.; Welch, M.J.; Siegel, B.A. *Eur. J. Nucl. Med. Molec. Imaging* **2003**, *30*, 844.
- [246] Dehdashti, F.; Grigsby, P.W.; Mintun, M.A.; Lewis, J.S.; Siegel, B.A.; Welch, M.J. *Int. J. Radiat. Oncol. Biol. Phys.* **2003**, *55*, 1233.
- [247] Koch, C.J.; Evans, S.M. *Adv. Exp. Med. Biol.* **2003**, *510*, 285.
- [248] Raleigh, J.A.; Franko, A.J.; Treiber, E.O.; Lunt, J.A.; Allen, P.S. *Int. J. Radiat. Oncol. Biol. Phys.* **1986**, *12*, 1243.
- [249] Maxwell, R.J.; Workman, P.; Griffiths, J.R. *Int. J. Radiat. Oncol. Biol. Phys.* **1989**, *16*, 925.
- [250] Jin, G.Y.; Li, S.J.; Moulder, J.E.; Raleigh, J.A. *Int. J. Radiat. Biol.* **1990**, *58*, 1025.
- [251] Li, S.J.; Jin, G.Y.; Moulder, J.E. *Cancer Commun.* **1991**, *3*, 133.
- [252] Kwock, L.; Gill, M.; McMurry, H.L.; Beckman, W.; Raleigh, J.A.; Joseph, A.P. *Radiat. Res.* **1992**, *129*, 71.
- [253] Workman, P.; Maxwell, R.J.; Griffiths, J.R. *NMR Biomed.* **1992**, *5*, 270.
- [254] Aboagye, E.O.; Maxwell, R.J.; Horsman, M.R.; Lewis, A.D.; Workman, P.; Tracy, M.; Griffiths, J.R. *Br. J. Cancer* **1998**, *77*, 65.
- [255] Aboagye, E.O.; Kelson, A.B.; Tracy, M.; Workman, P. *Anticancer Drug Des.* **1998**, *13*, 703.
- [256] Aboagye, E.O.; Maxwell, R.J.; Kelson, A.B.; Tracy, M.; Lewis, A.D.; Graham, M.A.; Horsman, M.R.; Griffiths, J.R.; Workman, P. *Cancer Res.* **1997**, *57*, 3314.
- [257] Aboagye, E.O.; Lewis, A.D.; Johnson, A.; Workman, P.; Tracy, M.; Huxham, I.M. *Br. J. Cancer* **1995**, *72*, 312.
- [258] Aboagye, E.O.; Lewis, A.D.; Graham, M.A.; Tracy, M.; Kelson, A.B.; Ryan, K.J.; Workman, P. *Anticancer Drug Des.* **1996**, *11*, 231.
- [259] Aboagye, E.O.; Lewis, A.D.; Tracy, M.; Workman, P. *Biochem. Pharmacol.* **1997**, *54*, 1217.
- [260] Raleigh, J.A.; Franko, A.J.; Kelly, D.A.; Trimble, L.A.; Allen, P.S. *Magn. Reson. Med.* **1991**, *22*, 451.
- [261] Aboagye, E.O.; Artemov, D.; Senter, P.D.; Bhujwalla, Z.M. *Cancer Res.* **1998**, *58*, 4075.
- [262] Seddon, B.M.; Maxwell, R.J.; Honess, D.J.; Grimshaw, R.; Raynaud, F.; Tozer, G.M.; Workman, P. *Clin. Cancer Res.* **2002**, *8*, 2323.
- [263] Clark Jr., L.C.; Gollan, F. *Science* **1966**, 1755.
- [264] Greenspan, J.S.; Fox, W.W.; Rubenstein, S.D.; Wolfson, M.R.; Spinner, S.S.; Shaffer, T.H. *Pediatrics* **1997**, *99*, E2.
- [265] Thomas, S.R.; Gradon, L.; Pratsinis, S.E.; Pratt, R.G.; Fotou, G.P.; McGoron, A.J.; Podgorski, A.L.; Millard, R.W. *Invest. Radiol.* **1997**, *32*, 29.
- [266] Huang, M.Q.; Ye, Q.; Williams, D.S.; Ho, C. *Magn. Reson. Med.* **2002**, *48*, 487.
- [267] Schreiber, W.G.; Markstaller, K.; Weiler, N.; Eberle, B.; Laukemper-Ostendorf, S.; Scholz, A.; Burger, K.; Thelen, M.; Kauczor, H.U. *Rofo Fortschr. Geb. Rontgenstr. Neuen. Bildgeb. Verfahr.* **2000**, *172*, 500.
- [268] Kauczor, H.U.; Heussel, C.P.; Schreiber, W.G.; Kreitner, K.F. *Radiologe* **2001**, *41*, 279.
- [269] Kuethe, D.O.; Behr, V.C.; Begay, S. *Magn. Reson. Med.* **2002**, *48*, 547.
- [270] Chen, X.J.; Moller, H.E.; Chawla, M.S.; Cofer, G.P.; Driehuis, B.; Hedlund, L.W.; Johnson, G.A. *Magn. Reson. Med.* **1999**, *42*, 721.
- [271] Ruppert, K.; Brookeman, J.; Hagspiel, K.D.; Mugler, J.P. *Magn. Reson. Med.* **2000**, *44*, 349.
- [272] Kauczor, H.U.; Chen, X.J.; van Beek, E.J.; Schreiber, W.G. *Eur. Respir. J.* **2001**, *17*, 1008.
- [273] Remy, W.F.; Geenen, R.W.; Hussain, S.M.; Cademartini, F.; Poley, J.W.; Siersema, P.D.; Krestin, G.P. *Radiograph.* **2004**, *24*, e18.
- [274] Rubin, D.L.; Falk, K.L.; Sperling, M.J.; Ross, M.; Saini, S.; Rothman, B.; Shellock, F.; Zerhouni, E.; Stark, D.; Outwater, E.K.; Schmiedl, U.; Kirby, L.C.; Chezmar, J.; Coates, T.; Chang, M.; Silverman, J.M.; Rofsky, N.; Burnett, K.; Engel, J.; Young, S.W. *JMRI* **7**, 865.
- [275] Hirohashi, S.; Uchida, H.; Yoshikawa, K.; Fujita, N.; Ohtomo, K.; Yuasa, Y.; Kawamura, Y.; Matsui, O. *Magn. Reson. Imaging* **1994**, *12*, 837.
- [276] Bisset, G.S.R.; Emery, K.H.; Meza, M.P.; Rollins, N.K.; Don, S.; Shorr, J.S. *Pediatric Radiol.* **1996**, *26*, 409.
- [277] Mattrey, R.F.; Trambert, M.A.; Brown, J.J.; Young, S.W.; Bruneton, J.N.; Wesbey, G.E.; Balsara, Z.N. *Radiology* **1994**, *191*, 841.
- [278] Schwarz, R.; Kaspar, A.; Seelig, J.; Kunnecke, B. *Magn. Reson. Med.* **2002**, *48*, 255.
- [279] Uzzan, B.; Nicolas, P.; Cucherat, M.; Perret, G.Y. *Cancer Res.* **2004**, *64*, 2941.
- [280] Robinson, S.P.; Rijken, P.F.; Howe, F.A.; McSheehy, P.M.; van der Sanden, B.P.; Heerschap, A.; Stubbs, M.; Van Der Kogel, A.J.; Griffiths, J.R. *J. Magn. Reson. Imaging* **2003**, *17*, 445.
- [281] Evelhoch, J.L. *JMRI* **1999**, *10*, 254.
- [282] Tofts, P.S.; Brix, G.; Buckley, D.L.; Evelhoch, J.L.; Henderson, E.; Knopp, M.V.; Larsson, H.B.; Lee, T.Y.; Mayr, N.A.; Parker, G.J.; Port, R.E.; Taylor, J.; Weisskoff, R.M. *J. Magn. Reson. Imaging* **1999**, *10*, 223.
- [283] Wang, Y.X.; Hussain, S.M.; Krestin, G.P. *Europ. Radiol.* **2001**, *11*, 2319.
- [284] Meyer, K.L.; Joseph, P.M.; Mukherji, B.; Livolsi, V.A.; Lin, R. *Invest. Radiol.* **1993**, *28*, 710.
- [285] Baldwin, N.J.; Wang, Y.; Ng, T.C. *Magn. Reson. Imaging* **1996**, *14*, 275.

- [286] Thomas, C.; Counsell, C.; Wood, P.; Adams, G.E. *JNCI* **1992**, *84*, 174.
- [287] Sogabe, T.; Imaizumi, T.; Mori, T.; Tominaga, M.; Koga, K.; Yabuuchi, Y. *Magn. Reson. Imaging* **1997**, *15*, 341.
- [288] Joseph, P.M.; Fishman, J.E.; Mukherji, B.; Sloviter, H.A. *J. Comp. Assist. Tomogr.* **1985**, *9*, 1012.
- [289] Ceckler, T.L.; Gibson, S.L.; Hilf, R.; Bryant, R.G. *Magn. Reson. Med.* **1990**, *13*, 416.
- [290] Negendank, W.G.; McCoy, L.E.; Crowley, M.G.; Corbett, T.H.; Schmidt, E.L. *Biomater Artif Cells Artif Organs* **1990**, *18*, 119.
- [291] Authier, B. *Magn. Reson. Med.* **1988**, *8*, 80.
- [292] Ewing, J.R.; Branch, C.A.; Fagan, S.C.; Helpert, J.A.; Simkins, R.T.; Butt, S.M.; Welch, K.M.A. *Stroke* **1990**, *21*, 100.
- [293] Leff, S.M.; Schnall, M.D.; Ligetti, L.; Osbakken, M.; Subramanian, V.H.; Chance, B.; Leigh, J.S. Jr. *Magn. Reson. Med.* **1988**, *7*, 412.
- [294] Ratner, A.V.; Quay, S.; Muller, H.H.; Simpson, B.B.; Hurd, R.; Young, S.W. *Invest. Radiol.* **1989**, *24*, 224.
- [295] Mehta, V.D.; Mason, R.P.; Kulkarni, P.V.; Lea, P.; Constantinescu, A.; Antich, P.P., In *¹⁹F MR characterization of fluorinated proteins and relaxation rate enhancement with Gd-DTPA for faster imaging*, E. H. Emram, Ed.; Plenum: New York, **1995**, 305.
- [296] Lee, H.; Price, R.R.; Holburn, G.E.; Partain, C.L.; Adams, M.D.; Cacheris, W.P. *J. Magn. Reson. Imaging* **1994**, *4*, 609.
- [297] Brix, G.; Bellemann, M.E.; Gerlach, L.; Haberkorn, U. *Radiology* **1998**, *209*, 259.
- [298] Fowler, J.S.; Volkow, N.D.; Wang, G.J.; Ding, Y.S. *Semin. Nucl. Med.* **2004**, *34*, 112.
- [299] Nakada, T.; Kwee, I.L.; Conboy, C.B. *J. Neurochem.* **1986**, *46*, 198.
- [300] Nakada, T.; Kwee, I.L. *Magn. Reson. Imaging* **1987**, *5*, 259.
- [301] Nakada, T.; Kwee, I.L. *Magn. Reson. Med.* **1987**, *4*, 366.
- [302] Nakada, T.; Kwee, I.L.; Card, P.J.; Matwiyoff, N.A.; Griffey, B.V.; Griffey, R.H. *Magn. Reson. Med.* **1988**, *6*, 307.
- [303] Nakada, T.; Kwee, I.L.; Griffey, B.V.; Griffey, R.H. *Magn. Reson. Imaging* **1988**, *6*, 633.
- [304] Nakada, T.; Kwee, I.L.; Griffey, B.V.; Griffey, R.H. *Radiology* **1988**, *168*, 823.
- [305] Kanazawa, Y.; Umayahara, K.; Shimmura, T.; Yamashita, T. *NMR Biomed.* **1997**, *10*, 35.
- [306] Nakada, T.; Kwee, I.L. *Magn. Reson. Med.* **1993**, *29*, 543.
- [307] Kanazawa, Y.; Yamane, H.; Shinohara, S.; Kuribayashi, S.; Momozono, Y.; Yamato, Y.; Kojima, M.; Masuda, K. *J. Neurochem.* **1996**, *66*, 2113.
- [308] Berkowitz, B.A.; Ackerman, J.J. *Biophys. J.* **1987**, *51*, 681.
- [309] O'Connell, T.M.; London, R.E. *J. Magn. Reson. B* **1995**, *109*, 264.
- [310] Kwee, I.L.; Nakada, T.; Card, P.J. *J. Neurochem.* **1987**, *49*, 428.
- [311] Karino, K.; Kador, P.F.; Berkowitz, B.; Balaban, R.S. *J Biol Chem* **1991**, *266*, 20970.
- [312] Kwee, I.L.; Nakada, T.; Suzuki, N. *NMR Biomed.* **1991**, *4*, 38.
- [313] Kwee, I.L.; Igarashi, H.; Nakada, T. *Neuroreport* **1996**, *7*, 726.
- [314] Presant, C.A.; Wolf, W.; Waluch, V.; Wiseman, C.; Kennedy, P.; Blayney, D.; Brechner, R.R. *The Lancet* **1994**, *343*, 1184.
- [315] Peters, G.F.J. *J. Clin. Oncol.* **1988**, *6*, 1653.
- [316] Hull, W.E.; Port, R.E.; Herrmann, R.; Britsch, B.; Kunz, W. *Cancer Res.* **1988**, *48*, 1680.
- [317] Koskinen-Kautilainen, M.; Luoma, H.; Tuomisto, J. *Magn. Trace Elem.* **1990**, *9*, 15.
- [318] Brix, G.; Bellemann, M.E.; Haberkorn, U.; Gerlach, L.; Lorenz, W.J. *Nucl. Med. Biol.* **1996**, *23*, 897.
- [319] Brix, G.; Bellemann, M.E.; Zabel, H.J.; Bachert, P.; Lorenz, W.J. *Magn. Reson. Imaging* **1993**, *11*, 1193.
- [320] Brix, G.; Bellemann, M.E.; Haberkorn, U.; Gerlach, L.; Bachert, P.; Lorenz, W.J. *Magn. Reson. Med.* **1995**, *34*, 302.
- [321] Guerquin-Kern, J.-L.; Leteurtre, F.; Croisy, A.; Lhoste, J.-M. *Cancer Res.* **1991**, *51*, 5770.
- [322] Ojugo, A.S.E.; McSheehy, P.M.J.; Stubbs, M.; Alder, G.; Bashford, C.L.; Maxwell, R.J.; Leach, M.O.; Judson, I.R.; Griffiths, J.R. *Br. J. Cancer* **1998**, *77*, 873.
- [323] Laurencot, C.M.; Kennedy, K.A. *Oncol. Res.* **1995**, *7*, 371.
- [324] Song, C.W.; Lyons, J.C.; Luo, Y., In *Intra-and extracellular pH in solid tumors: influence on therapeutic response*, B. A. Teicher, Ed.; Marcel Dekker: New York, **1993**, 25.
- [325] Raghunand, N.; Gillies, R.J. *Novartis Foundation Symposium* **2001**, *240*, 199.
- [326] Sijens, P.E.; Baldwin, N.J.; Ng, T.C. *Magn. Reson. Med.* **1991**, *19*, 337.
- [327] Stegman, L.D.; Rehemtulla, A.; Hamstra, D.A.; Rice, D.J.; Jonas, S.J.; Stout, K.L.; Chenevert, T.L.; Ross, B.D. *Gene Ther.* **2000**, *7*, 1005.
- [328] Aghi, M.; Kramm, C.M.; Chou, T.C.; Breakefield, X.O.; Chiocca, E.A. *J. Natl. Cancer Inst.* **1998**, *90*, 370.
- [329] Wyrwicz, A.M.; Li, Y.E.; Schofield, J.C.; Burt, C.T. *FEBS Letters* **1983**, *162*, 334.
- [330] Wyrwicz, A.M.; Conboy, C.B.; Nichols, B.G.; Ryback, K.R.; Eisele, P. *Biochim. Biophys. Acta* **1987**, *929*, 271.
- [331] Wyrwicz, A.M.; Conboy, C.B.; Ryback, K.R.; Nichols, B.G.; Eisele, P. *Biochim. Biophys. Acta* **1987**, *927*, 86.
- [332] Wyrwicz, A.M.; Conboy, C.B. *Magn. Reson. Med.* **1989**, *9*, 219.
- [333] Wyrwicz, A.M. *Ann. NY Acad. Sci.* **1991**, *625*, 733.
- [334] Venkatasubramanian, P.N.; Shen, Y.J.; Wyrwicz, A.M. *NMR Biomed.* **1993**, *6*, 377.
- [335] Venkatasubramanian, P.N.; Shen, Y.J.; Wyrwicz, A.M. *Biochim. Biophys. Acta* **1995**, *1245*, 262.
- [336] Venkatasubramanian, P.N.; Shen, Y.J.; Wyrwicz, A.M. *Magn. Reson. Med.* **1996**, *35*, 626.
- [337] Chew, W.M.; Moseley, M.E.; Mills, P.A.; Sessler, D.; Gonzalez-Mendez, R.; James, T.L.; Litt, L. *Magn. Reson. Imaging* **1987**, *5*, 51.
- [338] Hashimoto, T.; Ikehira, H.; Fukuda, H.; Ueshima, Y.; Tateno, Y. *Magn Reson Imaging* **1991**, *9*, 577.
- [339] Lockhart, S.H.; Cohen, Y.; Yasuda, N.; Freire, B.; Taheri, S.; Litt, L.; Eger, E.I., 2nd. *Anesthesiol.* **1991**, *74*, 575.
- [340] Litt, L.; Lockhart, S.; Cohen, Y.; Yasuda, N.; Kim, F.; Freire, B.; Laster, M.; Peterson, N.; Taheri, S.; Chang, L.H.; Sessler, D.I.; Moseley, M.; Eger, E.I.; James T.L. *Ann. NY Acad. Sci.* **1991**, *625*, 707.
- [341] Lockhart, S.H.; Cohen, Y.; Yasuda, N.; Kim, F.; Litt, L.; Eger, E.I., 2nd; Chang, L.H.; James, T. *Anesthesiol.* **1990**, *73*, 455.
- [342] Preece, N.E.; Challands, J.; Williams, S.C. *NMR Biomed.* **1992**, *5*, 101.
- [343] Selinsky, B.S.; Thompson, M.; London, R.E. *Biochem. Pharmacol.* **1987**, *36*, 413.
- [344] Selinsky, B.S.; Perlman, M.E.; London, R.E. *Molec. Pharmacol.* **1988**, *33*, 559.
- [345] Selinsky, B.S.; Perlman, M.E.; London, R.E. *Mol. Pharmacol.* **1988**, *33*, 567.
- [346] Kuethe, D.O.; Caprihan, A.; Fukushima, E.; Waggoner, R.A. *Magn. Reson. Med.* **1998**, *39*, 85.
- [347] Raleigh, J.; Franko, A.; Kelly, D.; Trimble, L.; Allen, P. *Magn. Reson. Med.* **1991**, *22*, 451.
- [348] Mehta, V.D.; Kulkarni, P.V.; Mason, R.P.; Constantinescu, A.; Aravind, S.; Goomer, N.; Antich, P.P. *FEBS Letters* **1994**, *349*, 234.
- [349] London, R.E.; Gabel, S.A. *Biochemistry* **1989**, *28*, 2378.
- [350] Ramasamy, R.; Zhao, P.; Gitomer, W.L.; Sherry, A.D.; Malloy, C.R. *Am. J. Physiol.* **1993**, *263*, H1958.
- [351] Berkowitz, B.A.; Handa, J.T.; Wilson, C.A. *NMR Biomed.* **1992**, *5*, 65.
- [352] Duong, T.Q.; Ackerman, J.J.; Ying, H.S.; Neil, J.J. *Magn. Reson. Med.* **1998**, *40*, 1.
- [353] Daugherty, A.; Becker, N.N.; Scherrer, L.A.; Sobel, B.E.; Ackerman, J.J.; Baynes, J.W.; Thorpe, S.R. *Biochem. J.* **1989**, *264*, 829.
- [354] Lanza, G.M.; Yu, X.; Winter, P.M.; Abendschein, D.R.; Karukstis, K.K.; Scott, M.J.; Chinen, L.K.; Fuhrhop, R.W.; Scherrer, D.E.; Wickline, S.A. *Circulation* **2002**, *106*, 2842.
- [355] Thomas, S.R.; Gradon, L.; Pratsinis, S.E.; Pratt, R.G.; Fotou, G.P.; McGoron, A.J.; Podgorski, A.L.; Millard, R.W. *Invest. Radiol.* **1997**, *32*, 29.
- [356] Robert, D.U.; Flatau, G.N.; Cambon, A.; Riess, J.G. *Tetrahedron* **1973**, *29*, 1877.
- [357] Morozova, T.V.; Chuvatkina, N.N.; Panteleeva, I.Y.; Boguslavskaya, L.S. *USSR Zh. Organ. Khim.* **1984**, *20*, 1379.
- [358] Hoffmann, F.W. *J. Org. Chem.* **1949**, *14*, 105.
- [359] Hu, C.; Qing, F.; Shen, C. *J. Chem. Soc., Perkin Trans. 1: Org. Bio-Org. Chem.* **1993**, *3*, 335.
- [360] Kurosawa, S.; Sekiya, A.; Arimura, T.; Yamada, T. *J. Fluorine Chem.* **1993**, *62*, 69.
- [361] Stepanov, I.V.; Burmakov, A.I.; Kunshenko, B.V.; Alekseeva, L.A.; Yagupol'skii, L.M. *Zhur. Organ. Khim.* **1983**, *19*, 273.

- [362] Fukuhara, T.; Yoneda, N.; Sawada, T.; Suzuki, A. *Synthetic Commun.* **1987**, *17*, 685.
- [363] Cacchi, S.; Fabrizi, G.; Goggiamani, A. *Organic Letters* **2003**, *5*, 4269.
- [364] Prakash, G.K.S.; Yudin, A.K. *Chem. Rev.* **1997**, *97*, 757.
- [365] Singh, R.P.; Shreeve, J.M. *Tetrahedron* **2000**, *56*, 7613.
- [366] Marban, E.; Kitakaze, M.; Kusuoka, H.; Porterfield, J.K.; Yue, D.T.; Chacko, V.P. *Proc. Natl. Acad. Sci. (USA)* **1987**, *84*, 6005.
- [367] Marban, E.; Kitakaze, M.; Chacko, V.P.; Pike, M.M. *Circ. Res.* **1988**, *63*, 673.
- [368] Shionoya, M.; Kimura, E.; Iitaka, Y. *J. Am. Chem. Soc.* **1990**, *112*, 9237.
- [369] Mason, R.P.; Jeffrey, F.M.H.; Malloy, C.R.; Babcock, E.E.; Antich, P.P. *Magn. Reson. Med.* **1992**, *27*, 310.
- [370] Berkowitz, B.A.; Wilson, C.A.; Hatchell, D.L.; London, R.E. *Magn. Reson. Med.* **1991**, *21*, 233.
- [371] Thomas, S.R.; Clark, Jr., L.C.; Ackerman, J.; Pratt, R.G.; Hoffmann, R.E.; Busse, L.J.; Kinsey, R.A.; Samaratunga, R.C. *J. Comp. Asst. Tomogr.* **1986**, *10*, 1.
- [372] Sotak, C.H.; Hees, P.S.; Huang, H.N.; Hung, M.H.; Krespan, C.G.; Reynolds, S. *Magn. Reson. Med.* **1993**, *29*, 188.
- [373] Papadopoulou, M.V.; Pouremad, R.; Rao, M.K.; Ji, M.; Bloomer, W.D. *In Vivo* **2001**, *15*, 365.

Synthesis and evaluation of novel enhanced gene reporter molecules: Detection of β -galactosidase activity using ^{19}F NMR of trifluoromethylated aryl β -D-galactopyranosides

Jianxin Yu, Li Liu, Vikram D. Kodibagkar, Weina Cui and Ralph P. Mason*

Department of Radiology, The University of Texas Southwestern Medical Center at Dallas, Dallas, TX, USA

Received 24 June 2005; revised 4 August 2005; accepted 5 August 2005

Available online 26 September 2005

Abstract—Gene therapy has emerged as a promising strategy for treatment of various diseases, but there is a pressing need for the development of non-invasive reporter techniques based on appropriate molecules and imaging modalities to assay gene expression. We now report the design, synthesis, and evaluation of novel enhanced reporter molecules, which reveal *lacZ* gene expression: trifluoromethylated aryl β -D-galactopyranosides. A series of five molecular structures were screened in solution and with stably transfected *lacZ* expressing human MCF7 breast cancer cells in vitro. *p*-Trifluoromethyl-*o*-nitrophenyl β -D-galactopyranoside (**PCF₃ONPG**) was found to exhibit valuable properties including a single ^{19}F NMR signal, stability in aqueous solution and with wild type cells, but a chemical shift response to enzyme cleavage ($\Delta\delta = 1.14$ ppm) in breast cancer cells transfected to stably express *lacZ*.

© 2005 Elsevier Ltd. All rights reserved.

1. Introduction

Strategies for identifying exogenous gene activity have been presented using radionuclide imaging,^{1,2} optical imaging,^{3,4} and NMR.^{5,6} In some cases, natural substrates are used, such as detection of fluorescent molecules or bioluminescence, but in other cases exogenous substrates have been designed to probe enzyme (viz., gene) activity. Recently, attention has turned to β -galactosidase (β -gal), since its introduction has become a standard means of assaying clonal insertion, transcriptional activation, protein expression, and protein interaction. Diverse colorimetric substrates have been developed suitable for histology.^{7,8} Tung et al.⁹ reported a near infrared active substrate and Louie et al.¹⁰ presented a proton MRI contrast agent. We have demonstrated the feasibility of using ^{19}F NMR to detect chemical shift changes accompanying enzyme-induced cleavage of fluorogalactopyranosides.^{11–14} We now report the synthesis of a series of trifluoromethyl (CF_3) aryl β -D-galactopyranosides designed to provide enhanced signal. We report synthesis, relevant characteris-

tics as β -gal substrates, and evaluation of their use to detect *lacZ* gene expression in breast cancer cells. Relative merits are compared with those of previous substrates.

2. Designs and synthesis

β -Galactosidase (β -gal) catalyzes the hydrolysis of galactopyranosides by cleavage of the C–O bonds between D-galactose and the aglycone.¹⁵ However, the enzyme shows remarkably broad substrate specificity. Based on our previous studies using a single fluorine atom as ^{19}F NMR sensitive reporter of β -gal activity,^{11–14} it appeared that introduction of a CF_3 group could be advantageous. Inherent signal to noise would be improved, allowing lower concentrations of reporter molecule to be applied, and hence, reducing issues of toxicity or substrate solubility. CF_3 groups are widely used in pharmaceuticals and agrochemicals since they resist enzyme degradation and the typical toxicity of mono- and difluoromethyl groups.¹⁴ Moreover, it has been observed that hydrogen bonding between the active site of the enzyme and the hydroxyl groups of the glycosidic substrate is important in the formation of the enzyme–substrate complex.^{16–18} Introduction of strong electron-withdrawing CF_3 group could increase

Keywords: β -Galactosidase; ^{19}F NMR; *lacZ*; Reporter gene.

* Corresponding author. Tel: +1 214 648 8926; fax: +1 214 648 4538;
e-mail: Ralph.Mason@UTSouthwestern.edu

the tendency to form the enzyme–substrate complex through the action of the fluorine as an acceptor in hydrogen bonding interactions in the ‘glycosylation’ step and make the phenolate anion a better leaving group in the ‘deglycosylation’ step.¹⁹

Following the successful high yield phase-transfer catalysis approach to the stereoselective syntheses of fluorinated aryl β -D-galactopyranosides,^{12,13} this versatile synthetic method was chosen for preparation of the target compounds **9–18** starting with commercially available trifluoromethylphenolic aglycones **2–8** (Fig. 1). The aglycones **2–8** reacted at 50 °C with 2,3,4,6-tetra-*O*-acetyl- α -D-galactopyranosyl bromide (**1**) in a dichloromethane–aqueous biphasic system (pH 8–9) using tetrabutylammonium bromide (TBAB) as the phase-transfer catalyst, affording trifluoromethyl aryl β -D-galactopyranoside tetraacetates **9–12** in near quantitative yield. However, **13** was obtained in poor yield (20%) and two of the trifluoromethyl phenols (3-trifluoromethylphenol **7** and 4-trifluoromethylphenol **8**) proved to be unreactive. To our knowledge molecules **9–18** are new, though we note that an isomer 4-nitro-2-trifluoromethylphenyl β -D-galactopyranoside has been reported previously in a patent related to CEDIA (cloned enzyme donor immunoassay).²⁰ That work did not appear to exploit the ¹⁹F NMR properties, but rather colorimetric changes accompanying β -gal induced cleavage. They reported a very poor yield using an alternate synthetic approach, though it may be characteristic of *o*-CF₃ groups since this was least successful in our hands.

The anomeric β -D-configuration of compounds **9–13** in the ⁴C₁ chair conformation was unambiguously established on the basis of the observed ¹H NMR chemical shifts (δ_{H} 4.98–5.25 ppm) of the anomeric protons, and the $J_{1,2}$ ($J \sim 8$ Hz) and $J_{2,3}$ ($J \sim 10$ Hz) coupling constants. The signals of the ¹³C NMR spectra of **9–13** were

assigned by comparison with the chemical shifts of *p*-nitrophenyl β -D-galactopyranosides.^{13,21} As expected, the anomeric carbon resonances appeared at 98–101 ppm in accord with the β -D-configuration.

Deacetylation of **9–13** with NH₃/MeOH from 0 °C to room temperature gave the free galactopyranosides **14–18** in quantitative yield. The signals of the ¹H NMR spectra of **14–18** were assigned by ¹H–¹H COSY spectra and D₂O exchange. The ¹H NMR chemical shifts (δ_{H} 5.00–5.15 ppm) of the anomeric protons and the $J_{1,2}$ ($J \sim 8$ Hz) and $J_{2,3}$ ($J \sim 11$ Hz) coupling constants showed that the free galactopyranosides **14–18** retained the anomeric β -D-configuration with the ⁴C₁ chair conformation.

3. ¹⁹F NMR

¹⁹F NMR spectra of the trifluoromethylphenyl β -D-galactopyranosides **14–18** were recorded in aqueous solutions with sodium trifluoroacetate (NaTFA) as an external chemical shift standard. Compounds **14–18** each gave a single narrow ¹⁹F NMR signal between δ 12–16 ppm essentially invariant ($\Delta\delta \leq 0.02$ ppm) with pH in the range 3 to 12 and temperatures from 25 to 37 °C in whole rabbit blood, 0.9% saline, or PBS. Addition of β -gal (G-2513) to **14–17** in PBS buffer (0.1 M, pH 7.4) at 37 °C led to rapid hydrolysis releasing the aglycones **2–5**, which appeared as single narrow ¹⁹F signals shifted downfield (Table 1). Compound **18** was cleaved comparatively slowly. The relative efficacy of **14** (PCF₃ONPG) and that of our previously reported *o*-fluoro-*p*-nitrophenyl β -D-galactopyranoside (OFPNPG) as β -gal substrate are shown in Figure 2. As expected, **14** provides about 3 times more signal, while cleavage rates are similar. Comparison of β -gal hydrolytic kinetics of **14–18** (Fig. 3) showed that each proceeded

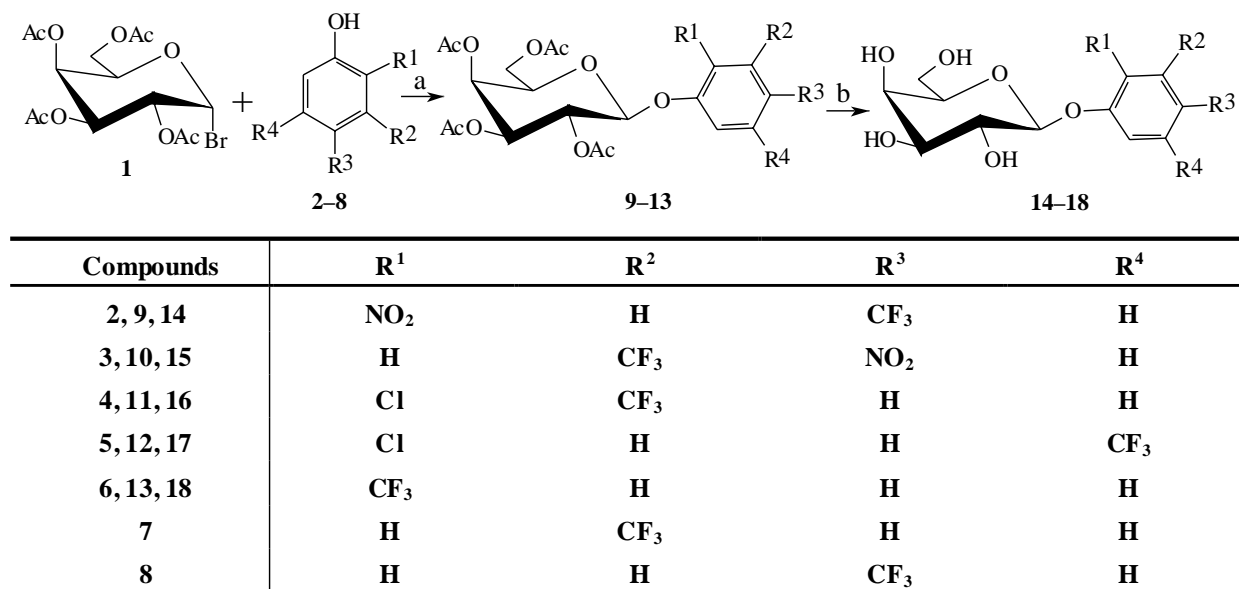


Figure 1. The reactions and the structures of **1–18**. Reaction and condition: (a) CH₂Cl₂–H₂O, pH 8–9, 50 °C, TBAB, \sim 1 h, near quantitative yield except **13** in only 20% yield; (b) NH₃–MeOH, 0 °C \rightarrow rt, 24 h, quantitative yields.

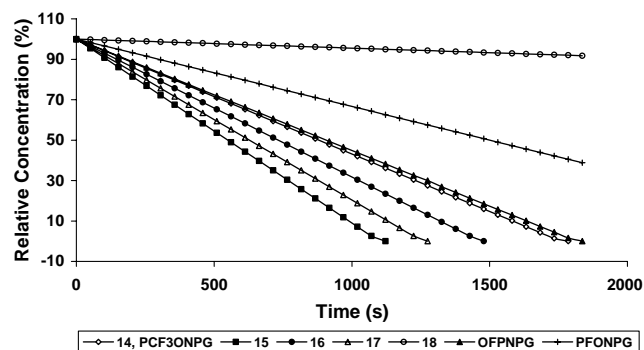
Table 1. ^{19}F chemical shifts^a and hydrolytic rates by β -gal^b

	14	15	16	17	18
$\delta_{\text{F}}(\text{substrate})$	13.40	15.23	13.24	12.70	14.11
$\delta_{\text{F}}(\text{product})$	14.54	15.43	13.94	12.95	14.61
$\Delta\delta_{\text{F}}$	1.14	0.20	0.70	0.25	0.50
$v(\mu\text{mol}/\text{min}/\text{U})$	33.0	52.8	39.6	46.2	2.61

^a ppm with respect to aq NaTFA.^b β -Gal (G-2513, 11 U) at 37 °C in PBS buffer (0.1 M, pH 7.4).

monotonically indicating straightforward first-order kinetics for all substrates and that the liberated aglycones **2–6** did not inhibit the β -gal. The substrates **14–17** exhibited rates in excess of 33 $\mu\text{mol}/\text{min}/\text{U}$ exceeding those of *p*-fluoro-*o*-nitrophenyl β -D-galactopyranoside (**PFONPG**; 19 $\mu\text{mol}/\text{min}/\text{U}$), **OFPNPG** (32 $\mu\text{mol}/\text{min}/\text{U}$), and even *o*-nitrophenyl β -D-galactopyranoside (**ONPG**; 32 $\mu\text{mol}/\text{min}/\text{U}$), which we have reported previously.^{11,13} The low hydrolysis rate of **18** may be due to the formation of an intramolecular $\text{F}\cdots\text{H}$ hydrogen bond between the 2- CF_3 and $\text{C}_1\text{--H}$ or steric effects, which plays an important role in the hydrolytic process rate.¹⁹

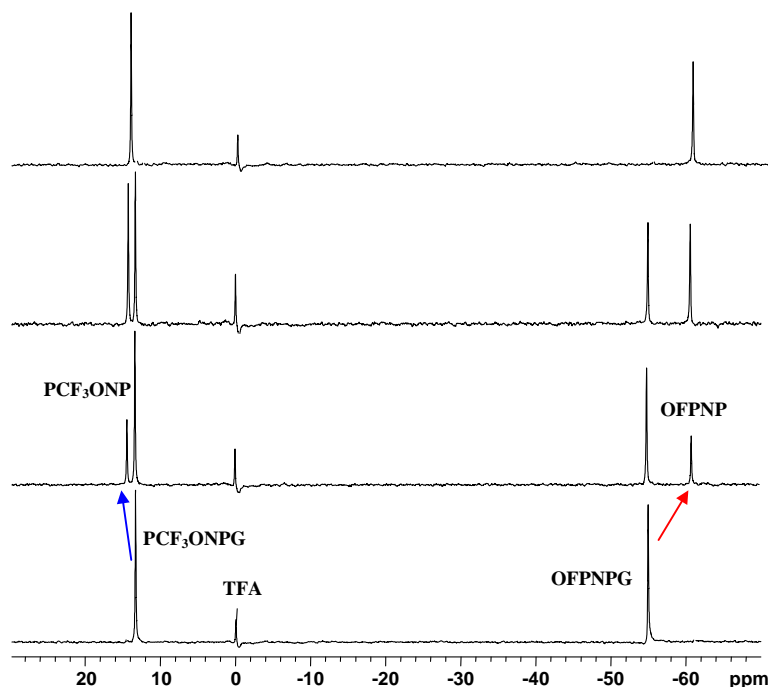
As expected, trifluoromethylphenyl β -D-galactopyranosides showed enhanced ^{19}F signal intensity on a molar basis compared with analogous fluorophenyl β -D-galactopyranosides, but the ^{19}F chemical shift changes were much smaller (Fig. 2, Table 1). The chemical shift ($\Delta\delta$ 1.14 ppm) accompanying cleavage of **14** is sufficient for investigations in vivo, but the other substrates **15–18** gave smaller values, which may be insufficient for effective studies. The aglycone *p*-trifluoromethyl-*o*-nitrophenol (**2**, **PCF₃ONP**) also exhibits a ^{19}F NMR chemical shift in response to pH ($\Delta\delta = \sim 1.00$ ppm) in the range of pH 4–7 (Fig. 4). Henderson–Hasselbalch coef-

**Figure 3.** Relative hydrolysis time courses of **14–18** (6.0 mmol), **OFPNPG**, and **PFONPG** (5.4 mmol) by β -gal (6 U) in PBS (0.1 M, 600 μL) at 37 °C.

ficients are $\text{p}K_{\text{a}} = 5.6$, $\delta_{\text{acid}} = 13.49$ ppm, $\delta_{\text{base}} = 14.52$, but importantly there is no overlap with the chemical shift of the substrate **14**.

4. In vitro evaluation

CF_3 - groups are often associated with increased lipophilicity. As expected, **PCF₃ONPG** has comparatively lower aqueous solubility than either **OFPNPG** or **PFONPG**. However, the higher ^{19}F signal intensity and sensitivity to β -gal allow use of lower concentrations of **PCF₃ONPG**, potentially circumventing issues of toxicity. **PCF₃ONPG** was stable in aqueous solution in the pH range 3–12 at temperatures from 25 to 37 °C over 5 days. Toxicity was evaluated for both aglycone **PCF₃ONP** and conjugate **PCF₃ONPG** using both wild type and *lacZ* expressing human MCF7 breast cancer

**Figure 2.** ^{19}F NMR spectra of **PCF₃ONPG** (1.1 mg, 3 mmol) and **OFPNPG** (2.87 mg, 9 mmol) with 1:3 molar ratios in the simultaneous hydrolysis by β -gal (11 U) in PBS (0.1 M, pH 7.4, 600 μL) at 37 °C.

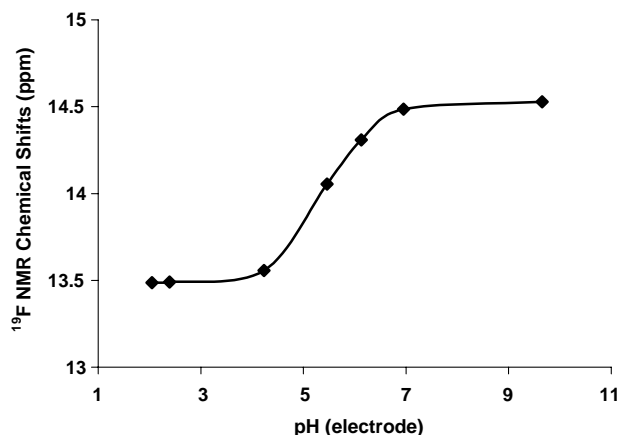


Figure 4. ¹⁹F NMR chemical shift pH titration curve of **2** (PCF₃ONPG) in saline at 37 °C.

cells. Cell viability assays²² showed that the aglycone PCF₃ONPG exhibited significant cytotoxicity even at 100 μM with both cell clones (Fig. 5). No toxicity was observed up to 1 mM for PCF₃ONPG over 96 h for wild type cells, but some toxicity was found with the *lacZ* expressing cells, presumably due to liberation of the aglycone.

When PCF₃ONPG was incubated with MCF7-WT cells for 5 h in PBS buffer at 37 °C under 5% CO₂ in air with

95% humidity, no changes were observed in the ¹⁹F NMR spectra. However, addition of PCF₃ONPG to cells stably transfected to express β-gal led to cleavage in a smooth monotonic manner releasing the aglycone PCF₃ONP (40.0 μmol/min per million MCF7-*lacZ* cells, Figs. 6, 7).

While the chemical shift response of the trifluoromethyl reporters is modest, we demonstrate that it is sufficient for chemical shift selective imaging (CSI) and we have observed the effect of MCF7-*lacZ* cells on PCF₃ONPG in vitro (Fig. 8).

5. Conclusion

The phase-transfer approach to synthesizing phenyl galactosides developed previously¹³ was also appropriate for several of the trifluoromethyl galactosides. The substrates are stable in aqueous solution and with wild type cancer cells, but the CF₃ agents are responsive to β-gal activity with rates exceeding those of the fluorophenyl analogs. Signal to noise is enhanced and although the ¹⁹F NMR chemical shift response to enzyme cleavage is smaller, it is adequate for detecting hydrolysis with PCF₃ONPG. Overall, the trifluoromethyl galactosides show promise as reporter molecules for β-gal activity and we are initiating investigations of *lacZ* expressing tumors in animals.

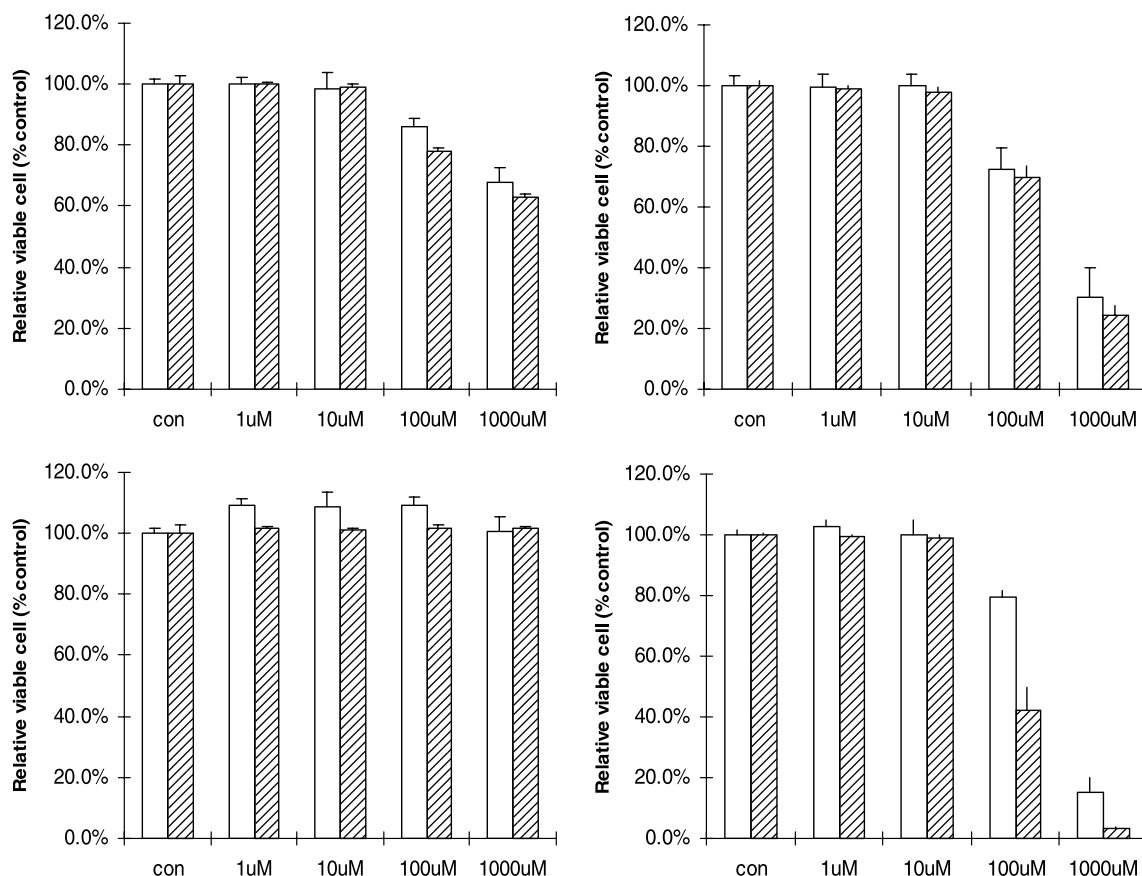


Figure 5. Cell viability of human MCF7 breast cancer cells in PBS (pH 7.4) with respect to exposure to substrate **14** (left panels) or aglycone **2** (right panels). Upper panels MCF7-*lacZ* cells; lower panels MCF7-WT. Open bars 48 h exposure; hatched bars 96 h exposure.

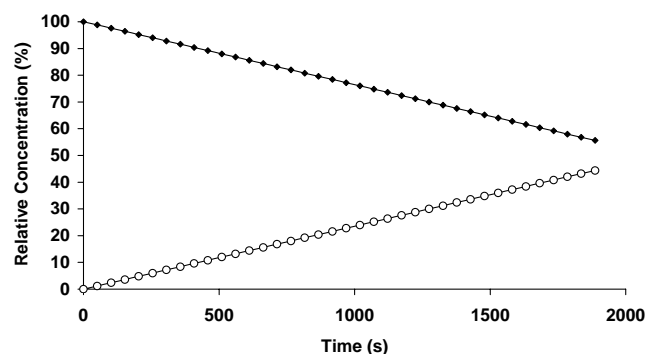


Figure 6. Hydrolysis of **14** (◆, 5.0 mmol) to **2** (○) by stably transfected MCF7-*lacZ* breast cancer cells (1.75×10^6) in PBS buffer at 37 °C.

6. Experimental

6.1. General methods

NMR spectra were recorded on a Varian Inova 400 spectrometer (400 MHz for ^1H , 100 MHz for ^{13}C , 376 MHz for ^{19}F) with CDCl_3 or $\text{DMSO}-d_6$ as solvents. ^1H and ^{13}C chemical shifts are referenced to TMS as internal standard and ^{19}F to dil sodium trifluoroacetate (NaTFA) in a capillary as external standard. All compounds were characterized by acquisition of ^1H , ^{13}C , DEPT, $^1\text{H}-^1\text{H}$, and COSY experiments at 25 °C and ^{19}F spectra at 37 °C. Imaging experiments used a Varian INOVA Unity scanner 4.7 T (188.2 MHz) with a 2D spin echo CSI sequence (FOV = 30×30 mm, spectral window = 30 ppm, slice thickness: 10 mm, matrix = 16×16 , and TR/TE = 1000/12 ms in 4.5 min per image). Microanalyses were performed on a Perkin-Elmer 2400CHN microanalyzer. Solutions in organic solvents were dried with anhydrous sodium sulfate and

concentrated in vacuo below 45 °C. Column chromatography was performed on silica gel (200–300 mesh) by elution with cyclohexane–EtOAc and silica gel GF₂₅₄ (Aldrich Chemical Company, St. Louis, MO) was used for analytical TLC. Detection was effected by spraying the plates with 5% ethanolic H_2SO_4 (followed by heating at 110 °C for 10 min) or by direct UV illumination of the plate.

For enzyme kinetic experiments, **PCF₃ONPG** (2.2 mg, 6 mmol) was dissolved in PBS (0.1 M, pH 7.4, 573 μL) and a PBS solution of β -gal (27 μL , G-2513 from *Escherichia coli*, 0.22 U/ μL , Aldrich) was added and NMR data were acquired immediately at 37 °C.

Human MCF7 breast cancer cells were stably transfected with recombinant vector phCMV/*lacZ*, which inserted the *E. coli lacZ* gene (from pSV- β -gal vector, Promega) to high expression human cytomegalovirus (CMV) immediate-early enhancer/promoter vector phCMV (Gene Therapy Systems, Inc) using Gene-PORTER2 (Gene Therapy Systems, Inc). For MCF7 cells, clonal selection was applied to identify those cells with highest β -gal expression. Control (wild type) and transfected (*lacZ*) cells were grown in culture dishes under standard conditions and harvested. **PCF₃ONPG** (2.2 mg) in PBS (70 μL) was added to a suspension of 10^6 cells in PBS (530 μL) and ^{19}F NMR spectra were acquired immediately and again after incubation for various times up to 5 h at 37 °C.

The sensitivities of MCF7-WT and -*lacZ* cells to **PCF₃ONPG** and **PCF₃ONP** were quantified using the Crystal Violet Mitogenic Assay²³ performed in triplicate using 24-well plates seeded with 2×10^4 cells per well in 1 mL DMEM supplemented with 10% FBS and 2 mM

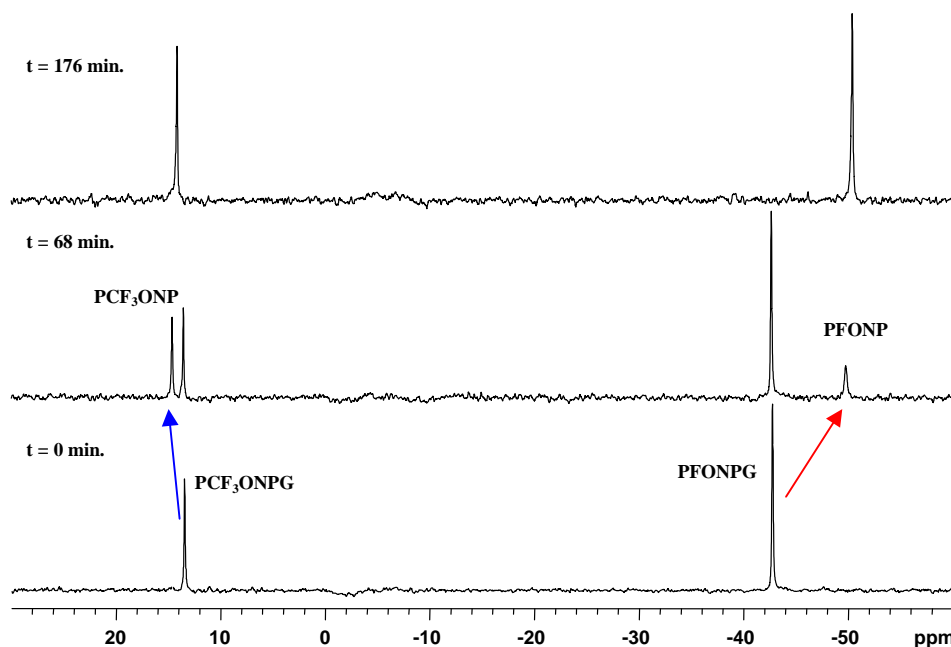


Figure 7. ^{19}F NMR spectra of **PCF₃ONPG** (1.7 mg, 4.5 mmol) and **PFONP** (6.0 mg, 18.8 mmol) showing simultaneous hydrolysis by stably transfected MCF7-*lacZ* cells (1.75×10^6) in PBS (0.1 M, pH 7.4, 600 μL) at 37 °C. Each spectrum acquired in 51 s.

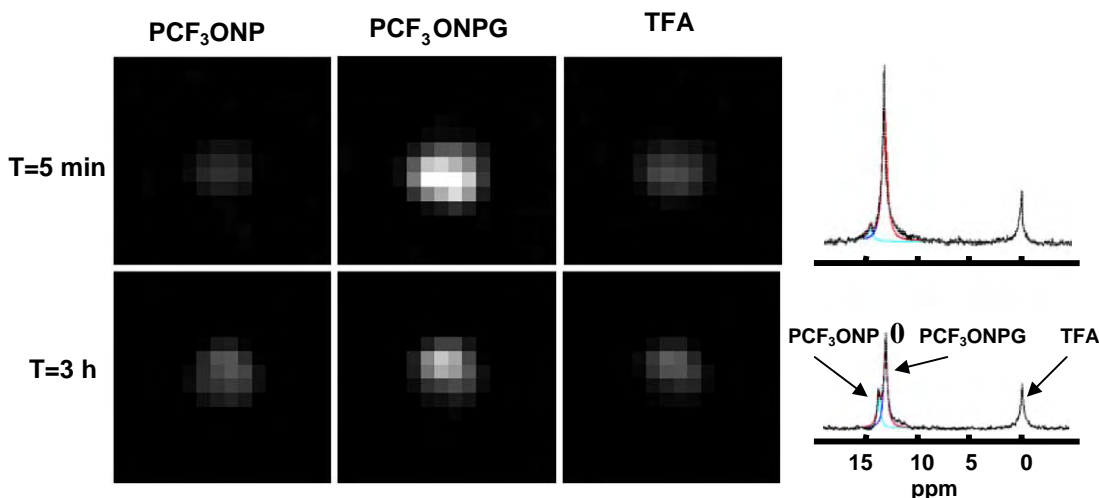


Figure 8. ^{19}F CSI of PCF_3ONPG (13.2 mg) and TFA (2.0 mg) during hydrolysis by stably transfected MCF7-*lacZ* cells (10^7) in PBS (0.1 M, pH 7.4, 700 μL) at 20 $^\circ\text{C}$. Upper images show data acquired in 4.5 min, ten minutes after addition of substrate to cells. The lower images were acquired 3 h later. At right are corresponding ^{19}F NMR spectra obtained from a single voxel in the image. The curve fits are also presented to demonstrate the deconvolution to allow CSI.

glutamine. After 24 h incubation, the medium was replaced with fresh DMEM containing 0.1% DMSO and various concentrations of PCF_3ONPG or PCF_3ONP (0–1 mM) and incubated for 48 or 96 h, followed by the Crystal Violet Mitogenic Assay.

6.2. Trifluoromethylphenyl β -D-galactopyranoside tetraacetates 9–13

6.2.1. General procedure. A solution of 2,3,4,6-tetra-*O*-acetyl- α -D-galactopyranosyl bromide (Sigma) (**1**) (1 mmol) and tetrabutyl-ammonium bromide (0.48 g, 1.5 mmol) in CH_2Cl_2 (5 mL) was stirred vigorously at 50 $^\circ\text{C}$ with the solution of fluorophenols (**2–8**) (1.2 mmol) in H_2O (5 mL; pH 8–9) until TLC showed complete reaction (~ 1 h). The organic layer was separated, washed, dried (Na_2SO_4), and evaporated under reduced pressure to give a syrup, which was purified by column chromatography on silica gel to give trifluoromethylphenyl β -D-galactopyranoside tetraacetates **9–13**.

2-Nitro-4-trifluoromethylphenyl 2,3,4,6-tetra-*O*-acetyl- β -D-galactopyranoside **9** (0.54 g, 99%) as white crystals, R_f 0.38 (3:2 cyclohexane/EtOAc), δ_{H} : 8.07 (1H, d, $J = 2.0$ Hz, Ar-H), 7.79 (1H, dd, $J = 1.6, 7.2$ Hz, Ar-H), 7.48 (1H, d, $J = 8.8$ Hz, Ar-H), 5.17 (1H, d, $J_{1,2} = 7.6$ Hz, H-1), 5.57 (1H, dd, $J_{2,3} = 10.4$ Hz, H-2), 5.12 (1H, dd, $J_{3,4} = 3.2$ Hz, H-3), 5.48 (1H, d, $J_{4,5} = 3.2$ Hz, H-4), 4.13 (1H, m, H-5), 4.24 (1H, dd, $J_{5,6a} = 4.4$ Hz, $J_{6a,6b} = 11.2$ Hz, H-6a), 4.18 (1H, dd, $J_{5,6b} = 5.6$ Hz, H-6b), 2.19, 2.15, 2.10, 2.01 (12H, 4s, $4 \times \text{CH}_3\text{CO}$) ppm; δ_{C} : 170.49, 170.31, 169.45 ($4 \times \text{CH}_3\text{CO}$), 140.93 (Ar-C_{1'}), 151.87 (Ar-C_{2'}), 130.74 (q, $^3J_{\text{F-C}} = 3.8$ Hz, Ar-C_{3'}), 126.14 (q, $^2J_{\text{F-C}} = 34.0$ Hz, Ar-C_{4'}), 123.10 (q, $^3J_{\text{F-C}} = 3.9$ Hz, Ar-C_{5'}), 119.59 (Ar-C_{6'}), 122.82 (q, $^1J_{\text{F-C}} = 284.0$ Hz, CF₃), 100.46 (C-1), 67.80 (C-2), 70.55 (C-3), 66.79 (C-4), 71.89 (C-5), 61.55 (C-6), 20.84, 20.80, 20.78, 20.73 ($4 \times \text{CH}_3\text{CO}$)

ppm. Anal. Calcd for $\text{C}_{21}\text{H}_{22}\text{NO}_{12}\text{F}_3$ (%): C, 46.92; H, 4.13; N, 2.61. Found: C, 46.90; H, 4.10; N, 2.58.

4-Nitro-3-trifluoromethylphenyl 2,3,4,6-tetra-*O*-acetyl- β -D-galactopyranoside **10** (0.54 g, 99%) as syrup, R_f 0.36 (3:2 cyclohexane/EtOAc), δ_{H} : 7.98 (1H, d, $J = 8.8$ Hz, Ar-H), 7.44 (1H, s, Ar-H), 7.28 (1H, d, $J = 9.2$ Hz, Ar-H), 5.25 (1H, d, $J_{1,2} = 8.0$ Hz, H-1), 5.57 (1H, dd, $J_{2,3} = 10$ Hz, H-2), 5.17 (1H, dd, $J_{3,4} = 2.8$ Hz, H-3), 5.50 (1H, d, $J_{4,5} = 3.2$ Hz, H-4), 4.15 (1H, m, H-5), 4.18 (2H, m, H-6), 2.20, 2.09, 2.07, 2.03 (12H, 4s, $4 \times \text{CH}_3\text{CO}$) ppm; δ_{C} : 170.61, 170.26, 170.16, 169.45 ($4 \times \text{CH}_3\text{CO}$), 142.91 (Ar-C_{1'}), 116.15 (q, $^3J_{\text{F-C}} = 6.1$ Hz, Ar-C_{2'}), 126.18 (q, $^2J_{\text{F-C}} = 34.4$ Hz, Ar-C_{3'}), 120.07 (Ar-C_{4'}), 127.91 (Ar-C_{5'}), 159.31 (Ar-C_{6'}), 121.76 (q, $^1J_{\text{F-C}} = 271.6$ Hz, CF₃), 98.70 (C-1), 68.30 (C-2), 70.65 (C-3), 67.01 (C-4), 71.99 (C-5), 61.95 (C-6), 20.82, 20.79, 20.71, 20.67 ($4 \times \text{CH}_3\text{CO}$) ppm. Anal. Calcd for $\text{C}_{21}\text{H}_{22}\text{NO}_{12}\text{F}_3$ (%): C, 46.92; H, 4.13; N, 2.61. Found: C, 46.89; H, 4.11; N, 2.60.

2-Chloro-3-trifluoromethylphenyl 2,3,4,6-tetra-*O*-acetyl- β -D-galactopyranoside **11** (0.50 g, 95%) as syrup, R_f 0.61 (3:2 cyclohexane/EtOAc), δ_{H} : 7.46 (1H, dd, $J = 1.2, 6.6$ Hz, Ar-H), 7.40 (1H, d, $J = 8.4$ Hz, Ar-H), 7.32 (1H, dd, $J = 7.8, 8.4$ Hz, Ar-H), 4.98 (1H, d, $J_{1,2} = 8.4$ Hz, H-1), 5.59 (1H, dd, $J_{2,3} = 10.5$ Hz, H-2), 5.11 (1H, dd, $J_{3,4} = 3.6$ Hz, H-3), 5.48 (1H, d, $J_{4,5} = 3.6$ Hz, H-4), 4.06 (1H, m, H-5), 4.25 (1H, dd, $J_{5,6a} = 6.6$ Hz, $J_{6a,6b} = 11.7$ Hz, H-6a), 4.16 (1H, dd, $J_{5,6b} = 6.0$ Hz, H-6b), 2.20, 2.10, 2.06, 2.02 (12H, 4s, $4 \times \text{CH}_3\text{CO}$) ppm; δ_{C} : 170.45, 170.42, 170.34, 169.42 ($4 \times \text{CH}_3\text{CO}$), 153.82 (Ar-C_{1'}), 122.39 (q, $^3J_{\text{F-C}} = 3.6$ Hz, Ar-C_{2'}), 130.11 (q, $^2J_{\text{F-C}} = 20.6$ Hz, Ar-C_{3'}), 122.39 (q, $^3J_{\text{F-C}} = 3.4$ Hz, Ar-C_{4'}), 127.42 (Ar-C_{5'}), 132.58 (Ar-C_{6'}), 124.01 (q, $^1J_{\text{F-C}} = 282.5$ Hz, CF₃), 100.83 (C-1), 68.28 (C-2), 70.69 (C-3), 66.87 (C-4),

71.47 (C-5), 61.42 (C-6), 20.92, 20.77, 20.70 ($4 \times \text{CH}_3\text{CO}$) ppm. Anal. Calcd for $\text{C}_{21}\text{H}_{22}\text{O}_{10}\text{ClF}_3$ (%): C, 47.90; H, 4.22. Found: C, 47.89; H, 4.20.

2-Chloro-5-trifluoromethylphenyl 2,3,4,6-tetra-*O*-acetyl- β -D-galactopyranoside **12** (0.51 g, 96%) as white crystals, R_f 0.56 (3:2 cyclohexane/EtOAc), δ_{H} : 7.51 (1H, s, Ar-H), 7.49 (1H, dd, $J = 1.8, 3.6$ Hz, Ar-H), 7.30 (1H, dd, $J = 1.2, 7.8$ Hz, Ar-H), 5.02 (1H, d, $J_{1,2} = 8.4$ Hz, H-1), 5.60 (1H, dd, $J_{2,3} = 10.2$ Hz, H-2), 5.12 (1H, dd, $J_{3,4} = 3.6$ Hz, H-3), 5.48 (1H, d, $J_{4,5} = 3.6$ Hz, H-4), 4.12 (1H, m, H-5), 4.22 (1H, dd, $J_{5,6a} = 4.2$ Hz, $J_{6a,6b} = 11.4$ Hz, H-6a), 4.17 (1H, dd, $J_{5,6b} = 7.8$ Hz, H-6b), 2.20, 2.10, 2.07, 2.02 (12H , 4s, $4 \times \text{CH}_3\text{CO}$) ppm; δ_{C} : 170.70, 170.27, 170.17, 169.40 ($4 \times \text{CH}_3\text{CO}$), 152.97 (Ar-C_{1'}), 109.92 (Ar-C_{2'}), 131.03 (Ar-C_{3'}), 115.13 (q, $^3J_{\text{F-C}} = 3.0$ Hz, Ar-C_{4'}), 130.34 (q, $^2J_{\text{F-C}} = 22.2$ Hz, Ar-C_{5'}), 121.06 (q, $^3J_{\text{F-C}} = 2.9$ Hz, Ar-C_{6'}), 122.59 (q, $^1J_{\text{F-C}} = 282.0$ Hz, CF₃), 100.65 (C-1), 68.13 (C-2), 70.62 (C-3), 67.21 (C-4), 71.95 (C-5), 62.31 (C-6), 20.89, 20.73, 20.50 ($4 \times \text{CH}_3\text{CO}$) ppm. Anal. Calcd for $\text{C}_{21}\text{H}_{22}\text{O}_{10}\text{ClF}_3$ (%): C, 47.90; H, 4.22. Found: C, 47.88; H, 4.21.

2-Trifluoromethylphenyl 2,3,4,6-tetra-*O*-acetyl- β -D-galactopyranoside **13** (0.30 g, 20%) as white crystals, R_f 0.54 (3:2 cyclohexane/EtOAc), δ_{H} : 7.60 (1H, dd, $J = 1.2, 7.8$ Hz, Ar-H), 7.50 (1H, m, Ar-H), 7.27 (1H, dd, $J = 1.8, 6.6$ Hz, Ar-H), 7.16 (1H, dd, $J = 7.8$ Hz, Ar-H), 5.06 (1H, d, $J_{1,2} = 8.4$ Hz, H-1), 5.58 (1H, dd, $J_{2,3} = 10.5$ Hz, H-2), 5.12 (1H, dd, $J_{3,4} = 3.6$ Hz, H-3), 5.47 (1H, dd, $J_{4,5} = 0.6$ Hz, H-4), 4.11 (1H, m, H-5), 4.27 (1H, dd, $J_{5,6a} = 6.0$ Hz, $J_{6a,6b} = 11.4$ Hz, H-6a), 4.17 (1H, dd, $J_{5,6b} = 6.0$ Hz, H-6b), 2.20, 2.08, 2.05, 2.01 (12H , 4s, $4 \times \text{CH}_3\text{CO}$) ppm; δ_{C} : 170.26, 170.20, 170.05, 169.10 ($4 \times \text{CH}_3\text{CO}$), 154.59 (Ar-C_{1'}), 120.10 (q, $^2J_{\text{F-C}} = 21.0$ Hz, Ar-C_{2'}), 127.03 (q, $^3J_{\text{F-C}} = 3.4$ Hz, Ar-C_{3'}), 122.80 (Ar-C_{4'}), 116.69 (Ar-C_{5'}), 133.30 (Ar-C_{6'}), 129.78 (q, $^1J_{\text{F-C}} = 208.4$ Hz, CF₃), 99.79 (C-1), 67.85 (C-2), 70.73 (C-3), 66.76 (C-4), 71.20 (C-5), 61.40 (C-6), 20.59, 20.36 ($4 \times \text{CH}_3\text{CO}$) ppm. Anal. Calcd for $\text{C}_{21}\text{H}_{23}\text{O}_{10}\text{F}_3$ (%): C, 51.21; H, 4.71. Found: C, 51.19; H, 4.69.

6.3. Trifluoromethylphenyl β -D-galactopyranosides 14–18

6.3.1. General procedure. A solution of trifluoromethylphenyl 2,3,4,6-tetra-*O*-acetyl- β -D-galactopyranoside (**9–13**) (0.4 g) in anhydrous MeOH (15 mL) containing 0.5 M NH_3 was vigorously stirred from 0 °C to room temperature overnight until TLC showed complete reaction and evaporated to dryness in vacuo. Chromatography of the crude syrup on silica gel with EtOAc–MeOH afforded the free β -D-galactopyranosides **14–18** in quantitative yield.

2-Nitro-4-trifluoromethylphenyl β -D-galactopyranoside **14** as white crystals, R_f 0.35 (1:9 MeOH/EtOAc), δ_{H} : 8.28 (1H, d, $J = 2.0$ Hz, Ar-H), 7.99 (1H, dd, $J = 2.0, 9.2$ Hz, Ar-H), 7.59 (1H, d, $J = 8.8$ Hz, Ar-H), 5.15 (1H, d, $J_{1,2} = 7.6$ Hz, H-1), 3.55 (1H, dd, $J_{2,3} = 8.9$ Hz, H-2), 3.50 (1H, dd, $J_{3,4} = 6.0$ Hz, H-3), 3.47 (1H, d, $J_{4,5} = 6.0$ Hz, H-4), 3.42 (1H, m, H-5), 3.67 (1H, m,

H-6), 5.24 (1H, d, $J_{\text{H-2,OH-2}} = 4.8$ Hz, HO-2), 4.63 (1H, d, $J_{\text{H-3,OH-3}} = 4.4$ Hz, HO-3), 4.92 (1H, d, $J_{\text{H-4,OH-4}} = 6.0$ Hz, HO-4), 4.69 (1H, t, $J_{\text{H-6,OH-6}} = 5.4, 5.6$ Hz, HO-6) ppm; δ_{C} : 152.18 (Ar-C_{1'}), 139.97 (Ar-C_{2'}), 130.82 (q, $^3J_{\text{F-C}} = 3.9$ Hz, Ar-C_{3'}), 122.06 (q, $^2J_{\text{F-C}} = 33.8$ Hz, Ar-C_{4'}), 122.42 (q, $^3J_{\text{F-C}} = 3.8$ Hz, Ar-C_{5'}), 117.91 (Ar-C_{6'}), 123.33 (q, $^1J_{\text{F-C}} = 270.9$ Hz, CF₃), 100.95 (C-1), 69.97 (C-2), 73.29 (C-3), 68.03 (C-4), 76.04 (C-5), 60.30 (C-6) ppm. Anal. Calcd for $\text{C}_{13}\text{H}_{14}\text{NO}_8\text{F}_3$ (%): C, 42.27; H, 3.82; N, 3.79. Found: C, 42.25; H, 3.80; N, 3.77.

4-Nitro-3-trifluoromethylphenyl β -D-galactopyranoside **15** as white crystals, R_f 0.40 (1:9 MeOH/EtOAc), δ_{H} : 8.16 (1H, d, $J = 8.8$ Hz, Ar-H), 7.53 (1H, d, $J = 2.8$ Hz, Ar-H), 7.49 (1H, dd, $J = 2.8, 8.8$ Hz, Ar-H), 5.08 (1H, d, $J_{1,2} = 7.6$ Hz, H-1), 3.53 (1H, dd, $J_{2,3} = 10.0$ Hz, H-2), 3.49 (1H, dd, $J_{3,4} = 5.2$ Hz, H-3), 3.44 (1H, d, $J_{4,5} = 2.4$ Hz, H-4), 3.61 (1H, m, H-5), 3.68 (2H, m, H-6), 5.33 (1H, d, $J_{\text{H-2,OH-2}} = 4.8$ Hz, HO-2), 4.60 (1H, d, $J_{\text{H-3,OH-3}} = 4.8$ Hz, HO-3), 4.96 (1H, d, $J_{\text{H-4,OH-4}} = 5.6$ Hz, HO-4), 4.70 (1H, dd, $J_{\text{H-6,OH-6}} = 5.2, 5.4$ Hz, HO-6) ppm; δ_{C} : 160.45 (Ar-C_{1'}), 115.95 (q, $^3J_{\text{F-C}} = 6.1$ Hz, Ar-C_{2'}), 123.67 (q, $^2J_{\text{F-C}} = 32.8$ Hz, Ar-C_{3'}), 141.10 (Ar-C_{4'}), 120.32 (Ar-C_{5'}), 128.48 (Ar-C_{6'}), 121.94 (q, $^1J_{\text{F-C}} = 271.7$ Hz, CF₃), 100.95 (C-1), 70.09 (C-2), 73.11 (C-3), 68.12 (C-4), 75.99 (C-5), 60.36 (C-6) ppm. Anal. Calcd for $\text{C}_{13}\text{H}_{14}\text{NO}_8\text{F}_3$ (%): C, 42.27; H, 3.82; N, 3.79. Found: C, 42.26; H, 3.79; N, 3.78.

2-Chloro-3-trifluoromethylphenyl β -D-galactopyranoside **16** as white crystals, R_f 0.48 (1:9 MeOH/EtOAc), δ_{H} : 8.28 (1H, d, $J = 2.0$ Hz, Ar-H), 7.99 (1H, dd, $J = 2.0, 9.2$ Hz, Ar-H), 7.59 (1H, d, $J = 8.8$ Hz, Ar-H), 5.15 (1H, d, $J_{1,2} = 7.6$ Hz, H-1), 3.55 (1H, dd, $J_{2,3} = 8.9$ Hz, H-2), 3.50 (1H, dd, $J_{3,4} = 6.0$ Hz, H-3), 3.47 (1H, d, $J_{4,5} = 6.0$ Hz, H-4), 3.42 (1H, m, H-5), 3.67 (2H, m, H-6), 5.24 (1H, d, $J_{\text{H-2,OH-2}} = 4.8$ Hz, HO-2), 4.63 (1H, d, $J_{\text{H-3,OH-3}} = 4.4$ Hz, HO-3), 4.92 (1H, d, $J_{\text{H-4,OH-4}} = 6.0$ Hz, HO-4), 4.69 (1H, dd, $J_{\text{H-6,OH-6}} = 5.4, 5.6$ Hz, HO-6) ppm; δ_{C} : 153.98 (Ar-C_{1'}), 120.13 (q, $^3J_{\text{F-C}} = 3.4$ Hz, Ar-C_{2'}), 128.48 (q, $^2J_{\text{F-C}} = 30.1$ Hz, Ar-C_{3'}), 131.62 (q, $^3J_{\text{F-C}} = 12.2$ Hz, Ar-C_{4'}), 128.32 (Ar-C_{5'}), 131.56 (Ar-C_{6'}), 124.70 (q, $^1J_{\text{F-C}} = 260.0$ Hz, CF₃), 100.95 (C-1), 69.97 (C-2), 73.29 (C-3), 68.03 (C-4), 76.04 (C-5), 60.30 (C-6) ppm. Anal. Calcd for $\text{C}_{13}\text{H}_{14}\text{ClO}_6\text{F}_3$ (%): C, 43.57; H, 3.94. Found: C, 43.55; H, 3.91.

2-Chloro-5-trifluoromethylphenyl β -D-galactopyranoside **17** as white crystals, R_f 0.50 (1:9 MeOH/EtOAc), δ_{H} : 7.69 (1H, d, $J = 8.0$ Hz, Ar-H), 7.55 (1H, d, $J = 0.6$ Hz, Ar-H), 7.59 (1H, dd, $J = 2.1, 8.8$ Hz, Ar-H), 5.11 (1H, d, $J_{1,2} = 8.4$ Hz, H-1), 3.53 (1H, dd, $J_{2,3} = 10.2$ Hz, H-2), 3.48 (1H, dd, $J_{3,4} = 5.2$ Hz, H-3), 3.48 (1H, d, $J_{4,5} = 6.4$ Hz, H-4), 3.44 (1H, m, H-5), 3.69 (2H, m, H-6), 5.20 (1H, d, $J_{\text{H-2,OH-2}} = 3.6$ Hz, HO-2), 4.58 (1H, d, $J_{\text{H-3,OH-3}} = 2.8$ Hz, HO-3), 4.91 (1H, d, $J_{\text{H-4,OH-4}} = 3.6$ Hz, HO-4), 4.65 (1H, dd, $J_{\text{H-6,OH-6}} = 5.0, 6.0$ Hz, HO-6) ppm; δ_{C} : 153.01 (Ar-C_{1'}), 109.31 (Ar-C_{2'}), 130.97 (Ar-C_{3'}), 112.90 (q, $^3J_{\text{F-C}} = 2.8$ Hz, Ar-C_{4'}), 122.32 (q, $^2J_{\text{F-C}} = 32.0$ Hz,

Ar-C_{5'}), 121.42 (q, $^3J_{F-C} = 2.7$ Hz, Ar-C_{6'}), 122.22 (q, $^1J_{F-C} = 262.0$ Hz, CF₃), 100.81 (C-1), 70.02 (C-2), 73.31 (C-3), 68.02 (C-4), 75.73 (C-5), 60.18 (C-6) ppm. Anal. Calcd for C₁₃H₁₄ClO₆F₃ (%): C, 43.57; H, 3.94. Found: C, 43.56; H, 3.93.

2-Trifluoromethylphenyl β-D-galactopyranoside **18** as white crystals, R_f 0.52 (1:9 MeOH/EtOAc), δ_H : 7.67 (1H, m, Ar-H), 7.60 (1H, dd, $J = 5.2, 5.6$ Hz, Ar-H), 7.33 (1H, d, $J = 5.6$ Hz, Ar-H), 7.12 (1H, dd, $J = 4.8, 5.2$ Hz, Ar-H), 5.00 (1H, d, $J_{1,2} = 7.8$ Hz, H-1), 3.62 (1H, dd, $J_{2,3} = 10.8$ Hz, H-2), 3.54 (1H, dd, $J_{3,4} = 4.8$ Hz, H-3), 3.49 (1H, dd, $J_{4,5} = 5.4, 6.0$ Hz, H-4), 3.40 (1H, m, H-5), 3.70 (2H, m, H-6), 4.97 (1H, d, $J_{H-2,OH-2} = 6.0$ Hz, HO-2), 4.57 (1H, d, $J_{H-3,OH-3} = 4.2$ Hz, HO-3), 4.91 (1H, d, $J_{H-4,OH-4} = 6.0$ Hz, HO-4), 4.65 (1H, dd, $J_{H-6,OH-6} = 5.4, 6.5$ Hz, HO-6) ppm; δ_C : 155.60 (Ar-C_{1'}), 131.65 (q, $^2J_{F-C} = 36.0$ Hz, Ar-C_{2'}), 126.49 (q, $^3J_{F-C} = 3.6$ Hz, Ar-C_{3'}), 121.14 (Ar-C_{4'}), 116.69 (Ar-C_{5'}), 133.95 (Ar-C_{6'}), 127.53 (q, $^1J_{F-C} = 208.4$ Hz, CF₃), 100.46 (C-1), 70.13 (C-2), 73.58 (C-3), 68.04 (C-4), 75.62 (C-5), 60.30 (C-6) ppm. Anal. Calcd for C₁₃H₁₅O₆F₃ (%): C, 48.14; H, 4.67. Found: C, 48.12; H, 4.66.

Acknowledgments

This work was supported by grants from the DOD Breast Cancer Initiative IDEA award DAMD17-03-1-0343-01 and the Cancer Imaging Program, NIH P20 CA 86354 (pre-ICMIC). NMR experiments were conducted at the Mary Nell and Ralph B. Rogers NMR Center, an NIH BTRP facility #P41-RR02584.

References and notes

- Gambhir, S. S.; Herschman, H. R.; Cherry, S. R.; Barrio, J. R.; Satyamurthy, N.; Toyokuni, T.; Phelps, M. E.; Larson, S. M.; Balatoni, J.; Finn, R.; Sadelain, M.; Tjuvajev, J.; Blasberg, R. *Neoplasia (New York)* **2000**, 2, 118.
- Haberkorn, U.; Mier, W.; Eisenhut, M. *Curr. Med. Chem.* **2005**, 12, 779.
- Contag, C. H.; Ross, B. D. *J. Magn. Reson. Imaging* **2002**, 16, 378.
- Hoffman, R. M. *Biotechniques* **2001**, 30, 1016.
- Ichikawa, T.; Hogemann, D.; Saeki, Y.; Tyminski, E.; Terada, K.; Weissleder, R.; Chiocca, E. A.; Basilion, J. P. *Neoplasia (New York)* **2002**, 6, 523.
- Zhang, Z.; Nair, S. A.; McMurphy, T. J. *Curr. Med. Chem.* **2005**, 12, 751.
- Pocsi, I.; Taylor, S. A.; Richardson, A. C.; Smith, B. V.; Price, R. G. *Biochim. Biophys. Acta* **1993**, 1163, 54.
- Heuermann, K.; Cosgrove, J. *Biotechniques* **2001**, 30, 1142.
- Tung, C. H.; Zeng, Q.; Shah, K.; Kim, D. E.; Schellingerhout, D.; Weissleder, R. *Cancer Res.* **2004**, 64, 1579.
- Louie, A. Y.; Huber, M. M.; Ahrens, E. T.; Rothbacher, U.; Moats, R.; Jacobs, R. E.; Fraser, S. E.; Meade, T. J. *Nat. Biotechnol.* **2000**, 18, 321.
- Cui, W.; Otten, P.; Li, Y.; Koeneman, K.; Yu, J.; Mason, R. P. *Magn. Reson. Med.* **2004**, 51, 616.
- Yu, J.; Ma, Z.; Li, Y.; Koeneman, K. S.; Liu, L.; Mason, R. P. *Med. Chem.* **2005**, 1, 255.
- Yu, J.; Otten, P.; Ma, Z.; Cui, W.; Liu, L.; Mason, R. P. *Bioconjugate Chem.* **2004**, 15, 1334.
- Yu, J.; Kodibagkar, V.; Cui, W.; Mason, R. P. *Curr. Med. Chem.* **2005**, 12, 818.
- Sinnott, M. L. *Chem. Rev.* **1990**, 90, 1171.
- Lemieux, R. U.; Hendricks, K. B.; Stick, R. V.; James, K. J. *J. Am. Chem. Soc.* **1975**, 97, 4056.
- Namchuk, M. N.; Withers, S. G. *Biochemistry* **1995**, 34, 16194.
- Sierks, M. R.; Svensson, B. *Biochemistry* **2000**, 39, 8585.
- McCarter, J. D.; Adam, M. J.; Withers, S. G. *Biochem. J.* **1992**, 286, 721.
- Guder, H. J.; Herrmann, R. Z.; Zdunek, D., in 'Preparation of nitrophenyl β-D-galactopyranosides as β-galactosidase substrates for cloned enzyme donor immunoassay (CEDIA),' German patent DE 4021063 A1 19920109, **1992**.
- Yoon, S.; Kim, H. G.; Chun, K. H.; Shin, J. E. N. *Bull. Korean Chem. Soc.* **1996**, 17, 599.
- Mosmann, T. *Immunol. Methods* **1983**, 65, 55.
- Kanamura, H.; Yoshida, O. *Urol. Res.* **1989**, 17, 259.

Synthesis and Characterization of Novel *lacZ* Gene Reporter Molecules: Detection of β -Galactosidase Activity by ^{19}F Nuclear Magnetic Resonance of Polyglycosylated Fluorinated Vitamin B₆

Jianxin Yu and Ralph P. Mason*

Department of Radiology, The University of Texas Southwestern Medical Center at Dallas, 5323 Harry Hines Boulevard, Dallas, Texas 75390-9058

Received October 18, 2005

Gene therapy has emerged as a promising strategy for treatment of various diseases. However, widespread implementation is hampered by difficulties in assessing the success of transfection, in particular, the spatial extent of expression in the target tissue and the longevity of expression. Thus, the development of noninvasive reporter techniques based on appropriate molecules and imaging modalities may help to assay gene expression. We have previously demonstrated the ability to detect β -galactosidase (β -gal) activity on the basis of ^{19}F NMR chemical shift associated with release of fluorophenyl aglycons from galactopyranoside conjugates. Use of fluoropyridoxol as the aglycon provides a potential less toxic alternative and we now report the design, synthesis, and structural analysis of a series of novel polyglycosylated fluorinated vitamin B₆ derivatives as ^{19}F NMR-sensitive aglycons for detection of *lacZ* gene expression. In particular, we report the activity of 3, α^4 , α^5 -tri-*O*-(β -D-galactopyranosyl)-6-fluoropyridoxol **4**, 3-*O*-(β -D-galactopyranosyl)- α^4 , α^5 -di-*O*-(β -D-glucopyranosyl)-6-fluoropyridoxol **12**, and 3-*O*-(β -D-galactopyranosyl)- α^4 , α^5 -di-*O*-(α -D-mannopyranosyl)-6-fluoropyridoxol **13**. Compounds **4**, **12**, and **13** all show promising characteristics including highly sensitive ^{19}F NMR response to β -gal activity ($\Delta\delta = 9.0 \sim 9.4$ ppm), minimal toxicity for substrate or aglycon, and good water solubility. However, the differential glycosylation of **12** and **13** appears more advantageous for assessing *lacZ* gene expression in vivo.

Introduction

Gene therapy holds great promise for the treatment of diverse diseases, but widespread implementation is hindered by difficulties in assessing the success of transfection. The development of noninvasive in vivo reporter techniques based on appropriate molecules and imaging modalities would be of considerable value for assessing the location, magnitude, and persistence of expression.

The *lacZ* gene encoding β -galactosidase (β -gal) is widely used in molecular biology as a reporter gene to assay clonal insertion, transcriptional activation, protein expression, and protein interaction. Many colorimetric reporter molecules have been described to detect β -gal activity and these form the basis of highly effective spectrophotometric assays in vitro.^{1–3} However, optical methods are less practical for applications in animals in vivo or ultimately in man in the clinic due to extensive light scattering and absorption by tissues. Toward such applications new reporter molecules are being developed. Recently, Tung et al.⁴ presented a near-infrared approach in vivo based on 9*H*-(1,3-dichloro-9,9-dimethylacridin-2-on-7-yl) β -D-galactopyranoside to detect β -gal activity in transfected tumors in live mice. Lee et al.⁵ described use of a radiolabeled competitive inhibitor 2-(4-[^{125}I / ^{123}I]iodophenyl)ethyl 1-thio- β -D-galactopyranoside to detect β -gal activity in mice. Louie et al.⁶ introduced an NMR approach using 1-[2-(β -D-galactopyranosyloxy)propyl]-4,7,10-tris(carboxymethyl)-1,4,7,10-tetraazacyclododecane)gadolinium(III) based on proton MRI contrast to detect β -gal activity in developing frog embryos following direct injection of substrate into eggs. We have been developing in vivo reporter molecules based on ^{19}F NMR with structures exploiting fluorophenol, trifluorophe-

nol, and fluoropyridoxol aglycons.^{7–11} To date our published investigations have focused on development of reporter molecules and we have demonstrated detection of β -gal activity in cultured tumor cells with preliminary examples of detectability in tumors in living mice.¹² In a continuing effort to develop enhanced approaches for in vivo detection of β -gal, we now report the synthesis and evaluation of polyglycosylated fluorinated vitamin B₆ reporter molecules, designed to enhance water solubility, cellular penetration, and enzyme response.

Design

The diversity of substrates and reporter molecules for β -gal activity is indicative of broad substrate specificity. Agents have been tailored for specific imaging modalities or with particular characteristics, such as thermal stability suitable for autoclaving. However, some substrates suffer from poor aqueous solubility and inability to reach targets in vivo and some aglycon products are toxic. Our initial investigations used fluorophenyl β -D-galactopyranosides.^{7,9} This approach was particularly facile, being a simple analogy of the classic “yellow” agent *o*-nitrophenyl β -D-galactopyranoside (ONPG). However, the product aglycon appears somewhat toxic, being closely similar to the uncoupler dinitrophenol. We were able to reduce the requisite concentration of reporter molecule by introducing a trifluoromethyl reporter moiety in place of a single fluorine atom, but this is characterized by a much smaller chemical shift response.¹¹ Toxicity could be largely avoided by using 6-fluoropyridoxol (**1**, FPOL) as the aglycon and we recently demonstrated proof of principle. Introduction of a D-galactose at the 3-phenolic group of FPOL, 3-*O*-(β -D-galactopyranosyl)-6-fluoropyridoxol (GFPOL), yielded a ^{19}F NMR gene expression reporter exhibiting a large chemical shift response to β -gal cleavage but having only moderate kinetic sensitivity to β -gal.⁸ GFPOL was also modestly water-soluble.

* Author to whom correspondence should be addressed: tel (214) 648-8926; fax (214) 648-4538; e-mail Ralph.Mason@UTSouthwestern.edu.

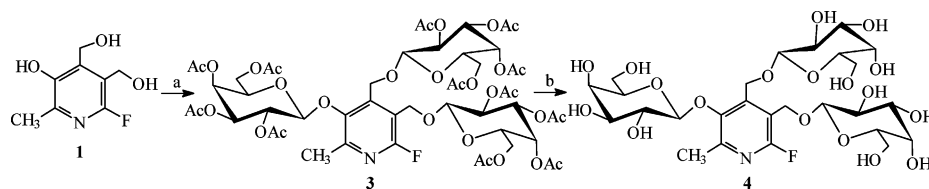


Figure 1. Reagents and conditions: (a) 2,3,4,6-tetra-*O*-acetyl- α -D-galactopyranosyl bromide **2**, Hg(CN)₂, 4 Å molecular sieve, CH₂Cl₂, RT, 12 h, 89%; (b) NH₃/MeOH, 0 °C \rightarrow RT, 24 h, quantitative yields.

We considered that introduction of additional sugar moieties could enhance water solubility and potentially improve enzyme sensitivity. Pertinent to this approach were reports that modification the α^4 - and α^5 -position hydroxymethyl moieties of FPOL produces modification of its pK_a with relatively minor changes in chemical shift and chemical shift range.¹³ Further, *Escherichia coli* (*lacZ*) β -gal catalyzes the hydrolysis of galactopyranosides by cleavage of the C–O bond between D-galactose and the aglycon with a double-displacement mechanism involving the formation (glycosylation step) and breakdown (deglycosylation step) of a glycosyl-enzyme intermediate via oxocarbenium ion-like transition states. It has been observed that hydrogen-bonding interaction between the enzyme and the glycosidic substrate is important in the formation of the enzyme–substrate complex and the hydrolysis rate.^{14,15} The involvement of fluorine atoms in hydrogen bonding is well documented and exemplified by some of the strongest known hydrogen bonds.¹⁶ Considerable evidence suggests that a C–F moiety can act as a weak proton acceptor and may form hydrogen bonds between the enzyme and the substrate.^{17–21}

We have found evidence of intramolecular hydrogen bonding between α^5 -OH and 6-F in ¹H NMR spectra of FPOL and its derivatives. For example, the signal of α^5 -OH in α^4 -OH and α^5 -OH unprotected analogues, such as FPOL or 3-*O*-(2,3,4,6-tetra-*O*-acetyl- β -D-galactopyranosyl)-6-fluoropyridoxol, always appears downfield and is coupled with 5-CH₂ as triplet due to the α^5 -OH exchange limitation by the α^5 -OH and 6-F hydrogen bonding. Meanwhile, α^4 -OH occurs as an upfield singlet. Introduction of two additional carbohydrate residues at α^4 - and α^5 -hydroxymethyl positions of GFPOL would inhibit α^5 -OH and 6-F hydrogen bonding and facilitate hydrogen bonding between the enzyme and the new substrates. Thus, substrate affinity should increase and both water solubility and enzyme sensitivity could be improved, while the virtues of GFPOL are retained.⁸

Results and Discussion

Syntheses. Our initial approach used a one-pot technique to introduce three D-galactose moieties at the 3 phenolic and α^4 , α^5 -hydroxymethyl sites, simultaneously. Reaction of **1** with 3.3 equiv of 2,3,4,6-tetra-*O*-acetyl- α -D-galactopyranosyl bromide **2** in anhydrous dichloromethane catalyzed by Hg(CN)₂ afforded the fully galactopyranosylated 6-fluoropyridoxol (**3**) in 89% yield, which was deacetylated with NH₃/MeOH, giving the free galactopyranoside 3, α^4 , α^5 -tri-*O*-(β -D-galactopyranosyl)-6-fluoropyridoxol (**4**) in quantitative yield (Figure 1). The ESI-MS of **3** showed the expected molecular ion at m/z 1178 and quasi-molecular ion at m/z 1179 [M + H], corresponding to the fully adorned derivative with three fully acetylated galactosides. The identity of **3** was established by ¹H and ¹³C NMR. The anomeric protons H-1', H-1'', and H-1''' of D-galactoses linked to 3, α^4 -, and α^5 -positions of FPOL at 5.24, 4.66, and 4.52 ppm, respectively, with three well-resolved doublets ($J_{1,2} = 8.0$ Hz), as well as $J_{2,3} \sim 10$ Hz, confirming that all D-galactoses are in the β -configuration with the ⁴C₁ chair conformation, whereas

in the ¹³C NMR spectrum, the anomeric carbons C-1', C-1'', and C-1''' occurred at 103.34 and 100.22 ppm.

Compound **4** was stable in buffer and gave a single sharp ¹⁹F NMR signal. Exposure of **4** to β -gal indicated that all three β -D-galactopyranosyl C_{1(gal)}–O linkages are sensitive resulting in multiple ¹⁹F signals around 3 ppm and 12–20 ppm (Figure 2). These results demonstrate the principle of polyglycosylation to enhance water solubility while retaining sensitivity to β -gal, but the complex spectra suggested a need for a more sophisticated approach. We therefore designed two further molecules, 3-*O*-(β -D-galactopyranosyl)- α^4 , α^5 -di-*O*-(β -D-glucopyranosyl)-6-fluoropyridoxol **12** and 3-*O*-(β -D-galactopyranosyl)- α^4 , α^5 -di-*O*-(α -D-mannopyranosyl)-6-fluoropyridoxol **13**, featuring differential glycosylation: galactosylation at the 3-phenolic group being sensitive to β -gal, and glucopyranosylation or mannopyranosylation at the α^4 , α^5 -hydroxymethyl groups to aid water solubility but resist β -gal activity. Retrosynthetic analysis suggested two approaches through differentially protected intermediates as key synthons.

6-Fluoro- α^4 , α^5 -isopropylidenepyridoxol **5** was previously prepared as part of the synthesis of 6-fluoro-3, α^4 -isopropylidenepyridoxol.^{8,13} Testing various acids as catalysts showed 2% H₂SO₄ acetone solution to provide the best yield of **5** (26%). The regioselectivity of the acetonation reaction was confirmed by comparing ¹H NMR of **5** and 6-fluoro-3, α^4 -isopropylidenepyridoxol, in which the 5-CH₂ signal of **5** appeared at 5.03 ppm as a singlet, while in 6-fluoro-3, α^4 -isopropylidenepyridoxol it appeared at 4.97 ppm as a doublet ($J_{H-5, HO-5} = 1.2$ Hz) due to the coupling of 5-OH.¹³ Treatment of **5** with **2** by the Koenigs–Knorr glycosylation gave 3-*O*-(2,3,4,6-tetra-*O*-acetyl- β -D-galactopyranosyl)- α^4 , α^5 -isopropylidene-6-fluoropyridoxol **6** in 85% yield. The $\delta_{H-1'}$ at 4.64 ppm is a well-resolved doublet ($J_{1,2} = 8.0$ Hz), and $\delta_{C-1'}$ at 100.03 ppm demonstrated that the D-galactose was in the β -configuration. The correlation between 2-CH₃ and H-1' of sugar ring from the NOESY spectrum of **6** verified that 2,3,4,6-tetra-*O*-acetyl- β -D-galactopyranosyl residue connected at the 3-phenolic site, providing further evidence that the acetonation had occurred regioselectively on 4,5-hydroxymethyl groups.

3-*O*-(2,3,4,6-Tetra-*O*-acetyl- β -D-galactopyranosyl)-6-fluoropyridoxol **7** was obtained by cleavage of acetonide **6**, but the yields were quite low ($\leq 15\%$), based on several hydrolysis conditions, such as 80% AcOH, 1% HCl, or 90% CF₃CO₂H in MeOH, CH₂Cl₂, or 1,4-dioxane at various temperatures (60–100 °C). A moderate amount of **1** was recoverable, indicating that the β -D-galactopyranosyl C_{1'(gal)}–O₃ bond became weak and sensitive to acid hydrolysis, presumably due to the presence of the 6-fluorine atom. Condensation of **7** with 2,3,4,6-tetra-*O*-acetyl- α -D-glucopyranosyl bromide **8** or 2,3,4,6-tetra-*O*-acetyl- α -D-mannopyranosyl bromide **9** in dry CH₂Cl₂ with Hg(CN)₂ as a promoter gave 3-*O*-(2,3,4,6-tetra-*O*-acetyl- β -D-galactopyranosyl)- α^4 , α^5 -di-*O*-(2,3,4,6-tetra-*O*-acetyl- β -D-glucopyranosyl)-6-fluoropyridoxol **10** or 3-*O*-(2,3,4,6-tetra-*O*-acetyl- β -D-galactopyranosyl)- α^4 , α^5 -di-*O*-(2,3,4,6-tetra-*O*-acetyl- α -D-mannopyranosyl)-6-fluoropyridoxol **11** in yields of 80% or 78%, respectively.

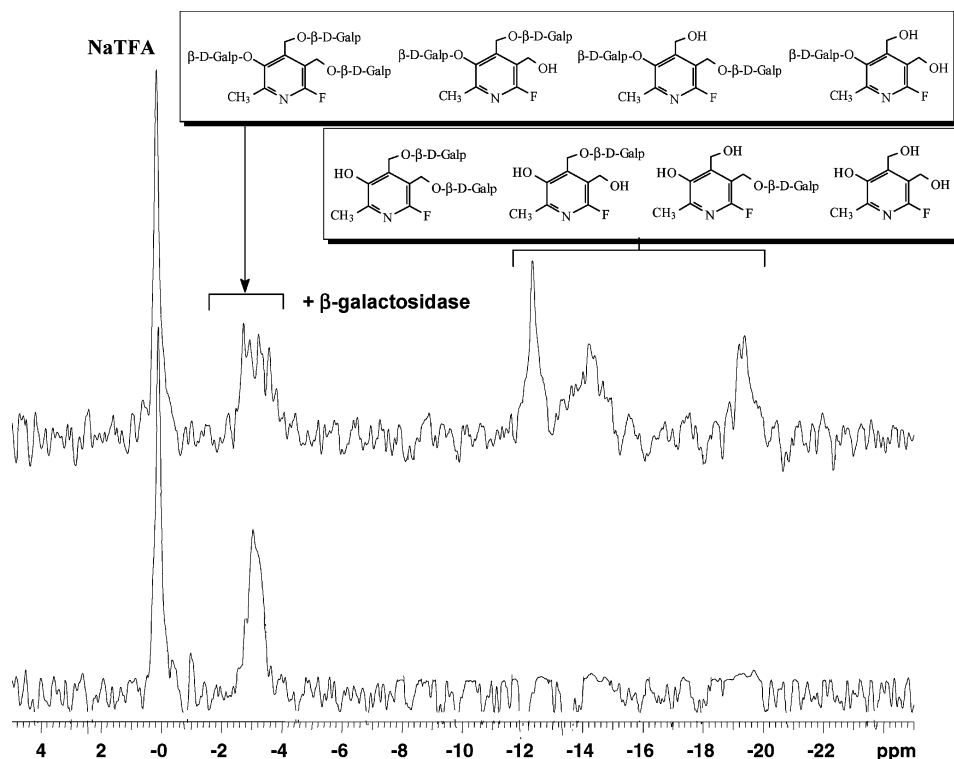


Figure 2. ^{19}F NMR spectra of 3, α^4 , α^5 -tri-*O*-(β -D-galactopyranosyl)-6-fluoropyridoxol **4** (10.1 mg, 15 mmol, lower trace) and its products resulting from addition of β -gal (E801A, 15 units) in PBS (pH = 7.4) at 37 °C (upper trace). Spectra were acquired in 51 s and enhanced with an exponential line broadening 40 Hz; β -D-Galp = β -D-galactopyranosyl.

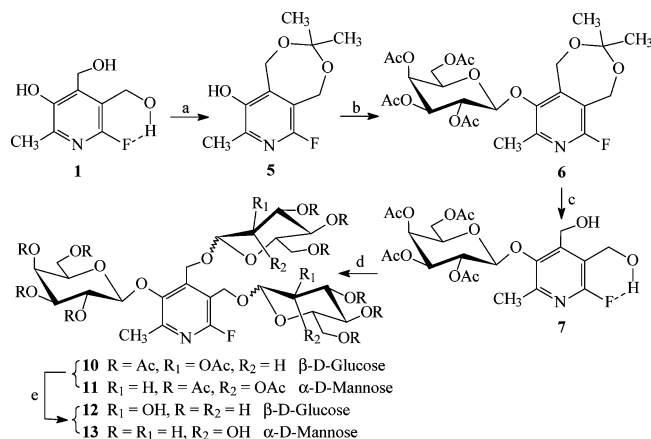


Figure 3. Reagents and conditions: (a) 2% H_2SO_4 , acetone, RT 4~5 h, 26%; (b) 2,3,4,6-tetra-*O*-acetyl- α -D-galactopyranosyl bromide **2**, Hg(CN) $_2$, 4 Å molecular sieve, CH_2Cl_2 , RT, 12 h, 85%; (c) 80% AcOH, 80 °C, 4~5 h, 15%; (d) 2,3,4,6-tetra-*O*-acetyl- α -D-glucopyranosyl bromide **8** or 2,3,4,6-tetra-*O*-acetyl- α -D-mannopyranosyl bromide **9**, Hg(CN) $_2$, 4 Å molecular sieve, CH_2Cl_2 , RT, 12 h, 80% (\rightarrow **10**) or 78% (\rightarrow **11**), respectively; (e) NH_3/MeOH , 0 °C \rightarrow RT, 24 h, quantitative yields.

Deacetylation of **10** or **11** in NH_3/MeOH from 0 °C to room temperature (RT) gave the target molecules **12** and **13** in quantitative yields (Figure 3). However, the overall yields for **12** and **13** through the five-step reactions were only 3%, with limiting steps in the α^4 , α^5 -isopropylidene group formation and hydrolysis procedures.

The acidic 3-phenolic group para to the 6-fluorine atom in FPOL should be easily converted into the monoanion under mild base conditions,^{8,13,22} suggesting an alternate approach to selectively benzylate the 3-OH under carefully controlled conditions. Benzyl bromide (1.1 equiv) was added dropwise over a period of 4~5 h to the well-stirred reaction mixture of **1** in a

dichloromethane/aqueous biphasic system (pH 10~11) with tetrabutylammonium bromide (TBAB) as the phase-transfer catalyst, yielding 3-*O*-benzyl-6-fluoropyridoxol **14** in 76% yield. The structure was established on the basis of the coupling characteristics of α^4 , α^5 -CH $_2$ as doublets ($J_{\text{H-4,HO-4}} = 6.0$ Hz, $J_{\text{H-5,HO-5}} = 5.4$ Hz) and α^4 , α^5 -OH as triplets in the ^1H NMR spectrum. Condensation of **14** with **8** or **9** gave 3-*O*-benzyl- α^4 , α^5 -di-*O*-(2,3,4,6-tetra-*O*-acetyl- β -D-glucopyranosyl)-6-fluoropyridoxol **15** or 3-*O*-benzyl- α^4 , α^5 -di-*O*-(2,3,4,6-tetra-*O*-acetyl- α -D-mannopyranosyl)-6-fluoropyridoxol **16** in satisfactory yields. Removal of the benzyl-protecting group afforded acceptors α^4 , α^5 -di-*O*-(2,3,4,6-tetra-*O*-acetyl- β -D-glucopyranosyl)-6-fluoropyridoxol **17** or α^4 , α^5 -di-*O*-(2,3,4,6-tetra-*O*-acetyl- α -D-mannopyranosyl)-6-fluoropyridoxol **18** in quantitative yields, which were subjected to a procedure similar to that described above for the preparation of galactosides, giving **10** or **11** in high yields (88% or 85%, respectively). After workup and deacetylation, the target compounds **12** and **13** were obtained in 57% and 52% overall yields over five-step reactions (Figure 4).

Recognizing the differential reactivity of the 3-phenolic group over the hydroxymethyl groups, most recently, we have successfully specifically galactopyranosylated **1** on the 3-phenolic group directly with **2** via the above phase-transfer catalysis technique, yielding **7**.⁸ Figure 5 depicts a very efficient route to synthesize the target compounds **12** and **13** in just three steps with higher overall yields (67% and 65%, respectively).

Characteristics. Compounds **4**, **12**, and **13** each gave a single narrow ^{19}F NMR signal between δ -2.0 and -3.3 ppm, essentially invariant ($\Delta\delta \leq 0.06$ ppm) with pH in the range 3~12 and temperatures from 25 to 37 °C in whole rabbit blood, 0.9% saline, or phosphate-buffered saline (PBS). Addition of β -gal (E801A) in PBS at 37 °C to **4**, **12** and **13** caused rapid hydrolysis, releasing the aglycons α^4 , α^5 -di-*O*-(β -D-galactopyranosyl)-6-fluoropyridoxol, α^4 , α^5 -di-*O*-(β -D-glucopyranosyl)-6-fluoropyridoxol, and α^4 , α^5 -di-*O*-(α -D-mannopyranosyl)-6-flu-

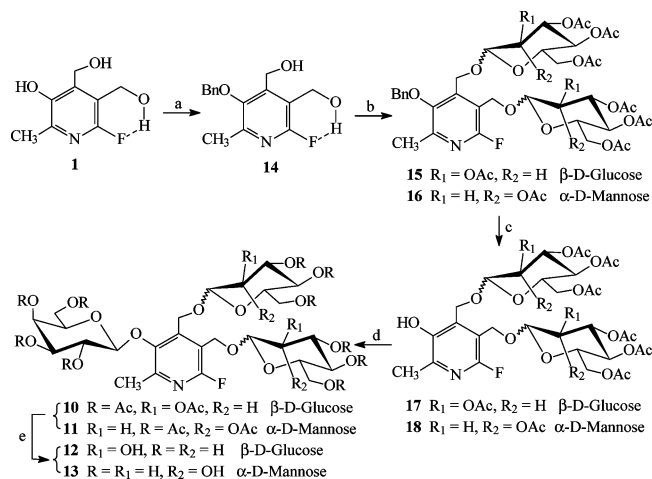


Figure 4. Reagents and conditions: (a) benzyl bromide (1.1 equiv), $\text{CH}_2\text{Cl}_2\text{-H}_2\text{O}$, pH 10–11, 50 °C, TBAB, 4–5 h, 76%; (b) 2,3,4,6-tetra-*O*-acetyl- α -D-glucopyranosyl bromide **8** or 2,3,4,6-tetra-*O*-acetyl- α -D-mannopyranosyl bromide **9**, $\text{Hg}(\text{CN})_2$, 4 Å molecular sieve, CH_2Cl_2 , RT, 12 h, 90% (\rightarrow **15**) or 85% (\rightarrow **16**), respectively; (c) 25 psi H_2 , Pd/C, RT, 12 h, quantitative yields; (d) 2,3,4,6-tetra-*O*-acetyl- α -D-galactopyranosyl bromide **2**, $\text{Hg}(\text{CN})_2$, 4 Å molecular sieve, CH_2Cl_2 , RT, 12 h, 88% (\rightarrow **10**) or 85% (\rightarrow **11**), respectively; (e) NH_3/MeOH , 0 °C \rightarrow RT, 24 h, 95% (\rightarrow **12**) or 94% (\rightarrow **13**), respectively.

oropyridoxol, which also appeared as single narrow ^{19}F signals between δ –11.20 and –12.40 ppm ($\Delta\delta$ = 9.0–9.4 ppm) (Table 1). Action of β -gal on **4** was complicated by action on each of the galactose residues, apparently randomly, to generate multiple signals representing **1** together with partially galactosylated products (Figure 2). The β -gal hydrolysis of **4**, **12**, and **13** proceeded in a smooth manner, indicating that the liberated aglycons have no inhibitory effects on β -gal (Figure 6). The kinetic curves suggest straightforward first-order kinetics, which were much more rapid for all substrates than for GFPOL. Compounds **12** and **13** gave single products upon exposure to β -gal (Figure 7). Addition of **12** and **13** to stably transfected human breast MCF-7-*lacZ* tumor cells showed cleavage of **12** or **13** (Figure 8) and this proceeded in an initially smooth monotonic manner at rates of 18.6 or 19.6 $\mu\text{mol min}^{-1}$ (million MCF7-*lacZ* cells) $^{-1}$, respectively. Compounds **12** and **13** have much higher aqueous solubility than GFPOL (GFPOL, 75 mM vs **12**, 196 mM, and **13**, 173 mM, all in PBS).

The products α^4, α^5 -di-*O*-(β -D-galactopyranosyl)-6-fluoropyridoxol (DGFPOL), α^4, α^5 -di-*O*-(β -D-glucopyranosyl)-6-fluoropyridoxol (DUFPOL), and α^4, α^5 -di-*O*-(α -D-mannopyranosyl)-6-fluoropyridoxol (DMFPOL) of the action of β -gal on **4**, **12**, and **13** also exhibit large ^{19}F NMR chemical shift response to pH ($\Delta\delta$ = \sim 11.0 ppm) in the range of pH 1–12 (Figure 9, Table 2), but there is no spectral overlap with the substrates.

Conclusion

These results provide further evidence for the broad specificity of β -gal and the feasibility of modifying substrate structures to enhance enzyme sensitivity and water solubility. The additional sugar residues in **4**, **12**, and **13** compared with GFPOL all lead to faster cleavage kinetics with β -gal. Significantly, the differential glycosylation provides structures that respond to β -gal with generation of single products. The results with stably transfected breast cancer cells indicate the potential for future studies in vivo.

Experimental Section

General Methods. NMR spectra were recorded on a Varian Inova 400 spectrometer (400 MHz for ^1H , 100 MHz for ^{13}C , 376 MHz for ^{19}F) with CDCl_3 or $\text{DMSO-}d_6$ as solvent. ^1H and ^{13}C chemical shifts are referenced to tetramethylsilane (TMS) as internal standard, and ^{19}F to a dilute solution of sodium trifluoroacetate (NaTFA) in a capillary as external standard (37 °C). Compounds were characterized by acquisition of ^1H , ^{13}C , distortionless enhancement by polarization transfer (DEPT), ^1H – ^1H correlation spectroscopy (COSY), or nuclear Overhauser enhancement spectroscopy (NOESY) experiments at 25 °C. Microanalyses were performed on a Perkin-Elmer 2400CHN microanalyzer. Mass spectra were obtained by positive and negative electrospray ionization mass spectrometry (ESI-MS) on a Micromass Q-TOF hybrid quadrupole/time-of-flight instrument (Micromass UK Ltd.). Reactions requiring anhydrous conditions were performed under nitrogen or argon. $\text{Hg}(\text{CN})_2$ was dried before use at 50 °C for 1 h, CH_2Cl_2 was dried over Drierite, and acetonitrile was dried on CaH_2 and kept over molecular sieves under N_2 . Solutions in organic solvents were dried with anhydrous sodium sulfate and concentrated in vacuo below 45 °C. 2,3,4,6-Tetra-*O*-acetyl- α -D-galactopyranosyl bromide **2** and 2,3,4,6-tetra-*O*-acetyl- α -D-glucopyranosyl bromide **8** were purchased from Sigma Chemical Co. 2,3,4,6-Tetra-*O*-acetyl- α -D-mannopyranosyl bromide **9** was prepared according to the literature method.²³ Column chromatography was performed on silica gel (200–300 mesh) by elution with cyclohexane/EtOAc, and silica gel GF₂₅₄ (Aldrich) was used for analytical thin-layer chromatography (TLC). Detection was effected by spraying the plates with 5% ethanolic H_2SO_4 (followed by heating at 110 °C for \sim 10 min) or by direct UV illumination of the plate.

For enzyme kinetic experiments, **4**, **12**, and **13** (10.1 mg, 15 μmol) were dissolved in PBS (0.1 M, pH = 7.4, 600 μL), and a PBS solution of β -gal (0.1 M, pH = 7.4, 15 μL , 1 unit/ μL , E801A, Promega, Madison, WI) was added and NMR data were acquired immediately at 37 °C.

MCF7-*lacZ* human breast cancer cells stably transfected to express β -gal were grown in culture under standard conditions and harvested. Compound **12** or **13** was added to suspension of cells (5×10^6) in PBS and observed by NMR for 1 h.

Syntheses: 3, α^4, α^5 -Tri-*O*-(2,3,4,6-tetra-*O*-acetyl- β -D-galactopyranosyl)-6-fluoropyridoxol **3.** A solution of 2,3,4,6-tetra-*O*-acetyl- α -D-galactopyranosyl bromide **2** (1.35 g, 3.3 mmol, 1.1 equiv) in anhydrous CH_2Cl_2 (8 mL) was added dropwise to a solution of 6-fluoropyridoxol **1** (0.18 g, 1.0 mmol) and $\text{Hg}(\text{CN})_2$ (1.01 g, 4.0 mmol) in dry MeCN (10 mL) containing powdered molecular sieves (4 Å, 2.0 g) with vigorous stirring at RT under argon in the dark for 12 h. The mixture was diluted with CH_2Cl_2 (30 mL), filtered through Celite, washed, dried (Na_2SO_4), and concentrated in vacuo. The residue was purified on a silica gel column (1:3 cyclohexane/EtOAc) to yield **3** (1.05 g, 89%) as syrup, R_f 0.30 (1:3 cyclohexane/EtOAc). NMR (CDCl_3) δ_{H} 5.24 (1H, d, $J_{1',2'} = 8.0$ Hz, H-1'), 5.04 (1H, dd, $J_{2',3'} = 9.8$ Hz, H-2'), 4.73 (1H, dd, $J_{3',4'} = 3.4$ Hz, H-3'), 3.98 (1H, dd, $J_{4',5'} = 2.4$ Hz, H-4'), 4.02–4.10 (3H, m, H-5' and H-6'), 4.66 (1H, d, $J_{1'',2''} = 8.0$ Hz, H-1''), 4.52 (1H, d, $J_{1''',2'''} = 8.0$ Hz, H-1'''), 5.15 (2H, dd, $J_{2'',3''} = J_{2''',3'''} = 10.0$ Hz, H-2'' and H-2'''), 5.07 (2H, dd, $J_{3'',4''} = J_{3''',4'''} = 3.6$ Hz, H-3'' and H-3'''), 5.52 (2H, dd, $J_{4'',5''} = J_{4''',5'''} = 3.2$ Hz, H-4'' and H-4'''), 3.88 (2H, m, H-5'' and H-5'''), 4.18 (2H, dd, $J_{5'',6a''} = J_{5''',6a'''} = 3.6$ Hz, $J_{6a'',6b''} = J_{6a''',6b'''} = 9.2$ Hz, H-6a'' and H-6a'''), 4.11 (2H, dd, $J_{5'',6b''} = J_{5''',6b'''} = 6.8$ Hz, H-6b'' and H-6b'''), 4.48 (2H, d, $J_{\text{CH}_2-4a, \text{CH}_2-4b} = J_{\text{CH}_2-5a, \text{CH}_2-5b} = 13.2$ Hz, CH₂-4a and CH₂-5a), 4.12 (2H, d, $J_{\text{CH}_2-4a, \text{CH}_2-4b} = J_{\text{CH}_2-5a, \text{CH}_2-5b} = 13.2$ Hz, CH₂-4b and CH₂-5b), 2.43 (3H, s, CH₃-2), 2.18, 2.17, 2.16, 2.15, 2.12, 2.11, 2.10, 2.09, 2.08, 2.07, 2.06, 2.05 (36H, 12s, 12 CH₃CO). δ_{C} 170.84, 170.79, 170.77, 170.73, 170.68, 170.54, 170.53, 170.49, 170.45, 170.35, 170.31, 170.28 (12 CH₃CO), 146.47 (d, $^3J_{\text{F-C}} = 14.5$ Hz, Py-C₂), 148.16 (d, $^4J_{\text{F-C}} = 3.8$ Hz, Py-C₃), 133.10 (s, Py-C₄), 112.51 (d, $^2J_{\text{F-C}} = 31.3$ Hz, Py-C₅), 155.04 (d, $^1J_{\text{F-C}} = 231.2$ Hz, Py-C₆), 103.34 (s, C-1'), 100.22 (s, C-1'' and

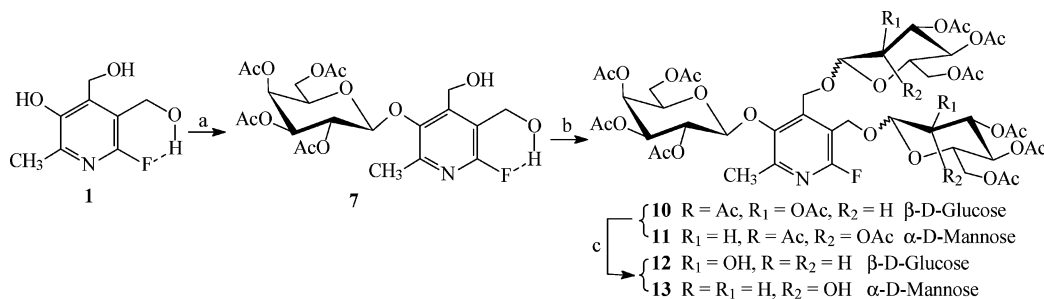


Figure 5. Reagents and conditions: (a) 2,3,4,6-tetra-*O*-acetyl- α -D-galactopyranosyl bromide **2**, CH_2Cl_2 - H_2O , pH 10~11, RT, TBAB, 4~5 h, 88%; (b) 2,3,4,6-tetra-*O*-acetyl- α -D-glucopyranosyl bromide **8** or 2,3,4,6-tetra-*O*-acetyl- α -D-mannopyranosyl bromide **9**, $\text{Hg}(\text{CN})_2$, 4 Å molecular sieve, CH_2Cl_2 , RT, 12 h, 80% (\rightarrow **10**) or 78% (\rightarrow **11**), respectively; (c) NH_3/MeOH , 0 °C \rightarrow RT, 24 h, 95% (\rightarrow **12**) or 94% (\rightarrow **13**), respectively.

Table 1. ^{19}F Chemical Shifts^a and Hydrolytic Rates^b

reporters	4	12	13	GFPOL
$\delta_{\text{F}}(\text{substrate})$	-3.02	-2.85	-2.14	-3.22
$\delta_{\text{F}}(\text{product})$	-12.37	-12.16	-11.22	-11.21
$\Delta\delta_{\text{F}}$	9.35	9.31	9.08	7.99
ν ($\mu\text{mol min}^{-1} \text{unit}^{-1}$)	34.0	35.0	38.0	4.3

^a Chemical shifts are given in parts per million (ppm) with respect to sodium trifluoroacetate. ^b β -gal (E801A) was added at 37 °C in PBS (0.1 M, pH = 7.4).

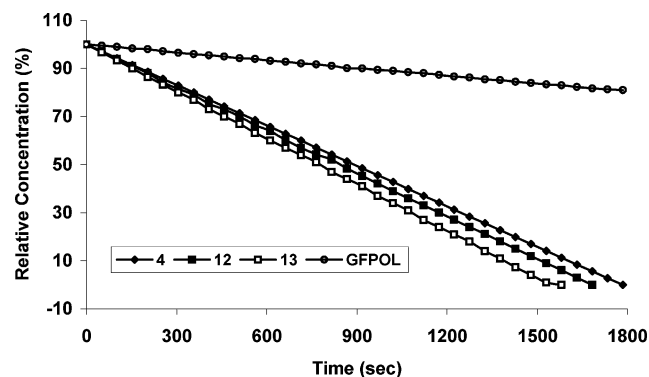


Figure 6. Kinetic hydrolysis time courses of **4** (\blacklozenge), **12** (\blacksquare), **13** (\square) (15.0 mmol each), and GFPOL (\circ) (10.0 mmol) by β -gal (E801A, 15 units) hydrolysis in PBS (0.1 M, pH = 7.4, 600 μL) at 37 °C.

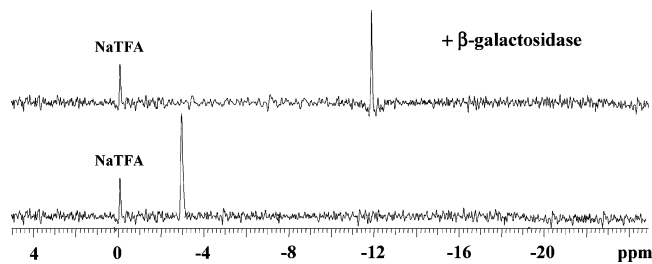


Figure 7. ^{19}F NMR spectra of 3-*O*-(β -D-galactopyranosyl)- α^4,α^5 -di-*O*-(β -D-glucopyranosyl)-6-fluoropyridoxol **12** (10.1 mg, 15 mmol, lower trace) and its hydrolysis by β -gal (E801A, 15 units) in PBS (0.1 M, pH = 7.4, 600 μL) at 37 °C (upper trace). Spectra were acquired in 205 s and enhanced with exponential line broadening = 40 Hz.

C-1'''), 70.75 (s, C-2'), 71.14 (s, C-3'), 70.61 (s, C-4'), 71.56 (s, C-5'), 67.03 (s, C-6'), 67.45 (s, C-2'' and C-2'''), 68.39 (s, C-3'' and C-3'''), 66.31 (s, C-4'' and C-4'''), 68.55 (s, C-5'' and C-5'''), 61.99 (s, C-6'' and C-6'''), 61.54 (s, CH_2 -4), 61.67 (s, CH_2 -5), 21.03, 20.94, 20.90, 20.89, 20.87, 20.85, 20.83, 20.79, 20.77, 20.76, 20.74, 20.72 (12s, 12 CH_3CO), 18.77 (s, CH_3 -3). ESI-MS m/z 1178 [M^+] (26%), 1179 [$\text{M} + 1$] (14%). Anal. Calcd for $\text{C}_{50}\text{H}_{64}\text{NO}_{30}\text{F}$: C, 50.96, H, 5.48, N, 1.19. Found: C, 50.93, H, 5.46, N, 1.15.

3,4,5-Tri-*O*-(β -D-galactopyranosyl)-6-fluoropyridoxol **4.** A solution of **3** (0.9 g) in anhydrous MeOH (20 mL) containing 0.5 M NH_3 was vigorously stirred from 0 °C to RT overnight, until TLC showed complete reaction, and then evaporated to dryness in

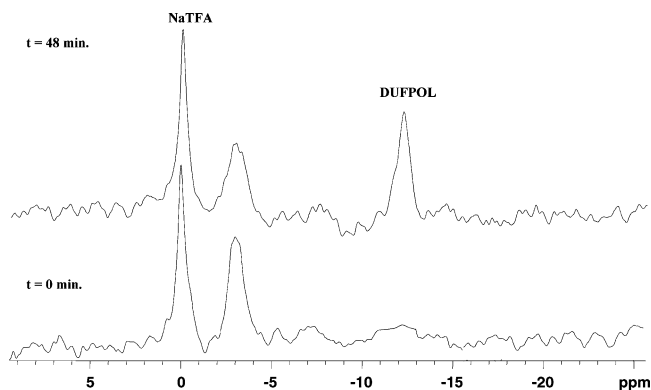


Figure 8. ^{19}F NMR spectra of 3-*O*-(β -D-galactopyranosyl)- α^4,α^5 -di-*O*-(β -D-glucopyranosyl)-6-fluoropyridoxol **12** (5.1 mg, 7.5 mmol) with stably transfected MCF7-*lacZ* cells (5×10^6) in PBS (0.1 M, pH = 7.4, 600 μL) at 37 °C. Spectra were acquired in 51 s and enhanced with an exponential line broadening = 100 Hz. [DUFPOL = α^4,α^5 -di-*O*-(β -D-glucopyranosyl)-6-fluoropyridoxol.]

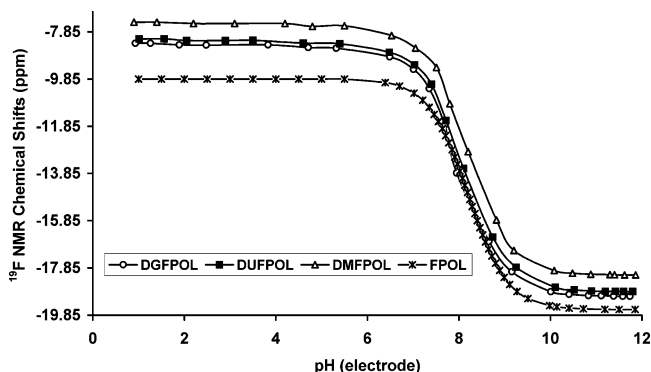


Figure 9. ^{19}F NMR chemical shift pH titration curve of DGFPOL, DUFPOL, and DMFPOL in 0.9% saline at 37 °C. [DGFPOL = α^4,α^5 -di-*O*-(β -D-galactopyranosyl)-6-fluoropyridoxol; DUFPOL = α^4,α^5 -di-*O*-(β -D-glucopyranosyl)-6-fluoropyridoxol; DMFPOL = α^4,α^5 -di-*O*-(α -D-mannopyranosyl)-6-fluoropyridoxol.]

Table 2. Acidities and ^{19}F NMR/pH Properties of DGFPOL, DUFPOL, DMFPOL, and FPOL in Saline at 25 °C^a

pH indicators	DGFPOL	DUFPOL	DMFPOL	FPOL ²⁴
pK_a	7.95	8.08	8.18	8.20
δ_{Facid}	-8.34	-8.15	-7.44	-9.85
δ_{Fbase}	-19.05	-18.85	-18.15	-19.61

^a Chemical shifts are given in parts per million (ppm) with respect to sodium trifluoroacetate.

vacuo. Chromatography of the crude syrup on silica gel with EtOAc/MeOH (4:1) afforded **4** (0.52 g) as a syrup in quantitative yield, R_f 0.10 (1:4 MeOH/EtOAc). NMR ($\text{DMSO}-d_6$) δ_{H} 4.95 (1H, d, $J_{1',2'} = 8.2$ Hz, H-1'), 4.76 (1H, dd, $J_{2',3'} = 10.0$ Hz, H-2'), 4.91 (1H, dd, $J_{3',4'} = 2.8$ Hz, H-3'), 5.11 (1H, dd, $J_{4',5'} = 2.3$ Hz, H-4'), 3.77 (1H, m, H-5'), 3.90 (1H, dd, $J_{5',6a'} = 6.4$ Hz, $J_{6a',6b'} = 12.4$ Hz,

H-6a'), 3.68 (1H, dd, $J_{5',6b'} = 3.6$ Hz, H-6b'), 4.22 (2H, d, $J_{1'',2''} = J_{1'',2'''} = 8.0$ Hz, H-1'' and H-1'''), 3.29 (2H, dd, $J_{2'',3''} = J_{2'',3'''} = 10.6$ Hz, H-2'' and H-2'''), 3.51 (2H, dd, $J_{3'',4''} = J_{3'',4'''} = 3.2$ Hz, H-3'' and H-3'''), 3.62 (2H, dd, $J_{4'',5''} = J_{4'',5'''} = 2.4$ Hz, H-4'' and H-4'''), 3.46 (2H, m, H-5'' and H-5'''), 3.66 (2H, dd, $J_{5'',6a''} = J_{5'',6a'''} = 3.6$ Hz, $J_{6a'',6b''} = J_{6a'',6b'''} = 10.4$ Hz, H-6a'' and H-6a'''), 3.39 (2H, dd, $J_{5'',6b''} = J_{5'',6b'''} = 6.6$ Hz, H-6b'' and H-6b'''), 4.48 (2H, d, $J_{CH_2-4a,CH_2-4b} = J_{CH_2-5a,CH_2-5b} = 13.0$ Hz, CH₂-4a and CH₂-5a), 4.44 (2H, d, $J_{CH_2-4a,CH_2-4b} = J_{CH_2-5a,CH_2-5b} = 13.0$ Hz, CH₂-4b and CH₂-5b), 2.32 (3H, s, CH₃-2). δ_C 144.65 (d, $^3J_{F-C} = 14.5$ Hz, Py-C₂), 147.87 (d, $^4J_{F-C} = 3.9$ Hz, Py-C₃), 137.36 (d, $^4J_{F-C} = 3.8$ Hz, Py-C₄), 115.15 (d, $^2J_{F-C} = 32.3$ Hz, Py-C₅), 154.26 (d, $^1J_{F-C} = 226.6$ Hz, Py-C₆), 103.19 (s, C-1'), 101.67 (s, C-1''), 101.67 (s, C-1'''), 70.36 (s, C-2'), 73.94 (s, C-3'), 69.44 (s, C-4'), 76.08 (s, C-5'), 62.88 (s, C-6'), 72.10 (s, C-2''), 73.50 (s, C-3''), 68.26 (s, C-4''), 75.02 (s, C-5''), 60.60 (s, C-6''), 68.77 (s, CH₂-4), 68.92 (s, CH₂-5), 19.19 (s, CH₃-3). ESI-MS m/z 673 [M⁺] (6%), 674 [M + 1] (10%). Anal. Calcd for C₂₆H₄₀NO₁₈F: C, 46.34, H, 5.99, N, 2.08. Found: C, 46.30, H, 5.96, N, 2.05.

α^4,α^5 -O-Isopropylidene-6-fluoropyridoxol 5. A suspension of **1** (0.50 g, 2.67 mmol) in anhydrous acetone (40 mL) containing 2% concentrated H₂SO₄ was stirred for 4~5 h, at the end of which time TLC (4:1 cyclohexane/EtOAc) indicated complete reaction, and then cold saturated Na₂CO₃ solution was added with vigorous stirring up to pH between 8 and 9. The precipitate was filtered off, and concentration of the reaction mixture under reduced pressure followed by purification on flash silica gel column (4:1 cyclohexane/EtOAc) gave **5** (0.64 g, 26%) as a syrup, R_f 0.34 (4:1 cyclohexane/EtOAc), NMR (CDCl₃) δ_H 7.45 (1H, s, HO-3), 5.03 (2H, s, CH₂-5), 4.57 (2H, s, CH₂-4), 2.33 (3H, s, CH₃-2), 1.55 (6H, s, 2 CH₃). δ_C 146.40 (d, $^3J_{F-C} = 14.5$ Hz, Py-C₂), 144.32 (d, $^4J_{F-C} = 3.8$ Hz, Py-C₃), 130.68 (s, Py-C₄), 111.21 (d, $^2J_{F-C} = 32.8$ Hz, Py-C₅), 152.20 (d, $^1J_{F-C} = 231.2$ Hz, Py-C₆), 100.15 (s, CMe₂), 58.70 (d, $^3J_{F-C} = 3.0$ Hz, CH₂-5), 54.51 (s, CH₂-4), 31.62 [s, C(CH₃)₂], 17.58 (s, CH₃-2). Anal. Calcd for C₁₁H₁₄NO₃F: C, 58.13, H, 6.21, N, 6.17. Found: C, 58.08, H, 6.16, N, 6.11.

3-O-(2,3,4,6-Tetra-O-acetyl- β -D-galactopyranosyl)- α^4,α^5 -O-isopropylidene-6-fluoropyridoxol 6. To a solution of **5** (0.62 g, 2.72 mmol) and Hg(CN)₂ (0.88 g, 3.50 mmol) in dry CH₂Cl₂ (10 mL) containing freshly activated 4 Å molecular sieves (2.0 g) was added dropwise compound **2** (1.23 g, 3.0 mmol, 1.1 equiv). The mixture was stirred overnight in the dark at RT under N₂ until TLC indicated complete reaction. Workup as for **3** gave **6** (1.29 g, 85%), R_f 0.40 (2:3 cyclohexane/EtOAc). NMR (CDCl₃) δ_H 4.64 (1H, d, $J_{1',2'} = 8.0$ Hz, H-1'), 5.25 (1H, dd, $J_{2',3'} = 10.0$ Hz, H-2'), 5.02 (1H, dd, $J_{3',4'} = 3.6$ Hz, H-3'), 5.41 (1H, dd, $J_{4',5'} = 3.2$ Hz, H-4'), 3.97 (1H, m, H-5'), 4.21 (1H, dd, $J_{5',6a'} = 4.4$ Hz, $J_{6a',6b'} = 11.2$ Hz, H-6a'), 4.13 (1H, dd, $J_{5',6b'} = 7.2$ Hz, H-6b'), 5.10 (1H, d, $J_{CH_2-4a,CH_2-4b} = 8.0$ Hz, CH₂-4a), 4.67 (1H, d, $J_{CH_2-4a,CH_2-4b} = 8.0$ Hz, CH₂-4b), 5.14 (1H, d, $J_{CH_2-5a,CH_2-5b} = 9.6$ Hz, CH₂-5a), 5.12 (1H, d, $J_{CH_2-5a,CH_2-5b} = 9.6$ Hz, CH₂-5b), 2.42 (3H, s, CH₃-2), 2.17, 2.09, 2.08, 1.99 (12H, 4s, 4 CH₃CO), 1.61, 1.59 (6H, 2s, 2 CH₃). δ_C 170.78, 170.39, 170.26, 170.11 (4s, 4 CH₃CO), 145.48 (d, $^3J_{F-C} = 15.2$ Hz, Py-C₂), 133.16 (d, $^4J_{F-C} = 4.0$ Hz, Py-C₃), 126.26 (s, Py-C₄), 116.95 (d, $^2J_{F-C} = 32.1$ Hz, Py-C₅), 154.30 (d, $^1J_{F-C} = 229.0$ Hz, Py-C₆), 101.41 (s, CMe₂), 100.03 (s, C-1'), 68.70 (s, C-2'), 70.82 (s, C-3'), 67.12 (s, C-4'), 71.53 (s, C-5'), 64.28 (s, C-6'), 55.38 (s, CH₂-4), 61.58 (s, CH₂-5), 31.88 (s, C(CH₃)₂), 20.90, 20.89, 20.82, 20.77 (4s, 4 CH₃CO), 18.77 (s, CH₃-2). Anal. Calcd for C₂₅H₃₂NO₁₂F: C, 53.84, H, 5.79, N, 2.51. Found: C, 53.79, H, 5.74, N, 2.49.

3-O-(2,3,4,6-Tetra-O-acetyl- β -D-galactopyranosyl)-6-fluoropyridoxol 7. A mixture of **6** (1.25 g, 2.50 mmol) in 80% AcOH (40 mL) was stirred at 80 °C for 4~5 h, till TLC (1:3 cyclohexane/EtOAc) showed complete reaction. The cooled mixture was neutralized with cold saturated Na₂CO₃ solution, extracted with EtOAc (4 × 30 mL), and concentrated and purified by flash silica gel column with 1:4 cyclohexane/EtOAc, giving **7** (0.17 g, 15%) as a syrup, R_f 0.18 (1:4 cyclohexane/EtOAc). NMR (CDCl₃) δ_H 4.79 (1H, d, $J_{1',2'} = 8.0$ Hz, H-1'), 5.55 (1H, dd, $J_{2',3'} = 10.6$ Hz,

H-2'), 5.10 (1H, dd, $J_{3',4'} = 3.6$ Hz, H-3'), 5.41 (1H, dd, $J_{4',5'} = 3.6$ Hz, H-4'), 3.88 (1H, m, H-5'), 4.24 (1H, dd, $J_{5',6a'} = 4.4$ Hz, $J_{6a',6b'} = 12.0$ Hz, H-6a'), 4.09 (1H, dd, $J_{5',6b'} = 6.0$ Hz, H-6b'), 5.01 (2H, d, $J_{CH_2-4a,CH_2-4b} = J_{CH_2-5a,CH_2-5b} = 12.4$ Hz, CH₂-4a and CH₂-5a), 4.62 (1H, d, $J_{CH_2-4a,CH_2-4b} = 12.4$ Hz, CH₂-4b), 4.66 (1H, d, $J_{CH_2-5a,CH_2-5b} = 12.4$ Hz, CH₂-5b), 3.50 (1H, m, α^4 -HO, exchangeable with D₂O), 3.56 (1H, m, α^5 -HO, exchangeable with D₂O), 2.47 (3H, s, CH₃-2), 2.23, 2.17, 2.02, 2.00 (12H, 4s, 4 CH₃CO). δ_C 170.32, 170.28, 170.18, 169.48 (4 CH₃CO), 150.33 (d, $^3J_{F-C} = 15.2$ Hz, Py-C₂), 147.62 (d, $^4J_{F-C} = 4.6$ Hz, Py-C₃), 146.32 (d, $^3J_{F-C} = 4.5$ Hz, Py-C₄), 120.17 (d, $^2J_{F-C} = 32.0$ Hz, Py-C₅), 157.60 (d, $^1J_{F-C} = 235.8$ Hz, Py-C₆), 102.39 (s, C-1'), 68.91 (s, C-2'), 70.74 (s, C-3'), 67.19 (s, C-4'), 71.93 (s, C-5'), 61.98 (s, C-6'), 55.91 (s, CH₂-4), 59.60 (s, CH₂-5), 20.99, 20.85, 20.70, 20.67 (4s, 4 CH₃CO), 19.46 (s, CH₃-2). Anal. Calcd for C₂₂H₂₈NO₁₂F: C, 51.05, H, 5.46, N, 2.71. Found: C, 51.00, H, 5.39, N, 2.68.

Alternately **7** was synthesized from **1** directly by phase transfer catalysis: to a well-stirred CH₂Cl₂ (10 mL)/H₂O (10 mL) biphasic mixture (pH 10~11) of **1** (0.5 g, 2.67 mmol) and TBAB (0.1 g, 0.31 mmol), a solution of **2** (1.21 g, 2.94 mmol, 1.1 equiv) in CH₂Cl₂ (10 mL) was added dropwise over a period of 4~5 h at RT, and the stirring continued for an additional hour. The products were extracted (EtOAc; 4 × 20 mL), washed free of alkali, dried (Na₂SO₄), and concentrated. The residue was purified by column chromatography on silica gel (1:4 cyclohexane/EtOAc) to afford **7** (1.08 g, 88%) as syrup, which is identical in all respects to the product obtained above.

3-O-(2,3,4,6-Tetra-O-acetyl- β -D-galactopyranosyl)- α^4,α^5 -di-O-(2,3,4,6-tetra-O-acetyl- β -D-glucopyranosyl)-6-fluoropyridoxol 10 and 3-O-(2,3,4,6-Tetra-O-acetyl- β -D-galactopyranosyl)- α^4,α^5 -di-O-(2,3,4,6-tetra-O-acetyl- α -D-mannopyranosyl)-6-fluoropyridoxol 11. Condensation of **7** (0.5 g, 1.1 mmol) with 2,3,4,6-tetra-O-acetyl- α -D-glucopyranosyl bromide **8** or 2,3,4,6-tetra-O-acetyl- α -D-mannopyranosyl bromide **9** (1.0 g, 2.40 mmol, 1.1 equiv) in dry CH₂Cl₂ (10 mL) with Hg(CN)₂ (0.63 g, 2.50 mmol) as a promoter, according to the procedures described for the preparation of **3** and **6**, furnished 3-O-(2,3,4,6-tetra-O-acetyl- β -D-galactopyranosyl)- α^4,α^5 -di-O-(2,3,4,6-tetra-O-acetyl- β -D-glucopyranosyl)-6-fluoropyridoxol **10** and 3-O-(2,3,4,6-tetra-O-acetyl- β -D-galactopyranosyl)- α^4,α^5 -di-O-(2,3,4,6-tetra-O-acetyl- α -D-mannopyranosyl)-6-fluoropyridoxol **11**, respectively.

3-O-(2,3,4,6-Tetra-O-acetyl- β -D-galactopyranosyl)- α^4,α^5 -di-O-(2,3,4,6-tetra-O-acetyl- β -D-glucopyranosyl)-6-fluoropyridoxol 10: 1.04 g, 80%, syrup, R_f 0.30 (1:3 cyclohexane/EtOAc). NMR (CDCl₃) δ_H 5.06 (1H, d, $J_{1',2'} = 7.8$ Hz, H-1'), 5.28 (1H, dd, $J_{2',3'} = 8.8$ Hz, H-2'), 4.98 (1H, dd, $J_{3',4'} = 4.8$ Hz, H-3'), 4.73 (1H, dd, $J_{4',5'} = 2.8$ Hz, H-4'), 3.95 (1H, m, H-5'), 4.19 (1H, dd, $J_{5',6a'} = 3.6$ Hz, $J_{6a',6b'} = 10.8$ Hz, H-6a'), 4.02 (1H, dd, $J_{5',6b'} = 5.2$ Hz, H-6b'), 5.36 (1H, d, $J_{1'',2''} = 8.0$ Hz, H-1''), 5.39 (1H, d, $J_{1'',2'''} = 8.0$ Hz, H-1'''), 5.12 (1H, dd, $J_{2'',3''} = 7.2$ Hz, H-2''), 5.15 (1H, dd, $J_{2'',3'''} = 6.8$ Hz, H-2'''), 5.04 (1H, dd, $J_{3'',4''} = 3.2$ Hz, H-3''), 5.07 (1H, dd, $J_{3'',4'''} = 3.6$ Hz, H-3'''), 4.76 (1H, dd, $J_{4'',5''} = 2.8$ Hz, H-4''), 4.78 (1H, dd, $J_{4'',5'''} = 2.8$ Hz, H-4'''), 3.91 (1H, m, H-5''), 3.93 (1H, m, H-5'''), 4.08 (1H, dd, $J_{5'',6a''} = 3.2$ Hz, $J_{6a'',6b''} = 9.4$ Hz, H-6a''), 4.10 (1H, dd, $J_{5'',6b''} = 3.0$ Hz, $J_{6a'',6b''} = 10.0$ Hz, H-6a'''), 4.04 (1H, dd, $J_{5'',6b''} = 7.6$ Hz, H-6b''), 4.07 (1H, dd, $J_{5'',6b''} = 6.8$ Hz, H-6b'''), 4.55 (2H, d, $J_{CH_2-4a,CH_2-4b} = J_{CH_2-5a,CH_2-5b} = 11.2$ Hz, CH₂-4a and CH₂-5b), 4.49 (1H, d, $J_{CH_2-4a,CH_2-4b} = 11.2$ Hz, CH₂-4b), 4.91 (1H, d, $J_{CH_2-5a,CH_2-5b} = 11.2$ Hz, CH₂-5a), 2.34 (3H, s, CH₃-2), 2.05, 1.98, 1.97, 1.96, 1.95, 1.94, 1.93, 1.92, 1.91, 1.90, 1.89, 1.88 (36H, 12s, 12 CH₃CO). δ_C 170.83, 170.80, 170.76, 170.72, 170.70, 170.56, 170.28, 170.20, 170.17, 170.00, 169.82, 169.75 (12 CH₃CO), 152.14 (d, $^3J_{F-C} = 16.0$ Hz, Py-C₂), 149.81 (s, Py-C₃), 138.42 (d, $^3J_{F-C} = 11.4$ Hz, Py-C₄), 117.48 (d, $^2J_{F-C} = 32.0$ Hz, Py-C₅), 157.56 (d, $^1J_{F-C} = 233.5$ Hz, Py-C₆), 102.66 (s, C-1'), 98.00 (s, C-1''), 98.06 (s, C-1'''), 71.09 (s, C-2'), 68.65 (s, C-2''), 68.95 (s, C-2'''), 74.46 (s, C-3'), 70.84 (s, C-3''), 71.51 (s, C-3'''), 70.05 (s, C-4'), 68.13 (s, C-4''), 68.22 (s, C-4'''), 75.10 (s, C-5'), 72.20 (s, C-5''), 74.24 (s, C-5'''), 63.75 (s, C-6'), 61.91 (s, C-6''), 63.86 (s, C-6'''), 56.77 (s, CH₂-4), 57.16 (s, CH₂-5), 21.20, 20.95, 20.93, 20.91, 20.89, 20.87, 20.85, 20.75, 20.67, 20.62, 20.58,

20.54 (12s, 12 CH_3CO), 19.76 (s, CH_3 -3). ESI-MS m/z 1178 [M^+] (28%), 1179 [$\text{M} + 1$] (12%). Anal. Calcd for $\text{C}_{50}\text{H}_{64}\text{NO}_{30}\text{F}$: C, 50.96, H, 5.48, N, 1.19. Found: C, 50.92, H, 5.44, N, 1.16.

3-*O*-(2,3,4,6-tetra-*O*-acetyl- β -D-galactopyranosyl)- α^4,α^5 -di-*O*-(2,3,4,6-tetra-*O*-acetyl- α -D-mannopyranosyl)-6-fluoropyridoxol 11: 1.01 g, 78%, syrup, R_f 0.35 (1:3 cyclohexane/EtOAc). NMR (CDCl_3) δ_{H} 4.80 (1H, d, $J_{1',2'} = 8.2$ Hz, H-1'), 5.13 (1H, dd, $J_{2',3'} = 9.8$ Hz, H-2'), 5.36 (1H, dd, $J_{3',4'} = 4.2$ Hz, H-3'), 5.30 (1H, dd, $J_{4',5'} = 3.6$ Hz, H-4'), 4.01 (1H, m, H-5'), 4.33 (1H, dd, $J_{5',6a'} = 3.2$ Hz, $J_{6a',6b'} = 10.0$ Hz, H-6a'), 4.11 (1H, dd, $J_{5',6b'} = 4.6$ Hz, H-6b'), 4.71 (2H, d, $J_{1'',2''} = J_{1''',2'''} = 2.4$ Hz, H-1'' and H-1'''), 4.74 (2H, dd, $J_{2'',3''} = J_{2''',3'''} = 6.2$ Hz, H-2'' and H-2'''), 5.22 (2H, dd, $J_{3'',4''} = J_{3''',4'''} = 3.8$ Hz, H-3'' and H-3'''), 3.95 (2H, dd, $J_{4'',5''} = J_{4''',5'''} = 2.0$ Hz, H-4'' and H-4'''), 4.02 (2H, m, H-5'' and H-5'''), 4.11 (2H, dd, $J_{5'',6a''} = J_{5''',6a'''} = 2.0$ Hz, $J_{6a'',6b''} = J_{6a''',6b'''} = 7.4$ Hz, H-6a'' and H-6a'''), 4.07 (2H, dd, $J_{5'',6b''} = J_{5''',6b'''} = 5.6$ Hz, H-6b'' and H-6b'''), 4.87 (2H, d, $J_{\text{CH}_2-4a, \text{CH}_2-4b} = J_{\text{CH}_2-5a, \text{CH}_2-5b} = 13.6$ Hz, CH_2 -4a and CH_2 -5b), 4.67 (1H, d, $J_{\text{CH}_2-4a, \text{CH}_2-4b} = J_{\text{CH}_2-5a, \text{CH}_2-5b} = 13.6$ Hz, CH_2 -4b and CH_2 -5a), 2.33 (3H, s, CH_3 -2), 2.07, 2.04, 2.03, 2.00, 1.99, 1.98, 1.97, 1.96, 1.95, 1.94, 1.93, 1.92 (36H, 12s, 12 CH_3CO). δ_{C} 171.27, 171.23, 171.15, 171.06, 170.87, 170.83, 170.76, 170.63, 170.58, 170.44, 170.29, 170.25 (12 CH_3CO), 153.06 (d, $^3J_{\text{F-C}} = 16.0$ Hz, Py-C₂), 149.41 (d, $^4J_{\text{F-C}} = 4.6$ Hz, Py-C₃), 145.38 (d, $^3J_{\text{F-C}} = 4.6$ Hz, Py-C₄), 117.21 (d, $^2J_{\text{F-C}} = 31.3$ Hz, Py-C₅), 159.55 (d, $^1J_{\text{F-C}} = 235.0$ Hz, Py-C₆), 103.62 (s, C-1'), 98.32 (s, C-1''), 98.61 (s, C-1'''), 70.75 (s, C-2'), 70.22 (s, C-2''), 70.26 (s, C-2'''), 71.83 (s, C-3'), 70.36 (s, C-3''), 70.39 (s, C-3'''), 69.38 (s, C-4'), 67.04 (s, C-4''), 68.60 (s, C-4'''), 72.54 (s, C-5'), 71.90 (s, C-5''), 72.45 (s, C-5'''), 61.47 (s, C-6'), 62.46 (s, C-6''), 63.53 (s, C-6'''), 56.44 (s, CH_2 -4), 56.46 (s, CH_2 -5), 21.29, 21.21, 21.19, 21.17, 21.13, 21.10, 21.08, 21.05, 21.00, 20.95, 20.90, 20.88 (12s, 12 CH_3CO), 20.35 (s, CH_3 -3). ESI-MS m/z 1178 [M^+] (20%), 1179 [$\text{M} + 1$] (17%). Anal. Calcd for $\text{C}_{50}\text{H}_{64}\text{NO}_{30}\text{F}$: C, 50.96, H, 5.48, N, 1.19. Found: C, 50.94, H, 5.45, N, 1.16.

3-*O*-(β -D-Galactopyranosyl)- α^4,α^5 -di-*O*-(β -D-glucopyranosyl)-6-fluoropyridoxol 12 and 3-*O*-(β -D-Galactopyranosyl)- α^4,α^5 -di-*O*-(α -D-mannopyranosyl)-6-fluoropyridoxol 13. Compounds **10** and **11** (1.00 g, 0.85 mmol) were deacetylated as described above for **4** to yield **12** and **13** in quantitative yields.

3-*O*-(β -D-Galactopyranosyl)- α^4,α^5 -di-*O*-(β -D-glucopyranosyl)-6-fluoropyridoxol 12: 0.57 g, foam solid, R_f 0.20 (1:4 MeOH/EtOAc). NMR ($\text{DMSO}-d_6$) δ_{H} 5.01 (1H, d, $J_{1',2'} = 8.2$ Hz, H-1'), 5.22 (1H, dd, $J_{2',3'} = 9.0$ Hz, H-2'), 4.92 (1H, dd, $J_{3',4'} = 4.6$ Hz, H-3'), 4.70 (1H, dd, $J_{4',5'} = 2.6$ Hz, H-4'), 3.91 (1H, m, H-5'), 4.12 (1H, dd, $J_{5',6a'} = 3.2$ Hz, $J_{6a',6b'} = 10.2$ Hz, H-6a'), 4.00 (1H, dd, $J_{5',6b'} = 5.6$ Hz, H-6b'), 5.14 (2H, d, $J_{1'',2''} = 10.0$ Hz, H-1'' and H-1'''), 4.82 (2H, dd, $J_{2'',3''} = J_{2''',3'''} = 8.2$ Hz, H-2'' and H-2'''), 4.69 (2H, dd, $J_{3'',4''} = J_{3''',4'''} = 3.4$ Hz, H-3'' and H-3'''), 4.93 (2H, dd, $J_{4'',5''} = J_{4''',5'''} = 3.2$ Hz, H-4'' and H-4'''), 3.65 (2H, m, H-5'' and H-5'''), 3.55 (2H, dd, $J_{5'',6a''} = J_{5''',6a'''} = 4.8$ Hz, $J_{6a'',6b''} = J_{6a''',6b'''} = 12.0$ Hz, H-6a'' and H-6a'''), 3.31 (2H, dd, $J_{5'',6b''} = J_{5''',6b'''} = 5.6$ Hz, H-6b'' and H-6b'''), 4.29 (1H, d, $J_{\text{CH}_2-4a, \text{CH}_2-4b} = 7.6$ Hz, CH_2 -4a), 4.36 (1H, d, $J_{\text{CH}_2-4a, \text{CH}_2-4b} = 7.6$ Hz, CH_2 -5a), 4.20 (2H, d, $J_{\text{CH}_2-4a, \text{CH}_2-4b} = J_{\text{CH}_2-5a, \text{CH}_2-5b} = 7.6$ Hz, CH_2 -4b and CH_2 -5b), 4.18~3.65 (12H, br, HO-2', 3', 4', 6', 2'', 3'', 4'', 6'', 2''', 3''', 4''', and 6''', exchangeable with D_2O), 2.42 (3H, s, CH_3 -2). δ_{C} 144.43 (d, $^3J_{\text{F-C}} = 15.0$ Hz, Py-C₂), 136.26 (d, $^4J_{\text{F-C}} = 3.8$ Hz, Py-C₃), 124.40 (d, $^3J_{\text{F-C}} = 3.8$ Hz, Py-C₄), 120.39 (d, $^2J_{\text{F-C}} = 32.8$ Hz, Py-C₅), 148.98 (d, $^1J_{\text{F-C}} = 259.7$ Hz, Py-C₆), 103.65 (s, C-1'), 101.76 (s, C-1'' and C-1'''), 72.34 (s, C-2'), 71.28 (s, C-2'' and C-2'''), 74.55 (s, C-3'), 73.88 (s, C-3'' and C-3'''), 69.82 (s, C-4'), 68.89 (s, C-4'' and C-4'''), 76.62 (s, C-5'), 77.29 (s, C-5'' and C-5'''), 61.36 (s, C-6'), 60.95 (s, C-6'' and C-6'''), 60.54 (s, CH_2 -4), 60.78 (s, CH_2 -5), 19.88 (s, CH_3 -3). ESI-MS m/z 673 [M^+] (8%), 674 [$\text{M} + 1$] (14%). Anal. Calcd for $\text{C}_{26}\text{H}_{40}\text{NO}_{18}\text{F}$: C, 46.34, H, 5.99, N, 2.07. Found: C, 46.32, H, 5.97, N, 2.07.

3-*O*-(β -D-Galactopyranosyl)- α^4,α^5 -di-*O*-(α -D-mannopyranosyl)-6-fluoropyridoxol 13: 0.57 g, foam solid, R_f 0.26 (1:4 MeOH/EtOAc). NMR ($\text{DMSO}-d_6$) δ_{H} 5.00 (1H, d, $J_{1',2'} = 8.0$ Hz, H-1'), 5.23 (1H, dd, $J_{2',3'} = 10.0$ Hz, H-2'), 5.16 (1H, dd, $J_{3',4'} = 3.8$ Hz, H-3'), 5.08 (1H, dd, $J_{4',5'} = 3.2$ Hz, H-4'), 4.21 (1H, m, H-5'), 4.51

(1H, dd, $J_{5',6a'} = 3.6$ Hz, $J_{6a',6b'} = 10.2$ Hz, H-6a'), 4.31 (1H, dd, $J_{5',6b'} = 4.8$ Hz, H-6b'), 4.84 (2H, d, $J_{1'',2''} = J_{1''',2'''} = 2.6$ Hz, H-1'' and H-1'''), 4.68 (2H, dd, $J_{2'',3''} = J_{2''',3'''} = 6.0$ Hz, H-2'' and H-2'''), 5.02 (2H, dd, $J_{3'',4''} = J_{3''',4'''} = 3.6$ Hz, H-3'' and H-3'''), 4.05 (2H, dd, $J_{4'',5''} = J_{4''',5'''} = 2.2$ Hz, H-4'' and H-4'''), 3.94 (2H, m, H-5'' and H-5'''), 4.21 (2H, dd, $J_{5'',6a''} = J_{5''',6a'''} = 2.4$ Hz, $J_{6a'',6b''} = J_{6a''',6b'''} = 8.4$ Hz, H-6a'' and H-6a'''), 4.17 (2H, dd, $J_{5'',6b''} = J_{5''',6b'''} = 6.5$ Hz, H-6b'' and H-6b'''), 4.77 (2H, d, $J_{\text{CH}_2-4a, \text{CH}_2-4b} = J_{\text{CH}_2-5a, \text{CH}_2-5b} = 11.6$ Hz, CH_2 -4a and CH_2 -5b), 4.57 (1H, d, $J_{\text{CH}_2-4a, \text{CH}_2-4b} = J_{\text{CH}_2-5a, \text{CH}_2-5b} = 11.6$ Hz, CH_2 -4b and CH_2 -5a), 2.45 (3H, s, CH_3 -2), 4.30~3.70 (12H, br, HO-2', 3', 4', 6', 2'', 3'', 4'', 6'', 2''', 3''', 4''', and 6''', exchangeable with D_2O). δ_{C} 151.07 (d, $^3J_{\text{F-C}} = 15.3$ Hz, Py-C₂), 148.61 (d, $^4J_{\text{F-C}} = 4.8$ Hz, Py-C₃), 144.27 (d, $^3J_{\text{F-C}} = 3.6$ Hz, Py-C₄), 116.29 (d, $^2J_{\text{F-C}} = 32.0$ Hz, Py-C₅), 157.25 (d, $^1J_{\text{F-C}} = 233.5$ Hz, Py-C₆), 103.68 (s, C-1'), 98.56 (s, C-1''), 98.68 (s, C-1'''), 71.76 (s, C-2'), 70.66 (s, C-2''), 70.86 (s, C-2'''), 72.38 (s, C-3'), 71.46 (s, C-3''), 71.32 (s, C-3'''), 70.48 (s, C-4'), 66.87 (s, C-4''), 67.90 (s, C-4'''), 73.64 (s, C-5'), 72.20 (s, C-5''), 72.65 (s, C-5'''), 62.77 (s, C-6'), 63.56 (s, C-6''), 64.83 (s, C-6'''), 57.54 (s, CH_2 -4), 58.41 (s, CH_2 -5), 20.12 (s, CH_3 -3). ESI-MS m/z 673 [M^+] (5%), 674 [$\text{M} + 1$] (9%). Anal. Calcd for $\text{C}_{26}\text{H}_{40}\text{NO}_{18}\text{F}$: C, 46.34, H, 5.99, N, 2.08. Found: C, 46.31, H, 5.97, N, 2.05.

3-*O*-Benzyl-6-fluoropyridoxol 14. To a well-stirred CH_2Cl_2 (10 mL)/ H_2O (10 mL) biphasic mixture (pH 10~11) of **1** (0.50 g, 2.67 mmol) and TBAB (0.10 g, 0.31 mmol), a solution of benzyl bromide (0.51 g, 2.94 mmol, 1.1 equiv) in CH_2Cl_2 (10 mL) was added dropwise over a period of 4~5 h, while the reaction temperature was maintained at 50 °C, and the stirring continued for an additional hour. Products were extracted (CH_2Cl_2 , 4 \times 20 mL), washed free of alkali, dried (Na_2SO_4), and concentrated, and the residue was purified by column chromatography on silica gel with 1:2 cyclohexane/EtOAc to afford major product **14** (0.56 g, 76%), white crystalline, R_f 0.38 (1:2 cyclohexane/EtOAc). NMR (CDCl_3) δ_{H} 7.39 (5H, m, Ar-H), 4.90 (2H, s, PhCH_2), 4.75 (2H, d, $J_{\text{H}-5, \text{HO}-5} = 5.4$ Hz, CH_2 -5), 4.72 (2H, d, $J_{\text{H}-4, \text{HO}-4} = 6.0$ Hz, CH_2 -4), 3.57 (1H, t, $J_{\text{H}-5, \text{HO}-5} = 5.4$ Hz, α^5 -OH, exchangeable with D_2O), 3.49 (1H, t, $J_{\text{H}-4, \text{HO}-4} = 6.0$ Hz, α^4 -OH, exchangeable with D_2O), 2.44 (3H, s, CH_3 -2). δ_{C} 151.34 (d, $^3J_{\text{F-C}} = 9.6$ Hz, Py-C₂), 146.97 (d, $^4J_{\text{F-C}} = 2.9$ Hz, Py-C₃), 149.55 (d, $^3J_{\text{F-C}} = 3.1$ Hz, Py-C₄), 119.09 (d, $^2J_{\text{F-C}} = 20.8$ Hz, Py-C₅), 156.30 (d, $^1J_{\text{F-C}} = 216.2$ Hz, Py-C₆), 136.33, 128.96, 128.88, 128.57 (Ph-C), 55.99 (s, PhCH_2 , CH_2 -4), 56.76 (s, CH_2 -5), 19.31 (s, CH_3 -2). Anal. Calcd for $\text{C}_{15}\text{H}_{16}\text{NO}_3\text{F}$: C, 64.96, H, 5.82, N, 5.05. Found: C, 64.95, H, 5.79, N, 5.04.

3-*O*-Benzyl- α^4,α^5 -di-*O*-(2,3,4,6-tetra-*O*-acetyl- β -D-glucopyranosyl)-6-fluoropyridoxol 15 and 3-*O*-Benzyl- α^4,α^5 -di-*O*-(2,3,4,6-tetra-*O*-acetyl- α -D-mannopyranosyl)-6-fluoropyridoxol 16. Glycosylation of **14** (0.46 g, 2.0 mmol) with **8** or **9** (1.83 g, 4.45 mmol, 1.1 equiv) was carried out as for **3**, **10**, and **11** to give **15** and **16**, respectively.

3-*O*-Benzyl- α^4,α^5 -di-*O*-(2,3,4,6-tetra-*O*-acetyl- β -D-glucopyranosyl)-6-fluoropyridoxol 15: 0.32 g, 95% syrup, R_f 0.35 (3:2 cyclohexane/EtOAc). NMR (CDCl_3) δ_{H} 7.41 (5H, m, Ar-H), 5.36 (1H, d, $J_{1',2'} = 8.2$ Hz, H-1'), 5.41 (1H, d, $J_{1'',2''} = 8.2$ Hz, H-1''), 5.14 (2H, dd, $J_{2',3'} = J_{2'',3''} = 7.4$ Hz, H-2' and H-2''), 4.45 (2H, dd, $J_{3',4'} = J_{3'',4''} = 3.3$ Hz, H-3' and H-3''), 4.84 (2H, dd, $J_{4',5'} = J_{4'',5''} = 3.8$ Hz, H-4' and H-4''), 3.96 (2H, m, H-5' and H-5''), 4.80 (2H, dd, $J_{5',6a'} = J_{5'',6a''} = 2.6$ Hz, $J_{6a',6b'} = J_{6a'',6b''} = 10.1$ Hz, H-6a' and H-6a''), 4.10 (2H, dd, $J_{5',6b'} = J_{5'',6b''} = 3.0$ Hz, H-6b' and H-6b''), 4.94 (2H, s, PhCH_2), 4.55 (1H, d, $J_{\text{CH}_2-4a, \text{CH}_2-4b} = 10.4$ Hz, CH_2 -4a), 4.48 (1H, d, $J_{\text{CH}_2-4a, \text{CH}_2-4b} = 10.4$ Hz, CH_2 -4b), 4.60 (1H, d, $J_{\text{CH}_2-5a, \text{CH}_2-5b} = 11.0$ Hz, CH_2 -5a), 4.52 (1H, d, $J_{\text{CH}_2-5a, \text{CH}_2-5b} = 11.0$ Hz, CH_2 -5b), 2.37 (3H, s, CH_3 -2), 2.00, 1.99, 1.98, 1.97, 1.96, 1.95, 1.94, 1.93 (24H, 8s, 8 CH_3CO). δ_{C} 170.84, 170.76, 170.31, 170.29, 170.26, 169.95, 169.92, 169.84 (8 CH_3CO), 152.18 (d, $^3J_{\text{F-C}} = 14.5$ Hz, Py-C₂), 142.64 (d, $^4J_{\text{F-C}} = 4.6$ Hz, Py-C₃), 150.12 (d, $^3J_{\text{F-C}} = 3.8$ Hz, Py-C₄), 116.20 (d, $^2J_{\text{F-C}} = 32.0$ Hz, Py-C₅), 157.40 (d, $^1J_{\text{F-C}} = 234.3$ Hz, Py-C₆), 136.37, 129.00, 128.94, 128.87, 128.16, 127.77 (Ph-C), 100.23 (s, C-1'), 100.41 (s, C-1''), 71.41 (s, C-2' and C-2''), 72.08 (s, C-3'), 72.19 (s, C-3''), 68.34 (s, C-4'), 68.51 (s, C-4''), 72.86 (s, C-5'), 72.93 (s, C-5''),

61.86 (s, C-6'), 61.98 (s, C-6''), 60.98 (s, CH₂-4), 61.28 (s, CH₂-5), 20.88, 20.85, 20.82, 20.75, 20.73, 20.60, 20.59, 20.58 (8s, 8 CH₃CO), 19.43 (s, CH₃-3). ESI-MS *m/z* 937 [M⁺] (35%), 938 [M + 1] (25%). Anal. Calcd for C₄₃H₅₂NO₂₁F: C, 55.05, H, 5.59, N, 1.49. Found: C, 55.03, H, 5.57, N, 1.48.

3-O-Benzyl- α^4,α^5 -di-O-(2,3,4,6-tetra-O-acetyl- α -D-mannopyranosyl)-6-fluoropyridoxol 16: 0.30 g, 90%, syrup, *R_f* 0.40 (3:2 cyclohexane/EtOAc). NMR (CDCl₃) δ _H 7.38 (5H, m, Ar-H), 5.38 (1H, d, *J*_{1',2'} = 2.6 Hz, H-1'), 5.41 (1H, d, *J*_{1'',2''} = 2.6 Hz, H-1''), 5.36~3.95 (18H, m, H-2', 3', 4', 5', 6', 2'', 3'', 4'', 5'', 6'', PhCH₂, CH₂-4, and CH₂-5), 2.38 (3H, s, CH₃-2), 2.02, 2.00, 1.99, 1.98, 1.97, 1.96, 1.95, 1.94 (24H, 8s, 8 CH₃CO). δ _C 171.25, 171.18, 170.89, 170.85, 170.78, 170.66, 170.60, 170.48 (8 CH₃CO), 153.28 (d, ³*J*_{F-C} = 15.8 Hz, Py-C₂), 145.48 (d, ⁴*J*_{F-C} = 4.8 Hz, Py-C₃), 150.16 (d, ³*J*_{F-C} = 3.8 Hz, Py-C₄), 116.30 (d, ²*J*_{F-C} = 31.0 Hz, Py-C₅), 157.77 (d, ¹*J*_{F-C} = 206.8 Hz, Py-C₆), 98.42 (s, C-1'), 100.03 (s, C-1''), 72.60~56.54 (13C, C-2', 3', 4', 5', 6', 2'', 3'', 4'', 5'', 6'', PhCH₂, CH₂-4, and CH₂-5), 21.23, 20.94, 20.92, 20.90, 20.88, 20.86, 20.84, 20.80, 20.78 (8s, 8 CH₃CO), 18.37 (s, CH₃-3). ESI-MS *m/z* 937 [M⁺] (32%), 938 [M + 1] (20%). Anal. Calcd for C₄₃H₅₂NO₂₁F: C, 55.05, H, 5.59, N, 1.49. Found: C, 55.01, H, 5.55, N, 1.45.

α^4,α^5 -Di-O-(2,3,4,6-tetra-O-acetyl- β -D-glucopyranosyl)-6-fluoropyridoxol 17 and α^4,α^5 -Di-O-(2,3,4,6-tetra-O-acetyl- α -D-mannopyranosyl)-6-fluoropyridoxol 18. A mixture of **15** or **16** (0.29 g, 0.30 mmol) and Pd-C (5%, 50 mg) in MeOH (40 mL) was stirred for 24 h at RT under H₂ (25 psi). Evaporated filtrate gave **17** and **18** in quantitative yields.

α^4,α^5 -Di-O-(2,3,4,6-tetra-O-acetyl- β -D-glucopyranosyl)-6-fluoropyridoxol 17: 0.26 g, syrup, *R_f* 0.28 (1:3 cyclohexane/EtOAc). NMR (CDCl₃) δ _H 7.33 (1H, s, HO-3, exchangeable with D₂O), 5.30 (1H, d, *J*_{1',2'} = 8.4 Hz, H-1'), 5.35 (1H, d, *J*_{1'',2''} = 8.4 Hz, H-1''), 5.09 (2H, dd, *J*_{2',3'} = *J*_{2'',3''} = 7.6 Hz, H-2' and H-2''), 4.35 (2H, dd, *J*_{3',4'} = *J*_{3'',4''} = 3.4 Hz, H-3' and H-3''), 4.80 (2H, dd, *J*_{4',5'} = *J*_{4'',5''} = 3.6 Hz, H-4' and H-4''), 3.89 (2H, m, H-5' and H-5''), 4.77 (2H, dd, *J*_{5',6a'} = *J*_{5'',6a''} = 2.4 Hz, *J*_{6a',6b'} = *J*_{6a'',6b''} = 10.6 Hz, H-6a' and H-6a''), 4.05 (2H, dd, *J*_{5',6b'} = *J*_{5'',6b''} = 3.2 Hz, H-6b' and H-6b''), 4.51 (1H, d, *J*_{CH2-4a,CH2-4b} = 10.3 Hz, CH₂-4a), 4.45 (1H, d, *J*_{CH2-4a,CH2-4b} = 10.3 Hz, CH₂-4b), 4.57 (1H, d, *J*_{CH2-5a,CH2-5b} = 11.1 Hz, CH₂-5a), 4.49 (1H, d, *J*_{CH2-5a,CH2-5b} = 11.1 Hz, CH₂-5b), 2.35 (3H, s, CH₃-2), 1.99, 1.98, 1.97, 1.96, 1.95, 1.94, 1.93, 1.91 (24H, 8s, 8 CH₃CO). δ _C 170.82, 170.78, 170.65, 170.58, 170.46, 169.85, 169.82, 169.80 (8 CH₃CO), 152.28 (d, ³*J*_{F-C} = 14.2 Hz, Py-C₂), 148.28 (d, ⁴*J*_{F-C} = 3.2 Hz, Py-C₃), 142.69 (d, ³*J*_{F-C} = 4.8 Hz, Py-C₄), 116.26 (d, ²*J*_{F-C} = 32.2 Hz, Py-C₅), 157.56 (d, ¹*J*_{F-C} = 231.4 Hz, Py-C₆), 100.35 (s, C-1'), 100.54 (s, C-1''), 71.37 (s, C-2' and C-2''), 72.18 (s, C-3'), 72.29 (s, C-3''), 68.38 (s, C-4'), 68.56 (s, C-4''), 72.83 (s, C-5'), 72.88 (s, C-5''), 61.82 (s, C-6'), 61.89 (s, C-6''), 60.90 (s, CH₂-4), 61.19 (s, CH₂-5), 20.85, 20.83, 20.82, 20.80, 20.78, 20.76, 20.73, 20.65 (8s, 8 CH₃CO), 19.32 (s, CH₃-3). ESI-MS *m/z* 847 [M⁺] (30%), 848 [M + 1] (21%). Anal. Calcd for C₃₆H₄₆NO₂₁F: C, 50.99, H, 5.47, N, 1.65. Found: C, 50.96, H, 5.45, N, 1.62.

α^4,α^5 -Di-O-(2,3,4,6-tetra-O-acetyl- α -D-mannopyranosyl)-6-fluoropyridoxol 18: 0.26 g, syrup, *R_f* 0.27 (1:3 cyclohexane/EtOAc). NMR (CDCl₃) δ _H 7.33 (1H, s, HO-3, exchangeable with D₂O), 5.33 (1H, d, *J*_{1',2'} = 2.7 Hz, H-1'), 5.37 (1H, d, *J*_{1'',2''} = 2.7 Hz, H-1''), 5.45~4.07 (16H, m, H-2', 3', 4', 5', 6', 2'', 3'', 4'', 5'', 6'', CH₂-4, and CH₂-5), 2.35 (3H, s, CH₃-2), 2.01, 2.00, 1.99, 1.98, 1.97, 1.96, 1.95, 1.94 (24H, 8s, 8 CH₃CO); δ _C: 171.33, 171.21, 170.85, 170.83, 170.76, 170.61, 170.56, 170.53 (8 CH₃CO), 153.67 (d, ³*J*_{F-C} = 15.8 Hz, Py-C₂), 149.08 (d, ⁴*J*_{F-C} = 3.0 Hz, Py-C₃), 145.68 (d, ³*J*_{F-C} = 4.6 Hz, Py-C₄), 118.23 (d, ²*J*_{F-C} = 31.2 Hz, Py-C₅), 157.59 (d, ¹*J*_{F-C} = 223.1 Hz, Py-C₆), 98.67 (s, C-1'), 100.33 (s, C-1''), 72.8~56.56 (12C, C-2', 3', 4', 5', 6', 2'', 3'', 4'', 5'', 6'', CH₂-4, and CH₂-5), 20.99, 20.97, 20.93, 20.90, 20.88, 20.86, 20.84, 20.80 (8s, 8 CH₃CO), 18.45 (s, CH₃-3). ESI-MS *m/z* 847 [M⁺] (25%), 848 [M + 1] (18%). Anal. Calcd for C₃₆H₄₆NO₂₁F: C, 50.99, H, 5.47, N, 1.65. Found: C, 50.97, H, 5.44, N, 1.63.

Acknowledgment. This work was supported by grants from the DOD Breast Cancer Initiative IDEA award, DAMD17-03-1-0343, and the Cancer Imaging Program, NIH P20 CA 86354 (pre-ICMIC). NMR experiments were conducted at the Mary Nell and Ralph B. Rogers NMR Center, an NIH BTRP facility P41-RR02584. We thank Dr. Li Liu for preparing the breast cancer cells.

References

- (1) Pocsí, I.; Taylor, S. A.; Richardson, A. C.; Smith, B. V.; Price, R. G. Comparison of several new chromogenic galactosides as substrates for various β -D-galactosidases. *Biochim. Biophys. Acta* **1993**, *1163*, 54–60.
- (2) Heuermann, K.; Cosgrove, J. S-Gal: an autoclavable dye for color selection of cloned DNA inserts. *BioTechniques* **2001**, *30*, 1142–1147.
- (3) Buller, C. J.; Zang, X. P.; Howard, E. W.; Pento, J. T. Measurement of beta-galactosidase tissue levels in a tumor cell xenograft model. *Methods Find. Exp. Clin. Pharmacol.* **2003**, *25*, 713–716.
- (4) Tung, C. H.; Zeng, Q.; Shah, K.; Kim, D. E.; Schellingerhout, D.; Weissleder, R. In vivo imaging of β -galactosidase activity using far red fluorescent switch. *Cancer Res.* **2004**, *64*, 1579–1583.
- (5) Lee, K. H.; Byun, S. S.; Choi, J. H.; Paik, J. Y.; Choe, Y. S.; Kim, B. T. Targeting of *lacZ* reporter gene expression with radiiodine-labeled phenylethyl- β -D-thiogalactopyranoside. *Eur. J. Nucl. Med. Mol. Imaging* **2004**, *31*, 433–438.
- (6) Louie, A. Y.; Huber, M. M.; Ahrens, E. T.; Rothbacher, U.; Moats, R.; Jacobs, R. E.; Fraser, S. E.; Meade, T. J. In vivo visualization of gene expression using magnetic resonance imaging. *Nat. Biotechnol.* **2000**, *18*, 321–325.
- (7) Cui, W.; Otten, P.; Li, Y.; Koeneman, K.; Yu, J.; Mason, R. P. A novel NMR approach to assessing gene transfection: 4-fluoro-2-nitrophenyl- β -D-galactopyranoside as a prototype reporter molecule for β -galactosidase. *Magn. Reson. Med.* **2004**, *51*, 616–620.
- (8) Yu, J. X.; Ma, Z.; Li, Y.; Koeneman, K. S.; Liu, L.; Mason, R. P. Synthesis and Evaluation of a Novel Gene Reporter Molecule: Detection of β -galactosidase activity Using ¹⁹F NMR of a Fluorinated Vitamin B6 conjugate. *Med. Chem.* **2005**, *1*, 255–262.
- (9) Yu, J. X.; Otten, P.; Ma, Z.; Cui, W.; Liu, L.; Mason, R. P. A Novel NMR Platform for Detecting Gene Transfection: Synthesis and Evaluation of Fluorinated Phenyl β -D-Galactosides with Potential Application for Assessing *lacZ* Gene Expression. *Bioconjugate Chem.* **2004**, *15*, 1334–1341.
- (10) Yu, J. X.; Kodibagkar, V.; Cui, W.; Mason, R. P. ¹⁹F: a versatile reporter for noninvasive physiology and pharmacology using magnetic resonance. *Curr. Med. Chem.* **2005**, *12*, 818–848.
- (11) Yu, J. X.; Liu, L.; Kodibagkar, V. D.; Cui, W.; Mason, R. P. Synthesis and Evaluation of Novel Enhanced Gene Reporter Molecules: Detection of β -Galactosidase Activity Using ¹⁹F NMR of Trifluoromethylated Aryl β -D-Galactopyranosides. *Bioorg. Med. Chem.* **2006**, *14*, 326–333.
- (12) Kodibagkar, V.; Yu, J.; Liu, L.; Brown, B.; Hetherington, H. P.; Gerard, R. D.; Mason, R. P. ¹⁹F CSI of gene-reporter molecule OFPNPG. ISMRM 13th Scientific Meeting, Miami Beach, FL, 2005.
- (13) He, S.; Mason, R. P.; Hunjan, S.; Mehta, V. D.; Arora, V.; Katipally, R.; Kulkarni, P. V.; Antich, P. P. Development of Novel ¹⁹F NMR pH Indicators: Synthesis and Evaluation of a Series of Fluorinated Vitamin B6 Analogues. *Bioorg. Med. Chem.* **1998**, *6*, 1631–1639.
- (14) Rye, C. S.; Withers, S. G. *Curr. Opin. Chem. Biol.* **2000**, *4*, 573–580.
- (15) Sinnott, M. L. Catalytic mechanism of enzymic glycosyl transfer. *Chem. Rev.* **1990**, *90*, 1171–1202.
- (16) Pauling, L. *The nature of the chemical bond*; Cornell University Press: Ithaca, NY, 1980.
- (17) McCarter, J. D.; Adam, M. J.; Withers, S. G. Binding energy and catalysis. Fluorinated and deoxygenated glycosides as mechanistic probes of *Escherichia coli* (*lacZ*) β -galactosidase. *Biochem. J.* **1992**, *286*, 721–727.
- (18) Street, I. P.; Armstrong, C. R.; Withers, S. G. Hydrogen bonding and specificity. Fluorodeoxy sugars as probes of hydrogen bonding in the glycogen phosphorylase–glucose complex. *Biochemistry* **1986**, *25*, 6021–6027.
- (19) Withers, S. G. 1998 Hoffmann la Roche Award Lecture – Understanding and exploiting glycosidases. *Can. J. Chem.* **1999**, *77*, 1–11.
- (20) Thoden, J. B.; Hegeman, A. D.; Wesenberg, G.; Chapeau, M. C.; Frey, P. A.; Holden, H. M. Structural analysis of UDP-sugar binding to UDP-galactose 4-epimerase from *Escherichia coli*. *Biochemistry* **1997**, *36*, 6294–6304.
- (21) White, A.; Tull, D.; Johns, K.; Withers, S. G.; Rose, D. R. Crystallographic observation of a covalent catalytic intermediate in a β -glycosidase. *Nat. Struct. Biol.* **1996**, *3*, 149–154.

- (22) Mason, R. P. Transmembrane pH gradients in vivo: measurements using fluorinated vitamin B6 derivatives. *Curr. Med. Chem.* **1999**, *6*, 481–499.
- (23) Lemieux, R. U. In *Methods in Carbohydrates Chemistry, Vol. II*; Whistler, R. L., Wolfrom, M. L., Eds.; Academic Press Inc.: London, 1963; pp 223–230.
- (24) Mehta, V. D.; Kulkarni, P. V.; Mason, R. P.; Constantinescu, A.; Aravind, S.; Goomer, N.; Antich, P. P. 6-Fluoropyridoxol: a novel probe of cellular pH using ^{19}F NMR spectroscopy. *FEBS Lett.* **1994**, *349*, 234–238.

JM051049O

Imaging β -galactosidase activity using ^{19}F chemical shift imaging of LacZ gene-reporter molecule 2-fluoro-4-nitrophenol- β -D-galactopyranoside

Vikram D. Kodibagkar^a, Jianxin Yu^a, Li Liu^a, Hoby P. Hetherington^b, Ralph P. Mason^{a,*}

^aDepartment of Radiology, University of Texas Southwestern Medical Center at Dallas, Dallas, TX 75390-9058, USA

^bDepartment of Radiology, Albert Einstein College of Medicine, Bronx, NY 10461, USA

Received 8 January 2006; accepted 8 April 2006

Abstract

2-Fluoro-4-nitrophenol- β -D-galactopyranoside (OFPNPG) belongs to a novel class of NMR active molecules (fluoroaryl- β -D-galactopyranosides), which are highly responsive to the action of β -galactosidase (β -gal). OFPNPG has a single ^{19}F peak (–55 ppm relative to aqueous sodium trifluoroacetate). Upon cleavage by β -gal, the pH sensitive aglycone 2-fluoro-4-nitrophenol (OFPNP) is observed at a chemical shift of –59 to –61 ppm. The chemical shift response is sufficient to observe β -gal activity using chemical shift imaging (CSI). ^{19}F CSI studies of enzyme activity and *lacZ* gene expression in 9L-glioma and MCF7 breast cancer cells are presented, providing further evidence for the utility of OFPNPG as a gene-reporter molecule for future in vivo studies.

© 2006 Elsevier Inc. All rights reserved.

Keywords: β -Galactosidase; ^{19}F NMR; CSI; *lacZ* gene reporter; Breast cancer; Phenylgalactopyranosides

1. Introduction

Although gene therapy has great potential for the treatment of diverse diseases, its widespread implementation is hindered by difficulties in assessing the success of transfection in terms of spatial extent, gene expression, and longevity of expression. Strategies for identifying exogenous gene activity have been presented using radio-nuclide imaging [1,2], optical imaging [3,4] and NMR [5,6].

β -Galactosidase (β -gal), the product of the *lacZ* gene, was the first expression system to be identified and characterized some 50 years ago, and it has become a fundamental tool in molecular biology as a reporter gene. Diverse colorimetric substrates have been developed suitable for in vitro or histological assays of β -gal [7]. More recently, Louie et al. [8] presented a proton MRI contrast agent, Tung et al. [9] used a near infrared active substrate and Lee et al. [10] reported a radioiodinated substrate to detect the activity of β -gal. An alternate strategy uses ^{19}F -labeled molecules as NMR active substrates, thus

exploiting the high NMR visibility of fluorine, the great NMR sensitivity of ^{19}F to the environmental milieu and the lack of background signal [11]. We have recently demonstrated the feasibility of using ^{19}F NMR to detect chemical shift changes accompanying β -gal-induced cleavage of the prototype reporter molecule, 2-nitro-4-fluorophenyl β -D-galactopyranoside (PFONPG) [12].

2-Fluoro-4-nitrophenyl- β -D-galactopyranoside (OFPNPG) is an isomer of PFONPG, which is highly responsive to the action of β -gal enzyme [13]. The molecule is stable in solution and with respect to wild-type cells, but β -gal causes rapid liberation of the aglycone 2-fluoro-4-nitrophenol (OFPNP), which has a pH-dependent ^{19}F NMR chemical shift, 4–6 ppm upfield from OFPNPG. We have chosen to develop imaging approaches using OFPNPG rather than PFONPG, since the aglycone appears to be less toxic and the pK_a is outside the normal physiological range. We now present ^{19}F NMR chemical shift imaging (CSI) studies of the conversion of OFPNPG to OFPNP β -gal enzyme in solution and *lacZ* transfected cancer cells lines.

2. Experimental

Human MCF7 breast cancer cells were stably transfected with recombinant vector *phCMV/lacZ* using

Presented in part at the 13th annual meeting of the International Society of Magnetic Resonance in Medicine, Miami, 2005.

* Corresponding author. Tel.: +1 214 648 8926; fax: +1 214 648 4538.

E-mail address: ralph.mason@utsouthwestern.edu (R.P. Mason).

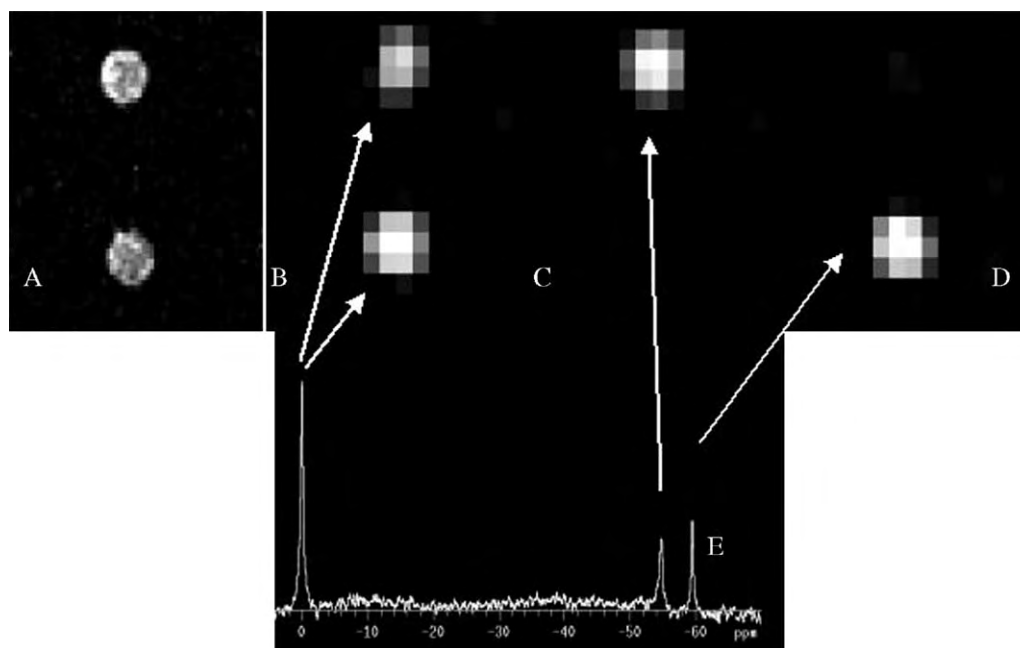


Fig. 1. ^{19}F CSI of OFPNPG and OFPNP. Two vials containing Na-TFA (75 mM) and OFPNPG (70 mM) or OFPNP (70 mM), respectively, were imaged by CSI: (A) spin echo proton scout image, ^{19}F CSI images of (B) Na-TFA, (C) OFPNPG and (D) OFPNP. (E) The corresponding bulk spectrum (with 30 Hz line broadening).

GenePORTER2 (Gene Therapy Systems), inserting the *E. coli lacZ* gene (from pSV- β -gal vector, Promega) under control of the high expression human cytomegalovirus (CMV) immediate-early enhancer/promoter vector phCMV (Gene Therapy Systems). Clonal selection was applied to identify those MCF-7 cells with the highest β -gal expression and these were grown in culture dishes under standard conditions and harvested [14]. 9L-Glioma cells stably

transfected to express lacZ were kindly provided by Dr. Steven Brown (Henry Ford Hospital, Detroit, MI, USA). Imaging experiments used a Varian INOVA Unity 4.7-T system (188.2 MHz for ^{19}F) with a standard 2D spin echo CSI sequence to image the conversion of OFPNPG to OFPNP. MRI parameters were as follows: field of view = 30×30 mm, spectral window = 70 ppm, slice thickness = 10 mm, matrix = 16×16 , TR/TE = 1000/12 ms. Chemical shift imaging data were reconstructed and analyzed with homebuilt programs written using the MATLAB programming language. Sodium trifluoroacetate (Na-TFA) (10 mg/ml) was used as internal standard. OFPNPG was dissolved in phosphate buffered saline (PBS) to yield a 70 mM solution, which was used in all experiments. For CSI studies with

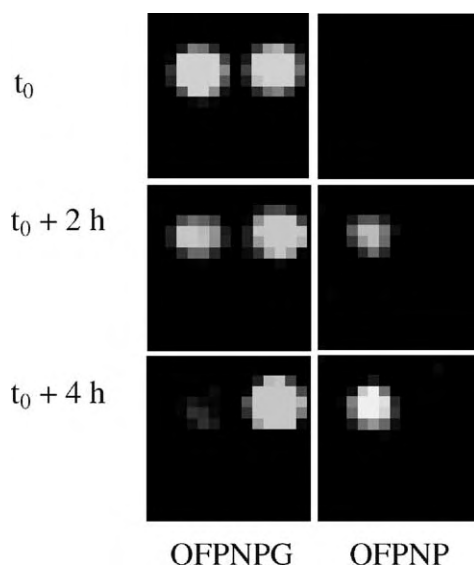


Fig. 2. Conversion of OFPNPG to OFPNP by β -gal enzyme. Two vials contained OFPNPG (70 mM). Upon addition of β -gal to the left vial, the intensity of OFPNPG signal was found to decrease, while that of OFPNP increased (right panel). Each image was acquired in $4\frac{1}{2}$ min.

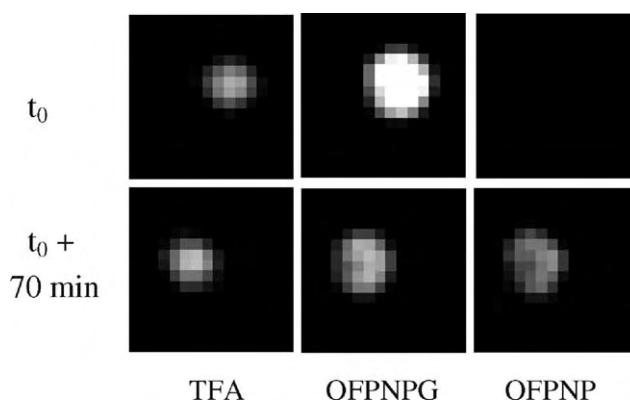


Fig. 3. Conversion of OFPNPG to OFPNP by 9L-lacZ rat glioma cells. 10^8 cells were added to a vial containing OFPNPG (70mM) and imaged. ^{19}F CSI revealed the conversion of OFPNPG to OFPNP over 70 min.

β -gal enzyme, a PBS solution of β -gal (180 μ l, G-2513, 0.22 unit/ μ l, Aldrich Chemical) was added to an aliquot of this solution and ^{19}F CSI data were acquired over 4 h at the ambient magnet bore temperature (18°C). For CSI studies with tumor cells, 10^8 9L-lacZ or 10^7 MCF7-lacZ cells were added to the solution of OFPNPG and imaged every 10 min over 70 min or 4 h, respectively. These samples were maintained at 37°C in a water bath between measurements.

3. Results

OFPNPG and OFPNP were easily distinguishable using ^{19}F CSI, as shown for two vials containing solutions of OFPNPG and OFPNP, respectively, with Na-TFA as internal chemical shift reference (Fig. 1). The conversion of OFPNPG to OFPNP by β -gal enzyme is shown in Fig. 2. Following addition of 80 U of β -gal enzyme to the left vial, conversion was detected by decrease in OFPNPG image intensity, which was accompanied by an increase in OFPNP image intensity. The OFPNPG intensity in the right vial (control) remained constant. Fig. 3 shows the conversion of OFPNPG to OFPNP by lacZ transfected rat 9L-glioma cells. Adding 10^8 9L-lacZ cells to a 70 mM solution of OFPNPG resulted in $\sim 40\%$ conversion to OFPNP over 70 min. Similar results were obtained with MCF-7-LacZ human breast cancer cells (Fig. 4). Over 4 h, 10^7 cells converted $\sim 40\%$ of OFPNPG to OFPNP.

4. Discussion

We previously demonstrated that OFPNPG and its analogues could be used to detect β -gal activity by NMR spectroscopy and identified OFPNPG as the best gene reporter molecule [13]. We now present a method to image β -gal activity in solution or in stably transfected cancer cells using ^{19}F CSI of OFPNPG. ^{19}F NMR provides a large chemical shift response to small changes in molecular structure or microenvironment [11]. Upon cleavage by β -gal, the substrate forms the aglycone OFPNP, which is shifted upfield by 4–6 ppm depending on pH [13]. Release of the pH-sensitive aglycones also suggests a novel approach to measuring pH at the site of enzyme activity. Rate of conversion in the presence of the enzyme found here was slower than our previous data since sample temperature was lower, in this case 18°C. The slower rate of conversion for the human breast cancer MCF7 cells compared to the glioma cells was due to lower cell number (by a factor of 10).

Although ^{19}F has a 100% natural abundance, signal/noise is of concern for any exogenously administered agent for in vivo imaging studies. We used a saturated solution of OFPNPG in PBS, but a further increase in solubility is possible by using aqueous DMSO. Trifluoromethyl analogues also provide a higher signal/noise, although the chemical shift response is much smaller

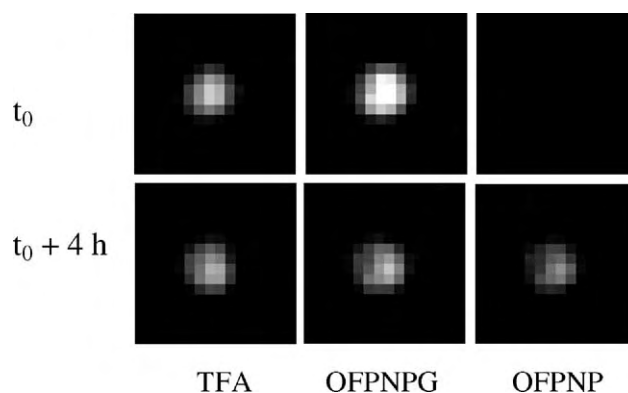


Fig. 4. Conversion of OFPNPG to OFPNP by MCF7-LacZ breast cancer cells detected using CSI. 10^7 cells were added to a vial containing OFPNPG (70 mM) and imaged over a period of 4 h.

($\Delta\delta = 1.5$ ppm) and may preclude effective imaging in vivo [14]. Other aglycones may also be introduced and we have shown that 6-fluoropyridoxol may be a less toxic substitute for nitrophenols [15]. OFPNPG specifically detected β -gal activity, but we note that ^{19}F NMR chemical shift response has been used by others to detect enzyme activity particularly with respect to pro-drug activation associated with gene-directed enzyme prodrug therapy. Others have examined fluorinated mustard drugs released by activity of glucuronidase [16] and carboxypeptidase G2 [17] and conversion of 5-fluorocytosine to 5-fluorouracil [6]. A major goal of our work was to seek minimally toxic gene reporter substrates and products, but we note that broad spectrum toxicity of nitrophenols could be applied to develop β -gal-activated chemotherapy using agents such as PFONPG.

We believe that noninvasive in vivo detection of gene reporter molecules will become increasingly important in biomedicine and it will be important to have diverse agents, genes and modalities for specific applications. Fluorophenyl β -D-galactosides offer a novel approach for determining β -gal activity. Key advantages of NMR reporters over radiolabeled substrates are the long shelf life, absence of radioactivity and the ability to distinguish between substrate and product. However, NMR does generally require millimolar reporter molecule concentrations, as opposed to micromolar (or lower) needed for optical and radionuclide approaches. The choice of appropriate probe and imaging modality depends critically on the nature of the problem at hand and an NMR approach could be suitable for many applications.

Acknowledgments

Supported in part by DOD Breast Cancer Initiative BC022001 DAMD17-03-1-0343 and the Cancer Imaging Program, NCI Pre-ICMIC P20 CA086354. NMR experiments were conducted at the Mary Nell and Ralph B. Rogers NMR Center, an NIH BTRP facility #P41-

RR02584. The glioma cells were a kind gift by Dr. Stephen Brown from the laboratory of Dr. Jae Ho Kim (Henry Ford Health System, Detroit, MI, USA).

References

- [1] Haberkorn U, Mier W, Eisenhut M. Scintigraphic imaging of gene expression and gene transfer. *Curr Med Chem* 2005;12:779–94.
- [2] Gambhir SS, Herschman HR, Cherry SR, Barrio JR, Satyamurthy N, Toyokuni T, et al. Imaging transgene expression with radionuclide imaging technologies [Review]. *Neoplasia (New York)* 2000;118–38.
- [3] Contag CH, Ross BD. It's not just about anatomy: in vivo bioluminescence imaging as an eyepiece into biology. *J Magn Reson Imaging* 2002;16:378–87.
- [4] Hoffman RM. Visualization of GFP-expressing tumors and metastasis in vivo. *Biotechniques* 2001;30:1016–22, 1024–6.
- [5] Ichikawa T, Hogemann D, Saeki Y, Tyminski E, Terada K, Weissleder R, et al. MRI of transgene expression: correlation to therapeutic gene expression. *Neoplasia (New York)* 2002;6:523–30.
- [6] Stegman LD, Rehemtulla A, Beattie B, Kievit E, Lawrence TS, Blasberg RG, et al. Noninvasive quantitation of cytosine deaminase transgene expression in human tumor xenografts with in vivo magnetic resonance spectroscopy. *Proc Natl Acad Sci U S A* 1999;96:9821–6.
- [7] Poci I, Taylor SA, Richardson AC, Smith BV, Price RG. Comparison of several new chromogenic galactosides as substrates for various β -D-galactosidases. *Biochim Biophys Acta* 1993;1163:54–60.
- [8] Louie AY, Huber MM, Ahrens ET, Rothbacher U, Moats R, Jacobs RE, et al. In vivo visualization of gene expression using magnetic resonance imaging. *Nat Biotechnol* 2000;18(3):321–5.
- [9] Tung CH, Zeng Q, Shah K, Kim DE, Schellingerhout D, Weissleder R. In vivo imaging of β -galactosidase activity using far red fluorescent switch. *Cancer Res* 2004;64(5):1579–83.
- [10] Lee KH, Byun SS, Choi JH, Paik JY, Choe YS, Kim BT. Targeting of lacZ reporter gene expression with radioiodine-labelled phenylethyl- β -D-thiogalactopyranoside. *Eur J Nucl Med Mol Imaging* 2004;31(3):433–8.
- [11] Yu JX, Kodibagkar VD, Cui W, Mason RP. ^{19}F : a versatile reporter for non-invasive physiology and pharmacology using magnetic resonance. *Curr Med Chem* 2005;12(7):819–48.
- [12] Cui W, Otten P, Li Y, Koeneman KS, Yu J, Mason RP. Novel NMR approach to assessing gene transfection: 4-fluoro-2-nitrophenyl- β -D-galactopyranoside as a prototype reporter molecule for β -galactosidase. *Magn Reson Med* 2004;51(3):616–20.
- [13] Yu J, Otten P, Ma Z, Cui W, Liu L, Mason RP. Novel NMR platform for detecting gene transfection: synthesis and evaluation of fluorinated phenyl β -D-galactosides with potential application for assessing LacZ gene expression. *Bioconjug Chem* 2004;15(6):1334–41.
- [14] Yu J, Liu L, Kodibagkar VD, Cui W, Mason RP. Synthesis and evaluation of novel enhanced gene reporter molecules: detection of β -galactosidase activity using ^{19}F NMR of trifluoromethylated aryl β -D-galactopyranosides. *Bioorg Med Chem* 2005;326–33.
- [15] Yu J, Ma Z, Li Y, Koeneman KS, Liu L, Mason RP. Synthesis and evaluation of a novel gene reporter molecule: detection of β -galactosidase activity using ^{19}F NMR of a fluorinated vitamin B₆ conjugate. *Med Chem* 2005;1(3):255–62.
- [16] Schmidt F, Monneret C. In vitro fluorine-19 nuclear magnetic resonance study of the liberation of antitumor nitrogen mustard from prodrugs. *J Chem Soc-Perkin Trans* 2002;1(10):1302–8.
- [17] Davies LC, Friedlos F, Hedley D, Martin J, Ogilvie LM, Scanlon IJ, et al. Novel fluorinated prodrugs for activation by carboxypeptidase G2 showing good in vivo antitumor activity in gene-directed enzyme prodrug therapy. *J Med Chem* 2005;48(16):5321–8.

**Non-invasive physiology and pharmacology
using ^{19}F magnetic resonance**

Jian-xin Yu, Weina Cui, Dawen Zhao, and Ralph P. Mason*

Laboratory of Prognostic Radiology, Department of Radiology,

The University of Texas Southwestern Medical Center at Dallas, Texas

* Author for correspondence.

Ralph P. Mason, Ph.D., CSci., C.Chem.

Department of Radiology

The University of Texas Southwestern Medical Center at Dallas

5323 Harry Hines Blvd,

Dallas, Texas 75390-9058

USA

Tel: USA (214)-648-8926, Fax: USA (214)-648-2991,

E-mail: Ralph.Mason@UTSouthwestern.edu.

Other authors Jian-xin.Yu@UTSouthwestern.edu; Weina.Cui@UTSouthwestern.edu;
Dawen.Zhao@UTSouthwestern.edu

Running title: ^{19}F NMR Reporter Molecules

Keywords: oxygen, pH, gene reporter, β -galactosidase, metal ions, 5FU, FDG, anesthetics

Abstract

^{19}F provides a powerful tool for nuclear magnetic resonance investigations. It has been widely exploited for both spectroscopic studies and increasingly for magnetic resonance imaging (MRI). The ^{19}F atom has high NMR sensitivity, while there is essentially no background signal in the body. Many diverse reporter molecules have been designed, which exploit the unique sensitivity of the fluorine atom to its microenvironment and these cover such diverse aspects as pO_2 , pH, metal ion concentrations (e.g., calcium, magnesium), gene reporter molecules, hypoxia reporters, vascular flow, and volume. There are also numerous drugs in clinical use (e.g., the cancer chemotherapeutics 5-fluorouracil and gemcitabine, anesthetics and psychoactive drugs such as fluoxetine) and agrochemicals, which include a fluorine atom. This review examines the properties of the fluorine atom that make it an ideal tool for NMR, consider the many properties that are available for interrogation and examine applications. NMR is a particularly flexible technology, since it can provide information through multiple parameters including chemical shift, relaxation processes (R_1 and R_2), scalar coupling, and chemical exchange. Moreover, fluorine NMR has a very large chemical shift range (~ 300 ppm) allowing multiple agents to be examined simultaneously.

1 Introduction

Magnetic resonance imaging has become the technology of choice for radiology and detection of many diseases. Today, clinical MRI uses almost exclusively the proton nucleus of the hydrogen atom, which occurs naturally in tissue water. Thus, there is a particularly strong signal, which is sensitive to tissue status and provides exquisite indications of soft tissue anatomy. Increasingly, the development of specific contrast agents and selective pulse sequences allows more detailed analysis of tissue properties such as diffusion, flow, and changes in vascular oxygenation [1, 2]. Much information may also be obtained from metabolites; however, these typically occur at millimolar concentrations (or less) requiring prodigious water suppression [3]. Heteronuclei can provide metabolic tracers and physiological reporters while avoiding the intense water and lipid signals. The ^{19}F atom has sensitivity of the order of 80% of that of proton, but there is essentially no endogenous signal from tissues. Most of the fluorine in the body is in the form of solid state fluoride ions, which give very broad lines, essentially undetectable using standard NMR equipment. There are also a few fluorine containing molecules that occur in nature, but these are almost exclusively in plants, are highly toxic, and thought to be part of inherent defense mechanisms [4]. Thus, any molecular fluorine introduced into the body in the form of reporter molecules or drugs is readily detected with high sensitivity.

The importance of fluorine in the Life Sciences continues to be recognized in journals such as the *Journal of Fluorine Chemistry*, reviews in regular journals devoted to technology, and the current series *Advances in Fluorine Science*. Many reviews beginning in the 1980s were devoted to fluorine NMR with seminal work from Thomas,

Selinsky and Burt, Prior, and London [5-8]. More recently, Mason reviewed the use of perfluorocarbons for measuring tissue oxygenation [9, 10] and fluorinated derivatives of vitamin B6 as probes of pH *in vivo* [11]. McSheehy *et al.* [12] discussed applications of fluorine NMR to oncology, Menon [13] examined fluorinated anesthetics, and Passe *et al.* [14] reviewed neuropsychiatric applications. Several reviews have concerned the pharmacokinetics of fluoropyrimidine drugs based on fluorine NMR including notable contributions from Bachert, Martino, and Wolf [15-17], and indeed, Wolf *et al.* contribute the succeeding article in this volume. Use of fluorine NMR to investigate physiology and pharmacology from an organic chemical perspective was the focus of a review by us [18]. Given the continuing appearance of novel applications in the field and developing interest in fluorine NMR, this current article will provide both a historical perspective and review state of the art. Readers are also directed to many relevant reviews that consider pharmacology, organic chemistry, or synthetic methods relating to fluorine [19-30]. Examples, include recent reviews from Jescke [26] on the unique role of fluorine in the design of active ingredients for modern crop protection, Dolbier, a review of fluorine chemistry at the millennium [21], Shimizu and Hiyama [24] examining modern synthetic methods for fluorine substituted target molecules, Isanbor and O'Hagan [28], reviewing fluorinated anti-cancer agents, Jäckel and Koksche [23], on fluorine in peptide design approaching engineering and Plenio, on the coordination chemistry of fluorine in fluorocarbons [25].

1.1 Context and perspective

In many disciplines, investigators have a deep understanding of their own specialty, but lack perspective of competing technologies. Historically, NMR investigators were physicists, who could develop sophisticated pulse sequences to manipulate nuclear spins, or radiofrequency engineers specialized in wave propagation and coil design. Alternatively, NMR investigators were chemists who could design new reporter molecules and assess metabolic processes. Today, the field is far more diverse. Beyond the integration of multiple disciplines into NMR, increasingly, there is recognition that often no single technology will optimally solve a problem, but multidisciplinary teams need to understand the strengths and weakness of diverse technologies and exploit multiple modalities. This review will promote the virtues and unique capabilities of ^{19}F NMR, but it is important to recognize competing technologies. In the United States increased emphasis on multimodality imaging and cross disciplinary research is now driven by the formation of the National Institute for Biomedical Imaging and Bioengineering (NIBIB) [31] and Cancer Imaging Program (CIP) of the NCI [32]. Moreover, new learned societies are dedicated to imaging in general, e.g., SMI-Society of Molecular Imaging [33], as opposed to being devoted to a specific modality (e.g., ISMRM-International Society of Magnetic Resonance in Medicine [34] or Society of Nuclear Medicine [35]) and many journals have published issues reviewing diverse imaging methods [36-39].

Proton MRI has the great advantage of using spin physics to interrogate tissue water revealing anatomy and pathophysiology based on cellular and tissue properties. Nonetheless, it is often enhanced by the introduction of paramagnetic contrast agents at micro molar concentrations. Fluorine MRI typically requires millimolar concentrations of

reporter molecules. In this respect, radionuclide and optical imaging techniques can offer far superior sensitivity, potentially with pico to nanomolar requirements. Fluorescence imaging is becoming more attractive with the commercial availability of many labeling kits [40] and new instrumentation, which allows spectral deconvolution [41]. However, fluorescence imaging can suffer from signal quenching and is generally a two dimensional technique. Recently, 3D fluorescence is becoming feasible in small animals [42, 43]. Nanoparticles (quantum dots) offer particularly high sensitivity although current generations would be inappropriate for human application, since they use highly toxic elements, such as cadmium and mercury [44]. Fluorescent proteins can also be generated *in situ*- cellular transfection can generate green fluorescence protein or longer wavelength proteins [45]. Alternatively, cells may be transfected with a bioluminescent imaging (BLI) reporter such as luciferase, which emits light upon interaction with luciferin substrate [38, 46]. Again, this is becoming feasible in three dimensions in small animals [47]. Generally, optical imaging technologies can use relatively cheap instrumentation.

Radionuclide imaging has similar sensitivity to optical imaging and is routinely used for studies of biodistribution, planar γ -scintigraphy, positron emission tomography (PET) and single photon emission computed tomography (SPECT) [48, 49]. A major drawback with radionuclides is the limited shelf life of substrates, which may either decay (short half life) or be subject to long-term radiolysis. Radioactivity also poses specific safety issues during production, reagent preparation, and ultimate disposal. Nonetheless, several PET and SPECT agents are in routine clinical use (*e.g.*, FDG, Prostascint, ^{99m}Tc [50-52]). Other materials are effective for tracing the

pharmacokinetics of labeled substrates. A major problem is ensuring that the label remains part of the molecule, since radioactivity provides no molecular characterization and unless specific analytical techniques such as HPLC are applied, only experience can indicate whether metabolic transformation has occurred

Ultrasound and x-ray imaging are routine in the clinic and examine endogenous molecules based on signal reflection and/or absorption. These are starting to find application in small animal research [53]. Currently, they provide primarily anatomical information, although addition of contrast agents promises new applications [54].

Relatively, ^{19}F NMR has multiple strengths and virtues as described in the following sections. Briefly, fluorine containing molecules tend to be metabolically stable and have indefinite shelf-life. The fluorine nucleus offers sufficient sensitivity for imaging, but also provides a very large chemical shift range immediately revealing metabolic transformations and allowing multiple molecules to be observed and identified simultaneously with potential applications to metabolomics. Fluorine MRI is readily combined with anatomical proton MRI providing high spatial resolution anatomy.

1.2 ^{19}F as an *in vivo* NMR probe

^{19}F is 100% naturally abundant and the only stable isotope of fluorine. The nucleus has a nuclear spin $I=1/2$ and a gyromagnetic ratio of 40.05 MHz/T, providing a sensitivity ~83% that of protons. The high gyromagnetic ratio generally allows the use of existing proton NMR instrumentation with the minimum of component adjustments. NMR has multiple strengths and virtues. Modern NMR instrumentation can be user friendly allowing a well-trained technician to undertake studies. However, NMR is

intrinsically a complex tool providing potentially a multitude of information based on diverse parameters including signal intensity (SI), chemical shift (δ), and changes of chemical shift ($\Delta\delta$). In addition, signals are characterized by the transverse dephasing rate ($R_2^* = 1/T_2^*$), spin-spin or transverse relaxation rate ($R_2 = 1/T_2$) and spin-lattice or longitudinal relaxation rate ($R_1 = 1/T_1$). Indeed, each of these parameters have been exploited for specific ^{19}F NMR reporter molecules (Table 1). With care, the NMR signal can be quantitative, so that the integral (area under the peak) of a signal is directly proportional to the amount of material being interrogated. However, NMR may be considered relatively insensitive compared with some other modalities. Typically, millimolar concentrations are required to achieve a good signal in a reasonable amount of time. The precise detection sensitivity is governed by numerous parameters including the volume of interrogation, the required spatial resolution, and relaxation properties of the molecule and its tendency to accumulate or disperse from a region of interest. Perhaps, most important is the temporal resolution since signals may be averaged over many hours. Increasingly there are attempts to target fluorinated agents to accumulate at a site of interest, e.g., using specific antibodies [55, 56] and low-molecular weight ligands [57].

The simplest concept of NMR is that of chemical shift. In this context, ^{19}F is exceptionally sensitive to molecular and microenvironmental changes. Fluorine NMR has a chemical shift range of ~ 300 ppm, as opposed to ~ 10 ppm for proton. Multiple different fluorinated agents may readily be detected simultaneously with minimal danger of signal overlap. To allow comparison between data from different molecules and different investigators chemical shifts must be referred to a standard. The IUPAC ^{19}F

NMR chemical shift standard is fluorotrichloromethane (CFCl_3) [58]. Using this agent, the range of chemical shifts of most organic fluorinated compounds is 0 ppm to -250 ppm. However, this volatile solvent is not convenient for most biomedical applications and thus, secondary standards are usually preferred. We favor sodium trifluoroacetate ($\text{CF}_3\text{CO}_2\text{Na}$ or NaTFA). This has the advantage of being readily available, quite non-toxic and may be used as either an external, or indeed, internal chemical shift standard in biological investigations. It should be noted that fluorine chemical shifts can be strongly solvent dependent and vary with dilution [59]. Fluorine may ultimately be described on a ϕ scale, extrapolated to infinite dilution, under which conditions $\text{CF}_3\text{CO}_2\text{H}$ is quoted as -76.530 ppm. For precise measurements, it may be critical for both the chemical shift standard and molecule of investigation to be under precisely the same conditions (necessitating an internal standard). External standards, e.g., in glass capillaries, may be subject to small susceptibility effects causing errors in estimation of absolute chemical shift. However, they provide more reliable quantitation standards for signal intensity. Chemical shift is the mainstay of detecting and classifying molecules and detecting and identifying metabolic products of agents. While there have been many theoretical exercises on fluorine chemical shift it can often be quite unpredictable and occurs across an exceptionally large range. In 1971 Emsley and Phillips [60] published a 520 page review of the theory relating to ^{19}F NMR chemical shifts followed by a 673 page compilation of coupling constants [61].

Scalar coupling constants of fluorine are typically much larger than proton. For geminal fluorine atoms $^2J_{\text{FF}}$ may be in the range of 200 – 800 Hz, while $^3J_{\text{FF}}$ is often less than 1 Hz, yet $^4J_{\text{FF}}$ may reach 20 Hz: such non-monotonicity can be confusing and

large long range couplings ${}^6\text{ or }{}^7J_{\text{FF}}$ are also encountered [18, 59, 61, 62]. Proton fluorine coupling constants are ${}^2J_{\text{FH}} \sim 45\text{-}90\text{ Hz}$ and ${}^3J_{\text{FH}} 0\text{-}53\text{ Hz}$. While fluorine carbon coupling is typically large (${}^1J_{\text{CF}} > 200\text{ Hz}$), it is generally not observed unless the carbon is enriched with ${}^{13}\text{C}$. However, as a corollary, fluorine coupling is observed clearly and extensively in ${}^{13}\text{C}$ NMR spectra. To avoid complexity of fluorine fluorine coupling, it may be important to include fluorine as a symmetrical moiety, e.g., a trifluoromethyl group, as opposed to asymmetric geminal fluorine atoms or a single fluorine atom. Likewise, a CF_3 moiety will generally avoid fluorine-hydrogen couplings. Since ${}^{19}\text{F}$ NMR is often detected by retuning a proton channel, proton decoupling may not be available.

Representative drugs, which include fluorine atoms and for which *in vivo* NMR has been reported are shown in Figure 1 [17, 63-73]. Furthermore, many drugs in early pre-clinical testing include fluorine atoms: the prevalence of fluorine atoms may reach 20% of all candidate agents [19]. Introduction of fluorine requires care. While the carbon fluorine bond is particularly strong, any release of fluoride or metabolites such as mono- or di-fluoroacetate can lead to exceedingly toxic products. For reporter molecules or pharmacological drugs, it is clearly important to minimize inadvertent toxicity. In this respect, the trifluoromethyl (CF_3) group is particularly suitable, since it resists degradation and for NMR avoids fluorine fluorine couplings. In pharmaceuticals and agrochemicals fluorine occurs in many forms ranging from a single fluorine atom to as many as six or nine identical fluorines (Table 2). In terms of NMR detection, the more equivalent fluorines, the stronger the signal. However, fluorine will modulate the properties of a molecule, since the fluorine atom is exceedingly electro-negative and the CF bond strongly polarized. While the van der Waals radius of a fluorine atom is quite

similar to a proton, the electronegativity alters electronic configuration modulating pKa. For the series of acetic acids $\text{pKa}(\text{CH}_3\text{CO}_2\text{H}) = 4.76$, $\text{pKa}(\text{CH}_2\text{FCO}_2\text{H}) = 2.59$, $\text{pKa}(\text{CHF}_2\text{CO}_2\text{H}) = 1.24$ and $\text{pKa}(\text{CF}_3\text{CO}_2\text{H}) = 0.23$ [19]. Similar changes have been reported for a series of fluoromethyl alanines (Table 3) [74]. The trifluoromethyl group is often considered to be equivalent to the introduction of an isopropyl group. Fluorine not only perturbs the electronic structure of a molecule, but also alters the hydrophobicity [75]. Indeed, in many cases, particularly for agrochemicals, fluorine is specifically added to reduce the water solubility of molecules, so they are retained more effectively on the waxy cuticle of plants [26]. Fluorine modifies lipophilicity and ability to cross membranes, such as the blood brain barrier, which is pertinent to the extensive applications in anesthetics and psychiatric drugs [76].

Fluorine chemistry has made major progress over the last 10 - 15 years and now many reagents are available for derivatization [24]. However, many require quite severe conditions using such materials as hydrogen fluoride [77], various metal halides such as SeF_4 [78], WF_6 [79], XeF_2 [80], and SbF_5 [81], or fluorine itself [82]. In some cases, a fluorine moiety may be introduced with S-ethyl trifluoroacetate (SETFA) [83] or trifluoroacetic anhydride [84]. It is often preferable to use a starting material that already includes a fluorine or multiple fluorine atoms, which may be introduced using relatively mild conditions, as explored extensively in the generation of fluorinated peptides [23].

While only a single isotope of fluorine is available for NMR, fluorine is finding increasing use as ^{18}F for positron emission tomography (PET; see other articles in this volume). While ^{18}F has a limited half life ($t_{1/2} = 110$ minutes), it has found major application in the detection of tumors including Medicare reimbursed studies with

fluorodeoxyglucose within the last five years. There is active interest in the pursuit of other ^{18}F agents to detect parameters such as hypoxia or mitosis [85-90]. The greatest strength of PET is that it may use nano to femtomolar concentrations, as opposed to the milli to micromolar concentrations required for NMR. However, ^{18}F simply provides a count of molecular concentration, *i.e.*, detecting radioactive decay with no indication of multiple substrates or metabolites. Thus, it may require rigorous HPLC or other analyses to strictly determine the fate of a drug. Meanwhile, ^{19}F can allow the detection of multiple agents, and metabolites simultaneously based on chemical shift. ^{19}F is indefinitely stable and the lack of radioactivity provides not only a long shelf life, but minimizes any issues of disposal of hazardous waste. Moreover, any fluorine MRI detection is readily correlated with the exquisite anatomy provided by routine proton MRI.

NMR is a particularly facile approach to analysis requiring minimal sample preparation: mixtures, turbid media, and organisms including biopsy specimens or living plants and animals or even patients may be examined directly. Feasibility is governed by sample volume and the need for appropriate magnetic resonance systems and RF coils [91, 92]. For small specimens (< 1 ml) magnetic fields exceed 22 tesla (950 MHz proton) and routine analysis is available at and above 7 T. These high field systems usually use vertical narrow bore magnets which can accommodate small samples of solutions (analytical and in vitro investigations) and sometimes mice. Small animal studies are most commonly performed in horizontal bore systems at 4.7 T, but increasingly systems are available at 7 and 9.4 T. Humans are now routinely studied at

3 T with research systems up to 12 T. Figure 1 shows representative drugs, which have been studied by ^{19}F NMR in clinical trials.

Proton NMR is potentially more versatile, since protons are essentially ubiquitous. However, this also provides a major drawback – crowded signals across limited chemical shift dispersion. Moreover, the water component of tissues can approach 70% water leading to signals approaching 80M, as compared with mM metabolites. Elegant water suppression methods have evolved over the years, but often obliterate extended spectral windows around water or are limited to specific molecular structures exhibiting multi quantum detectability [93-95]. Lipid signals may also interfere with detection. Samples may be subjected to D_2O exchange, but this is perturbing. Deuterium enrichment is feasible providing up to 6,400 fold amplification [96], but the gyromagnetic ratio (γ) is much lower reducing ultimate sensitivity. Carbon is also ubiquitous in biological systems, but only 1.1% is NMR active as ^{13}C . This does provide the opportunity for selective isotopic enrichment and has proven fruitful for many studies [97], though ^{13}C can be expensive. Again, the gyromagnetic ratio is relatively low, precluding effective clinical studies at low fields.

The virtues of ^{19}F have led to the design and use of many reporter molecules in pre-clinical investigations (Table 1 and Figure 1b). Since, there are few naturally occurring compounds containing fluorine, fluorinated molecules do not have to compete with background signal. Fluorine does occur extensively in bones and teeth, but the solid matrix causes very short T_2 values providing exceedingly broad signals, which can either be removed by deconvolution or electronic timing. Indeed, special rapid electronics are required for detecting solid state ^{19}F [98]. The spin lattice relaxation time

T_1 can be quite long, but efficient use of rapid pulsing at the Ernst angle can accelerate spectral acquisition [99]. For aqueous solutions, relaxation agents, such as Gd-DTPA, can be added to accelerate relaxation [100-102], and indeed, this has been used to identify cellular compartmentation based on the ability of the contrast agent to relax extracellular material, but not intracellular [103]. Data acquisition efficiency can also be enhanced by interleaving or acquiring simultaneously ^1H and ^{19}F NMR providing both anatomical and pharmacological/physiological data simultaneously [91, 92, 104, 105]. T_1 relaxation is extensively exploited with perfluorocarbons to measure $p\text{O}_2$, as described in detail in section 3.1.1.

A few natural organofluorine compounds exist, most notably in plants (Figure 1c). These are generally noted for their toxicity; most importantly fluoroacetate enters the tricarboxylic acid (TCA) cycle and as fluorocitrate inhibits cis-aconitase [4, 106, 107]. Of course, toxicity provides an opportunity to generate specific poisons and fluoroacetate is widely used as a rodenticide providing opportunities for NMR [108]. ^{19}F NMR has been used for extensive studies of body fluids such as milk and urine with respect to xenobiotica [109-115].

Fluorine is increasingly used in industrial products ranging from fluoropolymers (e.g., Teflon) and liquid crystal components to anesthetics (e.g., isoflurane) to refrigerants and fire suppressants (halocarbons), numerous agrochemicals and several medicines [21, 22, 26, 28]. While application of fluoro molecules will lead to increasingly crowded spectra, the large chemical shift range ensures that multiple molecules may be detected simultaneously. For example, in a study to investigate influence of tumor pH, on the anti-cancer drug 5FU in rat breast tumors, four molecules were detectable

simultaneously (Figure 2, the drug 5FU at -93.6 ppm, the extra cellular pH reporter CF₃POL at -16.69 ppm, a chemical shift standard NaTFA (0 ppm) and two signals for the gaseous veterinary anesthetic isoflurane (-5.1, -10.99 ppm)). As noted above, we favor NaTFA as an internal standard for biological investigation, as compared with the IUPAC standard (CFCI₃). In principle, the NaTFA was unnecessary here, since the isoflurane signals could have served as a secondary standard. However, it is important to note that the signals from anesthetics tend to have very short T_2^* [116-118], and thus, while they are visible in this pulse-acquire spectrum, they will tend to be “lost” in spin echo investigations, such as CSI (chemical shift imaging). While ¹⁹F NMR investigations can generally be performed using existing ¹H equipment, some care is required, since probe and RF components may include fluorinated material which can give rise to spurious signals [119].

In the following sections this review will separately consider industrial pharmacological and agro-chemical agents (Section 2) followed by active (Section 3) and passive (Section 4) reporter molecules. Active reporter molecules may further be differentiated as those based on physical interaction with a substrate (Section 3.1) or those that undergo a chemical reaction (Section 3.2).

2. ¹⁹F NMR for pharmacology

Fluorine is often added to modulate biological activity of pharmaceuticals. Numerous reports describe changes in pKa [74, 75] (see also Table 3), lipophilicity [19, 26, 75], retention, resistance to degradation [22], enhanced binding [19, 120] induced by selective incorporation of F atom or atoms. In other cases, F atoms have been used to

probe molecular interactions or binding sites in order to enhance drug design, even if fluorine is ultimately not included in the drugs. It has been recognized that ^{19}F chemical shift is not only highly dependant on molecular structure and ionization, but also on the microenvironment. In early work, Dwek [121] and Gerig [122] reported the use of F moieties to probe interactions of oxy- and deoxy-hemoglobin with co-factors such as diphosphoglycerate (DPG) under differential protonation [123]. Trifluoroacetylated chitotriose and N-trifluoroacetylglucosamine were used to probe active sites in lysozyme [124]. Many fluoro sugars have been used to study enzyme specificity, substrates, or inhibitors of enzymes such as glycogen phosphorylase and glucosidases [125-127].

Essentially no background ^{19}F signal occurs and the sensitivity is sufficient to examine biological mixtures, e.g., body fluids such as urine, blood, or milk for fluorinated metabolites [109-115, 128, 129]. This is being used both by academic laboratories and pharmaceutical companies to examine the fate of xenobiotica. In some cases metabolites (degradation products or excretory bioconjugates) are derived from fluorine containing drugs: in other cases ^{19}F labels may be added for the ADME (Absorption, Distribution, Metabolism, and Excretion Toxicity) process to learn about pathways, even though the labels are not included in the ultimate pharmaceuticals. In several cases glucuronides have been identified as key detoxification products [130-132]

2.1 Cancer Chemotherapeutics

2.1.1 Fluoropyrimidines

With the significant developments in fluorination technology, inclusion of F atoms into pharmaceuticals and agrochemicals is becoming more feasible and popular [26,

28]. Fluorine can yield subtle, but significant changes in drug activity [19, 22, 28]. The F atom is generally considered to have a structural size between H and OH, while CF₃ is similar to an isopropyl group [75]. The strong electro-negativity can modulate electronic distributions influencing pKa, particularly in proximity to delocalized aromatic structures [19, 75]. F may be involved in hydrogen bonding altering binding and entry into enzyme pockets [23]. Many new industrial pharmaceuticals and agrochemicals incorporate a fluorine group providing a tool for NMR investigations. Figure 1 show drugs, which have been examined by ¹⁹F NMR in clinical or advanced pre-clinical studies, while Table 2 shows diverse molecules including pharmaceuticals and agrochemicals, which could be strong candidates for ¹⁹F NMR investigations, but for which reports are lacking in the public domain. Most studies to date have examined pharmacokinetics and metabolism of fluoropyrimidines, particularly 5-fluorouracil (5FU). 5FU was first developed in the 1950s and remains a primary drug in treatment of many cancers, but it has a narrow range of efficacy/toxicity [28, 63, 133]. Presumably, both response and toxicity are related to pharmacokinetics and there is interest in assessing dynamics of uptake, biodistribution, and metabolism. Patients with enhanced tumor retention of 5FU ("trappers") may be expected to exhibit better response [134]. Such trapping is apparently a requisite, though not in itself sufficient for efficacy [17].

Given the importance and prevalence of 5FU, over 200 studies have reported ¹⁹F NMR investigations in clinical trials and evaluation in animal models. Several detailed reviews consider metabolism, pharmacokinetics, and detectability of 5FU and its metabolites and the reader is referred to these [15-17, 63]. 5FU requires anabolic conversion to nucleosides (e.g., FdUrd, FdUmp) and nucleotides for cytostatic activity,

requiring the activity of various kinases and phosphorylases [17]. However, competing catabolic reactions convert 5FU to 5,6-dihydrofluorouracil (DHFU) and α -fluoro β -alanine (FBAL) in liver, in addition to several other molecules offering little toxicity [15, 17, 135]. FBAL is excreted by the kidneys. Localized NMR spectroscopy and low resolution CSI have examined pharmacokinetics [103, 136-138]. NMR of excised tissue and body fluids has also provided insight into metabolism and can provide much higher sensitivity (e.g., μ M). While studies *in vivo* are most attractive, studies of cultured cells can also provide important information.

The pharmacokinetics of 5FU are reported to be pH sensitive, and thus measurements of tumor pH may have prognostic value for drug efficacy. In tumors with lower pH the retention of 5FU is considerably enhanced [139-141]. This has prompted investigations of the ability to alter pharmacokinetics by modulation of tumor pH to increase activity, e.g., by breathing carbogen [142, 143]. 5FU, its metabolites, and fluorinated pH reporter molecules can all be detected simultaneously by ^{19}F NMR (Figure 2). Intriguingly, fluoronucleotides derived *in vivo* from 5FU exhibit sensitivity to changes in pH and could be used to measure intracellular pH (pHi), although the presence of a mixture of products may complicate interpretation [141, 144, 145].

Given the inherent dose-limiting toxicity of 5FU, various pro-drugs and mixture formulations have been developed (e.g., capecitabine (Xeloda), Tegafur-uracil (Uftoral®) emitefur (3-(3-(6-benzoyloxy-3-cyano-2-pyridyloxycarbonyl)benzoyl)-1-ethoxymethyl-5-fluorouracil)) and ^{19}F NMR has played a role in analysis and development [16, 63]. A new and potentially exciting application is assessment of pro-drug therapy in conjunction with gene therapy, specifically the use of cytosine

deaminase, to convert the relatively innocuous 5-fluorocytosine (5FC) to 5FU [146-150]. Several investigations have now reported ^{19}F NMR of the conversion of 5FC to 5FU based on the ^{19}F NMR chemical shift, $\Delta\delta = 2$ ppm [18, 147, 150, 151].

Gemcitabine (Gemzar[®]) is a newer anticancer drug with a more favorable toxicity profile than 5FU. It comprises both sugar and pyrimidine moieties. In cells, it is phosphorylated and incorporated into DNA and to a lesser extent RNA, where it can inhibit DNA polymerases. It can also inhibit thymidine synthase. Given the significant clinical results and successful combination with radiotherapy, there is interest in optimizing activity based on ^{19}F NMR. Unlike 5FU, fluorine is now on the deoxyribosyl ring and the two geminal fluorines give rise to an AB quartet at -42 ppm ($\delta_{\text{TFA}} = 0$ ppm). This has been detected in human tumor xenografts by ^{19}F NMR following IP injection and kinetics have been investigated with respect to vasoactive drugs [65, 152]. Metabolite signals have been observed in liver and bladder using CSI [153]. At low pH, the signals appear as an AB quartet, but they appear to collapse and broaden to a single signal at pH 8 (Figure 3).

2.1.2. Other anticancer drugs

McSheehy *et al.* [154] presented a preliminary report of a novel thymidine synthase inhibitor, ZD9331, where both parent and metabolite peaks were detected at 4.7 T. Brix *et al.* [155] evaluated a trifluoromethylated derivative of 3-aminobenzamide, an inhibitor of poly (ADP-ribo) polymerase1 (PARP-1), as a potential radio sensitizer in Dunning prostate rat tumors and using CSI, detected separate signals from liver, muscle and tumor revealing maximum tissue signals after two days. Spees *et al.* [156]

followed pharmacokinetics of fluorine labeled methotrexate in sensitive and resistant tumor xenografts in mice and found an inverse correlation between surviving fraction and area under the curve.

2.2 Other drugs

Recognizing the exquisite sensitivity of ^{19}F NMR to microenvironment, inclusion of fluorine atoms in libraries of ligands has been used to probe molecular interactions based on changes in line width and chemical shift [157-160].

Following cancer chemotherapeutics, most *in vivo* ^{19}F NMR has examined psychiatric agents [14, 161]. These can be particularly favorable when they incorporate a CF_3 moiety. Several reports investigated fluoxetine (Prozac) with studies ranging from biopsy tissue extracts to preclinical animal models and human volunteers [70, 71, 162]. The primary goal has been correlation of concentration with efficacy, *e.g.*, Henry *et al.* [70] explored the relative brain concentrations of R and S enantiomers versus a racemic mixture of fluoxetine in separate groups of patients. Other studies have examined fluvoxamine (a selective serotonin reuptake inhibitor – SSRI) to counter a possessive compulsive disorder [71, 163]. Dexfenfluramine has been observed at brain concentrations $< 10\ \mu\text{M}$ [72]. ^{19}F NMR of trifluoperazine revealed multiple metabolites in rat brain extracts, but these were too weak and unresolved *in vivo* at 4.7 T [164]. Such studies have provided a single unlocalized spectrum corresponding to whole brain volume and lines are generally quite broad (2 – 3 ppm). Sassa *et al.* [165] used ^{19}F chemical shift imaging to detect haloperidol decanoate in schizophrenic patients

Other studies have examined fluoroquinolone antibiotics (fleroxacin) [166], antimicrobials (sitafloracin) [66] non-steroidal anti-inflammatory (niflumic acid [67]), anti-histamines (tecastemizole [68]), However, the tecastemizole was only detected from three of 23 patients and the retention was found to be much shorter than the psychotropic drugs such as fluoxetine. Attempts to detect dexamethasone in the eye at 1.5 T failed [167]. Perfluorocarbons (PFCs) have been used as a tamponade in eye surgery and residual PFC has been detected in patients at 1.5 T [168, 169]. Indeed, this allowed pO_2 measurements based on spin lattice relaxation, as discussed in detail in Section 3.1.1.1. The perfluorocarbon emulsion synthetic blood substitute Fluosol was proposed as a method of modulating tumor oxygenation [170] and it could be detected from surrounding tissues as long as one year after administration and tumor resection [171]. Perfluorononane has been used to explore GI tract in man and mice at 1.5 T [69]. This may provide insight into GI function or serve as a model for all drug delivery.

Many gaseous anesthetics are fluorinated, *e.g.*, halothane, enflurane isoflurane, sevoflurane, and desflurane. NMR studies of fluorinated anesthetics form some of the earliest *in vivo* applications of ^{19}F NMR [172-174]. Issues regarding the use of anesthetics are site of anesthetic action, duration of residence in the brain and toxicity of metabolic byproducts. The results have been a source of debate and controversy. Wyrwicz and co-workers [175] addressed the issue of residence times of anesthetics in the brain and observed signals for prolonged durations after cessation of anesthesia. Global spectroscopy is straightforward, but anesthetics have a short transverse relaxation time (T_2^*) and signals may be lost in localized spectroscopy or imaging approaches. Very few clinical studies have reported ^{19}F NMR of anesthetics in the

brain, though Menon *et al.* [13] demonstrated the feasibility of such studies and found halothane signal up to 90 min after the withdrawal of anesthetic. Lockwood *et al.* [176] studied isoflurane kinetics and showed biphasic elimination with decay halftimes of 9.5 and 130 min. Selinsky *et al.* [177, 178] have studied the metabolism of volatile anesthetics showing generation of potentially toxic metabolites such as methoxydifluoroacetate, dichloroacetate, and fluoride ion from methoxyflurane.

The ability to detect drugs *in vivo* depends on multiple considerations. Obviously, the concentration at which drugs are administered is important together with the tendency to localize or clear from tissues. One would also expect multiple fluorine atoms to provide enhanced signal to noise over a single fluorine atom. Of course, they must be spectrally equivalent. Table 2 shows multiple diverse commercial molecules from the pharmaceutical and agrochemical fields, each of which has one or more fluorine atoms. Although no particular *in vivo* fluorine NMR has been reported, they are clearly prime candidates. Indeed ^{19}F NMR has been exploited to assess pesticides as contaminants in food [179]: in oils and wine levels > 1 mg/l, while in food extracts detection levels may approach parts per billion [180]. In particular, we note that some agents have multiple equivalent fluorine atoms. Flutamide [181] has a trifluoromethyl group and while there appear to be no references to *in vivo* NMR, ^{19}F NMR has been used to investigate drug formulation [181, 182]. Bistrifluoron has two trifluoromethyl groups, but they are spectrally non equivalent. By contrast, T009317 [183], has a hydroxyditrifluoromethylisopropyl group would be expected to give high NMR sensitivity.

To obtain detectable signals (spectra, or images) sufficient fluorinated probe must be administered, though the concentration of probe in studies of living organisms should

be as low as possible to avoid physiological perturbations or toxic side effects. For pharmaceuticals, fluorine labels are added for development, but their ultimate presence depends on optimal drug activity. By contrast for reporter molecules, the fluorine atom is the key to efficacy and design is optimized for NMR detectability.

3 Active reporter molecules

Many reporter molecules have been designed specifically to exploit fluorine chemical shift, coupling, or relaxation to reveal physiological parameters. Active agents typically fall into three categories; i) molecules which enjoy a physical interaction, *e.g.*, perfluorocarbons, which exhibit exceptional gas solubility and reveal oxygen tension based on modification of relaxation parameters (Section 3.1.1); ii) Ligands designed to trap/bind specific entities, such as ions, specifically, but reversibly, *e.g.*, H^+ (pH) (Section 3.1.2), metal ions (Ca^{2+} , Mg^{2+}) (Section 3.1.3); iii) molecules which undergo irreversible chemical interaction modifying their structure, as revealed by a change in chemical shift (Section 3.2). These are represented by gene reporter molecules (Section 3.2.3), where substrates are cleaved by specific enzyme activity, and hypoxia agents (Section 3.2.2), which are modified by reductases and trapped. There are also passive agents, which occupy and hence reveal a space, compartment, or volume, *e.g.*, tumor blood volume (Section 4).

3.1 Physical Interactions

3.1.1 In vivo oximetry

Oxygen is vital to the well being of normal mammalian tissues and deficits are associated with myocardial infarct, stroke, diabetic neuropathy, and cancer. In each case, lack of oxygen is associated with poor prognosis and a clinical goal is often to enhance tissue oxygenation. There is increasing evidence that hypoxia influences such critical characteristics as angiogenesis, tumor invasion and metastasis [184-187]. Moreover, it has long been appreciated that hypoxic tumor cells are more resistant to radiotherapy [188]. Given that hypoxic tumors are more resistant to certain therapies, it becomes important to assess tumor oxygenation as part of therapeutic planning [189]. Patients could be stratified according to baseline hypoxia to receive adjuvant interventions designed to modulate pO_2 , or more intense therapy as facilitated by Intensity Modulated Radiation Therapy (IMRT). Tumors, which do not respond to interventions, may be ideal candidates for hypoxia selective cytotoxins (e.g., tirapazamine [190]).

Thus, there is a vital need to be able to measure tissue pO_2 and many diverse technologies have been presented, as reviewed previously [10, 191, 192]. Some, such as near infrared spectroscopy and blood oxygen level dependent (BOLD) contrast MRI provide an indication of vascular oxygenation [2, 193, 194]. PET has been used to examine oxygen extraction fraction and hence metabolic activity based on uptake of $^{15}O_2$, but the half-life of oxygen-15 is exceedingly short ($t_{1/2} \sim 2$ mins) [195, 196]. Other modalities provide an indication of hypoxia [197, 198]. In many cases, there is a desire to measure pO_2 directly and this may be achieved using polarographic electrodes [199, 200], fiber optic probes [201], free radical probes with electron spin resonance (ESR) [191, 202] or perfluorocarbon (PFC) probes with NMR [9, 10], as described below.

3.1.1.1 Perfluorocarbon pO₂ reporters

NMR oximetry is based on the paramagnetic influence of dissolved oxygen on the ¹⁹F NMR spin lattice relaxation rate of a perfluorocarbon, as reviewed previously [10]. The solubility of gas, notably oxygen, in PFCs occurs as an ideal gas liquid mixture, and thus, R₁ varies linearly with pO₂, as predicted by Henry's Law [5, 10, 203]. R₁ is sensitive to temperature, and magnetic field, but importantly, R₁ of PFCs is essentially unresponsive to pH, CO₂, charged paramagnetic ions, mixing with blood, or emulsification [204-206] and for the PFC emulsion of perfluorotributylamine (Oxypherol), we have shown that calibration curves obtained in solution are valid *in vivo* [207]. At any given magnetic field (B₀) and temperature (T)

$$R_1 = A + B \cdot pO_2, \quad [1]$$

where A is the anoxic relaxation rate, and B represents the sensitivity of the reporter molecule to the paramagnetic contribution of oxygen and the ratio $\eta = B/A$ has been proposed as a sensitivity index [208]. Several PFCs have been used successfully for NMR oximetry and characteristics are summarized in Table 4. A particular PFC molecule may have multiple ¹⁹F NMR resonances, and each resonance has a characteristic R₁ response to pO₂ and temperature [9, 62]. Many PFCs (*e.g.*, perfluorotributylamine (PFTB), perflubron (often referred to as perfluorooctylbromide; PFOB), and TheroxTM (F44-E)) have several ¹⁹F NMR resonances, which can be exploited to provide additional information in spectroscopic studies, but complicate effective imaging [209-211]. PFCs with a single resonance provide optimal signal to noise ratio (SNR) and simplify imaging: two agents hexafluorobenzene (HFB) [10] [36,

200, 212-217], and perfluoro-15-crown-5-ether (15C5) [218-221] have found extensive use. While most pO_2 investigations have exploited the R_1 sensitivity, R_2 is also sensitive as reported by Girard *et al.* [222]

R_1 is sensitive to temperature and even a relatively small error in temperature estimate can introduce a sizable discrepancy into the apparent pO_2 based on some PFCs. The relative error introduced into a pO_2 determination by a 1 °C error in temperature estimate ranges from 8 torr/°C for perfluorotributylamine [207], to 3 torr/°C for PFOB (perflubron) [223] or 15-Crown-5-ether [218], when pO_2 is actually 5 torr. HFB exhibits remarkable lack of temperature dependence and the comparative error would be 0.1 torr/°C [224]. Recognizing differential sensitivity of pairs of resonances within a single molecule to pO_2 and temperature Mason, *et al.* [207, 225] patented a method to simultaneously determine both parameters by solving simultaneous equations. However, generally it is preferable for a pO_2 sensor to exhibit minimal response to temperature, since this is not always known precisely *in vivo* and temperature gradients may occur across tumors.

PFCs are extremely hydrophobic and do not dissolve in blood directly, but may be formulated as biocompatible emulsions for intravenous (IV) infusion. PFC emulsions have been developed commercially both as potential synthetic blood substitutes [226-229] and as ultrasound contrast agents [230, 231]. Following IV infusion, a typical blood substitute emulsion circulates in the vasculature with a half-life of 12 h providing substantial clearance within two days [227]. Some investigators have examined tissue vascular pO_2 , while PFC remained in the blood [206, 232-235]. Flow can generate artifacts and correction algorithms have been proposed [236, 237]. Primary clearance is

by macrophage activity leading to extensive accumulation in the liver, spleen, and bone marrow [238, 239]. This is ideal for investigating pO_2 in the liver or spleen, but a major shortcoming for other tissues, since animals may exhibit extensive hepatomegaly or splenomegaly though there is no apparent toxicity [227, 238, 240]. Long term retention in tissues allows pO_2 measurements to be made *in vivo* and extensive studies have been reported in liver, spleen, abscess, perfused heart, and tumors [5, 9, 62, 218, 241-254].

3.1.1.2 Myocardial oxygenation

Due to motion, the heart is a particularly complex organ for measuring pO_2 , yet understanding myocardial physiology with respect to infarcts has important implications for the clinical practice. Sponsored by the American Heart Association, we sought to develop a non-invasive approach for monitoring dynamic changes in myocardial oxygenation [243]. In Figures 4 and 5, we present a case study demonstrating the ability to evaluate dynamic changes in myocardial oxygenation. Following IV or IP administration of PFC, some becomes sequestered in heart tissue. This is detectable using a surface coil placed over the heart of an open-chest rabbit, but for proof of principle investigations, we examined excised crystalloid perfused Langendorff rat hearts [243]. To achieve effective ^{19}F NMR signal Sprague-Dawley rats were loaded with perfluorotributylamine (Oxypherol; 1 ml/100g/day) for nine days via tail vein injections. Hearts containing the sequestered PFC were excised and retrograde perfused by the Langendorff method at a pressure of 70 cm H_2O with modified Krebs-Henseleit buffer. A fluid-filled latex balloon was inserted into the left ventricle and

connected to a pressure transducer to monitor developed pressure. Total global ischemia (TGI) was induced by halting flow to the aorta *in situ*. Cardiac arrest was induced by increasing the KCl in the perfusate to 20 mM.

In the absence of spatial selection, a ^{19}F NMR signal of perfluorotributylamine could be obtained representing the whole heart in one pulse at 7 T using a volume coil [243]. Using a full T_1 relaxation sequence (e.g., Figure 4), precise pO_2 values could be obtained. Global R_1 measurements provided an accuracy of 20 – 40 mm Hg (torr) and showed significant differences in cardiac tissue before and during ischemia ($p < 0.001$) and before and during KCl-induced cardiac arrest ($p < 0.001$, Figure 4b). However, it was apparent that pO_2 changes occurred far more rapidly than could be assessed using a full T_1 curve. More rapid T_1 estimates are feasible using fewer recovery time delays on the relaxation curve, and indeed, a two-point comparison based on partial saturation allowed dynamic changes in pO_2 to be assessed with one-second time resolution [243]. While any individual pO_2 estimate is less precise, the dynamics are apparent (Figure 5). The decline in myocardial tissue pO_2 in KCl arrested hearts undergoing ischemia was four to eight times slower than that of the normally beating hearts. Following the onset of ischemia, there was close correlation ($R = 0.93$) between the decline of pO_2 and developed pressure (Figure 5e).

Global measurements related to total global ischemia have some value, but clinical infarction is more likely to generate regional ischemia requiring spatial resolution for useful models. We have undertaken ^{19}F MRI of arrested hearts with respect to regional ischemia induced by ligation of the lower anterior descending (LAD) artery and found spatial heterogeneity of hypoxia [246]. However, acquisition times for the images

were excessive (hours), so that monitoring pO_2 dynamics in the heart is restricted to pre-clinical studies. Use of a PFC with a single resonance could improve SNR and reduce imaging times. Targeting cardiac tissue directly could also improve SNR and this has been a goal of Wickline *et al.* [56].

3.1.1.3 Tumor oxygenation

The most extensive use of ^{19}F NMR oximetry has been to investigate tumor oxygenation with both acute studies of interventions and chronic studies of growth. Many investigations, including our own initial studies, used PFC emulsions to probe tumor oxygenation. Uptake and deposition of PFC emulsions in tumors is highly variable and heterogeneous with most signal occurring in well perfused regions [242, 254]. Indeed, pO_2 values measured soon after intravenous infusion, but following vascular clearance (typically 2 days), are generally high, approaching arterial pO_2 [242]. Thus, physiological measurements with respect to intervention are biased towards the well perfused well oxygenated regions, which are often less important than hypoxic regions. Interestingly, following sequestration, PFC does not seem to redistribute within tissue, but remains associated with specific locations. Figure 6 shows residual PFC in the center of a tumor 18 days after systemic administration of Oxypherol. This was found to be essentially hypoxic tissue. When fresh PFC emulsion was administered and allowed to clear for two days, the original signal was still clearly delineated in both shape, form and intensity. However, a new signal was detected around the tumor periphery indicating the newly well-perfused regions. Such long term tissue marking has been proposed as a form of non-invasive histology [255]. Long tissue retention has the

advantage of facilitating chronic studies during tumor development and progressive tumor hypoxiation has been observed over many days [242, 245].

To avoid the bias towards well-perfused regions and need to await vascular clearance, we developed an approach using direct intratumoral (IT) injection of neat PFC, which allows any region of interest in a tumor to be interrogated immediately [10]. Use of a fine needle ensures minimal tissue damage. Direct injection of neat PFC has been used by others to investigate retinal oxygenation [256-258] and cerebral oxygenation in the interstitial and ventricular spaces [221] and for the first time here, we show results in rat thigh muscle (Figure 7).

We have identified hexafluorobenzene (HFB) as an ideal reporter molecule [224]. Symmetry provides a single narrow ^{19}F NMR signal and the spin lattice relaxation rate is highly sensitive to changes in pO_2 , yet minimally responsive to temperature [224, 259, 260]. HFB also has a long spin spin relaxation time (T_2), which is particularly important for imaging investigations. HFB is well characterized in terms of lack of toxicity [261, 262], exhibiting no mutagenicity [263], teratogenicity or fetotoxicity [264] and the manufacturer's material data safety sheet indicates $\text{LD}_{50} > 25 \text{ g/kg}$ (oral- rat) and $\text{LC}_{50} 95 \text{ g/m}^3/2 \text{ hours}$ (inhalation-mouse). HFB had been proposed as a veterinary anesthetic and has been used in many species including ponies, sheep, cats, dogs, rats and mice, but was abandoned due to its flammability [265]. Flammability is not a problem for NMR oximetry, where small quantities of liquid (typically, $50 \mu\text{l}$) are injected directly into the tumor.

Initial studies used $10\text{-}20 \mu\text{l}$ HFB injected directly into the center or periphery of a tumor and pO_2 measurements indicated tumor heterogeneity [224, 266]. Although data

were acquired using non-localized spectroscopy, the highly localized signal ensured that regional pO_2 was measured. Subsequently, we developed an imaging approach: *FREDOM* (Fluorocarbon Relaxometry using Echo planar imaging for Dynamic Oxygen Mapping) [10], which typically provides 50 to 150 individual pO_2 measurements across a tumor simultaneously in about 6.5 mins with a precision of 1 to 3 torr in relatively hypoxic regions based on 50 μ l injected dose (Figure 7). In both muscle and tumor tissues, pO_2 heterogeneity is apparent when rats breathe air (pO_2 ranged from 0 to 100 torr). Upon challenge with oxygen breathing, essentially all muscle regions showed a significant increase in oxygenation. Many tumors show little response to hyperoxic gas, but the 13762 NF mammary tumor generally shows extensive response [217], as seen in Figure 7. We have used *FREDOM* to examine the effects of vascular targeting agents [36, 267], vasoactive agents [215] and hyperoxic gases [10, 200, 212-217, 268-270]. We have shown that measurements are consistent with sequential determinations made using electrodes [271, 272] and fiber optic probes (FOXYTM and OxyLite[®]) [201, 216]. Repeat measurements are highly reproducible and generally quite stable in tumors under baseline conditions. Results are also consistent with hypoxia estimates using the histological marker pimonidazole [212]. Most significantly, estimates of pO_2 and modulation of tumor hypoxia are found to be consistent with modified tumor response to irradiation [213, 273]. Such prognostic capability could be important in the clinic, since it is known that relatively hypoxic tumors tend to be more aggressive and respond less well to radiation therapy [274-276]. Hitherto, we have lacked a ^{19}F MRI capability in our human systems in Dallas. However, Philips is promoting dual ^{19}F MRI capabilities on

the new 3 T human systems [91, 277] and we expect to be able to pursue translation of the *FREEDOM* approach in the near future.

3.1.2 pH

pH is an important indicator of tissue health and acidosis may reflect ischemia and hypoxia. Historically, tumors were believed to be acidic (Warburg hypothesis) and the detection of neutral or basic environments by NMR led to initial controversy [278]. It was ultimately realized that ^{31}P NMR of endogenous inorganic phosphate (Pi) reflects primarily the cytosolic pH, which is often in the range 7.0 to 7.4, whereas tumor interstitial (pHe) may indeed be acidic, as previously observed using polarographic electrodes. This reversed pH gradient has important implications for partitioning of weak acid or base drugs, and thus, considerably effort has been applied to developing robust reporter molecules. ^{19}F NMR pH indicators (Table 3) represent three strategies: i) development of molecules specifically designed for ^{19}F NMR, ii) fluorinated analogues of existing fluorescent indicators, iii) exploitation of the ^{19}F NMR chemical shift sensitivity inherent in cytotoxic drugs. Many molecules exhibit chemical shift response to changes in pH, e.g., the ^{19}F NMR resonance of 6-fluoropyridoxol [11, 279]. On the NMR time scale, protonated and deprotonated moieties are generally in fast exchange, so that a single signal is observed representing the amplitude weighted mean of acid and base forms. pH is measured using the Henderson-Hasselbalch equation:

$$\text{pH} = \text{pK}_a + \log_{10} \left[\frac{\delta_{\text{obs}} - \delta_{\text{acid}}}{\delta_{\text{base}} - \delta_{\text{obs}}} \right] \quad [2]$$

where δ_{acid} is the limiting chemical shift in acid, δ_{base} is the limiting chemical shift in base, and δ_{obs} is the chemical shift observed at a given pH. Due to the non-linear form of the equation, greatest sensitivity is found close to the pKa.

Reporter molecules may readily access the interstitial compartment, but intracellular measurements are more difficult. Deutsch *et al.* [74, 280] championed the use of ^{19}F NMR to measure intracellular pH primarily based on the series of agents 3-monofluoro-, 3,3-difluoro-, and 3,3,3-trifluoro-2-amino-2-methyl propanoic acid (Table 3). pH sensitivity is predicated on protonation of the amino group and it is immediately apparent that additional fluorine atoms influence the pKa. These molecules have been successfully applied to pH measurements in cells [74, 281-283] and isolated organs [74, 284]. A significant problem is loading indicators into cells, but esters are relatively permeable, stable in water, and undergo non-specific enzymatic hydrolysis intracellularly, liberating the pH-sensitive molecules [280]. This approach can lead to complex spectra including overlapping multi-line ester and liberated free acid resonances from both intra- and extracellular compartments (Figure 8) [285]. Widespread use of these molecules has been hindered by the problem of loading the indicators into cells and the relatively small chemical shift range ~ 2 ppm. Difluoromethyl ornithine (DFMO) represents another ^{19}F NMR sensitive amino acid, which is also a therapeutic drug. Unfortunately, its chemical shift response is even smaller and the chemical response is not monotonic, going through a reversal above the pKa [286]. A large chemical shift range is important to ensure precise measurements of pH. When multiple cellular compartments are present there is less problem with signal overlap. Perhaps more importantly, any chemical shift perturbations due to other factors, such as

susceptibly become less important [287-289]. Furthermore, the pKa should be matched to the pH range of interest since the largest chemical shift response occurs close to the pKa [74].

Aromatic reporter molecules tend to have a much larger chemical shift pH response. Analogs of vitamin B6, e.g., 6-fluoropyridoxol (6-FPOL) are highly sensitive to pH [11, 279, 290-292]. We showed that 6-FPOL itself readily enters cells and provides well resolved resonances reporting both intra- and extracellular pH (pHi and pHe), simultaneously, in whole blood (Figure 9) [279] and the perfused rat heart [290]. Ease of entry into blood cells may be related to facilitated transport, since vitamin B6 is naturally stored, transported, and redistributed by erythrocytes [293]. Intriguingly, most tumors cells show a single resonance only, suggesting that 6-FPOL does not enter. The somewhat basic pKa = 8.2 is appropriate for investigations of cellular alkalosis, but it is not ideal for studies in the normal physiological range (6.5-7.5) [290].

Ring substitution allowed us to alter the pKa and 6-fluoropyridoxamine (6-FPAM) offered superior characteristics with pKa 7.05 [291]. As for 6-FPOL, we have observed intra- and extracellular signals in whole blood and perfused rat hearts [11, 291], and in addition, specific tumor cells (Morris hepatoma MH-Tk) showed uptake [18]. While modification of the 4-hydroxymethyl group to aminomethyl altered the pKa favorably, the 5-isomer was minimally changed (Table 3) [291].

Noting the large chemical shift response of pyridines, we also explored fluorophenols as pH indicators. Like 6-FPOL, *p*-fluorophenols show a large chemical shift response $\Delta\delta$ 6.4 to 11.3 ppm, whereas *o*-fluorophenols have a smaller chemical shift range (~ 0.3 to 2.2 ppm) (Table 3) [294]. For comparison both 6-FPOL and PFONP

(*p*-fluoro-*o*-nitrophenol) are shown to reveal pH gradients in whole blood giving comparable results and consistent with electrode measurements (Figure 9). Fluorophenols must be used cautiously, since PFONP appears cytolytic for certain tumor cells and may act as an ionophore, by analogy with dinitrophenol.

Other aromatic pH reporters have been presented including analogs of fluorescent pH indicators. FQuene, a ^{19}F NMR sensitive analog of the fluorescent pH indicator quene-1, was used to measure intracellular pH in a perfused heart [295] and liver [296]. *o*-methoxy-*N*-(2-carboxyisopropyl)-4-fluoroaniline has a chemical shift range ~ 17 ppm, but the pK_a (5.8) is less suitable for *in vivo* investigations. Modification to *N,N*-(methyl-2-carboxyisopropyl)-4-fluoroaniline [297] retained a substantial chemical shift range ($\Delta\delta$ 12 ppm) and produced a physiologically suitable pK_a (6.8), however, no biological studies have been reported. Meta fluoro isomers showed considerably smaller chemical shift response to changes in pH. *N*-ethylaminophenol (NEAP) has been described with various analogs to detect pH or metal ions [298].

To enhance SNR, or reduce the required dose, a pH sensitive CF_3 moiety could be introduced in place of the F-atom. Trifluoromethylphenols show titration response, though by comparison with the fluorophenols (Table 3) the chemical shift response is typically smaller $\Delta\delta = 1.25$ ppm (*p*- CF_3ArOH , pK_a 8.5) to 0.4 ppm (*o*- $\text{CF}_3\text{-Ar}$, pK_a 7.92), as expected since electronic sensing must be transmitted through an additional C-C bond [299]. Importantly, the ^{19}F NMR signal occurs downfield from NaTFA, so that unlike 6-FPOL there is no interference from isoflurane signals [18]. While FPOL and FPAM provide both intra- and extracellular signals with varying ratios depending on cell type, 6-trifluoromethylpyridoxol (CF_3POL) is found to occur exclusively in the extra

cellular compartment, and thus reports pHe, or interstitial pH [18, 300]. Frenzel *et al.* [301] have described a fluoroaniline sulfonamide (ZK 150471) and its use has been demonstrated in mice and rats to investigate tumor pH [302, 303]. This molecule is restricted to the extracellular compartment only [301, 304], but combination with ^{31}P NMR of P_i to determine pH_i has been used to reveal the transmembrane pH gradient in mouse tumors [141]. A distinct problem with ZK150471 is that the pK_a differs in saline and plasma [304]. Most indicators require an additional chemical shift reference standard, *e.g.*, sodium trifluoroacetate, but NEAP [298], 6-FPOL-5- α -CF₃ [291] and ZK150471 [301] all have non-titrating intramolecular chemical shift references. pH measurements using 2-amino- 3,3- difluoro-2-methyl propanoic acid is based on changes in the splitting of the AB quartet and this again avoids need for a chemical shift reference, but the splitting increases the complexity of the spectrum and reduces SNR (Figure 8).

3.1.3 Metal ions

Since metal ions play key roles in cellular physiological processes many specific reporter molecules have been developed, mostly as fluorescent indicators incorporating extended aromatic and conjugated structures, where the wavelength of fluorescence depends upon specific binding of a metal ion. Several ^{19}F NMR reporters have been created by addition of fluorine atoms (Table 5).

Tsien [305] made an important breakthrough by establishing an approach for loading fluorescent metal ion chelators into cells using acetoxymethyl esters. He demonstrated 1,2-bis(o-aminophenoxy)ethane-N,N,N',N'-tetraacetic acid (BAPTA) for

detecting intracellular calcium ions and subsequently Metcalfe, *et al.* [295] added para-fluoro atoms to the aromatic ring yielding a ^{19}F NMR responsive agent (5,5-difluoro-1,2-bis(o-aminophenoxy)ethane-N,N,N',N'-tetraacetic acid (5FBAPTA)) (Table 5). Upon binding calcium, there is a change in chemical shift (Figure 10).

Ideally, such a reporter molecule would have high specificity for the metal ion of interest. In fact, the F-BAPTA agents are found to bind several divalent metal ions, including Ca^{2+} , Zn^{2+} , Pb^{2+} , Fe^{2+} , and Mn^{2+} (Figure 10) [306, 307], but importantly, each metal ion chelate has an individual chemical shift, so that they can be detected simultaneously [308]. 5FBAPTA includes two fluorine atoms symmetrically placed to provide a single signal. Upon binding there is slow exchange of Ca^{2+} , on and off the indicator, on the NMR time scale, so that separate signals are seen for the free and metal ion bound moieties, with chemical shifts of several ppm. Measurements are based on the signal ratio, avoiding the need for a chemical shift reference, in contrast to pH reporters, which are usually in the fast exchange regimen. Calcium concentration may be calculated from the formula [308]

$$[\text{Ca}^{2+}] = K_D[\text{Ca-FBAPTA}]/[\text{FBAPTA}] \quad [3].$$

However, the dissociation constant (K_D) does depend on pH, ionic strength, and the concentration of free Mg^{2+} , which need to be estimated independently. 5FBAPTA has been used extensively [308] in studies of cells [306, 309, 310], and the perfused beating heart, revealing calcium transients during the myocardial cycle (Figure 11) [311-313]. Kirschenlohr *et al.* [313] reported that developed pressure in the perfused heart was reduced after addition of 5FBAPTA, but this could be reversed by including 50 μM ZnCl_2 in the perfusion medium.

In an effort to find an optimal reporter, isomers and derivatives were developed (Figure 10). 4FBAPTA has a somewhat lower binding constant $K_D = 0.7 \mu\text{M}$, but exhibits fast exchange [308], so that the signals from the bound and unbound forms are averaged, and it is the absolute chemical shift, which is related to the ratio of the two components (Figure 10).

Plenio and Diodone have also reported fluorocrown ethers (Table 5), which exhibit chemical shift response upon binding Ca^{2+} [314]. Of course, calcium could potentially be analyzed directly by ^{43}Ca NMR, however, its natural abundance is $<0.2\%$, its sensitivity is $<1\%$ that of ^1H , and being quadrupolar, it is liable to extensive line broadening [59]. Thus, the application of ^{19}F NMR with appropriately designed reporter molecules gives insight into cytosolic $[\text{Ca}^{2+}]$.

Magnesium ions are also involved in biological processes and occur in cells at millimolar concentrations [315]. Magnesium can be estimated based on the chemical shift difference of the resonances of adenosine triphosphate (ATP) using ^{31}P NMR [316-318], though ^{31}P NMR has intrinsically low signal to noise, exacerbated under many pathophysiological conditions, such as ischemia. There are many fluorescent indicators for detection of $[\text{Mg}^{2+}]$ [319] and fluorinated NMR reporter have been proposed. The simplest is fluorocitrate [313], which shows a change in chemical shift upon binding Mg^{2+} . However, it is critical that the reporter molecule be used as the + isomer only, which has relatively little toxicity [320]. Levy, *et al.* [8, 321] developed the o-aminophenol-N,N,O-triacetic acid (APTRA) structure both for fluorescent application and by incorporation of fluorine atoms for ^{19}F NMR, which have been used in the perfused rat heart [322].

While indicators are normally designed for a specific ion they often also interact with other ions, *e.g.*, FBAPTA provides a unique chemical shift with many divalent metal ions (Figure 10) [306, 307] and has been used to estimate $[\text{Zn}^{2+}]$, $[\text{Pb}^{2+}]$ [323], and $[\text{Cd}^{2+}]$ [307]. Plenio and Diodone [314, 324] have developed series of fluorocyclophanes and fluoro crown ethers to explore specific cation binding (*e.g.*, K^+ , Li^+ , Na^+ , Ba^{2+} , Sr^{2+} , Ca^{2+} though in many cases multiple ions may be bound (Table 5, Figure 12). Takemura [325] reported macrocycles designed to bind K^+ , NH_4^+ and Ag^+ . In addition to the metal binding ligands shown in Table 5, many others have been reported, but these were selected since they exhibit particularly large chemical shift responses.

While most reporter molecules have been designed to interact with cations, Plenio and Diodone [326] reported fluorine containing cryptands, which interact with perchlorate. London and Gabel [327] reported fluorobenzene boronic acid, which interacted with specific sugars.

3.1.4 Caveats

A number of criteria are pertinent to the development and exploitation of reporter molecules. The fluorine NMR spectrum must respond to interaction with the ion of interest, *e.g.*, through the formation of a second signal, as in the slow exchange regime, or chemical shift in a fast exchange regime. For many ions, agents should be water soluble, although a degree of lipophilicity may help in transport. The reporter molecule must reach the cellular compartment of interest. Some molecules penetrate cells directly, while for others this is facilitated using acetoxymethyl esters. A critical issue for intracellular interrogation is loading the reporter molecule into cells. The tetra-

carboxylates do not penetrate cells, however, derivatization as acetoxymethyl esters, which has been very widely used in association with analogous fluorescent indicators provides a more lipophilic entity, which can equilibrate across cell membranes [305]. These esters are specifically designed so that intracellular esterases cleave the acetoxymethyl ester, releasing the charged reporter molecule, which is then essentially trapped in the intracellular compartment. The release of acetic acid and formaldehyde are considered to be relatively innocuous. In other cases specific cellular exclusion is important, so that any signal can unambiguously be attributed to the extra-cellular or interstitial compartment in a tissue. Such measurements would be analogous to electrode measurements.

It is critical that the reporter molecule not perturb the system under investigation. For ions, there is inevitably some binding and complexation. Provided there is sufficient reservoir of the ions, there can be rapid re-equilibration, and the concentration may give a realistic indication of the free concentration. In unregulated systems, this may be less reliable. The binding constant must be compatible with the typical concentration encountered *in vivo*. Ideally, the reporter ligand is highly selective for the ion of interest and of course the molecule should exhibit minimal toxicity. Signals should be narrow to enhance both the signal to noise and spectral resolution.

3.2 Chemical Interactions

In the previous section we considered reporter molecules, which interact reversibly in a physical sense, *e.g.*, solvation of gas, protonation, or binding of metal ion by a ligand. Other reporter molecules reveal activity based on irreversible bond

cleavage to release a distinct product. This may be more akin to the metabolism of drugs, but these reporters can be tailored to interrogate specific biological processes.

3.2.1 Metabolism of Fluorodeoxyglucose

Steric and electrostatic considerations allow a fluorine atom to replace a hydroxyl group in many sugars, while retaining enzyme substrate activity. Many tumors are characterized by a high glycolytic rate and fluorodeoxyglucose (FDG) is a fluorinated glucose analogue used in Positron Emission Tomography (PET) to measure metabolic activity [328]. It is particularly useful for staging tumors and monitoring metastases. FDG is recognized by glucose transporters and enters cells where it is effectively phosphorylated, trapping it intracellularly, but phosphorylated FDG (FDG-6-P) is not a substrate for phosphofructose isomerase. FDG accumulates in metabolically active cells, such as tumors, brain, and myocardium. FDG PET is currently the method of choice for detecting many cancer metastases and differentiating recurrent disease from scar tissue. While PET can assess retention with great sensitivity, it provides no metabolic information, whereas ^{19}F NMR can be used to differentiate individual metabolites from anabolic and catabolic processes. Of course NMR studies typically require mM concentrations as opposed to nM- μM for PET, and thus, metabolic fates may differ, but 2-FDG has been used in metabolic studies using ^{19}F NMR [329-332]. The 3-fluoro-3-deoxy-D-glucose isomer (3-FDG) has also been used in the eye, particularly with respect to exploring onset of cataracts [333, 334]. It is a poor substrate for hexokinase and the binding affinity of phosphohexose isomerase is low relative to glucose, but it has been used to probe aldose reductase activity in brain [335].

NMR not only provides spectral resolution for a given nucleus allowing multiple fluorine-labeled substrates to be observed simultaneously together with metabolic products, but other nuclei may also be detected. In particular ^{13}C and ^2H NMR have been used extensively to probe metabolism, both confirming well known pathways (e.g., glycolysis) and revealing novel detoxification products of xenobiotica [96, 97, 336, 337]. ^{13}C NMR may be considered preferable for such studies since isotopic enrichment is less perturbing than introduction of a fluorine label. As for ^{19}F NMR, ^{13}C NMR normally has minimal background signal, since the natural abundance of ^{13}C is only 1.1% allowing almost 100 fold enrichment. Isotopomer analysis can reveal substrate preferences and mechanisms of enzyme activity and kinetic isotope effects are minimal for ^{13}C , though may be sizable for ^2H examined substrates [338].

3.2.2 Hypoxia

While FDG has a role in detecting tumors, a new thrust is characterizing tumors so as to individualize therapy and optimize outcome. To this end, hypoxia is recognized as a critical characteristic. In Section 3.1.1, we described ^{19}F NMR methods for measuring pO_2 . As an alternative approach fluoronitroimidazoles have been used to detect hypoxia. Nitroimidazoles are bioreductive agents that are reduced by intracellular reductases to generate reactive intermediates. In the presence of oxygen, the intermediates are rapidly reoxidised and may clear from cells, but under hypoxic conditions they become covalently bound to cellular constituents, indicating the presence of cellular hypoxia. Nitroimidazoles have been used extensively in the past as hypoxic cell radiosensitizers [339] and more recently have gained a role as markers of

tumor hypoxia [85, 340-344]. EF5 and pimonidazole are widely used to assess hypoxia in histological analysis of biopsy specimens [198, 345-347], but non-invasive approaches would be preferable for therapeutic prognosis. Retention of ^{18}F misonidazole in hypoxic tumors has been observed using PET. Given the importance of hypoxia other PET and Single photon emission computed tomography (SPECT) sensitive agents have been proposed and tested (e.g., Cu-ATSM [348, 349] and iodinated azomycin galactoside (IAZG) [350]), but non-radioactive approaches would be preferable.

Fluorine-19 labels have been introduced into the nitroimidazole structure providing NMR sensitive agents [351, 352]. Studies have reported the fluorinated nitroimidazoles CCI-103F [353], Ro 07-0741 [354] and SR-4554 [351, 355, 356], which contain 6, 1, and 3 fluorine atoms per molecule, respectively (Table 6). Subsequent to administration, a washout period sufficient for elimination of unbound marker is required, since there is apparently no difference detectable *in vivo* in the chemical shifts of the parent molecule and the metabolites [351]. Li *et al.* [357] investigated the predictive potential of CCI-103F retention as an indicator of tumor radiosensitivity and found a weak correlation indicating that factors other than hypoxia are involved and glutathione concentration may be pertinent [351].

Aboagye *et al.* [358] found increased retention of SR-4554 in hypoxic tumors, but no linear correlation with pO_2 . Lack of correlation with pO_2 measurements [355, 358] and pimonidazole uptake [351] suggest that additional factors influence hypoxia marker retention and indeed blood flow/perfusion has been implicated [351]. Robinson and Griffiths found differential uptake of SR-4554 in diverse tumors known to exhibit different

levels of hypoxia. Surprisingly, there was no retention detected in C6 gliomas, which are widely reported to have extensive hypoxia (Figure 13). Trapping is predicated on nitroreductase activity, which may be lacking in some tumors. Unlike radiochemical approaches, which detect all labeled molecules, NMR offers potential benefits, but added complexity. Diverse adducts, and metabolites may exhibit multiple chemical shifts, each at very low concentration. There is also concern that polymeric adducts may have exceedingly short T_2 , so that they become essentially invisible for many NMR sequences [359]. The biggest problem with ^{19}F hypoxia agents is that they merely provide a qualitative impression of hypoxia rather than a definitive pO_2 . Seddon *et al.* [356] reported a correlation between retention of SR4554 and pO_2 , but a Phase I clinical ^{19}F NMR study [356] required infusion at doses of 400-1600 mg/m^2 , which could have adverse side effects.

3.2.3 Enzyme reporters

A ^{19}F atom can be substituted for a hydroxyl group in sugars with little overall structural perturbation. As such, fluorosugars were widely used to explore mechanisms of enzyme activity [124, 126, 360]. We adopted a different strategy by including ^{19}F into the aglycon moiety of a substrate to detect β -galactosidase activity (Figures 1 and 14, Table 7) [294]. This provides insight into activity of the *lacZ* gene, which has historically been the most popular reporter gene in molecular biology.

Gene therapy holds great promise for the treatment of diverse diseases. However, widespread implementation is hindered by difficulties in assessing the success of transfection in terms of spatial extent, gene expression, and longevity of expression. The development of non-invasive reporter techniques based on appropriate molecules

and imaging modalities may help to assay gene expression and this is often achieved by including a reporter gene in tandem with the therapeutic gene [38, 361]. Currently, reporter genes associated with optical imaging are most popular (e.g., bioluminescent imaging (BLI) of luciferase [38, 362] and fluorescent imaging of green fluorescent protein (GFP) and longer wavelength variants [45], since they are cheap modalities, and highly sensitive results are rapidly available. These techniques are very useful in superficial tissues and have extensive applications in mice, but application to larger bodies is limited by depth of light penetration. For deeper tissues and larger animals nuclear medicine approaches based on thymidine kinase or the sodium iodine symporter (hNIS) have been used [49, 363]. For cancer, thymidine kinase has the advantage that the gene serves not only as a reporter, but gene products can themselves have therapeutic value [146]. Cytosine deaminase (CD) activates the minimally toxic 5-fluorocytosine (5FC) to the highly toxic 5-fluorouracil (5FU) [146, 147]. The conversion of 5FC to 5FU causes a ^{19}F NMR chemical shift ~ 1.5 ppm, hence, revealing gene activity, which has been demonstrated in a number of systems *in vivo* [147, 150].

We have focused on substrates for lacZ, recognizing its popularity as a reporter gene. Given the popularity of lacZ [364-366] diverse reporter agents are commercially available, but mostly for optical and histological applications (e.g., X-gal, ONPG (o-nitrophenylgalactopyranoside), S-GalTM, and S-Galacton-StarTM) [367-369]. Recently, ^1H MRI [370], fluorescent [371] and radionuclide [372] substrates have been presented for *in vivo* work, prompting us to consider ^{19}F NMR active analogs. It appeared that introduction of a fluorine atom into the popular colorimetric biochemical indicator ortho-

nitrophenyl β -galactopyranoside (ONPG) could produce a strong candidate molecule. Fluoro-nitrophenol galactosides were used by Yoon *et al.* [373], to explore β -gal activity, but they placed the fluorine atom on the sugar moiety, which would be expected to provide much less chemical shift response to cleavage and they do not appear to have used ^{19}F NMR in these investigations.

Our prototype molecule 4-fluoro-2-nitrophenyl β -D-galactopyranoside (PFONPG, Table 7) proved effective as a substrate for β -galactosidase [374]. It provides a single ^{19}F NMR signal with a narrow line width and good stability in solution. It is stable in normal wild type cells and whole blood, but exposure to the enzyme or cells transfected to express β -galactosidase causes rapid cleavage in line with anticipated levels of transfection [374]. Upon cleavage of the glycosidic bond a chemical shift difference $\Delta\delta > 3.6$ ppm is observed, though the chemical shift of the product may have a range of about 9 ppm, since the released aglycone is pH sensitive and the pKa is in the physiological range. Significantly, there is no overlap between the chemical shift of the substrate and the product and the chemical shift difference is sufficient to permit chemical shift selective imaging to reveal distribution of each entity separately [375].

To seek optimal ^{19}F NMR reporters, we synthesized diverse agents and the broad range of substrate structures is consistent with enzyme promiscuity (lack of substrate specificity) (Table 7). The released aglycone PFONP is somewhat toxic and can cause lysis of fragile cells. We have synthesized series of analogues with the fluorine atom placed at various locations on the phenolic ring and incorporating alternate substituents, such as Cl and Br [294]. Each adduct and aglycone provides a unique chemical shift allowing ready comparison of susceptibility to enzyme activity.

The chemical shift accompanying cleavage depends strongly on the orientation of the F-atom with largest response for para-F and less for ortho-F. The rate of cleavage was closely related to the pKa of the aglycone [294] commensurate with enzyme studies reported previously [376].

One approach to reducing toxicity is introduction of a trifluoromethyl (CF₃) reporter group, as opposed to the single F-atom to enhance signal to noise. The chemical shift response is much smaller (Table 7), due to transmission of the electron density redistribution through an additional carbon-carbon bond [299]. Spectroscopic detection is still feasible *in vivo* and deconvolution allows CSI, but it is unlikely to be feasible *in vivo* [299]. Toxicity may also be altered by using alternate aglycons, such as the pH reporter 6-fluoropyridoxol [11]. 3-O-(β -D-galactopyranosyl)-6-fluoropyridoxol (GFPOL) is found to be a much less good substrate and reactivity is much slower [377]. It is also less water soluble. However, we have found that water solubility may be enhanced by polyglycosylation of the hydroxymethyl arms [378]. The polyglycosylated substrate was also highly reactive for β -gal, but when galactose was used for all sugar residues multiple products were rapidly generated causing complex spectra. Differential glycosylation using glucose or mannose as the secondary sugars overcame this problem [378].

Given the different chemical shifts of individual substrates and products, we believe there will be opportunities to use multiple reporters simultaneously. Indeed, we have investigated using 4-fluoro-2-nitrophenyl β -D-galactopyranoside (PFONPG) and 2-Fluorine-4-nitrophenyl β -D-galactopyranoside (OFPNPG) as substrates simultaneously to differentiate wild type and lacZ expressing tumors in mice [379].

4 Passive reporter molecules

Many active ^{19}F NMR reporter molecules have been designed, developed, and exploited, but other methods use a passive approach. In essence fluorinated molecules occupy a space and a signal magnitude provides an indication of anatomical properties such as lung volume, bowel function, vascular volume, or flow.

Perfluorocarbons exhibit remarkable gas solubility, and based on the high carrying capacity for oxygen and carbon dioxide, have been developed in emulsion form as synthetic blood substitutes [231]. PFCs may also be relevant as pure liquids. In a classic experiment, Clark and Gollan [380] submersed a living mouse in PFC liquid and far from drowning, it inhaled the PFC facilitating effective oxygen transport to the lungs. Thus, PFCs have potential application as surfactants to aid breathing in extremely premature infants, as explored in clinical trials [381]. PFC may be administered as liquid or aerosols. Thomas, *et al.* [382, 383] applied ^{19}F MRI to show the extent of lung filling. Further, by applying relaxation measurements (as described in Section 3.1) they could estimate regional pO_2 in the lungs of mice, rats, dogs and pigs [208, 383]. Various perfluorocarbons and perfluorocarbon emulsions have been introduced into the lung as aerosols, sometimes with animals under forced ventilation, following thorocotomy [383]. The ^{19}F signal provides an opportunity to image lungs. By contrast ^1H MRI is handicapped by lack of water signal. In a novel approach, Huang, *et al.*, [384] applied ^1H MRI to the water in a perfluorocarbon emulsion and found considerably enhanced structural information. Liquid and aerosol ventilation can be stressful, whereas inhalation of inert gas may be more practical, as shown by proof of principal using CF_4

or C_2F_6 [385]. More recent studies used SF_6 with potential application for detection of lung cancer, emphysema, or allograft rejection [386, 387]. Gas detection does require special MR instrumentation, due to the exceedingly short T_1 and T_2 relaxation.

Increasing awareness of colon cancer demands improved screening. Traditional barium meals provide contrast in CT, and virtual colonoscopy is competing with traditional fiber optic probes [388]. MR procedures have lagged behind CT, but several potential contrast agents have been presented, ranging from paramagnetic zeolite formulations [389] and ferric ammonium citrate [390] to PFC emulsions [391, 392] and recently images were shown in mice based on perfluorononane [69].

Angiogenesis is associated with tumor development and many clinical trials have found correlations between vascular density and prognosis. Traditional analysis required biopsy and histology, with CD31 antibodies to provide blood vessel counts [393], and dyes such as India ink or Hoechst 33342 to reveal perfusion [394]. ^{19}F NMR provides a robust indication of vascular volume *in vivo* based on intravenous perfluorocarbon emulsions, which are retained in the vasculature for a period of hours [395, 396]. Non-invasive measurements revealed acute modulation of tumor blood volume and have provided validation of non-invasive NIR methods [397, 398]. This approach has also been applied to other organs and tissues, *e.g.*, demonstrating reactive hyperemia in muscles [399]. Studies have validated signal using traditional radioisotope labeled approaches and dyes [400].

Fluorinated gases (*e.g.*, trifluoromethane (FC-23) and chlorofluoromethane (FC-22)) have been used to examine cerebral blood flow based on inflow and outflow kinetics, sometimes with pulsed delivery to facilitate compartmental analysis [401, 402].

The observation that HFB clears from tumors over a period of hours suggests this could provide insight into tissue perfusion [224, 266].

5 Potential innovations and improvements

Implementation and application of ^{19}F MRI in the clinic awaits further developments. As described above, many reporter molecules have been presented and are undergoing further refinement and evaluation. Sensitivity can be enhanced incrementally by exploiting molecular symmetry as emphasized in Table 2: bis fluorine atoms can enhance signal to noise ratio (SNR) two-fold, a CF_3 group three-fold, a bis- CF_3 six-fold and tris- CF_3 9-fold. Perhaps the most satisfying increase in SNR is gained by better targetability and localization following systemic delivery. Widespread utility of agents will depend on ready commercial availability. Other sensitivity gains can arise from enhanced radiofrequency coils and Parallel imaging (e.g., SMASH or SENSE technologies [403, 404]) and higher magnetic field. While ^{19}F MRI on human NMR systems is feasible, it still remains to be established as part of a routine commercial inventory. Clearly, use and need will stimulate widespread provision and availability which could occur quite rapidly.

6 Conclusions

Since there is essentially no ^{19}F NMR background signal in tissues, fluorinated drugs, and reporter molecules may be detected without interference. Huge diversity of application has been demonstrated in the biochemical and small animal areas, with some limited clinical application. To date clinical application is hindered by the lack of

availability of clinical ^{19}F NMR, but manufacturers are increasingly recognizing the value of including such capability. Given that ^{19}F NMR offers the potential to investigate many diverse parameters (Table 1) it will become increasingly available and useful in the future.

7 Acknowledgments

Supported in part by the Cancer Imaging Program, NCI Pre-ICMIC P20 CA086354, and IDEA awards from the DOD Breast Cancer Initiative DAMD 17-99-1-9381 and 17-03-1-0343 and Prostate Cancer Initiative W81XWH-06-1-0149. NMR experiments were conducted at the Mary Nell and Ralph B. Rogers NMR Center, an NIH BTRP facility #P41-RR02584. We are grateful to Drs. Mark Jeffrey, Himu Shukla, and Peter Peschke, for collegial support and allowing us to include unpublished collaborative studies here. Melody Simmons provided expert assistance in preparing this manuscript. Over the past 15 years our development of expertise in ^{19}F NMR has been supported by the NIH, Department of Defense Breast and Prostate Cancer Initiatives, the American Cancer Society, the American Heart Association, and The Whitaker Foundation.

Figure Legends

Figure 1 Representative fluorinated molecules

- a) Pharmaceuticals for which clinical or pre-clinical *in vivo* NMR studies have been reported: 5-fluorouracil (5FU) [16, 17, 63], gemcitabine [65] and capecitabine [73] are anti cancer drugs; fluoxetine [162] and dexfenfluramine [72] have neurological activity, sitafloxacin [66] is an antimicrobial, niflumic acid [67] is a non-steroidal anti inflammatory, tecastemzole [68] is an experimental antihistamine and perfluorononane has been proposed for GI imaging [69].
- b) Published ^{19}F NMR reporter molecules: 6-FPOL (6-fluoropyridoxol) is a pH reporter [11], HFB (hexafluorobenzene) is used for oximetry [10], PFONPG is a gene reporter for β -gal [294] and 5FBAPTA measures $[\text{Ca}^{2+}]$ [295].
- c) Natural products incorporating fluorine atoms: fluoroacetate, fluorocitrate, fluoroacetone and fluoro oleic acid [4].

Figure 2 Simultaneous detection of multiple fluorinated molecules *in vivo*.

To explore the hypothesis that uptake of the anti-cancer drug 5FU by tumors is pH dependant we infused 5FU (0.4 ml (50 mg/ml) IV), the extra cellular pH reporter CF_3POL (400 mg/kg IP), and the chemical shift standard NaTFA (200 mg/Kg IP) into an anesthetized rat (1% isoflurane) with a subcutaneous 13762NF breast tumor (1.4x1.5x1.1cm). 30 mins after administration all four molecules were detectable simultaneously in 17 mins. At this stage no metabolites of 5FU were detected.

Figure 3 ^{19}F NMR of gemcitabine

Lower spectrum shows a solution of gemcitabine hydrochloride at pH 3.2. For comparison the upper spectrum was obtained in the presence of sodium hydroxide at pH 8.4. Each spectrum required about 1 min at 376 MHz (9.4 T) (data acquired in collaboration with Dr. Peter Peschke, DKFZ, Heidelberg, Germany).

Figure 4 Monitoring myocardial oxygenation using ^{19}F NMR of sequestered perfluorotributylamine.

a) Spin lattice relaxation (R_1) recovery curve obtained in two minutes for the CF_3 resonance from an isolated Langendorff perfused rat heart that had sequestered Oxypherol. $R_1 = 2.11 \pm 0.08 \text{ s}^{-1}$ indicates 510 ± 30 torr at 37°C . Inset shows partial ^{19}F NMR spectrum with resolved downfield CF_3 and CF_2 resonances.

b) Steady state R_1 -measured pO_2 values of perfused rat hearts as percentage of normalized initial tissue pO_2 with respect to interventions. Hearts in Group A (\blacktriangle) showed pO_2 equivalent to zero torr during total global ischemia (TGI), but returned to 100% upon reperfusion. KCl arrest resulted in increased tissue pO_2 from the excess available oxygen. Elevated pO_2 was observed in hearts in both Group B (\blacksquare) (experiencing immediate arrest) and those in Group A (experiencing prior TGI). The previous ischemia experienced by Group A did not “condition” the hearts in terms of the R_1 -measured pO_2 . Global ischemia showed complete hypoxia for both groups with or without KCl arrest. Error bars represent one standard deviation of measurements from multiple hearts (data adapted from Ph.D. thesis of Himu Shukla, UT Southwestern 1994) [405].

Figure 5 Correlation of myocardial oxygenation and developed pressure in excised Langendorff perfused rat hearts

a) When NMR signals are acquired more rapidly than the time required for full relaxation, there is signal loss due to partial saturation. Comparing the intensity of a partially saturated signal to fully relaxed signal indicates R_1 , and hence, pO_2 . In "a" the larger CF_3 signal shows a decrease of about 15% compared with baseline under fully perfused, well oxygenated conditions. Induction of TGI caused rapid loss of signal commensurate with increasing T_1 and reduced pO_2 . Individual spectra were acquired in 1.1 s. The transition was complete within about 40 s. T_1 of the CF_3 resonance increased from 540 to 1240 ms causing the signal to decline from 86% to 68% accompanying TGI. The CF_2 resonance only changed from about 390 to 570 ms and this had minimal effect on signal intensity under these partial saturation conditions.

b) Dynamic data (the partial saturation spectra quantified using decay of the CF_3 resonance) from hearts made globally ischemic showed that an arrested heart ▲ consumed residual oxygen in the heart more slowly than a beating heart ○. Note that the arrested heart started from a higher state of tissue oxygenation due to reduced oxygen demand. The mono-exponential rate constants representing the loss of tissue pO_2 are: Beating $L=0.11\text{ s}^{-1}$, Arrested $L=0.02\text{ s}^{-1}$.

c) The pressure tracing of a perfused rat heart based on an intraventricular balloon catheter was digitized to quantitate the rate of ventricular pressure failure during ischemia. For this heart, a monoexponential curve fit to the pressure amplitude yielded a decay rate constant $P=0.085\text{ s}^{-1}$.

- d) Reperfusion following 5 mins TGI led to rapid reoxygenation of the rat hearts, revealed by increase in the CF_3 signal corresponding to shortening of T_1 .
- e) A strong linear relationship was found between the rate of heart tissue hypoxiation and ventricular pressure failure for rat hearts upon acute TGI ($r > 0.9$)

Figure 6 *In vivo* MR histology

Following administration of Oxypherol (perfluorocarbon blood substitute emulsion of perfluorotributylamine) to a Copenhagen rat bearing an AT1 tumor, ^{19}F NMR signal was initially detected around the tumor periphery [242]. Comparison of thin slices from 3D ^1H (a) and ^{19}F (b) MRI data sets obtained 18 days later showed that new tumor tissue grew around the labeled tissue and the ^{19}F label was exclusively in the central region and ^{19}F NMR oxygen tension measurements showed mean $\text{pO}_2 = 2.5$ torr for a group of six such tumors. When fresh Oxypherol was administered (4 x 2.5 ml IV) and allowed to clear for 48 h, the new PFC was found around the tumor periphery, but the original signal was retained in the center (c and d). These data reveal the differential perfusion of tumor regions and tendency of IV administered reporters to target well perfused regions (unpublished data obtained in collaboration with Drs. Anca Constantinescu and Peter Peschke).

Figure 7 *FREDOM*- tissue oxygen dynamics

- a) A linear relationship is found between the spin lattice relaxation rate R_1 of HFB and pO_2 (Reprinted from *Methods in Enzymology*, 386, Zhao D, Jiang L, Mason RP, Measuring Changes in Tumor Oxygenation., 378-418, Copyright (2004), with permission from Elsevier) [10].
- b) ^{19}F NMR relaxation curves from a single voxel in rat leg muscle after direct administration of 50 μ l HFB. Curves are shown during air breathing (circles; $T_1 = 7.37$ s, $pO_2 = 28$ torr) and following switch to oxygen for about 20 mins (crosses; $T_1 = 2.65$ s, $pO_2 = 156$ torr), respectively.
- c) pO_2 map of rat thigh muscle during air breathing. Data obtained in 6.5 mins, showing heterogeneity of baseline oxygenation. Mean $pO_2 = 20 \pm 1$ torr.
- d) Following 20 mins oxygen breathing all the voxels in 'C' showed increased pO_2 reaching a new mean $pO_2 = 158 \pm 6$ torr.
- e) pO_2 map of 13762NF rat breast tumor, while rat breathed air (mean $pO_2 = 13 \pm 2$ torr). Oxygenation is clearly lower than for muscle, above.
- f) During oxygen breathing tumor pO_2 increased, though showing considerable heterogeneity of response with mean $pO_2 = 52 \pm 4$ torr.

Figure 8 pH measurement in cells

^{19}F NMR of difluoromethylalanine para-chlorophenyl ester (1 mM) added to suspension of RINm5F cells (4% cytochrome c). Spectra were taken at 4-min intervals (1,600 scans, 30° pulse, repetition rate = 5/s) with broadband proton decoupling. The resonances marked e arise from the ester form of the amino acid. The resonances in

the lower spectrum marked o arise from extra cellular free amino acid, whereas those marked i arise from intracellular free amino acid. Spectrum A) 1-5 min; B) 5-9 min after addition of ester to the cell suspension. The ester quartet (e) lines decreased in intensity, while the quartets of lines from the product of ester hydrolysis, intracellular difluoromethylalanine (CF_{2i}) and extra cellular difluoromethylalanine (CF_{2e}), increased with time [Partial figure reproduced from J. Taylor and C. J. Deutsch, ^{19}F nuclear magnetic resonance: measurements of $[\text{O}_2]$ and pH in biological systems. *Biophys. J.* 1988;53:227-233 [406] with permission of the Biophysical Society].

Figure 9 Transmembrane pH gradient in red blood cells

^{19}F NMR of 6-fluoropyridoxol (4.2 mg), PFONP (4.8 mg), and NaTFA in fresh whole rabbit blood (600 μl). Both pH indicators show split peaks arising from intra- and extracellular signals. Extra cellular pH was measured using polarographic electrode $\text{pHe}=7.66$ and compared with $\text{pHe}_{(\text{PFONP})}=7.55$ and $\text{pHe}_{(\text{FPOL})}=7.55$. ^{19}F NMR showed intracellular pH $\text{pHi}_{(\text{PFONP})}=7.16$; $\text{pHi}_{(\text{FPOL})}=7.29$.

Figure 10 Detection of $[\text{Ca}^{2+}]$ using ^{19}F NMR of F-BAPTA

Left: molecular structures of three F-BAPTA isomers with Ca^{2+} binding constants.

Top right: Chemical shifts of F-BAPTA isomers upon binding divalent metal ions with respect to F-tryptophan.

Bottom right: ^{19}F NMR spectra of F-BAPTA in presence of Ca^{2+} . 5F-BAPTA is in slow exchange showing response for free and bound forms, whereas 4F-BAPTA is in fast

exchange showing weighted average (modified from Smith *et al. Proc. Natl. Acad. Sci. (USA) -Biological Sciences* 80, 7178-7182 (1983) - with permission [306]).

Figure 11 Changes in gated NMR spectra during the cardiac cycle.

Top panel: Isovolumic left ventricular pressure in a ferret heart paced at 0.99 Hz in 8 mM $[Ca^{2+}]$. NMR spectra were acquired at the two times indicated on the pressure record: a) 10 ms prior to stimulation; b) 75 ms after stimulation.

Middle panel shows gated ^{19}F NMR spectra (each from 800 acquisitions) recorded at a and b, as indicated. The bound (B) and free (F) peaks of 5F-BAPTA exhibit distinct chemical shifts at ~8 and 2 ppm, respectively, downfield from a standard of 1 mM 6-Ftryptophan at 0 ppm. It appears that the free $[Ca^{2+}]$ varied during the cardiac cycle.

Bottom panel shows gated ^{31}P spectra (400 scans) acquired at times a and b in the same heart. The major peaks correspond to phosphocreatine (0 ppm), ATP (the three peaks upfield from phosphocreatine), and inorganic phosphate (the small peak at 4-5 ppm) (Reproduced from Marban, *et al. Circ. Res.* 1988;63:673-678 [311] with permission of Lippincott, Williams & Wilkins).

Figure 12 ^{19}F NMR spectrum of FN_2O_4 ligand with mixture of mono and divalent cations: Li^+ , Na^+ , K^+ , Rb^+ , Mg^{2+} , Ca^{2+} , Sr^{2+} and Ba^{2+} . Due to slow exchange all species are detected simultaneously (Reprinted with permission from Plenio and Diodone, *JACS* **118**, 356-367 [314], Copyright 1996 American Chemical Society)

Figure 13 ^{19}F NMR of hypoxia reporter SR4554 in tumors

^{19}F NMR spectra obtained from (a) a vial containing 6 mg/ml SR-4554 resonating at ca. 45 ppm relative to a 5-fluorotryptophan (5-FTP) external standard, (b) a wild-type C6 glioma; (c) a RIF-1 fibrosarcoma; and (d) an HT29 colon adenocarcinoma all acquired 45 min after administration of 180 mg/kg SR-4554 IP. The degree of retention of the reduced adducts of SR-4554, measured by ^{19}F MRS, affords a non-invasive assessment of tumor hypoxia. No ^{19}F resonance was detected in C6 gliomas, although they are expected to exhibit considerable hypoxia. The RIF-1 fibrosarcoma grown in C3H mice and HT29 colon adenocarcinoma grown in nude mice showed clear ^{19}F resonances from SR-4554 (Reproduced with permission from Robinson and Griffiths, *Phil. Trans. R. Soc. London B Biol. Sci.* **359**, 987-996, Figure 6 (2004) [351]).

Figure 14 Detection of β -galactosidase activity in cells using ^{19}F NMR

Sequential ^{19}F NMR spectra of Lncap C4-2 prostate cancer cells transiently transfected with *lacZ* (1.0×10^7) in PBS (0.1 M, pH=7.4, 700 μL) at 37 °C following addition of GFPOL (1.84 mg, 5.27 mmol). ^{19}F NMR spectra were acquired in 102 s each, and enhanced with an exponential line broadening 40 Hz. In each spectrum GFPOL occurs on the left with liberated FPOL aglycon appearing at right (*).

Table 1 Fluorinated reporter molecules

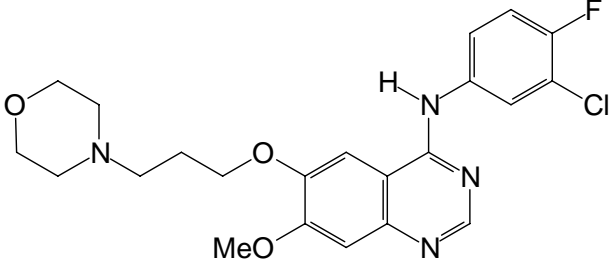
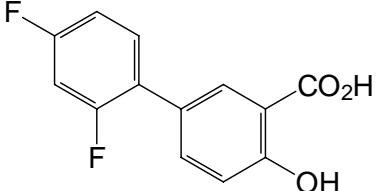
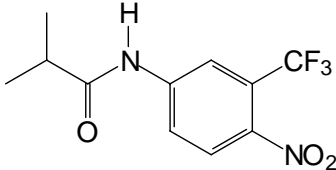
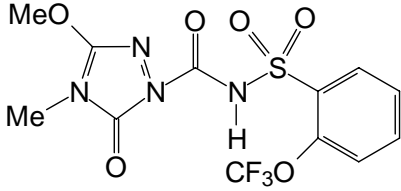
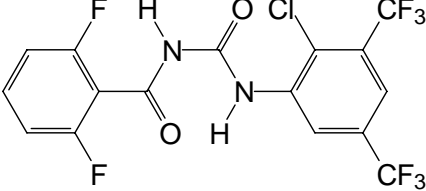
Parameter	Indicator	NMR	References
	(example)	Parameter	(representative)
Physical Interactions			
pO ₂	perfluorocarbons, e.g., hexafluorobenzene	R ₁ (R ₂) $\Delta\delta$	[9, 10, 222, 351, 407] [408]
pH	FPOL, DFMO, ZK150471	$\Delta\delta$, J	[11, 280, 301, 303, 409]
[Na ⁺]	F-cryp-1	δ , ratio	[410]
[Ca ²⁺]	5F-BAPTA	δ , ratio	[8, 295, 311]
[Mg ²⁺]	5F-APTRA	δ , ratio	[321]
Membrane/Chloride potential	TFA	ratio	[287, 411]
Chemical Interactions			
Gene activity	PFONPG, 5FC	$\Delta\delta$	[147, 294, 374, 378]
Nitric oxide	NN [•] <i>t</i>	$\Delta\delta$	[412]
Hypoxia	F-Misonidazoles	integral	[351, 413]
Glycolysis	FDG	integral	[331]
Drug metabolism	5-FU, gemcitabine	integral	[17, 63]
Protein catabolism	DLBA	integral	[414]
Disease specific receptors	nanoparticles	integral	[56, 57]
Passive Reporters			
Temperature	PFCs	ratio	[5, 207, 415]
Blood flow	Freon FC-23	Integral	[401]
Cell volume	TFM	integral	[287]
Diffusion	FDG	ADC	[416]
Vascular volume	Fluorocarbon emulsion	integral	[398, 417]
Lung function	PFC; SF ₆	integral	[384, 386, 387]
GI function	PFC	integral	[69, 392]

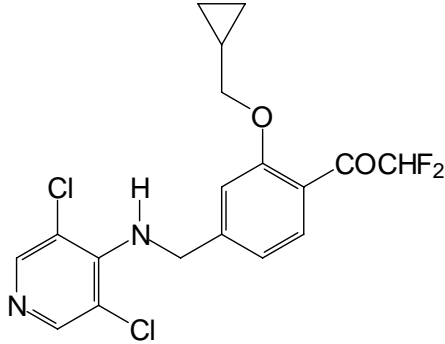
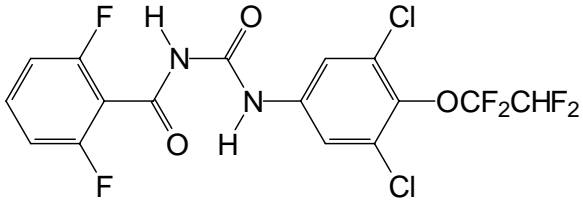
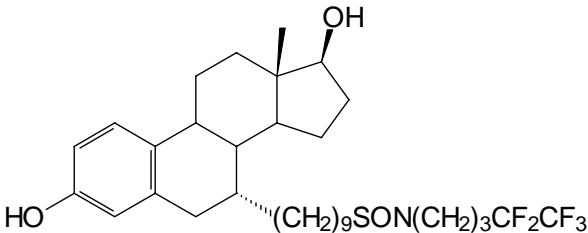
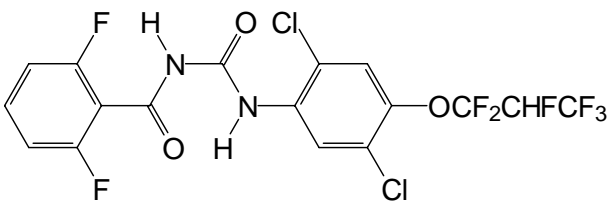
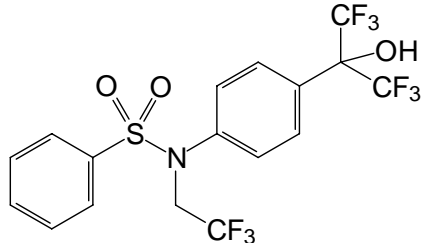
Myocardial infarction MP-312

integral [418]

t (2-(2,6-Difluorophenyl)-4,4,5,5-tetramethyl-4,5-dihydro-1*H*-imidazol-3-oxide-1-oxyl)

Table 2 Fluorine containing pharmaceuticals and agrochemicals [22, 26, 28]

Number of Equivalent F- Atoms	Molecular Structure	Name	Use	Relevant References
1		Gefitinib ZD1839 Iressa®	Anticancer Drug	[419, 420]
1+1		Diflunisal Dolobid®	Anti-Inflammatory Drug	[182]
3		Flutamide Eulexin®	Anti-Androgen Drug	[181, 421]
3		Flucarbazon	Herbicide	[422]
3+3 +2		Bistrifluron	Insecticide	[423]

2		Roflumilast	Anti inflammatory (asthma) Phosphodiesterase (PDE) 4 inhibitor	[424]
2+2+2		Hexaflumuron	Insecticide	[425]
3+2		Fulvestrant Faslodex [®]	Anti-Androgens Drug	[426]
3+2+2+1		Lufenuron	Insecticide	[427]
6+3		T 0901317	Anticancer Drug	[183]

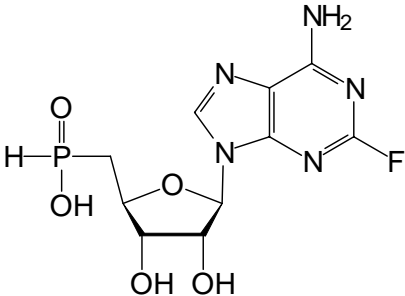
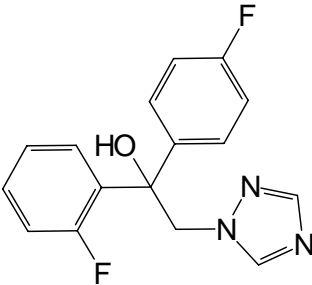
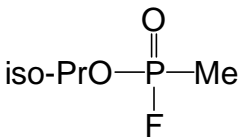
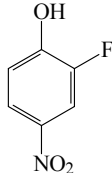
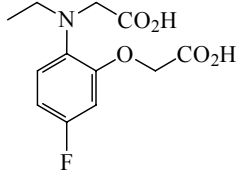
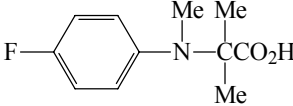
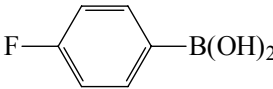
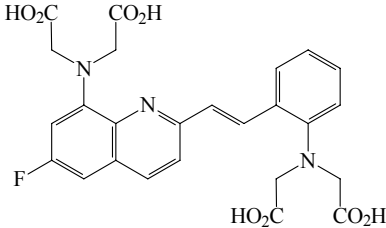
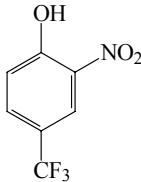
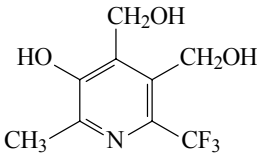
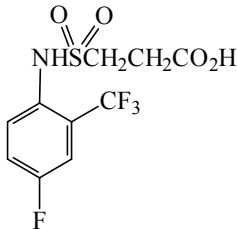
1		Fludarabine	Topo-isomerase Inhibitor	[428]
1+1		Flutriafol	Fungicide	[429]
1		Sarin	Toxicant	[430]

Table 3 ^{19}F NMR pH Indicators

Reporter	Structure	pK_a	$\delta_{\text{F(acid)}}^*$ (ppm)	$\delta_{\text{F(base)}}^*$ (ppm)	$\Delta\delta$ (ppm)	Reported Applications
3-fluoro-2-methyl alanine		8.5	-143.2	-145.3	2.05	Intracellular pH, perfused liver, lymphocytes [74]
3,3-difluoro-2-methyl alanine		7.3	-53.95	-55.95	2.00	Figure 8 [74]
3,3,3- trifluoro-2-methyl alanine		5.9	-0.25	-2.35	2.10	[74]
DFMO		6.4	4.60	4.30	0.30	[286]
6-FPOL		8.2	-9.84	-19.56	9.72	Transmembrane pH gradient, blood, heart, tumor [11, 290]
6-FPAM		7.05	-9.19	-19.19	10.07	Transmembrane pH gradient, blood, heart, tumor [11, 291]
6-FPOL-5- NH ₂		8.0	-7.57	-19.55	11.98	[291]
6-FPOL-5- α - CF ₃		7.6	-4.45	-14.09	9.64	[291]
PFONP		6.9	-44.44	-55.76	11.32	Transmembrane pH gradient, blood, [294, 374]

OFPNP		6.0	58.77	61.01	2.24	Extra cellular pH [294]
5FNEAP-1		6.85	35.60 **	24.70 **	10.90	Extra cellular pH [298]
N,N-(methyl-2-carboxyisopropyl)-4-fluoroaniline		6.8	-36.00	-49.50	13.50	in vivo pH measurement agents [297]
4-Fluoro benzene boronate (FBA)		8.7	-34.50	-43.50	8.80	in vivo pH measurement agents [431]
FQuene		6.7	11.82 ***	8.73 ***	3.09	Intracellular pH, Liver of rats [296]
PCF ₃ ONP		5.6	13.49	14.52	1.03	Extra cellular pH [299]
CF ₃ POL		6.8	15.15	16.76	1.7	Extra cellular pH [18]
ZK 150471		7.16	-52.74 ****	-62.87 ****	-10.13	in vivo pHe probe, tumor and tissue [301, 303, 304]

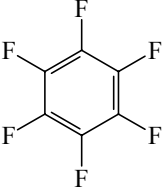
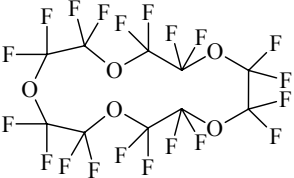
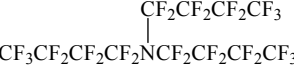
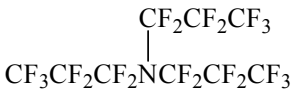
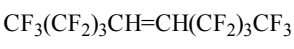
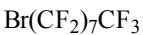
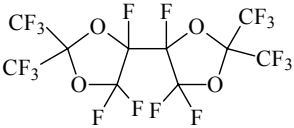
Unless otherwise noted, dilute CF_3CO_2^- was used as chemical shift reference;

** tetrafluoroterphthalic acid was used as standard, though variously in the experimental section NaF and hexafluorobenzene were used as standards;

*** chemicals shifts quoted with respect to 5FBAPTA;

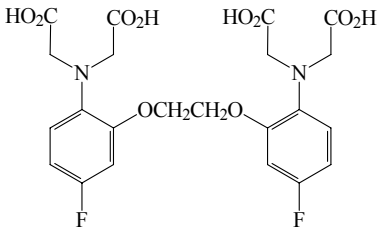
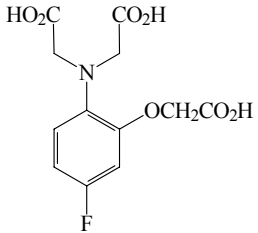
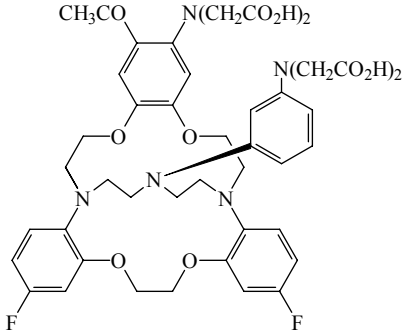
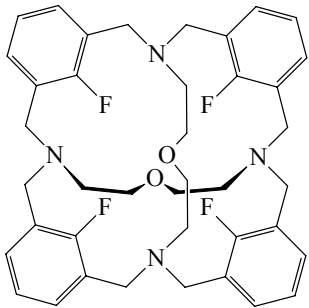
**** Intramolecular chemical shift difference.

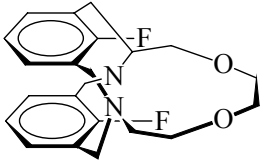
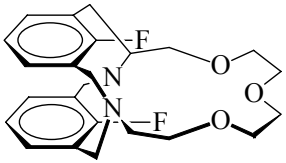
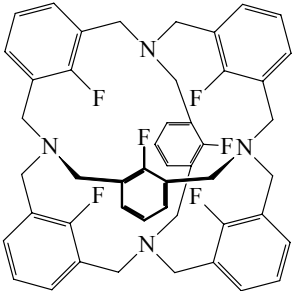
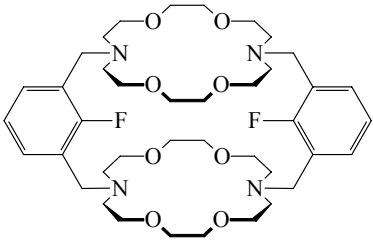
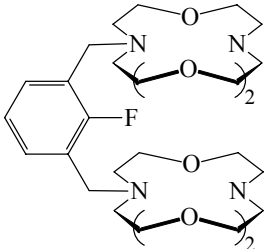
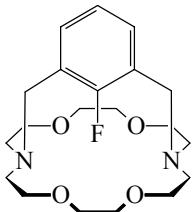
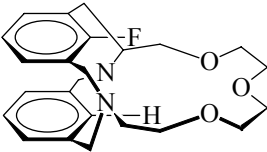
Table 4 ^{19}F NMR Characteristics and Applications of PFCs for Tissue Oximetry

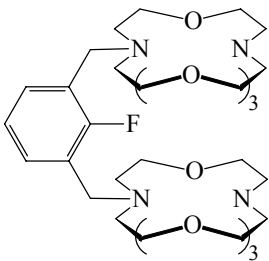
Name	Structure	Sensitivity to pO_2^a	Number of ^{19}F resonances	Applications
HFB		A=0.0835 B=0.001876	1	Rat breast tumor, prostate tumor, human lymphoma xenograft [10, 214, 215, 217, 267, 270] (Figure 7)
Perfluoro-15-crown-5-ether		A=0.345 B=0.0034	1	Tumor cells, mouse tumor, spleen, liver, rat breast tumor, rat brain [218, 247, 254]
FC-43 (Oxypherol)		A=1.09 B=0.00623	4	Liver, spleen, lung, eye, tumors, heart [5, 243, 244, 256]
PFTP (Fluosol)		A=0.301 B=0.00312	3	rat spleen, lung, tumors, cells [232, 252, 406]
F-44E (Therox)		A=0.2525 B=0.16527	4	rat spleen, liver, aorta, mouse Tumors [235, 253]
PFOB (Imagent, Oxygen)		A=0.2677 B=0.12259	7	rat heart, rat prostate tumor, rabbit liver, pig lungs, phantom [241, 250, 432, 433]
PTBD		A=0.50104 B=0.1672	2	Phantom [434]

$$^a R_1 (\text{s}^{-1}) = A + B \cdot \text{pO}_2 (\text{torr})$$

Table 5 ^{19}F NMR Metal Ions Indicators [¶]

Detected Ion	Agent	Structure	$\delta_{\text{F(Ligand)}}$ (ppm)	$\Delta\delta$ (ppm)	Ref.
[Ca ²⁺] [Zn ²⁺] [Pb ²⁺] [Cd ²⁺] [Hg ²⁺] [Co ²⁺] [Ni ²⁺] [Fe ²⁺]	5FBAPTA		2.08 ^{¶¶}	5.8 3.7 4.6 4.8 5.3 28.1 32.4 31.1	[307]
[Mg ²⁺]	5FAPTRA		0.80 ^{¶¶}	8.00	[322]
[Na ⁺]	F-cryp-1		5.50	1.9	[410]
[Li ⁺] [Na ⁺] [K ⁺] [Rb ⁺]	F ₄ -Cage		-116.70	4.20 -13.5 -6.8 -4.2	[325]

[Li ⁺]	F ₂ -[2.1.1]-Cryptand		-100.70	28.53	[324]
[Na ⁺]	F ₂ -[3.1.1]-Cryptand		-105.80	-16.00	[324]
[K ⁺]	F ₆ -Carcerand		-110.50	-15.76	[325]
[Rb ⁺]	(FN ₂ O ₄) ₂		-124.46	5.40	[25, 314]
[Cs ⁺]	F(NO ₄) ₂		-123.70	5.50	[25, 314]
[Ca ²⁺]	F-[2.2.1]-Cryptand		-114.38	-11.90	[25, 314]
[Sr ²⁺]	HF-[3.1.1]-Cryptand		-110.38	-5.87	[324]

[Ba ²⁺]	F(NO ₃) ₂		-123.78	7.90	[25, 314]
---------------------	----------------------------------	---	---------	------	--------------

¶ Unless otherwise noted, CFCl₃ was used as a chemical shift standard, solvent: CH₃CN. ¶¶ 6-Fluorotryptophan was used as a chemical shift standard.

Table 6
¹⁹F NMR Hypoxia Indicators

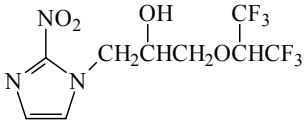
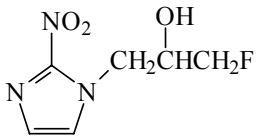
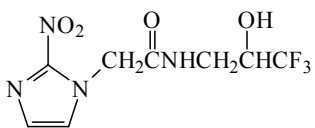
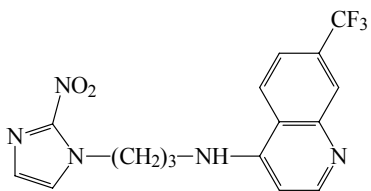
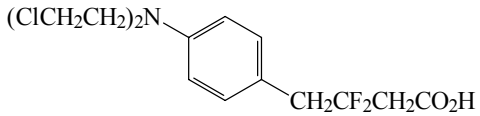
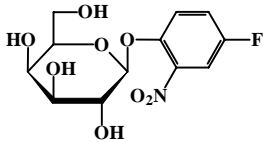
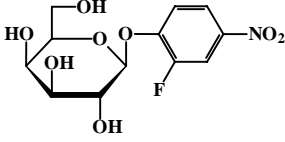
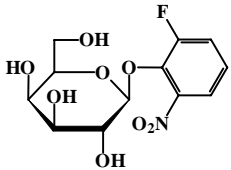
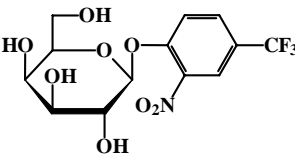
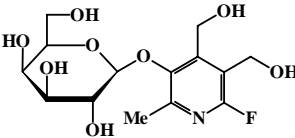
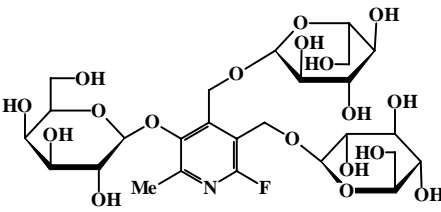
Name	Structure	Number of F atoms	Application
CCI 103F		6	Tumors, cells [353, 413]
RO 070741		1	Tumors, cells [354]
SR 4554		3	Tumors, cells [355, 356] [351]
NLTQ-1		3	Tumors, cells [435]
3,3-difluorochlorambucil		2 ABq	Tumors, cells [354]

Table 7 ^{19}F NMR lacZ Gene Reporters *

Reporter	Structure	$\delta_{\text{F(Substrate)}}$ (ppm)	$\delta_{\text{F(aglycone)}}$ (ppm)	$\Delta\delta$ (ppm)	References
PFONPG		-42.87	-52.71	-9.84	[374] [294]
OFPNPG		-54.93	-61.04	-6.11	[294] [375]
OFONPG		-50.67	-58.67	-8.00	[294]
PCF ₃ ONPG		13.40	14.54	1.14	[299]
GFPOL		-3.22	-11.21	-8.00	[377]
GDUFPOL		-2.85	-12.16	-9.31	[378]

* NaTFA was used as a chemical shift standard, in PBS (0.1M, pH = 7.4) buffer at 37 °C.

References

- [1] Z. Zhang, S. A. Nair and T. J. McMurry, Gadolinium Meets Medicinal Chemistry: MRI Contrast Agent Development, *Current Med. Chem.* 2005, **12**, 751-778.
- [2] C. Baudelet and B. Gallez, Current issues in the utility of blood oxygen level dependent MRI for the assessment of modulations in tumor oxygenation *Curr Med Imaging Rev.* 2005, **1**, 229-243.
- [3] D. Liebfritz in *Water suppression*, Vol. Eds.: J. D. de Certaines, W. M. M. J. Bovee and F. Podo), Pergamon, Oxford, **1992**, pp. 149-168.
- [4] D. O'Hagan and D. B. Harper, Fluorine-containing natural products, *J. Fluorine Chem.* 1999, **100**, 127-133.
- [5] S. R. Thomas in *The biomedical applications of Fluorine-19 NMR*, Vol. 2 Eds.: C. L. Partain, R. R. Price, J. A. Patton, M. V. Kulkarni and A. E. J. James), W.B. Saunders Co., London, **1988**, pp. 1536-1552.
- [6] B. S. Selinsky and C. T. Burt in *In vivo ¹⁹F NMR*, Vol. 11 Eds.: L. J. Berliner and J. Reuben), Plenum, New York, **1992**, pp. 241-276.
- [7] M. J. W. Prior, R. J. Maxwell and J. R. Griffiths in *Fluorine-¹⁹F NMR spectroscopy and imaging in-vivo*, Vol. (Ed. M. Rudin), Springer-Verlag, Berlin, **1992**, pp. 103-130.
- [8] R. E. London in *In vivo NMR studies utilizing fluorinated NMR probes*, Vol. (Ed. R. J. Gillies), Academic, San Diego, **1994**, pp. 263-277.
- [9] R. P. Mason, Non-invasive physiology: ¹⁹F NMR of perfluorocarbon, *Art. Cells, Blood Sub. & Immob. Biotech.* 1994, **22**, 1141-1153.
- [10] D. Zhao, L. Jiang and R. P. Mason, Measuring Changes in Tumor Oxygenation, *Methods Enzymol* 2004, **386**, 378-418.

- [11] R. P. Mason, Transmembrane pH gradients *in vivo*: measurements using fluorinated vitamin B6 derivatives, *Curr. Med. Chem.* 1999, **6**, 481-499.
- [12] P. M. J. McSheehy, L. P. Lemaire and J. R. Griffiths in *Fluorine-19 MRS: applications in oncology*, Vol. Eds.: D. M. Grant and R. K. Harris), Wiley, Chichester, **1996**, pp. 2048-2051.
- [13] D. K. Menon in *Fluorine-19 MRS: general overview and anesthesia*, Vol. (Ed. R. K. Harris), Wiley, Chichester, **1995**, pp. 2052-2063.
- [14] T. J. Passe, H. C. Charles, P. Rajagopalan and K. R. Krishnan, Nuclear magnetic resonance spectroscopy: a review of neuropsychiatric applications, *Nuclear magnetic resonance spectroscopy: a review of neuropsychiatric applications. Prog. Neuro-Psychopharmacol. Biol. Psych.* 1995, **19**, 541-563.
- [15] P. Bachert, Pharmacokinetics using fluorine NMR *in vivo*, *Prog. NMR Spectroscopy* 1998, **33**, 1-56.
- [16] R. Martino, M. Malet-Martino and V. Gilard, Fluorine nuclear magnetic resonance, a privileged tool for metabolic studies of fluoropyrimidine drugs, *Curr Drug Metab* 2000, **1**, 271-303.
- [17] W. Wolf, C. A. Presant and V. Waluch, ¹⁹F-MRS studies of fluorinated drugs in humans, *Adv. Drug Del. Rev.* 2000, **41**, 55-74.
- [18] J. X. Yu, V. Kodibagkar, W. Cui and R. P. Mason, ¹⁹F: a versatile reporter for non-invasive physiology and pharmacology using magnetic resonance, *Curr. Med. Chem.* 2005, **12**, 818-848.
- [19] H. J. Bohm, D. Banner, S. Bendels, M. Kansy, B. Kuhn, K. Muller, U. Obst-Sander and M. Stahl, Fluorine in medicinal chemistry, *Chembiochem* 2004, **5**, 637-643.

- [20] I. Ojima, Use of fluorine in the medicinal chemistry and chemical biology of bioactive compounds - A case study on fluorinated taxane anticancer agents, *Chembiochem* 2004, **5**, 628-635.
- [21] W. R. Dolbier, Fluorine chemistry at the millennium, *Journal of Fluorine Chemistry* 2005, **126**, 157-163.
- [22] B. K. Park, N. R. Kitteringham and P. M. O'Neill, Metabolism of fluorine-containing drugs, *Annual Review of Pharmacology and Toxicology* 2001, **41**, 443-470.
- [23] C. Jackel and B. Koksche, Fluorine in peptide design and protein engineering, *Eur. J. Org. Chem.* 2005, 4483-4503.
- [24] M. Shimizu and T. Hiyama, Modern synthetic methods for fluorine-substituted target molecules, *Angw. Chem.-Int. Ed.* 2005, **44**, 214-231.
- [25] H. Plenio, The coordination chemistry of fluorine in fluorocarbons, *Chembiochem* 2004, **5**, 650-655.
- [26] P. Jeschke, The unique role of fluorine in the design of active ingredients for modern crop protection, *Chembiochem* 2004, **5**, 570-589.
- [27] F. M. D. Ismail, Important fluorinated drugs in experimental and clinical use, *J. Fluorine Chem.* 2002, **118**, 27-33.
- [28] C. Isanbor and D. O'Hagan, Fluorine in medicinal chemistry: A review of anti-cancer agents, *J. Fluorine Chem.* 2006, **127**, 303-319.
- [29] C. E. Oyiliagu, M. Novalen and L. P. Kotra, Fluorine containing molecules for peptidomimicry: A chemical act to modulate enzymatic activity, *Mini-Rev. Organic Chem.* 2006, **3**, 99-115.

- [30] M. Zanda, Trifluoromethyl group: an effective xenobiotic function for peptide backbone modification, *New J. Chem.* 2004, **28**, 1401-1411.
- [31] <http://www.nibib.nih.gov/> in Vol. **2006**.
- [32] <http://imaging.cancer.gov/> in Vol. **2007**.
- [33] <http://www.molecularimaging.org>.
- [34] <http://www.ismrm.org/>.
- [35] <http://interactive.snm.org/> in Vol. **2007**.
- [36] R. P. Mason, S. Ran and P. E. Thorpe, Quantitative assessment of tumor oxygen dynamics: Molecular Imaging for Prognostic Radiology, *J. Cell. Biochem.* 2002, **87 suppl**, 45-53.
- [37] J. A. Karam, R. P. Mason, K. S. Koeneman, P. P. Antich, E. A. Benaim and J. T. Hsieh, Molecular imaging in prostate cancer, *J. Cell. Biochem.* 2003, **90**, 473-483.
- [38] C. H. Contag and B. D. Ross, It's not just about anatomy: In vivo bioluminescence imaging as an eyepiece into biology, *JMRI* 2002, **16**, 378-387.
- [39] R. Kumar and S. Jana, Positron emission tomography: an advanced nuclear medicine imaging technique from research to clinical practice., *Methods Enzymol.* 2004, **385**, 3-19.
- [40] <http://probes.invitrogen.com/handbook/> in Vol. **2007**.
- [41] <http://www.cri-inc.com/products/maestro.asp> in Vol. **2007**.
- [42] M. Oldham, H. Sakhalkar, T. Oliver, Y. M. Wang, J. Kirpatrick, Y. T. Cao, C. Badea, G. A. Johnson and M. Dewhirst, Three-dimensional imaging of xenograft tumors using optical computed and emission tomography, *Medical Physics* 2006, **33**, 3193-3202.
- [43] G. Zacharakis, H. Kambara, H. Shih, J. Ripoll, J. Grimm, Y. Saeki, R. Weissleder and V. Ntziachristos, Volumetric tomography of fluorescent proteins through small animals in vivo,

Proceedings of the National Academy of Sciences of the United States of America 2005, **102**, 18252-18257.

[44] A. M. Derfus, W. C. W. Chan and S. N. Bhatia, Probing the cytotoxicity of semiconductor quantum dots, *Nano Letters* 2004, **4**, 11-18.

[45] R. Hoffman, Green fluorescent protein imaging of tumour growth, metastasis, and angiogenesis in mouse models, *Lancet Oncol.* 2002, **3**, 546-556.

[46] C. H. Contag, S. D. Spilman, P. R. Contag, M. Oshiro, B. Eames, P. Dennerly, D. K. Stevenson and D. A. Benaron, Visualizing gene expression in living mammals using a bioluminescent reporter, *Photochem Photobiol.* 1997, **66**, 523-531.

[47] E. Richer, N. Slavine, M. A. Lewis, E. Tsyganov, G. C. Gellert, Z. Gunnur Dikmen, V. Bhagwandin, J. W. Shay, R. P. Mason and P. P. Antich, *Society of Molecular Imaging* (St. Louis) **2004**.

[48] F. Blankenberg, W. C. Eckelman, H. W. Strauss, M. J. Welch, A. Alavi, C. Anderson, S. Bacharach, R. G. Blasberg, M. M. Graham and W. Weber, Role of radionuclide imaging in trials of antiangiogenic therapy. [Review], *Acad. Radiol.* 2000, 851-867.

[49] U. Haberkorn, W. Mier and M. Eisenhut, Scintigraphic imaging of gene expression and gene transfer, *Curr. Med. Chem.* 2005, **12**, 779-794.

[50] D. Vranjesevic, J. E. Filmont, J. Meta, D. H. Silverman, M. E. Phelps, J. Rao, P. E. Valk and J. Czernin, Whole-body (18)F-FDG PET and conventional imaging for predicting outcome in previously treated breast cancer patients, *J. Nucl. Med.* 2002, **43**, 325-329.

[51] Y. Seo, B. L. Franc, R. A. Hawkins, K. H. Wong and B. H. Hasegawa, Progress in SPECT/CT imaging of prostate cancer, *Technology in Cancer Research & Treatment* 2006, **5**, 329-336.

- [52] C. Love, A. S. Din, M. B. Tomas, T. P. Kalapparambath and C. Palestro, Radionuclide bone imaging: An illustrative review, *Radiographics* 2003, **23**, 341-358.
- [53] E. Cherin, R. Williams, A. Needles, G. W. Liu, C. White, A. S. Brown, Y. Q. Zhou and F. S. Foster, Ultrahigh frame rate retrospective ultrasound microimaging and blood flow visualization in mice in vivo, *Ultrasound in Medicine and Biology* 2006, **32**, 683-691.
- [54] M. Tepel, P. Aspelin and N. Lameire, Contrast-induced nephropathy: a clinical and evidence-based approach., *Circulation* 2006 **113**, 1799-1806.
- [55] H. Mishima, T. Kobayashi, M. Shimizu, Y. Tamaki and M. Baba, In vivo F-19 chemical shift imaging with FTPA and antibody-coupled FMIQ, *JMRI* 1991, **1**, 705-709.
- [56] A. M. Morawski, P. M. Winter, X. Yu, R. Fuhrhop, M. J. Scott, F. Hockett, J. D. Robertson, P. J. Gaffney, G. M. Lanza and S. A. Wickline, Quantitative "magnetic resonance immunohistochemistry" with ligand-targeted (19)F nanoparticles., *Magn Reson Med* 2004, **52**, 1255-1262.
- [57] M. Higuchi, N. Iwata, Y. Matsuba, K. Sato, K. Sasamoto and T. C. Saido, F-19 and H-1 MRI detection of amyloid beta plaques in vivo, *Nature Neurosci.* 2005, **8**, 527-533.
- [58] R. K. Harris, E. D. Becker, S. M. Cabral de Menezes, R. Goodfellow and P. Granger, NMR nomenclature. Nuclear spin properties and conventions for chemical shifts (IUPAC Recommendations 2001) *Pure Appl. Chem.* 2001, **73**, 1795-1818.
- [59] F. A. Bovey, *Nuclear Magnetic Resonance Spectroscopy*, Academic Press, San Diego, **1988**, p. 653.
- [60] J. W. Emsley and L. Phillips, Fluorine chemical shifts, *Prog. NMR Spectrosc.* 1971, **7**, 1-520.

- [61] J. W. Emsley, L. Phillips and V. Wray, Fluorine coupling constants, *Prog. NMR Spec.* 1976, **10**, 83-756.
- [62] H. P. Shukla, R. P. Mason, D. E. Woessner and P. P. Antich, A comparison of three commercial perfluorocarbon emulsions as high field NMR probes of oxygen tension and temperature, *J. Magn. Reson. Series B* 1995, **106**, 131-114.
- [63] H. W. M. van Laarhoven, C. J. A. Punt, Y. J. L. Kamm and A. Heerschap, Monitoring fluoropyrimidine metabolism in solid tumors with in vivo ^{19}F magnetic resonance spectroscopy, *Crit. Rev. Oncol. /Hematol.* 2005, **56**, 321-343.
- [64] M. C. Malet-Martino, J. P. Armand, A. Lopez, J. Bernadou, J. P. Beteille, M. Bon and R. Martino, Evidence for the importance of 5'-deoxy-5-fluorouridine catabolism in humans from ^{19}F nuclear magnetic resonance spectrometry, *Cancer Res.* 1986, **46**, 2105-2112.
- [65] A. W. Blackstock, H. Lightfoot, L. D. Case, J. E. Tepper, S. K. Mukherji, B. S. Mitchell, S. G. Swarts and S. M. Hess, Tumor uptake and elimination of 2',2'-difluoro-2'-deoxycytidine (gemcitabine) after deoxycytidine kinase gene transfer: Correlation with in vivo tumor response, *Clin. Cancer Res.* 2001, **7**, 3263-3268.
- [66] G. S. Payne, D. J. Collins, P. Loynds, G. Mould, P. S. Murphy, A. S. K. Dzik-Jurasz, P. Kessar, N. Haque, M. Yamaguchi, S. Atarashi and M. O. Leach, Quantitative assessment of the hepatic pharmacokinetics of the antimicrobial sitafloxacin in humans using in vivo F-19 magnetic resonance spectroscopy, *Br. J. Clin. Pharmacol.* 2005, **59**, 244-248.
- [67] D. Bilecen, A. C. Schulte, A. Kaspar, E. Kustermann, J. Seelig, D. von Elverfeldt and K. Scheffler, Detection of the non-steroidal anti-inflammatory drug niflumic acid in humans: a combined F-19-MRS in vivo and in vitro study, *NMR Biomed.* 2003, **16**, 144-151.

- [68] E. Schneider, N. R. Bolo, B. Frederick, S. Wilkinson, F. Hirashima, L. Nassar, I. K. Lyoo, P. Koch, S. Jones, J. Hwang, Y. Sung, R. A. Villafuerte, G. Maier, R. Hsu, R. Hashoian and P. F. Renshaw, Magnetic resonance spectroscopy for measuring the biodistribution and in situ in vivo pharmacokinetics of fluorinated compounds: validation using an investigation of liver and heart disposition of tecastemizole, *J. Clin.Pharm. Therapeut.* 2006, **31**, 261-273.
- [69] R. Schwarz, A. Kaspar, J. Seelig and B. Kunnecke, Gastrointestinal transit times in mice and humans measured with ^{27}Al and ^{19}F nuclear magnetic resonance, *Magn. Reson. Med.* 2002, **48**, 255-261.
- [70] M. E. Henry, M. E. Schmidt, J. Hennen, R. A. Villafuerte, M. L. Butman, P. Tran, L. T. Kerner, B. Cohen and P. F. Renshaw, A Comparison of Brain and Serum Pharmacokinetics of R-Fluoxetine and Racemic Fluoxetine: A ^{19}F MRS Study, *Neuropsychopharmacol.* 2005, **30**, 1576-1583.
- [71] W. L. Strauss, A. S. Unis, C. Cowan, G. Dawson and S. R. Dager, Fluorine magnetic resonance spectroscopy measurement of brain fluvoxamine and fluoxetine in pediatric patients treated for pervasive developmental disorders, *Am. J. Psych.* 2002, **159**, 755-760.
- [72] J. D. Christensen, D. A. Yurgelun-Todd, S. M. Babb, S. A. Gruber, B. M. Cohen and P. F. Renshaw, Measurement of human brain dexfenfluramine concentration by ^{19}F magnetic resonance spectroscopy, *Brain Res.* 1999, **834**, 1-5.
- [73] Y. L. Chung, H. Troy, I. R. Judson, R. Leek, M. O. Leach, M. Stubbs, A. L. Harris and J. R. Griffiths, Noninvasive measurements of capecitabine metabolism in bladder tumors overexpressing thymidine phosphorylase by fluorine-19 magnetic resonance spectroscopy., *Clin. Cancer Res.* 2004 **10**, 3863-3870.

- [74] C. J. Deutsch and J. S. Taylor in *¹⁹F NMR measurements of intracellular pH*, Vol. (Ed. R. K. Gupta), CRC Press, Boca Raton, **1987**, pp. 55-73.
- [75] B. E. Smart, Fluorine substituent effects (on bioactivity), *J. Fluorine Chem.* 2001, **109**, 3-11.
- [76] G. Gerebtzoff, X. Li-Blatter, H. Fischer, A. Frentzel and A. Seelig, Halogenation of drugs enhances membrane binding and permeation, *Chembiochem* 2004, **5**, 676-684.
- [77] B. A. Shainyan, Y. S. Danilevich, A. A. Grigor'eva and Y. A. Chuvashov, Electrochemical fluorination of benzamide and acetanilide in anhydrous HF and in acetonitrile, *Russian J. Org. Chem. (Trans. Zh. Organ. Khim.)* 2004, **40**, 513-517.
- [78] G. A. Olah, M. Nojima and I. Kerekes, Synthetic methods and reactions. I. Selenium tetrafluoride and its pyridine complex. Convenient fluorinating agents for fluorination of ketones, aldehydes, amides, alcohols, carboxylic acids, and anhydrides, *J. Am. Chem. Soc.* 1974, **96**, 925-927.
- [79] A. Haas and T. Maciej, Fluorination by tungsten hexafluoride, *J. Fluorine Chem.* 1982, **20**, 581-587.
- [80] T. B. Patrick, L. Zhang and Q. Li, Rearrangement and double fluorination in the deiodinative fluorination of neopentyl iodide with xenon difluoride, *J. Fluorine Chem.* 2000, **102**, 11-15.
- [81] G. G. Belen'kii, V. A. Petrov and P. R. Resnick, Electrophilic, catalytic alkylation of polyfluoroolefins by some fluoroalkanes, *J. Fluorine Chem.* 2001, **108**, 15-20.
- [82] K. Adachi, Y. Ohira, G. Tomizawa, S. Ishihara and S. Oishi, Electrophilic fluorination with N,N'-difluoro-2,2'-bipyridinium salt and elemental fluorine, *J. Fluorine Chem.* 2003, **120**, 173-183.

- [83] V. Mehta, P. V. Kulkarni, R. P. Mason, A. Constantinescu and P. P. Antich, Novel molecular probes for ^{19}F magnetic resonance imaging: synthesis & characterization of fluorinated polymers, *Bioorg. Med. Chem. Lett.* 1992, **2**, 527-532.
- [84] J. Joubert, S. Roussel, C. Christophe, T. Billard, B. R. Langlois and T. Vidal, Trifluoroacetamides from amino alcohols as nucleophilic trifluoromethylating reagents, *Angew. Chem. Int. Ed.* 2003, **42**, 3133-3136.
- [85] J. S. Rasey, J. J. Casciari, P. D. Hofstrand, M. Muzi, M. M. Graham and L. K. Chin, Determining hypoxic fraction in a rat glioma by uptake of radiolabeled fluoromisonidazole, *Radiat Res* 2000, **153**, 84-92.
- [86] W. R. Dolbier, Jr. , A. R. Li, C. J. Koch, C. Y. Shiue and A. V. Kachur, [^{18}F]-EF5, a marker for PET detection of hypoxia: synthesis of precursor and a new fluorination procedure, *Appl. Radiat. Isotop.* 2001, **54**, 73-80.
- [87] C. S. Yap, J. Czernin, M. C. Fishbein, R. B. Cameron, C. Schiepers, M. E. Phelps and W. A. Weber, Evaluation of thoracic tumors with ^{18}F -fluorothymidine and ^{18}F -fluorodeoxyglucose-positron emission tomography, *Chest* 2006, **129**, 393-401.
- [88] P. Zanzonico, J. Campa, D. Polycarpe-Holman, G. Forster, R. Finn, S. Larson, J. Humm and C. Ling, Animal-specific positioning molds for registration of repeat imaging studies: comparative microPET imaging of F18-labeled fluoro-deoxyglucose and fluoro-misonidazole in rodent tumors, *Nucl. Med. Biol.* 2006 **33**, 65-70.
- [89] N. J. Spratt, U. Ackerman, H. J. Tochon-Danguy, G. A. Donnan and D. W. Howells, Characterization of fluoromisonidazole binding in stroke., *Stroke* 2006 **37**, 1862-1867.
- [90] J. Bussink, E. G. C. Troost, P. Laverman, M. Philipens, J. Lok, O. C. Boerman, J. Kaanders and A. J. van der Kogel, Characterization of human squamous cell head and neck

carcinoma xenografts using ^{18}F -FLT and ^{18}F -MISO autoradiography and immunohistochemistry, *Radiother. Oncol.* 2006, **78**, S33-S33.

[91] J. Keupp, P. C. Mazurkewitz, I. Gräßlin and T. Schaeffter, *Proc. Intl. Soc. Mag. Reson. Med.* **2006**, p. 102.

[92] G. Schnur, R. Kimmich and R. Lietzenmayer, Hydrogen/Fluorine retuning tomography. Applications to ^1H image-guided volume-selective ^{19}F spectroscopy and relaxometry of perfluorocarbon emulsions in tissue, *Magn. Reson. Med.* 1990, **13**, 478-489.

[93] J. Sanders and B. Hunter, *Modern NMR Spectroscopy*, Oxford University Press, New York, **1987**, p. 308.

[94] R. P. Mason, G. Cha, G. H. Gorrie, E. E. Babcock and P. P. Antich, Glutathione in whole blood: a novel determination using double quantum coherence transfer proton NMR spectroscopy, *FEBS Letters* 1993, **318**, 30-34.

[95] R. E. Hurd and D. M. Freeman, Metabolite Specific Proton Magnetic-Resonance Imaging, *Proc. Natl. Acad. Sci. (USA)* 1989, **86**, 4402-4406.

[96] R. P. Mason and J. K. M. Sanders, *In vivo* enzymology: a deuterium NMR study of formaldehyde dismutase in *Pseudomonas putida* F61a and *Staphylococcus aureus*, *Biochemistry* 1989, **28**, 2160-2168.

[97] R. P. Mason, J. K. M. Sanders, A. Crawford and B. K. Hunter, Formaldehyde metabolism by *E. Coli*: detection using *in vivo* ^{13}C NMR spectroscopy of $\underline{\text{S}}$ -(hydroxymethyl) glutathione as a transient intracellular intermediate, *Biochemistry*, 1986, **25**, 4504-4507.

[98] R. F. Code, J. E. Harrison, K. G. McNeill and M. Szykowski, *In vivo* ^{19}F spin relaxation in index finger bones, *Mag. Reson. Med.* 1990, **13**, 358-369.

- [99] D. W. J. Klomp, H. W. M. van Laarhoven, A. P. M. Kentgens and A. Heerschap, Optimization of localized F-19 magnetic resonance spectroscopy for the detection of fluorinated drugs in the human liver, *Magn. Reson. Med.* 2003, **50**, 303-308.
- [100] A. V. Ratner, S. Quay, H. H. Muller, B. B. Simpson, R. Hurd and S. W. Young, ^{19}F relaxation rate enhancement and frequency shift with Gd-DTPA, *Invest. Radiol.* 1989, **24**, 224-227.
- [101] V. D. Mehta, R. P. Mason, P. V. Kulkarni, P. Lea, A. Constantinescu and P. P. Antich in *^{19}F MR characterization of fluorinated proteins and relaxation rate enhancement with Gd-DTPA for faster imaging*, Vol. (Ed. E. H. Emram), Plenum, New York, **1995**, pp. 305-313.
- [102] H. Lee, R. R. Price, G. E. Holburn, C. L. Partain, M. D. Adams and W. P. Cacheris, In-Vivo F-19 MR-Imaging - Relaxation Enhancement with Gd-DTPA, *J. Magn. Reson. Imaging* 1994, **4**, 609-613.
- [103] G. Brix, M. E. Bellemann, L. Gerlach and U. Haberkorn, Intra- and extracellular fluorouracil uptake: assessment with contrast-enhanced metabolic F-19 MR imaging, *Radiology* 1998, **209**, 259-267.
- [104] B. S. Y. Li, G. S. Payne, D. J. Collins and M. O. Leach, H-1 decoupling for in vivo F-19 MRS studies using the time-share modulation method on a clinical 1.5 T NMR system, *Magnetic Resonance in Medicine* 2000, **44**, 5-9.
- [105] R. D. Kendrick and C. S. Yannoni, High-Power H-1-F-19 Excitation in a Multiple-Resonance Single-Coil Circuit, *J. Magn. Reson.* 1987, **75**, 506-508.
- [106] H. B. Lantum, R. B. Baggs, D. M. Krenitsky and M. W. Anders, Nephrotoxicity of chlorofluoroacetic acid in rats, *Toxicol. Sci.* 2002, **70**, 261-268.

- [107] B. Hassel, U. Sonnewald, G. Unsgard and F. Fonnum, Nmr-Spectroscopy of Cultured Astrocytes - Effects of Glutamine and the Gliotoxin Fluorocitrate, *J. Neurochem.* 1994, **62**, 2187-2194.
- [108] R. L. Frost, R. W. Parker and J. V. Hanna, Detection of the Pesticide Compound-1080 (Sodium Monofluoroacetate) Using F-19 Nuclear Magnetic-Resonance Spectroscopy, *Analyst* 1989, **114**, 1245-1248.
- [109] O. Corcoran, J. C. Lindon, R. Hall, I. M. Ismail and J. K. Nicholson, The potential of F-19 NMR spectroscopy for rapid screening of cell cultures for models of mammalian drug metabolism, *Analyst* 2001, **126**, 2103-2106.
- [110] M. Spraul, M. Hofmann, I. D. Wilson, E. Lenz, J. K. Nicholson and J. C. Lindon, Coupling of Hplc with F-19-NMR and H-1-NMR Spectroscopy to Investigate the Human Urinary-Excretion of Flurbiprofen Metabolites, *J.Pharmaceut. Biomed. Anal.* 1993, **11**, 1009-1015.
- [111] M. E. Bollard, E. Holmes, C. A. Blackledge, J. C. Lindon, I. D. Wilson and J. K. Nicholson, H-1 and F-19-nmr spectroscopic studies on the metabolism and urinary excretion of mono- and disubstituted phenols in the rat, *Xenobiotica* 1996, **26**, 255-273.
- [112] A. Preiss, J. Kruppa, J. Buschmann and C. Mugge, The determination of trifluoroacetic acid in rat milk samples by F-19-NMR spectroscopy and capillary gas chromatography, *J. Pharmaceut. Biomed. Anal.* 1998, **16**, 1381-1385.
- [113] M. Tugnait, E. M. Lenz, M. Hofmann, M. Spraul, I. D. Wilson, J. C. Lindon and J. K. Nicholson, The metabolism of 2-trifluormethylaniline and its acetanilide in the rat by ¹⁹F NMR monitored enzyme hydrolysis and ¹H/¹⁹F HPLC-NMR spectroscopy, *J. Pharmaceut. Biomed. Anal.* 2003, **30**, 1561-1574.

- [114] C. J. Duckett, J. C. Lindon, H. Walker, F. Abou-Shakra, I. D. Wilson and J. K. Nicholson, Metabolism of 3-chloro-4-fluoroaniline in rat using [C-14]-radiolabelling, F-19-NMR spectroscopy, HPLC-MS/MS, HPLC-ICPMS and HPLC-NMR, *Xenobiotica* 2006, **36**, 59-77.
- [115] C. A. Blackledge, J. K. Nicholson, J. A. Evans, C. Rodgers and I. D. Wilson, Application of H-1- and F-19-NMR spectroscopy in the investigation of the urinary and biliary excretion of 3,5-, 2,4-ditrifluoromethylbenzoic and pentafluorobenzoic acids in rat, *Xenobiotica* 2002, **32**, 605-613.
- [116] B. W. Dubois and A. S. Evers, ¹⁹F-NMR spin-spin relaxation (T₂) method for characterizing volatile anesthetic binding to proteins. Analysis of isoflurane binding to serum albumin., *Biochemistry*. 1992, **31**, 7069-7076.
- [117] W. M. Chew, M. E. Moseley, P. A. Mills, D. Sessler, R. Gonzalez-Mendez, T. L. James and L. Litt, Spin-echo fluorine magnetic resonance imaging at 2 T: in vivo spatial distribution of halothane in the rabbit head, *Magn. Reson. Imaging* 1987, **5**, 51-56.
- [118] D. K. Menon, G. G. Lockwood, C. J. Peden, I. J. Cox, J. Sargentoni, J. D. Bell, G. A. Coutts and J. G. Whitwam, In-Vivo F-19 Magnetic-Resonance Spectroscopy of Cerebral Halothane in Postoperative-Patients - Preliminary-Results, *Magn. Reson. Med.* 1993, **30**, 680-684.
- [119] E. E. Babcock, J. T. Vaughan, B. Lesan and R. L. Nunnally, Multinuclear NMR Investigations of Probe Construction Materials at 4.7-T, *Magn. Reson. Med.* 1990, **13**, 498-503.
- [120] T. A. Morinelli, A. K. Okwu, D. E. Mais, P. V. Halushka, V. John, C. K. Chen and J. Fried, Difluorothromboxane-A₂ and Stereoisomers - Stable Derivatives of Thromboxane-A₂ with

Differential-Effects on Platelets and Blood-Vessels, *Proc. Natl.Acad. Sci. (USA)* 1989, **86**, 5600-5604.

[121] R. A. Dwek in *The use of fluorine-19 as a detecting shift probe*, Vol. (Ed. R. A. Dwek), Clarendon, Oxford, **1975**, pp. 158-173.

[122] J. T. Gerig, Fluorine magnetic resonance of fluorinated ligands, *Methods Enzymol* 1989, **177**, 3-23.

[123] W. H. Huestis and M. A. Raftery, Study of cooperative interactions in hemoglobin using fluorine nuclear magnetic resonance, *Biochemistry* 1972 **11** 1648 - 1654

[124] F. Millett and M. A. Raftery, Fluorine-19 nuclear magnetic resonance study of the binding of trifluoroacetylglucosamine oligomers to lysozyme, *Biochemistry* 1972, **11** 1639 - 1643

[125] S. G. Withers, K. Rupitz and I. P. Street, 2-Deoxy-2-Fluoro-D-Glycosyl Fluorides - a New Class of Specific Mechanism-Based Glycosidase Inhibitors, *J. Biol. Chem.* 1988, **263**, 7929-7932.

[126] S. G. Withers, I. P. Street and M. D. Percival, Fluorinated Carbohydrates as Probes of Enzyme Specificity and Mechanism, *ACS Symposium Series* 1988, **374**, 59-77.

[127] W. G. Stirtan and S. G. Withers, Phosphonate and alpha-fluorophosphonate analogue probes of the ionization state of pyridoxal 5'-phosphate (PLP) in glycogen phosphorylase, *Biochemistry* 1996, **35**, 15057-15064.

[128] P. Szczecinski and D. Bartusik, F-19 NMR measurements - A potential tool for the determination of amino acids in body fluids, *Polish Journal of Chemistry* 2003, **77**, 321-328.

[129] L. A. Sylvia and J. T. Gerig, Fluorine Nmr-Studies of the Metabolism of Flumecinol (3-Trifluoromethyl-Alpha-Ethylbenzhydrol), *Drug Metabolism and Disposition* 1993, **21**, 105-113.

- [130] U. Sidelmann, S. H. Hansen, C. Gavaghan, A. W. Nicholls, H. A. J. Carless, J. C. Lindon, I. D. Wilson and J. K. Nicholson, Development of a simple liquid chromatographic method for the separation of mixtures of positional isomers and anomers of synthetic 2-, 3- and 4-fluorobenzoic acid glucuronides formed via acyl migration reactions, *Journal of Chromatography B: Biomedical Sciences and Applications* 1996, **685**, 113-122.
- [131] G. B. Scarfe, M. Tugnait, I. D. Wilson and J. K. Nicholson, Studies on the metabolism of 4-fluoroaniline and 4-fluoroacetanilide in rat: formation of 4-acetamidophenol (paracetamol) and its metabolites via defluorination and N-acetylation, *Xenobiotica* 1999, **29**, 205-216.
- [132] M. K. Ellis, J. L. Naylor, T. Green and M. A. Collins, Identification and Quantification of Fluorine-Containing Metabolites of 1-Chloro-2,2,2-Trifluoroethane (Hcfc133a) in the Rat by F-19-Nmr Spectroscopy, *Drug Metabolism and Disposition* 1995, **23**, 102-106.
- [133] C. Heidelberger, Fluorinated pyrimidines, a new class of tumour-inhibitory compounds, *Nature Chem. Biol.* 1957, **179** 663.
- [134] C. A. Presant, W. Wolf, V. Waluch, C. Wiseman, P. Kennedy, D. Blayney and R. R. Brechner, Association of intratumoral pharmacokinetics of fluorouracil with clinical response, *The Lancet* 1994, **343**, 1184-1187.
- [135] G. F. J. Peters, Fluorouracil: biochemistry and pharmacology, *J. Clin. Oncol.* 1988, **6**, 1653-1664.
- [136] G. Brix, M. E. Bellemann, U. Haberkorn, L. Gerlach and W. J. Lorenz, Assessment of the biodistribution of 5-fluorouracil as monitored by ¹⁸F PET and ¹⁹F MRI: a comparative animal study, *Nucl. Med. Biol.* 1996, **23**, 897-906.

- [137] G. Brix, M. E. Bellemann, L. Gerlach and U. Haberkorn, Direct detection of intratumoral 5-fluorouracil trapping using metabolic F-19 MR imaging, *Magn. Reson. Imaging* 1999, **17**, 151-155.
- [138] G. Brix, M. E. Bellemann, U. Haberkorn, L. Gerlach, P. Bachert and W. J. Lorenz, Mapping the Biodistribution and Catabolism of 5-Fluorouracil in Tumor-Bearing Rats by Chemical-Shift Selective F-19 MR-Imaging, *Magn. Reson. Med.* 1995, **34**, 302-307.
- [139] J.-L. Guerquin-Kern, F. Leteurtre, A. Croisy and J.-M. Lhoste, pH dependence of 5-fluorouracil uptake observed by *in vivo* ^{31}P and ^{19}F NMR spectroscopy, *Cancer Res.* 1991, **51**, 5770-5773.
- [140] A. S. E. Ojugo, P. M. J. McSheehy, M. Stubbs, G. Alder, C. L. Bashford, R. J. Maxwell, M. O. Leach, I. R. Judson and J. R. Griffiths, Influence of pH on the uptake of 5-fluorouracil into isolated tumour cells, *Br. J. Cancer* 1998, **77**, 873-879.
- [141] P. M. J. McSheehy, S. P. Robinson, A. S. E. Ojugo, E. O. Aboagye, M. B. Cannell, M. O. Leach, I. R. Judson and J. R. Griffiths, Carbogen breathing increases 5-Fluorouracil uptake and cytotoxicity in hypoxic Rif-1 tumors: a magnetic resonance study *in vivo*, *Cancer Res.* 1998, **58**, 1185-1194.
- [142] J. R. Griffiths, D. J. O. McIntyre, F. A. Howe, P. M. J. McSheehy, A. S. E. Ojugo, L. M. Rodrigues, P. Wadsworth, N. M. Price, F. Lofts, G. Nicholson, K. Smid, P. Noordhuis, G. J. Peters and M. Stubbs, Issues of normal tissue toxicity in patient and animal studies - Effect of carbogen breathing in rats after 5-fluorouracil treatment, *Acta Oncologica* 2001, **40**, 609-614.
- [143] H. van Laarhoven, G. Gambarota, J. Lok, M. Lammens, Y. Kamm, T. Wagener, C. Punt, A. van der Kogel and A. Heerschap, *Proc. Intl. Soc. Mag. Reson. Med. (Seattle)* **2006**, p. 1766.

- [144] P. E. Sijens, N. J. Baldwin and T. C. Ng, Multinuclear MR investigation of the metabolic response of murine RIF-1 tumor to 5-fluorouracil chemotherapy, *Magn. Reson. Med.* 1991, **19**, 337-385.
- [145] N. W. Lutz and W. E. Hull, Assignment and pH dependence of the ^{19}F -NMR resonances from the fluorouracil anabolites involved in fluoropyrimidine chemotherapy, *NMR Biomed.* 1999, **12**, 237-248.
- [146] S. O. Freytag, M. Khil, H. Stricker, J. Peabody, M. Menon, M. DePeralta-Venturina, D. Nafziger, J. Pegg, D. Paielli, S. Brown, K. Barton, M. Lu, E. Aguilar-Cordova and J. H. Kim, Phase I study of replication-competent adenovirus-mediated double suicide gene therapy for the treatment of locally recurrent prostate cancer., *Cancer Res.* 2002, **62**, 4968-4976.
- [147] L. D. Stegman, A. Rehemtulla, B. Beattie, E. Kievit, T. S. Lawrence, R. G. Blasberg, J. G. Tjuvajev and B. D. Ross, Noninvasive quantitation of cytosine deaminase transgene expression in human tumor xenografts with in vivo magnetic resonance spectroscopy, *PNAS (USA)* 1999, **96**, 9821-9826.
- [148] L. D. Stegman, A. Rehemtulla, D. A. Hamstra, D. J. Rice, S. J. Jonas, K. L. Stout, T. L. Chenevert and B. D. Ross, Diffusion MRI detects early events in the response of a glioma model to the yeast cytosine deaminase gene therapy strategy, *Gene Ther.* 2000, **7**, 1005-1010.
- [149] M. Aghi, C. M. Kramm, T. C. Chou, X. O. Breakefield and E. A. Chiocca, Synergistic anticancer effects of ganciclovir/thymidine kinase and 5-fluorocytosine/cytosine deaminase gene therapies, *J Natl Cancer Inst* 1998, **90**, 370-380.
- [150] H. Corban-Wilhelm, W. E. Hull, G. Becker, U. Bauder-Wust, D. Greulich and J. Debus, Cytosine deaminase and thymidine kinase gene therapy in a Dunning rat prostate tumour

model: absence of bystander effects and characterisation of 5-fluorocytosine metabolism with ^{19}F -NMR spectroscopy., *Gene Therapy* 2002, **9**, 1564-1575.

[151] T. Dresselaers, J. Theys, L. Dubois, W. Landuyt, P. Van Hecke and P. Lambin, *Proc. Intl. Soc. Mag. Reson. Med.* **2006**, p. 3175.

[152] G. O. Cron, N. Beghein, R. Ansiaux and B. Gallez, *Proc. Intl. Soc. Mag. Reson. Med.* (Seattle) **2006**, p. 1764.

[153] M. E. Bellemann, U. Haberkorn, L. Gerlach, J. Blatter and G. Brix, *7th Scientific Meeting ISMRM* (Philadelphia, PA) **1999**, p. 1352.

[154] P. M. J. McSheehy, A. S. E. Ojugo, M. O. Leach, I. R. Judson and J. R. Griffiths, *7th annual meeting ISMRM* (Philadelphia) **1999**, p. 1347.

[155] G. Brix, A. Schlicker, W. Mier, P. Peschke and M. E. Bellemann, Biodistribution and pharmacokinetics of the F-19-labeled radiosensitizer 3-aminobenzamide: assessment by F-19 MR imaging, *Magn. Reson. Imaging* 2005, **23**, 967-976.

[156] W. M. Spees, T. P. F. Gade, G. L. Yang, W. P. Tong, W. G. Bornmann, R. Gorlick and J. A. Koutcher, An F-19 magnetic resonance-based in vivo assay of solid tumor methotrexate resistance: Proof of principle, *Clin. Cancer Res.* 2005, **11**, 1454-1461.

[157] T. Tengel, T. Fex, H. Emtenas, F. Almqvist, I. Sethson and J. Kihlberg, Use of F-19 NMR spectroscopy to screen chemical libraries for ligands that bind to proteins, *Org. Biomolec. Chem.* 2004, **2**, 725-731.

[158] T. Tarrago, S. Frutos, R. A. Rodriguez-Mias and E. Giralt, Identification by F-19 NMR of traditional chinese medicinal plants possessing prolyl oligopeptidase inhibitory activity, *Chembiochem* 2006, **7**, 827-833.

- [159] S. Frutos, T. Tarrago and E. Giralt, A fast and robust F-19 NMR-based method for finding new HIV-1 protease inhibitors, *Bioorganic & Medicinal Chemistry Letters* 2006, **16**, 2677-2681.
- [160] L. P. Yu, P. J. Hajduk, J. Mack and E. T. Olejniczak, Structural studies of Bcl-xL/ligand complexes using F-19 NMR, *J. Biomolec. NMR* 2006, **34**, 221-227.
- [161] M. Bartels and K. Albert, Detection of psychoactive drugs using 19F MR spectroscopy. , *J Neural Transm Gen Sect.* 1995. , **99**, 1-6.
- [162] N. R. Bolo, Y. Hode and J. P. Macher, Long-term sequestration of fluorinated compounds in tissues after fluvoxamine or fluoxetine treatment: a fluorine magnetic resonance spectroscopy study in vivo., *Magma* 2004, **16**, 268-276.
- [163] W. L. Strauss, M. E. Layton and S. R. Dager, Brain Elimination Half-Life of Fluvoxamine Measured by 19F Magnetic Resonance Spectroscopy, *Am. J. Psych.* 1998, **155**, 380-384.
- [164] D. M. Lindquist, M. Dachtler, R. M. Hawk, C. N. Karson, K. Albert and R. A. Komoroski, Contribution of trifluoperazine metabolites to the in vivo F-19 NMR spectrum of rat brain, *Magn. Reson. Med.* 2000, **43**, 756-759.
- [165] T. Sassa, T. Suhara, H. Ikehira, T. Obata, F. Girard, S. Tanada and Y. Okubo, 19F-magnetic resonance spectroscopy and chemical shift imaging for schizophrenic patients using haloperidol decanoate. , *Psych. Clin. Neurosci.* 2002, **56**, 637-642.
- [166] P. Jynge, T. Skjetne, I. Gribbestad, C. H. Kleinbloesem, H. F. W. Hoogkamer, O. Antonsen, J. Krane, O. E. Bakoy, K. M. Furuheim and O. G. Nilsen, Invivo Tissue Pharmacokinetics by Fluorine Magnetic-Resonance Spectroscopy - a Study of Liver and Muscle Disposition of Fleroxacin in Humans, *Clin. Pharmacol. Therapeut.* 1990, **48**, 481-489.
- [167] O. Saether, A. Midelfart, O. Risa, O. Haraldseth and J. Krane, Proton decoupled F-19 NMR spectroscopy of drugs used in eye treatment, *Spectroscopy Letters* 2006, **39**, 135-144.

- [168] B. Gewiese, W. Noske, A. Schilling, D. Stiller, K. Wolf and M. Foerster, Human eye: visualization of perfluorodecalin with F-19 MR imaging, *Radiology* 1992, **185**, 131-133.
- [169] C. Wilson, B. Berkowitz, B. McCuen and C. Charles, Measurement of preretinal pO₂ in the vitrectomized human eye using ¹⁹F NMR, *Arch. Ophthalmol* 1992, **110**, 1098-1100.
- [170] R. P. Mason, E. E. Babcock, R. L. Nunnally and A. P. P., *Proc. XIII International Congress of Magnetic Resonance in Biological Systems* (Madison, WI) **1988**.
- [171] R. Nunnally, P. Antich, P. Nguyen, E. Babcock, G. McDonald and R. Mason, Fluosol adjuvant therapy in human cancer: examinations *in vivo* of perfluorocarbons by F-19 NM, *Proc. SMRM 7th Meeting San Francisco* 1988, 342.
- [172] A. M. Wyrwicz and C. B. Conboy, Multiecho ¹⁹F NMR imaging of halothane in rabbit brain., *Proc. 7th SMRM San Francisco* 1988, 597.
- [173] T. Takeda, K. Makita, S. Ishikawa, K. Kaneda, K. Yokoyama and K. Amaha, Uptake and elimination of sevoflurane in rabbit tissues - an *in vivo* magnetic resonance spectroscopy study, *Canadian Journal of Anaesthesia-Journal Canadien D Anesthesie* 2000, **47**, 579-584.
- [174] Y. Xu, P. Tang, W. G. Zhang, L. Firestone and P. M. Winter, F-19 Nuclear-Magnetic-Resonance Imaging and Spectroscopy of Sevoflurane Uptake, Distribution, and Elimination in Rat-Brain, *Anesthesiology* 1995, **83**, 766-774.
- [175] P. N. Venkatasubramanian, Y. J. Shen and A. M. Wyrwicz, *In vivo* ¹⁹F one-dimensional chemical shift imaging study of isoflurane uptake in rabbit brain., *NMR Biomed.* 1993, **6**, 377-382.
- [176] G. G. Lockwood, D. P. Dob, D. J. Bryant, J. A. Wilson, J. Sargentoni, S. M. SapsedByrne, D. N. F. Harris and D. K. Menon, Magnetic resonance spectroscopy of

isoflurane kinetics in humans .1. Elimination from the head, *Br. J. Anaesthes.* 1997, **79**, 581-585.

[177] B. S. Selinsky, M. E. Perlman and R. E. London, In vivo nuclear magnetic resonance studies of hepatic methoxyflurane metabolism. I. Verification and quantitation of methoxydifluoroacetate, *Molec. Pharmacol.* 1988, **33**, 559-566.

[178] B. S. Selinsky, M. E. Perlman and R. E. London, In vivo nuclear magnetic-resonance studies of hepatic methoxyflurane metabolism .2. A reevaluation of hepatic metabolic pathways, *Molec. Pharmacol.* **1988**, **33**, 567-573.

[179] E. P. Mazzola, A. P. Borsetti, S. W. Page and D. W. Bristol, Determination of Pesticide-Residues in Foods by F-19 Fourier-Transform Nuclear Magnetic-Resonance Spectroscopy, *Journal of Agricultural and Food Chemistry* 1984, **32**, 1102-1103.

[180] R. D. Mortimer and B. A. Dawson, Using F-19 Nmr for Trace Analysis of Fluorinated Pesticides in Food-Products, *Journal of Agricultural and Food Chemistry* 1991, **39**, 1781-1785.

[181] Z. Zuo, G. Kwon, B. Stevenson, J. Diakur and L. I. Wiebe, Flutamide - Hydroxypropyl-beta-cyclodextrin complex: Formulation, physical characterization, and absorption studies using the Caco-2 in vitro model, *J. Pharm. Pharmaceut. Sci.* 2000, **3**, 220-227.

[182] M. Masson, J. F. Sigurjonsdottir, S. Jonsdottir and T. Loftsson, Examination of F-19-NMR as a tool for investigation of drug-cyclodextrin complexes, *Drug Dev. Ind. Pharm.* 2003, **29**, 107-112.

[183] J. Fukuchi, J. M. Kokontis, R. A. Hiipakka, C. P. Chuu and S. Liao, Antiproliferative effect of liver X receptor agonists on LNCaP human prostate cancer cells., *Cancer Res.* 2004 **64**, 7686-7689.

- [184] E. K. Rofstad and T. Danielsen, Hypoxia-induced metastasis of human melanoma cells: involvement of vascular endothelial growth factor-mediated angiogenesis, *Br. J. Cancer* 1999., **80**, 1697-1707.
- [185] M. Höckel and P. Vaupel, Tumor Hypoxia: Definitions and Current Clinical, Biologic, and Molecular Aspects, *J Natl Cancer Inst* 2001, **93**, 266-276.
- [186] J. Folkman, Angiogenesis and apoptosis, *Seminars in Cancer Biol.* 2003, **13**, 159-167.
- [187] H. J. Knowles and A. L. Harris, Hypoxia and oxidative stress in breast cancer. Hypoxia and tumourigenesis. [Review], *Breast Cancer Res.* 2001., **3**, 318-322.
- [188] L. Gray, A. Conger, M. Ebert, S. Hornsey and O. Scott, The concentration of oxygen dissolved in tissues at time of irradiation as a factor in radiotherapy, *Br. J. Radiol* 1953, **26**, 638-648.
- [189] J. L. Tatum, G. J. Kelloff, R. J. Gillies, J. M. Arbeit, J. M. Brown, K. S. Chao, J. D. Chapman, W. C. Eckelman, A. W. Fyles, A. J. Giaccia, R. P. Hill, C. J. Koch, M. C. Krishna, K. A. Krohn, J. S. Lewis, R. P. Mason, G. Melillo, A. R. Padhani, G. Powis, J. G. Rajendran, R. Reba, S. P. Robinson, G. L. Semenza, H. M. Swartz, P. Vaupel, D. Yang, B. Croft, J. Hoffman, G. Liu, H. Stone and D. Sullivan, Hypoxia: Importance in tumor biology, noninvasive measurement by imaging, and value of its measurement in the management of cancer therapy, *Int. J. Radiat. Biol.* 2006, **82**, 699 - 757.
- [190] J. M. Brown, Exploiting the hypoxic cancer cell: mechanisms and therapeutic strategies, *Molec. Med. Today* 2000, **6**, 157-162.
- [191] H. M. Swartz and J. F. Dunn in *Measurements of oxygen in tissues: overview and perspectives on methods*, Vol. 530 Eds.: J. F. Dunn and H. M. Swartz), Kluwer Academic, New York, **2003**, pp. 1-12.

- [192] H. B. Stone, J. M. Brown, T. Phillips and R. M. Sutherland, Oxygen in human tumors: correlations between methods of measurement and response to therapy, *Radiat. Res.* 1993, **136**, 422-434.
- [193] H. Liu, Y. Gu, J. G. Kim and R. P. Mason, Near Infrared Spectroscopy and Imaging of Tumor Vascular Oxygenation, *Methods Enzymol.* 2004, **386**, 349-378.
- [194] R. P. Mason, Non-Invasive assessment of kidney oxygenation: a role for BOLD MRI, *Kidney Internat.* 2006, **70**, 10–11.
- [195] S. H. Yee, K. Lee, P. A. Jerabek and P. T. Fox, Quantitative measurement of oxygen metabolic rate in the rat brain using microPET imaging of briefly inhaled ^{15}O -labelled oxygen gas., *Nucl Med Commun* 2006 **27**, 573-581.
- [196] J. P. Coles, T. D. Fryer, P. G. Bradley, J. Nortje, P. Smielewski, K. Rice, J. C. Clark, J. D. Pickard and D. K. Menon, Intersubject variability and reproducibility of ^{15}O PET studies., *J Cereb Blood Flow Metab* 2006 **26**, 48-57.
- [197] C. J. Koch, Measurement of absolute oxygen levels in cells and tissues using oxygen sensors and 2 -nitroimidazole EF5, *Methods Enzymol.* 2002, **352**, 3-31.
- [198] J. A. Raleigh, S. C. Chou, G. E. Arteel and M. Horsman, Comparison among pimonidazole binding, oxygen electrode measurements, and radiation response in C3H mouse tumors, *Radiat. Res.* 1999, **151**, 580-589.
- [199] C. Song, I. Lee, T. Hasegawa, J. Rhee and S. Levitt, Increase in pO_2 and radiosensitivity of tumors by Fluosol and carbogen, *Cancer Res.* 1987, **47**, 442-446.
- [200] J. G. Kim, D. Zhao, A. Constantinescu, R. P. Mason and H. Liu, Interplay of Tumor Vascular Oxygenation and Tumor pO_2 Observed Using NIRS, Oxygen Needle Electrode, and ^{19}F MR pO_2 Mapping, *J. Biomed. Optics* 2003, **8**, 53-62.

- [201] Y. Gu, V. Bourke, J. G. Kim, A. Constantinescu, R. P. Mason and H. Liu, Dynamic Response of Breast Tumor Oxygenation to Hyperoxic Respiratory Challenge Monitored with Three Oxygen-Sensitive Parameters, *Applied Optics* 2003, **42**, 1-8.
- [202] B. Gallez, C. Baudelet and B. F. Jordan, Assessment of tumor oxygenation by electron paramagnetic resonance: principles and applications, *NMR Biomed.* 2004, **17**, 240 - 262.
- [203] P. Parhami and B. N. Fung, Fluorine-19 relaxation study of perfluorochemicals as oxygen carriers, *J. Phys. Chem.* 1983, **87**, 1928-1931.
- [204] S. R. Thomas, R. G. Pratt, R. W. Millard, R. C. Samaratunga, Y. Shiferaw, L. C. Clark Jr. and R. E. Hoffmann, Evaluation of the Influence of the Aqueous Phase Bioconstituent Environment on the F-19 T1 of Perfluorocarbon Blood Substitute Emulsions, *JMRI* 1994, **4**, 631-635.
- [205] C.-S. Lai, S. Stair, H. Miziorko and J. S. Hyde, Effect of oxygen and the spin label TEMPO-Laurate on ^{19}F and proton relaxation rates of the perfluorochemical blood substitute FC-43 emulsion, *J. Magn. Reson.* 1984, **57**, 447-452.
- [206] D. Eidelberg, G. Johnson, D. Barnes, P. S. Tofts, D. Delpy, D. Plummer and W. I. McDonald, ^{19}F NMR imaging of blood oxygenation in the brain, *Magn. Reson. Med.* 1988, **6**, 344-352.
- [207] R. P. Mason, H. P. Shukla and P. P. Antich, *In vivo* oxygen tension and temperature: Simultaneous determination using ^{19}F spectroscopy of perfluorocarbon, *Magn. Reson. Med.* 1993, **29**, 296-302.
- [208] S. R. Thomas, R. G. Pratt, R. W. Millard, R. C. Samaratunga, Y. Shiferaw, A. J. McGoron and K. K. Tan, *In vivo* pO_2 imaging in the porcine model with perfluorocarbon F-19 NMR at low field, *Magn. Reson. Imaging* 1996, **14**, 103-114.

- [209] R. P. Mason, N. Bansal, E. E. Babcock, R. L. Nunnally and P. P. Antich, A novel editing technique for ^{19}F MRI: molecule-specific imaging, *Magn. Reson. Imaging* 1990, **8**, 729-736.
- [210] E. E. Babcock, R. P. Mason and P. P. Antich, Effect of homonuclear J modulation on ^{19}F spin-echo images, *Magn. Reson. Med.* 1991, **17**, 178-188.
- [211] C. H. Sotak, P. S. Hees, H. N. Huang, M. H. Hung, C. G. Krespan and S. Raynolds, A new perfluorocarbon for use in fluorine-19 MRI and MRS, *Magn. Reson. Med* 1993, **29**, 188-195.
- [212] D. Zhao, S. Ran, A. Constantinescu, E. W. Hahn and R. P. Mason, Tumor oxygen dynamics: correlation of in vivo MRI with histological findings, *Neoplasia* 2003, **5**, 308-318.
- [213] D. Zhao, A. Constantinescu, C.-H. Chang, E. W. Hahn and R. P. Mason, Correlation of Tumor Oxygen Dynamics with Radiation Response of the Dunning Prostate R3327-HI Tumor, *Radiat. Res.* 2003, **159**, 621-631.
- [214] D. Zhao, C. Constantinescu, E. W. Hahn and R. P. Mason, Differential oxygen dynamics in two diverse Dunning prostate R3327 rat tumor sublines (MAT-Lu and HI) with respect to growth and respiratory challenge, *Int. J. Radiat. Oncol. Biol. Phys.* 2002, **53**, 744-756.
- [215] D. Zhao, A. Constantinescu, L. Jiang, E. W. Hahn and R. P. Mason, Prognostic Radiology: quantitative assessment of tumor oxygen dynamics by MRI, *Am. J. Clin. Oncol* 2001, **24**, 462-466.
- [216] D. Zhao, A. Constantinescu, E. W. Hahn and R. P. Mason, Tumor oxygen dynamics with respect to growth and respiratory challenge: investigation of the Dunning prostate R3327-HI tumor, *Radiat. Res.* 2001, **156**, 510-520.
- [217] Y. Song, A. Constantinescu and R. P. Mason, Dynamic Breast tumor oximetry: the development of Prognostic Radiology, *Technol. Cancer Res. Treat.* 2002, **1**, 471-478.

- [218] B. J. Dardzinski and C. H. Sotak, Rapid tissue oxygen tension mapping using ^{19}F Inversion-recovery Echo-planar imaging of Perfluoro-15-crown-5-ether, *Magn. Reson. Med.* 1994, **32**, 88-97.
- [219] Z. Wang, M.-Y. Su and O. Nalcioglu, Applications of Dynamic Contrast Enhanced MRI in Oncology: Measurement of Tumor Oxygen Tension, *Technol. Cancer Res. Treat.* 2002, **1**, 29-38.
- [220] B. J. P. van der Sanden, A. Heerschap, L. Hoofd, A. W. Simonetti, K. Nicolay, A. van der Toorn, W. N. M. Colier and A. J. van der Kogel, Effect of carbogen breathing on the physiological profile of human glioma xenografts, *Magn. Reson. Med.* 1999, **42**, 490-499.
- [221] T. Q. Duong, C. Iadecola and S. G. Kim, Effect of hyperoxia, hypercapnia, and hypoxia on cerebral interstitial oxygen tension and cerebral blood flow, *Magn. Reson. Med.* 2001, **45**, 61-70.
- [222] F. Girard, P. Poulet, I. J. Namer, J. Steibel and J. Chambron, Localized T-2 Measurements Using an Osiris-CPMG Method - Application to Measurements of Blood Oxygenation and Transverse Relaxation Free of Diffusion Effect, *NMR Biomed.* 1994, **7**, 343-348.
- [223] R. P. Mason, H. P. Shukla and P. P. Antich, Oxygent: a novel probe of tissue oxygen tension, *Biomater. Artif. Cells Immob. Biotechnol.* 1992, **20**, 929-935.
- [224] R. P. Mason, W. Rodbumrung and P. P. Antich, Hexafluorobenzene: a sensitive ^{19}F NMR indicator of tumor oxygenation, *NMR Biomed.* 1996, **9**, 125-134.
- [225] R. P. Mason and P. P. Antich in *Application of ^{19}F MR to non invasively assess $p\text{O}_2$ and temperature in vivo with rapid time resolution*, Vol. (Ed. US patent No.5, 562), **1995**.

- [226] J. G. Riess, Overview of progress in the fluorocarbon approach to *in vivo* oxygen delivery, *Biomat. Art. Cells Immob. Biotech.* 1992, **20**, 183-202.
- [227] R. J. Kaufman in *Medical oxygen transport using perfluorochemicals*, Vol. (Ed. J. Goldstein), Butterworth-Heinemann, N.Y., **1991**, pp. 127-158.
- [228] T. F. Zuck and J. G. Riess, Current status of injectable oxygen carriers. [Review], *Critical Rev. Clinical Lab. Sci.* 1994, **31**, 295-324.
- [229] M. P. Krafft, Fluorocarbons and fluorinated amphiphiles in drug delivery and biomedical research, *Adv. Drug Delivery Rev.* 2001, **47**, 209-228.
- [230] E. G. Schutt, D. H. Klein, R. M. Mattrey and J. G. Riess, Injectable microbubbles as contrast agents for diagnostic ultrasound imaging: the key role of perfluorochemicals, *Angew. Chem. Int. Ed.* 2003, **42**, 3218-3235.
- [231] J. G. Riess, Oxygen carriers ("blood substitutes")--raison d'etre, chemistry, and some physiology, *Chem. Rev.* 2001, **101**, 2797-2920.
- [232] J. E. Fishman, P. M. Joseph, T. F. Floyd, B. Mukherji and H. S. Sloviter, Oxygen-sensitive ^{19}F NMR imaging of the vascular system *in vivo*, *Magn. Reson. Imaging* 1987, **5**, 279-285.
- [233] J. E. Fishman, P. M. Joseph, M. J. Carvlin, M. Saadi-Elmandjra, B. Mukherji and H. S. Sloviter, *In vivo* measurements of vascular oxygen tension in tumors using MRI of a fluorinated blood substitute, *Invest. Radiol.* 1989, **24**, 65-71.
- [234] D. Eidelberg, G. Johnson, P. S. Tofts, J. Dobbin, H. A. Crockard and D. Plummer, ^{19}F imaging of cerebral blood oxygenation in experimental middle cerebral artery occlusion: preliminary results, *J. Cereb. Blood Flow Metab.* 1988, **8**, 276-281.

- [235] U. Noth, S. P. Morrissey, R. Deichmann, H. Adolf, C. Schwarzbauer, J. Lutz and A. Haase, In vivo measurement of partial oxygen pressure in large vessels and in the reticuloendothelial system using fast ^{19}F -MRI, *Magn Reson Med.* 1995, **34**, 738-745.
- [236] K. M. Hoard in *Measurement of flow rates using surface coil nuclear magnetic resonance*, Vol. MSc. UT Arlington, Arlington, **1989**.
- [237] T. Higuchi, S. Naruse, Y. Horikawa, K. Hirakawa and C. Tanaka, *In vivo* measurement of the partial pressure of oxygen in brain tissue using ^{19}F NMR., *7th SMRM* 1988, 435.
- [238] R. P. Mason, P. P. Antich, E. E. Babcock, J. L. Gerberich and R. L. Nunnally, Perfluorocarbon imaging *in vivo*: A ^{19}F MRI study in tumor-bearing mice, *Magn. Reson. Imaging* 1989, **7**, 475-485.
- [239] R. F. Mattrey and D. C. Long, Potential role of PFOB in diagnostic imaging, *Invest. Radiol* 1988, **23**, s298-301.
- [240] W. I. Rosenblum, M. G. Hadfield, A. J. Martinez and P. Schatzki, Alterations of liver and spleen following intravenous infusion of fluorocarbon emulsions, *Arch. Pathol. Lab. Med.* 1976, **100**, 213-217.
- [241] R. P. Mason and P. P. Antich, Tumor oxygen tension: measurement using Oxygent™ as a ^{19}F NMR probe at 4.7 T, *Artif. Cells Blood Subst. Immob. Biotechnol.* 1994, **22**, 1361-1367.
- [242] R. P. Mason, P. P. Antich, E. E. Babcock, A. Constantinescu, P. Peschke and E. W. Hahn, Non-invasive determination of tumor oxygen tension and local variation with growth, *Int. J. Radiat. Oncol. Biol. Phys.* 1994, **29**, 95-103.
- [243] R. P. Mason, F. M. H. Jeffrey, C. R. Malloy, E. E. Babcock and P. P. Antich, A noninvasive assessment of myocardial oxygen tension: ^{19}F NMR spectroscopy of sequestered perfluorocarbon emulsion, *Magn. Reson. Med.* 1992, **27**, 310-317.

- [244] R. P. Mason, R. L. Nunnally and P. P. Antich, Tissue oxygenation: a novel determination using ^{19}F surface coil spectroscopy of sequestered perfluorocarbon emulsion, *Magn. Reson. Med.* 1991, **18**, 71-79.
- [245] N. J. Baldwin and T. C. Ng, Oxygenation and metabolic status of KHT tumors as measured simultaneously by ^{19}F magnetic resonance imaging and ^{31}P magnetic resonance spectroscopy., *Magn. Reson. Imaging* 1996, **14**, 541-551.
- [246] H. P. Shukla, R. P. Mason, N. Bansal and P. P. Antich, Regional Myocardial Oxygen Tension: ^{19}F MRI of Sequestered Perfluorocarbon, *Magn. Reson. Med.* 1996, **35**, 827-833.
- [247] B. P. J. van der Sanden, A. Heerschap, A. W. Simonetti, P. F. J. W. Rijken, H. P. W. Peters, G. Stüben and A. J. van der Kogel, Characterization and validation of non-invasive oxygen tension measurements in human glioma xenografts by ^{19}F -MR relaxometry, *Int. J. Radiat. Oncol. Biol. Phys.* 1999, **44**, 649-658.
- [248] H. T. Tran, Q. Guo, D. J. Schumacher, R. B. Buxton and R. F. Mattrey, ^{19}F chemical shift imaging technique to measure intracellular pO_2 *in vivo* using perflubron, *Acad. Radiol.* 1995, **2**, 756-761.
- [249] K. G. Helmer, S. Han and C. H. Sotak, On the correlation between the water diffusion coefficient and oxygen tension in RIF-1 tumors, *NMR Biomed.* 1998, **11**, 120-130.
- [250] B. R. Barker, R. P. Mason, N. Bansal and R. M. Peshock, Oxygen tension mapping by ^{19}F echo planar NMR imaging of sequestered perfluorocarbon, *JMRI* 1994, **4**, 595-602.
- [251] X. Fan, J. N. River, M. Zamora, H. A. Al-Hallaq and G. S. Karczmar, Effect of carbogen on tumor oxygenation: combined fluorine-19 and proton MRI measurements, *Int. J. Radiat. Oncol. Biol. Phys.* 2002, **54**, 1202-1209.

- [252] S. K. Holland, R. P. Kennan, M. M. Schaub, M. J. D'Angelo and J. C. Gore, Imaging oxygen tension in liver and spleen by ^{19}F NMR, *Magn. Reson. Med.* 1993, **29**, 446-458.
- [253] P. S. Hees and C. H. Sotak, Assessment of changes in murine tumor oxygenation in response to nicotinamide using ^{19}F NMR relaxometry of a perfluorocarbon emulsion, *Magn. Reson. Med.* 1993, **29**, 303-310 and erratum 329 716 (1993).
- [254] D. J. O. McIntyre, C. L. McCoy and J. R. Griffiths, Tumour oxygenation measurements by ^{19}F MRI of perfluorocarbons, *Curr. Sci.* 1999, **76**, 753-762.
- [255] P. P. Antich, R. P. Mason, A. Constantinescu, P. Peschke and E. W. Hahn, MRI staining: a novel approach to tumor architecture using perfluorocarbons, *Proc. Soc. Nucl. Med.* 1994, **35(5)**, 216P.
- [256] B. A. Berkowitz, C. A. Wilson and D. L. Hatchell, Oxygen kinetics in the vitreous substitute perfluorotributylamine: a ^{19}F NMR study in vivo, *Invest. Ophthalmol. Vis. Sci.* 1991, **32**, 2382-2387.
- [257] C. A. Wilson, B. A. Berkowitz and D. L. Hatchell, Oxygen kinetics in preretinal perfluorotributylamine, *Exp. Eye Res.* 1992, **55**, 119-126.
- [258] W. Zhang, Y. Ito, E. Berlin, R. Roberts and B. A. Berkowitz, Role of hypoxia during normal retinal vessel development and in experimental retinopathy of prematurity, *Invest. Ophthalmol. Visual Sci.* 2003, **44**, 3119-3123.
- [259] J.-J. Delpuech, M. A. Hamza, G. Serratice and M.-J. Stébé, Fluorocarbons as oxygen carriers. I. An NMR study of oxygen solutions in hexafluorobenzene, *J. Chem. Phys.* 1979, **70**, 2680-2687.

- [260] M. A. Hamza, G. Serratice, M.-J. Stebe and J.-J. Delpuech, Solute-solvent interactions in perfluorocarbon solutions of oxygen. An NMR study, *J. Am. Chem. Soc.* 1981, **103**, 3733-3738.
- [261] I. M. C. M. Rietjens, A. Steensma, C. den Besten, G. van Tintelen, J. Haas, B. van Ommen and P. J. van Bladeren, Comparative biotransformation of hexachlorobenzene and hexafluorobenzene in relation to the induction of porphyria, *Eur. J. Pharmacol.* 1995, **293**, 292-299.
- [262] Y. S. Gorsman and T. A. Kapitonenko, Pharmacology and toxicology of hexafluorobenzene, *Izv. Estestvennonauchu. Inst. Pevinsk.* 1973, **15**, 155-163.
- [263] K. M. Mortelmans and V. F. Simmon, "In vitro" microbiological mutagenicity assays of eight fluorocarbon taggant samples., *Gov. Rep. Announce Index (US)* 1981, **81**, 2555-2587.
- [264] K. D. Courtney and J. E. Andrews, Teratogenic evaluation and fetal deposition of hexabromobenzene (HBB) and hexafluorobenzene (HFB) in CD-1 mice, *J. Environ. Sci. Health B* 1984, **19**, 83-94.
- [265] L. W. Hall, S. R. K. Jackson and G. M. Massey in *Hexafluorobenzene in veterinary anaesthesia*, Vol. Eds.: A. Arias, R. Llaurodo, M. A. Nalda and J. N. Lunn), Excerpta Medica, Oxford, **1975**, pp. 201-204.
- [266] S. Hunjan, R. P. Mason, A. Constantinescu, P. Peschke, E. W. Hahn and P. P. Antich, Regional tumor oximetry: ^{19}F NMR spectroscopy of hexafluorobenzene, *Int. J. Radiat. Oncol. Biol. Phys.* 1998, **40**, 161-171.
- [267] D. Zhao, L. Jiang, E. W. Hahn and R. P. Mason, Tumor physiological response to combretastatin A4 phosphate assessed by MRI, *Int. J. Radiat. Oncol. Biol. Phys* 2005, **62**, 872-880.

- [268] D. Le, R. P. Mason, S. Hunjan, A. Constantinescu, B. R. Barker and P. P. Antich, Regional tumor oxygen dynamics: ^{19}F PBSR EPI of hexafluorobenzene, *Magn. Reson. Imaging*, 1997, **15**, 971-981.
- [269] S. Hunjan, D. Zhao, A. Constantinescu, E. W. Hahn, P. P. Antich and R. P. Mason, Tumor Oximetry: demonstration of an enhanced dynamic mapping procedure using fluorine-19 echo planar magnetic resonance imaging in the Dunning prostate R3327-AT1 rat tumor, *Int. J. Radiat. Oncol. Biol. Phys.* 2001, **49**, 1097-1108.
- [270] M. Xia, V. Kodibagkar, H. Liu and R. P. Mason, Tumour oxygen dynamics measured simultaneously by near infrared spectroscopy and ^{19}F magnetic resonance imaging in rats, *Phys. Med. Biol.* 2006, **51**, 45-60.
- [271] R. P. Mason, S. Hunjan, A. Constantinescu, Y. Song, D. Zhao, E. W. Hahn, P. P. Antich and P. Peschke in *Tumor oximetry: Comparison of ^{19}F MR EPI and electrodes*, Vol. 530 Eds.: J. F. Dunn and H. M. Swartz), Kluwer, New York, **2003**, pp. 19-28.
- [272] R. P. Mason, A. Constantinescu, S. Hunjan, D. Le, E. W. Hahn, P. P. Antich, C. Blum and P. Peschke, Regional tumor oxygenation and measurement of dynamic changes, *Radiat. Res.* 1999, **152**, 239-249.
- [273] V. Bourke, J. Gilio, D. Zhao, A. Constantinescu, V. Kodibagkar, L. Jiang, E. W. Hahn and R. P. Mason, *Radiat. Res. Meeting* (St. Louis, Mo) **2004**.
- [274] E. K. Rofstad, K. Sundfor, H. Lyng and C. G. Trope, Hypoxia-induced treatment failure in advanced squamous cell carcinoma of the uterine cervix is primarily due to hypoxia-induced radiation resistance rather than hypoxia-induced metastasis., *Br. J. Cancer* 2000, **83**, 354-359.

- [275] A. W. Fyles, M. Milosevic, R. Wong, M.-C. Kavanagh, M. Pintile, A. Sun, W. Chapman, W. Levin, L. Manchul, T. J. Keane and R. P. Hill, Oxygenation predicts radiation response and survival in patients with cervix cancer, *Radiother. Oncol.* 1998, **48**, 149-156.
- [276] M. Höckel, K. Schlenger, B. Aral, M. Mitze, U. Schäffer and P. Vaupel, Hypoxia and radiation response in human tumors., *Semi. Radiat. Oncol.* 1996, **6**, 3-9.
- [277] J. Keupp and T. Schaeffter, *Proc. Intl. Soc. Mag. Reson. Med.* (Seattle) **2006**, p. 916.
- [278] J. R. Griffiths, Are cancer cells acidic?, *Br. J. Cancer* 1991, **64**, 425-427.
- [279] V. D. Mehta, P. V. Kulkarni, R. P. Mason, A. Constantinescu, S. Aravind, N. Goomer and P. P. Antich, 6-Fluoropyridoxol: a novel probe of cellular pH using ^{19}F NMR spectroscopy, *FEBS Letters* 1994, **349**, 234-238.
- [280] C. J. Deutsch and J. S. Taylor, Intracellular pH measured by ^{19}F NMR, *Ann. NY Acad. Sci.* 1987, **508**, 33-47.
- [281] C. Deutsch, J. S. Taylor and D. F. Wilson, Regulation of intracellular pH of human peripheral blood lymphocytes as measured by ^{19}F NMR, *Proc. Natl. Acad. Sci. (USA)* 1982, **79**, 7944-7948.
- [282] C. Deutsch, J. S. Taylor and M. Price, pH homeostasis in human lymphocytes: modulation by ions and mitogen, *J. Cell Biol.* 1984, **98**, 885-894.
- [283] T. Kashiwagura, C. J. Deutsch, J. Taylor, M. Erecinska and D. F. Wilson, Dependence of gluconeogenesis, urea synthesis, and energy metabolism of hepatocytes on intracellular pH, *J. Biol. Chem.* 1984, **259**, 237-243.
- [284] W. J. Thoma and K. Ugurbil, pH and compartmentation of isolated perfused rat liver studied by ^{19}F and ^{31}P NMR, *NMR Biomed.* 1988, **1**, 95-100.

- [285] J. S. Taylor and C. J. Deutsch, Fluorinated α -methylamino acids as ^{19}F NMR indicators of intracellular pH, *Biophys. J.* 1983, **43**, 261-267.
- [286] A. Joseph, C. Davenport, L. Kwock, C. T. Burt and R. E. London, Fluorine-19 NMR studies of tumor-bearing rats treated with difluoromethylornithine, *Magn. Reson. Med.* 1987, **4**, 137-143.
- [287] R. E. London and S. A. Gabel, Determination of membrane potential and cell volume by ^{19}F NMR using trifluoroacetate and trifluoroacetamide probes, *Biochemistry* 1989, **28**, 2378-2382.
- [288] A. S. L. Xu, J. R. Potts and P. W. Kuchel, The Phenomenon of Separate Intracellular and Extracellular Resonances of Difluorophosphate in P-31 and F-19 Nmr-Spectra of Erythrocytes, *Magn. Reson. Med.* 1991, **18**, 193-198.
- [289] A. S. L. Xu, A. R. Waldeck and P. W. Kuchel, Transmembrane F-19 Nmr Chemical-Shift Difference of Fluorinated Solutes in Liposomes, Erythrocytes and Erythrocyte-Ghosts, *NMR Biomed* 1993, **6**, 136-143.
- [290] S. Hunjan, R. P. Mason, V. D. Mehta, P. V. Kulkarni, S. Aravind, V. Arora and P. P. Antich, Simultaneous intra- and extra- cellular pH measurement using ^{19}F NMR of 6-Fluoropyridoxol, *Magn. Reson. Med.* 1998, **39**, 551-556.
- [291] S. He, R. P. Mason, S. Hunjan, V. D. Mehta, V. Arora, R. Katipally, P. V. Kulkarni and P. P. Antich, Development of Novel ^{19}F NMR pH Indicators: Synthesis and Evaluation of a Series of Fluorinated Vitamin B₆ Analogs, *Bioorg. Med. Chem.* 1998, **6**, 1631-1639.
- [292] W. Korytnyk and R. P. Singh, Proton magnetic resonance spectra of compounds in the vitamin B₆ group, *J. Am. Chem. Soc.* 1963, **85**, 2813-2817.

- [293] K. Yamada and M. Tsuji, Transport of vitamin B6 in human erythrocytes, *J. Vitaminol.* 1970, **16**, 237-242.
- [294] J. X. Yu, P. Otten, Z. Ma, W. Cui, L. Liu and R. P. Mason, A Novel NMR Platform for Detecting Gene Transfection: Synthesis and Evaluation of Fluorinated Phenyl β -D-Galactosides with Potential Application for Assessing LacZ Gene Expression, *Bioconj. Chem.* 2004, **15**, 1334-1341.
- [295] J. C. Metcalfe, T. R. Hesketh and G. A. Smith, Free cytosolic Ca^{2+} measurements with fluorine labelled indicators using ^{19}F NMR, *Cell Calcium* 1985, **6**, 183-195.
- [296] J. S. Beech and R. A. Iles, ^{19}F NMR indicators of hepatic intra cellular pH *in vivo*, *Biochem. Soc. Trans.* 1987, **15**, 871-872.
- [297] C. J. Deutsch and J. S. Taylor, New class of ^{19}F pH indicators: fluoroanilines, *Biophys. J.* 1989, **55**, 799-804.
- [298] C. K. Rhee, L. A. Levy and R. E. London, Fluorinated o-aminophenol derivatives for measurement of intracellular pH, *Bioconj. Chem.* 1995, **6**, 77-81.
- [299] J. X. Yu, L. Liu, V. D. Kodibagkar, W. Cui and R. P. Mason, Synthesis and Evaluation of Novel Enhanced Gene Reporter Molecules: Detection of β -Galactosidase Activity Using ^{19}F NMR of Trifluoromethylated Aryl β -D-Galactopyranosides, *Bioorg. Med. Chem.* 2006, **14**, 326-333.
- [300] W. Cui, P. Otten, J. Yu, V. Kodibagkar and R. P. Mason, *Proc. ISMRM* (Toronto, Canada) **2003**, p. 675.
- [301] T. Frenzel, S. Koszler, H. Bauer, U. Niedballa and H. J. Weinmann, Noninvasive *in vivo* pH measurement using a fluorinated pH probe and fluorine-19 magnetic resonance spectroscopy., *Invest. Radiol.* 1994, **29**, S220-222.

- [302] T. Miyazawa, Y. Aoki, K. Akagi, M. Takahashi, B. Fritz-Zieroth, T. Frenzel and H.-J. Weinmann, Application of ZK150 471, a fluorinated pH probe for ^{19}F MRS, to *in vivo* pH measurement after hyperthermic treatment of tumors in mice, *Acad. Radiol.* 1996, **3**, S363-364.
- [303] A. S. Ojugo, P. M. McSheehy, D. J. McIntyre, C. McCoy, M. Stubbs, M. O. Leach, I. R. Judson and J. R. Griffiths, Measurement of the extracellular pH of solid tumours in mice by magnetic resonance spectroscopy: a comparison of exogenous (^{19}F) and (^{31}P) probes, *NMR Biomed.* 1999, **12**, 495-504.
- [304] Y. Aoki, K. Akagi, Y. Tanaka, J. Kawai and M. Takahashi, Measurement of intratumor pH by pH indicator used in ^{19}F MR spectroscopy, *Invest. Radiol.* 1996, **31**, 680-689.
- [305] R. Y. Tsien, A non-disruptive technique for loading calcium buffers and indicators into cells, *Nature* 1981, **290**, 527-528.
- [306] G. A. Smith, R. T. Hesketh, J. C. Metcalfe, J. Feeney and P. G. Morris, Intracellular Calcium Measurements by F-19 Nmr of Fluorine-Labeled Chelators, *Proc. Natl. Acad. Sci. (USA)-Biological Sciences* 1983, **80**, 7178-7182.
- [307] J. Benders, U. Flogel, T. Schafer, D. Leibfritz, S. Hechtenberg and D. Beyersmann, Study of the interactions of cadmium and zinc ions with cellular calcium homoeostasis using F-19-NMR spectroscopy, *Biochem. J.* 1997, **322**, 793-799.
- [308] R. K. Gupta and R. J. Gillies in *^{19}F NMR measurement of intracellular free calcium ions in intact cells and tissues*, Vol. 2 (Ed. R. K. Gupta), CRC, Boca Raton, **1987**, pp. 45-53.
- [309] F. A. Schanne, J. R. Moskal and R. K. Gupta, Effect of lead on intracellular free calcium ion concentration in a presynaptic neuronal model: ^{19}F -NMR study of NG108-15 cells, *Brain Res.* 1989, **503**, 308-311.

- [310] F. A. Schanne, T. L. Dowd, R. K. Gupta and J. F. Rosen, Lead increases free Ca^{2+} concentration in cultured osteoblastic bone cells: simultaneous detection of intracellular free Pb^{2+} by ^{19}F NMR, *Proc. Natl. Acad. Sci. (USA)* 1989, **86**, 5133-5135.
- [311] E. Marban, M. Kitakaze, V. P. Chacko and M. M. Pike, Ca^{2+} Transients in Perfused Hearts Revealed by Gated F-19 Nmr-Spectroscopy, *Circ. Res.* 1988, **63**, 673-678.
- [312] H. Kusuoka, P. H. Backx, M. C. Camilion de Hurtado, M. Azan-Backx, E. Marban and H. E. Cingolani, Relative roles of intracellular Ca^{2+} and pH in shaping myocardial contractile response to acute respiratory alkalosis, *Am. J. Physiol.* 1993, **265**, H1696-1703.
- [313] H. L. Kirschenlohr, J. C. Metcalfe, P. G. Morris, G. C. Rodrigo and G. A. Smith, Ca^{2+} Transient, Mg^{2+} , and pH Measurements in the Cardiac Cycle by F-19 NMR, *Proc. Natl. Acad. Sci. (USA)* 1988, **85**, 9017-9021.
- [314] H. Plenio and R. Diodone, Covalently bonded fluorine as a σ -donor for groups I and II metal ions in partially fluorinated macrocycles, *JACS* 1996, **118**, 356-367.
- [315] J. L. Noronha and G. M. Matuschak, Magnesium in critical illness: metabolism, assessment, and treatment, *Intensive Care Medicine* 2002, **28**, 667-679.
- [316] R. K. Gupta and P. Gupta in ^{31}P NMR measurement of intracellular free magnesium in cells and organisms, Vol. 2 (Ed. R. K. Gupta), CRC, Boca Raton, **1987**, pp. 34-43.
- [317] E. Weller, P. Bachert, H. M. Meinck, B. Friedmann, P. Bartsch and H. Mairbaurl, Lack of effect of oral Mg-supplementation on Mg in serum, blood cells, and calf muscle, *Med. Sci. Sports Exe.* 1998, **30**, 1584-1591.
- [318] C. V. Odvina, R. P. Mason and C. Y. C. Pak, Prevention of Thiazide-induced Hypokalemia without Magnesium Depletion by Potassium-Magnesium Citrate, *Am. J. Therapeut.* 2006, **13**, 101–108.

- [319] E. Murphy, Measurement of Intracellular Ionized Magnesium, *Mineral and Electrolyte Metabolism* 1993, **19**, 250-258.
- [320] B. Tecle and J. E. Casida, Enzymatic defluorination and metabolism of fluoroacetate, fluoroacetamide, fluoroethanol, and (-)-erythro-fluorocitrate in rats and mice examined by ^{19}F and ^{13}C NMR, *Chem. Res. Toxicol.* 1989, **2**, 429-435.
- [321] L. A. Levy, E. Murphy, B. Raju and R. E. London, Measurement of cytosolic free magnesium concentration by ^{19}F NMR, *Biochemistry* 1988, **27**, 4041-4048.
- [322] E. Murphy, C. Steenbergen, L. A. Levy, B. Raju and R. E. London, Cytosolic Free Magnesium Levels in Ischemic Rat-Heart, *J. Biol. Chem.* 1989, **264**, 5622-5627.
- [323] G. J. Long, J. F. Rosen and F. A. X. Schanne, Lead Activation of Protein-Kinase-C from Rat-Brain - Determination of Free Calcium, Lead, and Zinc by F-19-Nmr, *J. Biol. Chem.* 1994, **269**, 834-837.
- [324] H. Plenio, J. Hermann and R. Diodone, The coordination chemistry of fluorocarbons: Difluoro-m-cyclophane-based fluorocryptands and their group I and II metal ion complexes, *Inorg. Chem.* 1997, **36**, 5722-5729.
- [325] H. Takemura, H. Kariyazono, M. Yasutake, N. Kon, K. Tani, K. Sako, T. Shinmyozu and T. Inazu, Syntheses of macrocyclic compounds possessing fluorine atoms in their cavities: Structures and complexation with cations, *Eur. J. Org. Chem.* 2000, **1**, 141-148.
- [326] H. Plenio and R. Diodone, A Fluorine-Containing Cryptand For The Complexation Of Anions And The Utility Of F-19 Nmr-Spectroscopy For The Determination Of Host Guest Association, *Z. Naturforsch. Section B- J. Chem. Sci.* 1995, **50**, 1075-1078.
- [327] R. E. London and S. A. Gabel, F-19 NMR-studies of fluorobenzenboronic acids .1. Interaction kinetics with biologically significant, *JACS* 1994, **116**, 2562-2569.

- [328] J. S. Fowler, N. D. Volkow, G. J. Wang and Y. S. Ding, 2-deoxy-2-[18F]fluoro-D-glucose and alternative radiotracers for positron emission tomography imaging using the human brain as a model., *Semin. Nucl. Med.* 2004, **34**, 112-121.
- [329] T. Nakada, I. L. Kwee and C. B. Conboy, *J. Neurochem.* 1986, **46**, 198.
- [330] T. Nakada, I. L. Kwee, P. J. Card, N. A. Matwiyoff, B. V. Griffey and R. H. Griffey, F-19 Nmr Imaging of Glucose-Metabolism, *Magn. Reson. Med.* 1988, **6**, 307-313.
- [331] T. Nakada, I. L. Kwee, B. V. Griffey and R. H. Griffey, F-19 Mr Imaging of Glucose-Metabolism in the Rabbit, *Radiology* 1988, **168**, 823-825.
- [332] B. A. Berkowitz and J. J. H. Ackerman, Proton Decoupled Fluorine Nuclear-Magnetic-Resonance Spectroscopy In situ, *Biophys. J.* 1987, **51**, 681-685.
- [333] M. J. Lizak, K. Mori and P. F. Kador, Determination of aldose reductase activity in the eye by localized magnetic resonance spectroscopy, *J. Ocular Pharmacol. Therapeut.* 2001, **17**, 475-483.
- [334] E. F. Secchi, M. J. Lizak, S. Sato and P. F. Kador, 3-fluoro-3-deoxy-D-galactose: A new probe for studies on sugar cataract, *Current Eye Research* 1999, **18**, 277-282.
- [335] I. L. Kwee, H. Igarashi and T. Nakada, Aldose reductase and sorbitol dehydrogenase activities in diabetic brain: In vivo kinetic studies using F-19 3-FDG NMR in rats, *Neuroreport* 1996, **7**, 726-728.
- [336] R. G. Shulman and D. L. Rothman, C-13 NMR of intermediary metabolism: Implications for systemic physiology, *Annual Review of Physiology* 2001, **63**, 15-48.
- [337] F. M. H. Jeffrey, A. Rajagopal, C. R. Malloy and A. D. Sherry, C-13-Nmr - a Simple yet Comprehensive Method for Analysis of Intermediary Metabolism, *Trends in Biochemical Sciences* 1991, **16**, 5-10.

- [338] R. P. Mason, J. K. M. Sanders and A. Cornish, *Invivo Enzymology - C-13 Nmr Measurement of a Kinetic Isotope Effect for Methanol Oxidation in Methylosinus-Trichosporium Ob3b*, *Febs Letters* 1987, **216**, 4-6.
- [339] I. J. Stratford and G. E. Adams in *Radiation sensitizers and bioreductive drugs*, Vol. Eds.: G. G. Steel, G. E. Adams and A. Horwich), Elsevier, Amsterdam, **1989**, pp. 145-162.
- [340] S. S. Foo, D. F. Abbott, N. Lawrentschuk and A. M. Scott, Functional imaging of intratumoral hypoxia, *Molecular Imaging Biol* 2004, **6**, 291-305.
- [341] A. Franko, C. Koch and D. Boisvert, Distribution of misonidazole adducts in gliosarcoma tumors and spheroids: implications for oxygen distribution, *Cancer Res* 1992, **52**, 3831-3837.
- [342] J. R. Ballinger, Imaging hypoxia in tumors, *Semin. Nucl. Med.* 2001, **31**, 321-329.
- [343] R. J. Hodgkiss, Use of 2-nitroimidazoles as bioreductive markers for tumour hypoxia, *Anti-cancer Drug Design* 1998, **13**, 687-702.
- [344] J. G. Rajendran and K. A. Krohn, Imaging hypoxia and angiogenesis in tumors. , *Radiol Clin North Am.* 2005 **43**, 169-187.
- [345] S. M. Evans, S. Hahn, D. R. Pook, W. T. Jenkins, A. A. Chalian, P. Zhang, C. Stevens, R. Weber, G. Weinstein, I. Benjamin, N. Mirza, M. Morgan, S. Rubin, W. G. McKenna, E. M. Lord and C. J. Koch, Detection of hypoxia in human squamous cell carcinoma by EF5 binding, *Cancer Res.* 2000, **60**, 2018-2024.
- [346] C. J. Koch, S. M. Hahn, K. J. Rockwell, J. M. Covey, W. G. McKenna and S. M. Evans, Pharmacokinetics of EF5 [2-(2-nitro-1-H-imidazol-1-yl)-N-(2,2,3,3,3-pentafluoropropyl) acetamide] in human patients: implications for hypoxia measurements in vivo by 2-nitroimidazoles., *Cancer Chemother. Pharmacol.* 2001, **48**, 177-187.

- [347] A. S. E. Ljungkvist, J. Bussink, P. F. J. W. Rijken, J. A. Raleigh, J. Denekamp and A. J. Van Der Kogel, Changes in tumor hypoxia measured with a double hypoxic marker technique., *Int. J. Radiat. Oncol. Biol. Phys.* 2000, **48**, 1529-1538.
- [348] J. S. Lewis, D. W. McCarthy, T. J. McCarthy, Y. Fujibayashi and M. J. Welch, Evaluation of Cu-64-ATSM in vitro and in vivo in a hypoxic tumor model, *J.Nucl. Med.* 1999, **40**, 177-183.
- [349] F. Dehdashti, P. W. Grigsby, M. A. Mintun, J. S. Lewis, B. A. Siegel and M. J. Welch, Assessing tumor hypoxia in cervical cancer by positron emission tomography with 60Cu-ATSM: relationship to therapeutic response-a preliminary report, *Int. J. Radiat. Oncol. Biol., Phys.* 2003, **55**, 1233-1238.
- [350] J. D. Chapman, E. L. Engelhardt, C. C. Stobbe, R. F. Schneider and G. E. Hanks, Measuring hypoxia and predicting tumor radioresistance with nuclear medicine assays, *Radiother. Oncol.* 1998, **46**, 229-237.
- [351] S. P. Robinson and J. R. Griffiths, Current issues in the utility of ^{19}F nuclear magnetic resonance methodologies for the assessment of tumour hypoxia, *Phil. Trans. R. Soc. London B Biol. Sci.* 2004, **359**, 987-996.
- [352] D. Procissi, F. Claus, J. Koziorowski, P. Burgman, C. Matei, S. Thakur, C. Ling and J. A. Koutcher, *Proc. Intl. Soc. Mag. Reson. Med.* **2006**, p. 1260.
- [353] J. M. Cline, G. L. Rosner, J. A. Raleigh and D. E. Thrall, Quantification of CCI-103F labeling heterogeneity in canine solid tumors, *Int. J. Radiat. Oncol. Biol. Phys.* 1997, **37**, 655-662.
- [354] P. Workman, R. J. Maxwell and J. R. Griffiths, Noninvasive MRS in New Anticancer Drug Development, *NMR Biomed.* 1992, **5**, 270-272.

- [355] B. M. Seddon, R. J. Maxwell, D. J. Honess, R. Grimshaw, F. Raynaud, G. M. Tozer and P. Workman, Validation of the fluorinated 2-nitroimidazole SR-4554 as a noninvasive hypoxia marker detected by magnetic resonance spectroscopy, *Clin. Cancer Res.* 2002, **8**, 2323-2335.
- [356] B. M. Seddon, G. S. Payne, L. Simmons, R. Ruddle, R. Grimshaw, S. Tan, A. Turner, F. Raynaud, G. Halbert, M. O. Leach, I. Judson and P. Workman, A phase I study of SR-4554 via intravenous administration for noninvasive investigation of tumor hypoxia by magnetic resonance spectroscopy in patients with malignancy, *Clin. Cancer Res.* 2003, **9**, 5101-5112.
- [357] S. J. Li, G. Y. Jin and J. E. Moulder, Prediction of Tumor Radiosensitivity by Hexafluoromisonidazole Retention Monitored by [H-1]/[F-19] Magnetic-Resonance Spectroscopy, *Cancer Commun.* 1991, **3**, 133-139.
- [358] E. O. Aboagye, R. J. Maxwell, M. R. Horsman, A. D. Lewis, P. Workman, M. Tracy and J. R. Griffiths, The relationship between tumour oxygenation determined by oxygen electrode measurements and magnetic resonance spectroscopy of the fluorinated 2-nitroimidazole SR-4554, *Br. J. Cancer* 1998, **77**, 65-70.
- [359] H. W. Salmon and D. W. Siemann, Utility of ¹⁹F MRS detection of the hypoxic cell marker EF5 to assess cellular hypoxia in solid tumors, *Radiother. Oncol.* 2004, **73**, 359-366.
- [360] J. K. Fairweather, M. Faijes, H. Driguez and A. Planas, Specificity studies of bacillus 1,3-1,4-beta-glucanases and application to glycosynthase-catalyzed transglycosylation., *Chembiochem.* 2002 **3**, 866-873.
- [361] T. Ichikawa, D. Hogemann, Y. Saeki, E. Tyminski, K. Terada, R. Weissleder, E. A. Chiocca and J. P. Basilion, MRI of transgene expression: correlation to therapeutic gene expression, *Neoplasia (New York)* 2002, **6**, 523-530.

- [362] Z. Paroo, R. A. Bollinger, D. A. Braasch, E. Richer, D. R. Corey, P. P. Antich and R. P. Mason, Validating bioluminescence imaging as a high-throughput, quantitative modality for assessing tumor burden, *Molecular Imaging* 2004, **3**, 117-124.
- [363] J. G. Tjuvajev, M. Doubrovin, T. Akhurst, S. Cai, J. Balatoni, M. M. Alauddin, R. Finn, W. Bornmann, H. Thaler, P. S. Conti and R. G. Blasberg, Comparison of radiolabeled nucleoside probes (FIAU, FHBG, and FHPG) for PET imaging of HSV1-tk gene expression, *J. Nucl. Med.* 2002, **43**, 1072-1083.
- [364] A. Kruger, V. Schirmacher and R. Khokha, The bacterial lacZ gene: An important tool for metastasis research and evaluation of new cancer therapies., *Cancer Metastasis Rev.*, 1999, **17**, 285-294.
- [365] I. G. Serebriiskii and E. A. Golemis, Uses of lacZ to study gene function: evaluation of beta-galactosidase assays employed in the yeast two-hybrid system, *Anal. Biochem.* 2000, **285**, 1-15.
- [366] J. R. Beckwith and D. Zipser in *The Lactose operon*, Vol. Cold Spring Harbor Laboratory, Cold Spring Harbor, **1970**, p. 435.
- [367] J. Kawaguchi, V. Wilson and P. J. Mee, Visualization of whole-mount skeletal expression patterns of LacZ reporters using a tissue clearing protocol., *Biotechniques* 2002, **32**, 68-73.
- [368] K. Heuermann and J. Cosgrove, S-Gal: an autoclavable dye for color selection of cloned DNA inserts, *Biotechniques* 2001, **30**, 1142-1147.
- [369] I. Bronstein, B. Edwards and J. C. Voyta, 1,2-Dioxetanes - Novel Chemi-Luminescent Enzyme Substrates - Applications To Immunoassays, *J. Chemilum. Biolum.* 1989, **4**, 99-111.

- [370] A. Y. Louie, M. M. Huber, E. T. Ahrens, U. Rothbacher, R. Moats, R. E. Jacobs, S. E. Fraser and T. J. Meade, In vivo visualization of gene expression using magnetic resonance imaging, *Nature Biotechnol.* 2000, **18**, 321-325.
- [371] C. H. Tung, Q. Zeng, K. Shah, D. E. Kim, D. Schellingerhout and R. Weissleder, In vivo imaging of beta-galactosidase activity using far red fluorescent switch., *Cancer Res.* 2004, **64**, 1579-1583.
- [372] K. H. Lee, S. S. Byun, J. H. Choi, J. Y. Paik, Y. S. Choe and B. T. Kim, Targeting of lacZ reporter gene expression with radioiodine-labelled phenylethyl-beta-d-thiogalactopyranoside, *Eur J Nucl Med Mol Imaging.* 2004, **31**, 433-438.
- [373] S. Yoon, H. G. Kim, K. H. Chun and J. E. N. Shin, 4-deoxy-analogs of p-nitrophenyl β -D-galactopyranosides for specificity study with β -galactosidase from escherichia coli, *Bull. Korean Chem. Soc.* 1996, **17**, 599-604.
- [374] W. Cui, P. Otten, Y. Li, K. Koeneman, J. Yu and R. P. Mason, A novel NMR approach to assessing gene transfection: 4-fluoro-2-nitrophenyl- β -D-galactopyranoside as a prototype reporter molecule for β -galactosidase, *Magn. Reson. Med.* 2004, **51**, 616-620.
- [375] V. D. Kodibagkar, J. Yu, L. Liu, H. P. Hetherington and R. P. Mason, Imaging β -galactosidase activity using ^{19}F chemical shift imaging of LacZ gene-reporter molecule 2-fluoro-4-nitrophenol- β -D-galactopyranoside, *Magn. Reson. Imaging* 2006, **24**, 959-962.
- [376] J. P. Richard, J. G. Westerfeld and S. Lin, Structure-reactivity relationships for beta-galactosidase (Escherichia coli, lac Z). 1. Bronsted parameters for cleavage of alkyl beta-D-galactopyranosides, *Biochemistry* 1995, **34**, 11703-11712.

- [377] J. X. Yu, Z. Ma, Y. Li, K. S. Koeneman, L. Liu and R. P. Mason, Synthesis and Evaluation of a Novel Gene Reporter Molecule: Detection of β -galactosidase activity Using ^{19}F NMR of a Fluorinated Vitamin B6 conjugate, *Med. Chem* 2005, **1**, 255-262.
- [378] J. X. Yu and R. P. Mason, Synthesis and Characterization of Novel lacZ Gene Reporter Molecules: Detection of β -Galactosidase Activity Using ^{19}F NMR of Polyglycosylated Fluorinated Vitamin B6, *J. Med. Chem.* 2006, **49**, 1991-1999.
- [379] V. Kodibagkar, J. Yu, L. Liu and R. P. Mason, *Proc. Society of Molecular Imaging* (Hawai'i) **2006**, p. in the press.
- [380] L. C. Clark Jr. and F. Gollan, Survival of mammals breathing organic liquids equilibrated with oxygen at atmospheric pressure, *Science* 1966, 1755-1756.
- [381] J. S. Greenspan, W. W. Fox, S. D. Rubenstein, M. R. Wolfson, S. S. Spinner and T. H. Shaffer, Partial liquid ventilation in critically ill infants receiving extracorporeal life support. Philadelphia Liquid Ventilation Consortium, *Pediatrics* 1997, **99**, E2.
- [382] S. R. Thomas, L. C. Clark Jr., J. Ackerman, R. G. Pratt, R. E. Hoffmann, L. J. Busse, R. A. Kinsey and R. C. Samaratunga, MRI imaging of the lung using liquid perfluorocarbons, *J. Comp. Asst. Tomogr.* 1986, **10**, 1-9.
- [383] S. R. Thomas, L. Gradon, S. E. Pratsinis, R. G. Pratt, G. P. Fotou, A. J. McGoron, A. L. Podgorski and R. W. Millard, Perfluorocarbon compound aerosols for delivery to the lung as potential ^{19}F magnetic resonance reporters of regional pulmonary pO_2 , *Invest. Radiol.* 1997, **32**, 29-38.
- [384] M. Q. Huang, Q. Ye, D. S. Williams and C. Ho, MRI of lungs using partial liquid ventilation with water-in-perfluorocarbon emulsions, *Magn. Reson. Med.* 2002, **48**, 487-492.

- [385] E. Heidelberger and P. C. Lauterbur, *Soc. Magn. Reson. Med.* (Boston, MA) **1982**, pp. 70-71.
- [386] D. O. Kuethe, V. C. Behr and S. Begay, Volume of rat lungs measured throughout the respiratory cycle using F-19 NMR of the inert gas SF₆, *Magnetic Resonance in Medicine* 2002, **48**, 547-549.
- [387] J. Ruiz-Cabello, J. M. Perez-Sanchez, R. P. de Alejo, I. Rodriguez, N. Gonzalez-Mangado, G. Peces-Barbas and M. Cortijo, Diffusion-weighted F-19-MRI of lung periphery: Influence of pressure and air-SF₆ composition on apparent diffusion coefficients, *Resp. Physiol. Neurobiol.* 2005, **148**, 43-56.
- [388] W. F. Remy, R. W. Geenen, S. M. Hussain, F. Cademartiri, J. W. Poley, P. D. Siersema and G. P. Krestin, CT and MR colonography: scanning techniques, postprocessing, and emphasis on polyp detection, *Radiograph.* 2004, **24**, e18.
- [389] D. L. Rubin, K. L. Falk, M. J. Sperling, M. Ross, S. Saini, B. Rothman, F. Shellock, E. Zerhouni, D. Stark, E. K. Outwater, U. Schmiedl, L. C. Kirby, J. Chezmar, T. Coates, M. Chang, J. M. Silverman, N. Rofsky, K. Burnett, J. Engel and S. W. Young, A multicenter clinical trial of Gadolite Oral Suspension as a contrast agent for MRI. [Clinical Trial. Clinical Trial, Phase II. Clinical Trial, Phase III, *JMRI* **7**, 865-872.
- [390] S. Hirohashi, H. Uchida, K. Yoshikawa, N. Fujita, K. Ohtomo, Y. Yuasa, Y. Kawamura and O. Matsui, Large scale clinical evaluation of bowel contrast agent containing ferric ammonium citrate in MRI., *Magn. Reson. Imaging* 1994, **12**, 837-846.
- [391] G. S. I. Bisset, K. H. Emery, M. P. Meza, N. K. Rollins, S. Don and J. S. Shorr, Perflubron as a gastrointestinal MR imaging contrast agent in the pediatric population, *Pediatric Radiol.* 1996., **26**, 409-415.

- [392] R. F. Mattrey, M. A. Trambert, J. J. Brown, S. W. Young, J. N. Bruneton, G. E. Wesbey and Z. N. Balsara, Perflubron as an oral contrast agent for MR imaging: results of a phase III clinical trial, *Radiology* 1994, **191**, 841-848.
- [393] B. Uzzan, P. Nicolas, M. Cucherat and G. Y. Perret, Microvessel density as a prognostic factor in women with breast cancer: a systematic review of the literature and meta-analysis, *Cancer Res.* 2004, **64**, 2941-2955.
- [394] S. P. Robinson, P. F. Rijken, F. A. Howe, P. M. McSheehy, B. P. van der Sanden, A. Heerschap, M. Stubbs, A. J. Van Der Kogel and J. R. Griffiths, Tumor vascular architecture and function evaluated by non-invasive susceptibility MRI methods and immunohistochemistry, *J. Magn. Reson. Imaging.* 2003, **17**, 445-454.
- [395] T. L. Ceckler, S. L. Gibson, R. Hilf and R. G. Bryant, *In situ* assessment of tumor vascularity using fluorine NMR imaging, *Magn. Reson. Med.* 1990, **13**, 416-433.
- [396] K. L. Meyer, P. M. Joseph, B. Mukherji, V. A. Livolsi and R. Lin, Measurement of Vascular Volume in Experimental Rat-Tumors by F-19 Magnetic-Resonance-Imaging, *Invest. Radiol.* 1993, **28**, 710-719.
- [397] T. Sogabe, T. Imaizumi, T. Mori, M. Tominaga, K. Koga and Y. Yabuuchi, Effects of vasodilators on the signal intensity of perfluorocarbon monitored by in vivo F-19-NMR spectroscopy, *Magn. Reson. Imaging* 1997, **15**, 341-345.
- [398] Y. Gu, R. P. Mason and H. Liu, Estimated fraction of tumor vascular blood contents sampled by near infrared spectroscopy and ¹⁹F magnetic resonance spectroscopy, *Optics Express* 2005, **13**, 1724-1733.
- [399] B. Authier, Reactive Hyperemia Monitored on Rat Muscle Using Perfluorocarbons and F-19 NMR, *Magn. Reson. Med.* 1988, **8**, 80-83.

- [400] N. J. Baldwin, Y. Wang and T. C. Ng, *In situ* ^{19}F MRS measurement of RIF-1 tumor blood volume: corroboration by radioisotope-labeled [^{125}I]-albumin and correlation to tumor size, *Magn. Reson. Imaging* 1996, **14**, 275-280.
- [401] J. R. Ewing, C. A. Branch, S. C. Fagan, J. A. Helpert, R. T. Simkins, S. M. Butt and K. M. A. Welch, Fluorocarbon-23 measure of cat cerebral blood flow by NMR, *Stroke* 1990, **21**, 100-106.
- [402] S. M. Eleff, M. D. Schnall, L. Ligetti, M. Osbakken, V. H. Subramanian, B. Chance and J. S. Leigh, Concurrent Measurements of Cerebral Blood-Flow, Sodium, Lactate, and High-Energy Phosphate-Metabolism Using F-19, Na-23, H-1, and P-31 Nuclear Magnetic-Resonance Spectroscopy, *Magn. Reson. Med.* 1988, **7**, 412-424.
- [403] J. S. van den Brink, Y. Watanabe, C. K. Kuhl, T. Chung, R. Muthupillai, M. Van Cauteren, K. Yamada, S. Dymarkowski, J. Bogaert, J. H. Maki, C. Matos, J. W. Casselman and R. M. Hoogeveen, Implications of SENSE MR in routine clinical practice, *Eur. J. Radiol.* 2003, **46**, 3-27.
- [404] K. P. Pruessmann, M. Weiger, M. B. Scheidegger and P. Boesiger, SENSE: Sensitivity encoding for fast MRI, *Magnetic Resonance in Medicine* 1999, **42**, 952-962.
- [405] H. P. Shukla in *Application of Perfluorocarbon Emulsions as Fluorine-19 Nuclear Magnetic Resonance Molecular Probes of Cardiac Tissue Oxygen Tension*, Vol. Ph.D. University of Texas Southwestern Graduate School of Biomedical Sciences, **1994**.
- [406] J. Taylor and C. J. Deutsch, ^{19}F nuclear magnetic resonance: measurements of $[\text{O}_2]$ and pH in biological systems, *Biophys. J.* 1988, **53**, 227-233.

- [407] Q. Guo, R. F. Mattrey, C. Guclu, R. B. Buxton and O. Nalcioğlu, Monitoring of pO₂ by spin-spin relaxation rate 1/T₂ of ¹⁹F in a rabbit abscess model, *Art. Cells, Blood Subs., Immob. Biotech.* 1994, **22**, 1449-1454.
- [408] J. J. Delpuech, M. A. Hamza and G. Serratrice, Determination of Oxygen by a Nuclear Magnetic-Resonance Method, *J. Magn. Reson.* 1979, **36**, 173-179.
- [409] N. Raghunand and R. J. Gillies, pH and chemotherapy, *Novartis Foundation Symposium* 2001, **240**, 199-211.
- [410] G. A. Smith, P. G. Morris, T. R. Hesketh and J. C. Metcalfe, Design of an indicator of intracellular free Na⁺ concentration using ¹⁹F-NMR, *Biochim. Biophys. Acta* 1986, **889**, 72-83.
- [411] R. Ramasamy, P. Zhao, W. L. Gitomer, A. D. Sherry and C. R. Malloy, Determination of chloride potential in perfused rat hearts by NMR spectroscopy, *Am. J. Physiol.* 1993, **263**, H1958-1962.
- [412] A. A. Bobko, S. V. Sergeeva, E. G. Bagryanskaya, A. L. Markel, V. V. Khrantsov, V. A. Reznikov and N. G. Kolosova, ¹⁹F NMR measurements of NO production in hypertensive ISIAH and OXYS rats, *Biochemical and Biophysical Research Communications* 2005, **330**, 367-370.
- [413] J. Raleigh, A. Franko, D. Kelly, L. Trimble and P. Allen, Development of an in vivo ¹⁹F MR method for measuring oxygen deficiency in tumors, *Magn. Reson. Med* 1991, **22**, 451-466.
- [414] A. Daugherty, N. N. Becker, L. A. Scherrer, B. E. Sobel, J. J. H. Ackerman, J. W. Baynes and S. R. Thorpe, Non-Invasive Detection of Protein-Metabolism In vivo by Nmr-Spectroscopy - Application of a Novel F-19-Containing Residualizing Label, *Biochem. J.* 1989, **264**, 829-835.

- [415] B. A. Berkowitz, J. T. Handa and C. A. Wilson, Perfluorocarbon temperature measurement using ^{19}F NMR, *NMR In Biomed.* 1992, **5**, 65-68.
- [416] T. Q. Duong, J. J. H. Ackerman, H. S. Ying and J. J. Neil, Evaluation of extra- and intracellular apparent diffusion in normal and globally ischemic rat brain via F-19 NMR, *Magn. Reson. Med.* 1998, **40**, 1-13.
- [417] C. Thomas, C. Counsell, P. Wood and G. E. Adams, Use of F-19 Nuclear-Magnetic-Resonance Spectroscopy and Hydralazine for Measuring Dynamic Changes in Blood Perfusion Volume in Tumors in Mice, *J. Natl. Cancer Inst.* 1992, **84**, 174-180.
- [418] R. L. Nunnally, E. E. Babcock, S. D. Horner and R. M. Peshock, Fluorine-19 NMR spectroscopy and imaging investigations of myocardial perfusion and cardiac function, *Magn. Reson. Imaging* 1985, **3**, 399-405.
- [419] R. Tibes, J. Trent and R. Kurzrock, Tyrosine kinase inhibitors and the dawn of molecular cancer therapeutics, *Ann. Rev. Pharmacol. Toxicol.* 2005, **45**, 357-+.
- [420] M. H. Cohen, G. A. Williams, R. Sridhara, G. Chen and R. Pazdur, FDA Drug Approval Summary: Gefitinib (ZD1839) (Iressa(R)) Tablets, *Oncologist* 2003, **8**, 303-306.
- [421] R. Neri, Pharmacology and Pharmacokinetics of Flutamide, *Urology* 1989, **34**, 19-21.
- [422] R. Eliason, J. J. Schoenau, A. M. Szmigielski and W. M. Lavery, Phytotoxicity and persistence of flucarbazone-sodium in soil, *Weed Sci.* 2004 **52**, 857-862.
- [423] J. K. Moon, J.-H. Kim, S. Rhee, G. Kim, H. Yun, B.-J. Chung, S. Lee and Y. Lim, Structural investigation of bistrifluron using X-ray crystallography, NMR spectroscopy, and molecular modeling., *Bull. Korean Chem. Soc.* 2002, **23**, 1545-1547.
- [424] P. Christie, Roflumilast: a selective phosphodiesterase 4 inhibitor, *Drugs Today* 2005, **41**, 667-675.

- [425] K. A. Haagsma and M. K. Rust, Effect of hexaflumuron on mortality of the Western subterranean termite (Isoptera: Rhinotermitidae) during and following exposure and movement of hexaflumuron in termite groups, *Pest Manag. Sci.* 2005 **61**, 517-531.
- [426] A. Howell, Fulvestrant ('Faslodex'): current and future role in breast cancer management, *Crit Rev Oncol Hematol.* 2006 **57**, 265-273.
- [427] K. A. Santora, M. Zakson-Aiken, C. Rasa and W. Shoop, Development of a mouse model to determine the systemic activity of potential flea-control compounds., *Vet Parasitol.* 2002 **104**, 257-264.
- [428] E. Van Den Neste, S. Cardoen, F. Offner and F. Bontemps, Old and new insights into the mechanisms of action of two nucleoside analogs active in lymphoid malignancies: fludarabine and cladribine (Review), *Int. J. Oncol.* 2005, **27**, 1113-1124.
- [429] C. Blasco, G. Font, J. Manes and Y. Pico, Solid-phase microextraction liquid chromatography/tandem mass spectrometry to determine postharvest fungicides in fruits., *Anal Chem.* 2003, **75**, 3606-3615.
- [430] A. W. Abu-Qare and M. B. Abou-Donia, Sarin: health effects, metabolism, and methods of analysis, *Food Chem. Toxicol.* 2002, **40**, 1327-1333.
- [431] R. E. London and S. A. Gabel, F-19 Nmr-Studies of Fluorobenzeneboronic Acids .1. Interaction Kinetics with Biologically Significant Ligands, *J. Am. Chem. Soc.* 1994, **116**, 2562-2569.
- [432] R. F. Mattrey, D. J. Schumacher, H. T. Tran, Q. Guo and R. B. Buxton, The use of Imagent in diagnostic imaging research and ¹⁹F magnetic resonance for pO₂ measurements, *Biomat Art Cells Immob Biotech* 1992, **20**, 917-920.

- [433] S. Laukemper-Ostendorf, A. Scholz, K. Burger, C. P. Heussel, M. Schmittner, N. Weiler, K. Markstaller, B. Eberle, H. U. Kauczor, M. Quintel, M. Thelen and W. G. Schreiber, 19F-MRI of perflubron for measurement of oxygen partial pressure in porcine lungs during partial liquid ventilation, *Magn Reson Med.* 2002, **47**, 82-89.
- [434] C. H. Sotak, P. S. Hees, H.-H. Huang, M.-H. Hung, C. G. Krespan and S. Reynolds, A new perfluorocarbon for use in fluorine-19 magnetic resonance spectroscopy, *Magn. Reson. Med.* 1993, **29**, 188-195.
- [435] M. V. Papadopoulou, R. Pouremad, M. K. Rao, M. Ji and W. D. Bloomer, In vitro evaluation of 4-[3-(2-nitro-1-imidazolyl)-propylamino]-7-trifluoromethylquinoline hydrochloride (NLTQ-1), a new bioreductive agent as a hypoxia marker by F-19-magnetic resonance spectroscopy (F-19-MRS), *In Vivo* 2001, **15**, 365-371.

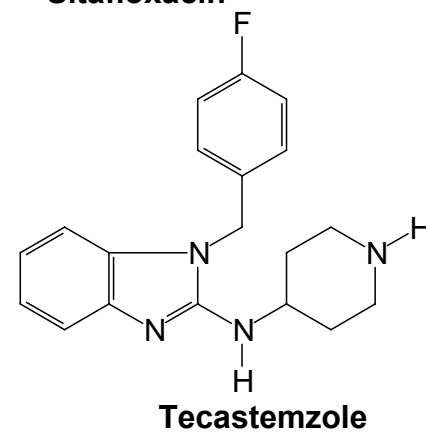
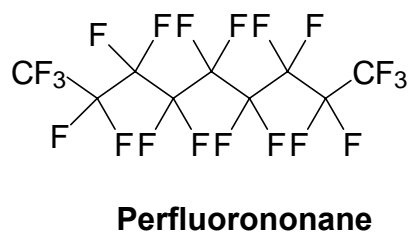
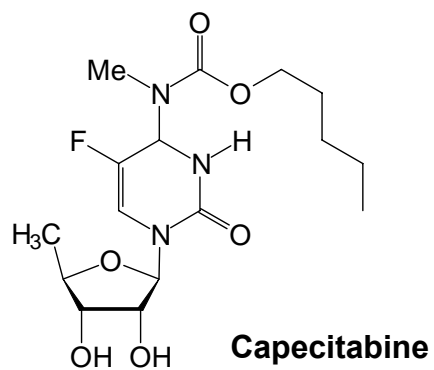
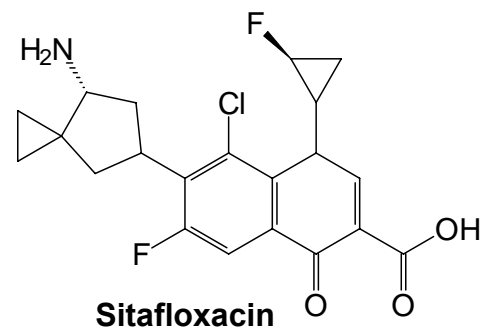
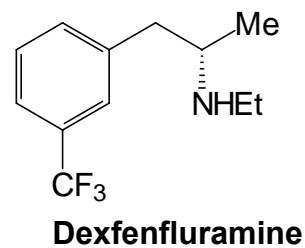
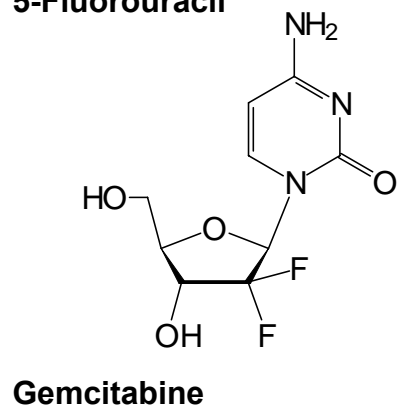
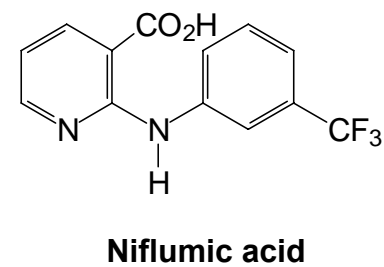
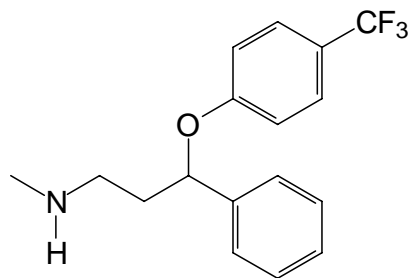
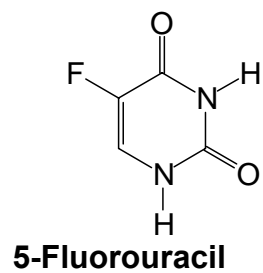
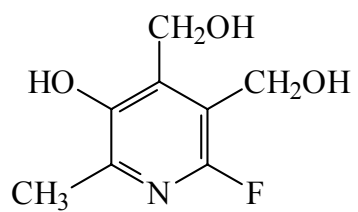
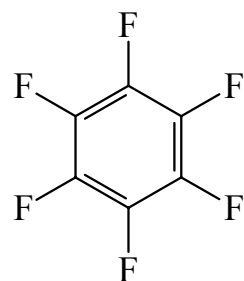


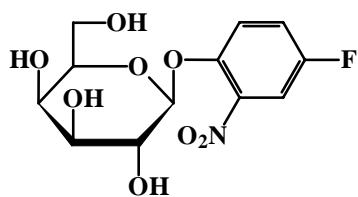
Fig 1a



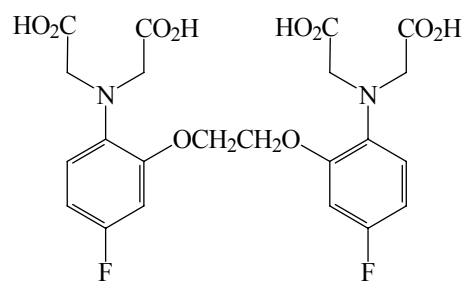
6-FPOL



HFB



PFONPG



5F-BAPTA

Fig 1b

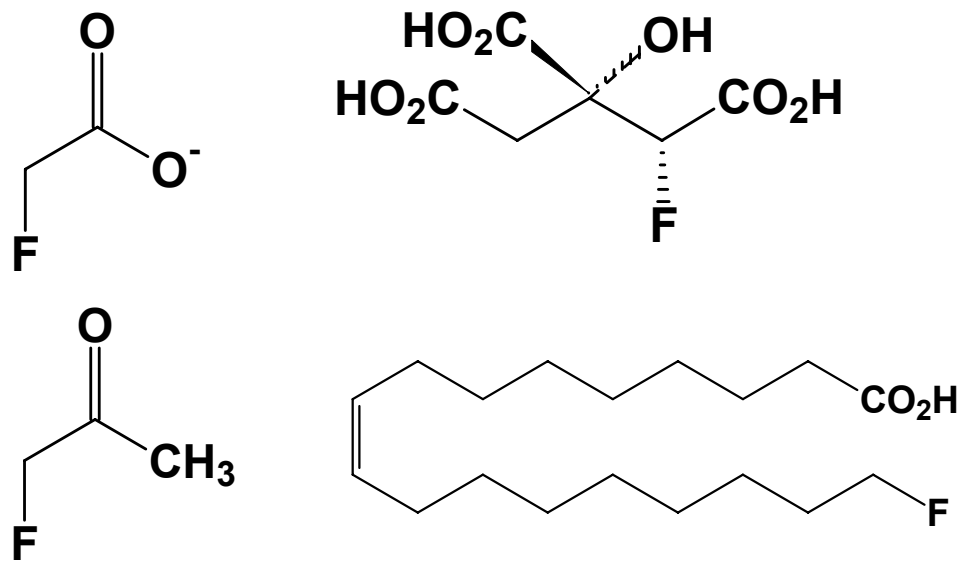


Fig 1c

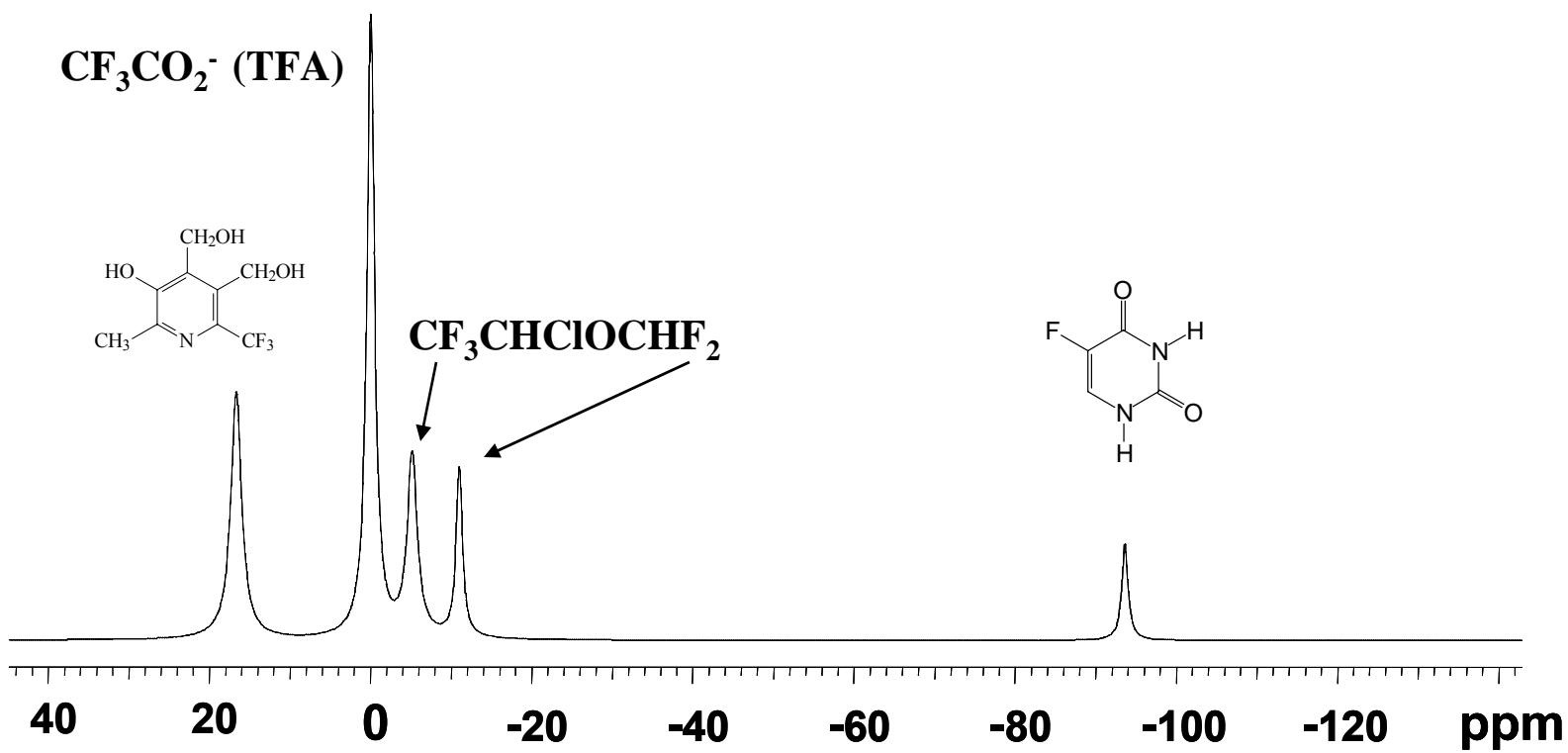


Fig 2

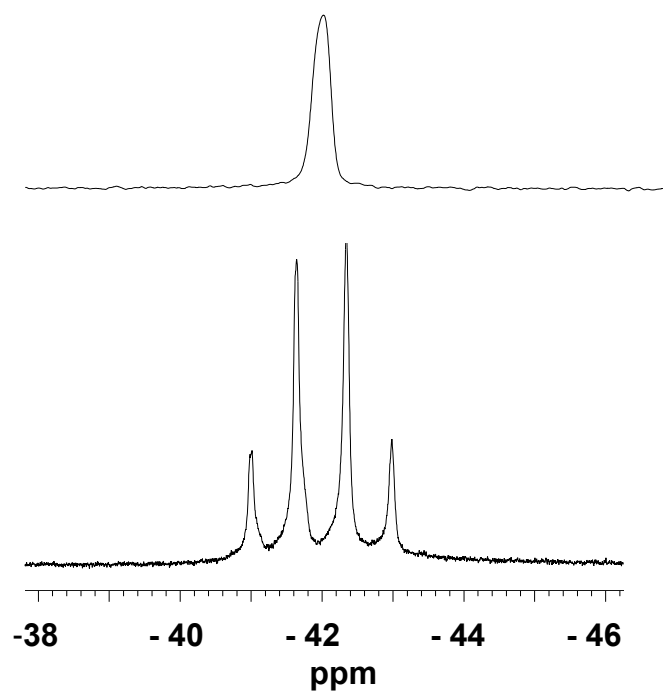


Fig 3

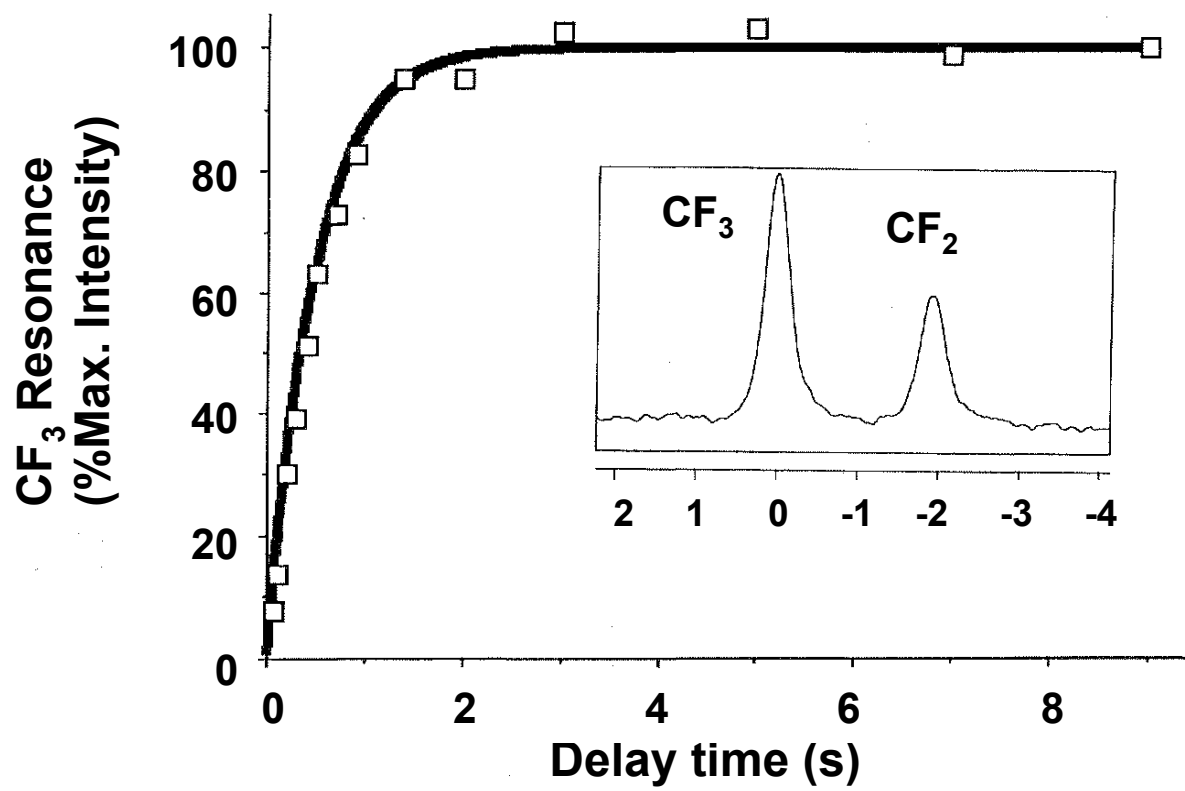


Fig 4a

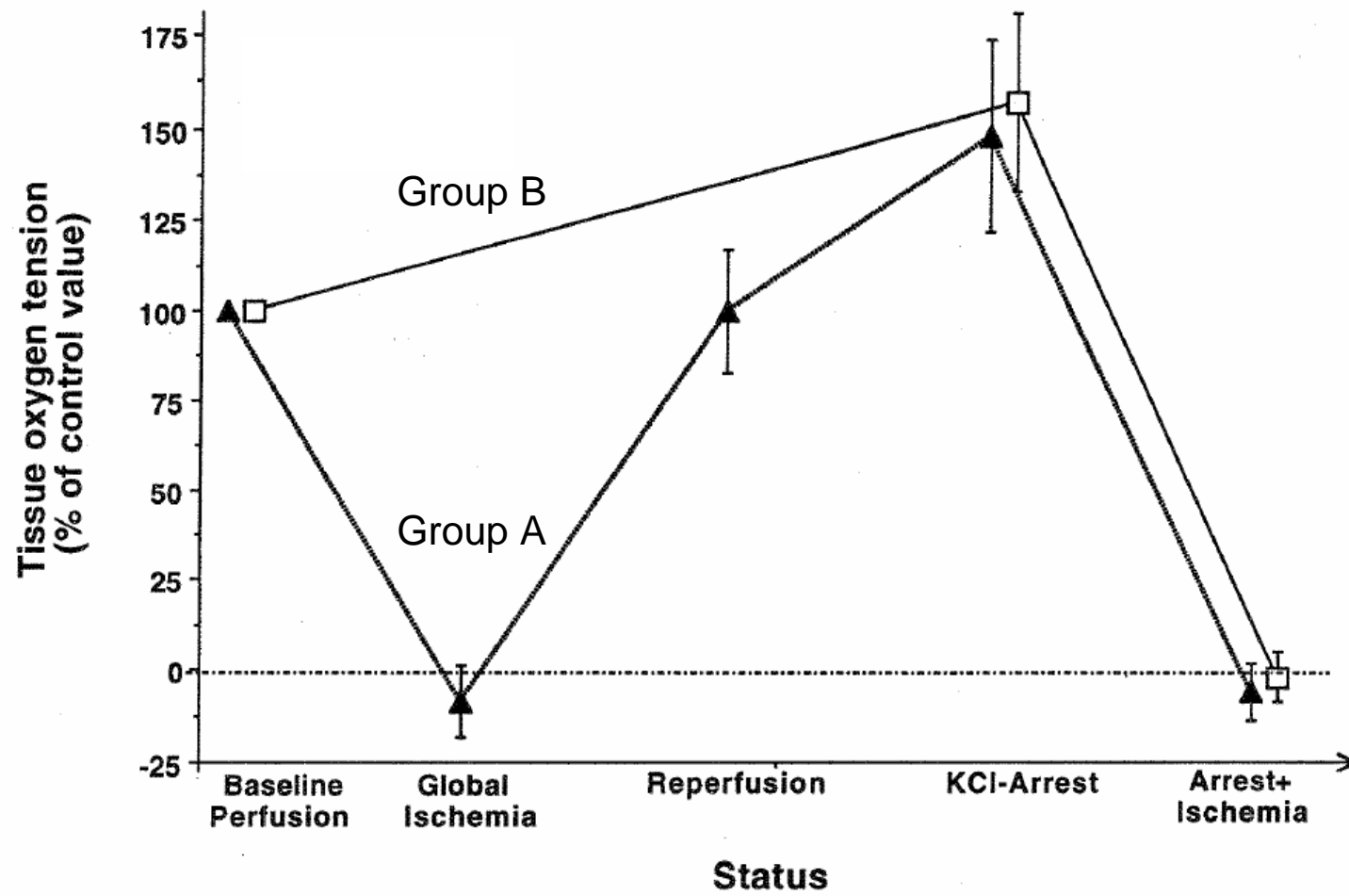


Fig 4b

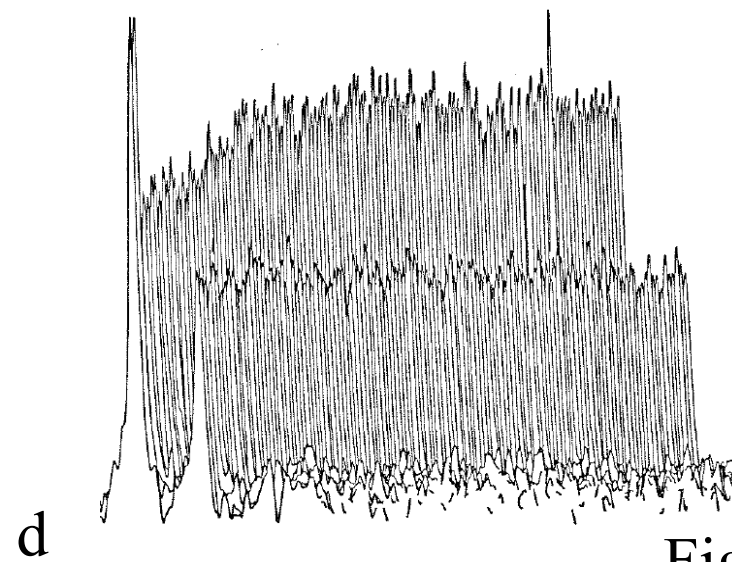
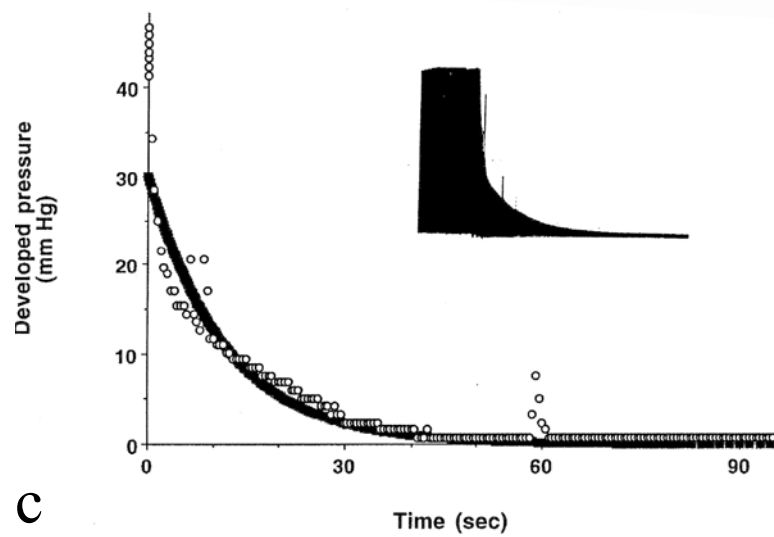
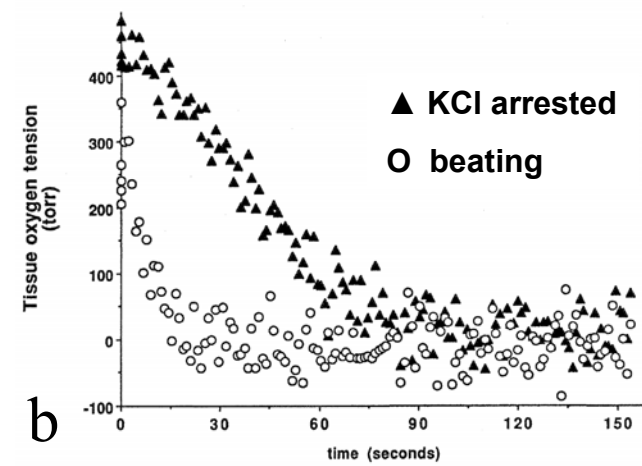
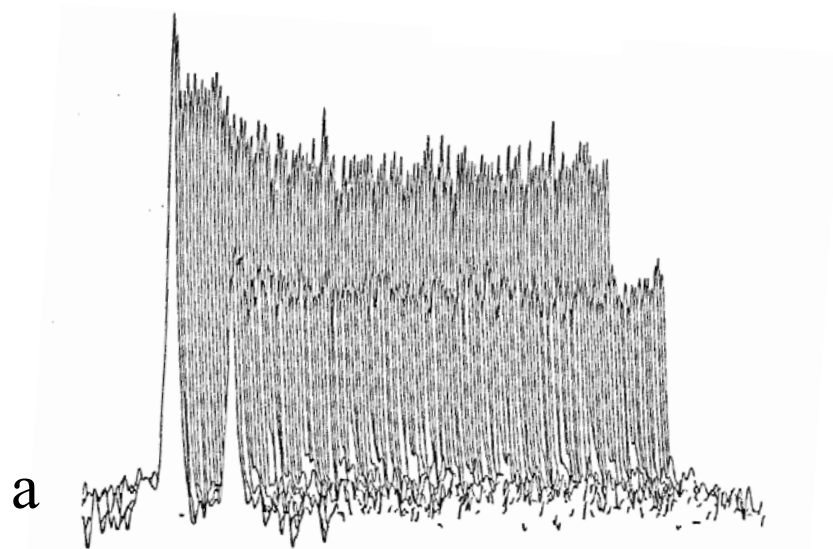


Fig 5

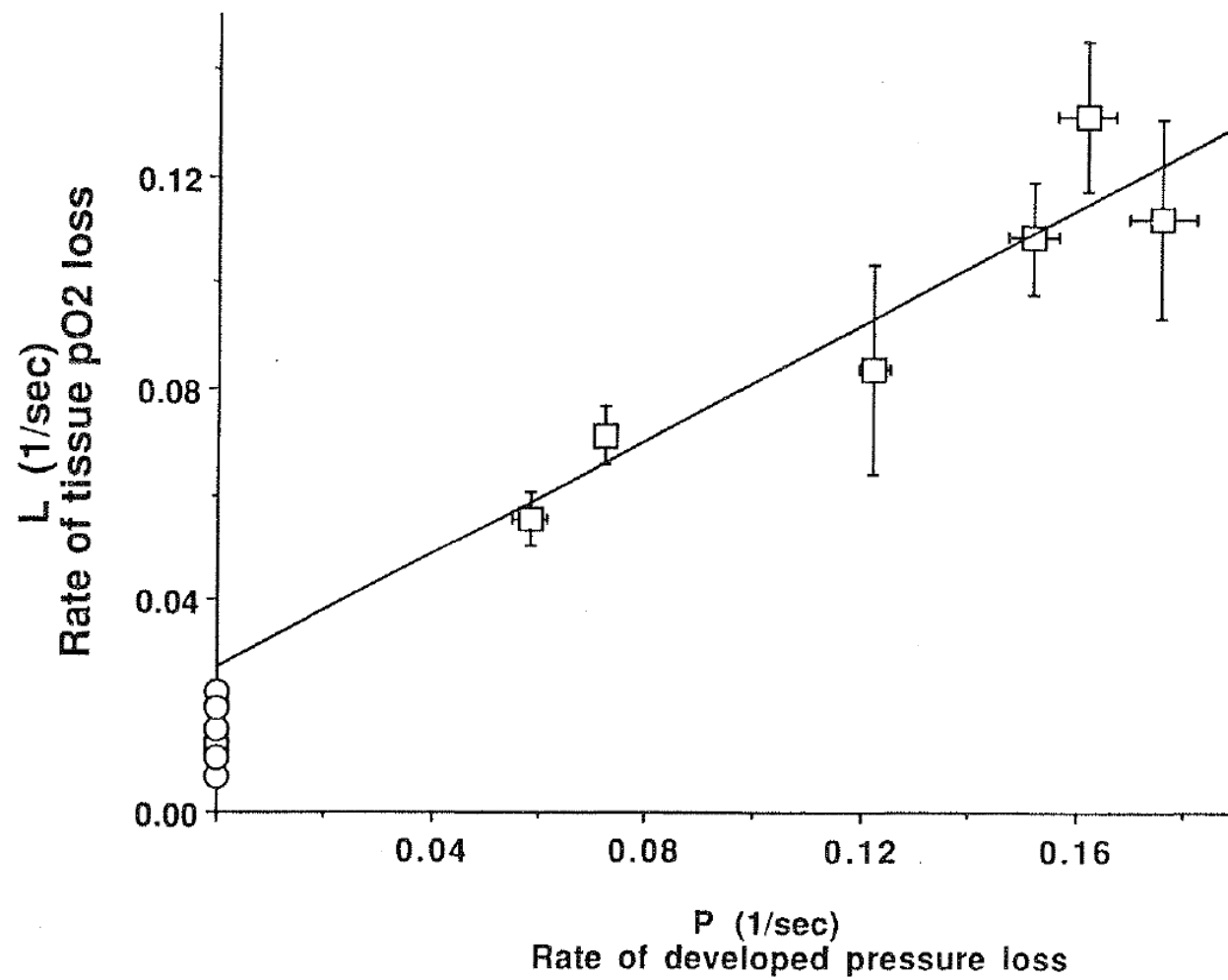


Fig 5e

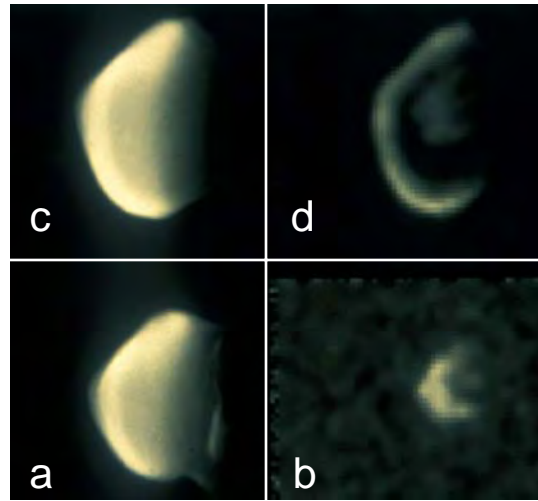
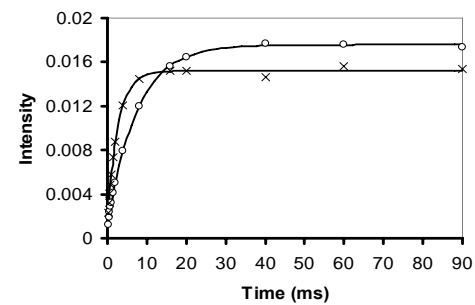
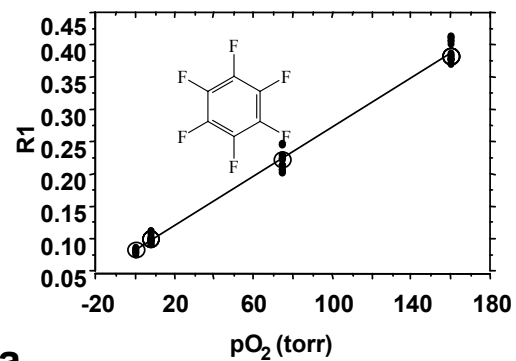


Fig 6



a

b

Air (21% O_2)

Oxygen (100% O_2)

Thigh muscle

c

d

13762NF

e

f

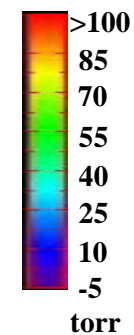


Fig 7

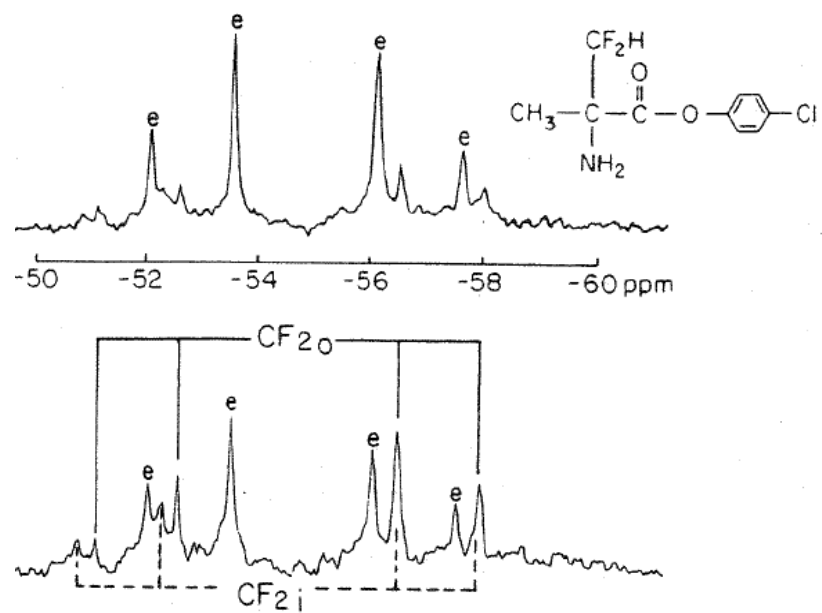


Fig 8

TFA

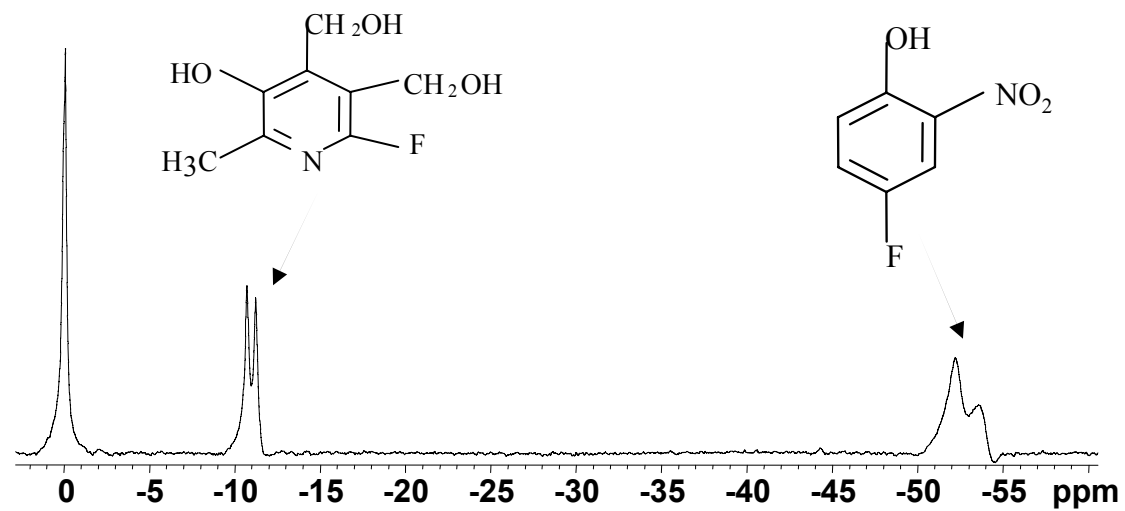
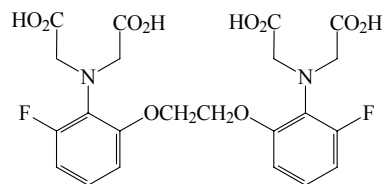
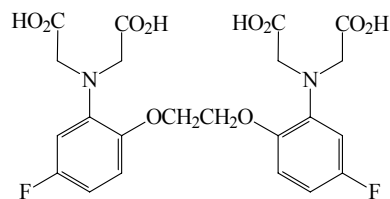


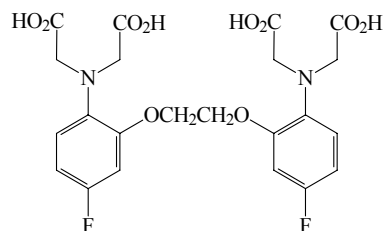
Fig 9



3F-BAPTA ($\log K_{Ca}$ 6.19)



4F-BAPTA ($\log K_{Ca}$ 5.6)



5F-BAPTA ($\log K_{Ca}$ 6.15)

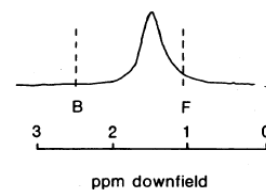
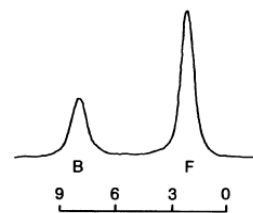
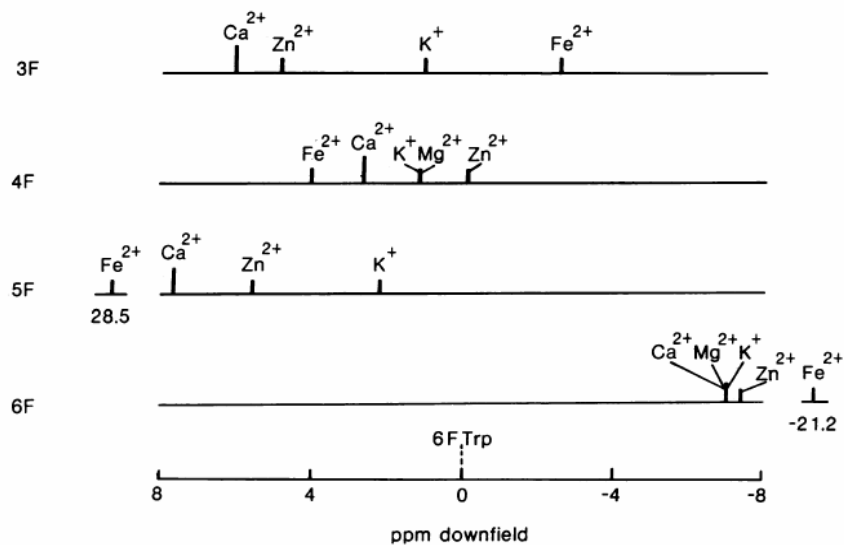


Fig 10

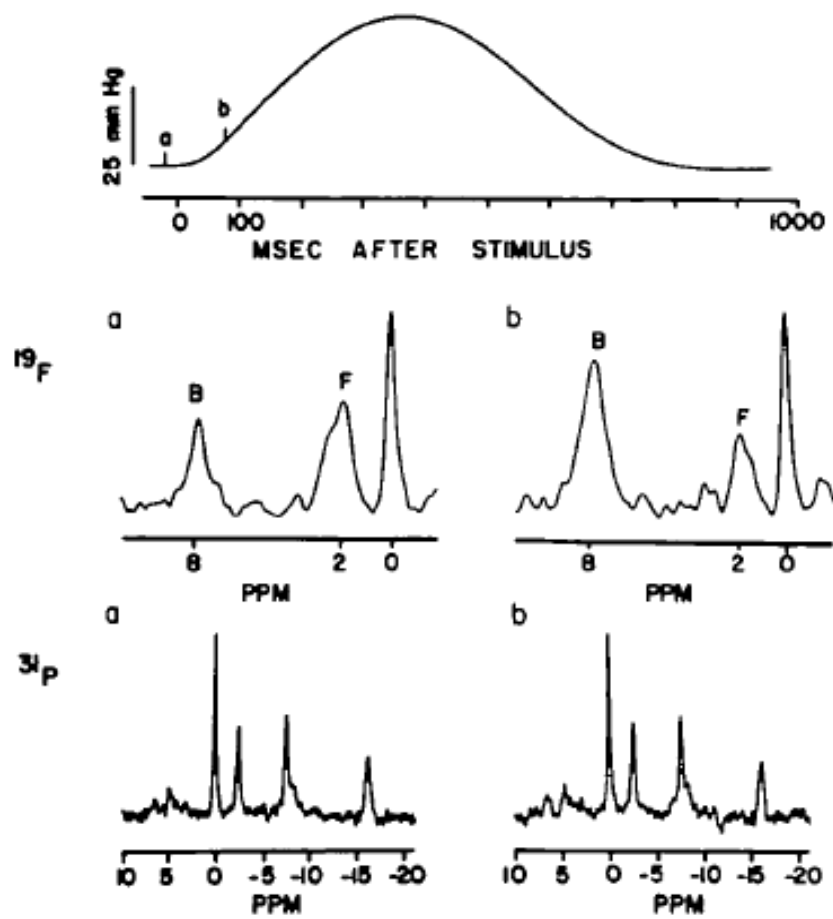


Fig 11

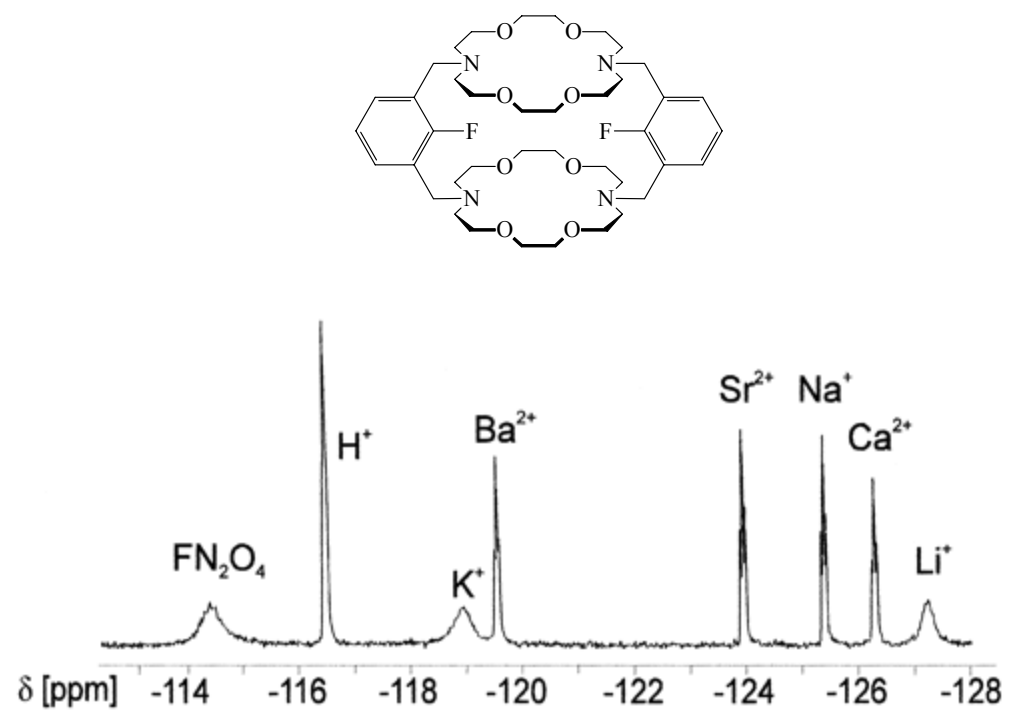


Fig 12

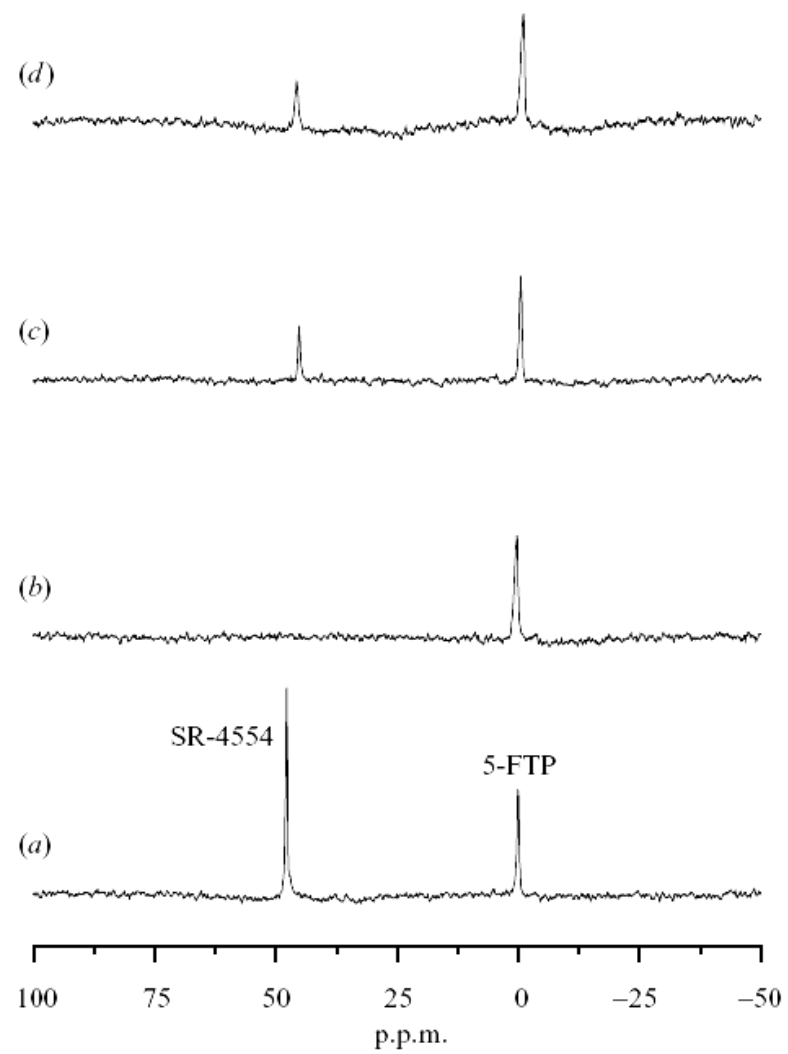


Fig 13

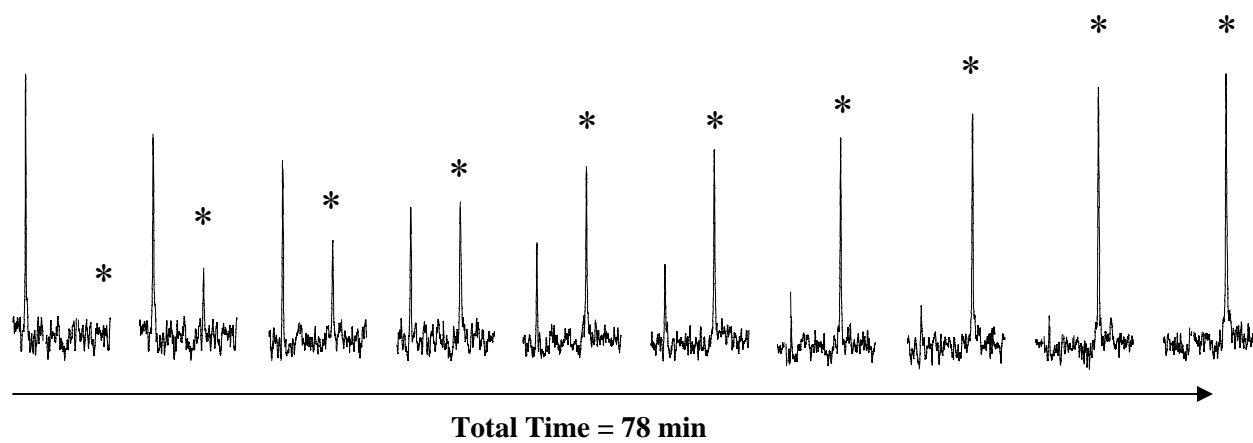


Fig 14

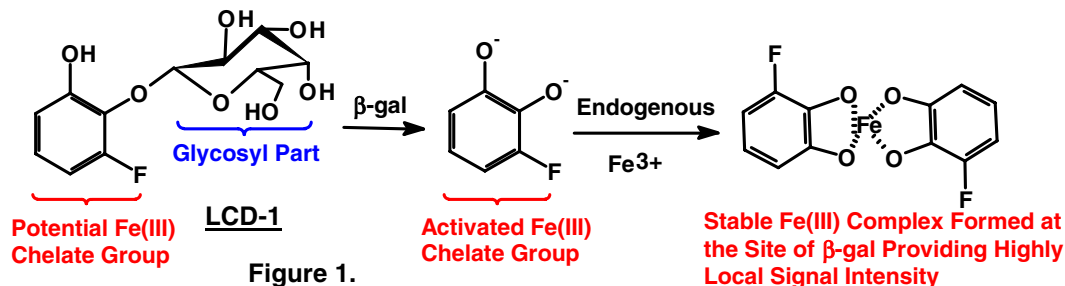
A Novel Approach in the Development of ^{19}F NMR Reporter to Assess LacZ Gene Expression

J.-X. Yu¹, R. Ren¹, R. P. Mason¹

¹Radiology, The University of Texas Southwestern Medical Center at Dallas, Dallas, Texas, United States

Introduction

The *lacZ* gene encoding β -gal is recognized as the most attractive reporter gene, and its introduction has become a standard means of assaying clonal insertion, transcriptional activation, protein expression, and protein interaction. Therefore, noninvasive *in vivo* detection of *lacZ* transgene expression and regulation would be of considerable value in many ongoing and future clinical cancer gene therapy trials. Weissleder *et al.*^[1] presented a near infrared *in vivo* approach based on DDAOG, Meade *et al.*^[2] reported a proton MRI approach using EgadMe. Recently, Mason *et al.* have presented both proton and ^{19}F NMR methods using S-galTM[3], AZD-3^[4] and fluorinated phenolic β -D-galactosides.^[5,6] A problem with the ^{19}F NMR approach was that product aglycones were not trapped at site of activity, but washed out and hence difficult to detect *in vivo*. Iron chelation therapy as novel strategies using some chemical chelators capturing iron in tumor has been applied to clinically treat some cancers. We now explore this new class of ^{19}F NMR reporter (LCD-1) exploiting enzyme-activated Fe-chelation formation to specifically retain the ^{19}F NMR reporter, aiming to increase signal-to-noise and potentially reducing the requisite doses of reporter molecule (Figure 1).



Materials and Methods

LCD-1 was stereo- and regio-selectively synthesized and characterized in our lab. ^{19}F NMR spectra were obtained using a Varian Unity INOVA 400 NMR spectrometer with a dilute solution of sodium trifluoroacetate (NaTFA) in a capillary as external standard (ppm) at 37°C.

Results

LCD-1 was stable in solution and gave a single sharp ^{19}F NMR signal. Addition of β -gal gave effective cleavage (215 $\mu\text{mol}/\text{min}$ per unit β -gal). Addition of LCD-1 to MCF7-*lacZ* cells caused rapid cleavage (Figure 2, 8 $\mu\text{mol}/\text{min}$ per million cells) generating two new signals, which we attribute to intra and extra cellular compartments. These provide an indication of transmembrane pH gradient. When ferric ammonium citrate (FAC) was included, cells generated a purple solution indicative of Fe-complex formation (Figure 3). Now only a single resonance was observed, which we believe represents the trapped complex.

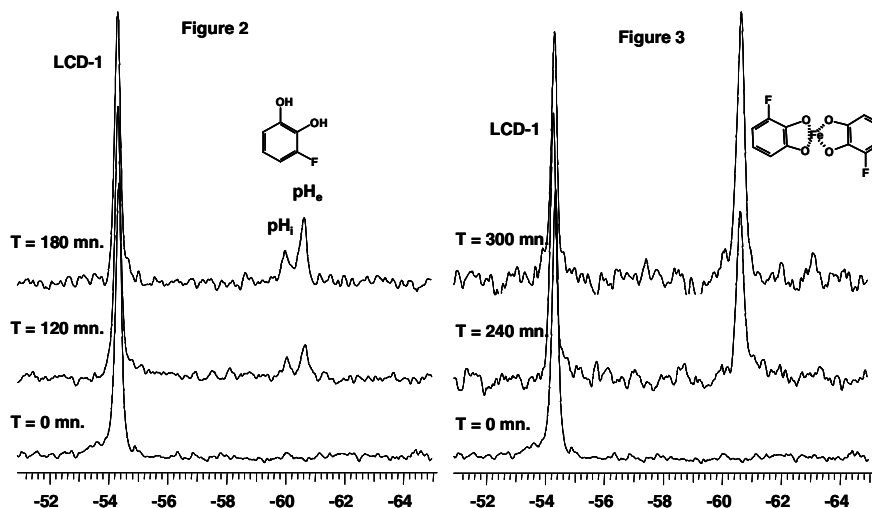
Conclusion

The reporter molecule specially accumulating, targeting or delivering to tumor cells is a great challenge for *in vivo* application with good sensitivity, specificity and spatial localization. These preliminary data demonstrate the feasibility of a novel approach to detecting β -gal activity, *i.e.*, generating complexes to trap the released reporter molecule products. Reassuringly, the product signals remain narrow and detectable, and we believe this fundamentally different approach shows promise for developing *in vivo* ^{19}F NMR platforms to gene reporter molecules.

Supported by DOD Breast Cancer Initiative IDEA award DAMD17-03-1-0343, Cancer Imaging Program P20 CA086354, and BTRP P41RR02584.

References

- [1] Tung *et al. Cancer Res.*, **2004**, 64, 1579-1583. [2] Louie *et al. Nature Biotechnol.*, **2000**, 18, 321-325. [3] Cui *et al. ISMRM*, Kyoto, #1712, **2004**. [4] Yu *et al. 13th ISMRM*, #0167, Florida, May, **2005**. [5] Yu *et al. Curr. Med. Chem.*, **2005**, 12, 819-848. [6] Yu *et al. Bioconjugate Chem.*, **2004**, 15, 1334-1341.



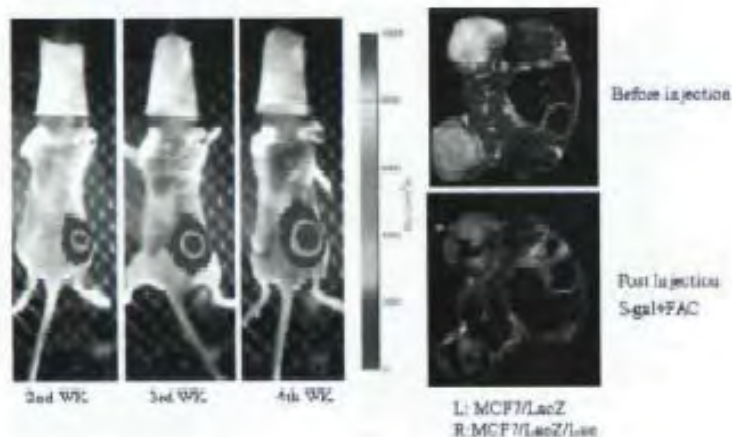
Abstracts from the Proceedings of the Society of Molecular Imaging Hawai'i 2006

Abstract ID: 312 Poster board space: 135

Detection of LacZ and Luciferase Double Gene Expression in Breast Cancer Xenograft by BLI and ^1H MRI.

Li Liu, Weina Cui, Angelina Contero, Ralph P. Mason. UT Southwestern Medical Center, Dallas, TX, USA. Contact e-mail: li.liu@utsouthwestern.edu.

LacZ and Luc have been used widely as reporter genes, to determine the location, the degree of activity and change in magnitude over time of the expression of therapeutic genes. We now report a novel double gene approach to detecting transgenic activity in tumors based on ^1H MRI of the "black stain", S-GalTM (3, 4-cyclohexenoesucletin- β -D-galactopyranoside) and BLI. MCF7 cells were transfected with pCMV/lacZ to generate MCF7/lacZ cells, these cells were further transfected by adenovirus system with Luc gene and the highest expressing clones from each isolated and implanted in flanks of nude female mice. Luciferin-D (450 mg/kg) was administered S.C. in the neck region and BLI acquired 10 mins later over 2 mins with a CCD camera. MRI was performed using a 4.7 T Varian Inova system with T2* weighted images obtained before, and 2 min after the intratumoral injection of 50 mg/kg S-gal-Na and 25 mg/kg ferric ammonium citrate (TR=500ms, TE=15ms, Flip angle=20, matrix=128x128). BLI showed a good linear relationship between light intensity and tumor growth curve in MCF7/lacZ/Luc, while no signal was found in the MCF7/lacZ tumor (left). Black paramagnetic precipitate was detected rapidly in both MCF7/lacZ/Luc and MCF7/lacZ tumors by ^1H MRI following S-gal + FAC injection, and confirmed by histology. Western blots and enzyme assay. This study demonstrates combined MRI and BLI to detect LacZ and Luc double gene expression in breast xenograft. BLI is relatively cheap and



facilitates high throughput interrogation, while MRI provides high spatial resolution. We believe this combined approach can become a valuable tool for assessing tumor growth (*e.g.*, constitutive Luc) together with *in situ* transfection.

Supported by DOD Breast Cancer Initiative IDEA Awards DAMD 170310363

Disclosure of author financial interests or relationships:

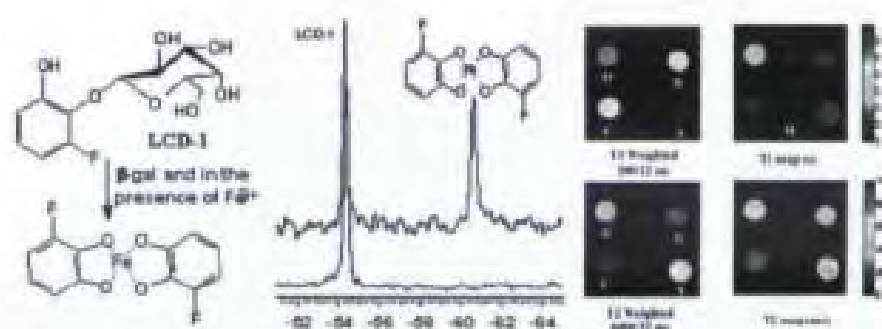
L. Liu, None; W. Cui, None; A. Contero, None; R. Mason, None.

Novel lacZ Gene Reporter with Dual Modalities: ^{19}F MRS and ^1H MRI.

Jian-Xin Yu, Vikram Kodibagkar, Ralph Mason. The University of Texas Southwestern Medical Center at Dallas, Dallas, TX, USA. Contact e-mail: Jian-Xin.Yu@UTSouthwestern.edu.

The *lacZ* gene encoding β -gal has been recognized as the most attractive reporter gene. Therefore, its noninvasive *in vivo* detection would be of considerable value in many ongoing and future clinical cancer gene therapy trials. Tung *et al.* presented a near infrared *in vivo* approach based on DDAOG, Louie *et al.* reported a ^1H MRI approach using EgadMe. Recently, Mason *et al.* presented ^1H MRI, ^{19}F MRS and CSI methods using S-galTM, AZD-3 and fluorinated phenolic β -D-galactosides. We now explore a new class of *lacZ* gene reporters with dual modalities (here LCD-1 as a representative), through enzyme-activated Fe-chelation formation to specifically localize ^{19}F NMR signal ($\Delta\delta$, 6.0ppm) and simultaneously *in situ* generate Fe-based ^1H MRI contrast agent, as shown in the Figure [^{19}F μRS : LCD-1 (2.6 mg, 9.5 μmol), $^4\text{CF-7-lacZ}$ cells (5×10^6) in PBS buffer (0.1M, pH=7.4, 600uL) and FAC (5.2mmol) at 37°C. ^1H MRI: **Conditions:** ^1H MRI, 200 MHz, 1mm slice, 128x128, 25.6x25.6 mm². (A) Control, LCD-1 (3.0 mg, 11 mmol), Fe^{3+} (5.0 mmol), TFA (2.0 mmol), PBS (650 uL); (B) LCD-1 (3.0 mg, 11 mmol), Fe^{3+} (5.0 mmol), MCF-7-*lacZ* cells (5×10^6), TFA (2.0 mmol), PBS (650 uL); (C) LCD-1 (5.8 mg, 21 mmol), Fe^{3+} (5.0 mmol), MCF-7-*lacZ* cells (5×10^6), TFA (2.0 mmol), PBS (650 uL); (D) LCD-1 (3.0 mg, 11 mmol), no Fe^{3+} , MCF-7-*lacZ* cells (5×10^6), TFA (2.0 mmol), PBS (650 uL)].

Acknowledgements Supported by the DOD Breast Cancer Initiative and NCI Pre-ICMIC P20 CA86354.



Disclosure of author financial interests or relationships:

J. Yu, None; V. Kodibagkar, None; R. Mason, None.

Abstract ID: 290 Poster board space: 90

Detection of LacZ Expression In Vivo in MCF-7 Breast Tumors Using Multiple Gene-Reporter Molecules.

Vikram Kodibagkar, Jian-xin Yu, Li Liu, **Ralph Mason**, UT Southwestern Medical Center, Dallas, TX, USA. Contact e-mail: ralph.mason@utsouthwestern.edu.

Gene therapy shows promise for treating cancer and has been successfully exploited in several clinical trials. A major hurdle is establishing a method of verifying transgene activity *in situ*. The *lacZ* gene encoding β -galactosidase (β -gal) has historically been the most popular reporter gene for molecular biology and we are designing non-invasive NMR approaches to reveal β -gal activity *in vivo*. 2-Fluoro-4-nitrophenol- β -D-galactopyranoside (OFPNPG) and 4-Fluoro-2-nitrophenol- β -D-galactopyranoside (PFONPG) belong to a novel class of NMR active molecules (fluorophenyl- β -D-galactopyranosides), which are highly responsive to the action of β -gal. We recently reported chemical shift MRI to detect β -gal activity based on substrate and product development in tumor cells. We now have extended the work by exploiting separate agents: OFPNPG and PFONPG both have a single ^{19}F peak at 55 ppm and 43 ppm, respectively, relative to aqueous sodium trifluoroacetate (NaTFA). Upon cleavage by β -gal, the pH sensitive aglycones OFPNP and PFONP are observed at a chemical shift of 59-61 ppm and 46.5-56 ppm, respectively. This difference in chemical shifts of the two substrates (OFPNPG and PFONPG) and their aglycones combined with a lack of overlap in the signals allowed us to simultaneously administer the two agents in different tumors (PFONPG in MCF-7 and OFPNPG in MCF-7-lacZ) on the same animals and compare the two tumor types with respect to β -gal activity.

Supported by DOD Breast Cancer Initiative DAMD 17-03-1-0343.

Disclosure of author financial interests or relationships:

V. Kodibagkar, None; **J. Yu**, None; **L. Liu**, None; **R. Mason**, None.

A MAGIC approach to gene expression (Magnetic resonance Assay of Gene Imaging Constructs)

Ralph P. Mason, Jian-Xin Yu, Li Liu, Weina Cui Jennifer McAnally, Vikram D. Kodibagkar
Cancer Imaging Program, Department of Radiology, UT Southwestern,
Dallas TX 75390-9058

Email: Ralph.Mason@UTSouthwestern.edu

Gene therapy holds great promise for the treatment of diverse diseases, but widespread implementation is hindered by difficulties in assessing the success of transfection: in particular, assessing the location, magnitude, and persistence of transgene expression. In some cases a single gene can serve as both therapeutic and reporter gene, e.g., thymidine kinase or cytosine deaminase. However, more usually specific reporter genes have been developed with accompanying assays, most notably optical (e.g., luciferase and fluorescent proteins) or radionuclide (hNIS). Optical approaches tend to be cheap and offer exceptionally high throughput, but while they are effective in mice, they tend to lack 3D spatial resolution and anatomical registration. Meanwhile, radionuclide approaches require skills, which are in short supply and agents may be limited by a short shelf life caused by decay or for longer lived isotopes radiolysis. Thus, there is a need for a robust novel technology and NMR appears attractive.

The lacZ gene encoding the enzyme β -galactosidase (β -gal), first described by Jacob and Monod, remains a very popular reporter gene in molecular biology. PCR and Western blotting are the most commonly used techniques for evaluation of gene expression and can be quantitative, but are highly invasive (require biopsy). A characteristic of β -gal is its extreme promiscuity (lack of substrate specificity), which can be exploited with varied substrate structures. Due to its popularity multiple colorimetric reporter substrates for β -gal have been demonstrated and some are commercially available for histology and *in vitro* detection. However, current methods of detecting β -gal activity are generally not suitable for applications *in vivo*. Therefore, development of reporter molecules for non-invasive detection of lacZ transgene expression *in vivo* would be of considerable value both for research and potentially future clinical gene therapy trials. Recently, Tung *et al.* (1) presented a near infrared fluorescent optical approach based on 9H-(1, 3-dichloro-9, 9-dimethylacridin-2-one-7-yl) β -D-galactopyranoside and detected β -gal expression in xenografts in mice. Lee *et al.* (2) described a radio labelled substrate 2-(4-[¹²⁵I/¹²³I]iodophenyl)ethyl-1-thio- β -D-galactopyranoside, which was used to detect β -gal activity in mice using a gamma camera. NMR approaches could be most attractive and Louie *et al* (3) reported a Gd(III)-based ¹H MRI approach using 1-[2-(β -D-galactopyranosyloxy)propyl]-4, 7, 10-

tris(carboxymethyl)-1, 4, 7, 10-tetraazacyclododecane) gadolinium (III), to assess β -gal activity in developing tadpoles. While a pioneering concept, this molecule is difficult to synthesize, provides modest contrast and requires direct intra cellular injection.

We sought alternative NMR active reporter molecules. One of the most fruitful resources for developing novel *in vivo* imaging agents is the body of knowledge associated with traditional histology and pathology. We were first attracted by the simplicity of the traditional “yellow” biochemical indicator ONPG (2-nitrophenol- β -D-galactopyranoside) and this prompted us to synthesize a series of fluorophenyl- β -D-galactopyranosides (FPGs) (4,5). The molecules show useful NMR characteristics with a single sharp ^{19}F NMR resonance, which is stable in whole blood and wild type tumor cells. Upon cleavage by β -gal, the single ^{19}F NMR peak of OFPNPG diminishes accompanied by appearance of a new signal 4-6 ppm upfield corresponding to the aglycon OFPNP. We have demonstrated proof of principle in cultures of cancer cells using ^{19}F NMR spectroscopy and ^{19}F Chemical Shift Imaging (CSI) (4,6) and most significantly demonstrated the ability to differentiate wild type and lacZ expressing breast and prostate tumor xenografts in mice using this approach (7,8).

Ideally, a reporter molecule would be highly sensitive, easy to synthesize and non-toxic. A characteristic of the FPGs is considerable toxicity (mM range) of the aglycon products. Thus, we considered analogs to minimize toxicity. Substitution of a CF_3 group for the fluorine atom enhances signal to noise allowing lower concentrations of substrate to be used. In cells transfected with lacZ to express β -gal, there was rapid release of product accompanied by generation of a new signal, but the chemical shift was much less potentially compromising *in vivo* investigations (9). Toxicity could also be mitigated by use of a fluoropyridoxol aglycon, while maintaining a large chemical shift response. In this case, both the reactivity and water solubility were severely reduced (10). However, introduction of additional sugar moieties enhanced water solubility and restored the reactivity (11). We continue to develop enhanced analogs, since we believe the ^{19}F spectroscopic approach will allow us to examine multiple substrates, potentially sensitive to multiple diverse enzymes simultaneously. As an example three substrates for β -gal and their products are observable simultaneously (Figure 1).

The ^{19}F NMR spectroscopy approach provides unequivocal evidence for gene activity, but proton MRI would have more immediate clinical application. Proton contrast MRI can potentially provide very high resolution in 3 dimensions in species ranging from small rodents to larger animals and ultimately the clinic. We recently showed that the “black stain”, S-GalTM ((3,4-cyclohexenoescoletin- β -D-galactopyranoside)) has potential as a proton MRI reporter (12). Upon cleavage by β -gal in the presence of ferric ions, the aglycon produces an intense black stain, which is not only visible, but also paramagnetic yielding strong T_2^* MRI contrast. We recently showed the first results *in vivo* demonstrating this novel approach to detecting gene activity in LacZ transfected

MCF7 tumor cells and MCF7/LacZ xenograft tumor (Figure 2) (13).

We believe the novel approaches based on Reporter Products for MRI (RPMs) hold great promise as a novel platform for imaging diverse gene activity and detecting gene function *in vivo*. More importantly, it could both accelerate the transfer of gene therapy to patients in the clinic and provide a new tool for the radiologist to evaluate gene therapy success.

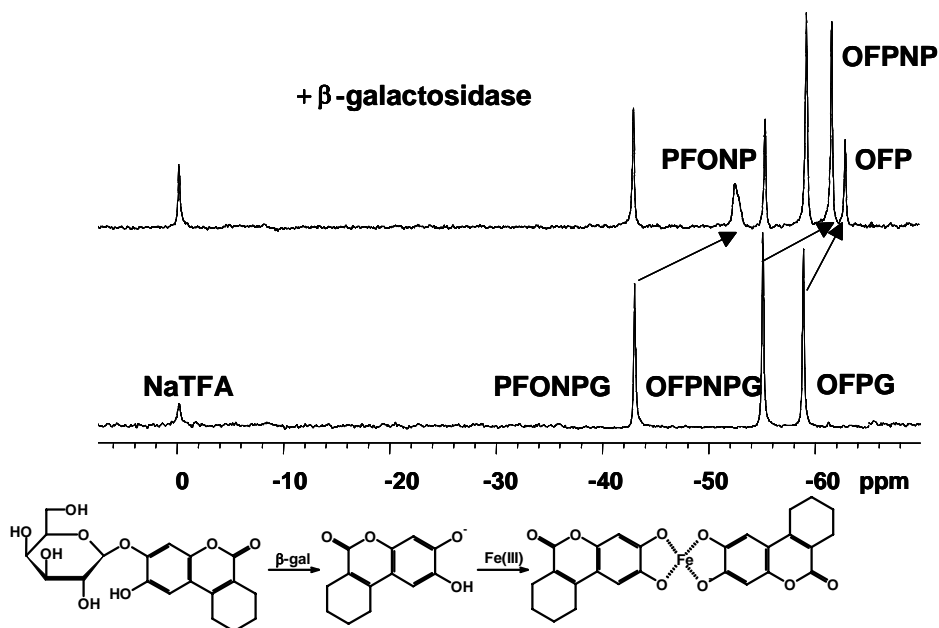


Figure 1 The conversion of three fluorophenyl- β -D-galactopyranosides (FPGs) detected by ^{19}F NMR simultaneously

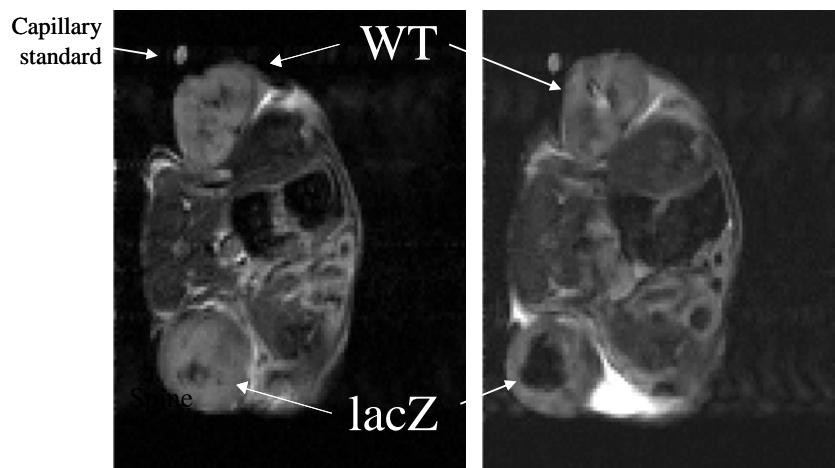


Figure 2 Above: the reaction for β -gal- activated precipitation of S-gal. Left: recognition of MCF7-lacZ tumor versus wild type xenograft in mouse by T2* weighed contrast at 4. 7 T following direct intra tumoral injection of S-gal + FAC.

Supported by the DOD Breast (DAMD 17-03-1-0343-01) and Prostate (17-03-1-0101) Cancer Initiatives. NMR experiments were conducted at the Advanced Imaging Research Center, an NIH BTRP facility #P41-RR02584.

References

1. Tung CH, Zeng Q, Shah K, Kim DE, Schellingerhout D, Weissleder R. In vivo imaging of beta-galactosidase activity using far red fluorescent switch. Cancer Res 2004;64:1579-

1583.

2. Lee KH, Byun SS, Choi JH, Paik JY, Choe YS, Kim BT. Targeting of lacZ reporter gene expression with radioiodine-labelled phenylethyl-beta-d-thiogalactopyranoside. *Eur J Nucl Med Mol Imaging* 2004;31:433-438.
3. Louie AY, Huber MM, Ahrens ET, Rothbacher U, Moats R, Jacobs RE, Fraser SE, Meade TJ. In vivo visualization of gene expression using magnetic resonance imaging. *Nature Biotechnol* 2000;18:321-325.
4. Cui W, Otten P, Li Y, Koeneman K, Yu J, Mason RP. A novel NMR approach to assessing gene transfection: 4-fluoro-2-nitrophenyl- β -D-galactopyranoside as a prototype reporter molecule for b-galactosidase. *Magn Reson Med* 2004;51:616-620.
5. Yu JX, Otten P, Ma Z, Cui W, Liu L, Mason RP. A Novel NMR Platform for Detecting Gene Transfection: Synthesis and Evaluation of Fluorinated Phenyl β -D-Galactosides with Potential Application for Assessing LacZ Gene Expression. *Bioconj Chem* 2004;15(6):1334-1341.
6. Kodibagkar VD, Yu J, Liu L, Hetherington HP, Mason RP. Imaging b-galactosidase activity using ^{19}F chemical shift imaging of LacZ gene-reporter molecule 2-fluoro-4-nitrophenol- β -D-galactopyranoside. *Magn Reson Imaging* 2006;24(7):959-962.
7. Kodibagkar V, Yu J, Liu L, Mason RP. Detection of LacZ expression *in vivo* in MCF-7 breast tumors using multiple gene-reporter molecules. 2006; Hawai'i.
8. Liu L, Kodibagkar VD, Yu JX, Mason RP. In vivo detection of β -gal in PC3 Prostate Xenograft by ^{19}F NMR 2006; Waikoloa Village, Hawai'i. p 372.
9. Yu JX, Liu L, Kodibagkar VD, Cui W, Mason RP. Synthesis and Evaluation of Novel Enhanced Gene Reporter Molecules: Detection of β -Galactosidase Activity Using ^{19}F NMR of Trifluoromethylated Aryl β -D-Galactopyranosides. *Bioorg Med Chem* 2006;14:326-333.
10. Yu JX, Ma Z, Li Y, Koeneman KS, Liu L, Mason RP. Synthesis and Evaluation of a Novel Gene Reporter Molecule: Detection of β -galactosidase activity using ^{19}F NMR of a Fluorinated Vitamin B6 conjugate. *Med Chem* 2005;1(3):255-262.
11. Yu JX, Mason RP. Synthesis and Characterization of Novel lacZ Gene Reporter Molecules: Detection of β -Galactosidase Activity Using ^{19}F NMR of Polyglycosylated Fluorinated Vitamin B6. *J Med Chem* 2006;49:1991-1999.
12. Cui W, Ma Z, Mason RP. S-GalTM, a novel ^1H MRI reporter for b-galactosidase. 2004; Kyoto, Japan. p 1712.
13. Mason RP, Yu Y, Liu L, Cui W, Kodibagkar V. Magnetic resonance assays of gene imaging constructs (MAGIC). 2005; Jackson Hole, WY.